Operator Theory
Advances and Applications
281

Fatihcan M. Atay
Pavel B. Kurasov
Delio Mugnolo
Editors

Discrete and Continuous Models in the Theory of Networks

Birkhäuser

Operator Theory: Advances and Applications

Volume 281

Founded in 1979 by Israel Gohberg

More information about this series at http://www.springer.com/series/4850

Fatihcan M. Atay • Pavel B. Kurasov •
Delio Mugnolo
Editors

Discrete and Continuous Models in the Theory of Networks

Birkhäuser

Editors
Fatihcan M. Atay
Department of Mathematics
Bilkent University
Ankara, Turkey

Pavel B. Kurasov
Department of Mathematics
Stockholm University
Stockholm, Sweden

Delio Mugnolo
Faculty of Mathematics
and Computer Science
FernUniversität in Hagen
Hagen, Germany

ISSN 0255-0156 ISSN 2296-4878 (electronic)
Operator Theory: Advances and Applications
ISBN 978-3-030-44096-1 ISBN 978-3-030-44097-8 (eBook)
https://doi.org/10.1007/978-3-030-44097-8

Mathematics Subject Classification: 34L15, 35R30, 81Q10

This book is published under the imprint Birkhäuser, www.birkhauser-science.com, by the registered company Springer Nature Switzerland AG.
The registered company address is: Gewerbestrasse 11, 6330 Cham, Switzerland

ZiF

Zentrum für interdisziplinäre Forschung
Center for Interdisciplinary Research
Universität Bielefeld

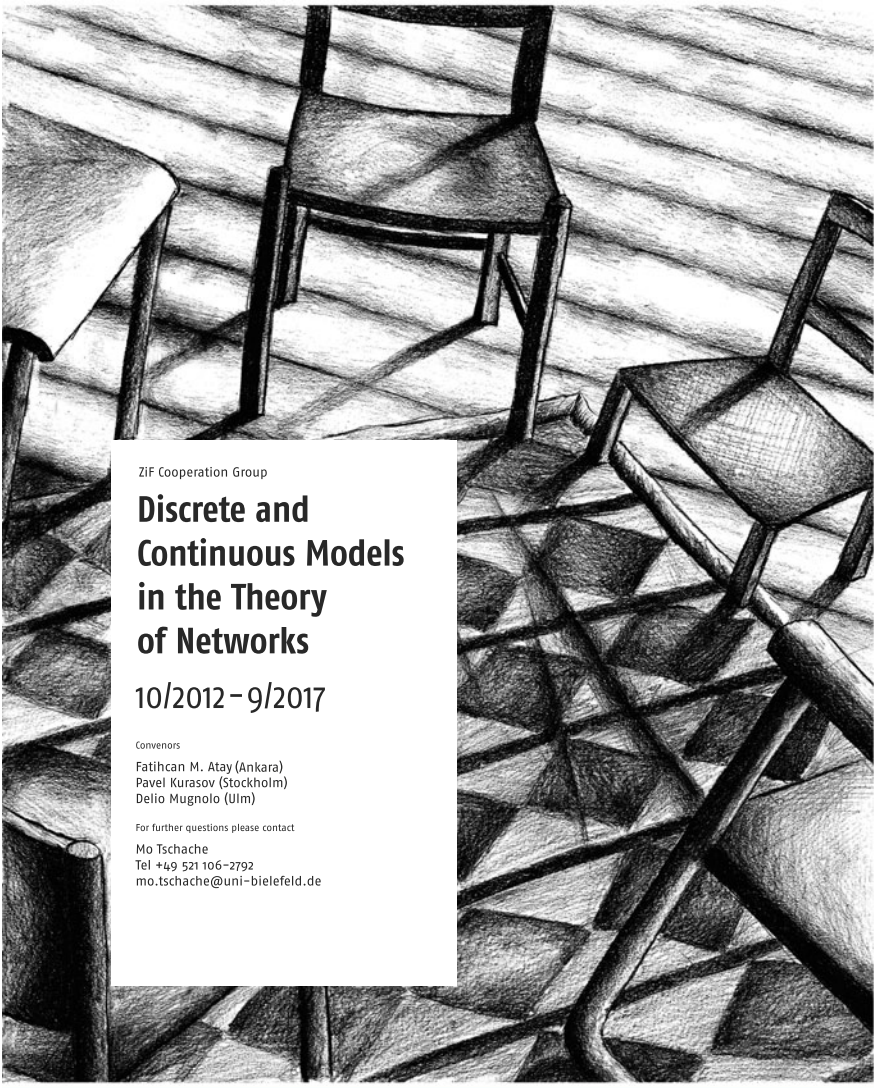

ZiF Cooperation Group

Discrete and Continuous Models in the Theory of Networks

10/2012 – 9/2017

Convenors

Fatihcan M. Atay (Ankara)
Pavel Kurasov (Stockholm)
Delio Mugnolo (Ulm)

For further questions please contact

Mo Tschache
Tel +49 521 106-2792
mo.tschache@uni-bielefeld.de

©ZiF, Felix Hüffelmann (Bielefeld), July 2013

Delio Mugnolo, Pavel B. Kurasov, and Fatihcan M. Atay

©ZiF, Alexandra Polina (Hamburg), September 2017

Pavel B. Kurasov, James Kennedy, and Delio Mugnolo

©ZiF, Alexandra Polina (Hamburg), May 2016

Gregory Berkolaiko

©ZiF, Alexandra Polina (Hamburg), May 2016

Pavel B. Kurasov

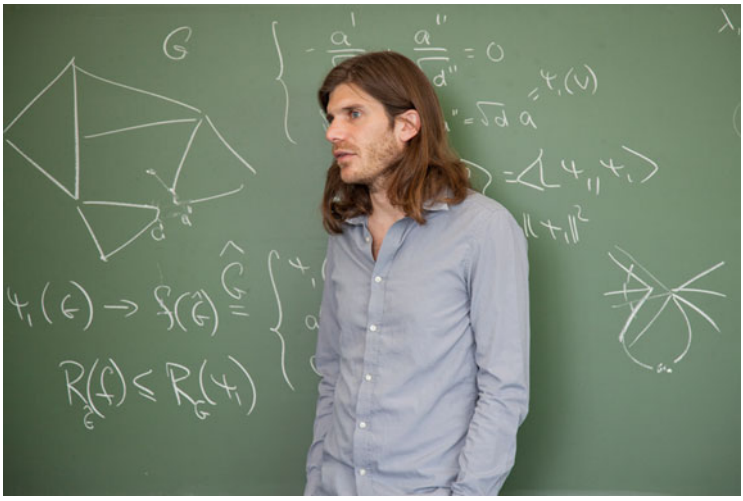

Delio Mugnolo

James Kennedy

ZiF

Zentrum für interdisziplinäre Forschung
Center for Interdisciplinary Research
Universität Bielefeld

Conference
27 November – 1 December 2017

Convenors
Delio Mugnolo (Hagen, GER)
Fatihcan Atay (Ankara, TUR)
Pavel Kurasov (Stockholm, SWE)

DISCRETE AND CONTINUOUS MODELS IN THE THEORY OF NETWORKS

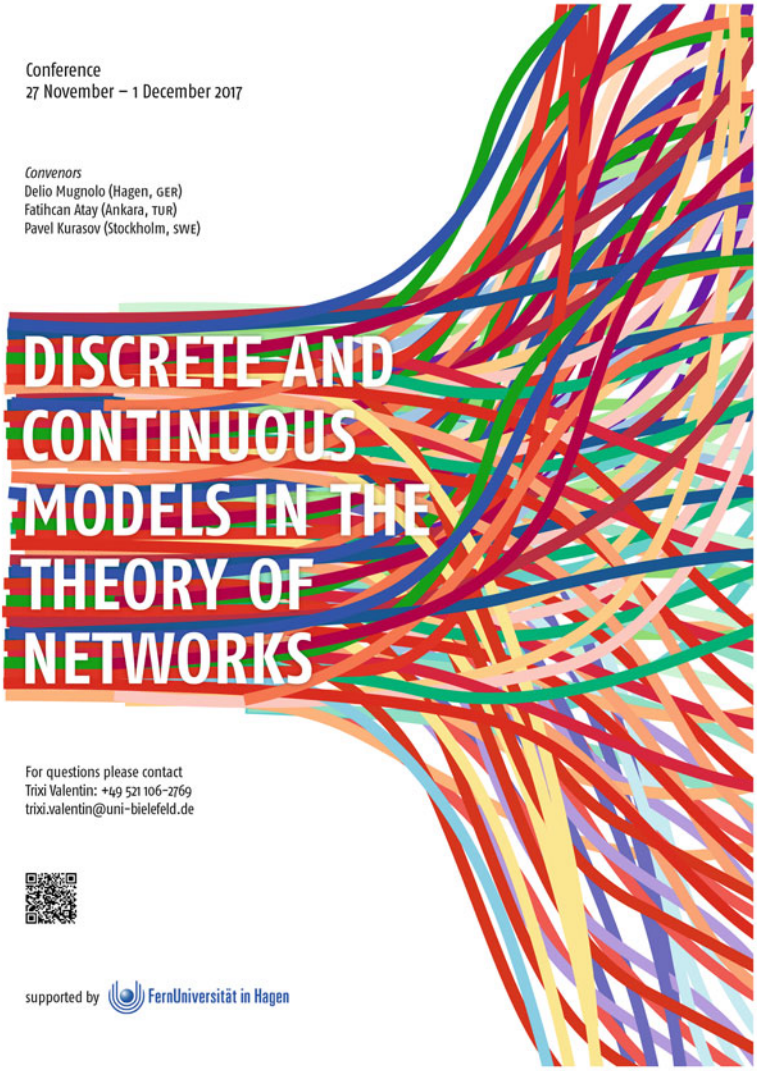

For questions please contact
Trixi Valentin: +49 521 106-2769
trixi.valentin@uni-bielefeld.de

supported by FernUniversität in Hagen

Uzy Smilansky

**First two rows: Shiping Liu, Joachim von Below,
Delio Mugnolo, and Felix Ali Mehmeti**

©ZiF, Alexandra Polina (Hamburg), November 2017

Anders Karlsson

©ZiF, Alexandra Polina (Hamburg), November 2017

Rami Band

©ZiF, Alexandra Polina (Hamburg), November 2017

Closing conference, December 2017

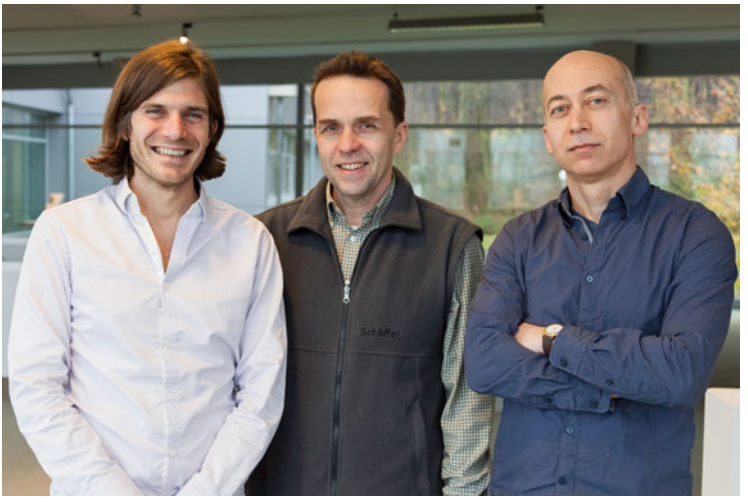

©ZiF, Alexandra Polina (Hamburg), November 2017

Delio Mugnolo, Pavel B. Kurasov, and Fatihcan M. Atay

Preface

The cooperation group “Discrete and Continuous Methods in the Theory of Networks” was granted financial support by

Zentrum für interdisziplinäre Forschung (Centre for Interdisciplinary Research) at Bielefeld University in the summer of 2012 and has begun its investigations in the spring of 2013.

When originally designing this programme, our goal was twofold: on the one hand, we wanted to investigate the possibility of formalising questions from applied sciences—including, but not limited to, theoretical physics and biology—in a graph- or network-based language, making them feasible by mathematical methods. On the other hand, we wanted to bridge the distance between the analysis of difference operators on graphs and differential operators on metric graphs, which 10 years ago used to be studied by different and mostly disconnected communities active in the areas of spectral graph theory, potential theory, spectral geometry, Dirichlet form theory, stochastic analysis, semigroup theory, or dynamical systems.

In the framework of this cooperation group, we have organised a series of short, regular meetings spread all over the 5 years our group was supported. This format has allowed us to work intensively, concentrating meeting-wise on a specific subject; to elaborate our thoughts over time, multiplying our output and adapting our topics to the newest circumstances of research in the fields related to network science; to rebuild our team of collaborators according to our previous experiences, especially promoting productive attitude, interest in/ability at interactions with other group members, intellectual curiosity, promising ideas. We—three mathematicians—have been on our mettle to adapt and respect different scientific cultures concerning diverse issues like speed of publication, hierarchy of research work by graduate students, readiness for idea exchanges before publications, understanding of what kind of advances are worth a publication, and what the main content of an article

should be (Simply a proof? A new experiment? A new phenomenon observed heuristically?).

Throughout the years, we have invited to attend our meetings at the **ZiF** physicists, mathematicians, biologists, neuroscientists, theoreticians of complex networks, a linguist, a logistician, a computer scientist. Reflecting the interdisciplinary mission and the agreeable lack of output pressure of **ZiF**, these open discourses have provided the group with new challenges. Many scientific discussions were led within our group, which highly profited from the stimulating atmosphere at **ZiF**: the activity of dozens of invited scientists resulted in over a hundred published articles. The current volume collects a selection of interesting, original contributions based on scientific questions aroused during the workshops or on topics presented at the conclusive conference held in Bielefeld in December 2017.

In spite of the interdisciplinary nature of our past activities, when planning this volume we have decided to rather focus on our programme's mathematical core: we believe that our knowledge and skills are the best we can contribute to other scientific fields as well as to other mathematical areas.

Selecting papers for this publication was also a way to reflect the current status of the theory of networks and its manifold applications as well as to indicate research directions which we consider most interesting and promising in the medium term. Especially, the last decade saw the birth and the development of investigations on spectral estimates for quantum graphs, much along the lines of classical spectral geometry for manifolds; it is not immodest to say that our programme at **ZiF** was partially responsible for the outburst of this topic. We are glad to present, among others, five papers from this ever-growing area. Also, the dichotomy between graphs and metric graphs has been surpassed and the distance between the theories of finite and infinite graphs is being progressively bridged.

The topics of the papers in this volume can be roughly clustered as follows:

- **Spectral quantum graph geometry**: papers by J.B. Kennedy; by J. Rohleder and C. Seifert; by N. Nicolussi;
- **Spectral theory of discrete graphs**: papers by H. Ge, B. Hua, and A. Lin; by S. Liu, N. Peyerimhoff, and A. Vdovina;
- **Quantum graphs as chaotic systems**: papers by M. Ławniczak, M. Białous, V. Yunko, S. Bauch, and L. Sirko; by H.A. Weidenmüller;
- **Approximations of quantum graphs**: paper by C. Cacciapuoti;
- **Zeta functions for graphs**: paper by A. Karlsson;
- **Few-body systems on metric graphs**: papers by J. Bolte and J. Kerner; by S. Egger;
- **Non-linear differential equations on metric graphs**: papers by S. Dovetta and L. Tentarelli; by J. von Below and J.A. Lubary;
- **Complex networks**: papers by M.-T. Hütt and A. Lesne; by K. Taglieber and U. Freiberg.
- **Applications of networks**: papers by S. Bonaccorsi and S. Turri (epidemics); by M.T. Fairhurst (social networks).

Most of the contributions have direct implications in the study of fundamental problems in natural sciences (close to applications), while also more traditional topics often contain radical ideas opening new perspectives in research.

ZiF's generous support to our research may have ended, but this does certainly not imply the end of our scientific collaborations. We continue to work on the related subjects, keeping contacts established during our meetings at **ZiF**.

This is also the right place to thank all our invitees of the last years, without whom our project could have never be so successful: Riccardo Adami, Felix Ali Mehmeti, Lior Alon, Patricia Alonso Ruiz, Ramy Badr, Rami Band, Moritz Beber, Till Becker, Joachim von Below, Gregory Berkolaiko, Ginestra Bianconi, Türker Biyikoğlu, Jens Bolte, Stefano Bonaccorsi, Jonathan Breuer, Claudio Cacciapuoti, Radu C. Cascaval, Vsevolod Chernyshev, Andrea Corli, Taskin Deniz, Simone Dovetta, Sebastian Egger, Merle Fairhurst, Mareike Fischer, Uta Freiberg, Christoph Fretter, Júlia Gallinaro, Nebojša Gašparović, Federica Gregorio, Jiao Gu, Michael Hinz, Matthias Hofmann, Danijela Horak, Bobo Hua, Marc-Thorsten Hütt, Dina Irofti, Patrick Joly, Jürgen Jost, Stojan Jovanović, Maryna Kachanovska, Cristopher Kaiser-Bunbury, Michael Kaplin, Anders Karlsson, Moritz Kaßmann, Matthias Keller, James Kennedy, Joachim Kerner, Kosmas Kosmidis, Aleksey Kostenko, Maria Kozlova, Marjeta Kramar Fijavž, Hafida Laasri, Francisco Lacerda, Fereshteh Lagzi, Michał Ławniczak, Corentin Léna, Annick Lesne, Jiří Lipovský, Shiping Liu, Wenlian Lu, Alexander Lück, Yuri Maistrenko, Gabriela Malenová, Claudio Marchi, Benjamin Mauroy, Bojan Mohar, Fumito Mori, Jacob Muller, Anna Muranova, Serge Nicaise, Noema Nicolussi, Diego Noja, Philipp-Jens Ostermeier, Gábor Pete, Mats-Erik Pistol, Matteo Polettini, Mason A. Porter, Olaf Post, Jonathan Rohleder, Stefan Rotter, Mostafa Sabri, Sadrah Sadeh, Ruben Sanchez Garcia, Holger Schanz, Jonathan Schiefer, Marcel Schmidt, Michael Schwarz, Andrea Serio, Leszek Sirko, Uzy Smilansky, Adrian Spener, Rune Suhr, Klemens Taglieber, Lorenzo Tentarelli, Christiane Tretter, Françoise Truc, Konstantinous Tsougkas, Francesco Tudisco, Hande Tunçel Gölpek, Stephen J. Watson, Hans Arwed Weidenmüller, Melchior Wirth, Wolfgang Woess, and Verena Wolf.

Last but not least, we would like to express our warmest thanks to the whole staff of the **ZiF** and in particular to the executive secretary Dr Britta Padberg, who throughout these years provided us with an exceptional and highly stimulating environment for research and exchange of ideas and skills—and did so in a competent, interested, and hearty way; to the research secretary Ms Mo Tschache and to the academic coordinator Dr Marc Schalenberg, who constantly supported us with the planning and the everyday management of our workshops; and to Ms Trixi Valentin and Ms Marina Hoffmann of the conference office for their invaluable assistance as the conference was organised and then carried out.

Ankara, Turkey — Fatihcan M. Atay
Stockholm, Sweden — Pavel B. Kurasov
Hagen, Germany — Delio Mugnolo
December 2019

Contents

Stability Matters for Reaction–Diffusion–Equations on Metric Graphs Under the Anti-Kirchhoff Vertex Condition

Joachim von Below and José A. Lubary

Abstract The stability properties of stationary nonconstant solutions of reaction–diffusion–equations $\partial_t u_j = \partial_j^2 u_j + f(u_j)$ on the edges k_j of a finite metric graph G under the so–called anti–Kirchhoff condition (KC) at the vertices v_i of the graph are investigated. The latter one consists in the following two requirements at each node.

$$\sum_{v_i \in k_j} u_j(v_i, t) = 0,$$

$$k_j \cap k_s = \{v_i\} \implies d_{ij}\partial_j u_j(v_i, t) = d_{is}\partial_s u_s(v_i, t),$$

where $d_{ij}\partial_j u_j(v_i, t)$ denotes the outer normal derivative of u_j at v_i on the edge k_j. Though on any finite metric graph there is a simple nonlinearity leading to a unique stable nonconstant stationary solution, there are classes of reaction-terms allowing only stable stationary solutions that are constant on each edge. For example, odd nonlinearities allow only such stable stationary solutions, in particular they only allow the trivial solution as stable one on trees.

The second author was supported by the MINECO grant MTM2017-84214-C2-1-P and is part of the Catalan research group 2017 SGR 1392.

J. von Below (✉)
LMPA Joseph Liouville ULCO, FR CNRS Math. 2956, Universités Lille Nord de France ULCO, Calais, France
e-mail: below@univ-littoral.fr

J. A. Lubary
Departament de Matemàtiques, Universitat Politècnica de Catalunya, Campus Nord, Edifici Ω, Barcelona, Spain

F. M. Atay et al. (eds.), *Discrete and Continuous Models in the Theory of Networks*, Operator Theory: Advances and Applications 281,
https://doi.org/10.1007/978-3-030-44097-8_1

Keywords Reaction–diffusion–equations · Metric graphs · Quantum graphs · Networks · Attractors · Stability · Anti-Kirchhoff condition

MSC (2010) 35K57, 35B35, 35B41, 35R02, 35J25

Among the classical and often considered transition conditions at the nodes of a metric graph we find the continuity condition at the ramification nodes

$$\forall v_i \in V_{\mathrm{r}} : \; k_j \cap k_s = \{v_i\} \implies u_j(v_i) = u_s(v_i), \tag{1}$$

and Kirchhoff's flow law at all the nodes v_i

$$\sum_{j=1}^{N} d_{ij}\partial_j u_j(v_i, \cdot) = 0 \quad \text{for} \quad 1 \le i \le n. \tag{2}$$

We shall cite both conditions (1) and (2) together as (CK). They have been treated by many authors, including generalizations as weighted Kirchhoff conditions and dynamical ones, and are of interest in many settings and applications.

However, when treating wave dispersion or splitting problems on graphs e.g., or as in many other quantum graph problems, the (CK)-condition is not suitable and should be replaced by its *orthogonal* condition, the so-called *anti-Kirchhoff condition* (KC), see [1, 9, 12, 14] and the references therein. It is given by the continuity of the outer normal derivatives at the ramification nodes (5) and by vanishing potential sums at all vertices (4). Mathematically it stems from the self-adjoint orthogonal boundary condition in the sense of the Y-boundary conditions associated to corresponding Bochner-spaces, see [9].

As for the condition (CK), the fundamental paper by E. Yanagida [19] contains a list of five exceptional graphs that do not allow stable nonconstant stationary solutions. Moreover, he established some basic instability tools, as the instability criterion in the presence of two different critical points in one edge. In 2015 the authors [7] showed that the same exclusion result for any metric graph with sufficiently small edge lengths, as well as for any metric graph for the cubic balanced case $f(u) = u - u^3$, for $f(u) = \eta \sin(u)$ and for some other nonlinearities. Other recent instability criteria, also for dynamical Kirchhoff conditions, can be found in [10]. Finally, the authors [8] showed that in the fully autonomous case, there are no stable stationary nonconstant solutions at all.

The present paper deals with the stability of stationary solutions of the flow on a metric graph governed by autonomous reaction-diffusion edge equations under the anti-Kirchhoff condition. To be more specific, on the edges k_j of a metric graph we

consider the problem

$$\begin{cases} u_j \in \mathcal{C}([0,\ell_j]\times[0,\infty))\cap\mathcal{C}^{2,1}([0,\ell_j]\times(0,\infty)) & \text{for } 1\le j\le N,\\ \partial_t u_j = \partial_j^2 u_j + f(u_j) \quad \text{on } k_j & \text{for } 1\le j\le N,\\ u=\big(u_j\big)_{N\times 1} \text{ satisfies (4) and (5)} \end{cases} \tag{3}$$

with the transition condition at the vertices v_i

$$\sum_{v_i\in k_j} u_j(v_i,t)=0 \quad \text{for} \quad 1\le i\le n, \tag{4}$$

$$k_j\cap k_s=\{v_i\} \implies d_{ij}\partial_j u_j(v_i,t)=d_{is}\partial_s u_s(v_i,t) \quad \text{for} \quad 1\le i\le n. \tag{5}$$

Conceivably, we shall cite both conditions (4) and (5) together as (KC). Note that (4) reduces to the 0-Dirichlet condition at boundary vertices.

The presentation is organized as follows. After some prerequisites and graph theoretical preliminaries in Sects. 1 and 2 presents some basic facts about stationary solutions, while Sect. 3 presents basic tools for the stability analysis for stationary solutions. In particular, instability criteria in connection with the Rayleigh quotient of the linearized eigenvalue equations at a stationary solution will be presented. In Sect. 4 nonlinearities vanishing at 0 will be treated, in particular on trees and non bipartite unicyclic graphs. In Sect. 5 it will be shown that on any finite metric graph G, there is a nonlinearity such that there exists a stable nonconstant stationary solution on G. This exhibits a remarkable difference with the (CK)-case, where Yanagida's exceptional graphs or others do never allow such solutions. In Sect. 6 it will be shown that odd nonlinearities always exclude stable nonconstant stationary solution eventually except those solutions that are constant on each edge and belong to the kernel of the signless incidence matrix. This implies that on trees, odd nonlinearities allow only the trivial solution as stable one. Finally, under the condition $f(0)=0$, it will be shown in Sect. 7 that problem (3) never has stable nontrivial stationary solutions on a loop.

1 Metric Graphs

For any graph $\Gamma=(V,E,\in)$, the vertex set is denoted by $V=V(\Gamma)$, the edge set by $E=E(\Gamma)$ and the incidence relation by $\in\subset V\times E$. The valency of each vertex v is denoted by $\gamma(v)=\#\{k\in E \,\big|\, v\in k\}$. Unless otherwise stated, all graphs considered in this paper are assumed to be nonempty, connected and finite with

$$n=\#V, \qquad N=\#E.$$

The vertices will be numbered by $v_1, \ldots, v_n$, the respective valencies by $\gamma_1, \ldots, \gamma_n$, and the edges by $k_1, \ldots, k_N$. The *boundary vertices* $V_{\rm b} = \{v_i \in V \,\big|\, \gamma_i = 1\}$ will be distinguished from the *ramification nodes* $V_{\rm r} = \{v_i \in V \,\big|\, \gamma_i \geq 2\}$ and the *essential ramification nodes* $V_{\rm ess} = \{v_i \in V \,\big|\, \gamma_i \geq 3\}$. By definition, a *circuit* is a connected and regular graph of valency 2. A *path* is a connected graph with two distinct vertices of valency 1 while the other vertices are all of valency 2. For further graph theoretical terminology we refer to [11, 18].

Moreover, we consider each graph as a connected *topological graph* in $\mathbb{R}^m$, i.e. $V(\Gamma) \subset \mathbb{R}^m$ and the edge set consists in a collection of Jordan curves

$$E(\Gamma) = \{\pi_j : [0, \ell_j] \to \mathbb{R}^m \,\big|\, 1 \leq j \leq N\}$$

with the following properties: Each support $k_j := \pi_j\left([0, \ell_j]\right)$ has its endpoints in the set $V(\Gamma)$, any two vertices in $V(\Gamma)$ can be connected by a path with arcs in $E(\Gamma)$, and any two edges $k_j \neq k_h$ satisfy $k_j \cap k_h \subset V(\Gamma)$ and $\#(k_j \cap k_h) \leq 2$. The arc length parameter of an edge k_j is denoted by x_j. Unless otherwise stated, we identify the graph $\Gamma = (V, E, \in)$ with its associated *metric graph*, *network* or *quantum graph*

$$G = \bigcup_{j=1}^{N} \pi_j\left([0, \ell_j]\right),$$

especially each edge π_j with its support k_j. Throughout it will be assumed that all $\pi_j \in \mathcal{C}^2([0, \ell_j], \mathbb{R}^m)$. Thus, endowed with the induced topology G is a connected and compact space in $\mathbb{R}^m$. Throughout, we shall denote the total graph length by

$$L = L(\Gamma) = \sum_{j=1}^{N} \ell_j.$$

The orientation of the graph Γ is given by the *incidence matrix* $\mathcal{D}(\Gamma) = (d_{ik})_{n \times N}$ with

$$d_{ij} = \begin{cases} 1 & \text{if } \pi_j(\ell_j) = v_i, \\ -1 & \text{if } \pi_j(0) = v_i, \\ 0 & \text{otherwise.} \end{cases}$$

For functions defined on the edges $u_j : [0, \ell_j] \to \mathbb{C}$ we use the abbreviations

$$u_j(v_i) := u_j(\pi_j^{-1}(v_i)), \quad \partial_j u_j(v_i) := \frac{\partial}{\partial x_j} u_j(x_j)\Big|_{\pi_j^{-1}(v_i)} \quad \text{etc.}$$

Moreover, using $u := \left(u_j\right)_{N\times 1}$, we shall abbreviate

$$\int_G u\,dx = \sum_{j=1}^{N} \int_0^{\ell_j} u_j(x_j)\,dx_j.$$

Endowed with a usual product norm we introduce the following vector spaces for $k \in \mathbb{N}$ and $p \in [1,\infty]$.

$$\mathcal{V}^k(G) = \prod_{j=1}^{N} \mathcal{C}^k[0,\ell_j], \quad \mathcal{C}^k(G) = \{u \in \mathcal{V}^k(G) \,\big|\, u \text{ satisfies } (1)\},$$

$$L^p(G) = \prod_{j=1}^{N} L^p(0,\ell_j), \quad H^k(G) = \prod_{j=1}^{N} H^k(0,\ell_j),$$

$$\mathcal{H}^k_{KC}(G) = \left\{u \in H^k(G) \,\big|\, u = \left(u_j\right)_{N\times 1} \text{ satisfies (4) and (5)}\right\},$$

$$\mathcal{H}^k_{K_0}(G) = \left\{u \in H^k(G) \,\big|\, u = \left(u_j\right)_{N\times 1} \text{ satisfies (4)}\right\}.$$

The validity of the anti-Kirchhoff conditions (4) and (5) in a function space will be indicated by the subscript (KC), the one of (4) only by the subscript K_0. The validity of the classical Kirchhoff flow condition in spaces of continuous functions on G will be indicated by the subscript K, e.g. $\mathcal{C}^1_K(G)$ etc.

Note that $\mathcal{V}^0_{K_0}(G)$ is a closed subspace of $\mathcal{V}^0(G)$ endowed with the norm of uniform convergence. As $\left\{u \in \mathcal{C}^1[0,1] \,\big|\, u'(0) = u'(1) = 0\right\}$ is a dense subspace of $\mathcal{C}[0,1]$, $\mathcal{V}^1_{KC}(G)$ is a dense subspace of $\mathcal{V}^0_{K_0}(G)$. This will permit to minimize the Rayleigh quotient introduced in (9) in $\mathcal{H}^1_{K_0}(G)$ or in suitable subspaces of it.

2 Stationary Solutions

In the present context of reaction–diffusion–equations, a *stationary solution* is by definition a solution that does not depend on time. Stationary solutions of Problem 3 satisfy $\int_G f(u)dx = 0$ in the (CK)-case. This is no longer true under (KC). Set

$$v_i = d_{ij}\,\partial_j u_j(v_i,t) \tag{6}$$

for some incident edge k_j with v_i.

Lemma 2.1 *A stationary solution u of (3) satisfies* $\int_G f(u)dx = -\sum_{i=1}^{n} \gamma_i v_i$ *and*

$$\int_G f(u)\, u\, dx = \|u\|^2_{H_0^1(G)}\,.$$

Proof The first assertion follows readily from the edge differential equations. As for the second one, we conclude

$$\sum_j \int_0^{\ell_j} f(u_j)\, u_j\, dx_j = \sum_j \int_0^{\ell_j} \left(\partial_j u_j\right)^2 dx_j - \sum_j \left[\partial_j u_j(x_j)\, u_j\,(x_j)\right]_0^{\ell_j}$$

$$= \sum_j \int_0^{\ell_j} \left(\partial_j u_j\right)^2 dx_j - \sum_i v_i \sum_{v_i \in e_j} u_j(v_i) = \sum_j \int_0^{\ell_j} \left(\partial_j u_j\right)^2 dx_j.$$

■

Lemma 2.2 *A stationary solution u of (3) on a bipartite graph satisfies*

$$\int_G \partial u\, dx = 0.$$

Proof Using a source-sink-orientation of Γ, we conclude

$$\int_G \partial u\, dx = \sum_j \left[\, u_j\,(x_j)\right]_0^{\ell_j} = \sum_j \left(u_j(\ell_j) - u_j(0)\right) = 0.$$

■

Closing this section we pursue a Lyapunov-energy-calculus with

$$\mathcal{E}(u) = \int_G \frac{(\partial u)^2}{2} - F(u)\, dx, \quad F(s) = \int_0^s f(\eta)\, d\eta.$$

Lemma 2.3 *Let u be a solution of (3). Along u the energy decreases:*

$$\dot{\mathcal{E}}(u) := \frac{d}{dt}\mathcal{E}(u) = -\int_G (\partial_t u)^2\, dx.$$

Proof We can follow a standard density argument using conditions (4) and (5):

$$\begin{aligned}\dot{\mathcal{E}}(u) &= \int_G \partial_{xt} u \partial_x u - f(u)\partial_t u \, dx \\ &= \underbrace{\sum_j \left[\partial_t u_j \; \partial_j u_j\right]_0^{\ell_j}}_{=0} - \int_G \partial_t u \underbrace{\left(\partial_x^2 u + f(u)\right)}_{\partial_t u} dx = -\int_G (\partial_t u)^2 \, dx,\end{aligned}$$

since

$$\sum_j \left[\partial_t u_j \; \partial_j u_j\right]_0^{\ell_j} = \sum_i \sum_j \underbrace{d_{ij}\partial_j u_j(v_i,t)}_{v_i(t)} \partial_t u_j(v_i,t) = \sum_i v_i(t)\partial_t \underbrace{\Big(\sum_j d_{ij}^2 u_j(v_i,t)\Big)}_{=0} = 0.$$

■

In order to establish the application of Lasalle's principle, we have to add an extra condition on F. For example, under the hypothesis

$$\left\{z \in \mathbb{R} \;\middle|\; F(z) \geq 0\right\} \text{ bounded} \tag{7}$$

we obtain with $M := \max_{\mathbb{R}} F^+ < \infty$ that $\mathcal{E}(u) \geq -\int_G F(u)\,dx \geq -ML$. This enables the application of Lasalle's Principle [2] in order to conclude the following

Corollary 2.4 *Under condition (7) the solutions u belonging to* $\mathcal{C}\left([0,\infty); H^1(\Gamma)\right) \cap \mathcal{C}^1\left((0,\infty); \mathcal{H}^1_{KC}(\Gamma)\right)$ *of (3) tend to stationary solutions as* $t \to \infty$ *with respect to* $\|u\|_{H^1(\Gamma)}$*, since their ω-limits belong to the set of functions satisfying* $\dot{\mathcal{E}}(u) = 0$.

3 Stability

Throughout, we use Lyapunov's notion of stability. Conceivably, a stationary solution w of problem (3) is called *stable* with respect to some norm $\|\cdot\|_G$ on G if for each $\epsilon > 0$, there exists a $\delta > 0$ such that, for each initial data $u_0 \in \mathcal{C}(G)$ with $\|u_0 - w\|_G < \delta$ the solution of (3) exists in $[0,\infty)$ and satisfies

$$\forall t > 0 \; : \|u(\cdot,t) - w\|_G < \epsilon.$$

Unless otherwise stated, we shall consider stability with respect to the L^∞-norm. Some important instability criteria can be established with the aid of the Rayleigh quotient $R(\varphi; u)$ of the linearized eigenvalue problem (8) at a stationary solution u

as under (CK):

$$\begin{cases} \varphi \in \mathcal{H}^2_{KC}(G), \\ \partial_j^2 \varphi_j + f'(u_j)\varphi_j = -\lambda \varphi_j \quad \text{on } k_j, \quad 1 \le j \le N, \end{cases} \tag{8}$$

$$R(\varphi; u) = \frac{\displaystyle\sum_{j=1}^{N} \int_0^{\ell_j} \left(\partial_j \varphi_j\right)^2 - f'(u_j)\varphi_j^2 dx_j}{\displaystyle\sum_{j=1}^{N} \int_0^{\ell_j} \varphi_j^2 dx_j}. \tag{9}$$

Negative values of the Rayleigh quotient lead to instability of u. Note that the only possible equilibrium under (KC) is the trivial solution, whether Γ contains boundary vertices or not. However, in contrast to the (CK)-case, we can allow (KC)-test functions here that are constant on each edge. Introduce

$$\Pi^+(\Gamma) = \left\{ c = \left(c_j\right)_{N\times 1} \in \mathbb{R}^N \,\middle|\, \forall i \in \{1, \ldots, n\} : \sum_{j=1}^{N} d_{ij}^2 c_j = 0 \right\} \tag{10}$$

In fact, $\Pi^+(\Gamma)$ is the kernel of the signless incidence matrix of Γ, see also Sect. 4. Its dimension amounts to $N - n + c^+(\Gamma)$, where $c^+(\Gamma)$ denotes the number of bipartite connected components of Γ.

Lemma 3.1 *Let u be a stationary solution of (3).*

(a) If $\Pi^+(\Gamma) \neq \{0\}$ and

$$M = M(\Gamma) := \max \left\{ \sum_{j=1}^{N} c_j^2 \int_0^{\ell_j} f'(u_j) dx_j \;\middle|\; c \in \Pi^+, \sum_{j=1}^{N} c_j^2 = 1 \right\} > 0,$$

then u is unstable.

(b) If Γ contains an even circuit ζ such that $\displaystyle\int_\zeta f'(u)dx > 0$, then u is unstable.

(c) If Γ contains an Eulerian bipartite subgraph Z such that $\displaystyle\int_Z f'(u)dx > 0$, then u is unstable.

(d) If Γ contains a subgraph Σ with $M(\Sigma) > 0$, then $M(\Gamma) > 0$, and u is unstable.

Proof

(a) By compactness, the maximum M is attained for some $c \in \Pi^+$ with $\|c\|_2 = 1$. Then $R(c) < 0$, and u has to be unstable.

(b) Under the hypothesis, Π^+ contains an alternating element belonging to Π^+ with entries ± 1 along its support ζ that leads to $M > 0$.

(c) By hypothesis, Z is the superposition of edge disjoint even circuits. The proof is the same as for (b) with Z replacing ζ and an element belonging to Π^+ with entries ± 1 along its support Z that leads to $M > 0$.
(d) A maximizer c_Σ of M on Σ can be extended to an admissible element to the remaining edges in Γ by 0 leading to $M(\Gamma) > 0$. ■

This clearly suggests that stability of a stationary solution is a rare property. The Lemma applies e.g. to the nonlinearities $f(u) = u^{2k+1}$. Note that (d) does not mean that M is strictly increasing with respect to the subgraph relation. Moreover, one cannot conclude from $\int_0^{\ell_j} f'(u_j)dx_j > 0$ on a sole edge k_j that $M(\Gamma) > 0$, since on a single edge graph Π^+ reduces to $\{0\}$. As

$$\prod_{j=1}^{N} H_0^1(0, \ell_j) \leq \mathcal{H}^1_{K_0}(\Gamma),$$

a negative value of one sole edge Rayleigh quotient

$$\frac{\int_0^{\ell_j} \left(\partial_j \varphi_j\right)^2 - f'(u_j)\varphi_j^2 dx_j}{\int_0^{\ell_j} \varphi_j^2 dx_j}$$

leads to instability of a stationary solution of (3), since the zero extension of φ_j to Γ is an admissible function for $R(\varphi; u)$. Thus we can state the following

Corollary 3.2 *Let u be a stationary solution of* (3).

(a) If on some edge k_j there exists $\varphi_j \in H_0^1[0, \ell_j]$ such that

$$\int_0^{\ell_j} \left(\partial_j \varphi_j\right)^2 - f'(u_j)\varphi_j^2 dx_j < 0,$$

then u is unstable.
(b) If $f'(u_j) > \frac{\pi^2}{\ell_j^2}$ on some edge k_j, then u is unstable.

Proof It remains to show (b). Let φ be an eigenfunction of $\varphi'' + \lambda_1 \varphi = 0$ on $[0, \ell_j]$ belonging to $\lambda_1 = \frac{\pi^2}{\ell_j^2}$ with $\varphi(0) = \varphi(\ell_j) = 0$ and $\int_0^{\ell_j} \varphi^2 \, dx_j = 1$. Extend φ to Γ by 0. Then φ is admissible for $R(\cdot; u)$ and

$$R(\varphi; u) = \int_0^{\ell_j} \left(\partial_j \varphi_j\right)^2 - f'(u_j)\varphi_j^2 \, dx_j = \int_0^{\ell_j} \left\{\lambda_1 - f'(u_j)\right\} \varphi_j^2 \, dx_j < 0.$$

Now (a) permits to conclude. ■

We note in passing that the last assertions are also valid under (CK).

Lemma 3.3 *If a stationary solution u of (3) satisfies*

$$\int_G f'(u)\,u^2 dx > \int_G f(u)\,u dx,$$

then u is unstable.

Proof

$$\|u\|^2_{L^2(G)}\,R(u;u) = \int_G (\partial u)^2\,dx - \int_G f'(u)\,u^2 dx = \int_G f(u)u dx - \int_G f'(u)\,u^2 dx < 0.$$

■

This applies e.g. to the nonlinearity $f(u) = u^3 - u$, since $\int_G f'(u)\,u^2 - f(u)\,u dx = 2\int_G u^4 dx$. Thus, there is no stable stationary solution of (3) except the equilibrium 0, whose domain of attraction contains all solutions u of (3) belonging to $\prod_j \mathcal{C}\left(\left[0,\ell_j\right]\times[0,\infty);[-\alpha,\alpha]\right)\cap\mathcal{C}^{2,1}\left(\left[0,\ell_j\right]\times(0,\infty)\right)$ for all $[-\alpha,\alpha]\subset(-1,1)$. This can be seen with the aid of the L^2-norm as follows. Set

$$y(t) = \|u(\cdot,t)\|^2_{L^2(G)} \quad \text{and} \quad y_0 = y(0) = \|u_0\|^2_{L^2(G)},$$

multiply all edge differential equations by u, integrate over G and use $\|u\|^4_{L^4(G)} \le y\alpha^2$ in order to get

$$\frac{1}{2}\dot{y} = \int_G u\partial_x^2 u + u^4 - u^2\,dx = -\|u(\cdot,t)\|^2_{H_0^1(G)} + \|u(\cdot,t)\|^4_{L^4(G)} - y \le \left(\alpha^2 - 1\right)y.$$

Thus,

$$y(t) \le y_0\,e^{2\left(\alpha^2-1\right)t}$$

and $\lim_{t\to\infty} y(t) = 0$. As the ω-limit of $t \mapsto u(\cdot,t)$ belongs to $H_0^1\left[0,\ell_j\right]$ on each edge, see Corollary 2.4, we conclude

$$\lim_{t\to\infty} \|u(\cdot,t)\|_{\infty,G} = 0.$$

Next, we carry over Yanagida's Two Points Lemma under (CK) [7, 8, 19] to the anti-Kirchhoff condition (KC).

Lemma 3.4 *Suppose that u is a stationary solution of (3) that is nonconstant on some edge k_j. If there are two points on k_j with $0 \le z_1 < z_2 \le \ell_j$ such that*

$$\partial_j u_j(z_1) = \partial_j u_j(z_2) = 0,$$

then u is unstable.

Proof Define $\psi \in \prod_k H_0^1[0, \ell_k]$ by

$$\psi_k(x_k) = \begin{cases} \partial_j u_j(x_j) & \text{if } j = k \text{ and } z_1 \le x_k \le z_2, \\ 0 & \text{otherwise.} \end{cases}$$

Then ψ is admissible in the Rayleigh quotient of u, and $R(\psi; u)$ vanishes since its numerator amounts to

$$\int_{z_1}^{z_2} (\partial_j \psi_j)^2 - f_j'(u_j)\psi_j^2 dx_j = \left[\partial_j^2 u_j \partial_j u_j\right]_{z_1}^{z_2} - \int_{z_1}^{z_2} \partial_j \left\{\partial_j^2 u_j + f(u_j)\right\} \psi_j dx_j = 0.$$

Now consider the edge k_j separately, on which ψ_j solves the linearized equation $\partial_j^2 \psi_j + f'(u_j)\psi_j = 0$ in $H_0^1[0, \ell_j]$. Thus, ψ_j is an eigenfunction belonging to the eigenvalue 0 in $H_0^1[0, \ell_j]$. If

$$z_2 - z_1 < \ell_j,$$

ψ_j cannot belong to the minimal eigenvalue λ_1 of the operator $\partial_j^2 + f'(u_j)$ in $H_0^1[0, \ell_j]$, since the simple eigenvalue λ_1 possesses an eigenfunction $\eta \in H_0^1[0, \ell_j]$ that is positive in $(0, \ell_j)$. Thus, $\lambda_1 < 0$ and

$$\int_0^{\ell_j} \left(\partial_j \eta\right)^2 - f'(u_j)\eta^2 dx_j = \lambda_1 \int_0^{\ell_j} \eta^2 dx_j < 0.$$

Now Corollary 3.2 permits to conclude in the case $z_2 - z_1 < \ell_j$. If

$$z_1 = 0, \qquad z_2 = \ell_j,$$

then we have to apply a different argument. Note that an argument with a positive eigenfunction in the whole graph does not apply, since the smallest eigenvalue of the operator $\left(\partial_j^2 + f'(u_j)\right)_{N\times 1}$ on Γ is not simple in general, see [9] and Sect. 4. However, if $\lambda_0 = \min\left\{R(\varphi; u) \,\middle|\, \varphi \in \mathcal{H}^1_{K_0}(G)\right\} = 0$, then ψ is not only an eigenfunction as above, but a minimizer of $R(\cdot; u)$ and, thereby, satisfies (KC). This can be seen as follows. Choose an arbitrary $\xi \in \mathcal{H}^1_{K_0}(G)$. Then the minimizer

property leads to

$$\frac{d}{ds} R\,(\psi + s\xi; u)\Big|_{s=0} = 0$$

and

$$\int_G \partial\psi\partial\xi - f'(u)\psi\xi\, dx = R(\psi; u) \int_G \psi\xi\, dx. \tag{11}$$

For the special case of the eigenfunction ψ fulfilling the linearized edge equations this leads to

$$\forall \xi \in \mathcal{H}^1_{K_0}(G) : \partial_j\psi_j(\ell_j)\,\xi_j(\ell_j) - \partial_j\psi_j(0)\,\xi_j(0) = 0.$$

Thus, ψ fulfills (KC), in particular $\partial_j\psi_j(\ell_j) = \partial_j\psi_j(0) = 0$. Consequently, as a solution of a linear 2nd order equation, ψ has to vanish on k_j which is impossible. Again $\lambda_0 < 0$, and in both cases u is shown to be unstable. ■

We note in passing that (11) is a key step in showing that a minimizer of $R(\cdot; u)$ satisfies (KC) using the Y-boundary condition setting [9].

Lemma 3.5 *Suppose that the nonlinearity f is an odd function and that u is a stationary solution of (3) that is nonconstant on some edge k_j. If there are two points on k_j with $0 \le z_1 < z_2 \le \ell_j$ such that*

$$u_j(z_1)\partial_j u_j(z_1) = 0 = u_j(z_2)\partial_j u_j(z_2),$$

then u is unstable.

Proof Write $v_1 := \pi_j(0)$ and $v_2 := \pi_j(\ell_j)$. In the mixed case $u_j(z_1) = \partial_j u_j(z_2) = 0$, we construct a modified graph $\widetilde{\Gamma}$ as follows, (see Fig. 1). Omit k_j, add at v_1 an edge k_{N+1} of length z_1 with boundary vertex v_{n+1}. On k_{N+1} define u by restricting u_j to $[0, z_1]$ correspondingly.

At v_2 replace u_j by $\widetilde{u_j}$ on a new edge k_j of length $\tilde{\ell}_j = \ell_j - 3z_1 + 2z_2$ between v_2 and a new boundary vertex $v_{n+2} = \pi_j(0)$ as follows:

$$\tilde{u}_j(\tilde{x}_j) = \begin{cases} -u_j\left(\tilde{x}_j + z_1\right) & \text{if } 0 \le \tilde{x}_j \le z_2 - z_1, \\ -u_j\left(2z_2 - z_1 - \tilde{x}_j\right) & \text{if } z_2 - z_1 \le \tilde{x}_j \le 2z_2 - 2z_1, \\ u_j\left(\tilde{x}_j - 2z_2 + 3z_1\right) & \text{if } 2z_2 - 2z_1 \le \tilde{x}_j \le \ell_j + 2z_2 - 3z_1. \end{cases}$$

Note that $-u_j$ is a solution of the same elliptic equation on k_j since f is odd. Moreover, $\tilde{u}_j$ displays even reflexion of u_j at $\tilde{x}_j = z_2 - z_1$ and odd reflexion of u_j at $\tilde{x}_j = 2z_2 - 2z_1$. By the imposed conditions, $\tilde{u}_j \in \mathcal{C}^2[0, \tilde{\ell}_j]$. On the remaining edges $\tilde{u}$ is defined by u. Now $\tilde{u}$ is well-defined on the resulting graph $\widetilde{\Gamma}$, in which

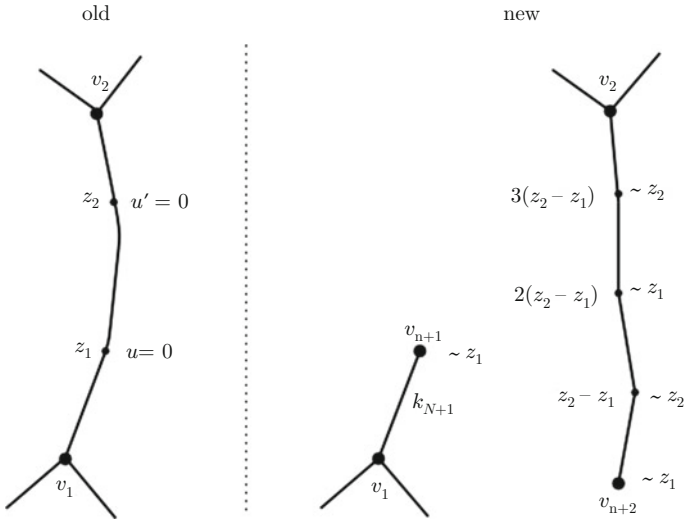

Fig. 1 Proof of Lemma 3.5. On the l.h.s.: the edge k_j in Γ; on the r.h.s. replacing k_j by two edges incident to boundary vertices in $\widetilde{\Gamma}$

$\partial_j \tilde{u}_j$ has two distinct zeros $0 < z_2 - z_1$ and $3z_2 - 3z_1$ on the new k_j. Thus, by Lemma 3.4, $\tilde{u}$ cannot be stable on $\widetilde{\Gamma}$, neither u can do so on Γ, since (KC) at a boundary vertex reduces to the 0-Dirichlet condition, and, thereby, the stability notions under (KC) on $\widetilde{\Gamma}$ and Γ are equivalent.

In the case $u_j(z_1) = u_j(z_2) = 0$, $\partial_j u_j$ vanishes at some $z_3 \in [z_1, z_2]$ and the mixed case shown above permits to conclude. ■

Note that without the hypothesis on f being odd, the assertion of Lemma 3.5 is no longer true as it is well displayed by Example 5.1. A first application of Lemma 3.5 settles the case when some u_j vanishes in the nodes incident to the edge k_j.

Corollary 3.6 *Let the nonlinearity f be odd. If $u_j \in H_0^1[0, \ell_j]$ is nontrivial and belongs to a stationary solution u of problem (3), then u is unstable.*

Proof As u_j cannot be constant, $\partial_j u_j$ has a zero in $[0, \ell_j]$ which permits to conclude with lemma (3.5) or with Picard–Lindelöff's Theorem if the zero coincides with one of the vertices of k_j. ■

In particular, with an odd nonlinearity f, $\prod_{j=1}^N H_0^1(0, \ell_j)$ can never contain a stable nontrivial stationary solution of the flow defined by problem (3) in $\mathcal{H}^1_{K_0}(\Gamma)$. On the other hand, they can occur under even nonlinearities, as it is well displayed by Example 5.1. Moreover, nontrivial stable stationary solutions belonging to Π^+ can occur under odd f, see Sect. 6.

4 Nonlinearities Vanishing at 0

It is well-known [9] that

$$\lambda_0(\Gamma) := \min \sigma \left(-\Delta^{KC}; \Gamma\right)$$

satisfies $\lambda_0(\Gamma) = \lambda_1 > 0$ if and only if Γ is a tree or a non bipartite unicyclic graph and $\lambda_0(\Gamma) = 0$ in all the other cases.

Lemma 4.1 *Suppose $f(0) = 0$. If $f'(0) > 0$, then the equilibrium 0 is unstable. If $f'(0) < -\lambda_0$, then 0 is linearly stable.*

Proof The linearized eigenvalue edge equations read $\partial_j \varphi_j = \left(-\lambda - f'(0)\right)\varphi_j$. In the first case $\min R(\varphi; 0) < 0$, while in the second one $\min R(\varphi; 0) > 0$. ■

In fact, there is a much better result, though, in general, a comparison principle [5–7] as under (CK) is not available under (KC).

Theorem 4.2 *Suppose $f(0) = 0$ and $f'(0) < 0$. Then 0 is a local attractor in $\mathcal{V}^0(G; [-1, 1]) = \prod_{j=1}^N \mathcal{C}^0\left([0, \ell_j]; [-1, 1]\right)$. More precisely, there are constants $\beta > 0$ and $1 > \delta > 0$ such that for all $2 \le p < \infty$ and for all solutions belonging to $\mathcal{V}^0(G; [-\delta, \delta])$*

$$\|u\|_{L^p(G)} < \delta L^{\frac{1}{p}} \exp\left(-\frac{2\beta}{p}t\right).$$

In particular, 0 is stable with respect to $\|\cdot\|_{L^p(G)}$ for all $2 \le p \le \infty$, and for all solutions belonging to $\mathcal{V}^0(G; [-\delta, \delta])$,

$$\lim_{t\to\infty} \|u(\cdot, t)\|_{\infty, G} = 0.$$

Proof As $f'(0) < 0$, there are constants $\beta > 0$ and $0 < \delta < 1$ such that

$$\frac{f(z)}{z} \le -\beta < 0 \quad \text{for all} \quad |z| \le \delta.$$

In particular, for functions taking their values in $[-\delta, \delta]$ we have

$$f(u)u \le -\beta u^2.$$

Set $y(t) = \|u(\cdot, t)\|^2_{L^2(G)}$ and $y_0 := y(0) = \|u_0\|^2_{L^2(G)}$. Then by (KC) as above,

$$\frac{1}{2}\dot{y} = \int_G u\partial_x^2 u + f(u)u\, dx \le -\beta y.$$

This shows that

$$0 \leq y(t) \leq y_0\, e^{-2\beta t} \leq y_0 < \delta^2 L$$

and $\lim_{t\to\infty} y(t) = 0$. Moreover, working with functions taking their values in $[-1, 1]$ and using $\|u\|_{L^p(G)} < y^{\frac{1}{p}}$, we get

$$\|u\|_{L^p(G)} < \delta^{\frac{2}{p}} L^{\frac{1}{p}} \exp\left(-\frac{2\beta}{p}t\right).$$

This shows first that all $\|u\|_{L^p(G)}$ are uniformly bounded from above by $\delta \max\{1, L\}$ and for all $t \geq 0$, which in turn implies that

$$\forall t \geq 0 : \lim_{p\to\infty} \|u(\cdot, t)\|_{L^p(G)} = \|u(\cdot, t)\|_{\infty,G} \leq \delta \max\{1, L\}.$$

This shows that 0 is stable. Moreover, as the ω-limit of $t \mapsto u(\cdot, t)$ belongs to $H_0^1\left[0, \ell_j\right]$ on each edge, see Sect. 2, we conclude

$$\lim_{t\to\infty} \|u(\cdot, t)\|_{\infty,G} = 0.$$

■

Remark 4.3 The stability result for 0 in Theorem 4.2 would follow readily by considering a local positive maximum or a negative minimum and the edge differential equations if a control at the nodes by a comparison principle would be possible. Clearly one would like to conclude from $\|u_0\|_{\infty,G} < \delta$ alone that $\|u(\cdot, t)\|_{\infty,G} < \delta$ for $t > 0$, where u is a solution of problem (3) with initial data u_0. But, as typical for parabolic systems, this is very crucial. In fact, using the classical invariance principle for parabolic systems, see e.g. [17], we can replace the requirement $u(\cdot, t) \in \mathcal{V}^0(G; [-\delta, \delta])$ by

$$u(\cdot, t) \in \left\{\varphi \in \mathcal{V}^0(G) \;\middle|\; \max\left\{|\varphi(v_i)| \;\middle|\; 1 \leq i \leq n\right\} \leq \delta\right\} \quad \text{for } t \geq 0,$$

since the flow generated by $\dot{z} = f(z)$ has 0 as a global attractor in $S := [-\delta, \delta]^N$ and since a.e. on ∂S, the scalar product of f with the outer normal vector field of ∂S is nonpositive.

It has been shown in [9] that 0 is not an eigenvalue of Δ^{KC} on trees or on non bipartite unicyclic graphs, since its algebraic multiplicity amounts to $N-n+1$ or to $N-n$, according to its parity. The proof given there is readily extended to arbitrary edge lengths. First, we note that a harmonic function on an arbitrary finite metric

graph under (KC) is constant on each edge, since

$$0 = \sum_j \int_0^{\ell_j} \left(\partial_j^2 u_j\right) u_j dx_j = -\sum_j \int_0^{\ell_j} \left(\partial_j u_j\right)^2 dx_j + \sum_i v_i \sum_{v_i \in k_j} u_j(v_i)$$
$$= -\sum_j \int_0^{\ell_j} \left(\partial_j u_j\right)^2 dx_j.$$

Thus, the eigenspace belonging to 0 of the Laplacian under (KC) is

$$E_0(\Gamma; \Delta^{KC}) = \Pi^+(\Gamma).$$

Denote the adjacency relation between vertices by $\sim$ and introduce

$$\mathcal{M}(\Gamma) = \left\{ M \,\middle|\, M = (m_{ih})_{n\times n}\,,\ \forall i, h \in \{1, \ldots, n\} :\ v_i \not\sim v_h \Rightarrow m_{ih} = 0 \right\}$$

and, using $\mathbf{e} = (1)_{n\times 1}$,

$$\mathcal{M}^+(\Gamma) = \left\{ M \in \mathcal{M}(\Gamma) \,\middle|\, M^* = M,\ M\mathbf{e} = 0 \right\}.$$

Using [3, Section 6] we are led to the following conclusion.

Lemma 4.4 *If Γ is a finite connected graph, then the geometric and algebraic multiplicity of 0 as eigenvalue of Δ^{KC} amount to*

$$m(0) = \dim \mathcal{M}^+(\Gamma) = \begin{cases} N - n + 1 & \text{if } \Gamma \text{ is bipartite,} \\ N - n & \text{if } \Gamma \text{ is not bipartite.} \end{cases}$$

In particular, there are no nontrivial harmonic functions under (KC) if and only if Γ is a tree or a non bipartite unicyclic graph.

Thus, the minimal eigenvalue λ_1 of the Laplacian under (KC) of these graphs is positive. This permits to deduce an unrestricted Poincaré inequality. As it stands, the general case is more complicated than in the (KC)-case. Conceivably, we restrict ourselves to the considered graph class. For the homogeneous eigenvalue problem

$$\begin{cases} u \in \mathcal{H}^2_{KC}(G), \\ \partial_j^2 u_j = -\lambda u_j \quad \text{on } k_j \quad \text{for } 1 \le j \le N, \end{cases}$$

the minimal Laplacian eigenvalue $\lambda_1 > 0$ on Γ is given by

$$\lambda_1 = \min \left\{ \|u\|^{-2}_{L^2(G)} \sum_{j=1}^N \int_0^{\ell_j} (\partial_j u_j)^2 dx_j \,\middle|\, u \in \mathcal{H}^1_{K_0}(G) \right\}.$$

Thus, we can state the following

Lemma 4.5 *Let Γ be a tree or a non bipartite unicyclic graph. Then $u \in \mathcal{H}^1_{K_0}(\Gamma)$ satisfies*

$$\|u\|^2_{L^2(\Gamma)} = \int_\Gamma u^2 dx \le \frac{1}{\lambda_1} \sum_{j=1}^N \int_0^{\ell_j} (\partial_j u_j)^2 dx_j = \frac{1}{\lambda_1} \|u\|^2_{H^1_0(\Gamma)}.$$

This enables the following exclusion of nonconstant stationary solutions.

Theorem 4.6 *Let Γ be a tree or a non bipartite unicyclic graph. Suppose $f(0) = 0$. Let $\mathrm{Lip}(f)$ denote the Lipschitz constant of f in some interval $[z_{\min}, z_{\max}]$ containing 0. Then for all real η with*

$$0 < \eta < \frac{\lambda_1}{\mathrm{Lip}(f)} \tag{12}$$

the elliptic problem

$$\begin{cases} u \in \mathcal{H}^2_{KC}(\Gamma), \\ \partial_j^2 u_j + \eta f(u_j) = 0 \ \text{on}\ k_j, \quad 1 \le j \le N, \end{cases} \tag{13}$$

has no nontrivial solution taking values in $[z_{\min}, z_{\max}]$. In particular, problem (13) cannot have nontrivial stable stationary solutions with the latter property.

Proof Let u be a solution of (13). According to Lemmas 2.1 and 4.5,

$$\sum_j \int_0^{\ell_j} \left(\partial_j u_j\right)^2 dx_j = \eta \sum_j \int_0^{\ell_j} f(u_j) u_j dx_j = \eta \sum_j \int_0^{\ell_j} \left(f(u_j) - f(0)\right) u_j dx_j$$

$$\le \eta\, \mathrm{Lip}(f)\, \|u\|^2_{L^2(\Gamma)} \le \frac{\eta\, \mathrm{Lip}(f)}{\lambda_1} \sum_j \int_0^{\ell_j} \left(\partial_j u_j\right)^2 dx_j.$$

This permits to conclude that u is constant on each edge, i.e. $u \in \Pi^+$. But for a tree or a non bipartite unicyclic graph $\Pi^+ = \{0\}$, which permits to conclude. ■

With the same rescaling technique as in [7, Corollary 4.9] we are led to the following

Corollary 4.7 *Let Γ be a tree or a non bipartite unicyclic graph. Suppose $f(0) = 0$. If the edge lengths of the metric graph G are sufficiently small, then the elliptic problem*

$$\begin{cases} u \in \mathcal{H}^2_{KC}(\Gamma), \\ \partial_j^2 u_j + f(u_j) = 0 \ \text{on}\ k_j, \quad 1 \le j \le N, \end{cases}$$

has no nontrivial solution. In particular, there are no nonconstant, stationary (stable) solutions of the parabolic problem (3).

For graphs of higher corank, the dimension of the eigenspace belonging to 0 can be rather high by Lemma 4.4, and its orthogonal complement in $L^2(G)$ does not allow a simple characterization as in the (CK)-case unless the tautological one in order to get a suitable Poincaré inequality. We omit the details of the corresponding exclusion result. Moreover, it seems that the condition $f(0) = 0$ is essential, as will be illustrated in the following section.

5 Constant Nonlinearities

Example 5.1 Let Γ be a graph with all edge lengths equal to ℓ. Suppose $f \equiv C$ with a non zero constant C, and consider on Γ the parabolic problem

$$\begin{cases} u_j \in \mathcal{C}([0,\ell]\times[0,\infty)) \cap \mathcal{C}^{2,1}([0,\ell]\times(0,\infty)) & \text{for } 1 \le j \le N, \\ \partial_t u_j = \partial_j^2 u_j + C \quad \text{on } k_j & \text{for } 1 \le j \le N, \\ u = \big(u_j\big)_{N\times 1} \text{ satisfies } (KC). \end{cases} \tag{14}$$

Then $w = \big(w_j\big)_{N\times 1}$ defined by

$$w_j(x) = \frac{C}{2} x(\ell - x)$$

is the only stationary solution of (14). This follows readily by considering $u'' = -C$ on a single edge and on a circuit. Then reason by recurrence on N for the general case.

Consider first the case that Γ is a tree or a non bipartite unicyclic graph with all edge lengths equal to ℓ. Then, in fact, w is a global attractor in $\mathcal{V}^0(G)$ (or $L^2(G)$), and thereby stable, since for every solution u of (14),

$$\delta := u - w \in \Big(\mathcal{C}([0,\ell]\times[0,\infty)) \cap \mathcal{C}^{2,1}([0,\ell]\times(0,\infty))\Big)^N$$

solves the heat equation

$$\begin{cases} \partial_t \delta_j = \partial_j^2 \delta_j \quad \text{on } [0,\ell] & \text{for } 1 \le j \le N, \\ \delta = \big(\delta_j\big)_{n\times 1} \text{ satisfies } (KC). \end{cases}$$

But the minimal eigenvalue of the Laplacian under (KC) on Γ satisfies $\lambda_1 > 0$. Thus, eigenfunction expansion and Dirichlet's Theorem yield

$$\|u(\cdot,t) - w\|_{\infty,G} \le \text{const.}\, e^{-\lambda_1 t}\, \|u(\cdot,0) - w\|_{\infty,G}\,.$$

If Γ is neither a tree, nor a non bipartite unicyclic graph, then the minimal eigenvalue of the Laplacian under (KC) is 0, and w is still seen to be stable, since

$$\|u(\cdot,t)-w\|_{\infty,G} \leq \text{const. } \|u(\cdot,0)-w\|_{\infty,G}\,.$$

We note in passing that for $C=0$, the trivial solution clearly is stable on any graph. On the energy level, though we cannot apply Lasalle's Principle, we calculate

$$\mathcal{E}(u(\cdot,t)) \searrow \mathcal{E}(w) = N\left(\frac{C^2}{24}-\frac{C}{12}\right).$$

Note that w is the only stationary solution of (14) on any finite metric graph with equal edge lengths. This leads to the following

Corollary 5.2 *On each finite metric graph with equal edge lengths, there is a nonlinearity such that problem* (3) *has a stable stationary nonconstant solution. More precisely, if* Γ *is a tree or a non bipartite unicyclic graph, then* (14) *has a global attractor belonging to* $\prod_{j=1}^{N} H_0^1(0,\ell_j)$ *that is the only stationary solution. If* Γ *is neither a tree nor unicyclic non bipartite, then* (14) *has a unique stationary solution belonging to* $\prod_{j=1}^{N} H_0^1(0,\ell_j)$ *that is stable and nonconstant.*

Thus, there are no exceptional abstract graphs under (KC), in contrast to Condition (CK). According to a result by Yanagida [19] there are five exceptional graphs that do not allow any stable stationary nonconstant solutions for any nonlinearity f under (CK). But, we can also show the above result without the edge restriction.

Theorem 5.3 *On each finite metric graph* Γ *there is a nonlinearity such that problem* (3) *has a stable stationary nonconstant solution. More precisely, if* Γ *is a tree or a non bipartite unicyclic graph, then the parabolic problem*

$$\begin{cases} u_j \in \mathcal{C}([0,\ell_j]\times[0,\infty))\cap\mathcal{C}^{2,1}([0,\ell_j]\times(0,\infty)) & \text{for } 1\leq j\leq N,\\ \partial_t u_j = \partial_j^2 u_j + C \quad \text{on } k_j & \text{for } 1\leq j\leq N,\\ u=(u_j)_{N\times 1} \text{ satisfies } (KC) \end{cases} \tag{15}$$

with an arbitrary nonvanishing constant C, has a global attractor that is the only stationary solution. If Γ *is neither a tree nor unicyclic non bipartite, then* (15) *has a unique stationary solution that is stable and nonconstant.*

Proof In order to establish the existence of a unique stationary solution, the edge differential equations lead to the following ansatz with $w=(w_j)_{N\times 1}$ defined by

$$w_j(x_j) = -\frac{C}{2}x_j^2 + b_j x_j + c_j$$

with suitable coefficients b_j and c_j. Condition (4) leads at each vertex v_i to

$$\sum_{d_{ij}=-1} c_j + \sum_{d_{ij}=1} \left[b_j \ell_j + c_j \right] = \frac{C}{2} \sum_{d_{ij}=1} \ell_j^2 \tag{16}$$

Denoting the edges incident with the ramification node v_i by $k_{i1}, \ldots, k_{i\gamma_i}$, condition (5) leads at each such v_i to

$$\forall \nu \in \{2, \ldots, \gamma_i\} : \; d_{i,i1} b_{i1} - d_{i,i\nu} b_{i\nu} = \frac{1 + d_{i,i\nu}}{2} \ell_{i\nu} - \frac{1 + d_{i,i1}}{2} \ell_{i1}, \tag{17}$$

bearing in mind that

$$d_{ij} \partial_j w_j(v_i) = \frac{1 + d_{ij}}{2} \ell_j + d_{ij} b_j = \begin{cases} -b_j & \text{if } d_{ij} = -1 \\ b_j - \ell_j & \text{if } d_{ij} = 1 \\ 0 & \text{otherwise.} \end{cases}$$

Write the coefficients b_j and c_j in one $2N$-column vector

$$\mathbf{y} = \begin{pmatrix} b_1 \\ \vdots \\ b_N \\ c_1 \\ \vdots \\ c_N \end{pmatrix}.$$

Equations (16) and (17) form $2N$ linear inhomogeneous equations that define a $2N \times 2N$-matrix $\mathbf{M}$ by the Hand Shaking Lemma. It is well-known [4, 6, 15, 16] that $\mathbf{M}$ has full rank, since $\mathbf{M}$ is equivalent with a block diagonal matrix composed by n blocks, each of them corresponding to a vertex v_i and being of the form

$$\begin{pmatrix} * & * & * & \cdots & * \\ 1 & -1 & 0 & \cdots & 0 \\ 1 & 0 & -1 & \cdots & 0 \\ \vdots & \vdots & \ddots & \ddots & 0 \\ 1 & 0 & \cdots & 0 & -1 \end{pmatrix}_{\gamma_i \times \gamma_i}.$$

The symbol $*$ stands for the entries 1 and ℓ_j stemming from (16). Thus, there is a unique solution of $\mathbf{My} = \mathbf{g}$, where $\mathbf{g}$ stands for the corresponding inhomogeneous terms defined by the edges lengths and the incidence factors contained in (16) and (17). In turn, there is a unique nonconstant stationary solution w of (15).

It remains to show the attractor and stability assertions about w, but as this proof is identical with the argument in Example 5.1, we omit the details and conclude. ■

Note that in Example 5.1 the vector $\mathbf{y}$ is given by $b_j = \frac{1}{2}C$ and $c_j = 0$. Note furthermore that under (CK) there are no stationary solutions $u \in \mathcal{C}^2_K(G)$ of problem (15) at all on any finite metric graph, since such a solution would have to fulfill $\int_G \partial^2 u \, dx = 0$ by the Kirchhoff condition (2).

6 Odd Nonlinearities

If the nonlinearity f is an odd function, then u is a solution of (3) if and only if $-u$ shares the same property, and u is a stable stationary solution if and only if $-u$ is such a solution. If Γ consists in a single edge, we are looking for stationary solutions of $\partial_t u = \partial^2 u + f(u)$ in $\mathcal{C}^2_0[0, \ell]$. Then Rolle's Theorem and Lemma 3.5 or Picard–Lindelöff's Theorem lead to the exclusion of nontrivial stable stationary solutions on an interval. In fact, it will be shown that on any finite graph, odd nonlinearities admit only stable stationary solution u of (3) that belong to $\Pi^+(\Gamma)$, in particular, for $\Pi^+(\Gamma) = \{0\}$, only the trivial solution can be stable. In order to illustrate the anti-Kirchhoff condition (KC), let us anticipate the proof for star graphs. If $\#V_{\mathrm{ess}}(\Gamma) = 1$, then $u = 0$ at $V_{\mathrm{b}}(\Gamma)$ and the identical $d_{1j}\partial_j u_j(v_1)$ at the ramification node v_1 lead to a zero of some $\partial_j u_j$ on some edge k_j. Then Lemma 3.5 permits to conclude. Next, the general bipartite case will be treated.

Theorem 6.1 *If the nonlinearity f is an odd function, and if Γ is bipartite, then a stable stationary solution u of (3) belongs to $\Pi^+(\Gamma)$, i.e. u is constant on each edge.*

Proof As a bipartite graph, we can endow Γ with a sink-source-orientation, i.e. at each node v_i either all incident $d_{ij} = -1$ or all incident $d_{ij} = 1$. Let w be a stable stationary solution of (3) on Γ that is nonconstant on some edges. On these edges ∂w vanishes at most once. Moreover, a sign change of ∂w cannot take place in a vertex, unless all the incident derivatives vanish there.

By (KC) and by the sink–source–orientation, ∂w defines a continuous function on Γ. Accordingly, Γ can be decomposed into connected components, where ∂w is of constant sign. Thus, adding to $V(\Gamma)$ the interior edge points where ∂w vanishes at the boundary of such a connected component, we get an enlarged graph, that is bipartite since on a circuit the number of sign changes of ∂w has to be even. Now replace w by $-w$ on appropriate components in order to achieve $\partial \tilde{w} \geq 0$ on an enlarged bipartite graph $\tilde{\Gamma}$, where all the entities on the new graph will be marked by $\tilde{\cdot}$. Clearly, at the new nodes $\tilde{w}$ fulfills (KC), and $\tilde{w}$ is a stable stationary solution of (3) on $\tilde{\Gamma}$. By connectedness of Γ and $\tilde{\Gamma}$, not counting the edges on which $\tilde{w}$ is constant, it follows that $\partial \tilde{w} > 0$ on all remaining edges of Γ except at most N points. This is absurd, since $\int_{\tilde{G}} \partial \tilde{w} \, d\tilde{x} = 0$ by Lemma 2.2. ■

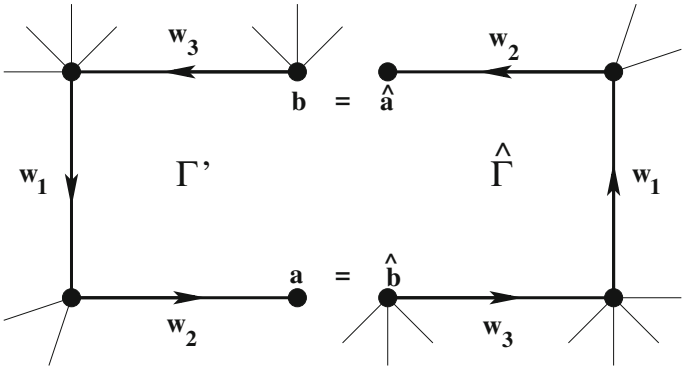

Fig. 2 Proof of Theorem 6.3. Constructing the graph $\tilde{\Gamma}_1$ by identifying a with $\hat{b}$ and b with $\hat{a}$

Corollary 6.2 *If the nonlinearity f is an odd function, and if Γ is a tree, then a stable stationary solution u of (3) vanishes on the whole tree Γ.*

Theorem 6.3 *If the nonlinearity f is an odd function, then a stable stationary solution u of (3) belongs to $\Pi^+(\Gamma)$, i.e. u is constant on each edge.*

Proof We have to find a bipartite enlargement $\tilde{\Gamma}$ of Γ such that a presumed stationary solution w of (3) on Γ is unstable if its extension $\tilde{w}$ is unstable on $\tilde{\Gamma}$. This can be achieved by using the fact that a graph is bipartite if and only if it contains only circuits of even lengths. In fact, we can apply a well-known bipartite covering technique form abstract graph theory (see Fig. 2). Suppose that Γ contains an odd circuit ζ with M edges and vertices numbered by $1, \dots, M$ such that v_i and v_{i+1} are adjacent, and such that the incidence $\mod M$ is given by

$$d_{ij} = \begin{cases} -1 & \text{if } i = j, \\ 1 & \text{if } i = j+1, \\ 0 & \text{otherwise.} \end{cases} \tag{18}$$

Split the node v_M into two nodes a and b of a modified graph Γ' such that $a = \pi_{M-1}(\ell_{M-1})$ is a boundary vertex and such that $b = \pi_M(0)$ has valency $\gamma_M(\Gamma) - 1$ in Γ'. Let π denote the path formed by the edges of ζ of length M in Γ'. Now take a copy $\hat{\Gamma}$ of Γ' whose entities are all indicated by $\hat{}$ and on which w is identically copied, i.e. $\hat{w}_j = w_j$ for all $1 \le j \le N$. Next, identify a with $\hat{b}$ and b with $\hat{a}$ and get a new graph $\tilde{\Gamma}_1$, in which π and $\hat{\pi}$ form a circuit of length $2M$. Moreover, by construction, $\tilde{w}^{(1)} \in \mathcal{V}^2_{KC}(\tilde{\Gamma}_1)$ is well-defined by w and $\hat{w}$, and w is stable on Γ if and only if $\tilde{w}$ is stable on $\tilde{\Gamma}_1$.

If $\tilde{\Gamma}_1$ is not yet bipartite, choose an odd circuit ξ and the corresponding $\hat{\xi}$ and proceed with both of them in one step in order to get a graph $\tilde{\Gamma}_2$, in which ξ and $\hat{\xi}$ are replaced by circuits of double length, and on which $\tilde{w}^{(2)} \in \mathcal{V}^2_{KC}(\tilde{\Gamma}_2)$ is stable if and only if w is stable on Γ.

If the original graph Γ has r odd circuits, then repeating this construction in at most r steps leads to the desired bipartite graph $\tilde{\Gamma}$ on which the corresponding stationary solution $\tilde{w}$ is stable on $\tilde{\Gamma}$ if and only if w is stable on Γ. Note that in the k-th step leading to $\tilde{\Gamma}_k$, 2^k copies of the same odd circuit of Γ are treated as above and replaced by circuits of common double length. This guarantees that after at most r steps, the resulting graph is bipartite.

As at each step the stability or instability of the involved stationary solution are maintained, Theorem 6.1 permits to conclude. ■

In particular, for non bipartite unicyclic graphs, only the trivial solution can be stable. In fact, the proof of Theorem 6.3 has shown the following

Corollary 6.4 *Let f be a nonlinearity such that on all bipartite graphs Γ all possible stable stationary solutions of* (3) *can only belong to $\Pi^+(\Gamma)$. Then the same is true for arbitrary metric graphs.*

We close the section with an example that displays exactly two attractors under (KC), as well as under (CK). It has been shown in [7] that on each finite graph under (CK), the only stable stationary solutions of the edge differential equations in (3) with $f(u) = u - u^3$ are the equilibria ± 1. Here, we consider the same balanced cubic nonlinearity under (KC) on an even circuit ζ with $N = n$ vertices and edges. Number the vertices and the edges such that $d_{jj} = -1$ and $d_{j+1,j} = 1$ with indices being taken modulo N. Then Lemma 3.1(b) applies in order to show the instability of the one and only equilibrium 0. Moreover, $\Phi : \mathcal{C}^1_K(\zeta) \to \mathcal{V}^1_{KC}(\zeta)$ defined by

$$\Phi(w) = \left((-1)^j w_j\right)_{N\times 1}$$

establishes an isometric isomorphism with respect to the norms $\|\cdot\|_{L^\infty(\zeta)}$, $\|\cdot\|_{L^2(\zeta)}$, $\|\cdot\|_{H^1(\zeta)}$ and $\|\cdot\|_{H^1_0(\zeta)}$. As f is an odd function, $u \in \mathcal{C}^{2,1}_K(\zeta \times [0,T])$ is a solution of all edge equations

$$\partial_t u_j = \partial_j^2 u_j + u_j - u_j^3, \tag{19}$$

if and only if $\Phi(u) \in \mathcal{V}^{2,1}_{KC}(\zeta \times [0,T])$ solves all Eqs. (19). Thus, under (KC), $\Phi(1)$ and $\Phi(-1)$ are the only stable stationary solutions on the even circuit ζ, and the asymptotic solution behaviour under (CK) and (KC) correspond to each other by the mapping Φ.

Clearly, this reasoning seems to be rather specific to even circuits and not to be available on more general Eulerian graphs. However, it helps in determining

the domains of attraction of $\Phi(1) = \left((-1)^j\right)_{N\times 1} \in \Pi^+(\zeta)$ and $\Phi(-1) = \left((-1)^{j+1}\right)_{N\times 1} \in \Pi^+(\zeta)$. Using the results from [7], those turn out to be

$$\mathcal{D}\left(\Phi(-1)\right) = \left\{ w_0 \in \mathcal{V}^0_{K_0}(\zeta) \,\middle|\, \lim_{t\to\infty} \int_\zeta \Phi\left(w(\cdot,t)\right) dx = -L(\zeta) \right\},$$

$$\mathcal{D}\left(\Phi(1)\right) = \left\{ w_0 \in \mathcal{V}^0_{K_0}(\zeta) \,\middle|\, \lim_{t\to\infty} \int_\zeta \Phi\left(w(\cdot,t)\right) dx = L(\zeta) \right\}.$$

Besides these two attractors, however, there are solutions tending to the unstable equilibrium 0, namely

$$\mathcal{D}\left(0\right) = \left\{ w_0 \in \mathcal{V}^0_{K_0}(\zeta) \,\middle|\, \lim_{t\to\infty} \mathcal{E}(w(\cdot,t)) = 0 \right\}.$$

7 Loops

If Γ is a loop, then the stationary case of problem (3) reduces to the antiperiodic ordinary BVP on the interval $[0, \ell]$

$$\begin{cases} u \in \mathcal{C}^2([0,\ell]) \\ u'' + f(u) = 0 \quad \text{on } [0,\ell] \\ u(0) = -u(\ell) \\ u'(0) = -u'(\ell) \end{cases} \tag{20}$$

According to [13, p. 214], the minimal eigenvalue of the linearized EVP

$$\begin{cases} \varphi \in H^2[0,\ell] \\ \varphi'' + f'(u)\varphi = -\lambda\varphi \quad \text{on } [0,\ell] \\ \varphi(0) = -\varphi(\ell) \\ \varphi'(0) = -\varphi'(\ell) \end{cases} \tag{21}$$

has only eigenfunctions with exactly one zero in $[0, \ell)$, and it is the only eigenvalue bearing this property. If f is an odd function, then Theorem 6.3 assures that problem (20) has no stable nontrivial solution. But, here a quite elementary argument can be applied: $\psi = u'$ is an eigenfunction belonging to $\lambda = 0$ and satisfies both boundary conditions in (20) by the differential equation for u, as f is odd. If ψ has two zeros in $[0, \ell)$, then u is unstable by Lemma 3.4. Thus, ψ is an eigenfunction belonging to the minimal eigenvalue of (21), namely 0, and has exactly one zero $z_1 \in [0, \ell)$. Now either Lemma 3.5 and the Intermediate Value

Theorem apply, or, in the case of a double zero z_1 of u, the unique solvability of the Cauchy problem at z_1 permits to conclude.

In the case of the cubic $f(u) = u - u^3$ e.g., the corresponding Hamiltonian phase plane displays very well that there is no stable nontrivial stationary solution. The part of the trajectory corresponding to the solution φ of (20) and connecting $\big(\varphi(0), \varphi'(0)\big)$ with $-\big(\varphi(0), \varphi'(0)\big)$ has to cross the φ-axis and the φ'-axis. Then Lemma 3.5 settles the instability. For general $f \in \mathcal{C}^1$, the procedure is more complicated.

Theorem 7.1 *If the nonlinearity fulfills $f(0) = 0$, then problem (20) has no stable nontrivial solution on a loop.*

Proof Clearly, the only possible constant solution of (20) is the trivial one. Suppose that u is a nonconstant solution of (20). If $u'(0) = 0$, then $u'(\ell) = 0$, and Lemma 3.4 permits to conclude. Thus we can assume

$$u'(0) = -u'(\ell) \neq 0.$$

By the Intermediate Value Theorem, there exists $0 < z_1 < \ell$ such that $u'(z_1) = 0$, say $0 < z_1 \leq \frac{\ell}{2}$. Then, by uniqueness of the corresponding Cauchy problems at z_1,

$$\forall x \in [0, z_1] : \, u\,(2z_1 - x) = u(x),$$

in particular

$$u\,(2z_1) = u(0) = -u(\ell), \qquad u'\,(2z_1) = -u'(0) = u'(\ell).$$

If $z_1 = \frac{\ell}{2}$, then $u(\ell) = u(0) = -u(\ell)$ and $u(\ell) = u(0) = 0$. Thus, $u \in \mathcal{C}_0[0, \ell]$. Then we can reduce the loop problem to a sphere $\mathbb{S}^1$ of length 2ℓ with (CK) as follows. Clearly, u has a sign, otherwise there would be another zero of u'. Say $u < 0$ in $(0, \ell)$. Set

$$\tilde{u}(x) = \begin{cases} u(x) & \text{if } 0 \leq x \leq \ell, \\ -u\,(2\ell - x) & \text{if } \ell \leq x \leq 2\ell, \end{cases}$$

$$\tilde{f}(z) = \begin{cases} f(z) & \text{if } z \leq 0, \\ -f(-z) & \text{if } z \geq 0. \end{cases}$$

Then $\tilde{u} \in \mathcal{C}^2\,[0, 2\ell]$, $\tilde{f} \in \mathcal{C}^1(\mathbb{R})$, and $\tilde{u}$ solves $\tilde{u}'' + \tilde{f}(\tilde{u}) = 0$ in $[0, 2\ell]$ under the conditions $\tilde{u}(0) = \tilde{u}(2\ell) = 0$, $\tilde{u}'(0) = \tilde{u}'(2\ell)$, and $\tilde{u}''(0) = \tilde{u}''(2\ell)$. Thus, $\tilde{u}$ is a stationary solution on the sphere that cannot be stable according to [19]. By construction, u must be unstable on the loop.

Thus, we can suppose

$$z_1 < \frac{\ell}{2}.$$

If $u'(z_2) = 0$ with some $2z_1 \le z_2 \le \ell$, Lemma 3.4 permits to conclude that u is unstable, since $z_1 < z_2$ by construction. This applies in particular, if $u(2z_1) = 0$, since then $u(2z_1) = u(0) = u(\ell) = 0$, which yields another zero of u' lying in $[2z_1, \ell]$ by Rolle's Theorem. Thus, we can assume that $u(2z_1) \neq 0$ and

$$\forall x \in [2z_1, \ell] : u'(x) \neq 0.$$

As $u(2z_1) = -u(\ell)$, there exists a unique $z_3 \in (2z_1, \ell)$ such that $u(z_3) = 0$ by the Intermediate Value Theorem. Consider the uniquely extended solution v of

$$\begin{cases} v \in \mathcal{C}^2([-z_3 + 2z_1, z_3]) \\ v'' + f(v) = 0 \quad \text{on } [-z_3 + 2z_1, z_3] \\ v(-z_3 + 2z_1) = v(z_3) = 0 \\ v'(-z_3 + 2z_1) = -v'(z_3) \end{cases} \tag{22}$$

that coincides with u on $[0, z_3]$. With the same reasoning as in the case $z_1 = \frac{\ell}{2}$, it follows that u is unstable in $\mathcal{C}[-z_3 + 2z_1, z_3]$. In detail,

$$\exists \varepsilon_0 > 0 \, \forall \delta > 0 \, \exists \varphi_0 \in \mathcal{C}[-z_3 + 2z_1, z_3] : \ \|\varphi_0 - u\|_{\infty,[-z_3+2z_1,z_3]} < \delta$$
$$\& \, \exists t_1 > 0 : \ \|\varphi(\cdot, t_1) - u\|_{\infty,[-z_3+2z_1,z_3]} \ge \varepsilon_0.$$

But, u restricted to $[2z_1, z_3]$ and $v(-x)$ evaluated in $[0, z_3 - 2z_1]$ coincide by solution uniqueness for the Cauchy problems at $2z_1$ and 0, respectively. By the continuity of the flow and by solution uniqueness on $[0, \ell]$, we conclude that u is unstable on the loop under (KC). ■

Example 5.1 yields a global attractor $w(x) = \frac{1}{2}x(\ell - x)$ for the nonlinearity $f \equiv 1$ on the loop and shows again that condition $f(0) = 0$ is essential for the assertion of Theorem 7.1.

By the scalar character of problem (20), the classical attractivity and stability criteria as in [7, Theorem 4.1] hold correspondingly.

Theorem 7.2 *Suppose there are constants A and C with $-\infty < A < 0 < C \le \infty$ such that*

$$f(0) = 0, \quad f'(0) < 0, \quad f > 0 \text{ in } (A, 0) \quad \text{and} \quad f < 0 \text{ in } (0, C). \tag{23}$$

If $u \in \mathcal{C}([0,\ell]\times[0,\infty)) \cap \mathcal{C}_K^{2,1}([0,\ell]\times(0,\infty))$ *is a solution of* (20) *with an initial condition* $u(\cdot,0) \in \mathcal{C}([0,\ell];[A,C))$ *such that* $u \not\equiv A$*, then*

$$\lim_{t\to\infty} \|u(\cdot,t)\|_{\infty,[0,\ell]} = 0.$$

Acknowledgments Joachim von Below is grateful to the research group GREDPA at UPC Barcelona for the invitation in 2017. José A. Lubary is grateful to the LMPA Joseph Liouville at ULCO in Calais for the invitation in 2018.

References

1. Albeverio, S., Cacciapuoti, C., and Finco, D., Coupling in the singular limit of thin quantum waveguides. *J. Math. Phys.* **48** (2007) 032103.
2. Amman, H., *Ordinary differential equations*, de Gruyter Berlin 1990.
3. Below, J. von, A characteristic equation associated with an eigenvalue problem on C^2-networks. *Lin. Algebra Appl.* **71** (1985) 309–325.
4. Below, J. von, Classical solvability of linear parabolic equations on networks, *J. Differential Equ.* **72** (1988) 316–337.
5. Below, J. von, A maximum principle for semilinear parabolic network equations, in: J. A. Goldstein, F. Kappel, W. Schappacher (eds.), Differential equations with applications in biology, physics, and engineering, *Lect. Not. Pure and Appl. Math.* **133**, M. Dekker Inc. New York, 1991, pp. 37–45.
6. Below, J. von, *Parabolic network equations,* 2nd ed. Tübingen 1994.
7. Below, J. von and Lubary, J.A., Instability of stationary solutions of reaction–diffusion–equations on graphs. *Results. Math.* **68** (2015),171–201.
8. Below, J. von and Lubary, J. A., Stability implies constancy for fully autonomous reaction–diffusion equations on finite metric graphs. *Networks and Heterogeneous Media* **13** (2018),691–717.
9. Below, J. von and Mugnolo, D., The spectrum of the Hilbert space valued second derivative with general self-adjoint boundary conditions. *Linear Algebra and its Applications* **439** (2013) 1792–1814.
10. Below, J. von and Vasseur, B., Instability of stationary solutions of evolution equations on graphs under dynamical node transition, in: *Mathematical Technology of Networks*, ed. by Delio Mugnolo, *Springer Proceedings in Mathematics & Statistics* **128** (2015), 13–26.
11. Biggs, N. L., Algebraic graph theory. *Cambridge Tracts Math. 67*, Cambridge University Press, 1967.
12. Cardanobile, S. and Mugnolo, D., Parabolic systems with coupled boundary conditions. *J. Differ. Equ.* **247** (2009) 1229–1248.
13. Coddington, Earl N. and Levinson, N.. *Theory of Ordinary Differential Equations* (1955) Mc Graw Hill.
14. Fulling, S.A., Kuchment, P., and Wilson, J.H., Index theorems for quantum graphs. *J. Phys. A* **40** (2007) 14165–14180.
15. Lubary, J.A., Multiplicity of solutions of second order linear differential equations on networks. *Lin. Alg. Appl.* **274** (1998) 301–315.
16. Lubary, J.A., On the geometric and algebraic multiplicities for eigenvalue problems on graphs, in: Partial Differential Equations on Multistructures, *Lecture Notes in Pure and Applied Mathematics* Vol. **219**, Marcel Dekker Inc. New York, (2000) 135–146.

17. Weinberger, H. F., Invariant sets for weakly coupled parabolic and elliptic systems. *Rendiconti di Mat.* **8** (1975) 295–310.
18. Wilson, R. J.. Introduction to graph theory, Oliver & Boyd Edinburgh, 1972.
19. Yanagida, E., Stability of nonconstant steady states in reaction–diffusion systems on graphs. *Japan J. Indust. Appl. Math.* **18** (2001) 25–42.

Many-Particle Quantum Graphs: A Review

Jens Bolte and Joachim Kerner

Abstract In this paper we review recent work that has been done on quantum many-particle systems on metric graphs. Topics include the implementation of singular interactions, Bose-Einstein condensation, solvable models and spectral properties of some simple models in connection with superconductivity in quantum wires.

1 Introduction

Quantum graph models describe the motion of particles along the edges of a metric graph. They have become popular models in various areas of physics and mathematics as they combine the simplicity of one-dimensional models with the potential complexity of graphs. One-particle quantum graphs and their applications are described in detail in [KS99b, GS06, EKK08, BK13a].

Many-particle quantum systems are of fundamental importance in condensed matter as well as in statistical physics, see [MR04a, Sch06, CCG11]. In particular, phenomena like Bose-Einstein condensation, Anderson localisation and superconductivity have attracted much attention both in a phenomenological and a mathematical context. However, those phenomena are notoriously difficult to address, so that models that are promising to yield interesting results while still being sufficiently accessible are in demand. This was a major reason to develop and study quantum many-particle models on graphs. Another reason lies in the growing importance of one-dimensional, nano-technological devices [HV16, GG08].

J. Bolte (✉)
Department of Mathematics, Royal Holloway, University of London, Egham, UK
e-mail: jens.bolte@rhul.ac.uk

J. Kerner
Department of Mathematics and Computer Science, FernUniversität in Hagen, Hagen, Germany
e-mail: Joachim.Kerner@fernuni-hagen.de

F. M. Atay et al. (eds.), *Discrete and Continuous Models in the Theory of Networks*, Operator Theory: Advances and Applications 281,
https://doi.org/10.1007/978-3-030-44097-8_2

Among early quantum graph examples are models of two particles with singular interactions on simple graphs [MP95, CC07, Har07, Har08], where some basic spectral properties were studied. Other approaches involve quantum field theory on graphs (see, e.g., [BM06, Sch09]) where, due to the presence of vertices and the finite lengths of edges, translation invariance is broken. This leads to the presence of symmetry algebras that are of interest in their own right [MR04b]. In the context of quantum integrability, these symmetry algebras play a role in the construction of many-particle quantum models on graphs in which one can represent eigenfunctions in terms of a Bethe-ansatz [CC07, BG17, BG18]. In this context also extensive studies of non-linear Schrödinger equations (see, e.g., [Noj14, Cau15]) are of particular interest.

The phenomenon of Anderson localisation, which is known to occur in a large class of systems governed by random Schrödinger operators [CFKS87, Sto01], has been investigated for interacting particles on graphs in [Sab14].

When particles are indistinguishable, the particle exchange symmetry has to be implemented. In three or more dimensions this leads to the well-known Fermi-Bose alternative. However, in lower dimensions more options may become available including, e.g., the possibility of anyons in two dimensions [LM77]. In models of discrete quantum graphs the possible exchange symmetry representations were identified in [HKR11, HKRS14], and a whole range of exotic options were found; see also [MS17] for recent developments in this direction.

In this paper we mainly review our own contributions to many-particle quantum graphs. This includes the construction of two types of singular pair interactions. The first one [BK13b] is closely related to vertices and can be seen as a model of interactions between particles that is mediated by the presence of an impurity (thought of as being located in a vertex); this type of interactions is similar to the one introduced in [MP95]. The second type of singular interactions [BK13c] are the more familiar δ-pair interactions. They are models of very short-range, or contact interactions. When implemented for bosons, these interactions lead to a Lieb-Liniger gas [LL63] on a graph, and in the limit of hardcore interaction they lead to a Tonks-Giradeau gas [Gir60]. For all of these models it has been shown that they can be rigorously implemented with self-adjoint Hamiltonians and it has been proven that their spectra are discrete and the eigenvalues follow a Weyl law.

Due to a well-known theorem of Hohenberg [Hoh67], free Bose gases in one dimension are often said to not display Bose-Einstein condensation (BEC). This statement, however, is only true if in finite volume one imposes Dirichlet or other standard boundary conditions. It has been known though that non-standard boundary conditions may lead to cases where a finite number of eigenvalues are negative and remain so in the thermodynamic limit, such that in this limit a spectral gap below the continuum develops. Such a scenario then leads to BEC into the negative-energy ground state [LW79, Ver11]. A similar behaviour occurs for free bosons on graphs, and it is possible to fully characterise all boundary conditions where this is the case [BK14]. For a gas of bosons with pairwise repulsive hardcore interactions, a suitable Fermi-Bose mapping, however, shows that no condensation can be expected. Furthermore, it can be shown that arbitrarily small repulsive

pair interactions prohibit a Bose gas on a graph to condense into the free ground state [BK16].

In statistical mechanics solvable models play a significant role. In this context solvability refers to the fact that eigenfunctions of the Hamiltonan have a simple representation in terms of a so-called Bethe ansatz [Bet31, Gau14]. This form of the eigenfunctions also leads to a characterisation of eigenvalues through finitely many secular equations. The Lieb-Liniger gas [LL63] of N bosons with δ-interactions on a circle is an example of a solvable model and its version on an interval [Gau71] can be seen as a first example where vertices play a role. Vertices of degree two (and higher) present obstacles to the solvability of models with δ-interactions. A modification of the interactions that preserves solvability when one vertex of degree two is present was found in [CC07]. The basic idea behind this construction can be extended to arbitrarily (finitely) many vertices of any (finite) degree [BG17], as well as to any (finite) number of particles [BG18].

In the final section we are concerned with a two-particle model on a simple non-compact quantum graph, namely the half-line $\mathbb{R}_+$, which can be thought of as a quantum wire. Besides singular interactions localised on the vertex at zero [KM16, EK17] and contact interactions of the Lieb-Liniger type, we introduce a binding potential that leads to a pairing of the two particles [KM17, Kerb, Ker18]. We also provide generalisations of this model by considering singular two-particle interactions whose locations are randomly distributed along the half-line [Kera], and by taking into account surface defects in coupling the continuous half-line to a discrete graph [Kerc]. In all of these cases we are mainly interested in describing spectral properties of the associated Hamiltonians. Using the acquired knowledge about the spectrum we are able to investigate Bose-Einstein condensation of pairs. In this sense, these results can be seen as statements related to superconductivity in quantum wires. Note here that arguably the first results regarding the superconductivity on graphs were obtained in [dG81a, dG81b, Ale83].

2 Preliminaries

2.1 One-Particle Quantum Graphs

A quantum graph is a metric graph Γ with a differential operator that serves as Hamiltonian operator describing the motion of a particle along the edges of the graph, see [GS06, BK13a]. A metric graph is a (finite) combinatorial graph with a metric structure that arises from assigning lengths to edges. Let $\mathcal{V}$ be the set of vertices and $\mathcal{E} = \mathcal{E}_{\text{int}} \cup \mathcal{E}_{\text{ext}}$ be the set of edges. Then every $e \in \mathcal{E}_{\text{int}}$, an internal edge, is adjacent to two distinct vertices, and every $e \in \mathcal{E}_{\text{ext}}$, an external edge, is adjacent to a single vertex. A metric structure is introduced by assigning finite lengths to internal edges; external edges are considered to be of infinite length. In this way every $e \in \mathcal{E}_{\text{int}}$ is identified with an interval $[0, l_e]$ whereas every $e \in \mathcal{E}_{\text{ext}}$ is

identified with a copy of the real semi-axis $[0, \infty)$. Graphs without external edges, $\mathcal{E} = \mathcal{E}_{\text{int}}$, are compact.

One now introduces functions on Γ,

$$\psi = (\psi_1, \ldots, \psi_E) \,, \tag{2.1}$$

where $E = |\mathcal{E}|$ and $\psi_e : [0, l_e] \to \mathbb{C}$ for internal edges and $\psi_e : [0, \infty) \to \mathbb{C}$ for external edges. In this way one defines the Hilbert space

$$L^2(\Gamma) := \bigoplus_{e \in \mathcal{E}_{\text{int}}} L^2(0, l_e) \bigoplus_{e \in \mathcal{E}_{\text{ext}}} L^2(0, \infty) \,, \tag{2.2}$$

as well as the Sobolev spaces

$$H^m(\Gamma) := \bigoplus_{e \in \mathcal{E}_{\text{int}}} H^m(0, l_e) \bigoplus_{e \in \mathcal{E}_{\text{ext}}} H^m(0, \infty) \,. \tag{2.3}$$

A Hamiltonian operator $H = -\Delta + V$ is a self-adjoint operator (in many cases with domain $\mathcal{D} \subset H^2(\Gamma)$) that acts on functions on an edge as

$$(H\psi)_e = -\psi_e'' + V_e \psi_e \,, \tag{2.4}$$

where $V = (V_1, \ldots, V_E)$ is a potential function. In many quantum graph models, however, one considers the case $V = 0$.

In the following we shall restrict our attention to compact graphs, although the examples in Sect. 6 will be non-compact; the necessary modifications are more or less obvious.

In order to characterise domains $\mathcal{D}$ of self-adjointness one has to impose boundary conditions at the vertices on functions in the domain. We denote boundary values of functions as

$$\psi_{bv} = \big(\psi_1(0), \ldots \psi_E(0), \psi_1(l_1), \ldots, \psi_E(l_E)\big) \,, \tag{2.5}$$

and of inward derivatives as

$$\psi'_{bv} = \big(\psi_1'(0), \ldots \psi_E'(0), -\psi_1'(l_1), \ldots, -\psi_E'(l_E)\big) \,. \tag{2.6}$$

Self-adjoint realisations of H can be obtained as maximal symmetric extensions of the operator with minimal domain $C_0^\infty(\Gamma)$ (see, e.g., [KS99a]). Their domains can be uniquely parametrised in terms of an orthogonal projector P and a self-adjoint map L, such that $P^\perp L P^\perp = L$, on the space $\mathbb{C}^{2E}$ of boundary values, as [Kuc04]

$$\mathcal{D}(P, L) = \big\{\psi \in H^2(\Gamma) : \; (P + L)\psi_{bv} + P^\perp \psi'_{bv} = 0\big\} \,. \tag{2.7}$$

It is often useful to work with quadratic forms instead of self-adjoint operators, making use of the fact that a semi-bounded (from below) self-adjoint operator defines a unique, semi-bounded and closed quadratic form, and vice versa [BHE08]. The form associated with a quantum graph Laplacian $-\Delta$ on the domain (2.7) is [Kuc04]

$$\mathcal{Q}[\psi] = \int_\Gamma |\nabla\psi|^2 \,\mathrm{d}x - \langle \psi_{bv}, L\psi_{bv}\rangle_{\mathbb{C}^{2E}} \,, \tag{2.8}$$

with form domain

$$\mathcal{D}_\mathcal{Q} = \left\{\psi \in H^1(\Gamma) : \; P\psi_{bv} = 0\right\} . \tag{2.9}$$

The boundary conditions prescribed in (2.7) and (2.9) do not necessarily respect the connectivity of the combinatorial graph. The latter will, however, be the case for local boundary conditions, where

$$P = \bigoplus_{v\in\mathcal{V}} P_v \quad \text{and} \quad L = \bigoplus_{v\in\mathcal{V}} L_v \,, \tag{2.10}$$

and P_v, L_v act on the subspace $\mathbb{C}^{d_v}$ of boundary values at the edge ends adjacent to the vertex $v \in \mathcal{V}$. Here d_v is the degree of the vertex v.

A quantum graph Hamiltonian $H = -\Delta + V$ defined on a domain (2.7) is self-adjoint, bounded from below, and has compact resolvent (note that the latter fails to hold for non-compact graphs). Hence its spectrum is real, bounded from below, discrete and eigenvalues accumulate only at infinity. In the most relevant case of $V = 0$, one can characterise eigenvalues through a secular determinant. One first defines a (vertex) scattering matrix

$$S(k) := -P - (L + \mathrm{i}kP^\perp)^{-1}(L - \mathrm{i}kP^\perp) \,, \tag{2.11}$$

where $k \in \mathbb{C}$ is such that k^2 is a spectral parameter for $-\Delta$, and then a matrix

$$T(k) := \begin{pmatrix} 0 & \mathrm{e}^{\mathrm{i}k\boldsymbol{l}} \\ \mathrm{e}^{\mathrm{i}k\boldsymbol{l}} & 0 \end{pmatrix} \tag{2.12}$$

encoding the metric information about Γ. Here $\mathrm{e}^{\mathrm{i}k\boldsymbol{l}}$ is a diagonal $E \times E$ matrix with diagonal entries $\mathrm{e}^{\mathrm{i}kl_e}$, $e = 1, \ldots, E$. Defining $U(k) := S(k)T(k)$, one can show [KS06] that k^2 is a non-zero eigenvalues of $-\Delta$ of multiplicity $m(k)$, iff k is a zero of

$$\det\big(\mathbb{1} - U(k)\big) \tag{2.13}$$

of order $m(k)$. An eigenvalue zero has to be treated separately, see [KS06, BE09, BES15]. A similar, slightly more complicated condition can be obtained for operators of the form $H = -\Delta + V$, see [BER15].

The secular equation (2.13) can be used to derive a trace formula [Rot83, KS99b, KN05, Win08, BE09] that expresses spectral functions in terms of sums over periodic orbits on the graph.

2.2 Many-Particle Kinematics

Following the general construction of systems of several (distinguishable) particles from given one-particle systems in quantum mechanics, the Hilbert space of N distinguishable particles on a metric graph Γ is

$$\mathcal{H}_N = L^2(\Gamma) \otimes \cdots \otimes L^2(\Gamma) \,. \tag{2.14}$$

Vectors in the tensor product are collections of functions $\psi_{e_1 \ldots e_N} \in L^2([0, l_{e_1}] \times \cdots \times [0, l_{e_N}])$. These are functions of N variables describing the positions of the particles on the N edges $e_1, \ldots, e_N$, which do not need to be all different. In a slight abuse of notation we shall view these collections of functions as functions on the domain

$$D_\Gamma^{(N)} := \bigcup_{e_1 \ldots e_N} (0, l_{e_1}) \times \cdots \times (0, l_{e_N}) \,, \tag{2.15}$$

such that we shall also use the notation $\mathcal{H}_N = L^2(D_\Gamma^{(N)})$.

N-particle observables are self-adjoint operators on $\mathcal{H}_N$. An operator O that respects the tensor product structure (2.14) of the Hilbert space,

$$O = \sum_{i=1}^{N} \mathbb{1} \otimes \cdots \otimes \mathbb{1} \otimes O_i \otimes \mathbb{1} \cdots \otimes \mathbb{1} \,, \tag{2.16}$$

does not detect any correlations or interactions between particles. A Hamiltonian describing particle interactions, therefore, cannot be of this product form. In other words, particle interactions will be implemented by choosing a Hamiltonian that does not have the product structure. This can be achieved either in the form of, say, a potential

$$V(x_1, \ldots, x_N) = \sum_{i,j=1}^{N} V_p(x_i, x_j) \tag{2.17}$$

with explicit pair interactions. However, one can also implement interactions by choosing an operator domain for an N-particle Laplacian $-\Delta_N$, acting as

$$(-\Delta_N \psi)_{e_1 \dots e_N} = -\frac{\partial^2 \psi_{e_1 \dots e_N}}{\partial x_{e_1}^2} - \dots - \frac{\partial^2 \psi_{e_1 \dots e_N}}{\partial x_{e_N}^2} , \tag{2.18}$$

that does not respect the tensor product structure for the operator.

When the N particles are indistinguishable, the exchange symmetry has to be implemented in the kinematic set up of the quantum system. If one adopts the Bose-Fermi alternative, the only relevant representations of the symmetric group will be the totally symmetric one (for bosons) and the totally anti-symmetric one (for fermions). The quantum state spaces then are the totally symmetric and the totally anti-symmetric subspaces $\mathcal{H}_{N,B}$ and $\mathcal{H}_{N,F}$, respectively, of (2.14).

3 Singular Pair Interactions

A possible way of introducing interactions is to violate the tensor product structure (2.16) with boundary conditions, either at the boundaries of the domains $[0, l_{e_1}] \times \dots \times [0, l_{e_N}]$, or at additional boundaries introduced for the purpose of generating other types of interactions. Typically, such boundary conditions will lead to singular interactions that can formally be expressed in terms of δ-functions, see e.g. [BEKS94, BMLL13].

3.1 Vertex-Induced Singular Interactions

Boundary conditions imposed at the boundaries of $[0, l_{e_1}] \times \dots \times [0, l_{e_N}]$ alone correspond to interactions that act when at least one particle sits in a vertex (corresponding to $x_{e_j} = 0$ or $x_{e_j} = l_{e_j}$). Hence we say that such interactions are vertex induced. An example for a pair of particles on the same edge (of length l) would be the two-dimensional Laplacian plus a formal potential of the form

$$v(x_1, x_2)\big[\delta(x_1) + \delta(x_1 - l) + \delta(x_2) + \delta(x_2 - l)\big] . \tag{3.1}$$

A version of such an interaction on a Y-shaped graph can be found in [MP95].

Constructing N-particle Laplacians with boundary conditions is not as straight forward as for one-particle Laplacians. The reason for this is that the minimal symmetric operator, which is an N-particle Laplacian with domain $C_0^\infty(D_\Gamma^{(N)})$, does not have finite deficiency indices. For that reason it is more appropriate to construct self-adjoint realisations of the N-particle Laplacian via their associated sesqui-linear forms.

In the following we restrict our attention to $N = 2$, noting that this case contains all the essential steps in order to construct N-particle Hamiltonians with pair interactions. As a first step we simplify the notation in that we define

$$\psi_{e_1e_2}(x_{e_1}, y_{e_2}) = \psi_{e_1e_2}(l_{e_1}x, l_{e_2}y) \tag{3.2}$$

with $x, y \in (0, 1)$. The $4E^2$ boundary values of functions $\psi \in H^1(D_\Gamma^{(2)})$ and derivatives of functions $\psi \in H^2(D_\Gamma^{(2)})$ then are

$$\psi_{bv}(y) = \begin{pmatrix} \sqrt{l_{e_2}}\psi_{e_1e_2}(0, l_{e_2}y) \\ \sqrt{l_{e_2}}\psi_{e_1e_2}(l_{e_1}, l_{e_2}y) \\ \sqrt{l_{e_1}}\psi_{e_1e_2}(l_{e_1}y, 0) \\ \sqrt{l_{e_1}}\psi_{e_1e_2}(l_{e_1}y, l_{e_2}) \end{pmatrix} \quad \text{and} \quad \psi'_{bv}(y) = \begin{pmatrix} \sqrt{l_{e_2}}\psi_{e_1e_2,x}(0, l_{e_2}y) \\ -\sqrt{l_{e_2}}\psi_{e_1e_2,x}(l_{e_1}, l_{e_2}y) \\ \sqrt{l_{e_1}}\psi_{e_1e_2,y}(l_{e_1}y, 0) \\ -\sqrt{l_{e_1}}\psi_{e_1e_2,y}(l_{e_1}y, l_{e_2}) \end{pmatrix}. \tag{3.3}$$

Here $y \in [0, 1]$ and the indices e_1e_2 run over all E^2 possible pairs with $e_1, e_2 = 1, \ldots, E$.

With the one-particle form domain (2.9) in mind we now introduce bounded and measurable maps $P, L : [0, 1] \to \mathrm{M}(4E^2, \mathbb{C})$ such that for a.e. $y \in [0, 1]$,

1. $P(y)$ is an orthogonal projector,
2. $L(y)$ is a self-adjoint endomorphism on $\ker P(y)$.

With these maps we can define the quadratic form,

$$\begin{aligned} Q^{(2)}_{P,L}[\psi] &:= \langle \nabla\psi, \nabla\psi \rangle_{L^2(D_\Gamma)} - \langle \psi_{bv}, L(\cdot)\psi_{bv} \rangle_{L^2(0,1)\otimes\mathbb{C}^{4E^2}} \\ &= \sum_{e_1,e_2=1}^{E} \int_0^{l_{e_2}} \int_0^{l_{e_1}} \left(\left|\psi_{e_1e_2,x}(x, y)\right|^2 + \left|\psi_{e_1e_2,y}(x, y)\right|^2 \right) \mathrm{d}x\, \mathrm{d}y \\ &\quad - \int_0^1 \langle \psi_{bv}(y), L(y)\psi_{bv}(y) \rangle_{\mathbb{C}^{4E^2}}\, \mathrm{d}y\,, \end{aligned} \tag{3.4}$$

and prove the following result [BK13b].

Theorem 3.1 *Given maps $P, L : [0, 1] \to \mathrm{M}(4E^2, \mathbb{C})$ as above that are bounded and measurable, the quadratic form (3.4) with domain*

$$\mathcal{D}_{Q^{(2)}} = \{\psi \in H^1(D_\Gamma) : \ P(y)\psi_{bv}(y) = 0 \text{ for a.e. } y \in [0, 1]\} \tag{3.5}$$

is closed and semi-bounded (from below).

The semi-bounded, self-adjoint operator associated with this form via the representation theorem for quadratic forms [BHE08] can be identified as a self-

adjoint realisation of the Laplacian when its domain is contained in $H^2(D_\Gamma^{(2)})$; in this case the form is said to be regular.

In order to identify regular forms we need to impose further restrictions on the maps P and L. The first one is that they are block-diagonal, in the form

$$M(y) = \begin{pmatrix} \tilde{M}(y) & 0 \\ 0 & \tilde{M}(y) \end{pmatrix} , \tag{3.6}$$

with respect to an arrangement of the components of (3.3) where the upper two components for all pairs e_1, e_2 are separated from the lower two components. Then we obtain the following result [BK13b].

Theorem 3.2 *Let L be Lipschitz continuous on $[0, 1]$ and let P be of the block-diagonal form (3.6). Assume that the matrix entries of $\tilde{P}$ are in $C^3(0, 1)$ and possess extensions of class C^3 to some interval $(-\eta, 1 + \eta)$, $\eta > 0$. Moreover, when $y \in [0, \varepsilon_1] \cup [l - \varepsilon_2, l]$, with some $\varepsilon_1, \varepsilon_2 > 0$, suppose that $L(y) = 0$ and that $\tilde{P}(y)$ is diagonal with diagonal entries that are either zero or one. Then the quadratic form $Q^{(2)}_{P,L}$ is regular. The associated semi-bounded, self-adjoint operator is a Laplacian with domain*

$$\mathcal{D}_2(P, L) := \{\psi \in H^2(D_\Gamma^{(2)}) : \ (P(y)+L(y))\psi_{bv}(y)+P^\perp(y)\psi'_{bv}(y) = 0 \text{ for a.e. } y \in [0, 1]\} . \tag{3.7}$$

Note the similarity of (3.7) with (2.7).

As one would expect from a quantum systems with a configuration space of finite volume, the spectrum of a two-particle Laplacian with domain (3.7) is discrete. Moreover, a Weyl law for the eigenvalue count holds: Let λ_n, $n \in \mathbb{N}$, denote the eigenvalues of the operator, then

$$N(\lambda) := \#\{n \in \mathbb{N} : \ \lambda_n \leq \lambda\} \sim \frac{\mathcal{L}^2}{4\pi} , \quad \lambda \to \infty , \tag{3.8}$$

where $\mathcal{L} = l_{e_1} + \cdots + l_{e_E}$ is the total length of the metric graph, see [BK13b].

The constructions above can be carried over to bosonic or fermionic systems in a straight forward manner; for details see [BK13b].

3.2 Contact Interactions

Realistic two-particle interactions are often of the form (2.17). When the range of the interaction is small one can model the pair potential with a Dirac-δ, so that the formal N-particle Hamiltonian is

$$H_N = -\Delta_N + \alpha \sum_{i<j} \delta(x_i - x_j) . \tag{3.9}$$

Here Δ_N denotes the N-particle Laplacian and $\alpha \in \mathbb{R}$ is a constant determining the interaction strength. In this way an interaction takes place when (at least) two particles are at the same position and, therefore, one speaks of a contact interaction. In order to implement contact interactions in a self-adjoint operator one has to impose boundary conditions along hyperplanes in the configuration space of N particles that are characterised by equations $x_i = x_j$. Contact interactions for bosons on a circle have, e.g., been studied in much detail in the form of the Lieb-Liniger model [LL63], and for distinguishable particles on infinite star graphs in [Har07, Har08].

A self-adjoint operator representing the formal expression (3.9) can be defined as an extension of the N-particle Laplacian with domain $C_0^\infty(D_\Gamma^{(N)})$. This can be done much in the same way as above for the vertex-induced singular interactions after additional boundaries have been introduced to the domain (2.15). As contact interactions require two particles to be on the same edge, components in (2.15) where $e_1, \dots, e_N$ are N distinct edges do not contribute. Taking the example of $N = 2$ as for the vertex-induced singular interactions above, one introduces the subdivision

$$D_{ee} := [0, l_e] \times [0, l_e] = D_{ee}^+ \cup D_{ee}^- \,, \tag{3.10}$$

of diagonal domains, where

$$D_{ee}^+ := \{(x, y) \in D_{ee} : x \geq y\} \quad \text{and} \quad D_{ee}^- := \{(x, y) \in D_{ee} : x \leq y\} \,. \tag{3.11}$$

These subdivisions modify the total domain $D_\Gamma^{(2)}$, see (2.15). The resulting domain with the additional boundaries is denoted as $D_\Gamma^{*(2)}$.

Boundary values of components $\psi_{e_1e_2}$ of functions $\psi \in H^2(D_\Gamma^{*(2)})$ and their derivatives are as in (3.3) when $e_1 \neq e_2$. For the remaining components, however, the additional boundaries lead to the boundary values

$$\psi_{ee,bv}(y) := \begin{pmatrix} \sqrt{l_e}\psi_{ee}^-(0, l_e y) \\ \sqrt{l_e}\psi_{ee}^+(l_e, l_e y) \\ \sqrt{l_e}\psi_{ee}^+(l_e y, 0) \\ \sqrt{l_e}\psi_{ee}^-(l_e y, l_e) \\ \sqrt{l_e}\psi_{ee}^+(l_e y, l_e y) \\ \sqrt{l_e}\psi_{ee}^-(l_e y, l_e y) \end{pmatrix} \quad \text{and} \quad \psi'_{ee,bv}(y) := \begin{pmatrix} \sqrt{l_e}\psi_{ee,x}^-(0, l_e y) \\ -\sqrt{l_e}\psi_{ee,x}^+(l_e, l_e y) \\ \sqrt{l_e}\psi_{ee,y}^+(l_e y, 0) \\ -\sqrt{l_e}\psi_{ee,y}^-(l_e y, l_e) \\ \sqrt{2l_e}\psi_{ee,n}^+(l_e y, l_e y) \\ \sqrt{2l_e}\psi_{ee,n}^-(l_e y, l_e y) \end{pmatrix} , \tag{3.12}$$

for $y \in [0, 1]$. Here $\psi_{ee}^\pm : D_{ee}^\pm \to \mathbb{C}$ and

$$\psi_{ee,n}^\pm := \frac{\pm 1}{\sqrt{2}}\big(\psi_{ee,x}^\pm - \psi_{ee,y}^\pm\big) \tag{3.13}$$

is the normal derivative along the diagonal part of the boundary.

The space $\mathbb{C}^{n(E)}$, $n(E) = 4E^2 + 2E$, of boundary values decomposes into a $4E^2$-dimensional subspace W_{vert} of vertex-induced boundary values as in Sect. 3.1, and a $2E$-dimensional subspace W_{cont} of boundary values on diagonals associated with contact interactions. Introducing maps P and L on $[0, 1]$ that take values in the orthogonal projectors and self adjoint maps on $W_{vert} \oplus W_{cont}$, respectively, in the same way as in Sect. 3.1, their restrictions to W_{vert} should satisfy the same properties as above. The restrictions to the edge-e subspace of W_{cont} should take the form

$$P_{cont,e} = \frac{1}{2}\begin{pmatrix} 1 & -1 \\ -1 & 1 \end{pmatrix} \quad \text{and} \quad L_{cont,e} = -\frac{1}{2}\alpha(y)\mathbb{1}_2 \,, \tag{3.14}$$

where $\alpha : [0, 1] \to \mathbb{R}$ is a possibly varying, Lipschitz-continuous interaction strength. With boundary conditions as described in (3.7) this choice implies continuity of functions across diagonals,

$$\psi^+_{ee}(l_e y, l_e y) = \psi^-_{ee}(l_e y, l_e y) \,, \tag{3.15}$$

and satisfies jump conditions for the normal derivatives,

$$\psi^+_{ee,n}(l_e y, l_e y) + \psi^-_{ee,n}(l_e y, l_e y) = \frac{1}{\sqrt{2}}\alpha(y)\psi^{\pm}_{ee}(l_e y, l_e y) \,. \tag{3.16}$$

These conditions ensure a rigorous, self-adjoint realisation of the δ-type contact interactions (3.9). The operator is a two-particle Laplacian with domain (3.7), where now

$$P = P_{vert} \oplus P_{cont} \quad \text{and} \quad L = L_{vert} \oplus L_{cont} \,. \tag{3.17}$$

Hardcore contact interactions correspond to Dirichlet conditions along all diagonal boundaries. These conditions follow from δ-type interactions by taking the limit $\alpha \to \infty$ (the convergence is in the sense of forms, see [Kat95]). For more detail see [BK13c].

As in the case of vertex-induced singular interactions, the spectrum of the two-particle Laplacian with domain (3.7) and (3.17) is discrete and the Weyl law (3.8) holds [BK13c].

3.3 A Lieb-Liniger Model on Graphs

The contact interactions of Sect. 3.2 offer an opportunity to extend the Lieb-Liniger model of N bosons with δ-interactions on a circle to arbitrary metric graphs. Implementing bosonic symmetry first requires to restrict the N-particle Hilbert space $\mathcal{H}_N$, see (2.14), to its totally symmetric subspace $\mathcal{H}_{N,B}$. The projector Π_B

to that subspace acts on vector $\psi \in \mathcal{H}_N$ as

$$(\Pi_B \psi)_{e_1 \dots e_N} = \frac{1}{N!} \sum_{\pi \in S_N} \psi_{e_{\pi(1)} \dots e_{\pi(N)}} \,, \tag{3.18}$$

where S_N denotes the symmetric group. In order to implement δ-type contact interactions one has to dissect the hyper-rectangles $(0, l_{e_1}) \times \cdots \times (0, l_{e_N})$ with at least two coinciding edges, $e_i = e_j$ with $i \neq j$, along the hyperplanes $x_{e_i} = x_{e_j}$. The resulting configuration space is $D_\Gamma^{*(N)}$. On the hyperplanes we impose boundary conditions that are equivalent to (3.15)–(3.16).

The remaining, vertex related boundary values can be simplified by making use of the particle exchange symmetry. For functions $\Psi \in H_B^1(D_\Gamma^{*(N)})$ they are

$$\psi_{bv,vert}(\boldsymbol{y}) = \begin{pmatrix} \sqrt{l_{e_2} \dots l_{e_N}}\, \psi_{e_1 \dots e_N}(0, l_{e_2} y_1, \dots, l_{e_N} y_{N-1}) \\ \sqrt{l_{e_2} \dots l_{e_N}}\, \psi_{e_1 \dots e_N}(l_{e_1}, l_{e_2} y_1, \dots, l_{e_N} y_{N-1}) \end{pmatrix} \,, \tag{3.19}$$

and for derivatives,

$$\psi'_{bv,vert}(\boldsymbol{y}) = \begin{pmatrix} \sqrt{l_{e_2} \dots l_{e_N}}\, \psi_{e_1 \dots e_N, x_{e_1}^1}(0, l_{e_2} y_1, \dots, l_{e_N} y_{N-1}) \\ -\sqrt{l_{e_2} \dots l_{e_N}}\, \psi_{e_1 \dots e_N, x_{e_1}^1}(l_{e_1}, l_{e_2} y_1, \dots, l_{e_N} y_{N-1}) \end{pmatrix} \,, \tag{3.20}$$

where $\boldsymbol{y} = (y_1, \dots, y_{N-1}) \in [0,1]^{N-1}$.

Introducing maps $L_{vert}, P_{vert} : [0,1]^{N-1} \to M(2E^N, \mathbb{C})$ in analogy to (3.17), we are now in a position to introduce the quadratic form

$$\begin{aligned} Q_B^{(N)}[\psi] = {} & N \sum_{e_1 \dots e_N} \int_0^{l_{e_1}} \dots \int_0^{l_{e_N}} |\psi_{e_1 \dots e_N, x_{e_1}}(x_{e_1}, \dots, x_{e_N})|^2 \, \mathrm{d}x_{e_N} \dots \mathrm{d}x_{e_1} \\ & - N \int_{[0,1]^{N-1}} \langle \psi_{bv,vert}, L_{vert}(\boldsymbol{y}) \psi_{bv,vert} \rangle_{\mathbb{C}^{2E^N}} \, \mathrm{d}\boldsymbol{y} \\ & + \frac{N(N-1)}{2} \sum_{e_2 \dots e_N} \int_{[0,1]^{N-1}} \alpha(y_1) \, |\sqrt{l_{e_2} \dots l_{e_N}}\, \psi_{e_2 e_2 \dots e_N}(l_{e_2} y_1, \boldsymbol{l}\boldsymbol{y})|^2 \, \mathrm{d}\boldsymbol{y} \,, \end{aligned} \tag{3.21}$$

where $\boldsymbol{l}\boldsymbol{y} = (l_{e_2} y_1, l_{e_3} y_2, \dots, l_{e_N} y_{N-1})$, with form domain

$$\mathcal{D}_{Q_B^{(N)}} = \{ \psi \in H_B^1(D_\Gamma^{*(N)}); \; P_{vert}(\boldsymbol{y}) \psi_{bv,vert}(\boldsymbol{y}) = 0 \text{ for a.e. } \boldsymbol{y} \in [0,1]^{N-1} \} \,. \tag{3.22}$$

The first two lines in (3.21) define a bosonic N-particle Laplacian with vertex-related boundary conditions, whereas the last line yields pairwise, δ-type contact interactions.

The hardcore limit, $\alpha \to \infty$ (see above), of the Lieb-Liniger gas is the so-called Tonks-Girardeau gas [Gir60].

4 Bose-Einstein Condensation

One of the most interesting questions arising for bosonic many-particle systems is whether they show the phenomenon of Bose-Einstein condensation (BEC). This occurs when below a critical temperature the particles condense into the same one-particle state [PO56]. The original version of BEC [Ein25] was found for free, i.e., non-interacting bosons in three dimensions that are confined to box of finite volume and whose wave functions satisfy standard conditions at the boundary of the box; it occurs in the thermodynamic limit of increasing the particle number and the volume of the box while keeping the particle density fixed. One can readily show that this form of BEC does not occur in one dimension as long as standard boundary conditions are imposed. However, it has long been known that BEC for free bosons does occur in one dimension when the boundary conditions are changed in such a way that the free, one-particle Hamiltonian has a negative eigenvalue and in the thermodynamic limit a gap remains in the spectrum between the ground state and the continuum above zero [LW79, Ver11].

4.1 Free Bosons

In a many-particle system of N free bosons, the Hamiltonian is a symmetrised version of an operator with the tensor product structure (2.16). Its eigenvalues are of the form $k_{n_1}^2 + \cdots + k_{n_N}^2$, where k_n^2 is an eigenvalue of the one-particle Hamiltonian, which we assume to be a Laplacian with domain (2.7). The number of negative eigenvalues is controlled by the self-adjoint map L in the characterisation of the domain [BL10], and this determines whether or not BEC is found in the thermodynamic limit. In this limit the volume growth is achieved by stretching all edge lengths with the same factor, $l_e \mapsto \eta l_e$, $\eta > 0$. Hence, the thermodynamic limit can be performed by sending the total length $\mathcal{L} = \sum_e l_e$ to infinity.

The first result required in order to prove BEC establishes a gap in the spectrum [BK14].

Proposition 4.1 *Let $-\Delta$ be a one-particle Laplacian on a compact metric graph with domain (2.7). Assume that L has at least one positive eigenvalue and let L_{max} be the largest eigenvalue. Then the ground state eigenvalue $k_0^2(\mathcal{L})$ of the Laplacian at total length $\mathcal{L}$ converges to $-L_{max}$ in the thermodynamic limit $\mathcal{L} \to \infty$.*

In the grand canonical ensemble of statistical mechanics (see, e.g., [Sch06] for details), the density of particles $\rho_n(\beta, \mu_{\mathcal{L}})$ in an eigenstate with eigenvalue $k_n^2(\mathcal{L})$ is

$$\rho_n(\beta, \mu_{\mathcal{L}}) = \frac{1}{\mathcal{L}} \frac{1}{\mathrm{e}^{\beta(k_n^2(\mathcal{L})-\mu_{\mathcal{L}})} - 1} , \tag{4.1}$$

where $\beta = 1/k_B T$ is the inverse temperature and $\mu_{\mathcal{L}} \leq k_0^2(\mathcal{L})$ is the so-called chemical potential which itself depends on $\mathcal{L}$. More explicitly, $\mu_{\mathcal{L}}$ is chosen such that

$$\rho = \frac{1}{\mathcal{L}} \sum_{n=0}^{\infty} \frac{1}{\mathrm{e}^{\beta(k_n^2(\mathcal{L})-\mu_{\mathcal{L}})} - 1} \tag{4.2}$$

is the fixed density of particles on the graph for all values of $\mathcal{L}$.

Definition 4.2 We say that an eigenstate with eigenvalue $k_n^2(\mathcal{L})$ is macroscopically occupied in the thermodynamic limit if

$$\limsup_{\mathcal{L}\to\infty} \rho_n(\beta, \mu_{\mathcal{L}}) > 0 . \tag{4.3}$$

If such an eigenstate exists we say that there is BEC into this eigenstate.

For a more general definition of BEC that also holds for interacting systems, see [PO56]. With these observations one is able to obtain a complete characterisation of free Bose gases on compact graphs in terms of BEC [BK14].

Theorem 4.3 *Let Γ be a compact metric graph with one-particle Laplacian defined on the domain (2.7). If L is negative semi-definite, no BEC occurs at finite temperature in the thermodynamic limit.*

If, however, L has at least one positive eigenvalue, there exists a critical temperature $T_c > 0$ such that BEC occurs below T_c in the thermodynamic limit.

The one-particle ground state eigenfunction into which all particles condense below the critical temperature is peaked around the vertices and hence is not homogeneous, as it would be in the classical case of particles in a box with Dirichlet boundary conditions, see also [LW79].

4.2 Interacting Bosons

For interacting bosons it is much harder to prove that BEC either holds or is absent (see, e.g., [LS02, LVZ03] for a discussion of BEC in interacting systems with a mean-field scaling). In the case of the Tonks-Girardeau gas [Gir60] of particles with hardcore interactions on a graph, however, one can use a Fermi-Bose mapping in order to prove the absence of phase transitions which then indicates an

absence of BEC. The Fermi-Bose mapping is a bijection between the set of bosonic many-particle Laplacians with hardcore interactions and the set of free fermionic Laplacians on the same compact, metric graph. The fermionic N-particle Hilbert space $\mathcal{H}_{N,F}$ is the totally antisymmetric subspace of $\mathcal{H}_N$, i.e., the image of the projector

$$(\Pi_F \psi)_{e_1 \dots e_N} = \frac{1}{N!} \sum_{\pi \in S_N} (-1)^{\operatorname{sgn} \pi} \psi_{e_{\pi(1)} \dots e_{\pi(N)}} , \tag{4.4}$$

compare (3.18). One notices that the antisymmetry implies that continuous fermionic functions vanish along diagonal hyperplanes $x_{e_i} = x_{e_j}$, where $e_i = e_j$ but $i \neq j$, as do functions in the domain of a bosonic Laplacian with hardcore interactions. Using appropriate permutations of edges one can construct a bijection between bosonic and fermionic functions in such a way that the latter are in the domain of a fermionic quadratic form that is associated with a free fermionic Laplacians. As the forms coincide, the Fermi-Bose mapping is isospectral. For details of the construction we refer to [BK14]. In fermionic systems BEC is well known to be absent. In the present case one calculates the free-energy density of free fermions (with Dirichlet boundary conditions in the vertices) in the thermodynamic limit,

$$f_{D,F}(\beta, \mu) = \limsup_{\mathcal{L} \to \infty} \frac{1}{\beta \mathcal{L}} \operatorname{Tr} \mathrm{e}^{-\beta H_N} = -\frac{1}{\beta} \int_0^\infty \log(1 + \mathrm{e}^{-\beta(k^2 - \mu)}) \, \mathrm{d}k, \tag{4.5}$$

see [BK14]. This energy density is smooth and has no singularities in β which shows that there is no phase transition, consequently indicating an absence of BEC.

Other forms of (repulsive) interactions can be modelled by pair potentials of the type (2.17). On a metric graph this takes the form

$$(V_{N,\mathcal{L}} \psi)_{e_1 \dots e_N}(x_{e_1}, \dots, x_{e_N}) = \sum_{i<j} V_{p,\mathcal{L}}(x_{e_i} - x_{e_j}) \psi_{e_1 \dots e_N}(x_{e_1}, \dots, x_{e_N}) , \tag{4.6}$$

and gives rise to the (bosonic) N-particle Hamiltonian

$$H_N = -\Delta_N + V_{N,\mathcal{L}} . \tag{4.7}$$

The pair potentials are repulsive when the functions $V_{p,\mathcal{L}}$ are non-negative, and for technical reasons we assume that for all $\mathcal{L} > 0$ there exist $A_\mathcal{L} > 0$ and $\epsilon_\mathcal{L} > 0$ such that $V_{p,\mathcal{L}}(x) \geq \epsilon_\mathcal{L}$ for all $x \in [-A_\mathcal{L}, A_\mathcal{L}]$. Moreover, the L^1-norm of $V_{p,\mathcal{L}}$ is assumed to be independent of $\mathcal{L}$. These assumptions are consistent with choosing functions $V_{p,\mathcal{L}}$ that are a δ-series in the thermodynamic limit $\mathcal{L} \to \infty$. One can, e.g., take $V_{p,\mathcal{L}}(x) = \mathcal{L} v(\mathcal{L} x)$ with $v \in C_0^\infty(\mathbb{R})$, $v \geq 0$ and $\|v\|_1 = \alpha$ so that $\lim_{\mathcal{L} \to \infty} V_{p,\mathcal{L}}(x) = \alpha \delta(x)$. With this choice the Lieb-Liniger model will be recovered in the thermodynamic limit.

A Gibbs state at inverse temperature $\beta > 0$ is defined via

$$\omega_\beta(O) := \frac{\mathrm{Tr}\left(O\,\mathrm{e}^{-\beta H_N}\right)}{\mathrm{Tr}\,\mathrm{e}^{-\beta H_N}}\,, \tag{4.8}$$

where O is a (bounded) observable, i.e., a (bounded and) self-adjoint operator. If now ψ_0 is the ground state of the free bosonic system, i.e., composed of the ground state eigenfunction ϕ_0 of the one-particle Laplacian and $N(\phi_0)$ is the particle number operator in this ground state one can infer from Theorem 4.3 whether or not the non-interacting system shows BEC. Assuming this to be the case, one can ask what the effect of adding a repulsive interaction (4.6) is. It can be shown [BK16] that in the theromodynamic limit the occupation of this ground state vanishes,

$$\limsup_{\mathcal{L}\to\infty} \frac{\omega_\beta(N(\phi_0))}{\mathcal{L}} = 0\,. \tag{4.9}$$

According to a direct analogue of Definition 4.2, this means that there is no BEC into the free ground state. Hence, although BEC into the ground state was present in the free bosonic system, even the smallest perturbation by repulsive pair interactions of the type (2.17) make this condensation disappear.

Summarising, although free bosons on a compact metric graph may display BEC, an addition of repulsive interactions is likely to destroy the condensate. The BEC that can occur is caused by δ-type, attractive, one-particle potentials in the vertices and the associated condensate is not homogeneous, but concentrated around the vertices.

5 Exactly Solvable Many-Particle Quantum Graphs

Much of the success of one-particle quantum graph models relies on the fact that eigenvalues possess a simple characterisation in terms of a secular equation based on the finite-dimensional determinant (2.13). On the one hand this enables one to compute eigenvalues by searching for zeros of a low-dimensional determinant, and on the other hand it leads to a trace formula that is an identity [Rot83, KS99b, BE09] rather than a semiclassical approximation as in other, typical models of quantum systems (see, e.g., [Gut90]).

The secular equation rests on the fact that the edge-e component of an eigenfunction must be of the form

$$\psi_e(x_e) = a_e\,\mathrm{e}^{\mathrm{i}kx_e} + b_e\,\mathrm{e}^{-\mathrm{i}kx_e}\,, \tag{5.1}$$

with some coefficients $a_e, b_e \in \mathbb{C}$. It provides a sufficient condition that the $2E$ coefficients must satisfy in order to yield an eigenfunction. Components of N-particle eigenfunctions with eigenvalue λ are functions of N variables, $x_{e_1}, \ldots, x_{e_N}$,

so that, in general, they are of the form

$$\psi_{e_1\dots e_n}(x_{e_1},\dots,x_{e_N}) = \int_{\mathbb{R}^N} a_{e_1\dots e_n}(k_1,\dots,k_N)\,\delta(k_1^2+\dots+k_N^2-\lambda) \\ \mathrm{e}^{\mathrm{i}(k_1 x_{e_1}+\dots+k_N x_{e_N})}\,\mathrm{d}^N k\,. \tag{5.2}$$

Hence, instead of the need to determine constants, in generic cases with $N \geq 2$ a replacement for the secular equation needs to determine coefficient functions $a_{e_1\dots e_n}(\cdot)$. This would therefore be a condition imposed on elements of an infinite dimensional space.

However, under certain circumstances such conditions may collapse to a finite dimensional subspace. This, indeed, will be the case if certain integrability conditions are satisfied which imply that eigenfunctions can be represented by a so-called Bethe-ansatz [Gau14]. In essence, a Bethe-ansatz is a finite sum of plane waves,

$$\psi_{\mathrm{Bethe}}(x_1,\dots,x_N) = \sum_{\alpha\in J} A_\alpha\,\mathrm{e}^{\mathrm{i}(k_1^\alpha x_1+\dots+k_N^\alpha x_N)}\,, \tag{5.3}$$

where J is a finite index set, such that the vectors $(k_1^\alpha,\dots,k_N^\alpha)$ with $(k_1^\alpha)^2+\dots+(k_N^\alpha)^2=\lambda$ are drawn from a finite subset of $\mathbb{R}^N$. Contrasting this with the general form (5.2) of an N-particle eigenfunction suggests that a Bethe-ansatz will only be possible under some strict conditions. These integrability conditions (see, e.g., [Gau14, CC07]) are also behind the Lieb-Liniger model, for which it has long been known that eigenfunctions can be characterised in terms of a finite number of coefficients [LL63] and take a Bethe-ansatz form (5.3). The first example of a quantum graph with a non-trivial vertex where a Bethe-ansatz was shown to work is a particle on a line or ring with one vertex, where non-Kirchhoff conditions are imposed [CC07]. Since N particles on a graph have a configuration space that is composed of subsets of $\mathbb{R}^N$, a further class of examples in this spirit where a Bethe-ansatz for the eigenfunctions is known to exist is given by the Dirichlet- or Neumann Laplacian on a fundamental domain for the action of a Weyl group [Bőö80]. Indeed, the mechanism behind these examples can be carried over to a class of quantum graph models, generalising the approach of [CC07]. This has been done in [BG17, BG18], and in the following we will review those results.

The simplest example is that of two bosons on an interval $[0,l]$ with Dirichlet boundary conditions at the interval ends and a δ-interaction (3.9) between the particles. This is a modification of the Lieb-Liniger model first studied by Gaudin [Gau71]. The two-particle Hilbert space is

$$\mathcal{H}_2 = L^2(0,l)\otimes L^2(0,l) \cong L(D)\,, \tag{5.4}$$

where D is the square (3.10) that will be dissected as in (3.11). Accordingly, $\psi^{\pm} \in L^2(D^{\pm})$, for which the Bethe-ansatz

$$\psi^{\pm}(x_1, x_2) = \sum_{P \in \mathcal{W}_2} A_P^{\pm} \, \mathrm{e}^{\mathrm{i}(k_{P(1)}x_1 + k_{P(2)}x_2)} \,, \tag{5.5}$$

can be shown to lead to eigenfunctions. Here $\mathcal{W}_2$ is a Weyl group, which is a finite group with eight elements. The fact that the ansatz (5.5) is consistent comes from the conditions an eigenfunction has to satisfy:

(i) $-\Delta\psi = \lambda\psi$;
(ii) $\psi(x_1, x_2) = \psi(x_2, x_1)$;
(iii) $\left(\frac{\partial}{\partial x_1} - \frac{\partial}{\partial x_2}\right)\psi(x, x) = \alpha\psi(x, x)$;
(iv) $\psi(0, x) = \psi(l, x) = 0$.

These conditions are compatible with the plane-wave form $A\,\mathrm{e}^{\mathrm{i}(k_1x_1 + k_2x_2)}$ and only require substitutions of the wave vectors (k_1, k_2) with either (k_2, k_1), $(-k_1, k_2)$, or combinations thereof. These operations, seen as an action of a group on $\mathbb{R}^2$, generate the action of the Weyl group $\mathcal{W}_2 = \mathbb{Z}/2\mathbb{Z} \rtimes S_2$. An interesting interpretation of this in terms of reflected rays can be found in [McG64]. The conditions (i)–(iv) also yield a restriction on the allowed wave vectors,

$$\mathrm{e}^{-2\mathrm{i}k_n l} = \frac{k_n + k_m - \mathrm{i}\alpha}{k_n + k_m + \mathrm{i}\alpha} \, \frac{k_n - k_m - \mathrm{i}\alpha}{k_n - k_m + \mathrm{i}\alpha} \,, \tag{5.6}$$

for all $n \neq m \in \{1, 2\}$. Solutions $(k_1, k_2) \neq (0, 0)$ with $0 \leq k_1 \leq k_2$ then give eigenvalues $\lambda = k_1^2 + k_2^2$.

The above model, for N bosons, was first studied by Gaudin [Gau71, Gau14]. The original Lieb-Liniger model [LL63], however, was formulated for particles on a circle. Instead of the Dirichlet conditions (iv) one then has to require periodic boundary conditions, which renders the reflection $(k_1, k_2) \mapsto (-k_1, k_2)$ expendable. The Bethe ansatz for the Lieb-Liniger model, therefore, only requires a summation over the symmetric group S_2, rather than over the Weyl group $\mathcal{W}_2 = \mathbb{Z}/2\mathbb{Z} \rtimes S_2$ as in (5.5). Hence, one concludes that the boundaries of the interval are responsible for the additional reflections necessary in the Bethe ansatz. In a graph language, the interval ends are vertices of degree one. Adding a vertex of degree two in the context of a Bethe ansatz was first done in [CC07], where is was found that this is incompatible with δ-pair interactions. Instead, the interactions were modified to include another contribution that formally looks like $\delta(x_1 + x_2)$. This means that the particles do not only interact when they touch, but also when they are the same distance away from the vertex on either of the edges connected by the vertex. If then this interaction is provided with a variable strength that is supported in a neighbourhood of the vertex, this will still be a localised interaction.

An extension of this method to arbitrary metric graphs with generalisations of the interactions introduced in [CC07] has been done in [BG17], and an extension

to N particles can be found in [BG18]. The first step is to define the singular pair interactions, and this is most clearly done on a star graph of d half-lines. Then a given metric graph is first converted into its star representation, consisting of $|\mathcal{V}|$ star graphs, i.e., one for each $v \in \mathcal{V}$ of degree d_v. A Bethe ansatz is made for each star graph, and then the boundary conditions that represent the pair interactions on each star, as well as the matching conditions that allow to recover the original graph from its star representation imply conditions that characterise eigenvalues of the Laplacian with the singular pair interactions.

If now Γ_v is the star graph with d_v half-lines that is associated with the vertex $v \in \mathcal{V}$, the Hilbert space is $\oplus_{ee'} L^2(D_{ee'})$; here e and e' are edge labels and $D_{ee'} = \mathbb{R}^2_+$ is the two-particle configuration space when one particle is on edge e and the other one on e'. These configuration spaces are dissected into $D^+_{ee'}$ and $D^-_{ee'}$, which are defined in analogy to (3.11), and the restrictions of functions $\psi_{ee'}$ to $D^\pm_{ee'}$ are denoted as $\psi^\pm_{ee'}$. One then requires that

$$\begin{aligned} \psi^+_{ee'}(x,x) &= \psi^-_{e'e}(x,x)\,, \\ \left(\frac{\partial}{\partial x_1} - \frac{\partial}{\partial x_2} - 2\alpha\right)\psi^+_{ee'}(x,x) &= \left(\frac{\partial}{\partial x_1} - \frac{\partial}{\partial x_2}\right)\psi^-_{e'e}(x,x)\,. \end{aligned} \tag{5.7}$$

These conditions are similar to those generating δ-interactions. However, they apply to all pairs of edges, not only the diagonal ones. Hence there is a singular interaction, also across edges, whenever two particles are the same distance away from the vertex. A Bethe ansatz (5.5) is then introduced for the functions $\psi^\pm_{ee'}$, with the yet to be determined coefficients $A^\pm_{P,ee'}$. In a next step one has to cut the edges of the stars to the finite lengths that are required and then glue the stars to finally yield the original compact graph. In this glueing process it has to be ensured that the interactions only take place when two edges are connected in the same vertex, and not arbitrarily across the graph. In addition to (5.7), this yields conditions to be imposed on the coefficients $A^\pm_{P,ee'}$. These conditions can be formulated in terms of secular equations involving determinants

$$Z(k_1,k_2) = \det\big(\mathbb{1} - U(k_1,k_2)\big), \tag{5.8}$$

where

$$U(k_1,k_2) = E(k_2)Y(k_2-k_1)(\mathbb{1}_2 \otimes S(k_2) \otimes \mathbb{1}_{2E})Y(k_1+k_2), \tag{5.9}$$

and

$$\begin{aligned} Y(k) &= \frac{1}{k+i\alpha}\begin{pmatrix} -i\alpha & k \\ k & -i\alpha \end{pmatrix} \otimes \boldsymbol{\alpha} + \begin{pmatrix} 0 & 1 \\ 1 & 0 \end{pmatrix} \otimes (\mathbb{1}_{E^2} - \boldsymbol{\alpha})\mathbb{T}_{E^2} \\ E(k) &= \mathbb{1}_{4E} \otimes \begin{pmatrix} 0 & 1 \\ 1 & 0 \end{pmatrix} \otimes \mathrm{e}^{\mathrm{i}k\boldsymbol{l}}; \end{aligned} \tag{5.10}$$

Here $\mathbb{T}_{E^2}$ is a permutation matrix, and $\boldsymbol{\alpha}$ is a diagonal matrix with the interaction strengths (which could, in principal, be different for each pair of edges) $\alpha_{ee'}$ on the diagonal. More details can be found in [BG17]. The final result is the following statement.

Theorem 5.1 *Let $-\Delta_2$ be a two-particle Laplacian on a compact metric graph with pair interactions as described above. Then the zeros (k_1, k_2), where $0 \leq k_1 \leq k_2$, of $Z(k_i, k_j)$ for $i \neq j \in \{1, 2\}$ of order m correspond to eigenvalues $k_1^1 + k_2^2$ of $-\Delta_2$.*

We note that, with (5.8) in mind, the secular equations are reminiscent of the one-particle case (2.13). Some special cases and numerical results in some example can be found in [BG17]. The generalisation to N particles follows the same lines and is contained in [BG18].

6 Many-Particle Models on a Quantum Wire

In this section we are concerned with interacting two-particle systems on a simple non-compact quantum graph, namely the positive half-line $\mathbb{R}_+ = (0, \infty)$ which can be seen as a quantum wire. More specifically, the Hamiltonian has several contributions: a hard-wall binding potential and two singular contributions, one of which is of the vertex-induced type defined in Sect. 3.1 and the other one representing the contact interactions introduced in Sect. 3.2. The Hamiltonian is formally given by

$$H = -\frac{\partial^2}{\partial x^2} - \frac{\partial^2}{\partial y^2} + v_b(|x-y|) + v(x,y)\,[\delta(x) + \delta(y)] + \alpha(y)\delta(x-y)\,, \qquad (6.1)$$

where $v_b : \mathbb{R}_+ \to \overline{\mathbb{R}}$ is a (hard-wall) binding potential that is (formally) defined via

$$v_b(x) := \begin{cases} 0 & \text{for} \quad x < d\,, \\ \infty & \text{otherwise}\,, \end{cases} \qquad (6.2)$$

where $d > 0$ characterises the size of the pair. We realise this formal potential by requiring Dirichlet boundary conditions at $|x - y| = d$. Furthermore, $v : \mathbb{R}_+^2 \to \mathbb{R}$ is supposed to be a real-valued, symmetric and bounded potential, $v \in L^\infty(\mathbb{R}_+^2)$. Note that setting $d = \infty$ corresponds to the case where no binding potential in (6.1) is added. Also note that we always assume $\alpha(\cdot) \in L^\infty(\mathbb{R}_+)$.

It is important to note that interactions of the form (6.1) generically break translation invariance, even with potentials $v(x, y) = v(|x - y|)$, and consequently lead to non-separable many-body problems. Although only rarely discussed in the literature, they have important applications in various areas of physics [Gla93, GN05].

Other important situations in which singular interactions of the above form are expected can be found in solid-state physics. For example, similar to the Cooper pairing mechanism of superconductivity [Coo56], two electrons in a metal can effectively interact with each other through the interaction of each individual particle with the lattice via electron-phonon-electron interactions. Hence, if a metal exhibits spatially localised defects, there will be effective, spatially localised two-particle interactions.

Furthermore, the idea to consider a binding potential in (6.1), which effectively leads to a 'molecule', or a pair of particles, also originated from Cooper's work [Coo56]; another example can be found in [QU16], where the scattering of a bound pair of particles at mirrors is investigated. As a matter of fact, it was Cooper who realised that electrons in a metal will form pairs (Cooper pairs), if the metal is in the superconducting phase, i.e., is cooled below some critical temperature [BCS57, MR04a]. Hence, the Hamiltonian (6.1), or versions thereof, provide toy models to investigate bound pairs of particles in a quantum wire with defects [KM17, Kera]. Most importantly, in this model one can derive rigorous results related to the superconducting behaviour of quantum wires [Kerb, Kerc, Ker18].

6.1 The Model Without Hard-Wall Binding Potential

In this subsection we present results regarding the Hamiltonian (6.1) without binding potential, i.e., $v_b \equiv 0$. For more detail, we refer to [BK13b, BK13c, KM16, EK17] from which most of the results are taken.

In a first step one has to give a rigorous meaning to the Hamiltonian (6.1), which is only formally defined due the δ-distributions. This requires a suitable variant of Theorem 3.1 and Sect. 3.2. (Note that here the two-particle configuration space without binding potential is $\mathbb{R}^2_+$). In order to do this one constructs a quadratic form on $L^2(\mathbb{R}^2_+)$,

$$q^\infty_{\alpha,\sigma}[\varphi] := \int_{\mathbb{R}^2_+} |\nabla\varphi|^2 \,\mathrm{d}x - \int_0^\infty \sigma(y)|\gamma(\varphi)|^2 \mathrm{d}y + \int_0^\infty \alpha(y)|\varphi(y,y)|^2 \,\mathrm{d}y\,, \tag{6.3}$$

where $\sigma(y) := -v(0,y)$ is a real-valued boundary potential and $\gamma(\varphi) := (\varphi(y,0), \varphi(0,y))^T$ are the boundary values of $\varphi \in H^1(\mathbb{R}^2_+)$, which are well-defined in $L^2(\partial\mathbb{R}^2_+)$ due to the trace theorem for Sobolev functions [Dob05]. In the same way one defines $\varphi|_{x=y}$ as the trace of $\varphi \in H^1(\mathbb{R}^2_+)$ along the diagonal $x = y$.

Theorem 6.1 *For any given $\sigma, \alpha \in L^\infty(\mathbb{R}_+)$ the form $\left(q^\infty_{\alpha,\sigma}, H^1(\mathbb{R}^2_+)\right)$ is bounded from below and closed.*

Hence, according to the representation theorem for quadratic forms [BHE08] there exists a unique self-adjoint operator associated with the form $q^\infty_{\alpha,\sigma}$. We denote this operator by $-\Delta^{d=\infty}_{\sigma,\alpha}$. Since the only volume term in (6.3) is associated with the

∇-operator, this operator acts as the standard two-dimensional Laplacian $-\Delta$ on functions $\varphi \in \mathcal{D}(-\Delta_{\sigma,\alpha}^{d=\infty}) \subset H^1(\mathbb{R}^2_+)$. The boundary integrals in (6.3), on the other hand, reflect boundary conditions. More explicitly, one has coordinate-dependent Robin conditions along $\partial\mathbb{R}^2_+$, and coordinate-independent jump conditions along the diagonal $x = y$, see [BK13c, KM16] for more details.

In a next step we characterise the spectrum of the self-adjoint operator $-\Delta_{\sigma,\alpha}^{d=\infty}$.

Theorem 6.2 *For any given $\sigma, \alpha \in L^\infty(\mathbb{R}_+)$ one has $[0,\infty) \subset \sigma_{ess}(-\Delta_{\sigma,\alpha}^{d=\infty})$. Furthermore, if $\sigma(y), \alpha(y) \to 0$ as $y \to \infty$ one has $\sigma_{ess}(-\Delta_{\sigma,\alpha}^{d=\infty}) = [0,\infty)$.*

Proof We adapt [Theorem 3.1, [KM16]] where the case $\alpha = 0$ has been considered. In order to show that $[0,\infty)$ is contained in the essential spectrum, we construct a suitable Weyl sequence: Let $\tau : \mathbb{R} \to \mathbb{R}$ be a smooth test function such that $\tau \geq 0$, $\tau(t) = 1$ for $t \geq 1$ and $\tau(t) = 0$ for $t \leq 0$. We define, for $a_R, b_R > 0$ and any $k \in [0,\infty)$,

$$\varphi_{a_R,b_R,k}(x,y) := \tau\left(x - (a_R - 1)\right)\tau\left(y - (b_R - 1)\right) e^{ik(x+y)} \tau\left((2a_R + 1) - x\right) \\ \tau\left((2b_R + 1) - x\right).$$

Hence, $\varphi_{a_R,b_R,k}$ is supported on the rectangle $[a_R - 1, 2a_R + 1] \times [b_R - 1, 2b_R + 1]$. We now choose a_R and b_R such that they tend to infinity as $R \to \infty$ and such that the support of $\varphi_{a_R,b_R,k}$ excludes the diagonal $x = y$.

Regarding the norm we obtain

$$\|\varphi_{a_R,b_R,k}\|^2_{L^2(\mathbb{R}^2_+)} \geq a_R b_R/2\,,$$

for R large enough. A direct calculation then shows that, using a shorthand notation,

$$\begin{aligned}(\partial_{xx}\varphi_{a_R,b_R,k})(x,y) = &-k^2\tau(\cdot)\tau(\cdot)e^{ik(x+y)}\tau(\cdot)\tau(\cdot) + \tau''(\cdot)\tau(\cdot)e^{ik(x+y)}\tau(\cdot)\tau(\cdot) \\ &+ 2ik\tau'(\cdot)\tau(\cdot)e^{ik(x+y)}\tau(\cdot)\tau(\cdot) - 2ik\tau(\cdot)\tau(\cdot)e^{ik(x+y)}\tau'(\cdot)\tau(\cdot) \\ &- 2\tau'(\cdot)\tau(\cdot)e^{ik(x+y)}\tau'(\cdot)\tau(\cdot) + \tau(\cdot)\tau(\cdot)e^{ik(x+y)}\tau''(\cdot)\tau(\cdot)\,.\end{aligned}$$

A similar expression is obtained for $\partial_{yy}\varphi_{a_R,b_R,k}$. Since the derivatives of τ appearing are bounded and non-zero only over a interval of length one, we directly obtain

$$\frac{\|-\Delta\varphi_{a_R,b_R,k} - 2k^2\varphi_{a_R,b_R,k}\|^2_{L^2(\mathbb{R}^2_+)}}{\|\varphi_{a_R,b_R,k}\|^2_{L^2(\mathbb{R}^2_+)}} \to 0\,,$$

as $R \to \infty$. This proves that $2k^2 \in \sigma_{ess}(-\Delta_{\sigma,\alpha}^{d=\infty})$ and hence the statement.

The second part of the statement is proved via a bracketing argument. In a first step one writes $\mathbb{R}^2_+ = B_R(\mathbb{R}^2_+) \cup (\mathbb{R}^2_+ \setminus B_R(\mathbb{R}^2_+))$ where $B_R(\mathbb{R}^2_+) := \{(x, y) \in \mathbb{R}^2_+ : x^2 + y^2 < R^2\}$ and introduces the comparison operator

$$-\Delta_{B_R(\mathbb{R}^2_+)} \oplus -\Delta_{\mathbb{R}^2_+ \setminus B_R(\mathbb{R}^2_+)} \tag{6.4}$$

which is a direct sum of two two-dimensional Laplacians with the same boundary conditions as $-\Delta^{d=\infty}_{\sigma,\alpha}$, except for additional Neumann boundary conditions along the dissecting line. The first Laplacian in (6.4) has purely discrete spectrum only and hence does not contribute to the essential spectrum. Furthermore, for any $\varphi \in H^1(\mathbb{R}^2_+)$ one has the estimates

$$\left| \int_R^\infty \sigma(y) |\gamma(\varphi)|^2 \mathrm{d}y \right| \leq \|\sigma \chi_{[R,\infty)}]\|_\infty \left(c_1 \|\nabla \varphi\|^2_{L^2(\mathbb{R}^2_+)} + c_2 \|\varphi\|^2_{L^2(\mathbb{R}^2_+)} \right)$$

and

$$\left| \int_R^\infty \alpha(y) |\varphi(y, y)|^2 \mathrm{d}y \right| \leq \|\alpha \chi_{[R,\infty)}]\|_\infty \left(c_1 \|\nabla \varphi\|^2_{L^2(\mathbb{R}^2_+)} + c_2 \|\varphi\|^2_{L^2(\mathbb{R}^2_+)} \right)$$

for some constants $0 < c_1 < 1$ and $c_2 > 0$; e.g., see [BK13b, BK13c]. Hence, with $\mathbb{1}$ denoting the identity operator, we obtain

$$-\Delta_{\mathbb{R}^2_+ \setminus B_R(\mathbb{R}^2_+)} \geq -c_2 \left(\|\sigma \chi_{[R,\infty)}]\|_\infty + \|\alpha \chi_{[R,\infty)}]\|_\infty \right) \cdot \mathbb{1}$$

and since $R > 0$ can be chosen arbitrarily, we conclude that $\inf \sigma_{ess}(-\Delta^{d=\infty}_{\sigma,\alpha}) = 0$. □

The discrete part of the spectrum, i.e., isolated eigenvalues with finite multiplicity, is characterised in the following statement.

Theorem 6.3 *Assume that* $\sigma, \alpha \in L^1(\mathbb{R}_+) \cap L^\infty(\mathbb{R}_+)$ *and that* $\inf \sigma_{ess}(-\Delta^{d=\infty}_{\sigma,\alpha}) = 0$. *Then, if*

$$\int_{\mathbb{R}_+} [2\sigma(y) - \alpha(y)] \, \mathrm{d}y > 0 \,, \tag{6.5}$$

negative eigenvalues will exist.

Proof As in the proof of [Theorem 3.3, [KM16]] one picks the test function $\varphi_\varepsilon(r) := e^{-r^\varepsilon}$, $\varepsilon > 0$, defined in polar coordinates. Evaluating $q^\infty_{\alpha,\sigma}[\varphi_\varepsilon]$ one performs the limit $\varepsilon \to 0$ to conclude that $q^\infty_{\alpha,\sigma}[\varphi_\varepsilon] < 0$ for small enough ε. The statement then follows by the variational principle [BHE08]. Note that the factor of 2 is due to the fact the there are two boundary segments of $\mathbb{R}^2_+$. □

Lemma 6.4 *Assume that* $\sigma, \alpha \in L^\infty(\mathbb{R}_+)$ *have bounded support. Then there exist only finitely many negative eigenvalues.*

Proof The statement follows from a bracketing argument, see [BHE08] for a general discussion and [KM16, KM17] for applications of this technique.

In a first step one writes $\mathbb{R}^2_+ = B_R(\mathbb{R}^2_+) \cup (\mathbb{R}^2_+ \setminus B_R(\mathbb{R}^2_+))$ where $B_R(\mathbb{R}^2_+) := \{(x, y) \in \mathbb{R}^2_+ : x^2 + y^2 < R^2\}$. The comparison operator then is a direct sum of two two-dimensional Laplacians, i.e.,

$$-\Delta_{B_R(\mathbb{R}^2_+)} \oplus -\Delta_{\mathbb{R}^2_+ \setminus B_R(\mathbb{R}^2_+)} \tag{6.6}$$

with the same boundary conditions as $-\Delta^{d=\infty}_{\sigma,\alpha}$, except for additional Neumann boundary conditions along the dissecting line. We then choose R large enough so that $\sigma = \alpha = 0$ in $\mathbb{R}^2_+ \setminus B_R(\mathbb{R}^2_+)$. Accordingly, $-\Delta_{\mathbb{R}^2_+ \setminus B_R(\mathbb{R}^2_+)}$ is a positive operator. On the other hand, $-\Delta_{B_R(\mathbb{R}^2_+)}$ is defined on a bounded Lipschitz domain and hence has purely discrete spectrum, i.e., its essential spectrum is empty and there are only finitely many negative eigenvalues. Consequently, the operator bracketing

$$-\Delta_{B_R(\mathbb{R}^2_+)} \oplus -\Delta_{\mathbb{R}^2_+ \setminus B_R(\mathbb{R}^2_+)} \leq -\Delta^{d=\infty}_{\sigma,\alpha} \tag{6.7}$$

implies the statement. □

6.2 The Model with a Hard-Wall Binding Potential

The model with non-vanishing binding potential, but vanishing contact interaction, was first studied in [KM17]. The first important difference to the case where $v_b \equiv 0$ is that the two-particle configuration space is reduced from $\mathbb{R}^2_+$ to the 'pencil-shaped' domain

$$\Omega := \{(x, y) \in \mathbb{R}^2_+ : |x - y| < d\} . \tag{6.8}$$

Hence, the underlying Hilbert space is $L^2(\Omega)$ rather than $L^2(\mathbb{R}^2_+)$. As before, a rigorous realisation of (6.1) is obtained via the form

$$q^d_{\alpha,\sigma}[\varphi] := \int_\Omega |\nabla\varphi|^2 \, \mathrm{d}x - \int_0^d \sigma(y)|\gamma(\varphi)|^2 \mathrm{d}y + \int_0^\infty \alpha(y)|\varphi(y, y)|^2 \, \mathrm{d}y \, , \tag{6.9}$$

which is defined on $\mathcal{D}_q := \{\varphi \in H^1(\Omega) : \varphi|_{\partial\Omega_D} = 0\}$, where $\partial\Omega_D := \{(x, y) \in \mathbb{R}^2_+ : |x - y| = d\}$. Note that the Dirichlet boundary conditions along $\partial\Omega_D$ are due to the choice of the hard-wall binding potential.

Theorem 6.5 *For every $\sigma, \alpha \in L^\infty(\mathbb{R}_+)$ the form $\left(q^d_{\alpha,\sigma}, \mathcal{D}_q\right)$ is bounded from below and is closed.*

As before, the representation theorem of forms assures the existence of a unique self-adjoint operator associated with $q^d_{\alpha,\sigma}$ which shall be denoted by $-\Delta^d_{\sigma,\alpha}$. Again, this operator acts as the standard two-dimensional Laplacian with coordinate dependent Robin boundary conditions along the boundary segments with $x = 0$ or $y = 0$ as well as a jump condition along the diagonal $x = y$ as before, see [Remark 1, [KM17]] for a more details.

So far the presence of a binding potential made no difference. However, as soon as we characterise the spectrum of $-\Delta^d_{\sigma,\alpha}$, the effect of the binding potential becomes obvious.

Theorem 6.6 *Assume that $\sigma, \alpha \in L^\infty(\mathbb{R}_+)$ are given. Then $[2\pi^2/d^2, \infty) \subset \sigma_{ess}(-\Delta^d_{\sigma,\alpha})$. Furthermore, if $\alpha(y) \to 0$ as $y \to \infty$ one has $\sigma_{ess}(-\Delta^d_{\sigma,\alpha}) = [\pi^2/2d^2, \infty)$.*

Proof We only add some remarks, see [Theorem 2, [KM17]] and the proof of Theorem 6.2 for more details. We also note that the first part readily follows from the proof of second part as presented below.

In a first step we note that we can equivalently consider the Laplacian on the domain $\widetilde{\Omega}$ that is obtained from Ω by a clockwise rotation about an angle $\pi/4$. On this domain we consider the Weyl sequence, $R > 0$ large enough and $k \in [0, \infty)$,

$$\varphi_{R,k}(x, y) := \psi_0(y)\tau\left(x - (R-1)\right) e^{ikx}\tau\left((2R+1) - x\right) ,$$

where $\tau : \mathbb{R} \to \mathbb{R}$ is a smooth function with $\tau(x) = 0$ for $x \leq 0$, $\tau(x) = 1$ for $x \geq 1$ and $\tau(x) \geq 0$ otherwise. Furthermore, ψ_0 is the ground state of the one-dimensional Dirichlet-Laplacian on the interval $[-d/\sqrt{2}, +d/\sqrt{2}]$.

One has $\|\varphi_{R,k}\|^2_{L^2(\widetilde{\Omega})} > R/2$ for R large enough. Furthermore, using a shorthand notation, we calculate

$$\begin{aligned}
-\Delta\varphi_{R,k} &= -\partial_{xx}\varphi_{R,k} + \frac{\pi^2}{2d^2}\varphi_{R,k} \\
&= \psi_0(y)(-k^2\tau(\cdot)e^{ikx}\tau(\cdot) + \tau''(\cdot)e^{ikx}\tau(\cdot) + \tau(\cdot)e^{ikx}\tau''(\cdot) + 2ik\tau'(\cdot)e^{ikx}\tau(\cdot) \\
&\quad - 2\tau'(\cdot)e^{ikx}\tau'(\cdot) - 2ik\tau(\cdot)e^{ikx}\tau'(\cdot)) + \frac{\pi^2}{2d^2}\varphi_{R,k} .
\end{aligned}$$

Hence,

$$\frac{\| - \Delta\varphi_{R,k} - \left(k^2 + \frac{\pi^2}{2d^2}\right)\varphi_{R,k}\|^2_{L^2(\widetilde{\Omega})}}{\|\varphi_{R,k}\|^2_{L^2(\widetilde{\Omega})}} \to 0$$

as $R \to \infty$. Consequently, for any $\psi \in H^1(\widetilde{\Omega})$ that fulfils Dirichlet boundary conditions along the corresponding line segments and R large enough,

$$\begin{aligned} s(\varphi_{R,k}, \psi) &= \int_{\widetilde{\Omega}} \overline{\nabla \varphi_{R,k}}(x) \nabla \psi(x) \, \mathrm{d}x + \frac{1}{\sqrt{2}} \int_{R-1}^{\infty} \alpha(x) \overline{\varphi_{R,k}}(x,0) \psi(x,0) \, \mathrm{d}x \\ &= -\int_{\widetilde{\Omega}} \overline{\Delta \varphi_{R,k}}(x) \psi(x) \, \mathrm{d}x + \frac{1}{\sqrt{2}} \int_{R-1}^{\infty} \alpha(x) \overline{\varphi_{R,k}}(x,0) \psi(x,0) \, \mathrm{d}x \, , \end{aligned}$$

using an integration by parts. Note that $s(\cdot, \cdot)$ denotes the sesquilinear form associated with the rotated version of the quadratic form. Using the estimate, with some constant $c > 0$,

$$\left| \int_{R-1}^{\infty} \alpha(x) \overline{\varphi_{R,k}}(x,0) \psi(x,0) \, \mathrm{d}x \right| \leq c \|\alpha \chi_{[R-1,\infty)}\|_{\infty} \|\varphi_{R,k}\|_{H^1(\widetilde{\Omega})} \|\psi\|_{H^1(\widetilde{\Omega})}$$

we conclude that

$$\sup_{\psi} \left| s\left(\frac{\varphi_{R,k}}{\|\varphi_{R,k}\|_{L^2(\widetilde{\Omega})}}, \psi \right) - \left(k^2 + \frac{\pi^2}{2d^2} \right) \left\langle \frac{\varphi_{R,k}}{\|\varphi_{R,k}\|_{L^2(\widetilde{\Omega})}}, \psi \right\rangle_{L^2(\widetilde{\Omega})} \right| \to 0 \, ,$$

as $R \to \infty$ by Hölder's inequality. Note here that the supremum is taken over all functions in the form domain with form norm smaller or equal to one, see [Proposition 5.1, [PS12]]. This shows that $k^2 + \frac{\pi^2}{2d^2} \in \sigma_{ess}(-\Delta^d_{\sigma,\alpha})$ for any $k \in [0, \infty)$. □

Theorem 6.6 illustrates that, as long as the contact interaction strength converges to zero, the binding potential leads to a shift of the essential spectrum by at least $\pi^2/2d^2$. As for the effect on the discrete spectrum we first note that whenever $d = \infty$, by Theorem 6.2 this is trivial for $\sigma = \alpha = 0$. From a physical point of view this seems reasonable since there is no attractive potentials that could lead to bound states. However, quite surprisingly, for $d < \infty$ and $\sigma = \alpha = 0$ we have the following result [Theorem 3, [KM17]].

Theorem 6.7 *Consider the self-adjoint operator $-\Delta^d_{\sigma=0,\alpha=0}$, i.e., we assume that $\sigma = \alpha = 0$. Then*

$$\sigma_d(-\Delta^d_{\sigma=0,\alpha=0}) \neq \emptyset \, . \tag{6.10}$$

In other words, there exist eigenvalues below $\pi^2/2d^2$.

Note that the existence of eigenvalues smaller than $\pi^2/2d^2$ for vanishing boundary and contact potential is a purely quantum mechanical effect. Furthermore, it is a geometrical effect since no non-trivial discrete spectrum would exist if one considered the two-particle system on the full line $\mathbb{R}$ instead of the half-line $\mathbb{R}_+$, see [Remark 4, [KM17]].

Of course, if one assumes that $\sigma(y) \geq 0$ for a.e. $y \in [0, d]$, and $\alpha(y) \leq 0$ for a.e. $y \in [0, \infty)$, the discrete spectrum will also be non-empty since the boundary integrals in $q^d_{\alpha,\sigma}$ are negative (note here the minus sign in the definition of the boundary potential σ). However, one may ask what happens when a positive boundary potential σ becomes large. Since this implies a strong repulsive singular two-particle interaction localised at the origin, bound states may no longer exist. Indeed, we have the following result.

Theorem 6.8 *There exists a constant $\gamma < 0$ such that $\sigma_d(-\Delta^d_{\sigma,\alpha}) = \emptyset$ whenever $\sigma(y) \leq \gamma$ for a.e. $y \in [0, d]$, $\alpha(y) \geq 0$ for a.e. $y \in [0, \infty)$ and $\alpha(y) \to 0$ as $y \to \infty$.*

Proof Without contact potential α this result has been shown in [Theorem 4, [KM17]].

Now, by Theorem 6.6 we conclude that $\inf \sigma_{ess}(-\Delta^d_{\sigma,\alpha}) = \pi^2/2d^2$. Furthermore, since α is assumed to be strictly positive, the corresponding operator is larger (in the sense of an operator bracketing) than the operator with same boundary potential σ, but without contact potential. Consequently, if there existed an eigenvalue smaller than $\pi^2/2d^2$ the same would hold for the operator without contact potential. This, however, is in contradiction with [Theorem 4, [KM17]].

□

Theorem 6.8 shows that strong singular interactions at the origin (without contact interaction) destabilise the system in the sense that no discrete spectrum is present anymore when compared to the free system with $\sigma = \alpha = 0$.

6.3 Random Singular Pair Interactions

In this subsection we consider a generalisation of the Hamiltonian (6.1) in the sense that the singular, vertex-induced pair interactions are not only present in the origin or the vertex of the graph. This seems desirable since, as described previously, localised two-particle interactions can be associated with defects in the metal and such defects occur, of course, not only at the origin but everywhere in the wire. We note that this model was formulated in [Kera] to which we also refer for more detail.

Since the spatial positions of defects in a real metal varies from metal to metal it seems reasonable not to work with a specific (deterministic) two-particle Hamiltonian, but with a random one. In other words, in this section we enter the realm of random Schrödinger operators which have become an important research area [Sto01, Kir08]. Most importantly, using the language of random Schrödinger operators, one has been able to give a rigorous description of various phenomena in physics such as Anderson localisation [And58, CFKS87].

Turning to our model, we consider a system of two particles on the half-line $\mathbb{R}_+$ whose random Hamiltonian shall formally be given by

$$H_\omega = -\frac{\partial^2}{\partial x^2} - \frac{\partial^2}{\partial y^2} + v_b(|x-y|) + \sum_{i=1}^{\infty} v_i(x,y)\left[\delta(x-a_i(\omega)) + \delta(y-a_i(\omega))\right] , \tag{6.11}$$

where $(a_i(\omega))_{i\in\mathbb{N}}$ are the random positions of the defects, called atoms in the sequel. As before we assume that $(v_i)_{i\in\mathbb{N}}$ are real-valued, bounded and symmetric, $v_i(x,y) = v_i(y,x)$. Furthermore, we define $l_i(\omega) := a_i(\omega) - a_{i-1}(\omega)$ for $i \geq 1$ and set $a_0(\omega) := 0$. In other words, $l_i(\omega)$ is the random distance between the $i-1$-st and the i-th atom.

Now we consider the lengths $(l_i(\omega))_{i\in\mathbb{N}}$ as a family of independent random variables over some probability space $(\Pi, \xi, \mathbb{P})$ generated by a Poisson process, see [Sto95] for more detail. More explicitly, we assume that the probability for the length $l_i(\omega)$ to be in the interval $[a,b]$ is given by

$$\mathbb{P}[l_i \in [a,b]] = \nu \int_a^b \mathrm{e}^{-\nu l}\mathrm{d}l , \tag{6.12}$$

with $\nu > 0$ denoting the Poisson density.

Again, due to the presence of δ-potentials in (6.11) we shall use a suitable quadratic form to rigorously construct a self-adjoint operator that is associated with the formal expression (6.11). We introduce

$$q_\omega[\varphi] = \int_\Omega |\nabla\varphi|^2 \,\mathrm{d}x + \sum_{i=1}^{\infty} \int_{\Gamma_i(\omega)} \sigma_i(y)|\gamma_i(\varphi)|^2 \,\mathrm{d}y , \tag{6.13}$$

where $\gamma_i(\varphi)$ denotes the restriction (in the sense of traces of Sobolev functions) to

$$\Gamma_i(\omega) := \{(x,y) \in \Omega : x = a_i(\omega) \text{ or } y = a_i(\omega)\} . \tag{6.14}$$

Furthermore, we set $\sigma_i(y) := -v_i(0,y)$. Due to the infinite sum appearing in (6.13) it may not be possible to define q_ω on all $H^1(\Omega)$. Since we want to find a closed realisation of the form q_ω we have to guess a suitable sub-domain. Indeed, one has the following result [Theorem 2.1, [Kera]].

Theorem 6.9 *Let $(\sigma_i(\omega))_{i\in\mathbb{N}} \subset L^\infty(\mathbb{R}_+)$ be given. Then the form q_ω on the domain*

$$\mathcal{D}_q(\omega) = \{\varphi \in H^1(\Omega) : q_\omega[\varphi] < \infty\} \tag{6.15}$$

is positive and closed for almost every $\omega \in \Pi$.

We denote the unique self-adjoint operator associated with the form q_ω as $-\Delta_\sigma(\omega)$.

The random Schrödinger operators usually considered in the literature have an astonishing property, namely that the spectrum is almost surely non-random [PF92, Kir08], which is due to a certain ergodicity property of the models. For our model, we will see that only the essential part of the spectrum is non-random. The discrete part, however, is random. Indeed we have the following results [Theorem 3.1, Lemma 3.4, Theorem 3.5 [Kera]].

Theorem 6.10 *Let* $(\sigma_i(\omega))_{i\in\mathbb{N}} \subset L^\infty(\mathbb{R}_+)$ *be given. Then*

$$\sigma_{ess}(-\Delta_\sigma(\omega)) = [\pi^2/2d^2, \infty) \tag{6.16}$$

almost surely.

The discrete part of the spectrum, on the other hand, is random. More explicitly, we obtain the following result.

Theorem 6.11 *Let* $(\sigma_i(\omega))_{i\in\mathbb{N}} \subset L^\infty(\mathbb{R}_+)$ *be given. Then*

$$\mathbb{P}[\sigma_d(-\Delta_\sigma(\omega)) \neq \emptyset] > 0\,. \tag{6.17}$$

Furthermore, there exists a constant $\gamma = \gamma(d) > 0$ *such that if* $\inf\sigma_k > \gamma$ *for one* $k \in \mathbb{N}$ *then*

$$\mathbb{P}[\sigma_d(-\Delta_\sigma(\omega)) = \emptyset] > 0\,. \tag{6.18}$$

Theorem 6.11 tells us that the discrete part of the spectrum is destroyed with finite probability as well as conserved with finite probability. This leads to an interesting physical implication: In general, disorder is associated with a suppression of transport as in the Anderson localisation phenomenon due to the presence of a dense pure point spectrum. In the above model, however, disorder may lead to an improvement of transport through the destruction of the discrete part of the spectrum. Indeed, according to 'Fermi's golden rule' the transition rate of going from one state to another depends on the density of final states. Hence, if no discrete spectrum is present, a transition is possible also for small excitation energies since there does not exist a finite energy gap in the spectrum.

6.4 The Condensation of Electron Pairs in a Quantum Wire

In this subsection we want to report on the results that were obtained in [Kerb, Kerc, Ker18]. Since we are interested in pairs of particles, we consider the case where $d < \infty$, i.e., we assume that a hard-wall binding potential v_b is present. In the previous sections we worked on the full Hilbert space $L^2(\Omega)$ describing two distinguishable and spinless particles. However, since we are interested in applying the Hamiltonian (6.1) to understand phenomena related to superconductivity, and

which involves electrons, we need to implement the exchange symmetry of identical particles.

In this review we restrict ourselves to the case considered in [Kerb] where the two electrons are assumed to have the same spin. This leads to the requirement that the two-particle wave function has to be anti-symmetric. The case of opposite spin, which is realised in actual Cooper pairs, is considered in [Ker18]. We only mention here that the results regarding the condensation there are comparable.

In order to ensure anti-symmetry of the wave function we work in the anti-symmetric subspace

$$L^2_a(\Omega) := \{\varphi \in L^2(\Omega) : \ \varphi(x, y) = -\varphi(y, x)\} . \tag{6.19}$$

We then introduce the quadratic form

$$q^d_\sigma[\varphi] := \frac{\hbar^2}{2m_e} \int_\Omega |\nabla\varphi|^2 \, \mathrm{d}x - \int_0^d \sigma(y)|\gamma(\varphi)|^2 \mathrm{d}y , \tag{6.20}$$

where $\sigma \in L^\infty(\mathbb{R}_+)$, on this subspace. Here we added physical constants with m_e denoting the electron mass. The domain of the form is given by $\mathcal{D}_q := \{\varphi \in H^1(\Omega) \cap L^2_a(\Omega) : \ \varphi|_{\partial\Omega_D} = 0$ and $\varphi(x, x) = 0\}$. Again, this form is closed and bounded from below, and hence there exists a unique self-adjoint operator associated with this form. This is the Hamiltonian of our two-particle system. We denote this operator, which again acts as the standard two-dimensional Laplacian, as $-\Delta^d_\sigma$.

Theorem 6.12 ([Kerb]) *One has*

$$\sigma_{ess}(-\Delta^d_\sigma) = [\hbar^2\pi^2/m_e d^2, \infty) . \tag{6.21}$$

Furthermore, if $\sigma = 0$ *then*

$$\sigma_d(-\Delta^d_{\sigma=0}) = \{E_0\} , \tag{6.22}$$

i.e., there is exactly one eigenvalue with multiplicity one below the bottom of the essential spectrum. In addition, one has

$$0.25 \cdot \frac{\hbar^2\pi^2}{m_e d^2} \leq E_0 \leq 0.93 \cdot \frac{\hbar^2\pi^2}{m_e d^2} . \tag{6.23}$$

Theorem 6.12 has an interesting physical consequence: one important measurable quantity associated with the superconducting phase of a metal is the so-called spectral gap $\Delta > 0$, see [MR04a]. This spectral gap is responsible, for example, for the exponential decay of the specific heat at temperatures lower than the critical one. It is one of the successes of the BCS-theory that the spectral gap can be interpreted as the binding energy of a single Cooper pair. In other words, the spectral gap measures the energy necessary to break up one Cooper pair. Due to the choice of the hard-wall

binding potential, in our model the pair cannot be broken up. However, it is possible to excite a pair. Since, as we will see later, the pairs condense into the ground state it seems reasonable to identify the spectral gap as the excitation of a pair from the ground state to the first excited states. In other words, in our model one obtains the relation

$$\Delta = \Delta(d) \sim \frac{\hbar^2 \pi^2}{m_e d^2} \tag{6.24}$$

for the spectral gap. This relation establishes a direct link between the spatial extension of a pair and the spectral gap. In particular, since the spectral gap in superconducting metals is of order 10^{-3} eV [MR04a], the relation (6.24) implies that d is of the order 10^{-6} m. Interestingly, this agrees with Cooper's estimate as presented in [Coo56].

In order to study the condensation phenomenon (similar to BEC as in Sect. 4) of electron pairs one has to employ methods from quantum statistical mechanics (see, e.g., [Sch06]). In particular, one has to perform a thermodynamic limit as in Sect. 4, and this requires to restrict the system from the half-line to the interval $(0, L)$. The underlying Hilbert space then is $L^2_a(\Omega_L)$, with

$$\Omega_L := \{(x, y) \in \Omega : 0 < x, y < L\} . \tag{6.25}$$

The natural generalisation of (6.20) is defined on the domain $\mathcal{D}_{q_L} := \{\varphi \in H^1(\Omega_L) \cap L^2_a(\Omega_L) : \varphi|_{\partial\Omega_{L,D}} = 0 \text{ and } \varphi(x, x) = 0\}$ with $\partial\Omega_{L,D} := \{(x, y) \in \partial\Omega_L : |x - y| = d \text{ or } x = L \text{ or } y = L\}$. In other words, one introduces additional Dirichlet boundary conditions along the dissecting lines $x = L$ and $y = L$. We denote the associated self-adjoint operator by $-\Delta^d_{\sigma,L}$.

Since Ω_L is a bounded Lipschitz domain, $-\Delta^d_{\sigma,L}$ has purely discrete spectrum. We denote its corresponding eigenvalues, counted with multiplicity, by $\{E^\sigma_n(L)\}_{n\in\mathbb{N}_0}$.

Lemma 6.13 *Assume that $\sigma = 0$. Then*

$$\lim_{L\to\infty} E^{\sigma=0}_0(L) = E_0 . \tag{6.26}$$

Furthermore, $E^{\sigma=0}_n(L) \geq \frac{\hbar^2\pi^2}{m_e d^2}$ for all $n \geq 1$ and $L > d$.

Lemma 6.13 implies the existence of a finite spectral gap in the thermodynamic limit which eventually is responsible for the condensation of the pairs.

Recalling Definition 4.2, we can now establish the main result of this section.

Theorem 6.14 *For $\sigma = 0$ there exists a critical density $\rho_{crit}(\beta)$ such that the ground state is macroscopically occupied in the thermodynamic limit for all pair densities $\rho > \rho_{crit}(\beta)$. Furthermore, there exists a constant $\gamma < 0$ such that, for all pair densities $\rho > 0$, no eigenstate is macroscopically occupied if $\|\sigma\|_\infty < \gamma$.*

Proof For the proof see the proofs of [Theorems 3.3 and 3.6, [Kerb]] as well as [Theorem 4.4, [Ker18]]. □

Theorem 6.14 shows that the pairs condense in the quantum wire given that there are no repulsive singular two-particle interactions localised at the origin. However, if the singular interactions are strong enough, the condensate in the ground state will be destroyed. Hence, if one identifies a 'superconducting phase' with the presence of a condensate of pairs (here in an eigenstate for non-interacting pairs), Theorem 6.14 shows that a superconducting phase in a quantum wire can be destroyed by singular two-particle interactions.

6.5 *The Impact of Surface Defects on a Condensate of Electrons*

In this final section we report on yet another application of the two-particle model introduced above which was presented in [Kerc]. More explicitly, we extend the model characterised by the form (6.20) and the associated Hamiltonian $-\Delta_\sigma^d$ defined on the anti-symmetric Hilbert space $L_a^2(\Omega)$. However, we will only consider the case where there are no singular, vertex-induced two-particle interactions at the origin, i.e., we set $\sigma = 0$.

In Sect. 6.4 we investigated the (Bose-Einstein) condensation of pairs of electrons. Theorem 6.14 shows that the pairs condense into the ground state if no singular interactions are present and given the pair density $\rho > 0$ is large enough. Also, the presence of condensation is paramount for the existence of the superconducting phase. Real metals are never perfect and there exist defects that affect the behaviour of electrons in the bulk. However, besides defects in the bulk, a real metal will also exhibit defects on the surface, i.e., a real surface will not be arbitrarily smooth. Note that the existence of a surface is, to a first approximation, not taken into account in most discussions in solid state physics, since the solid is modelled to be infinitely extended in order to conserve periodicity. However, it has also long become clear that surface effects cannot be neglected altogether [FS04]. It is the aim of this section to introduce a model to investigate the effect of surface defects on a condensate of electron pairs as described in the previous section.

In order to take surface defects into account we have to extend our Hilbert space. More explicitly, we set

$$\mathcal{H} := L_a^2(\Omega) \oplus \ell^2(\mathbb{N}) , \tag{6.27}$$

where $\ell^2(\mathbb{N})$ is the space of square-summable sequences. Consequently, a given pair of electrons is described by a state of the form $(\varphi, f)^T$, with $\varphi \in L_a^2(\Omega)$ and $f \in \ell^2(\mathbb{N})$. This means that we model the surface defects as the vertices of the discrete graph $\mathbb{N}$, which seems reasonable in a regime where the spatial extension of those defects is small compared to the bulk.

The Hamiltonian of a free pair of electrons on $\mathcal{H}$ is given by

$$H_p := -\Delta^d_{\sigma=0} \oplus \mathcal{L}(\gamma) \,, \tag{6.28}$$

where $\mathcal{L}(\gamma)$ is the (weighted) discrete Laplacian acting via

$$(\mathcal{L}(\gamma) f)(n) = \sum_{m=1}^{\infty} \gamma_{mn} \left(f(m) - f(n) \right) \,, \tag{6.29}$$

with $(\gamma)_{mn} =: \gamma_{mn} = \delta_{|n-m|,1} e_n$ for $n \geq m$, $\gamma = \gamma^T$, and $(e_n)_{n\in\mathbb{N}} \subset \mathbb{R}_+$.

Now, since we are interested in the condensation phenomenon we have to restrict the system to a finite volume as we have done in the previous section. More explicitly, the finite volume Hilbert space is given by

$$\mathcal{H}_L := L^2_a(\Omega_L) \oplus \mathbb{C}^{n(L)} \,, \tag{6.30}$$

where $n(L) \in \mathbb{N}$ denotes the number of surface defects in the interval $[0, L]$. On this Hilbert space one considers H^L_p, i.e., the restriction of H_p to the finite-volume Hilbert space $\mathcal{H}_L$. This operator has purely discrete spectrum and the eigenvalues are the union of those coming from $-\Delta^d_\sigma|_{L^2_a(\Omega_L)}$ (where this operator is defined as in the previous section) and $\mathcal{L}(\gamma)|_{\mathbb{C}^{n(L)}}$.

In order to formulate the model it is convenient to use the formalism of second quantisation [MR04a]. This means that one works on the Fock space over $\mathcal{H}_L$, rather than on $\mathcal{H}_L$ itself. The second quantisation of H^L_p is given by

$$\Gamma(H^L_p) = \sum_{n=0}^{\infty} E^{\sigma=0}_n(L) a^*_n a_n + \sum_{k=1}^{n(L)} \lambda_k(L) b^*_k b_k \,, \tag{6.31}$$

where $(E^{\sigma=0}_n(L))_{n\in\mathbb{N}_0}$ are the eigenvalues of $-\Delta^d_{\sigma=0}|_{L^2_a(\Omega_L)}$ and $(\lambda_k(L))_{k=1,\ldots,n(L)}$ are the eigenvalues of $\mathcal{L}(\gamma)|_{\mathbb{C}^{n(L)}}$, counted with multiplicity. Furthermore, (a^*_n, a_n) are the creation and annihilation operators of the states $\varphi_n \oplus 0$, where $\varphi_n \in L^2_a(\Omega_L)$ are the corresponding eigenstate of $-\Delta^d_{\sigma=0}|_{L^2_a(\Omega_L)}$. In contrast, (b^*_k, b_k) are the creation and annihilation operators of the states $0 \oplus f_n$, where $f_n \in \mathbb{C}^{n(L)}$ are the corresponding eigenstates of $\mathcal{L}(\gamma)|_{\mathbb{C}^{n(L)}}$. To obtain the full Hamiltonian of the model we extend the free Hamiltonian (6.31) and write

$$H_L(\rho_s, \alpha, \lambda) = \Gamma(H^L_p) - \alpha \sum_{k=1}^{n(L)} b^*_k b_k + \lambda \rho_s(\mu_L, L) \sum_{k=1}^{n(L)} b^*_k b_k \,, \tag{6.32}$$

where $\alpha \geq 0$ describes the surface tension; $\lambda \geq 0$ is an interaction strength associated with the repulsion of the pairs in the surface defects and $\rho_s(\mu_L, L)$ is the density of pairs on $\mathbb{C}^{n(L)}$, see the equation below. Note here that $\sum_{k=1}^{n(L)} b^*_k b_k$ is

the (surface-) number operator whose expectation value equals the number of pairs in the surface defects. Also, the third term in (6.32) is added to take into account repulsive interactions between electron pairs accumulating in the surface defects which are expected since the surface defects are imagined to be relatively small. The explicit form of this term follows from a simplification of standard mean-field considerations where the interaction term is generally of the form $\lambda \hat{N}^2/V$, where $\hat{N}$ is the number operator and V is the volume of the system. In other words, we have replaced $\hat{N}/V$ by the density $\rho_s(\mu_L, L)$ for which

$$\rho_s(\mu_L, L) := \frac{\omega_{\beta,\mu_L}^{H_L(\rho_s,\alpha,\lambda)}\left(\sum_{k=1}^{n(L)} b_k^* b_k\right)}{n(L)} \tag{6.33}$$

holds with $\omega_{\beta,\mu_L}^{H_L(\rho_s,\alpha,\lambda)}(\cdot)$ denoting the Gibbs state of the grand-canonical ensemble at inverse temperature $\beta = 1/T$ and chemical potential μ_L.

The advantage of the Hamiltonian $H(\rho_s, \alpha, \lambda)$ is that it can be rewritten as

$$H_L(\rho_s, \alpha, \lambda) = \sum_{n=0}^{\infty} E_n^{\sigma=0}(L) a_n^* a_n + \sum_{k=1}^{n(L)} \left(\lambda_k(L) + \lambda\rho_s(\mu_L, L) - \alpha\right) b_k^* b_k \,, \tag{6.34}$$

which yields an effective, non-interacting many-pair model with shifted eigenvalues for the discrete part. Note that, in particular, (6.34) implies $\mu_L < \min\{\lambda\rho_s(\mu_L, L) - \alpha, E_0(L)\}$, taking into account that $\lambda_1(L) = 0$.

The goal then is to investigate the macroscopic occupation of the ground state $\varphi_0 \oplus 0$ in a suitable thermodynamic limit (see [Kerc] for details) for the Hamiltonian (6.34). It turns out that a key quantity is the inverse density of surface defects $\delta > 0$ defined as

$$\delta := \lim_{L\to\infty} \frac{L}{n(L)} \,. \tag{6.35}$$

One obtains the following result.

Theorem 6.15 *If*

$$2\lambda \cdot \delta \cdot \rho < E_0 + \alpha \tag{6.36}$$

holds, no eigenstate $\varphi_n \oplus 0$ is macroscopically occupied in the thermodynamic limit. This means, in particular, that the condensate is destroyed for arbitrary pair densities whenever $\lambda = 0$.

Theorem 6.15 has the remarkable consequence that the condensation is destroyed for all pair densities $\rho > 0$ in the following cases: the pairs do not repel each other which allows them to accumulate in the surface defects or the number of surface defects is very large.

Finally, we obtain the following result.

Theorem 6.16 *Assume that* $\delta, \lambda > 0$. *Then there exists a critical pair density* $\rho_{crit} = \rho_{crit}(\beta, \delta, \alpha, \lambda) > 0$ *such that for all pair densities* $\rho > \rho_{crit}$ *the state* $\varphi_0 \oplus 0$ *is macroscopically occupied in the thermodynamic limit.*

Theorem 6.16 shows that the condensate can be recovered given the interaction strength $\lambda > 0$ is non-zero and, most importantly, given the number of surface impurities is not too large.

References

[Ale83] S. Alexander, *Superconductivity of networks. A percolation approach to the effects of disorder*, Phys. Rev. B **27** (1983), 1541–1557.

[And58] P. W. Anderson, *Absence of diffusion in certain random lattices*, Phys. Rev. **109** (1958), 1492–1505.

[Bő80] P.H. Bérard, *Spectres et groupes cristallographiques. I. Domaines euclidiens*, Invent. Math. **58** (1980), no. 2, 179–199.

[BCS57] J. Bardeen, L. N. Cooper, and J. R. Schrieffer, *Theory of superconductivity*, Phys. Rev. **108** (1957), 1175–1204.

[BE09] J. Bolte and S. Endres, *The trace formula for quantum graphs with general self-adjoint boundary conditions*, Ann. H. Poincare **10** (2009), 189–223.

[BEKS94] J. F. Brasche, P. Exner, Y. A. Kuperin, and P. Seba, *Schrödinger-operators with singular interactions*, Journal of Mathematical Analysis and Applications **184** (1994), no. 1, 112 – 139.

[BER15] J. Bolte, S. Egger, and R. Rueckriemen, *Heat-kernel and resolvent asymptotics for Schrödinger operators on metric graphs*, Appl. Math. Res. Express. AMRX (2015), no. 1, 129–165.

[BES15] J. Bolte, S. Egger, and F. Steiner, *Zero modes of quantum graph Laplacians and an index theorem*, Ann. H. Poincaré **16** (2015), no. 5, 1155–1189.

[Bet31] H. Bethe, *Zur Theorie der Metalle I.*, Z. Phys. **71** (1931), 205–226.

[BG17] J. Bolte and G. Garforth, *Exactly solvable interacting two-particle quantum graphs*, J. Phys. A: Math. Theo. **50** (2017), no. 10, 105101, 27.

[BG18] ——, *Solvable models of interacting n-particle systems on quantum graphs*, Mathematical problems in quantum physics, Contemp. Math., vol. 717, Amer. Math. Soc., Providence, RI, 2018, pp. 117–128.

[BHE08] J. Blank, M. Havliček, and P. Exner, *Hilbert space operators in quantum physics*, Springer Verlag, 2008.

[BK13a] G. Berkolaiko and P. Kuchment, *Introduction to quantum graphs*, American Mathematical Society, Providence, RI, 2013.

[BK13b] J. Bolte and J. Kerner, *Quantum graphs with singular two-particle interactions*, J. Phys. A: Math. Theo. **46** (2013), no. 4, 045206.

[BK13c] ——, *Quantum graphs with two-particle contact interactions*, J. Phys. A: Math. Theo. **46** (2013), no. 4, 045207.

[BK14] ——, *Many-particle quantum graphs and Bose-Einstein condensation*, Journal of Mathematical Physics **55** (2014), no. 6.

[BK16] J. Bolte and J. Kerner, *Instability of Bose-Einstein condensation into the one-particle ground state on quantum graphs under repulsive perturbations*, J. Math. Phys. **57** (2016), no. 4, 043301, 9.

[BL10] J. Behrndt and A. Luger, *On the number of negative eigenvalues of the Laplacian on a metric graph*, J. Phys. A: Math. Theo. **43** (2010), 1–10.

[BM06] B. Bellazzini and M. Mintchev, *Quantum fields on star graphs*, J. Phys. A: Math. Gen. **39** (2006), no. 35, 11101–11117.

[BMLL13] J. Behrndt, Matthias M. Langer, and V. Lotoreichik, *Schrödinger operators with δ and δ'-potentials supported on hypersurfaces*, Ann. H. Poincaré **14** (2013), no. 2, 385–423.

[Cau15] V. Caudrelier, *On the inverse scattering method for integrable PDEs on a star graph*, Comm. Math. Phys. **338** (2015), no. 2, 893–917.

[CC07] V. Caudrelier and N. Crampé, *Exact results for the one-dimensional many-body problem with contact interaction: including a tunable impurity*, Rev. Math. Phys. **19** (2007), no. 4, 349–370.

[CCG11] M.A. Cazalilla, R. Citro, T. Giamarchi, E. Orignac, and M. Rigol, *One dimensional bosons: From condensed matter systems to ultracold gases*, Rev. Mod. Phys. **83** (2011), no. 4, 1405.

[CFKS87] H. L. Cycon, R. G. Froese, W. Kirsch, and B. Simon, *Schrödinger operators with application to quantum mechanics and global geometry*, Texts and Monographs in Physics, Springer-Verlag, Berlin, 1987.

[Coo56] Leon N. Cooper, *Bound electron pairs in a degenerate Fermi gas*, Phys. Rev. **104** (1956), 1189–1190.

[dG81a] P. G. de Gennes, C. R. Acad, Sci. B **292** (1981), 279.

[dG81b] P. G. de Gennes, C. R. Acad. Sci. Ser. B **292** (1981), 9.

[Dob05] M. Dobrowolski, *Angewandte Funktionalanalysis: Funktionalanalysis, Sobolev-Räume und Elliptische Differentialgleichungen*, Springer-Verlag, Berlin, 2005.

[Ein25] A. Einstein, Sitzber. Kgl. Preuss. Akadm. Wiss. (1925), 3.

[EK17] S. Egger and J. Kerner, *Scattering properties of two singularly interacting particles on the half-line*, Rev. Math. Phys. **29** (2017), no. 10.

[EKK08] P. Exner, J. P. Keating, P. Kuchment, T. Sunada, and A. Teplyaev (eds.), *Analysis on graphs and its applications*, Proceedings of Symposia in Pure Mathematics, vol. 77, American Mathematical Society, Providence, RI, 2008.

[FS04] K. Fossheim and A. Sudboe, *Superconductivity: Physics and applications*, Wiley, 2004.

[Gau71] M. Gaudin, *Boundary energy of a Bose gase in one dimension*, Phys. Rev. A **4** (1971), 386–394.

[Gau14] ——, *The Bethe wavefunction*, Cambridge University Press, New York, 2014, Translated from the 1983 French original by Jean-Sébastien Caux.

[GG08] N. Goldman and P. Gaspard, *Quantum graphs and the integer quantum Hall effect*, Phys. Rev. B **77** (2008), 024302.

[Gir60] M. D. Girardeau, *Relationship between systems of impenetrable bosons and fermions in one dimension*, J. Math. Phys. **1** (1960), 516–523.

[Gla93] M. L. Glasser, *A solvable non-separable quantum two-body problem*, J. Phys. A: Math. Gen. **26** (1993), no. 17, L825.

[GN05] M. L. Glasser and L. M. Nieto, *Solvable quantum two-body problem: entanglement*, J. Phys. A: Math. Gen. **38** (2005), no. 24, L455.

[GS06] S. Gnutzmann and U. Smilansky, *Quantum graphs: Applications to quantum chaos and universal spectral statistics*, Taylor and Francis. Advances in Physics **55** (2006), 527–625.

[Gut90] M.C. Gutzwiller, *Chaos in classical and quantum mechanics*, Interdisciplinary Applied Mathematics, vol. 1, Springer-Verlag, New York, 1990.

[Har07] M. Harmer, *Two particles on a star graph, I*, Russian Journal of Mathematical Physics **14** (2007), 435–439.

[Har08] ——, *Two particles on a star graph, II*, Russian Journal of Mathematical Physics **15** (2008), 473–480.

[HKR11] J. M. Harrison, J. P. Keating, and J. M. Robbins, *Quantum statistics on graphs*, Proc. R. Soc. Lond. Ser. A Math. Phys. Eng. Sci. **467** (2011), no. 2125, 212–233.

[HKRS14] J. M. Harrison, J. P. Keating, J. M. Robbins, and A. Sawicki, *n-particle quantum statistics on graphs*, Comm. Math. Phys. **330** (2014), no. 3, 1293–1326.

[Hoh67] P. C. Hohenberg, *Existence of long-range order in one and two dimensions*, Phys. Rev. **158** (1967), 383–386.

[HV16] P. Harrison and A. Valavanis, *Quantum wells, wires and dots*, Wiley, 2016.

[Kat95] T. Kato, *Perturbation theory for linear operators*, Classics in Mathematics, Springer-Verlag, Berlin, 1995.

[Kera] J. Kerner, *A remark on the effect of random singular two-particle interactions*, Arch. Math. (Basel) **112** (2019), no. 6, 649–659.

[Kerb] J. Kerner, *On bound electron pairs on the half-line*, Rep. Math. Phys. **83** (2019), no. 1, 129–138.

[Kerc] J. Kerner, *Impact of surface defects on a condensate of electron pairs in a quantum wire*, Theor. Math. Phys. **203** (2020), no. 2, 691–699.

[Ker18] J. Kerner, *On pairs of interacting electrons in a quantum wire*, J. Math. Phys. **59** (2018), no. 6, 063504.

[Kir08] W. Kirsch, *An invitation to random Schrödinger operators*, Random Schrödinger operators, Panor. Synthèses, vol. 25, Soc. Math. France, Paris, 2008, pp. 1–119.

[KM16] J. Kerner and T. Mühlenbruch, *Two interacting particles on the half-line*, J. Math. Phys. **57** (2016), no. 2, 023509, 10. MR 3455670

[KM17] ——, *On a two-particle bound system on the half-line*, Rep. Math. Phys. **80** (2017), no. 2, 143–151.

[KN05] P. Kurasov and M. Nowaczyk, *Inverse spectral problem for quantum graphs*, J. Phys. A: Math. Gen. **38** (2005), no. 22, 4901.

[KS99a] V. Kostrykin and R. Schrader, *Kirchhoff's rule for quantum wires*, J. Phys. A: Math. Gen. **32** (1999), 595–630.

[KS99b] T. Kottos and U. Smilansky, *Periodic orbit theory and spectral statistics for quantum graphs*, Ann. Phys. (NY) **274** (1999), 76–124.

[KS06] V. Kostrykin and R. Schrader, *Laplacians on metric graphs: Eigenvalues, resolvents and semigroups*, Contemporary Mathematics **415** (2006), 201–225.

[Kuc04] P. Kuchment, *Quantum graphs. I. Some basic structures*, Waves Random Media **14** (2004), S107–S128.

[LL63] E. Lieb and W. Liniger, *Exact analysis of an interacting Bose gas. I. The general solution and the ground state*, Phys. Rev. **130** (1963), 1605–1616.

[LM77] J.M. Leinaas and J. Myrheim, *On the theory of identical particles*, Il Nouvo Cimento B **37** (1977), no. 1, 1–23.

[LS02] E. H. Lieb and R. Seiringer, *Proof of Bose-Einstein condensation for dilute trapped gases*, Phys. Rev. Lett. **88** (2002), 170409.

[LVZ03] J. Lauwers, A. Verbeure, and V.A. Zagrebnov, *Proof of Bose-Einstein condensation for interacting gases with a one-particle gap*, J. Phys. A: Math. Gen. **36** (2003), 169–174.

[LW79] L. J. Landau and I. F. Wilde, *On the Bose-Einstein condensation of an ideal gas*, Comm. Math. Phys. **70** (1979), no. 1, 43–51.

[McG64] J. B. McGuire, *Study of exactly soluble one-dimensional N-body problems*, J. Math. Phys. **5** (1964), 622–636.

[MP95] Yu. B. Melnikov and B. S. Pavlov, *Two-body scattering on a graph and application to simple nanoelectronic devices*, J. Math. Phys. **36** (1995), 2813–2825.

[MR04a] P. A. Martin and F. Rothen, *Many-Body Problems and Quantum Field Theory*, Springer Verlag, Berlin-Heidelberg, 2004.

[MR04b] M. Mintchev and E. Ragoucy, *Interplay between Zamolodchikov-Faddeev and reflection-transmission algebras*, J. Phys. A: Math. Gen. **37** (2004), no. 2, 425–431, Special issue on recent advances in the theory of quantum integrable systems.

[MS17] T. Maciążek and A. Sawicki, *Homology groups for particles on one-connected graphs*, J. Math. Phys. **58** (2017), no. 6, 062103.

[Noj14] D. Noja, *Nonlinear Schrödinger equation on graphs: recent results and open problems*, Philos. Trans. R. Soc. Lond. Ser. A Math. Phys. Eng. Sci. **372** (2014), no. 2007, 20130002, 20.

[PF92] L. Pastur and A. Figotin, *Spectra of random and almost-periodic operators*, Grundlehren der Mathematischen Wissenschaften, vol. 297, Springer-Verlag, Berlin, 1992.

[PO56] O. Penrose and L. Onsager, *Bose-Einstein condensation and liquid helium*, Phys. Rev. **104** (1956), 576–584.

[PS12] J. Perez and P. Stollmann, *Heat kernel estimates for the Neumann problem on g-manifolds*, Manuscripta Mathematica **138** (2012), no. 3, 371–394.

[QU16] F. Queisser and W. G. Unruh, *Long-lived resonances at mirrors*, Phys. Rev. D **94** (2016), 116018, 9.

[Rot83] J.-P. Roth, *Spectre du laplacien sur un graphe*, C. R. Acad. Sci. Paris Sér. I Math. **296** (1983), 793–795.

[Sab14] M. Sabri, *Anderson localization for a multi-particle quantum graph*, Rev. Math. Phys. (2014), no. 1, 1350020, 52.

[Sch06] F. Schwabl, *Statistical mechanics*, Springer-Verlag, 2006.

[Sch09] R. Schrader, *Finite propagation speed and causal free quantum fields on networks*, J. Phys. A: Math. Theo. **42** (2009), no. 49, 495401, 39.

[Sto95] G. Stolz, *Localization for random Schrödinger operators with Poisson potential*, Ann. Inst. H. Poincaré Phys. Théor. **63** (1995), no. 3, 297–314.

[Sto01] P. Stollmann, *Caught by disorder: bound states in random media*, vol. 20, Springer Science & Business Media, 2001.

[Ver11] A.F. Verbeure, *Many-body boson systems*, Theoretical and Mathematical Physics, Springer-Verlag London, Ltd., London, 2011, Half a century later.

[Win08] B. Winn, *A conditionally convergent trace formula for quantum graphs*, Analysis on graphs and its applications, Proc. Sympos. Pure Math., vol. 77, Amer. Math. Soc., Providence, RI, 2008, pp. 491–501.

Deterministic and Stochastic Mean-Field SIRS Models on Heterogeneous Networks

Stefano Bonaccorsi and Silvia Turri

Abstract In this paper we study a model for the spread of an SIRS-type epidemics on a network, both in a deterministic setting and under the presence of a random environment, that enters in the definition of the infection rates of the nodes. Accordingly, we model the infection rates in the form of independent stochastic processes. To analyze the problem, we apply a mean field approximation that is known in the literature as NIMFA model, which allows to get a differential equation for the probability of infection in each node. We discover a sufficient condition which guarantees the extinction of the epidemics both in the deterministic and in the stochastic setting.

1 Introduction

Differential models for population dynamics are necessary tools to make predictions and analysis in many fields of science, starting from the early contributions in epidemic models due to Kermack and McKendrick [11] which were concerned with the spread of infectious diseases.

The name *epidemic model*, that in the origin was actually referred to the spread of infections in human populations, is currently used to cover the spreading of many other threats in a population, cultural beliefs [5, 25], drug and alcohol addictions [19], as well as digital populations: diffusion of computer viruses and worms, spreading of informations (news, rumors, messages) in on-line social networks [23].

The epidemic models generally assume that individuals are divided into classes that represent the status of the individual itself. The main classes are: susceptibles (S), that are healthy and can contract the infection, infected and infectious (I) and recovered and immune (R). In general, the model assumes that susceptible individuals can get infected, usually, through interaction with other infected indi-

S. Bonaccorsi (✉) · S. Turri
University of Trento, Department of Mathematics, Povo, Trento, Italy
e-mail: stefano.bonaccorsi@unitn.it

F. M. Atay et al. (eds.), *Discrete and Continuous Models in the Theory of Networks*, Operator Theory: Advances and Applications 281,
https://doi.org/10.1007/978-3-030-44097-8_3

viduals. An infected individual remains in such state for a certain period of time, and then recovers: in classical SIS models, the recovered individual returns to the class of susceptibles, while in SIR models it becomes immune for the remaining time (perfect vaccination). In this paper, we consider a SIRS model, that is an intermediate case between SIS and SIR dynamics. The recovered individual receives a temporary immunity, i.e. the immunity wanes after some time (called latency period) before the individual returns to the susceptible class [2, 8]. In order to introduce heterogeneity of the population it is necessary to introduce a network-based approach, where inhomogeneous contact rates and individual responses to the infection are introduced [4, 14, 18].

Under some standard mathematical simplification, we can describe the epidemic spreading using the theory of Markov chains in discrete and continuous time [1]. This approach is often use to describe epidemic models based on their deterministic formulations. In most cases, the deterministic model is a good representation of the process, however, is important to include in the analysis also a stochastic effect in order to cover more realistic situations.

There are different possible way to include stochasticity in the model, both from a mathematical and a biological perspective, one of the approaches is to consider stochastic differential equations [1]. Another way to introduce a stochastic perturbation consists of replacing one or more parameters of the deterministic model by the corresponding stochastic counterparts, indeed, the parameters may have a great variability [6, 16].

Our epidemic spreading process is described by an individual-based mean-field approximation [20]. The idea is to write down the equations of the evolution in time of the probability of every node to be in each class assuming independence between the state of every couples of nodes.

After a mean-field approximation, the non linear system considered has two different solutions, the first is the trivial one that represent the absorbing state, the second is the nonzero steady-state solution called metastable state [13, 20]. This behaviour depends on the effective infection rate $\tau = \beta/\delta$, the ratio between infection rate and curing rate. If this quantity is above a critical threshold τ_c i.e., $\tau > \tau_c$, the infection spreads and there exist a nonzero fraction of infected nodes, while, if $\tau \leq \tau_c$, the epidemic dies out quickly.

Computing the critical threshold for the SIRS mean-field model in the discrete homogeneous case, we observe that it coincides with the critical threshold for the SIS model and the metastable state of the SIRS case is proportional to that of the SIS model.

Throughout the paper we shall discuss the long time behaviour of the solution both in deterministic and stochastic case finding conditions which guarantee the extinction of the epidemics. For the asymptotic stability of the stochastic case we use a result in [17] and we found a sufficient condition for the exponential stability of the solution. Since the condition is only sufficient, in some cases the solution wanes even if the condition is not satisfied; we analyse this behaviour by means of some simulations in a given graph.

The paper is organized as follows. In Sect. 2 we describe the SIRS model in the deterministic case and we introduce the related individual-based mean-field approximation that we use to obtain a system of differential equation for each node. Then, in Sect. 3 we study the behaviour of the solution over time, finding the stability properties of the system obtained. At first, we consider the homogeneous case and we study the epidemic spreading to changing the effective infection rate which is the ratio between the infection rate β and the recovery rate δ. Then we extend the results to the heterogeneous setting. In Sect. 5 we include stochasticity in the parameters of the model, we prove that the unique global solution remains in $(0, 1)^{3N}$ whenever it starts from this region and we study the stability properties. Finally, in Sect. 4 we provide some numerical results for the heterogeneous case in order to better investigate the behaviour of the solution.

2 The Deterministic Model

The spatial structure of the population is encoded by a *network*, i.e., an undirected graph $G(E, V)$ with set of vertices (nodes) $V = \{\mathsf{v}_1, \ldots, \mathsf{v}_N\}$ (N being the total amount of the population) and set of links E. The geometry of the network is described by the symmetric adjacency matrix A, in which the element $a_{ij} = a_{ji}$ is either 1 if the nodes v_i and v_j are connected, or 0 otherwise. We shall further denote d_i the degree of the node v_i.

In a classical SIS model, the state of an individual at time t is represented by a Bernoulli random variable $X_i(t)$, where $X_i = 0$ represents the healthy, susceptible state and $X_i = 1$ the infected state. Therefore, the state of the system can be represented by the quantity $p_i(t) = \mathbb{P}(X_i(t) = 1)$, which represents the probability that the i-individual is infectious at time t.

On the other hand, in a SIRS model the random variable $X_i(t)$ needs to take three different values (which represent the states S, I and R, respectively) and the state is described by three quantities, $x_i(t) = \mathbb{P}(X_i(t) = S)$, $y_i(t) = \mathbb{P}(X_i(t) = I)$ and $z_i(t) = \mathbb{P}(X_i(t) = R)$. The total probability theorem implies that

$$x_i(t) + y_i(t) + z_i(t) = 1 \tag{1}$$

for every time $t \geq 0$.

The infection of an individual i is a Poisson process with rate $b_i(t)$ which depends on the state of the other individuals. More precisely, the probability that a node i in a susceptible state receives infections from its neighbors is given by

$$b_i(t) = 1 - \prod_{j:j \text{ neighbors of } i} (1 - \beta_j y_j(t)),$$

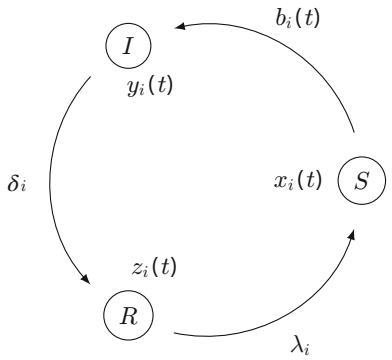

Fig. 1 State transition diagram for node v_i

where β_j is the rate at which individual j tries to infect its neighbors. By means of the adjacency matrix A, previous expression becomes

$$b_i(t) = 1 - \prod_{j=1}^{N} (1 - a_{ij}\beta_j y_j(t)). \tag{2}$$

We assume that the curing process per the node v_i is a Poisson process with rate δ_i, and that the period of latency is exponentially distributed with rate λ_i, All involved Poisson processes are independent (Fig. 1).

We are thus lead to the following *mean field* model for the SIRS epidemics

$$\begin{cases} x_i'(t) = -b_i(t)x_i(t) + \lambda_i z_i(t) \\ y_i'(t) = b_i(t)x_i(t) - \delta_i y_i(t) \\ z_i'(t) = \delta_i y_i(t) - \lambda_i z_i(t) \end{cases} \tag{3}$$

Obviously, it is sufficient to solve just two of them, thanks to (1).

A justification of Eq. (3) can be given in terms of a mean-field approximation for the exact Markov process on the space $\{S, I, R\}^N$, following the ideas in [20]. For instance, the exact Markovian equation governing the state of individual i implies that the transition probability for the node v_i to move from the susceptible to the infected state is given by

$$B_i(t) = 1 - \prod_{j=1}^{N} \left(1 - \beta_j a_{ij} \mathbf{1}_{X_j(t)=I}\right)$$

where the indicator function is 1 if the node v_j is in the state I at time t and it is 0 otherwise. Therefore, this coupling is a random variable, and the process is, in some sense, "doubly stochastic" and actually not Markovian.

Van Mieghem [20, 21] proposed to replace the actual, random infection rate $B_i(t)$ with its average $b_i(t)$, which can be interpreted as a mean-field approximation of the exact model.

A different, but related, justification of Eq. (3) can be given by taking expectation in the governing equation of transition rate for the Markov process on the space $\{S, I, R\}^N$. The equation for the probability of node i being in state I is given by

$$\frac{d}{dt}\mathbb{E}[\mathbf{1}_I(X_i(t))] = \mathbb{E}\left[-\delta_i \mathbf{1}_I(X_i(t)) + \mathbf{1}_S(X_i(t))1 - \prod_{j=1}^{N}\left(1 - \beta_j a_{ij}\mathbf{1}_{X_j(t)=I}\right)\right]$$

As one can see, the equation contains the joint probabilities for the random variables $X_i(t)$. Therefore, the system does not contain enough equations for getting a solution. However, instead of adding more and more equations, which should allow to solve also for the joint probabilities, we propose to close the system by assuming independence between the infection state of every couple of nodes. This approximation is also called a mean-field approximation [24].

It shall be noticed that this second approach leads to a model which is formally defined by Eq. (3), but in this case the coefficients $b_i(t)$ have a different expression, i.e.,

$$\tilde{b}_i(t) = \sum_{j=1}^{N} a_{ij}\beta_j y_j(t).$$

We shall often use, in the sequel, the following observation.

Remark 1 The function $\tilde{b}_i(t)$ is a first-order approximation of $b_i(t)$ for small values of the parameters β.

3 The Critical Threshold

Since the early models, it is known that the time behavior of an epidemics' spreading depends on the ratio $\tau = \beta/\delta$ between infection rate over the curing rate[1]: if this quantity is below a critical threshold τ_c then the epidemics dies out exponentially

[1] In demography, this quantity is referred to as the *basic reproduction number*, [7], and in classical SIS models without spatial structure the critical threshold is equal to 1

fast, otherwise the epidemics becomes endemic in the population, meaning that there exists a positive lower bound on the probability of being infected [15].

It is our interest to extend the above result to a spatially structured population. In the analysis of a SIS epidemics in an homogeneous population, the analysis in [20] provides the determination of the epidemic threshold $\tau_c = 1/\lambda_1$ of the mean-field N-intertwined model as the inverse of the largest eigenvalue λ_1 of the adjacency matrix A. It is our aim the extension of this result to the SIRS epidemic model.

In the first part of this section, we provide a sufficient condition for the epidemics to die out exponentially fast. In order to simplify the analysis, we explicitly solve the steady state problem associated to (3) in case of constant parameters β, δ and λ. Actually, it becomes necessary to solve the system

$$\begin{cases} y_i'(t) = (1 - y_i(t) - z_i(t))\, b_i(t) - \delta y_i(t) \\ z_i'(t) = \delta y_i(t) - \lambda z_i(t) \end{cases} \tag{4}$$

Since both functions $y_i(t)$ and $z_i(t)$ take values in $[0, 1]$, we can bound the first equation as

$$\begin{cases} y_i'(t) \leq 1 - \prod_{j=1}^{N} (1 - a_{ij}\beta y_j(t)) - \delta y_i(t) \\ z_i'(t) = \delta y_i(t) - \lambda z_i(t) \end{cases}$$

Taking into account the first order expansion of the product in previous formula, i.e.,

$$\prod_{j=1}^{N} (1 - a_{ij}\beta y_j(t)) \geq 1 - \sum_{j=1}^{N} a_{ij}\beta y_j(t)$$

we obtain the following

$$\begin{cases} y_i'(t) \leq \beta \sum_{j=1}^{N} a_{ij} y_j(t) - \delta y_i(t) \\ z_i'(t) = \delta y_i(t) - \lambda z_i(t) \end{cases} \tag{5}$$

Define the vector $\eta = (y_1, \ldots, y_n, z_1, \ldots, z_n)^\star \in \mathbb{R}^{2n}$ and consider the block matrix

$$C = \left(\begin{array}{c|c} \beta A - \delta I_n & 0 \\ \hline \delta I_n & -\lambda I_n \end{array} \right)$$

We consider the differential systems

$$\begin{aligned} \eta'(t) &\leq C\eta(t) \\ \eta(0) &= \eta_0 \end{aligned} \tag{6}$$

and

$$\begin{aligned} \tilde{\eta}'(t) &= C\tilde{\eta}(t) \\ \tilde{\eta}(0) &= \eta_0 \end{aligned} \tag{7}$$

Let us recall that a comparison principle for linear equations implies that for $0 \leq \eta_{0;i} \leq 1$ then $0 \leq \eta_i(t) \leq \tilde{\eta}_i(t)$ for every $t > 0$. Moreover, the null solution of the linear differential system (7) is asymptotically stable if and only if the real parts of every eigenvalue of C is negative.

Theorem 1 *Assume that the ratio $\tau = \beta/\delta$ satisfies*

$$\tau < 1/\lambda_1(A). \tag{8}$$

Then the SIRS epidemic model (3) vanishes exponentially fast for every possible initial condition.

The proof follows from the analysis of the eigenvalues of the matrix C. The real parts of every eigenvalue of C have to be negative.

Using the properties of block matrices we have that the eigenvalues of C are: $-\lambda$, coming from the second block on the diagonal, that is negative, and

$$\lambda_i(\beta A - \delta I_n) = \beta\lambda_i(A) - \delta$$

and, in order to get the asymptotically stability we have to impose the following condition

$$\lambda_1(\beta A - \delta I_n) = \beta\lambda_1(A) - \delta < 0$$

which reads

$$\frac{\beta}{\delta} < \frac{1}{\lambda_1(A)}.$$

We see that the presence of a latency period does not affect the critical threshold. We then proceed to analyse how the latency rate λ influence the model above threshold.

Our aim is the computation of the steady-state vector $\eta_\infty(y_1, \dots, y_n, z_1, \dots, z_n)^\star \in \mathbb{R}^{2n}$ that satisfies

$$\begin{cases} 0 = (1 - y_i - z_i)\, b_i - \delta y_i \\ 0 = \delta y_i - \lambda z_i \end{cases} \tag{9}$$

where

$$b_i = 1 - \prod_{j=1}^{N} (1 - a_{ij}\beta y_j).$$

We can assume that near the critical threshold the steady-state has the form

$$\eta = \varepsilon \tilde{\eta},$$

where $\tilde{\eta}$ is a vector with all positive elements (compare e.g. [22]). Then we proceed to analyse Eq. (9). Using the second equation in system (9) we obtain that the system is determined by the value of the projection of η on the first n components: $Y = (y_1, \dots, y_n)^\star$

$$\delta y_i = (1 - (1 + \frac{\delta}{\lambda}) y_i)\, b_i$$

We expect $y_i = \varepsilon \tilde{y}_i$, hence we perform an asymptotic expansion in the small parameter ε;

$$\delta \varepsilon \tilde{y}_i = (1 - \varepsilon(1 + \frac{\delta}{\lambda})\tilde{y}_i) \left(\sum_{j=1}^{N} \beta a_{ij} \varepsilon \tilde{y}_j + O(\varepsilon^2) \right).$$

If we simplify previous expression and take the limit for $\varepsilon \to 0$, we see that under condition (8) there exists only the null solution to previous equation, while a non trivial stable state $\eta = \varepsilon\tilde{\eta}$ exists if τ is larger than the critical threshold. We summarise what we've found in the following

Theorem 2 *Under condition (8), there exists only one stable solution for the SIRS model (3) that is the trivial one, and the system converges to the trivial solution exponentially fast.*

If the ratio $\tau = \beta/\delta$ satisfies $\tau > 1/\lambda_1(A)$, then the trivial steady state is unstable and there exists a non-trivial steady state η_∞ that is asymptotically stable.

3.1 Computing the Meta-Stable State

In this section we are interested in the computation of the meta-stable state for the SIRS model (3) in the over-critical case $\tau > 1/\lambda_1(A)$. We shall provide a description of the situation in either the case described by the mean field model with infection rate $b_i(t)$ and in the first order approximation $\tilde{b}_i(t)$.

At first, we give an explicit formula for the solution in the case of the approximating infection rate $\tilde{b}_i(t)$. In order to compute the value of $\eta_\infty = (Y, Z)^\star$, we consider the system

$$\begin{cases} 0 = (1 - y_i - z_i)\,\tilde{b}_i - \delta y_i \\ 0 = \delta y_i - \lambda z_i \end{cases} \tag{10}$$

Then, by the second equation we get that

$$z_i = \frac{\delta}{\lambda} y_i$$

and we arrive at the equation

$$\delta y_i = \left(1 - \left(1 + \tfrac{\delta}{\lambda}\right) y_i\right) \beta (AY)_i$$

Let us introduce $\lambda^* = 1 + \frac{\delta}{\lambda}$; then a little algebra leads to

$$\lambda^* y_i = 1 - \frac{1}{1 + \tau (A\lambda^* y)_i}$$

The above system for the unknowns $Y = (y_1, \ldots, y_n)$ can be solved by means of a recursive argument

$$\lambda^* y_i^{(k+1)} = 1 - \frac{1}{1 + \tau (A\lambda^* y^{(k)})_i}$$

which, even after a few iterations, gives a good approximation of the exact value. Moreover, we recognize the above formula from the analog computation in the SIS case [21].

A similar computation can be made for the SIRS model described in model (3) with infection rate $b_i(t)$.

We aim to emphasize that the first order approximation shows a good agreement with the mean field model. Let us consider for instance the spread of an SIRS epidemics on the network plotted in Fig. 3a, which corresponds to a graph with $|V| = 18$ nodes and $|E| = 25$ vertices. In Fig. 2 we provide a numerical computation for the overall percentage of infected individuals in the meta-stable state for the mean field approximation model (with coefficients $b_i(t)$) and its first

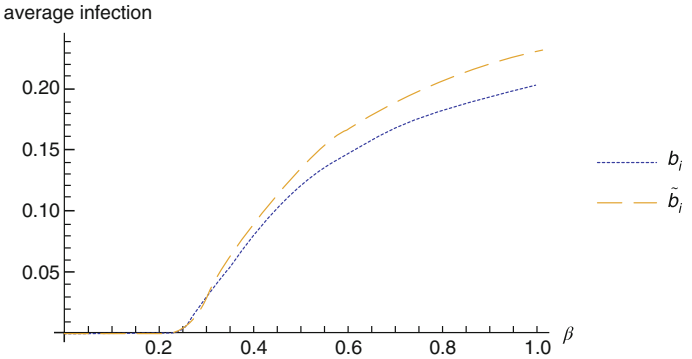

Fig. 2 In this graph, we plot the overall infected individuals in the meta-stable state as the (uniform) infection rate in the nodes β varies between 0 and 1, in either the case of mean field approximation model (with coefficients $b_i(t)$) and its first order approximation (with coefficients $\tilde{b}_i(t)$). The underlying network is depicted in Fig. 3a. The other parameters are $\delta = 1$ (arbitrary units), $\lambda = 0.5$ (latency period is the double of the curing period). Critical threshold $\tau_c = 1/\lambda_1(A) = 0.24263$

order approximation (with coefficients $\tilde{b}_i(t)$). It is apparent that these models share the same qualitative features.

Theorem 3 *The average incidence of the epidemics for the SIRS model, in the over-threshold case $\tau > 1/\lambda_1(A)$ (that coincides with the critical region for the SIS model), is equal to that of the SIS model rescaled by a factor $\frac{\lambda}{\lambda+\delta} < 1$ which depends on the latency rate λ.*

In the meta-stable state, the average number of susceptible, infected and recovered individuals is given by, respectively,

$$S = \sum_{i=1}^{n} x_i(t) = N\left(1 - \frac{\lambda+\delta}{\lambda}\frac{I}{N}\right),$$

$$I = \sum_{i=1}^{n} y_i(t), \qquad R = \sum_{i=1}^{n} z_i(t) = \frac{\delta}{\lambda} I.$$

For a latency period going to 0 (which corresponds to $\lambda \to \infty$) we get that the SIRS model converges to the SIS model; conversely, if $\lambda \to 0$ (there is no return to the susceptible state), then the quantity of infected individuals converges to 0, as in the SIR model.

3.2 The Heterogeneous Case

In this section we extend the above result to the heterogeneous setting, where we include the possibility for both the infection rates and the curing rates to be different for each node. As we have seen before, in this case, the governing equation is given by system (3). Actually, it is necessary to solve

$$\begin{cases} y_i'(t) = (1 - y_i(t) - z_i(t))\, b_i(t) - \delta_i y_i(t) \\ z_i'(t) = \delta_i y_i(t) - \lambda_i z_i(t) \end{cases} \tag{11}$$

Taking into account that $y_i(t)$ and $z_i(t)$ take values in $[0, 1]$ and considering the first order expansion of the product in $b_i(t)$ i.e.

$$\prod_{j=1}^{N} (1 - a_{ij}\beta y_j(t)) \geq 1 - \sum_{j=1}^{N} a_{ij}\beta y_j(t)$$

we obtain a generalization of the system (5)

$$\begin{cases} y_i'(t) \leq \displaystyle\sum_{j=1}^{N} a_{ij}\beta_j y_j(t) - \delta_i y_i(t) \\ z_i'(t) = \delta_i y_i(t) - \lambda_i z_i(t) \end{cases}$$

As in the homogeneous case we consider the block matrix

$$C = \left(\begin{array}{c|c} A\,\mathrm{diag}(\beta_i) - \mathrm{diag}(\delta_i) & 0 \\ \hline \mathrm{diag}(\delta_i) & -\mathrm{diag}(\lambda_i) \end{array} \right)$$

and the differential systems

$$\begin{aligned} \eta'(t) &\leq C\eta(t) \\ \eta(0) &= \eta_0 \end{aligned} \tag{12}$$

and

$$\begin{aligned} \tilde{\eta}'(t) &= C\tilde{\eta}(t) \\ \tilde{\eta}(0) &= \eta_0 \end{aligned} \tag{13}$$

In order to understand when the null solution of the linear differential system (13) is asymptotically stable we analyse the eigenvalue of the matrix C. We have to study when the real part of every eigenvalue of C is negative. For the property of the

block matrix it is sufficient to understand when the matrix $A\mathrm{diag}(\beta_i) - \mathrm{diag}(\delta_i)$ is semidefinite negative.

Since the sign of the matrix $A\mathrm{diag}(\beta_i) - \mathrm{diag}(\delta_i)$ is equivalent to that of the matrix $A - \mathrm{diag}(\delta_i/\beta_i)$, a sufficient condition for this matrix to be (semi-)negative defined is

$$\lambda_1(A) \leq \min\left\{\frac{\delta_i}{\beta_i}\right\} \tag{14}$$

We can improve previous estimate. Recall that the discrete Laplacian operator $\mathcal{L} = \mathrm{diag}(\mathsf{d}(\mathsf{v}_i)) - A$ is semi-definite positive, where $\mathsf{d}(\mathsf{v})$ is the degree of vertex v [22]; hence, writing

$$A - \mathrm{diag}(\delta_i/\beta_i) = \left[A - \mathrm{diag}(\mathsf{d}(\mathsf{v}_i))\right] + \left[\mathrm{diag}(\mathsf{d}(\mathsf{v}_i)) - \mathrm{diag}(\delta_i/\beta_i)\right]$$

we obtain the following sufficient condition for the matrix $A\mathrm{diag}(\beta_i) - \mathrm{diag}(\delta_i)$ to be (semi-)negative defined:

$$\max\left\{\mathsf{d}(\mathsf{v}_i) - \frac{\delta_i}{\beta_i}\right\} \leq 0 \tag{15}$$

For a regular graph, say of degree $\mathsf{d}(\mathsf{v}) = r$, it holds that $\lambda_1(A) = r$, which means that conditions (14) and (15) coincide.

Remark 2 In order to justify our preference for condition (15), we propose the following problem. We are given a population, whose spatial structure is described by a graph G with adjacency matrix A. Assume that the infection rates are constant throughout the population at a level β. Assume that a cure is available, and can be distributed to the population, with a cost for each individual that is proportional to the efficiency (measured in terms of the rate δ_i). Then, according to the policy in (14), it is necessary to distribute (pay) a quantity proportional to $N\lambda_1(A)$ units in order to guarantee the vanishing of the epidemics.

However, according to the policy in (15), the total cost of the cure is proportional to $\sum_{i=1}^{N} \mathsf{d}(\mathsf{v}_i)$. Since $N\lambda_1(A) \geq \sum_{i=1}^{N} \mathsf{d}(\mathsf{v}_i)$ (compare [22, Eq.(3.31)]), it follows that condition (15) is globally better than (14).

Now, we compute the metastable state for the SIRS model in the heterogeneous case. We consider the system

$$\begin{cases} 0 = (1 - y_i - z_i)\,\tilde{b}_i - \delta y_i \\ 0 = \delta_i y_i - \lambda_i z_i \end{cases} \tag{16}$$

from which we get

$$\delta_i y_i = \left(1 - \left(1 + \tfrac{\delta_i}{\lambda_i}\right) y_i\right) \sum_{j=1}^{N} a_{ij} \beta_j y_j$$

that yields the nodal steady state equation

$$\sum_{j=1}^{N} a_{ij} \beta_j y_j = \frac{\delta_i y_i}{1 - \left(1 + \tfrac{\delta_i}{\lambda_i}\right) y_i}$$

We recognize the above formula from the heterogeneous SIS case [21, Eq.(6)]. In particular, we see that for a latency period going to 0 (which corresponds to $\lambda \to \infty$) we get that the SIRS model converges to the SIS model.

4 Simulations for the Deterministic Heterogeneous Case

In the first example, described in Fig. 3, we consider the sufficient condition (14). We associate to every node a different value of the infection rate β_i chosen arbitrarily in the interval $(0.1, 0.23)$. The sufficient condition for stability, stated in (14), is $\max\{\beta_i\} \leq \frac{1}{\lambda_1(A)} = 0.242431$; therefore, our system is in the under-threshold regime. The simulation shows that the epidemic level decreases to zero uniformly in the whole network.

The next example shows that the sufficient conditions (15) and (14) are not necessary. Consider the simple graph in Fig. 4. We observe the following behaviours, according to the different values of the parameters β_j: when the sufficient condition (15) is verified, then the graph converges exponentially fast to the zero solution (absence of infection). Otherwise, the topological structure of the graph shall play a rôle. In both the examples depicted in Fig. 5, the system does not satisfy the sufficient conditions above. As far as condition (14) is concerned, we have $\frac{1}{\lambda_1(A)} = 0.306579$ but $\max\{\beta_i\} = 0.8$, hence the inequality is not satisfied. Moreover, condition (15) requires $\max\{\beta_i \mathsf{d}(\mathsf{v}_i)\} \leq 1$. Since in (a): $\beta_4 \mathsf{d}(\mathsf{v}_4) = 4$ while in (b) $\beta_6 \mathsf{d}(\mathsf{v}_6) = 1.6$, condition (15) fails to hold too.

However, in the case in Fig. 5a, when the central node has a large infectivity rate, the system converges to a metastable state where the average infection rate of the nodes is positive ($\bar{y} = 0.0235458$), while in case (b), when the large infectivity rate is associated with a peripheral node, the system converges to zero.

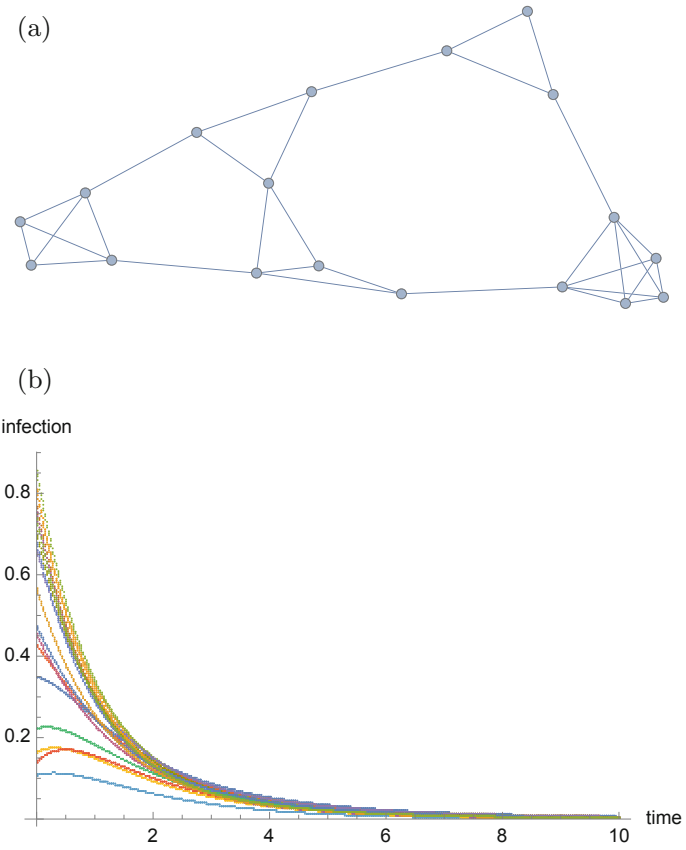

Fig. 3 In (**b**), the rate of infection in the network provided in (**a**) as a function of time, for different values of the initial infection rate. In the simulation we fix $\delta = 1$, $\lambda = 0.5$ and we choose arbitrary values β_i such that $\max\{\beta_i\} \leq \frac{1}{\lambda_1(A)} = 0.242431$. (**a**) The model network for this simulation. It contains $|V| = 18$ nodes and $|E| = 25$ edges. (**b**) Total rate of infection for the above network in the under-threshold regime

5 Stochastic SIRS Model

In order to make things formal, we shall introduce a standard n-dimensional Brownian motion $W(t) = (w_1(t), \ldots, w_n(t))$ defined on a stochastic basis $(\Omega, \mathcal{F}, \{\mathcal{F}_t\}, \mathbb{P})$ that satisfies the standard assumptions.

In the epidemiology literature, despite the potential importance of the environmental noise, stochastic models have received relatively little attention. In the aggregated models, there are mainly two ways to introduce a stochastic perturbation. In the first, one replaces one or more of the parameters of the deterministic model by the corresponding stochastic counterparts (see for instance [16]). In a second way, one can add randomly fluctuation affecting directly the deterministic model (see for instance [9, 10]).

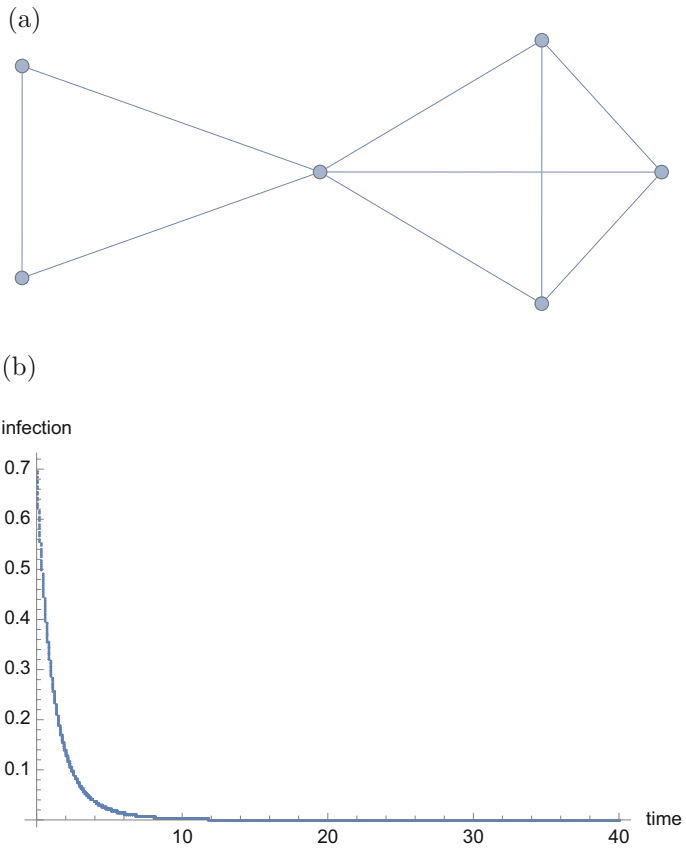

Fig. 4 In the simulation we fix $\delta = 1$, $\lambda = 0.5$ and the we choose arbitrary values β_i such that $\max\{\beta_i\} \leq \frac{1}{\lambda_1(A)} = 0.306579$. (**a**) The model network for this simulation. It contains $|V| = 6$ nodes and $|E| = 9$ edges. (**b**) Total rate of infection for the above network in the under-threshold regime

Here, we consider the mean field model for the SIRS epidemics (3), and we assume that the infection rate $b_i(t)$ is perturbed by a stochastic term having the form $\sigma_i \frac{y_i(t)}{1+\alpha y_i(t)} \dot{w}_i(t)$ (compare system (2) in [12] or [6]), thus leading to the stochastic differential system

$$\begin{cases} \mathrm{d}x_i(t) = [-b_i(t)x_i(t) + \lambda_i z_i(t)]\,\mathrm{d}t - \sigma_i \dfrac{x_i(t)y_i(t)}{1+\alpha y_i(t)}\,\mathrm{d}w_i(t) \\ \mathrm{d}y_i(t) = [b_i(t)x_i(t) - \delta_i y_i(t)]\,\mathrm{d}t + \sigma_i \dfrac{x_i(t)y_i(t)}{1+\alpha y_i(t)}\,\mathrm{d}w_i(t) \\ \mathrm{d}z_i(t) = [\delta_i y_i(t) - \lambda_i z_i(t)]\,\mathrm{d}t \end{cases} \tag{17}$$

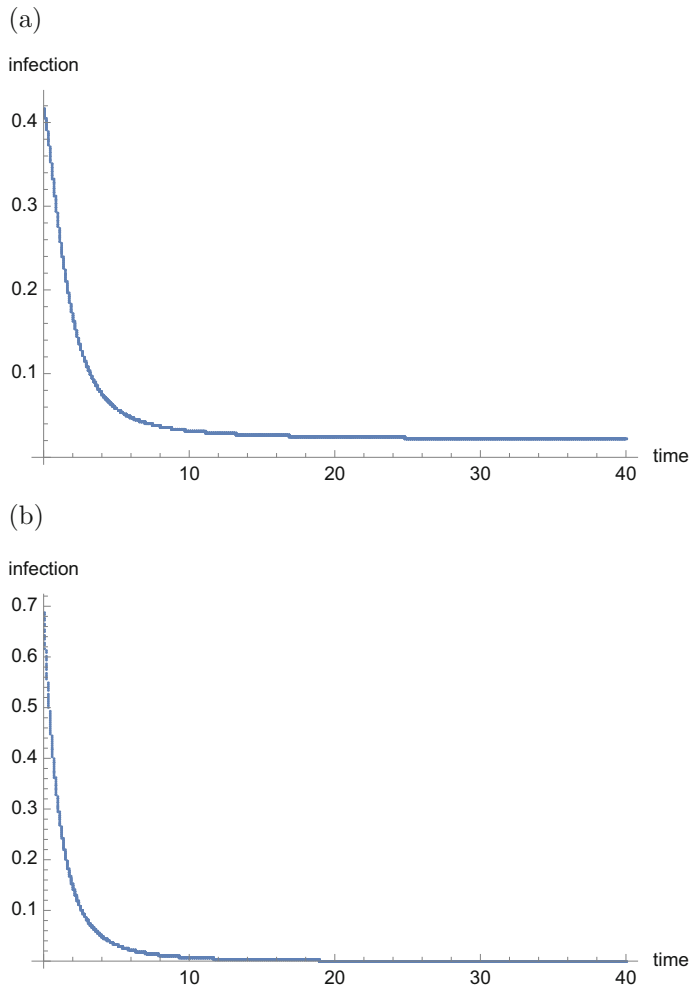

Fig. 5 In the simulation we fix $\delta = 1, \lambda = 0.5$. In (**a**) we consider all $\beta_i = 0.2$ except $\beta_4 = 0.8$ (v_4 is the central node). The system converges to a meta-stable state. In (**b**) we consider all $\beta_i = 0.2$ except $\beta_6 = 0.8$ (v_6 is the rightmost node). The system converges to the null state. Sufficient conditions for stability: (14) means $\max\{\beta_i\} \leq \frac{1}{\lambda_1(A)} = 0.306579$, which fails to hold, while condition (15) requires $\max\{\beta_i \mathsf{d}_i\} \leq 1$. Since $\mathsf{d}_6 = 2$, condition (15) fails to hold too. (**a**) Total rate of infection in the network in Fig. 4a when the central node is highly infective. (**b**) Total rate of infection in the network in Fig. 4a when only a peripheral node is highly infective

We shall denote $P(t) = \left(\underline{x}(t), \underline{y}(t), \underline{z}(t)\right)$ the solution of (17) with the standard notation $\underline{x} = (x_1, \ldots, x_n)$.

Remark 3 In (17) we have chosen the stochastic perturbation term in such a way that the disturbance is small provided that the state of the node is far from infection. This also implies the viability of the system in the set $[0, 1]^{3N}$, since a diffusion coefficient independent of the infection level would have implied a stochastic variability also near the zero level, thus allowing the solution to go below zero, which does not have any physical meaning.

Theorem 4 *For any initial condition $(\underline{x}, \underline{y}, \underline{z}) \in D := (0, 1)^{3N}$ the solution of system (17) has an infinite life-span and, moreover, it remains inside the domain D for all times, almost surely.*

Since the coefficients of the equation are locally Lipschitz continuous, for any given initial value $P(0) = (\underline{x}, \underline{y}, \underline{z})$ there is a unique local solution on $t \in [0, \tau_e)$, where τ_e is the explosion time (see for instance [3]).

To show this solution is global, we need to show that $\tau_e = \infty$ a.s. This is achieved if we prove a somehow stronger property of the solution, namely that it never leaves the domain D. The following computations are somehow standard (compare for instance [6]). Let $N_0 > 0$ be sufficiently large for $p_i(0) \geq \frac{1}{N_0}$, $p \in \{x, y, z\}$, for all $i = 1, \ldots n$. For each integer $N \geq N_0$, define the stopping time

$$\tau_N = \inf \left\{ t \in [0, \tau_e) : \inf_{p \in \{x,y,z\}, i \in \{1,\ldots,n\}} p_i(t) < 1/N \right\},$$

where, as customary, $\inf \emptyset = +\infty$ (with $\emptyset$ denoting the empty set).

Clearly τ_N is increasing as $N \to \infty$ and letting $\tau_\infty = \lim_{n\to\infty} \tau_N$, we have $\tau_\infty \leq \tau_e$ a.s. Hence we basically need to show that $\tau_\infty = \infty$ a.s; if this were not so, there would exists a pair of constants $T > 0$ and $\epsilon \in (0, 1)$ such that

$$\mathbb{P}\{\tau_\infty \leq T\} > \epsilon.$$

Accordingly, there is an integer $N_1 \geq N_0$ such that

$$\mathbb{P}\{\tau_N \leq T\} \geq \epsilon/2 \qquad \forall N \geq N_1. \tag{18}$$

Now we define a function $V : D \to \mathbb{R}^+$ as

$$V(P(t)) = -\sum_{i=1}^{n} \log\left[x_i(t) y_i(t) z_i(t)\right].$$

By Itô's formula we have

$$\begin{aligned} \mathrm{d}V(P(t)) = \sum_{i=1}^{n} \Bigg(& b_i(t) + \delta_i + \lambda_i + \frac{1}{2}\sigma_i^2 \frac{x_i(t)^2 + y_i(t)^2}{(1+\alpha y_i(t))^2} \\ & - \lambda_i \frac{z_i(t)}{x_i(t)} - b_i(t)\frac{x_i(t)}{y_i(t)} - \delta_i \frac{y_i(t)}{z_i(t)} \Bigg) \, \mathrm{d}t \\ & + \sum_{i=1}^{n} \sigma_i \frac{y_i(t) - x_i(t)}{1+\alpha y_i(t)} \, \mathrm{d}w_i(t) \end{aligned}$$

Therefore, in $[0, \tau_N)$ we have, by using the positivity of the components of $P(t)$, and the simple bounds $b_i(t) \le 1$ and $x_i^2 + y_i^2 \le 2$:

$$\begin{aligned} V(P(t)) - V(P(0)) \le & \sum_{i=1}^{n} \left(1 + \delta_i + \lambda_i + \sigma_i^2\right) t \\ & + M(t) \end{aligned} \tag{19}$$

where $M(t)$ is the (local) martingale defined by

$$M(t) = \sum_{i=1}^{n} \sigma_i \int_0^t \frac{y_i(s) - x_i(s)}{1+\alpha y_i(s)} \, \mathrm{d}w_i(s).$$

Taking the expectation in (19) we arrive to

$$\begin{aligned} \mathbb{E}[V\,(P(\tau_n \wedge T))] &\le \mathbb{E}[V(P(0))] + K\,\mathbb{E}(\tau_n \wedge T) \\ &\le \mathbb{E}[V(P(0))] + KT. \end{aligned} \tag{20}$$

Set $\Omega_N = \{\tau_N \le T\}$ for $N \ge N_1$. By (18) we have $P(\Omega_N) \ge \epsilon/2$. Since for every $\omega \in \Omega_N$, there is at least one of the $p_i(\tau_N, \omega)$, $p \in \{x, y, z\}$, equal to $1/N$, then it holds

$$V\,(P(\tau_N, \omega)) \ge -\log \frac{1}{N}. \tag{21}$$

Then from (20) and (21) it follows that

$$V(P(0)) + KT \ge \mathbb{E}\left[\chi_{\Omega_N} V\,(P(\tau_N, \omega))\right] \ge \epsilon/2 \log(N)$$

where χ_{Ω_N} is the indicator function of Ω_N. Letting $N \to \infty$ we have the following contradiction

$$\infty > V(P(0)) + KT \geq \lim_{N\to\infty} \epsilon/2 \log(N) = \infty,$$

that is a contraddiction. Hence we must have $\tau_\infty = \infty$ a.s. and the proof is complete.

The concept of asymptotic stability for dynamical system was introduced in 1892 by Lyapunov: roughly speaking, it means that the system converges to the equilibrium solution for large time, independently by the initial condition. Later, in the 1960s, the concept was extended to stochastic systems by Bucy, Arnold, Has'minskii and many others. Let us briefly recall the main definitions we shall need in this section.

Definition 5 The trivial solution of the equation

$$\begin{aligned} \mathrm{d}x(t) &= f(t, x(t))\,\mathrm{d}t + g(t, x(t))\,\mathrm{d}W(t) \\ x(0) &= x_0 \end{aligned} \tag{22}$$

is said to be stochastically asymptotically stable if

(i) it is stochastically stable:

$$\mathbb{P}\{|x(t; x_0) < r \text{ for all } t > 0\} \geq 1 - \varepsilon$$

(ii) moreover, for every $\varepsilon \in (0, 1)$, there exists a $\delta_0 = \delta_0(\varepsilon) > 0$ such that

$$\mathbb{P}\{\lim_{t\to\infty} |x(t; x_0) = 0\} \geq 1 - \varepsilon$$

whenever $|x_0| < \delta_0$.

In the sequel, we adapt the presentation of Arnold [3] to our case. In particular, we shall exploit the invariance of the domain D and consider all the following construction restricting the functions, and inequalities, to D.

A continuous function $V(x)$ defined on $D \cap B_h(0)$ is said to be positive-definite (in the sense of Lyapunov) if $V(0) = 0$ and $V(x) > 0$ on $|x| > 0$.

A function V is said to be negative-definite if $-V$ is positive-definite.

The diffusion operator associated to (22) is

$$Lv(x) = \left(\sum f_i(t, x)\frac{\partial}{\partial x_i} + \frac{1}{2}\sum \left[g(t, x)g^\star(t, x)\right]_{ij} \frac{\partial^2}{\partial_i x_j}\right) v(x).$$

In order to prove asymptotic stability of the solution, we shall appeal to the following result (compare [17, Ch.4, Thm.2.2]).

Proposition 6 *If there exists a positive-definite function $V(x)$ such that $LV(x)$ is negative-definite, then the trivial solution of Eq. (22) is stochastically asymptotically stable.*

It shall be noted that in the above result the functions V and LV are given in the whole space. However, since we only allow initial conditions in the invariant domain D, a sufficient condition for the relevant inequality $\mathbb{E}LV(X_t^x) \leq 0$ is $LV(x)$ negative defined in D.

In this section we consider the unknown $P(t) = (\underline{y}(t), \underline{z}(t))$ and the corresponding equation

$$\begin{cases} \mathrm{d}y_i(t) = [b_i(t)(1 - y_i(t) - z_i(t)) - \delta_i y_i(t)]\,\mathrm{d}t + \sigma_i \dfrac{(1 - y_i(t) - z_i(t))y_i(t)}{1 + \alpha y_i(t)}\,\mathrm{d}w_i(t) \\ \mathrm{d}z_i(t) = [\delta_i y_i(t) - \lambda_i z_i(t)]\,\mathrm{d}t \end{cases} \tag{23}$$

In order to study asymptotic stability, we consider the function $V(P) = \sum \log(1 + y_i) + \varepsilon \sum z_i$ on the domain $D \cap B_h(0)$ for some $h > 0$. This function is positive-definite (in the sense of Lyapunov), hence we shall prove that $LV(P)$ is negative-definite, where

$$\begin{aligned} LV(P) = &\sum_{i=1}^{n} [b_i(t)(1 - y_i(t) - z_i(t)) - \delta_i y_i(t)] \frac{1}{1 + y_i(t)} \\ &- \sum_{i=1}^{n} \left(\sigma_i \frac{(1 - y_i(t) - z_i(t))y_i(t)}{1 + \alpha y_i(t)} \right)^2 \frac{1}{(1 + y_i(t))^2} \\ &+ \varepsilon \sum_{i=1}^{n} [\delta_i y_i(t) - \lambda_i z_i(t)] \end{aligned}$$

Claim 1 It holds that $b_i(t) \leq \tilde{b}_i(t)$ for $P \in D \cap B_h(0)$.

Proof We compute

$$\begin{aligned} b_i(t) &= 1 - \prod_{j=1}^{N} (1 - a_{ij}\beta_j y_j(t)) = 1 - (1 - a_{i1}\beta_1 y_1)(1 - a_{i2}\beta_2 y_2) \dots (1 - a_{iN}\beta_N y_N) \\ &= 1 - (1 - \sum_{j=1}^{N} a_{ij}\beta_j y_j + \sum_{j,k=1}^{N} a_{ij}a_{ik}\beta_j\beta_k y_j y_k - \dots) \\ &= \sum_{j=1}^{N} a_{ij}\beta_j y_j - (\sum_{j,k=1}^{N} a_{ij}a_{ik}\beta_j\beta_k y_j y_k - \sum_{j,k,l=1}^{N} a_{ij}a_{ik}a_{il}\beta_j\beta_k\beta_l y_j y_k y_l + \dots) \end{aligned}$$

where, taking into account that $0 \leq y_i \leq h$, for h small enough, we get

$$\sum_{j,k=1}^{N} a_{ij}a_{ik}\beta_j\beta_k y_j y_k \geq \sum_{j,k,l=1}^{N} a_{ij}a_{ik}a_{il}\beta_j\beta_k\beta_l y_j y_k y_l \geq \dots$$

and all the differences between successive pair of sums inside the brackets are positive. This implies that

$$b_i(t) \leq \sum_{j=1}^{N} a_{ij}\beta_j y_j = \tilde{b}_i(t)$$

as claimed. □

We thus estimate

$$LV(P) \leq -\sum_{i=1}^{n}\left(-\beta\deg(\mathsf{v}_i) + \delta_i\left(\frac{1}{1+h} - \varepsilon\right)\right) y_i$$
$$-\varepsilon\sum_{i=1}^{n}\lambda_i z_i$$

(the diffusion term is negative and goes to zero as y^2 hence it is negligible) and, due to the arbitrariness of h and ε, we arrive at the following result.

Theorem 7 *The sufficient condition* (15) *for the exponential stability of the solution of the deterministic problem* (3) *is also a sufficient condition for the exponential stability of the solution of the stochastic problem* (17).

6 Conclusion

In this paper we study the behaviour of an epidemics spreading in a population with homogeneous and inhomogeneous contact rates, where the rates at which each individual can be infected from its neighbours are considered as independent stochastic processes.

We start from the deterministic case obtained after a mean field approximation, where the infection rate β between each two given individuals is either zero, if they are not in contact, or a given constant, if they are connected.

However, since epidemic processes are usually affected by random disturbances, we introduce in this model a stochastic heterogeneity of the population by taking into account a variability in time of the parameters. Precisely, we assume that the rate of receiving the infection, for each individual, varies around a common average

value under the action of a family of independent, identically distributed Brownian motions.

We observe that the steady state solution of the SIRS model can be exactly mapped to that of the SIS model, via the identification of the density of infected individuals. Therefore, all the critical properties of the SIRS model are very similar to the SIS model.

In the last part, we consider the stochastic system and we prove that $(0, 1)^{3N}$ is invariant. We study the asymptotic behaviour of the solution finding a sufficient condition for the stochastic asymptotic stability of the solution.

Acknowledgments The authors wish to thank dr. Stefania Ottaviano and prof. Delio Mugnolo for many interesting discussions, and the anonymous referee for the invaluable help to improve the presentation of the paper.

References

1. L.J.Allen, *An introduction to stochastic epidemic models*, Mathematical Epidemiology, Springer, 2008, pp. 81–130
2. R.M. Anderson and R.M. May, **Infectious Diseases in Humans: Dynamics and Control**. Oxford University Press, Oxford, 1991.
3. Ludwig Arnold, **Stochastic differential equations: theory and applications**. Wiley-Interscience [John Wiley & Sons], New York-London-Sydney, 1974.
4. S. Bansal, B.T. Grenfell and L.A. Meyers, *When individual behaviour matters: homogeneous and network models in epidemiology*, Journal of the Royal Society Interface, **4**, 879–891 (2007)
5. Luís M.A. Bettencourt, Ariel Cintrón-Arias, David I. Kaiser and Carlos Castillo-Chávez, *The power of a good idea: Quantitative modeling of the spread of ideas from epidemiological models*, Physica A: Statistical Mechanics and its Applications **364**, 513–536, (2006)
6. Stefano Bonaccorsi and Stefania Ottaviano, *Epidemics on networks with heterogeneous population and stochastic infection rates*, Mathematical Biosciences, **279**, 43–52 (2016). https://doi.org/10.1016/j.mbs.2016.07.002
7. Tom Britton, *Stochastic epidemic models: a survey*, arXiv:0910.4443, (2009)
8. W. Hethcote, *Qualitative analyses of communicable disease models*, Mathematical Biosciences **28**(3–4), 335–356 (1976). https://doi.org/10.1016/0025-5564(76)90132-2
9. L. Imhof and S. Walcher, *Exclusion and persistence in deterministic and stochastic chemostat models*, J. Differential Equations, **217**, 26–53 (2005)
10. Daqing Jiang, Jiajia Yu, Chunyan Ji, and Ningzhong Shi, *Asymptotic behavior of global positive solution to a stochastic SIR model*, Mathematical and Computer Modelling **54**(1–2), 221–232 (2011). https://doi.org/10.1016/j.mcm.2011.02.004
11. W. O. Kermack and A. G. McKendrick, *A contribution to the mathematical theory of epidemics*, Proc. Roy. Soc. Lond. A, **115**, 700–721 (1927)
12. A. Lahrouz, L. Omari, and D. Kiouach, *Global analysis of a deterministic and stochastic nonlinear SIRS epidemic model*, Nonlinear Analysis: Modelling and Control **16**(1), 59–76 (2011)
13. Cong Li, Ruud van de Bovenkamp, and Piet Van Mieghem, *Susceptible-infected-susceptible model: A comparison of N-intertwined and heterogeneous mean-field approximations*, Physical Review E **86**, 026116 (2012)
14. Chun-Hsien Li, Chiung-Chiou Tsai and Suh-Yuh Yang, *Analysis of epidemic spreading of an SIRS model in complex heterogeneous networks*, Communications in Nonlinear Science and Numerical Simulation, **19**(4), 1042–1054 (2014). https://doi.org/10.1016/j.cnsns.2013.08.033

15. Dan Li, Shengqiang Liu, and Jing'an Cui, *Threshold dynamics and ergodicity of an SIRS epidemic model with Markovian switching*, Journal of Differential Equations, **263**(12), 8873–8915 (2017). https://doi.org/10.1016/j.jde.2017.08.066
16. Qiuying Lu, *Stability of SIRS system with random perturbations*, Physica A: Statistical Mechanics and its Applications **388**(18), 3677–3686 (2009). https://doi.org/10.1016/j.physa.2009.05.036
17. Mao, X., **Stochastic Differential Equations and Applications**, 2nd Edition, Horwood Publishing, Chichester, 2007.
18. R. Pastor-Satorras, A. Vespignani *Epidemic dynamics in scale-free networks*, Phys Rev Lett, **86**, 3200 (2001)
19. F. Sánchez, X. Wang, C. Castillo-Chávez, D. M. Gorman and P. J. Gruenewald, *Drinking as an Epidemic-A Simple Mathematical Model with Recovery and Relapse*, in: **Therapist's Guide to Evidence-Based Relapse Prevention**. Elsevier Inc., 353–368 (2007). https://doi.org/10.1016/B978-012369429-4/50046-X
20. P. Van Mieghem, J., Omic and R., Kooij, *Virus Spread in Networks*, IEEE/ACM Transactions on Networking **17**(1), 1–14 (2009). https://doi.org/10.1109/TNET.2008.925623
21. Piet Van Mieghem and Jasmina Omic, *In-homogeneous Virus Spread in Networks*, arXiv:1306.2588 (2008)
22. Piet van Mieghem, **Graph Spectra for Complex Networks**, Cambridge University Press (2011)
23. Piet Van Mieghem, *The viral conductance of a network*, Computer Communications **35**, 1494–1506 (2012)
24. Piet Van Mieghem, *Exact Markovian SIR and SIS epidemics on networks and an upper bound for the epidemic threshold*, arXiv:1402.1731 (2014)
25. Duncan J. Watts, *A simple model of global cascades on random networks*, P. Natl. Acad. Sci. USA **99**(9), 5766–5771 (2002). https://doi.org/10.1073/pnas.082090499

Kreĭn Formula and Convergence of Hamiltonians with Scaled Potentials in Dimension One

Claudio Cacciapuoti

Abstract In this brief report we study the convergence of the Hamiltonian $h^\varepsilon := -(\cdot)'' + V(x/\varepsilon)/\varepsilon^2$ in dimension one as ε goes to zero. This problem has already been studied in several former works (also in the more general setting of metric graphs) and the results that we present here are not new. Aim of this work is to formulate the problem in the setting of metric graphs and to exploit an approach based on a Kreĭn formula for the resolvent of h^ε. Such a formula allows to mark out the rôle of the zero eigenvalue for an auxiliary Hamiltonian. The existence of the zero eigenvalue is responsible of the coupling in the limiting Hamiltonian, otherwise h^ε converges in norm resolvent sense to the direct sum of two Dirichlet Laplacians on the half-line. In a forthcoming paper such approach will be generalized to the study of an analogous problem on metric graphs with a small compact core.

Keywords Kreĭn formula · Point interactions · Scaling limit · Metric graphs

MSC 2010 81Q35, 47A10, 34B45

1 Introduction

In this brief report we discuss the limit of the one-dimensional Hamiltonian

$$h^\varepsilon := -\frac{d^2}{dx^2} + \frac{1}{\varepsilon^2} V(\cdot/\varepsilon) \tag{1.1}$$

as ε goes to zero. Where V is a bounded real valued, compactly supported function.

The author is indebted to the anonymous referee whose comments helped to improve the manuscript.

C. Cacciapuoti (✉)
Dipartimento di Scienza e Alta Tecnologia, Università dell'Insubria, Como, Italy
e-mail: claudio.cacciapuoti@uninsubria.it

F. M. Atay et al. (eds.), *Discrete and Continuous Models in the Theory of Networks*, Operator Theory: Advances and Applications 281,
https://doi.org/10.1007/978-3-030-44097-8_4

The results we present here are not new. Indeed, a proper understanding of the limit of h^ε dates back to the paper [1], where it was shown (under the additional assumption $\int_{\mathbb{R}} V \neq 0$) that the limit strongly depends on the existence of a *zero energy resonance* for the unscaled Hamiltonian $h \equiv h^{\varepsilon=1}$.

The Hamiltonian h has a zero energy resonance if there exists a function $\varphi \in L^\infty(\mathbb{R})$, such that $\varphi \notin L^2(\mathbb{R})$, and $h\varphi = 0$ in distributional sense.

If h has not a zero energy resonance the limit of h^ε (in norm resolvent sense) is the Laplacian on $L^2(\mathbb{R})$ with domain $\{f \in H^2(\mathbb{R}\backslash\{0\}) | f(0^+) = f(0^-) = 0\}$. Note that this operator can be understood as the direct sum of two Laplacians on the half-line with a Dirichlet condition in the origin, in this case the parts of the real line at the right and at the left hand side of the origin are completely decoupled.

If h has a zero energy resonance, the limiting operator allows a coupling between the right and left side of the origin. In particular, the result in [1] can be rephrased as follows: one can define two constants $c_\pm := \lim_{x\to\pm\infty} \varphi(x)$ (φ can be chosen so that $c_\pm$ are real valued and $c_+^2 + c_-^2 = 1$), and the limiting operator (in norm resolvent sense) is the Laplacian on the real line with domain $\{f \in H^2(\mathbb{R}\backslash\{0\}) | c_- f(0^+) = c_+ f(0^-)\,;\; c_+ f'(0^+) = c_- f'(0^-)\}$.

The proof in [1] was based on the unitary equivalence between the operators $(h^\varepsilon - z)^{-1}$ and $\varepsilon^2(h - \varepsilon^2 z)^{-1}$. As a consequence, the limit (in norm resolvent sense) of h^ε as $\varepsilon \to 0$ can be understood by exploiting some former results by [4] on the low energy expansion of the resolvents of one dimensional Schrödinger operators in the presence of zero energy resonances.

The same problem has been studied in several other works, for example in [7] the effect of an additional term $\lambda V(x/\varepsilon)/\varepsilon$, $\lambda \in \mathbb{R}$, is considered. We mention the work [15] in which the authors, besides dropping the assumption $\int_{\mathbb{R}} V \neq 0$, note that the condition on the existence of a zero energy resonance can also be formulated as follows. Assume that the potential V is compactly supported in $(-1, 1)$ and consider the auxiliary Hamiltonian

$$\mathring{h} : L^2(-1, 1) \to L^2(-1, 1) \tag{1.2}$$

$$D(\mathring{h}) := \left\{ f \in H^2(-1, 1) | f'(1) = f'(-1) = 0 \right\} \;; \qquad \mathring{h} := -\frac{d^2}{dx^2} + V. \tag{1.3}$$

$\mathring{h}$ has purely discrete spectrum moreover its eigenvalues are simple. For $n \in \mathbb{N}$, denote by λ_n its eigenvalues (arranged in increasing order) and by $\{\varphi_n\}_{n\in\mathbb{N}}$ a corresponding set of orthonormal eigenfunctions. The existence of a zero energy resonance for h is equivalent to $\mathring{h}$ having zero as an eigenvalue. In particular, if $\lambda_{n^*} = 0$ is an eigenvalue for $\mathring{h}$ the constants $c_\pm$ defined above (up to an inessential multiplication factor) are given by $c_\pm = \varphi_{n^*}(\pm 1)$, and the limiting Hamiltonian is the one described above. Otherwise, if zero is not an eigenvalue for $\mathring{h}$, the limiting Hamiltonian is the direct sum of Dirichlet Laplacians on the half-lines. We refer to [15], for a discussion on the limit of Hamiltonians of the form (1.1) and for further references. The approach presented in this report was partially developed in [6].

The aim of our report is twofold.

On one side, we want to reformulate the problem in a way that can be naturally adapted to the study of an analogous problem on metric graphs with a "small" compact core. For an introduction to the theory of metric graphs we refer to the monograph [2]. Let $\mathcal{K}$ be a compact metric graph, and define $\mathcal{K}^\varepsilon$ by squeezing uniformly $\mathcal{K}$, i.e., $\mathcal{K}^\varepsilon = \varepsilon\mathcal{K}$. Then consider the graph $\mathcal{G}^\varepsilon$ obtained by attaching several half-lines or edges of finite length (not dependent on ε) to $\mathcal{K}^\varepsilon$; we say that $\mathcal{G}^\varepsilon$ is a graph with a small compact core, and divide $\mathcal{G}^\varepsilon$ in an *inner* part (the compact core $\mathcal{K}^\varepsilon$) and an *outer* part (the additional edges). In a forthcoming paper we plan to study the limit of Hamiltonians (with suitable scaling properties) defined on $L^2(\mathcal{G}^\varepsilon)$. For this reason, in the analysis of the operator h^ε, we want to decompose the Hilbert space $L^2(\mathbb{R})$ in an *inner* Hilbert space $L^2(-\varepsilon, \varepsilon)$ (playing the role of $\mathcal{K}^\varepsilon$) and an *outer* Hilbert space $L^2(0, +\infty) \oplus L^2(0, +\infty)$. We note that problems on graphs with a small compact core have been studied in several papers in the case in which $\mathcal{G}^\varepsilon$ is a star-graph or its outer part is made up of half-lines, see, e.g., [8–11, 17–19]. In particular, the rôle of zero energy resonances (or, equivalently, zero energy eigenvalues for an auxiliary Hamiltonian) has already been pointed out, see, e.g., [10, 11, 17–19]. In the latter series of works, it was proved that the scaled Hamiltonian converges (in the norm resolvent sense) to a limiting one defined through the eigenfunctions of the zero eigenvalue similarly to as described above for h^ε. We also mention the recent work [3] in which the convergence of Schrödinger operators on metric graphs with shrinking edges is analyzed. The problem studied in [3] is closely related to the problem studied in our report, with the difference that in [3] the potential term is scaled differently and does not affect substantially the vertex conditions in the limiting operator.

On the other side, we want to exploit a method to study the convergence based on a Kreĭn formula for the resolvent of the Hamiltonian h^ε (more precisely, for an equivalent Hamiltonian on the Hilbert space decomposed in inner and outer part). Such a formula allows us to reduce the analysis to relatively simple ε-dependent operators (in some cases these are just matrices) and to isolate the rôle of the zero eigenvalue. In a forthcoming work, such a formula will be the main tool to study the problem on graphs with a small compact core, also in the case in which the outer part of the graph has edges of finite length.

The structure of the paper is the following. In Sect. 2 we set up the problem and state the main result, see Theorem 1. In Sect. 3 we obtain the Kreĭn resolvent formula, see Theorem 2. In Sect. 4 we prove Theorem 1.

In what follows C denotes a generic positive constant not dependent on ε.

Given a self-adjoint operator A we denote by $\rho(A)$ the resolvent set of A.

Given two Hilbert spaces X and Y, we denote by $\mathcal{B}(X, Y)$ (or simply by $\mathcal{B}(X)$ if $X = Y$) the space of bounded operators from X to Y, and by $\|\cdot\|_{\mathcal{B}(X,Y)}$ the corresponding norm. For any $a \in \mathbb{R}$, we use the notation $\mathcal{O}_{\mathcal{B}(X,Y)}(\varepsilon^a)$ to denote a generic operator from X to Y whose norm is bounded by $C\varepsilon^a$ for ε small enough.

2 Main Result

As a first step we formulate the problem in a metric graph setting.

We identify the real line $\mathbb{R}$ with the graph $\mathcal{G}^\varepsilon$ made up of three edges (e_1^{out}, e_2^{out}, and $e^{in,\varepsilon}$) and two vertices (v_1 and v_2): $e_1^{out} := [0, +\infty)$, $e_2^{out} := [0, +\infty)$, and $e^{in,\varepsilon} := [-\varepsilon, \varepsilon]$; the points $0 \in e_1^{out}$ and $\varepsilon \in e^{in,\varepsilon}$ are both identified with the vertex v_1; while the points $0 \in e_2^{out}$ and $-\varepsilon \in e^{in,\varepsilon}$ are both identified with the vertex v_2.

Additionally, we divide the graph $\mathcal{G}^\varepsilon$ into an *inner part* and an *outer part*; the inner part coincides with the edge $e^{in,\varepsilon}$ the outer part is constituted by the edges e_1^{out} and e_2^{out}. Associated to this splitting are the Hilbert spaces

$$\mathcal{H}^{out} := L^2(e_1^{out}) \oplus L^2(e_2^{out}) \qquad \text{and} \qquad \mathcal{H}^{in,\varepsilon} := L^2(e^{in,\varepsilon}).$$

The space $\mathcal{H}^\varepsilon := L^2(\mathcal{G}^\varepsilon)$ of square integrable functions on $\mathcal{G}^\varepsilon$ can be understood as the direct sum

$$\mathcal{H}^\varepsilon = \mathcal{H}^{out} \oplus \mathcal{H}^{in,\varepsilon}. \tag{2.1}$$

Given a function $f \in \mathcal{H}^\varepsilon$ we shall denote by f^{out} and f^{in} its components in the decomposition (2.1), and write $f = (f^{out}, f^{in})$; moreover, we shall denote by f_1^{out} and f_2^{out} the components of f^{out} in the decomposition $\mathcal{H}^{out} = L^2(e_1^{out}) \oplus L^2(e_2^{out})$.

We denote by $\mathcal{H}_2^{out}$ and $\mathcal{H}_2^{in,\varepsilon}$ the spaces

$$\mathcal{H}_2^{out} := H^2(e_1^{out}) \oplus H^2(e_2^{out}) \qquad \text{and} \qquad \mathcal{H}_2^{in,\varepsilon} := H^2(e^{in,\varepsilon});$$

and by $\mathcal{H}_2^\varepsilon$ the direct sum

$$\mathcal{H}_2^\varepsilon := \mathcal{H}_2^{out} \oplus \mathcal{H}_2^{in,\varepsilon}.$$

Note that functions in $\mathcal{H}_2^\varepsilon$ are continuous with continuous derivative on the edges of the graph $\mathcal{G}^\varepsilon$ but do not need to be continuous in the vertices.

Set $V^\varepsilon(x) = \varepsilon^{-2} V(x/\varepsilon)$, and assume that V is a bounded real valued function with compact support in $(-1, 1)$.

To rewrite the Hamiltonian h^ε (see Eq. (1.1)) as an operator in $\mathcal{H}^\varepsilon$, we define two maps $\mathbf{\Gamma}_0^\varepsilon$ and $\mathbf{\Gamma}_1^\varepsilon$ as follows

$$\mathbf{\Gamma}_0^\varepsilon : \mathcal{H}_2^\varepsilon \to \mathbb{C}^4\,; \qquad \mathbf{\Gamma}_1^\varepsilon : \mathcal{H}_2^\varepsilon \to \mathbb{C}^4 \tag{2.2}$$

$$\mathbf{\Gamma}_0^\varepsilon f := \begin{pmatrix} f_1^{out}(0) \\ f_2^{out}(0) \\ f^{in\prime}(\varepsilon) \\ -f^{in\prime}(-\varepsilon) \end{pmatrix}; \qquad \mathbf{\Gamma}_1^\varepsilon f := \begin{pmatrix} f_1^{out\prime}(0) \\ f_2^{out\prime}(0) \\ f^{in}(\varepsilon) \\ f^{in}(-\varepsilon) \end{pmatrix}. \tag{2.3}$$

Let us denote by $\mathbf{\Theta}$ be the 4×4 matrix

$$\mathbf{\Theta} := \begin{pmatrix} \mathbb{O}_2 & \mathbb{I}_2 \\ \mathbb{I}_2 & \mathbb{O}_2 \end{pmatrix}, \tag{2.4}$$

and define the self-adjoint operator $\mathbf{H}^\varepsilon$ as

$$D(\mathbf{H}^\varepsilon) := \{ f \in \mathcal{H}_2^\varepsilon |\, \mathbf{\Gamma}_1^\varepsilon f = \mathbf{\Theta} \mathbf{\Gamma}_0^\varepsilon f \} \tag{2.5}$$

$$(\mathbf{H}^\varepsilon f)^{out} = -f^{out\prime\prime}; \qquad (\mathbf{H}^\varepsilon f)^{in} = -f^{in\prime\prime} + V^\varepsilon f^{in} \tag{2.6}$$

(here $f^{out\prime\prime}$ denotes the function in $\mathcal{H}^{out}$ such that $(f^{out\prime\prime})_j = f_j^{out\prime\prime}$, $j = 1, 2$).

It is easy to convince oneself that $\mathbf{H}^\varepsilon$ can be identified, through an obvious identification map between $\mathcal{H}^\varepsilon$ and $L^2(\mathbb{R})$, with the Hamiltonian h^ε defined by Eq. (1.1) on the domain $H^2(\mathbb{R})$. Indeed the *gluing conditions* $\mathbf{\Gamma}_1^\varepsilon f = \mathbf{\Theta} \mathbf{\Gamma}_0^\varepsilon f$ guarantee the continuity of the function and of its first derivative in the vertices v_1 and v_2; the minus sign in the definition of the map $\mathbf{\Gamma}_0^\varepsilon$ takes into account the direction of the derivatives.

In the analysis of the limit, we want to compare the Hamiltonian $\mathbf{H}^\varepsilon$ with limiting operators acting only on the outer Hilbert space $\mathcal{H}^{out}$ (which can obviously be identified with $L^2(\mathbb{R})$ itself). As for $\mathbf{H}^\varepsilon$, to define such operators, we start by defining two maps Γ_0^{out} and Γ_1^{out} as follows

$$\Gamma_0^{out} : \mathcal{H}_2^{out} \to \mathbb{C}^2; \qquad \Gamma_1^{out} : \mathcal{H}_2^{out} \to \mathbb{C}^2$$

$$\Gamma_0^{out} f^{out} := \begin{pmatrix} f_1^{out}(0) \\ f_2^{out}(0) \end{pmatrix}; \qquad \Gamma_1^{out} f^{out} := \begin{pmatrix} f_1^{out\prime}(0) \\ f_2^{out\prime}(0) \end{pmatrix},$$

and denote by $\mathring{H}^{out}$ the self-adjoint operator

$$D(\mathring{H}^{out}) := \{ f^{out} \in \mathcal{H}_2^{out} | \Gamma_0^{out} f^{out} = 0 \}; \qquad \mathring{H}^{out} f^{out} = -f^{out\prime\prime}.$$

Indeed $\mathring{H}^{out}$ is nothing else that the direct sum of two Dirichlet Laplacians on the half-lines identified by e_1^{out} and e_2^{out}.

To cover all the possible limits of $\mathbf{H}^\varepsilon$ we will need also the Hamiltonian defined as follows. For a vector $\underline{\beta} = (\beta_1, \beta_2)^T \in \mathbb{C}^2$ let P_β be the orthogonal projection on its span:

$$P_\beta := \frac{1}{|\underline{\beta}|^2} \begin{pmatrix} |\beta_1|^2 & \beta_1 \bar{\beta}_2 \\ \beta_2 \bar{\beta}_1 & |\beta_2|^2 \end{pmatrix} \equiv \frac{1}{|\underline{\beta}|^2} \underline{\beta} (\underline{\beta}, \cdot)_{\mathbb{C}^2}, \tag{2.7}$$

with $|\underline{\beta}|^2 = |\beta_1|^2 + |\beta_2|^2$; then H_β^{out} denotes the self-adjoint operator

$$D(H_\beta^{out}) := \{f^{out} \in \mathcal{H}_2^{out} | P_\beta^\perp \Gamma_0^{out} f^{out} = 0\,,\ P_\beta \Gamma_1^{out} f^{out} = 0\} \quad H_\beta^{out} f^{out} = -f^{out\prime\prime}. \tag{2.8}$$

We note that H_β^{out} coincides with the "coupling" Hamiltonian described in the introduction with $c_+ = \beta_1$ and $c_- = \beta_2$ (and up to an obvious identification map).

Before stating our main result we still need to introduce: the auxiliary Hamiltonian, that allows us to distinguish between the decoupling and the coupling limiting operators; some identification maps that allow us to compare $\mathbf{H}^\varepsilon$ with $\mathring{H}^{out}$ (or H_β^{out}) as they act on different Hilbert spaces, $\mathcal{H}^\varepsilon$ and $\mathcal{H}^{out}$ respectively.

Set $\mathcal{H}^{in} \equiv \mathcal{H}^{\varepsilon=1,in} = L^2(-1, 1)$ and define the operator

$$\mathring{H}^{in} : \mathcal{H}^{in} \to \mathcal{H}^{in} \tag{2.9}$$

$$D(\mathring{H}^{in}) := \{f^{in} \in \mathcal{H}_2^{in} \equiv H^2(-1, 1) | f^{in\prime}(1) = f^{in\prime}(-1) = 0\} \tag{2.10}$$

$$\mathring{H}^{in} f^{in} := -f^{in\prime\prime} + V f^{in} \tag{2.11}$$

This Hamiltonian coincides with $\mathring{h}$ introduced in Eqs. (1.2)–(1.3). It is well known (see, e.g., [25, Th. 5.7]) that its spectrum consists of discrete and simple eigenvalues, moreover the corresponding eigenfunctions form an orthonormal basis of $\mathcal{H}^{in}$. For $n \in \mathbb{N}$, we denote by λ_n the eigenvalues of $\mathring{H}^{in}$ (arranged in increasing order) and by $\{\varphi_n\}_{n\in\mathbb{N}}$ a corresponding set of orthonormal eigenfunctions.

In the analysis of the limit we distinguish two cases:

Generic (or Non-Resonant) Case. 0 is not an eigenvalue of the operator $\mathring{H}^{in}$.
Non-Generic (or Resonant) Case. 0 is an eigenvalue of the operator $\mathring{H}^{in}$.

In the non-generic case we assume that $\lambda_{n^*} = 0$ and denote by $\varphi_* \equiv \varphi_{n^*}$ the corresponding eigenfunction (of unit norm). Moreover, we define the vector $\underline{c}_* := (\varphi_*(1), \varphi_*(-1))^T \in \mathbb{C}^2$, and the Hamiltonian H_{c_*}, defined through $\underline{c}_*$ according to Eq. (2.8).

Concerning the identification maps, we denote by J the operator which maps $\mathcal{H}^{out}$ in $\mathcal{H}^\varepsilon$. J is defined by

$$J : \mathcal{H}^{out} \to \mathcal{H}^\varepsilon, \qquad Ju = (u, 0) \quad \text{for all } u \in \mathcal{H}^{out}.$$

Its adjoint J^* maps $\mathcal{H}^\varepsilon$ in $\mathcal{H}^{out}$, and is given by:

$$J^* : \mathcal{H}^\varepsilon \to \mathcal{H}^{out}, \qquad J^* f = f^{out} \quad \text{for all } f = (f^{out}, f^{in}) \in \mathcal{H}^\varepsilon.$$

Remark 2.1 $J^* J = \mathbb{I}^{out}$, where $\mathbb{I}^{out}$ is the identity in $\mathcal{H}^{out}$.

To analyze the convergence of operators acting on different Hilbert spaces we use the notion of δ^ε-quasi unitary equivalence introduced by P. Exner and O. Post in the series of works [12–14, 22, 23], see, in particular, [14, Sec. 3.2] and [23, Ch. 4]. We remark that the approach used in [3] is also based on the notion of δ^ε-quasi unitary equivalence of operators acting on different Hilbert spaces (there referred to as convergence in *generalized norm resolvent sense*, see [3, Sec. 5]).

Keeping in mind Rem. 2.1, we have that the operator $\mathbf{H}^\varepsilon$ is δ^ε-quasi unitarily equivalent to a self-adjoint operator H^{out} in $\mathcal{H}^{out}$ if

$$\left\|(\mathbb{I}-JJ^*)(\mathbf{H}^\varepsilon-z)^{-1}\right\|_{\mathcal{B}(\mathcal{H}^\varepsilon)}\leq C\delta^\varepsilon \quad \text{and} \quad \left\|J(H^{out}-z)^{-1}-(\mathbf{H}^\varepsilon-z)^{-1}J\right\|_{\mathcal{B}(\mathcal{H}^{out},\mathcal{H}^\varepsilon)}\leq C\delta^\varepsilon,$$

for some $z\in\mathbb{C}\backslash\mathbb{R}$ with $|\operatorname{Im} z|$ large enough.

Our main result is the following:

Theorem 1 *In the generic case the operator $\mathbf{H}^\varepsilon$ is ε-quasi unitarily equivalent to the operator $\mathring{H}^{out}$; in the non-generic case, the operator $\mathbf{H}^\varepsilon$ is $\varepsilon^{1/2}$-quasi unitarily equivalent to the operator $H^{out}_{c_*}$.*

In particular, for any $z\in\mathbb{C}\backslash\mathbb{R}$ there exist positive constants ε_0 and C such that for all $0<\varepsilon<\varepsilon_0$:

$$\left\|J(\mathring{H}^{out}-z)^{-1}-(\mathbf{H}^\varepsilon-z)^{-1}J\right\|_{\mathcal{B}(\mathcal{H}^{out},\mathcal{H}^\varepsilon)}\leq C\varepsilon \tag{2.12}$$

and

$$\left\|(\mathbb{I}-JJ^*)(\mathbf{H}^\varepsilon-z)^{-1}\right\|_{\mathcal{B}(\mathcal{H}^\varepsilon)}\leq C\varepsilon^{3/2} \tag{2.13}$$

in the generic case; and

$$\left\|J(H^{out}_{c_*}-z)^{-1}-(\mathbf{H}^\varepsilon-z)^{-1}J\right\|_{\mathcal{B}(\mathcal{H}^{out},\mathcal{H}^\varepsilon)}\leq C\varepsilon^{1/2} \tag{2.14}$$

and

$$\left\|(\mathbb{I}-JJ^*)(\mathbf{H}^\varepsilon-z)^{-1}\right\|_{\mathcal{B}(\mathcal{H}^\varepsilon)}\leq C\varepsilon^{1/2} \tag{2.15}$$

in the non-generic case.

Remark 2.2 By Theorem 1 we infer that:

$$\left\|(\mathring{H}^{out}-z)^{-1}J^*-J^*(\mathbf{H}^\varepsilon-z)^{-1}\right\|_{\mathcal{B}(\mathcal{H}^\varepsilon,\mathcal{H}^{out})}\leq C\varepsilon \tag{2.16}$$

in the generic case; and

$$\left\|(H^{out}_{c_*}-z)^{-1}J^*-J^*(\mathbf{H}^\varepsilon-z)^{-1}\right\|_{\mathcal{B}(\mathcal{H}^\varepsilon,\mathcal{H}^{out})}\leq C\varepsilon^{1/2} \tag{2.17}$$

in the non-generic case. Equation (2.16) follows by the trivial inequality

$$\begin{aligned}&\left\|(\mathring{H}^{out}-z)^{-1}J^*-J^*(\mathbf{H}^{\varepsilon}-z)^{-1}\right\|_{\mathcal{B}(\mathcal{H}^{\varepsilon},\mathcal{H}^{out})}\\ \leq&\left\|J^*\big(J(\mathring{H}^{out}-z)^{-1}-(\mathbf{H}^{\varepsilon}-z)^{-1}J\big)J^*\right\|_{\mathcal{B}(\mathcal{H}^{\varepsilon},\mathcal{H}^{out})}+\left\|J^*(\mathbf{H}^{\varepsilon}-z)^{-1}(JJ^*-\mathbb{I})\right\|_{\mathcal{B}(\mathcal{H}^{\varepsilon},\mathcal{H}^{out})}\end{aligned}$$

together with the bounds (2.12) and (2.13), and by using

$$\|J^*\|_{\mathcal{B}(\mathcal{H}^{\varepsilon},\mathcal{H}^{out})}=1\quad\text{and}\quad\left\|(\mathbf{H}^{\varepsilon}-z)^{-1}(JJ^*-\mathbb{I})\right\|_{\mathcal{B}(\mathcal{H}^{\varepsilon})}=\left\|(JJ^*-\mathbb{I})(\mathbf{H}^{\varepsilon}-\bar{z})^{-1}\right\|_{\mathcal{B}(\mathcal{H}^{\varepsilon})}.$$

The bound (2.17), is obtained in a similar way. We refer to [23] for a comprehensive discussion on the comparison between operators acting on different spaces.

3 Kreĭn resolvent Formula

Aim of this section is to obtain a Kreĭn-type formula for the resolvent of $\mathbf{H}^{\varepsilon}$, defined as $\mathbf{R}^{\varepsilon}(z):=(\mathbf{H}^{\varepsilon}-z)^{-1}$, for $z\in\rho(\mathbf{H}^{\varepsilon})$. We shall use some known result of self-adjoint theory of symmetric operators and boundary triples, see, e.g, [5, 16, 20, 21, 24]. For the most we shall follow the approach and notation from [20, 21, 24].

We shall define first several operators in the outer (see Sect. 3.1) and inner (see Sect. 3.2) space. The formula for $\mathbf{R}^{\varepsilon}(z)$ is obtained in Sect. 3.3.

3.1 Operators in the Outer Space

It is well known that the resolvent set of the operator $\mathring{H}^{out}$ is $\rho(\mathring{H}^{out})=\mathbb{C}\backslash[0,+\infty)$. For all $z\in\mathbb{C}\backslash[0,+\infty)$ we denote by $\mathring{R}^{out}(z)$ the resolvent of $\mathring{H}^{out}$, defined as $\mathring{R}^{out}(z):=(\mathring{H}^{out}-z)^{-1}$. The explicit form of $\mathring{R}^{out}(z)$ is given by

$$\mathring{R}^{out}(z)=\mathrm{diag}(r_0(z),r_0(z)).$$

By the latter formula we mean: $(\mathring{R}^{out}(z)f^{out})_j=r_0(z)f_j^{out}$. Here $r_0(z)$ is the resolvent of the Dirichlet Laplacian in $L^2(0,+\infty)$, its integral kernel (denoted by the same symbol) is

$$r_0(z;x,y)=\frac{ie^{i\sqrt{z}|x-y|}}{2\sqrt{z}}-\frac{ie^{i\sqrt{z}(x+y)}}{2\sqrt{z}}\qquad z\in\mathbb{C}\backslash[0,+\infty)\,,\ \mathrm{Im}\,\sqrt{z}>0\,,\ x,y\in\mathbb{R}_+.$$

We define the map

$$\breve{G}^{out}(z):\mathcal{H}^{out}\to\mathbb{C}^2\,;\qquad\breve{G}^{out}(z):=\Gamma_1^{out}\,\mathring{R}^{out}(z)\,;\qquad z\in\mathbb{C}\backslash[0,+\infty).$$

Note that

$$(\breve{G}^{out}(z)f^{out})_j = (r_0(z)f_j^{out})'(0) = \int_0^\infty e^{i\sqrt{z}y} f_j^{out}(y)dy \qquad j = 1, 2.$$

One can write $\breve{G}^{out}(z) = \mathrm{diag}((\overline{e^{i\sqrt{z}\cdot}}, \cdot)_{L^2(e_1^{out})}, (\overline{e^{i\sqrt{z}\cdot}}, \cdot)_{L^2(e_2^{out})})$. The map $\breve{G}^{out}(z)$ is bounded as an operator from $\mathcal{H}^{out}$ to $\mathbb{C}^2$.

We denote by $G^{out}(z)$ the adjoint of $\breve{G}^{out}(\bar{z})$

$$G^{out}(z) : \mathbb{C}^2 \to \mathcal{H}^{out}\ ; \qquad G^{out}(z) := (\breve{G}^{out}(\bar{z}))^*.$$

It is easy to see that for any vector $\underline{v} \in \mathbb{C}^2$

$$(G^{out}(z)\underline{v})_j = e^{i\sqrt{z}x} v_j\,, \qquad j = 1, 2\,,\ x \in [0, +\infty);$$

one can write $G^{out}(z) = \mathrm{diag}(e^{i\sqrt{z}\cdot}, e^{i\sqrt{z}\cdot})$. The map $G^{out}(z)$ is bounded as an operator from $\mathbb{C}^2$ to $\mathcal{H}^{out}$. Finally we define the map

$$Q^{out}(z) : \mathbb{C}^2 \to \mathbb{C}^2\ ; \qquad Q^{out}(z) := \Gamma_1^{out}\, G^{out}(z).$$

It is easy to see that $Q^{out}(z)$ is the 2×2 matrix given by $Q^{out}(z) = i\sqrt{z}\,\mathbb{I}_2$.

For all $z \in \rho(H_\beta^{out})$ we denote by $R_\beta^{out}(z)$ the resolvent of the Hamiltonian H_β^{out} defined in Eq. (2.8), $R_\beta^{out}(z) := (H_\beta^{out} - z)^{-1}$. $R_\beta^{out}(z)$ can be expressed through the Kreĭn formula

$$R_\beta^{out}(z) = \mathring{R}^{out}(z) - \frac{1}{i\sqrt{z}} G^{out}(z) P_\beta \breve{G}^{out}(z). \tag{3.1}$$

That $R_\beta^{out}(z)$ is the resolvent of H_β^{out} can be checked by an explicit calculation, noticing that for all $f^{out} \in \mathcal{H}^{out}$ one has $R_\beta^{out}(z)f^{out} \in D(H_\beta^{out})$ and $-\big(R_\beta^{out}(z)f^{out}\big)'' - zR_\beta^{out}(z)f^{out} = f^{out}$. It is also easy to convince oneself that $\rho(H_\beta^{out}) = \mathbb{C}\backslash[0, +\infty)$.

3.2 Operators in the Inner Space

We define two maps $\Gamma_0^{in,\varepsilon}$ and $\Gamma_1^{in,\varepsilon}$ as follows

$$\Gamma_0^{in,\varepsilon} : \mathcal{H}_2^{in,\varepsilon} \to \mathbb{C}^2\ ; \qquad \Gamma_1^{in,\varepsilon} : \mathcal{H}_2^{in,\varepsilon} \to \mathbb{C}^2$$

$$\Gamma_0^{in,\varepsilon} f^{in} := \begin{pmatrix} f^{in\prime}(\varepsilon) \\ -f^{in\prime}(-\varepsilon) \end{pmatrix}\ ; \qquad \Gamma_1^{in,\varepsilon} f^{in} := \begin{pmatrix} f^{in}(\varepsilon) \\ f^{in}(-\varepsilon) \end{pmatrix}$$

Let $\mathring{H}^{in,\varepsilon}$ denote the self-adjoint operator

$$D(\mathring{H}^{in,\varepsilon}) := \{f^{in} \in \mathcal{H}_2^{in,\varepsilon} | \Gamma_0^{in,\varepsilon} f^{in} = 0\}\,; \qquad \mathring{H}^{in,\varepsilon} f^{in} = -f^{in\prime\prime} + V^{\varepsilon} f^{in}. \tag{3.2}$$

For all $z \in \rho(\mathring{H}^{in,\varepsilon})$ we denote by $\mathring{R}^{in,\varepsilon}(z)$ the resolvent of $\mathring{H}^{in,\varepsilon}$, defined as $\mathring{R}^{in,\varepsilon}(z) := (\mathring{H}^{in,\varepsilon} - z)^{-1}$.

The spectrum of $H^{in,\varepsilon}$ consists of isolated simple eigenvalues. To write down its resolvent we use a decompositions in eigenfunctions. For $n \in \mathbb{N}$ we denote by λ_n^{ε} the eigenvalues of $H^{in,\varepsilon}$ (arranged in increasing order) and by $\{\varphi_n^{\varepsilon}\}_{n\in\mathbb{N}}$ a corresponding set of orthonormal eigenfunctions. We have that

$$\mathring{R}^{in,\varepsilon}(z; x, y) = \sum_{n\in\mathbb{N}} \frac{\varphi_n^{\varepsilon}(x)\varphi_n^{\varepsilon}(y)}{\lambda_n^{\varepsilon} - z} \qquad z \in \mathbb{C}\,,\ z \neq \lambda_n^{\varepsilon}.$$

For any fixed $\varepsilon > 0$, this series converges uniformly because λ_n^{ε} diverges as n^2 as $n \to \infty$ and φ_n^{ε} are uniformly bounded, see, e.g., [26, Sec. 1.12].

We want to define maps which are analogous to $G^{out}(z)$, $\breve{G}^{out}(z)$, $Q^{out}(z)$. To get explicit formulae we introduce the following notation: For any eigenfunction φ_n^{ε} we define the vector $\underline{c}_n^{\varepsilon} := (\varphi_n^{\varepsilon}(\varepsilon), \varphi_n^{\varepsilon}(-\varepsilon))^T \in \mathbb{C}^2$

Next, we define the map

$$\breve{G}^{in,\varepsilon}(z) : \mathcal{H}^{in,\varepsilon} \to \mathbb{C}^2\,; \qquad \breve{G}^{in,\varepsilon}(z) := \Gamma_1^{in,\varepsilon}\, \mathring{R}^{in,\varepsilon}(z) \qquad z \in \mathbb{C}\,,\ z \neq \lambda_n^{\varepsilon}.$$

Note that

$$\breve{G}^{in,\varepsilon}(z) = \sum_{n\in\mathbb{N}} \frac{\underline{c}_n^{\varepsilon}(\varphi_n^{\varepsilon}, \cdot)_{\mathcal{H}^{in,\varepsilon}}}{\lambda_n^{\varepsilon} - z}.$$

We denote by $G^{in,\varepsilon}(z)$ the adjoint of $\breve{G}^{\varepsilon,in}(\bar{z})$

$$G^{in,\varepsilon}(z) : \mathbb{C}^2 \to \mathcal{H}^{in,\varepsilon}\,; \qquad G^{in,\varepsilon}(z) := (\breve{G}^{in,\varepsilon}(\bar{z}))^*,$$

it is easy to see that

$$G^{in,\varepsilon}(z) = \sum_{n\in\mathbb{N}} \frac{\varphi_n^{\varepsilon}(\underline{c}_n^{\varepsilon}, \cdot)_{\mathbb{C}^2}}{\lambda_n^{\varepsilon} - z}.$$

Finally we define the map (2×2 z-valued matrix)

$$Q^{in,\varepsilon}(z) : \mathbb{C}^2 \to \mathbb{C}^2\,; \qquad Q^{in,\varepsilon}(z) := \Gamma_1^{in,\varepsilon}\, G^{in,\varepsilon}(z).$$

It is easy to see that

$$Q^{in,\varepsilon}(z) = \sum_{n\in\mathbb{N}} \frac{\underline{c}_n^{\varepsilon}(\underline{c}_n^{\varepsilon},\cdot)_{\mathbb{C}^2}}{\lambda_n^{\varepsilon} - z}.$$

3.3 Operator in the Full Space

Keeping in mind the decomposition $\mathcal{H}^{\varepsilon} = \mathcal{H}^{out} \oplus \mathcal{H}^{in,\varepsilon}$ we note that the maps $\mathbf{\Gamma}_0^{\varepsilon}$ and $\mathbf{\Gamma}_1^{\varepsilon}$ defined in Eqs. (2.2) and (2.3) can be written as $\mathbf{\Gamma}_0^{\varepsilon} = \mathrm{diag}(\Gamma_0^{out}, \Gamma_0^{in,\varepsilon})$ and $\mathbf{\Gamma}_1^{\varepsilon} = \mathrm{diag}(\Gamma_1^{out}, \Gamma_1^{in,\varepsilon})$.

For all $z \in \rho(\mathbf{H}^{\varepsilon})$ we denote by $\mathbf{R}^{\varepsilon}(z)$ the resolvent of $\mathbf{H}^{\varepsilon}$, defined as $\mathbf{R}^{\varepsilon}(z) := (\mathbf{H}^{\varepsilon} - z)^{-1}$.

We look for a Kreĭn resolvent formula for $\mathbf{R}^{\varepsilon}(z)$. To this aim we define first the operator

$$\mathring{\mathbf{H}}^{\varepsilon} := \mathrm{diag}(\mathring{H}^{out}, \mathring{H}^{in,\varepsilon});$$

it is worth noticing that

$$D(\mathring{\mathbf{H}}^{\varepsilon}) = \{f \in \mathcal{H}_2^{\varepsilon} |\, \mathbf{\Gamma}_0^{\varepsilon} f = 0\}.$$

Moreover, since the operator is diagonal in the direct sum $\mathcal{H}^{out} \oplus \mathcal{H}^{in,\varepsilon}$, one has that

$$\mathring{\mathbf{R}}^{\varepsilon}(z) := (\mathring{\mathbf{H}}^{\varepsilon} - z)^{-1} = \mathrm{diag}(\mathring{R}^{out}(z), \mathring{R}^{in,\varepsilon}(z)).$$

We define the maps

$$\breve{\mathbf{G}}^{\varepsilon}(z) : \mathcal{H}^{\varepsilon} \to \mathbb{C}^4\,; \qquad \breve{\mathbf{G}}^{\varepsilon}(z) := \mathbf{\Gamma}_1^{\varepsilon}\,\mathring{\mathbf{R}}^{\varepsilon}(z)$$

and

$$\mathbf{G}^{\varepsilon}(z) : \mathbb{C}^4 \to \mathcal{H}^{\varepsilon}\,; \qquad \mathbf{G}^{\varepsilon}(z) := (\breve{\mathbf{G}}^{\varepsilon}(\bar{z}))^*.$$

It is easy to convince oneself that

$$\breve{\mathbf{G}}^{\varepsilon}(z) = \mathrm{diag}(\breve{G}^{out}(z), \breve{G}^{in,\varepsilon}(z)) \qquad \text{and} \qquad \mathbf{G}^{\varepsilon}(z) = \mathrm{diag}(G^{out}(z), G^{in,\varepsilon}(z)).$$

We apply $\mathbf{\Gamma}_1^{\varepsilon}$ to $\mathbf{G}^{\varepsilon}(z)$ and define the map (z-dependent 4×4 matrix)

$$\mathbf{Q}^{\varepsilon}(z) : \mathbb{C}^4 \to \mathbb{C}^4\,; \qquad \mathbf{Q}^{\varepsilon}(z) := \mathbf{\Gamma}_1^{\varepsilon}\,\mathbf{G}^{\varepsilon}(z). \tag{3.3}$$

One has that

$$\mathbf{Q}^{\varepsilon}(z) = \begin{pmatrix} i\sqrt{z}\,\mathbb{I}_2 & \mathbb{O}_2 \\ \mathbb{O}_2 & Q^{in,\varepsilon}(z) \end{pmatrix}.$$

We remark that $\mathbf{G}^{\varepsilon}(z)$ and $\mathbf{Q}^{\varepsilon}(z)$ are the *gamma-field* and the *Weyl-function* associated to the boundary triple $(\mathbb{C}^4, \mathbf{\Gamma}_0^{\varepsilon}, \mathbf{\Gamma}_1^{\varepsilon})$ for the operator $\mathbf{H}_{max}^{\varepsilon *}$, we refer to the proof of Theorem 2 below for more details.

Theorem 2 *Let* $\mathbf{\Theta}$ *be as in Eq.* (2.4)*. For any* $z \in \rho(\mathbf{H}^{\varepsilon}) \cap \rho(\mathring{\mathbf{H}}^{\varepsilon})$ *the map*

$$(\mathbf{Q}^{\varepsilon}(z) - \mathbf{\Theta}) : \mathbb{C}^4 \to \mathbb{C}^4$$

is invertible and the resolvent $\mathbf{R}^{\varepsilon}(z)$ *is given by*

$$\mathbf{R}^{\varepsilon}(z) = \mathring{\mathbf{R}}^{\varepsilon}(z) - \mathbf{G}^{\varepsilon}(z)\big(\mathbf{Q}^{\varepsilon}(z) - \mathbf{\Theta}\big)^{-1}\check{\mathbf{G}}^{\varepsilon}(z). \tag{3.4}$$

Proof Denote by $\mathbf{H}_{min}^{\varepsilon}$ the restriction of $\mathring{\mathbf{H}}^{\varepsilon}$ to the domain

$$D(\mathbf{H}_{min}^{\varepsilon}) := \{f \in \mathcal{H}_2^{\varepsilon} |\, \mathbf{\Gamma}_0^{\varepsilon} f = 0;\ \mathbf{\Gamma}_1^{\varepsilon} f = 0\}.$$

$\mathbf{H}_{min}^{\varepsilon}$ is a densely defined symmetric operator on $\mathcal{H}^{\varepsilon}$. Its adjoint $\mathbf{H}_{max}^{\varepsilon} := \mathbf{H}_{min}^{\varepsilon *}$ is

$$D(\mathbf{H}_{max}^{\varepsilon}) = \mathcal{H}_2^{\varepsilon}$$

$$(\mathbf{H}_{max}^{\varepsilon} f)^{out} = -f^{out\prime\prime}; \qquad (\mathbf{H}_{max}^{\varepsilon} f)^{in} = -f^{in\prime\prime} + V^{\varepsilon} f^{in}.$$

We note that $(\mathbb{C}^4, \mathbf{\Gamma}_0^{\varepsilon}, \mathbf{\Gamma}_1^{\varepsilon})$ is a boundary triple for $\mathbf{H}_{max}^{\varepsilon *}$, i.e.,

$$(f, \mathbf{H}_{max}^{\varepsilon *} g)_{\mathcal{H}^{\varepsilon}} - (\mathbf{H}_{max}^{\varepsilon *} f, g)_{\mathcal{H}^{\varepsilon}} = (\mathbf{\Gamma}_0^{\varepsilon} f, \mathbf{\Gamma}_1^{\varepsilon} g)_{\mathbb{C}^4} - (\mathbf{\Gamma}_1^{\varepsilon} f, \mathbf{\Gamma}_1^{\varepsilon} g)_{\mathbb{C}^4}$$

for all $f, g \in D(\mathbf{H}_{max}^{\varepsilon *})$, and the mapping $\mathbf{\Gamma}^{\varepsilon} : D(\mathbf{H}_{max}^{\varepsilon *}) \to \mathbb{C}^4 \oplus \mathbb{C}^4$, $\mathbf{\Gamma}^{\varepsilon} f := (\mathbf{\Gamma}_0^{\varepsilon} f, \mathbf{\Gamma}_1^{\varepsilon} f)$ is surjective. For an introduction to the theory of boundary triples we refer to [24, Ch. 14], see also [5].

In what follows we will show that the map $\mathbf{G}^{\varepsilon}(z)$ is the gamma-field associated to the triple $(\mathbb{C}^4, \mathbf{\Gamma}_0^{\varepsilon}, \mathbf{\Gamma}_1^{\varepsilon})$, i.e., it is the inverse of the map $\mathbf{\Gamma}_0^{\varepsilon}$ restricted to $\mathrm{Ker}(\mathbf{H}_{max}^{\varepsilon *} - z)$, $\mathbf{\Gamma}_0^{\varepsilon} \restriction_{\mathrm{Ker}(\mathbf{H}_{max}^{\varepsilon *} - z)} : \mathrm{Ker}(\mathbf{H}_{max}^{\varepsilon *} - z) \to \mathbb{C}^4$, see [24, Def. 14.4].

For each $z \in \rho(\mathring{\mathbf{H}}^{\varepsilon})$, the map $\mathbf{\Gamma}_0^{\varepsilon} \restriction_{\mathrm{Ker}(\mathbf{H}_{max}^{\varepsilon *} - z)}$ is invertible, see [24, Lem. 14.13]. Hence, for any $\underline{v} \in \mathbb{C}^4$ there exists a unique $f_v \in \mathrm{Ker}(\mathbf{H}_{max}^{\varepsilon *} - z)$ such that $\mathbf{\Gamma}_0^{\varepsilon} f_v = \underline{v}$.

For any $g \in \mathcal{H}^\varepsilon$ one has that

$$\begin{aligned}(\mathbf{G}^\varepsilon(z)\underline{v}, g)_{\mathcal{H}^\varepsilon} = (\underline{v}, \check{\mathbf{G}}^\varepsilon(\bar{z})g)_{\mathbb{C}^4} &= (\mathbf{\Gamma}_0^\varepsilon f_v, \mathbf{\Gamma}_1 \mathring{\mathbf{R}}^\varepsilon(\bar{z})g)_{\mathbb{C}^4} \\ &= (\mathbf{\Gamma}_0^\varepsilon f_v, \mathbf{\Gamma}_1 \mathring{\mathbf{R}}^\varepsilon(\bar{z})g)_{\mathbb{C}^4} - (\mathbf{\Gamma}_1^\varepsilon f_v, \mathbf{\Gamma}_0 \mathring{\mathbf{R}}^\varepsilon(\bar{z})g)_{\mathbb{C}^4} \\ &= \big(f_v, (\mathbf{H}_{max}^{\varepsilon *} - \bar{z})\mathring{\mathbf{R}}^\varepsilon(\bar{z})g\big)_{\mathcal{H}^\varepsilon} - \big((\mathbf{H}_{max}^{\varepsilon *} - z) f_v, \mathring{\mathbf{R}}^\varepsilon(\bar{z})g\big)_{\mathcal{H}^\varepsilon} \\ &= \big(f_v, g\big)_{\mathcal{H}^\varepsilon}\end{aligned}$$

hence, $\mathbf{G}^\varepsilon(z)\underline{v} = f_v \in \mathrm{Ker}(\mathbf{H}_{max}^{\varepsilon *} - z)$ for all $\underline{v} \in \mathbb{C}^4$. By the latter identity it immediately follows that $\mathbf{\Gamma}_0^\varepsilon \mathbf{G}^\varepsilon(z)\underline{v} = \underline{v}$ for all $\underline{v} \in \mathbb{C}^4$.

By [24, Def. 14.4], the map $\mathbf{Q}^\varepsilon(z)$ defined in Eq. (3.3), is the Weyl-function of the operator $\mathring{\mathbf{H}}^\varepsilon$ associated with the boundary triple $(\mathbb{C}^4, \mathbf{\Gamma}_0^\varepsilon, \mathbf{\Gamma}_1^\varepsilon)$.

By Eq. (14.13), and Th. 14.18 (see Eq. (14.43)) in [24], it follows that the map $(\mathbf{Q}^\varepsilon(z) - \mathbf{\Theta}) : \mathbb{C}^4 \to \mathbb{C}^4$ is invertible for all $z \in \rho(\mathbf{H}^\varepsilon) \cap \rho(\mathring{\mathbf{H}}^\varepsilon)$, and $\mathbf{R}^\varepsilon(z)$ in Eq. (3.4) is the resolvent of the operator $\mathbf{H}^\varepsilon$ defined by Eqs. (2.5) and (2.6). □

We conclude this section by noticing that, by using the inversion formula for block matrices, one has

$$\big(\mathbf{Q}^\varepsilon(z) - \mathbf{\Theta}\big)^{-1} = \begin{pmatrix} Q^{in,\varepsilon}(z)(i\sqrt{z}Q^{in,\varepsilon}(z) - \mathbb{I}_2)^{-1} & (i\sqrt{z}Q^{in,\varepsilon}(z) - \mathbb{I}_2)^{-1} \\ (i\sqrt{z}Q^{in,\varepsilon}(z) - \mathbb{I}_2)^{-1} & i\sqrt{z}(i\sqrt{z}Q^{in,\varepsilon}(z) - \mathbb{I}_2)^{-1} \end{pmatrix}$$

and that the second term in Eq. (3.4), to be understood as an operator in $\mathcal{H}^{out} \oplus \mathcal{H}^{in,\varepsilon}$, can be written as

$$\begin{aligned}&\mathbf{G}^\varepsilon(z)\big(\mathbf{Q}^\varepsilon(z) - \mathbf{\Theta}\big)^{-1}\check{\mathbf{G}}^\varepsilon(z) \\ &= \begin{pmatrix} G^{out}(z)Q^{in,\varepsilon}(z)(i\sqrt{z}Q^{in,\varepsilon}(z) - \mathbb{I}_2)^{-1}\check{G}^{out}(z) & G^{out}(z)(i\sqrt{z}Q^{in,\varepsilon}(z) - \mathbb{I}_2)^{-1}\check{G}^{in,\varepsilon}(z) \\ G^{in,\varepsilon}(z)(i\sqrt{z}Q^{in,\varepsilon}(z) - \mathbb{I}_2)^{-1}\check{G}^{out}(z) & i\sqrt{z}\,G^{in,\varepsilon}(z)(i\sqrt{z}Q^{in,\varepsilon}(z) - \mathbb{I}_2)^{-1}\check{G}^{in,\varepsilon}(z) \end{pmatrix}.\end{aligned} \tag{3.5}$$

4 Limit of $\mathbf{R}^\varepsilon(z)$

In this section we study the limit of $\mathbf{R}^\varepsilon(z)$ as $\varepsilon \to 0$. To understand the limit we must understand the asymptotic properties of the items in formula (3.5).

We start by pointing out a scaling property of the operator $\mathring{H}^{in,\varepsilon}$, see Eq. (3.2). Recall that $\mathcal{H}^{in,\varepsilon} = L^2(e^{in,\varepsilon}) = L^2(-\varepsilon, \varepsilon)$ and we have set $\mathcal{H}^{in} \equiv \mathcal{H}^{\varepsilon=1,in}$. Define the unitary scaling group

$$U^\varepsilon : \mathcal{H}^{in} \to \mathcal{H}^{in,\varepsilon}\,; \qquad (U^\varepsilon f^{in})(x) := \varepsilon^{-1/2} f^{in}(x/\varepsilon),$$

and its inverse

$$U^{\varepsilon-1}:\mathcal{H}^{in,\varepsilon}\to\mathcal{H}^{in}\,;\qquad (U^{\varepsilon-1}f^{in})(x):=\varepsilon^{1/2}f^{in}(\varepsilon x).$$

It is easy to check that $\mathring{H}^{in,\varepsilon}=\varepsilon^{-2}U^{\varepsilon}\mathring{H}^{in}U^{\varepsilon-1}$, where $\mathring{H}^{in}$ is the auxiliary Hamiltonian defined in Eqs. (2.9)–(2.11). Due to the unitary scaling $\mathring{H}^{in,\varepsilon}=\varepsilon^{-2}U^{\varepsilon}\mathring{H}^{in}U^{\varepsilon-1}$ we have that

$$\lambda_n^{\varepsilon}=\varepsilon^{-2}\lambda_n\,;\qquad \varphi_n^{\varepsilon}(x)=\varepsilon^{-1/2}\varphi_n(x/\varepsilon).$$

Hence, we can write the integral kernel of the resolvent $\mathring{R}^{in,\varepsilon}(z)$ as

$$\mathring{R}^{in,\varepsilon}(z;x,y)=\varepsilon^2\sum_{n\in\mathbb{N}}\frac{\varphi_n^{\varepsilon}(x)\varphi_n^{\varepsilon}(y)}{\lambda_n-\varepsilon^2 z}=\varepsilon\sum_{n\in\mathbb{N}}\frac{\varphi_n(x/\varepsilon)\varphi_n(y/\varepsilon)}{\lambda_n-\varepsilon^2 z}\qquad x,y\in[-\varepsilon,\varepsilon]. \tag{4.1}$$

In a similar way, we can write the operators $\breve{G}^{in,\varepsilon}(z)$ and $G^{in,\varepsilon}(z)$ and the matrix $Q^{in,\varepsilon}(z)$. We proceed as we did in Sect. 3.2 and for any eigenfunction φ_n we define the vector $\underline{c}_n$ as $\underline{c}_n=(\varphi_n(1),\varphi_n(-1))^T\in\mathbb{C}^2$. Obviously, one has that $\underline{c}_n^{\varepsilon}=\varepsilon^{-1/2}\underline{c}_n$, where $\underline{c}_n^{\varepsilon}$ was defined in Sect. 3.2. By using the scaling properties in the formula for the operators we are interested in, we obtain

$$\breve{G}^{in,\varepsilon}(z)=\varepsilon^{3/2}\sum_{n\in\mathbb{N}}\frac{\underline{c}_n(\varphi_n^{\varepsilon},\cdot)_{\mathcal{H}^{in,\varepsilon}}}{\lambda_n-\varepsilon^2 z}\,;\qquad G^{in,\varepsilon}(z)=\varepsilon^{3/2}\sum_{n\in\mathbb{N}}\frac{\varphi_n^{\varepsilon}(\underline{c}_n,\cdot)_{\mathbb{C}^2}}{\lambda_n-\varepsilon^2 z}, \tag{4.2}$$

and

$$Q^{in,\varepsilon}(z)=\varepsilon\sum_{n\in\mathbb{N}}\frac{\underline{c}_n(\underline{c}_n,\cdot)_{\mathbb{C}^2}}{\lambda_n-\varepsilon^2 z}. \tag{4.3}$$

These formulae will be used in the study of the limit of $\mathbf{R}^{\varepsilon}(z)$.

4.1 Limiting Hamiltonian: Generic Case

In this section we study the limit of the relevant quantities and prove Theorem 1 in the generic case.

Proposition 4.1 *Let $z\in\mathbb{C}\backslash\mathbb{R}$. In the generic case,*

$$\mathring{R}^{in,\varepsilon}(z)=\mathcal{O}_{\mathcal{B}(\mathcal{H}^{in,\varepsilon})}(\varepsilon^2); \tag{4.4}$$

$$\breve{G}^{in,\varepsilon}(z)=\mathcal{O}_{\mathcal{B}(\mathcal{H}^{in,\varepsilon},\mathbb{C}^2)}(\varepsilon^{3/2})\,;\qquad G^{in,\varepsilon}(z)=\mathcal{O}_{\mathcal{B}(\mathbb{C}^2,\mathcal{H}^{in,\varepsilon})}(\varepsilon^{3/2}). \tag{4.5}$$

Proof We prove first claim (4.4). For any $f^{in} \in \mathcal{H}^{in,\varepsilon}$, since $\{\varphi_n^\varepsilon\}_{n\in\mathbb{N}}$ is an orthonormal set of eigenfunctions in $\mathcal{H}^{in,\varepsilon}$, and by Eq. (4.1), we infer

$$\|\mathring{R}^{in,\varepsilon}(z)f^{in}\|_{\mathcal{H}^{in,\varepsilon}} = \varepsilon^2\left(\sum_{n\in\mathbb{N}}\frac{|(\varphi_n^\varepsilon, f^{in})_{\mathcal{H}^{in,\varepsilon}}|^2}{|\lambda_n-\varepsilon^2 z|^2}\right)^{1/2} \leq C\varepsilon^2\|f^{in}\|_{\mathcal{H}^{in,\varepsilon}},$$

where in the latter inequality we used the bound $1/|\lambda_n-\varepsilon^2 z|^2 \leq \frac{4}{|\lambda_n|^2} \leq C$, which holds true in the generic case because $|\lambda_n-\varepsilon^2 z| \geq |\lambda_n|/2 \geq C$ for all $n\in\mathbb{N}$ and ε small enough.

To prove the first claim in Eq. (4.5), note that for any $f^{in} \in \mathcal{H}^{in,\varepsilon}$, by Eq. (4.2) and Cauchy-Schwarz inequality, one has

$$\|\check{G}^{in,\varepsilon}(z)f^{in}\|_{\mathbb{C}^2} \leq \varepsilon^{3/2}\|f^{in}\|_{\mathcal{H}^{in,\varepsilon}}\left(\sum_{n\in\mathbb{N}}\frac{\|\underline{c}_n\|_{\mathbb{C}^2}^2}{|\lambda_n-\varepsilon^2 z|^2}\right)^{1/2} \leq C\,\varepsilon^{3/2}\|f^{in}\|_{\mathcal{H}^{in,\varepsilon}},$$

because $\|\underline{c}_n\|_{\mathbb{C}^2}^2 \leq C$ and $\sum_{n\in\mathbb{N}}\frac{1}{|\lambda_n-\varepsilon^2 z|^2} \leq C\sum_{n\in\mathbb{N}}\frac{1}{|\lambda_n|^2} \leq C$. This proves the first statement in claim (4.5). The second claim is trivial, being $G^{in,\varepsilon}(z)$ the adjoint of $\check{G}^{in,\varepsilon}(\bar{z})$. □

Proposition 4.2 *Let $z\in\mathbb{C}\backslash\mathbb{R}$. In the generic case,*

$$Q^{in,\varepsilon}(z) = \mathcal{O}_{\mathcal{B}(\mathbb{C}^2)}(\varepsilon).$$

Proof We note that $\left|\sum_{n\in\mathbb{N}}\frac{\varphi_n(\pm1)\varphi_n(\pm1)}{\lambda_n-\varepsilon^2 z}\right| \leq C\sum_{n\in\mathbb{N}}\frac{1}{|\lambda_n-\varepsilon^2 z|} \leq C$, hence, by Eq. (4.3), it follows that $\|Q^{in,\varepsilon}(z)\|_{\mathcal{B}(\mathbb{C}^2)} \leq C\,\varepsilon$. □

We are now ready to prove the main theorem on the convergence of the resolvent in the generic case.

Proof of Theorem 1: Generic Case We prove first that

$$J\mathring{R}^{out}(z) - \mathbf{R}^\varepsilon(z)J = \mathcal{O}_{\mathcal{B}(\mathcal{H}^{out},\mathcal{H}^\varepsilon)}(\varepsilon). \tag{4.6}$$

We note that in this case $(i\sqrt{z}Q^{in,\varepsilon}(z)-\mathbb{I}_2)^{-1} = \mathcal{O}_{\mathcal{B}(\mathbb{C}^2)}(1)$. Moreover we have the identity

$$J\mathring{R}^{out}(z) - \mathbf{R}^\varepsilon(z)J = \mathbf{G}^\varepsilon(z)\big(\mathbf{Q}^\varepsilon(z)-\mathbf{\Theta}\big)^{-1}\check{\mathbf{G}}^\varepsilon(z)J.$$

Hence, see Eq. (3.5), claim (4.6) follows from

$$G^{out}(z)Q^{in,\varepsilon}(z)(i\sqrt{z}Q^{in,\varepsilon}(z)-\mathbb{I}_2)^{-1}\check{G}^{out}(z) = \mathcal{O}_{\mathcal{B}(\mathcal{H}^{out},\mathcal{H}^{out})}(\varepsilon)$$

and

$$G^{in,\varepsilon}(z)(i\sqrt{z}Q^{in,\varepsilon}(z)-\mathbb{I}_2)^{-1}\breve{G}^{out}(z)=\mathcal{O}_{\mathcal{B}(\mathcal{H}^{out},\mathcal{H}^{in,\varepsilon})}(\varepsilon^{3/2}). \tag{4.7}$$

We are left to prove that

$$(\mathbb{I}-JJ^*)\mathbf{R}^{\varepsilon}(z)=\mathcal{O}_{\mathcal{B}(\mathcal{H}^{\varepsilon})}(\varepsilon^{3/2}). \tag{4.8}$$

We start by noticing the identity $(\mathbb{I}-JJ^*)\mathbf{R}^{\varepsilon}(z)f=(0,(\mathbf{R}^{\varepsilon}(z)f)^{in})$, from which it follows that $\|(\mathbb{I}-JJ^*)\mathbf{R}^{\varepsilon}(z)f\|_{\mathcal{H}^{\varepsilon}}=\|(\mathbf{R}^{\varepsilon}(z)f)^{in}\|_{\mathcal{H}^{in,\varepsilon}}$, for all $f=(f^{out},f^{in})\in\mathcal{H}^{\varepsilon}$. Next, note that by Eqs. (3.4) and (3.5) it follows that

$$\begin{aligned}(\mathbf{R}^{\varepsilon}(z)f)^{in}=&\mathring{R}^{in,\varepsilon}(z)f^{in}-i\sqrt{z}\,G^{in,\varepsilon}(z)(i\sqrt{z}Q^{in,\varepsilon}(z)-\mathbb{I}_2)^{-1}\breve{G}^{in,\varepsilon}(z)f^{in}\\&-G^{in,\varepsilon}(z)(i\sqrt{z}Q^{in,\varepsilon}(z)-\mathbb{I}_2)^{-1}\breve{G}^{out}(z)f^{out}.\end{aligned} \tag{4.9}$$

The latter term at the r.h.s. is bounded by $C\varepsilon^{3/2}\|f^{out}\|_{\mathcal{H}^{out}}$ by Eq. (4.7). Concerning the first two terms at the r.h.s., we note that

$$\begin{aligned}\mathring{R}^{in,\varepsilon}(z)-i\sqrt{z}\,G^{in,\varepsilon}(z)(i\sqrt{z}Q^{in,\varepsilon}(z)-\mathbb{I}_2)^{-1}\breve{G}^{in,\varepsilon}(z)&=\mathcal{O}_{\mathcal{B}(\mathcal{H}^{in,\varepsilon})}(\varepsilon^2)+\mathcal{O}_{\mathcal{B}(\mathcal{H}^{in,\varepsilon})}(\varepsilon^3)\\&=\mathcal{O}_{\mathcal{B}(\mathcal{H}^{in,\varepsilon})}(\varepsilon^2)\end{aligned}$$

by Proposition 4.1 and since $(i\sqrt{z}Q^{in,\varepsilon}(z)-\mathbb{I}_2)^{-1}=\mathcal{O}_{\mathcal{B}(\mathbb{C}^2)}(1)$.

This concludes the proof of Theorem 1 in the generic case. The non-generic Case is analyzed in the next section. □

4.2 *Limiting Hamiltonian: Non-generic Case*

In this section we study the limit of the relevant quantities and prove Theorem 1 in the non-generic case.

Proposition 4.3 *Let $z\in\mathbb{C}\backslash\mathbb{R}$. In the non-generic case*

$$\mathring{R}^{in,\varepsilon}(z)=-\frac{\varphi^{\varepsilon}_*(\varphi^{\varepsilon}_*,\cdot)_{\mathcal{H}^{in,\varepsilon}}}{z}+\mathcal{O}_{\mathcal{B}(\mathcal{H}^{in,\varepsilon})}(\varepsilon^2); \tag{4.10}$$

$$\breve{G}^{in,\varepsilon}(z)=-\frac{\underline{c}_*(\varphi^{\varepsilon}_*,\cdot)_{\mathcal{H}^{in,\varepsilon}}}{\varepsilon^{1/2}z}+\mathcal{O}_{\mathcal{B}(\mathcal{H}^{in,\varepsilon},\mathbb{C}^2)}(\varepsilon^{3/2}); \tag{4.11}$$

$$G^{in,\varepsilon}(z)=-\frac{\varphi^{\varepsilon}_*(\underline{c}_*,\cdot)_{\mathbb{C}^2}}{\varepsilon^{1/2}z}+\mathcal{O}_{\mathcal{B}(\mathbb{C}^2,\mathcal{H}^{in,\varepsilon})}(\varepsilon^{3/2}). \tag{4.12}$$

Proof We prove first claim (4.10). By Eq. (4.1), we infer

$$\mathring{R}^{in,\varepsilon}(z) = -\frac{\varphi_*^\varepsilon(\varphi_*^\varepsilon,\cdot)_{\mathcal{H}^{in,\varepsilon}}}{z} + \varepsilon^2 \sum_{n\in\mathbb{N},n\neq n^*} \frac{\varphi_n^\varepsilon(\varphi_n^\varepsilon,\cdot)_{\mathcal{H}^{in,\varepsilon}}}{\lambda_n - \varepsilon^2 z}.$$

Taking into account the fact that $\{\varphi_n^\varepsilon\}_{n\in\mathbb{N}}$ in an orthonormal set of eigenfunctions in $\mathcal{H}^\varepsilon$, it follows that, for all $f^{in} \in \mathcal{H}^{in,\varepsilon}$,

$$\left\| \varepsilon^2 \sum_{n\in\mathbb{N},n\neq n^*} \frac{\varphi_n^\varepsilon(\varphi_n^\varepsilon, f^{in})_{\mathcal{H}^{in,\varepsilon}}}{\lambda_n - \varepsilon^2 z} \right\|_{\mathcal{H}^{in,\varepsilon}} = \varepsilon^2 \left(\sum_{n\in\mathbb{N},n\neq n^*} \frac{|(\varphi_n^\varepsilon, f^{in})_{\mathcal{H}^{in,\varepsilon}}|^2}{|\lambda_n - \varepsilon^2 z|^2} \right)^{1/2} \leq C\varepsilon^2 \|f^{in}\|_{\mathcal{H}^{in,\varepsilon}},$$

see also the proof of claim (4.4).

To prove claim (4.11), we start by noticing that by Eq. (4.2)

$$\check{G}^{in,\varepsilon}(z) = -\frac{\underline{c}_*(\varphi_*^\varepsilon,\cdot)_{\mathcal{H}^{in,\varepsilon}}}{\varepsilon^{1/2} z} + \varepsilon^{3/2} \sum_{n\in\mathbb{N},n\neq n^*} \frac{\underline{c}_n(\varphi_n^\varepsilon,\cdot)_{\mathcal{H}^{in,\varepsilon}}}{\lambda_n - \varepsilon^2 z},$$

and reason in the same way as in the proof of Proposition 4.1. Claim (4.12) follows straightforwardly, being $G^{in,\varepsilon}(z)$ the adjoint of $\check{G}^{in,\varepsilon}(\bar{z})$. □

We denote by P_{c_*} the projection obtained by setting $\underline{\beta} = \underline{c}_*$ in Eq. (2.7).

Proposition 4.4 *Let $z \in \mathbb{C}\backslash\mathbb{R}$. In the non-generic case,*

$$Q^{in,\varepsilon}(z) = -\frac{|\underline{c}_*|^2}{\varepsilon z} P_{c_*} + \mathcal{O}_{\mathcal{B}(\mathbb{C}^2)}(\varepsilon). \tag{4.13}$$

Moreover,

$$(i\sqrt{z}Q^{in,\varepsilon}(z) - \mathbb{I}_2)^{-1} = \frac{i\varepsilon\sqrt{z}}{|\underline{c}_*|^2} P_{c_*} + \mathcal{O}_{\mathcal{B}(\mathbb{C}^2)}(\varepsilon^2) - P_{c_*}^\perp(\mathbb{I}_2 + \mathcal{O}_{\mathcal{B}(\mathbb{C}^2)}(\varepsilon)), \tag{4.14}$$

$$= \frac{i\varepsilon\sqrt{z}}{|\underline{c}_*|^2} P_{c_*} + \mathcal{O}_{\mathcal{B}(\mathbb{C}^2)}(\varepsilon^2) - (\mathbb{I}_2 + \mathcal{O}_{\mathcal{B}(\mathbb{C}^2)}(\varepsilon)) P_{c_*}^\perp, \tag{4.15}$$

and

$$Q^{in,\varepsilon}(z)(i\sqrt{z}Q^{in,\varepsilon}(z) - \mathbb{I}_2)^{-1} = \frac{1}{i\sqrt{z}} P_{c_*} + \mathcal{O}_{\mathcal{B}(\mathbb{C}^2)}(\varepsilon). \tag{4.16}$$

Proof Claim (4.13) immediately follows after noticing that

$$Q^{in,\varepsilon}(z) = -\frac{\underline{c}_*(\underline{c}_*,\cdot)_{\mathbb{C}^2}}{\varepsilon z} + \varepsilon \sum_{n\in\mathbb{N}, n\neq n^*} \frac{\underline{c}_n(\underline{c}_n,\cdot)_{\mathbb{C}^2}}{\lambda_n - \varepsilon^2 z}.$$

Next we prove claim (4.14). We start by noticing the a-priori bound

$$(i\sqrt{z}Q^{in,\varepsilon}(z) - \mathbb{I}_2)^{-1} = \mathcal{O}_{\mathcal{B}(\mathbb{C}^2)}(1). \tag{4.17}$$

To prove bound (4.17) we use the trivial identity

$$(i\sqrt{z}Q^{in,\varepsilon}(z) - \mathbb{I}_2)^{-1} = -i(Q^{in,\varepsilon}(z) + i\mathbb{I}_2/\sqrt{z})^{-1}/\sqrt{z},$$

and the identities

$$Q^{in,\varepsilon}(z) - Q^{in,\varepsilon}(\bar{z}) = 2i\,\breve{G}^{in,\varepsilon}(\bar{z})G^{in,\varepsilon}(z)\,\mathrm{Im}\,z, \qquad (Q^{in,\varepsilon}(z))^* = Q^{in,\varepsilon}(\bar{z}),$$

see, e.g., [24, Prop. 14.15] or [20, Eqs. (5) and (7.1)]. The latter identities, taking into account also $G^{in,\varepsilon}(z) = (\breve{G}^{in,\varepsilon}(\bar{z}))^*$ and the expansion (4.12), give

$$\begin{aligned}\mathrm{Im}(\underline{v}, Q^{in,\varepsilon}(z)\underline{v})_{\mathbb{C}^2} =& \frac{\big(\underline{v}, (Q^{in,\varepsilon}(z) - Q^{in,\varepsilon}(\bar{z}))\underline{v}\big)_{\mathbb{C}^2}}{2i} = \|G^{in,\varepsilon}(z)\underline{v}\|^2_{\mathcal{H}^{in,\varepsilon}}\,\mathrm{Im}\,z \\ =& \frac{|(\underline{c}_*, \underline{v})_{\mathbb{C}^2}|^2}{\varepsilon|z|^2}\,\mathrm{Im}\,z + \mathcal{O}(\varepsilon).\end{aligned}$$

Hence,

$$\begin{aligned}|(\underline{v}, (Q^{in,\varepsilon}(z) + i\mathbb{I}_2/\sqrt{z})\underline{v})_{\mathbb{C}^2}| \geq& |\,\mathrm{Im}(\underline{v}, (Q^{in,\varepsilon}(z) + i\mathbb{I}_2/\sqrt{z})\underline{v})_{\mathbb{C}^2}| \\ =& \left|\frac{|(\underline{c}_*, \underline{v})_{\mathbb{C}^2}|^2}{\varepsilon|z|^2}\,\mathrm{Im}\,z + \mathcal{O}(\varepsilon) + \frac{\|\underline{v}\|^2_{\mathbb{C}^2}}{|z|}\,\mathrm{Re}\,\sqrt{z}\right|.\end{aligned} \tag{4.18}$$

Recalling that $z \in \mathbb{C}\backslash\mathbb{R}$ and that our choice for the determination of the square root is $\mathrm{Im}\,\sqrt{z} > 0$, we have that $\mathrm{Im}\,z$ and $\mathrm{Re}\,\sqrt{z}$ are both not zero and have the same sign. From the latter considerations, and from the lower bound (4.18), we infer that for ε small enough

$$|(\underline{v}, (Q^{in,\varepsilon}(z) + i\mathbb{I}_2/\sqrt{z})\underline{v})_{\mathbb{C}^2}| \geq \frac{1}{2}\left|\frac{|(\underline{c}_*, \underline{v})_{\mathbb{C}^2}|^2}{\varepsilon|z|^2}\,\mathrm{Im}\,z + \frac{\|\underline{v}\|^2_{\mathbb{C}^2}}{|z|}\,\mathrm{Re}\,\sqrt{z}\right| > 0$$

for all $\underline{v} \neq 0$, which in turn implies (4.17).

To obtain (4.14), we use the identity

$$
\begin{aligned}
(i\sqrt{z}Q^{in,\varepsilon}(z)-\mathbb{I}_2)^{-1} &= \left(i\sqrt{z}\left(Q^{in,\varepsilon}(z)+\frac{|\underline{c}_*|^2}{\varepsilon z}P_{c_*}\right)-\frac{i|\underline{c}_*|^2}{\varepsilon\sqrt{z}}P_{c_*}-\mathbb{I}_2\right)^{-1}\\
&= -\left(\frac{i|\underline{c}_*|^2}{\varepsilon\sqrt{z}}P_{c_*}+\mathbb{I}_2\right)^{-1}+i\sqrt{z}\left(\frac{i|\underline{c}_*|^2}{\varepsilon\sqrt{z}}P_{c_*}+\mathbb{I}_2\right)^{-1}\\
&\quad\left(Q^{in,\varepsilon}(z)+\frac{|\underline{c}_*|^2}{\varepsilon z}P_{c_*}\right)(i\sqrt{z}Q^{in,\varepsilon}(z)-\mathbb{I}_2)^{-1}.
\end{aligned}
$$

Since

$$
\left(\frac{i|\underline{c}_*|^2}{\varepsilon\sqrt{z}}P_{c_*}+\mathbb{I}_2\right)^{-1}=\left(\frac{i|\underline{c}_*|^2}{\varepsilon\sqrt{z}}+1\right)^{-1}P_{c_*}+P_{c_*}^{\perp}=-\frac{i\varepsilon\sqrt{z}}{|\underline{c}_*|^2}P_{c_*}+\mathcal{O}_{\mathcal{B}(\mathbb{C}^2)}(\varepsilon^2)+P_{c_*}^{\perp},
$$

and by using the expansion (4.13) and the a-priori bound (4.17), we obtain

$$
\begin{aligned}
&(i\sqrt{z}Q^{in,\varepsilon}(z)-\mathbb{I}_2)^{-1}\\
=&\frac{i\varepsilon\sqrt{z}}{|\underline{c}_*|^2}P_{c_*}+\mathcal{O}_{\mathcal{B}(\mathbb{C}^2)}(\varepsilon^2)-P_{c_*}^{\perp}+\left(-\frac{i\varepsilon\sqrt{z}}{|\underline{c}_*|^2}P_{c_*}+\mathcal{O}_{\mathcal{B}(\mathbb{C}^2)}(\varepsilon^2)+P_{c_*}^{\perp}\right)\mathcal{O}_{\mathcal{B}(\mathbb{C}^2)}(\varepsilon)\\
=&\frac{i\varepsilon\sqrt{z}}{|\underline{c}_*|^2}P_{c_*}+\mathcal{O}_{\mathcal{B}(\mathbb{C}^2)}(\varepsilon^2)-P_{c_*}^{\perp}(\mathbb{I}_2+\mathcal{O}_{\mathcal{B}(\mathbb{C}^2)}(\varepsilon)).
\end{aligned}
$$

Since $(Q^{in,\varepsilon}(\bar{z}))^* = Q^{in,\varepsilon}(z)$ and $\overline{i\sqrt{\bar{z}}} = i\sqrt{z}$, we have that $(i\sqrt{\bar{z}}Q^{in,\varepsilon}(\bar{z})-\mathbb{I}_2)^{-1*} = (i\sqrt{z}Q^{in,\varepsilon}(z)-\mathbb{I}_2)^{-1}$, from which we obtain formula (4.15).

Claim (4.16) follows immediately by taking into account expansions (4.13) and (4.14). □

We are now ready to prove the main theorem on the convergence of the resolvent in the non-generic case.

In what follows we denote by $R_{c_*}^{out}(z)$ the resolvent of the Hamiltonian $H_{c_*}^{out}$, its expression is obtained by setting $\underline{\beta} = \underline{c}_*$ in Eq. (3.1).

***Proof of Theorem** 1: Non-generic Case* We start by proving the bound (2.14), i.e., that

$$
J R_{c_*}^{out}(z) - \mathbf{R}^{\varepsilon}(z)J = \mathcal{O}_{\mathcal{B}(\mathcal{H}^{out},\mathcal{H}^{\varepsilon})}(\varepsilon^{1/2}). \tag{4.19}
$$

We have the identity

$$
J R_{c_*}^{out}(z) - \mathbf{R}^{\varepsilon}(z)J = \mathbf{G}^{\varepsilon}(z)\big(\mathbf{Q}^{\varepsilon}(z)-\mathbf{\Theta}\big)^{-1}\breve{\mathbf{G}}^{\varepsilon}(z)J - J\frac{1}{i\sqrt{z}}G^{out}(z)P_{c_*}\breve{G}^{out}(z),
$$

which is a direct consequence of Eqs. (3.1) (with $\underline{\beta} = \underline{c}_*$) and Eq. (3.4). Taking into account the explicit formula (3.5), claim (4.19) follows from

$$G^{out}(z)\left(Q^{in,\varepsilon}(z)(i\sqrt{z}Q^{in,\varepsilon}(z)-\mathbb{I}_2)^{-1}-\frac{1}{i\sqrt{z}}P_{c_*}\right)\check{G}^{out}(z)=\mathcal{O}_{\mathcal{B}(\mathcal{H}^{out},\mathcal{H}^{out})}(\varepsilon)$$

and

$$G^{in,\varepsilon}(z)(i\sqrt{z}Q^{in,\varepsilon}(z)-\mathbb{I}_2)^{-1}\check{G}^{out}(z)=\mathcal{O}_{\mathcal{B}(\mathcal{H}^{out},\mathcal{H}^{in,\varepsilon})}(\varepsilon^{1/2}). \tag{4.20}$$

Note that in the latter step we used the fact that the term $P_{c_*}^{\perp}\mathcal{O}_{\mathcal{B}(\mathbb{C}^2)}(1)$ in Eq. (4.14) does not produce a factor $\varepsilon^{-1/2}$ from the expansion in Eq. (4.12) because $(\underline{c}_*, P_{c_*}^{\perp}\underline{v})_{\mathbb{C}^2}=0$ for all $\underline{v}\in\mathbb{C}^2$.

We are left to prove the bound (2.15), i.e., that

$$(\mathbb{I}-JJ^*)\mathbf{R}^{\varepsilon}(z)=\mathcal{O}_{\mathcal{B}(\mathcal{H}^{\varepsilon})}(\varepsilon^{1/2}).$$

Reasoning as in the proof of claim (4.8), see also Eq. (4.9), we have that a contribution of order $\varepsilon^{1/2}$ comes from the term in Eq. (4.20). For the remaining terms in Eq. (4.9) we have the bound

$$\mathring{R}^{in,\varepsilon}(z)-i\sqrt{z}\,G^{in,\varepsilon}(z)(i\sqrt{z}Q^{in,\varepsilon}(z)-\mathbb{I}_2)^{-1}\check{G}^{in,\varepsilon}(z)=\mathcal{O}_{\mathcal{B}(\mathcal{H}^{in,\varepsilon})}(\varepsilon). \tag{4.21}$$

To prove the latter, we use expansions (4.11), (4.12), and (4.14) to obtain

$$\begin{aligned}
&i\sqrt{z}\,G^{in,\varepsilon}(z)(i\sqrt{z}Q^{in,\varepsilon}(z)-\mathbb{I}_2)^{-1}\check{G}^{in,\varepsilon}(z)\\
&\quad=i\sqrt{z}\left(-\frac{\varphi_*^{\varepsilon}(\underline{c}_*,\cdot)_{\mathbb{C}^2}}{\varepsilon^{1/2}z}+\mathcal{O}_{\mathcal{B}(\mathbb{C}^2,\mathcal{H}^{in,\varepsilon})}(\varepsilon^{3/2})\right)\\
&\qquad\left(\frac{i\varepsilon\sqrt{z}}{|\underline{c}_*|^2}P_{c_*}+\mathcal{O}_{\mathcal{B}(\mathbb{C}^2)}(\varepsilon^2)+P_{c_*}^{\perp}\mathcal{O}_{\mathcal{B}(\mathbb{C}^2)}(1)\right)\\
&\qquad\left(-\frac{\underline{c}_*(\varphi_*^{\varepsilon},\cdot)_{\mathcal{H}^{in,\varepsilon}}}{\varepsilon^{1/2}z}+\mathcal{O}_{\mathcal{B}(\mathcal{H}^{in,\varepsilon},\mathbb{C}^2)}(\varepsilon^{3/2})\right).
\end{aligned}$$

Taking into account the fact that $(\underline{c}_*, P_{c_*}^{\perp}\underline{v})_{\mathbb{C}^2}$ and $P_{c_*}\underline{c}_*=\underline{c}_*$, we obtain

$$\begin{aligned}
&i\sqrt{z}\,G^{in,\varepsilon}(z)(i\sqrt{z}Q^{in,\varepsilon}(z)-\mathbb{I}_2)^{-1}\check{G}^{in,\varepsilon}(z)\\
&\quad=i\sqrt{z}\left(-\frac{i\varepsilon^{1/2}}{|\underline{c}_*|^2\sqrt{z}}\varphi_*^{\varepsilon}(\underline{c}_*,\cdot)_{\mathbb{C}^2}+\mathcal{O}_{\mathcal{B}(\mathbb{C}^2,\mathcal{H}^{in,\varepsilon})}(\varepsilon^{3/2})\right)\\
&\qquad\left(-\frac{\underline{c}_*(\varphi_*^{\varepsilon},\cdot)_{\mathcal{H}^{in,\varepsilon}}}{\varepsilon^{1/2}z}+\mathcal{O}_{\mathcal{B}(\mathcal{H}^{in,\varepsilon},\mathbb{C}^2)}(\varepsilon^{3/2})\right)\\
&\quad=-\frac{\varphi_*^{\varepsilon}(\varphi_*^{\varepsilon},\cdot)_{\mathcal{H}^{in,\varepsilon}}}{z}+\mathcal{O}_{\mathcal{B}(\mathcal{H}^{in,\varepsilon})}(\varepsilon),
\end{aligned}$$

which together with expansion (4.10), gives Eq. (4.21) and concludes the proof of the non-generic case in Theorem 1. □

References

1. Albeverio, S., Cacciapuoti, C., and Finco, D., *Coupling in the singular limit of thin quantum waveguides*, J. Math. Phys. **48** (2007), 032103.
2. Berkolaiko, G. and Kuchment, P., *Introduction to quantum graphs*, Mathematical Surveys and Monographs, vol. 186, American Mathematical Society, Providence, RI, 2013.
3. Berkolaiko, G., Latushkin, Y., and Sukhtaiev, S., *Limits of quantum graph operators with shrinking edges*, Adv. Math. **352** (2019), 632–669.
4. Bollé, D., Gesztesy, F., and Wilk, S. F. J., *A complete treatment of low-energy scattering in one dimension*, J. Operator Theory **13** (1985), no. 1, 3–32.
5. Brüning, J., Geyler, V., and Pankrashkin, K., *Spectra of self-adjoint extensions and applications to solvable Schrödinger operators*, Rev. Math. Phys. **20** (2008), no. 1, 1–70.
6. Cacciapuoti, C., *Graph-like asymptotics for the Dirichlet Laplacian in connected tubular domains*, Analysis, Geometry and Number Theory **2** (2017), 25–58.
7. Cacciapuoti, C. and Exner, P., *Nontrivial edge coupling from a Dirichlet network squeezing: the case of a bent waveguide*, J. Phys. A **40** (2007), no. 26, F511–F523.
8. Cheon, T. and Exner, P., *An approximation to δ' couplings on graphs*, J. Phys. A **37** (2004), no. 29, L329–L335.
9. Cheon, T., Exner, P., and Turek, O., *Approximation of a general singular vertex coupling in quantum graphs*, Ann. Physics **325** (2010), no. 3, 548–578.
10. Exner, P. and Man'ko, S. S., *Approximations of quantum-graph vertex couplings by singularly scaled potentials*, J. Phys. A **46** (2013), no. 34, 345202.
11. Exner, P. and Man'ko, S. S., *Approximations of quantum-graph vertex couplings by singularly scaled rank-one operators*, Lett. Math. Phys. **104** (2014), no. 9, 1079–1094.
12. Exner, P. and Post, O., *Convergence of spectra of graph-like thin manifolds*, J. Geom. Phys. **54** (2005), 77–115.
13. Exner, P. and Post, O., *Quantum networks modelled by graphs*, AIP Conference Proceedings **998** (2008), no. 1, 1–17.
14. Exner, P. and Post, O., *Approximation of quantum graph vertex couplings by scaled Schrödinger operators on thin branched manifolds*, J. Phys. A **42** (2009), 415305, 22pp.
15. Golovaty, Yu D. and Hryniv, R. O., *On norm resolvent convergence of Schrödinger operators with δ'-like potentials*, J. Phys. A **43** (2010), no. 15, 155204.
16. Gorbachuk, V. I. and Gorbachuk, M. L., *Boundary value problems for operator differential equations*, Mathematics and its Applications (Soviet Series), vol. 48, Kluwer Academic Publishers Group, Dordrecht, 1991, Translated and revised from the 1984 Russian original.
17. Man'ko, S. S., *Schrödinger operators on star graphs with singularly scaled potentials supported near the vertices*, J. Math. Phys. **53** (2012), no. 12, 123521, 13.
18. Man'ko, S. S., *Quantum-graph vertex couplings: some old and new approximations*, Math. Bohem. **139** (2014), no. 2, 259–267.
19. Man'ko, S. S., *On δ'-couplings at graph vertices*, Mathematical results in quantum mechanics, World Sci. Publ., Hackensack, NJ, 2015, pp. 305–313.
20. Posilicano, A., *A Kreĭn-like formula for singular perturbations of self-adjoint operators and applications*, J. Funct. Anal. **183** (2001), no. 1, 109–147.
21. Posilicano, A., *Self-adjoint extensions of restrictions*, Oper. Matrices **2** (2008), no. 4, 483–506.
22. Post, O., *Spectral convergence of quasi-one-dimensional spaces*, Ann. Henri Poincaré **7** (2006), 933–973.

23. Post, O., *Spectral analysis on graph-like spaces*, vol. 2039, Springer Science & Business Media, 2012.
24. Schmüdgen, K., *Unbounded self-adjoint operators on Hilbert space*, Graduate Texts in Mathematics, vol. 265, Springer, Dordrecht, 2012.
25. Teschl, G., *Ordinary differential equations and dynamical systems*, Graduate Studies in Mathematics, vol. 140, American Mathematical Society, Providence, RI, 2012.
26. Titchmarsh, E. C., *Eigenfunction expansions associated with second-order differential equations. Part I*, Second Edition, Clarendon Press, Oxford, 1962.

Ground States of the L^2-Critical NLS Equation with Localized Nonlinearity on a Tadpole Graph

Simone Dovetta and Lorenzo Tentarelli

Abstract The paper aims at giving a first insight on the existence/nonexistence of ground states for the L^2-critical NLS equation on metric graphs with localized nonlinearity. As a consequence, we focus on the tadpole graph, which, albeit being a toy model, allows to point out some specific features of the problem, whose understanding will be useful for future investigations. More precisely, we prove that there exists an interval of masses for which ground states do exist, and that for large masses the functional is unbounded from below, whereas for small masses ground states cannot exist although the functional is bounded.

Keywords Minimization · Metric graphs · Critical growth · Nonlinear Schrödinger equation · Localized nonlinearity

AMS Subject Classification 5R02, 35Q55, 81Q35, 49J40

1 Introduction

The study of evolution equations on *metric graphs* or networks has gained a great popularity in recent years, since they represent effective models for the study of the dynamics of physical systems living in branched spatial structures (see, e.g., [10, 12] and the references therein). More precisely, a particular interest has been addressed

S. Dovetta (✉)
Istituto di Matematica Applicata e Tecnologie Informatiche "E. Magenes", Consiglio Nazionale delle Ricerche, Pavia, Italy

Dipartimento di Matematica "G. Peano", Università degli Studi di Torino, Torino, Italy
e-mail: simone.dovetta@imati.cnr.it

L. Tentarelli
Dipartimento di Scienze Matematiche "G.L. Lagrange", Politecnico di Torino, Torino, Italy
e-mail: lorenzo.tentarelli@polito.it

F. M. Atay et al. (eds.), *Discrete and Continuous Models in the Theory of Networks*, Operator Theory: Advances and Applications 281,
https://doi.org/10.1007/978-3-030-44097-8_5

to the investigation of the *focusing* nonlinear Schrödinger (a.k.a. NLS) equation, namely

$$\imath\dot{\psi} = -\psi'' - |\psi|^{p-2}\psi \qquad (p \geq 2) \tag{1}$$

with suitable boundary conditions at the vertices of the graph, as it is supposed to well approximate, for $p = 4$, the behavior of Bose–Einstein condensates in ramified traps (see, e.g., [22]).

From the mathematical point of view, the discussion is mainly focused on the study of the stationary solutions of (1), that is functions of the form $\psi(t, x) = e^{i\lambda t}u(x)$, with $\lambda \in \mathbb{R}$, solving the stationary equation associated to (1)

$$u'' + |u|^{p-2}u = \lambda u\,.$$

In this perspective, the first pioneering works (e.g., [1–3], and subsequently [4]) concern the study of the so-called *infinite N-star* graph (see Fig. 1), with boundary conditions of *δ-type* or *δ′-type*.

On the other hand, in the case of *Kirchhoff conditions*, that is functions with the sum of the derivatives equal to zero at the vertices (see (7) below), more complex topologies have been managed (e.g., Fig. 2). In [7–9, 23] there is a discussion of the existence of *ground states*, namely solutions of (1) arising as global minimizers of the NLS energy functional

$$E(u) := \frac{1}{2}\int_{\mathcal{G}} |u'|^2\,dx - \frac{1}{p}\int_{\mathcal{G}} |u|^p\,dx \tag{2}$$

among functions with fixed mass $\mu > 0$, i.e. $\int_{\mathcal{G}} |u|^2\,dx = \mu$. Precisely, [7, 8] investigate the so-called L^2-subcritical regime $p \in (2, 6)$, while [9] treats the critical case $p = 6$. Furthermore, in [11, 15, 27, 28] the investigation has been extended to more general stationary solutions that do not necessarily minimize the energy functional.

A modification of this model, proposed e.g. by Gnutzmann et al. [21] and Noja [26], arises when one assumes that the nonlinearity affects only the *compact core*

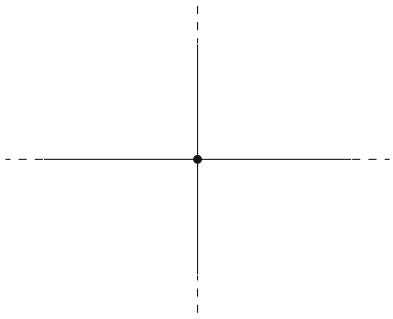

Fig. 1 Infinite N-star graph ($N = 4$)

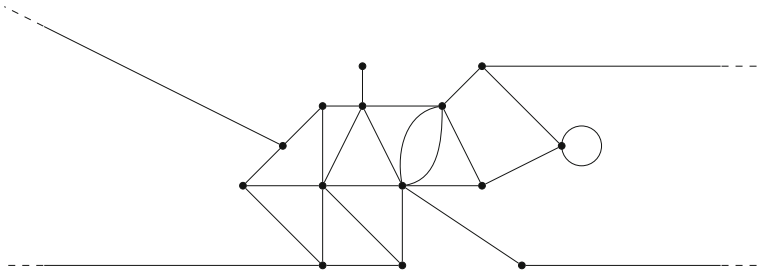

Fig. 2 A general noncompact metric graph

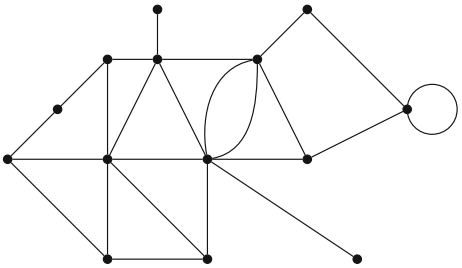

Fig. 3 The compact core of the graph in Fig. 2

$\mathcal{K}$ of the graph, namely the subgraph consisting of all its bounded edges (e.g., the compact core of Fig. 1 is empty, while the one of Fig. 2 is given by Fig. 3). In this case, the stationary equation of interest reads as

$$u'' + \chi_{\mathcal{K}}|u|^{p-2}u = \lambda u \qquad (+\text{ Kirch. cond.}), \tag{3}$$

with $\chi_{\mathcal{K}}$ denoting the characteristic function of $\mathcal{K}$.

The existence of solutions to this problem has been widely investigated in the L^2-subcritical case in [30–32]. In particular, [32] discusses the existence of the ground states of the modified energy functional

$$E(u,\mathcal{K}) := \frac{1}{2}\int_{\mathcal{G}} |u'|^2\,dx - \frac{1}{p}\int_{\mathcal{K}} |u|^p\,dx, \tag{4}$$

while [30, 31] manage more general stationary solutions.

In this paper we aim at giving a first insight on the existence/nonexistence of ground states of the problem with the *localized nonlinearity* in the critical case $p = 6$. In particular, as a preliminary study, we explore a specific graph, the *tadpole* graph (see Fig. 4), which allows to point out some peculiar features of the problem whose understanding will suggest interesting perspectives for future investigations. More precisely, in our main result (namely, Theorem 2.1) we prove, first, that there exists a threshold mass μ_1 under which ground states cannot exist even though the

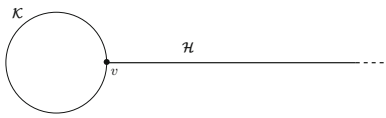

Fig. 4 A tadpole graph

functional $E(\cdot, \mathcal{K})$ is bounded from below. Therefore, we establish the existence of another threshold $\mu_2 \geq \mu_1$ such that, if $\mu \in [\mu_2, \mu_{\mathbb{R}}]$ (where $\mu_{\mathbb{R}}$ is the *critical mass* of the real line defined by (8)), then a ground state does exist; and, finally, that, for all $\mu > \mu_{\mathbb{R}}$, $E(\cdot, \mathcal{K})$ is unbounded from below.

For the sake of completeness we also mention some other recent works on the stationary solutions of the NLS equation on graphs. Problems with a wide class of δ-type conditions and external potentials are managed in [14, 16]. On the other hand, [18, 24] discuss compact graphs, while [5, 6, 20, 29] focus on periodic graphs (i.e., graphs whose noncompactness is not due to the presence of half-lines, but to the infinite number of edges). Finally, it is worth quoting three further works on evolution equations on graphs. The former is [19], where is presented a preliminary result of Control Theory on graphs for the bi-linear Schrödinger equation; then [25] introduces the study of the Airy equation (thus opening to the application of metric graphs in hydrodynamics); and, finally, [13] discusses the bound states of another important dispersive equation on graph, the NonLinear Dirac (NLD) equation.

The paper is organized as follows. In Sect. 2 we present a precise setting of the problem and we state our main result (Theorem 2.1). In Sect. 3 we show some preliminary results, mainly concerning compactness issues, while Sect. 4 provides the proof of the main theorem of the paper.

2 Setting and Main Results

We consider the *tadpole* graph $\mathcal{T}$ (Fig. 4), that is a connected noncompact metric graph consisting of a compact circle $\mathcal{K}$ and a half-line $\mathcal{H}$ (endowed with the usual intrinsic parametrization—see [7]) incident at the vertex v.

A function $u : \mathcal{T} \to \mathbb{R}$ can be seen as a couple of functions (v, w), with $v : \mathcal{K} \to \mathbb{R}$ and $w : \mathcal{H} \to \mathbb{R}$, and thus Lebesgue and Sobolev spaces can be defined as usual

$$L^p(\mathcal{T}) := \{u : \mathcal{T} \to \mathbb{R} : v \in L^p(\mathcal{K}),\ w \in L^p(\mathcal{H})\}$$

and

$$H^1(\mathcal{T}) := \{u : \mathcal{T} \to \mathbb{R} \text{ continuous} : v \in H^1(\mathcal{K}),\ w \in H^1(\mathcal{H})\}.$$

We also define, for $\mu > 0$,

$$H^1_\mu(\mathcal{T}) := \left\{ u \in H^1(\mathcal{T}) : \int_{\mathcal{T}} |u|^2 \, dx = \mu \right\}.$$

We address the problem of the existence of a function $u \in H^1_\mu(\mathcal{T})$ such that $E(u, \mathcal{K}) = \mathcal{E}_{\mathcal{K}}(\mu)$, where

$$E(u, \mathcal{K}) := \frac{1}{2} \int_{\mathcal{T}} |u'|^2 \, dx - \frac{1}{6} \int_{\mathcal{K}} |u|^6 \, dx \tag{5}$$

and

$$\mathcal{E}_{\mathcal{K}}(\mu) := \inf_{u \in H^1_\mu(\mathcal{T})} E(u, \mathcal{K}). \tag{6}$$

It is clear that such a minimizer u, usually called *ground state*, satisfies

$$\begin{cases} v'' + |v|^4 v = \lambda v \\ w'' = \lambda w \end{cases}$$

(for some $\lambda > 0$) and

$$v'(0) - v'(L) + w'(0) = 0 \tag{7}$$

where $L := |\mathcal{K}|$ and we have considered an anti-clockwise parametrization of $\mathcal{K}$, i.e. u solves the stationary NLS equation (3) on $\mathcal{T}$.

Remark 2.1 We limit ourselves to consider real valued functions in the search of ground states since it can be shown that minimizers of the NLS energy are always real valued up to the multiplication times a constant phase (for more see [7, 32]). It is also possible to prove, by an easy regularity argument, that a ground state cannot be equal to zero at any point of the graph.

Before stating the main result of the paper, it is worth recalling some well-known facts on the ground states of the complete problem, i.e. with the nonlinearity extended on the whole graph. Precisely, we have to introduce the concept of *critical mass*, as the existence of a minimizer in the critical case $p = 6$ is strictly connected to the value of the mass.

When $\mathcal{G} = \mathbb{R}$ (see [17]),

$$\inf_{u \in H^1_\mu(\mathbb{R})} E(u) = \begin{cases} 0 & \text{if } \mu \le \mu_{\mathbb{R}} \\ -\infty & \text{if } \mu > \mu_{\mathbb{R}} \end{cases} \qquad \left(\mu_{\mathbb{R}} = \frac{\sqrt{3}}{2}\pi\right) \tag{8}$$

and the infimum is attained only at $\mu = \mu_{\mathbb{R}}$; whereas, when $\mathcal{G} = \mathbb{R}^+$,

$$\inf_{u \in H^1_\mu(\mathbb{R}^+)} E(u) = \begin{cases} 0 & \text{if } \mu \leq \mu_{\mathbb{R}^+} \\ -\infty & \text{if } \mu > \mu_{\mathbb{R}^+} \end{cases} \qquad (\mu_{\mathbb{R}^+} = \frac{\sqrt{3}}{4}\pi)$$

and the infimum is attained only at $\mu = \mu_{\mathbb{R}^+}$. The values $\mu_{\mathbb{R}}$ and $\mu_{\mathbb{R}^+}$ are said to be the critical masses of the line and of the half-line (respectively).

Concerning the tadpole $\mathcal{G} = \mathcal{T}$, as a consequence of Theorem 3.3 in [9], it has been proved that

$$\inf_{u \in H^1_\mu(\mathcal{T})} E(u) \begin{cases} \geq 0 & \text{if } \mu \leq \mu_{\mathbb{R}^+} \\ < 0 & \text{if } \mu \in (\mu_{\mathbb{R}^+}, \mu_{\mathbb{R}}] \\ = -\infty & \text{if } \mu > \mu_{\mathbb{R}} \end{cases}$$

and global minimizers of the energy exist if and only if $\mu \in (\mu_{\mathbb{R}^+}, \mu_{\mathbb{R}}]$.

We can now present the main result of this paper.

Theorem 2.1 *There exist two values $\mu_1, \mu_2 \in (\mu_{\mathbb{R}^+}, \mu_{\mathbb{R}})$, with $\mu_1 < \mu_2$, such that*

(i) if $\mu \leq \mu_1$, then $\mathcal{E}_{\mathcal{K}}(\mu) = 0$ and it is not attained;
(ii) if $\mu_2 \leq \mu \leq \mu_{\mathbb{R}}$, then there exists a ground state of mass μ.
(iii) if $\mu > \mu_{\mathbb{R}}$, then $\mathcal{E}_{\mathcal{K}}(\mu) = -\infty$.

Furthermore, ground states always realize strictly negative energy levels.

We point out that the previous result displays a different phenomenology with respect to the analogous in the everywhere nonlinear problem. Indeed, even though ground states are proved to exist only for some intervals of masses in both cases, Theorem 2.1 suggests that these intervals are actually different. Specifically, it appears that concentrating the nonlinearity on the compact core does not allow the presence of global minimizers if the mass is too close to $\mu_{\mathbb{R}^+}$, and a new lower threshold must arise. However, we are not able to detect the sharp values of μ_1 and μ_2 at the moment, so that it is still an open problem to determine μ^* such that ground states with concentrated nonlinearity exist if and only if $[\mu^*, \mu_{\mathbb{R}}]$. We will address this issue in a forthcoming paper.

3 Preliminaries and Compactness

First, let us recall some previous results on noncompact metric graphs, highlighting the consequences they have on the problem we discuss in the paper.

It is well-known (see for instance [7, 32]) that the following Gagliardo–Nirenberg inequalities

$$\|u\|_{L^6(\mathcal{T})}^6 \leq C_{\mathcal{T}} \|u\|_{L^2(\mathcal{T})}^4 \|u'\|_{L^2(\mathcal{T})}^2, \tag{9}$$

$$\|u\|_{L^\infty(\mathcal{T})} \leq C_\infty \|u\|_{L^2(\mathcal{T})}^{1/2} \|u'\|_{L^2(\mathcal{T})}^{1/2} \tag{10}$$

hold for every $u \in H^1(\mathcal{T})$ (here $C_{\mathcal{T}}, C_\infty$ denote the optimal constants). Furthermore, a modified version of (9) has been established in [9, Lemma 4.4]. Precisely, for every $u \in H^1_\mu(\mathcal{T})$, there exists $\theta_u := \theta(u) \in [0, \mu]$, such that

$$\|u\|_{L^6(\mathcal{T})} \leq 3\left(\frac{\mu - \theta_u}{\mu_{\mathbb{R}}}\right)^2 \|u'\|_{L^2(\mathcal{T})}^2 + C\sqrt{\theta_u} \tag{11}$$

with $C > 0$ independent of u.

In addition, recalling the definition of the complete NLS energy given by (2) with $\mathcal{G} = \mathcal{T}$, we know (again from [9]) that

$$(i) \quad \mu \leq \mu_{\mathbb{R}^+} \qquad \Longrightarrow E(u) > 0, \qquad \forall u \in H^1_\mu(\mathcal{T});$$

$$(ii) \quad \mu_{\mathbb{R}^+} < \mu \leq \mu_{\mathbb{R}} \qquad \Longrightarrow -\infty < \inf_{u \in H^1_\mu(\mathcal{T})} E(u) < 0$$

$$(iii) \ \mu < \mu_{\mathbb{R}} \qquad \Longrightarrow \inf_{u \in H^1_\mu(\mathcal{T})} E(u) = -\infty.$$

Moreover, global minimizers exist only in case (ii).

Since it is straightforward that, for every $u \in H^1(\mathcal{T})$,

$$E(u, \mathcal{K}) \geq E(u),$$

the previous observations have some relevant consequences on the problem with localized nonlinearity too. In fact, we have that

$$E(u, \mathcal{K}) > 0, \qquad \forall u \in u \in H^1_\mu(\mathcal{T}), \tag{12}$$

for every $\mu \leq \mu^+_{\mathbb{R}}$, and that

$$\mathcal{E}_{\mathcal{K}}(\mu) > -\infty, \qquad \forall \mu \in (\mu_{\mathbb{R}^+}, \mu_{\mathbb{R}}]. \tag{13}$$

On the other hand, arguing exactly as in [9], one can show that,

$$\mathcal{E}_{\mathcal{K}}(\mu) = -\infty, \qquad \forall \mu > \mu_{\mathbb{R}},$$

which immediately proves item *(iii)* of Theorem 2.1.

We conclude this section establishing a compactness result, valid only for localized nonlinearities, which ensures that ground states exist if and only if the infimum of the energy is strictly negative and finite.

Lemma 3.1 *Let $\mu \in (0, \mu_{\mathbb{R}}]$. If*

$$-\infty < \mathcal{E}_{\mathcal{K}}(\mu) < 0 \tag{14}$$

then, there exists a ground state of $E(\cdot, \mathcal{K})$ of mass μ. If, on the contrary, $E(u, \mathcal{K}) > 0$ for every $u \in H^1_\mu(\mathcal{T})$, then

$$\mathcal{E}_{\mathcal{K}}(\mu) = 0 \tag{15}$$

and it is not attained.

Proof We start by showing that, for every $\mu \in (0, \mu_{\mathbb{R}}]$,

$$\mathcal{E}_{\mathcal{K}}(\mu) \leq 0\,. \tag{16}$$

For every $n \in \mathbb{N}$, define

$$u_n(x) := \begin{cases} \alpha_n, & \text{if } x \in (1, n) \cap \mathcal{H}, \\ \alpha_n x, & \text{if } x \in [0, 1] \cap \mathcal{H}, \\ \alpha_n (n + 1 - x), & \text{if } x \in [n, n + 1] \cap \mathcal{H}, \\ 0, & \text{elsewhere on } \mathcal{T}, \end{cases}$$

where $\{\alpha_n\}_{n\in\mathbb{N}}$ is chosen so that $\|u_n\|^2_{L^2(\mathcal{T})} = \mu$, for every $n \in \mathbb{N}$ (note that this entails $\alpha_n \to 0$, as $n \to +\infty$). It is, then, easy to check that $u_n \to 0$ strongly in $H^1(\mathcal{T})$, thus implying that $E(u_n, \mathcal{K}) \to 0$, as $n \to +\infty$, and hence that (16) is satisfied.

On the other hand, if $E(u, \mathcal{K}) > 0$ for every $u \in H^1_\mu(\mathcal{T})$, then (16) yields (15) and, consequently, the infimum cannot be attained.

Finally, suppose that, on the contrary, (14) holds and let $\{u_n\}_{n\in\mathbb{N}} \subset H^1_\mu(\mathcal{T})$ be a minimizing sequence for $E(\cdot, \mathcal{K})$. Then, for large n, $E(u_n, \mathcal{K}) \leq -c$, with $c > 0$, and, combining with (11), this entails

$$\frac{1}{2}\|u_n'\|^2_{L^2(\mathcal{T})}\left[1 - \frac{(\mu - \theta_{u_n})^2}{\mu^2_{\mathbb{R}}}\right] - C\sqrt{\theta_{u_n}} \leq E(u_n, \mathcal{G}) \leq -c < 0$$

with $\theta_{u_n} \in [0, \mu]$. Thus, one finds that $\theta_{u_n} \geq \widetilde{c} > 0$, so that $\left(\frac{\mu-\theta_{u_n}}{\mu_{\mathbb{R}}}\right)^2 < 1$ and hence $\{u_n\}_{n\in\mathbb{N}}$ is bounded in $H^1_\mu(\mathcal{T})$. As a consequence, $u_n \rightharpoonup u$ in $H^1(\mathcal{T})$ and

$u_n \to u$ in $L^6_{loc}(\mathcal{T})$ (up to subsequences), and thus

$$E(u, \mathcal{K}) \leq \liminf_n E(u_n, \mathcal{K}) = \mathcal{E}_{\mathcal{K}}(\mu).$$

It is, then, left to prove that $\|u\|^2_{L^2(\mathcal{T})} =: m = \mu$.

First we see that, if $m = 0$, then $u \equiv 0$, and hence

$$\mathcal{E}_K(\mu) = \liminf_n E(u_n, \mathcal{K}) \geq E(u, \mathcal{K}) = 0,$$

which contradicts (14). On the other hand, if $m < \mu$, then there exists $\sigma > 1$ satisfying $\|\sigma u\|^2_{L^2(\mathcal{T})} = \mu$. However, this implies that

$$E(\sigma u, \mathcal{K}) = \frac{\sigma^2}{2} \int_{\mathcal{T}} |u'|^2 \, dx - \frac{\sigma^6}{6} \int_{\mathcal{K}} |u|^6 \, dx < \sigma^2 E(u, \mathcal{K}) < E(u, \mathcal{K}),$$

which is again a contradiction. Hence, $m = \mu$, which concludes the proof. □

4 Proof of Theorem 2.1

This section is devoted to the proof of items *(i)* and *(ii)* of Theorem 2.1 (item *(iii)* has been already discussed in the previous section).

Proof of Theorem 2.1: Item (i) First, note that, whenever $\mu \leq \mu_{\mathbb{R}^+}$, combining (12) and Lemma 3.1, one easily sees that no ground state may exist.

On the other hand, assume (by contradiction) that there exists a ground state of $E(\cdot, \mathcal{K})$ of mass μ, for every $\mu \in (\mu_{\mathbb{R}^+}, \mu_{\mathbb{R}}]$. Then, let $\{\mu_\varepsilon\}_{\varepsilon>0}$ be a sequence such that $\mu_\varepsilon \to \mu_{\mathbb{R}^+}$, as $\varepsilon \to 0$, and let u_ε be (one of) the associated ground state(s).

Now, it is immediate that $E(u_\varepsilon, \mathcal{K}) \leq 0$. As a consequence, exploiting the modified Gagliardo–Nirenberg inequality (11) as in the proof of Lemma 3.1, there results

$$\|u'_\varepsilon\|^2_{L^2(\mathcal{T})} \leq \frac{\mu_\varepsilon^2}{\mu_{\mathbb{R}}^2} \|u'_\varepsilon\|^2_{L^2(\mathcal{T})} + C\sqrt{\mu_{\mathbb{R}}}.$$

Therefore $\{u_\varepsilon\}_{\varepsilon>0}$ is bounded in $H^1(\mathcal{T})$ and there exists $u \in H^1(\mathcal{T})$ such that $u_\varepsilon \rightharpoonup u$ in $H^1(\mathcal{T})$ and $u_\varepsilon \to u$ in $L^6_{loc}(\mathcal{T})$ (up to subsequences), as $\varepsilon \to 0$.

Furthermore, using (10) and (again) the negativity of the energy, one finds

$$\|u'_\varepsilon\|^2_{L^2(\mathcal{T})} < \frac{1}{3}\|u_\varepsilon\|^6_{L^6(\mathcal{K})} \leq \frac{L}{3}\|u_\varepsilon\|^6_{L^\infty(\mathcal{K})} \leq \frac{L}{3}\|u_\varepsilon\|^6_{L^\infty(\mathcal{T})}$$

$$\leq \frac{C_\infty^6 L}{3}\|u_\varepsilon\|^3_{L^2(\mathcal{T})}\|u'_\varepsilon\|^3_{L^2(\mathcal{T})} = \frac{C_\infty^6 L}{3}\mu_\varepsilon^{3/2}\|u'_\varepsilon\|^3_{L^2(\mathcal{T})},$$

which yields (as $\|u_\varepsilon'\|^2_{L^2(\mathcal{T})} \neq 0$)

$$\|u_\varepsilon'\|_{L^2(\mathcal{T})} \geq \frac{3}{C_\infty^6 L \mu_{\mathbb{R}}^{3/2}}, \qquad \forall \varepsilon > 0, \tag{17}$$

thus preventing $u \equiv 0$. Indeed, if $u \equiv 0$, then $u_\varepsilon \to 0$ in $L^\infty(\mathcal{K})$ (from compact embeddings) and, as $E(u_\varepsilon, \mathcal{K}) \leq 0$,

$$\|u_\varepsilon'\|^2_{L^2(\mathcal{T})} < \frac{1}{3}\|u_\varepsilon\|^6_{L^6(\mathcal{K})} \leq \frac{1}{3} L \|u_\varepsilon\|^6_{L^\infty(\mathcal{K})} \to 0, \qquad \text{as } \varepsilon \to 0,$$

but this contradicts (17).

Finally, by the weak lower semicontinuity, we have

$$\|u\|^2_{L^2(\mathcal{T})} \leq \liminf_{\varepsilon \to 0} \mu_\varepsilon = \mu_{\mathbb{R}^+}$$

and

$$E(u, \mathcal{K}) \leq \liminf_{\varepsilon \to 0} E(u_\varepsilon, \mathcal{K}) \leq 0.$$

Hence, u is a function in $H^1_m(\mathcal{T})$, for some $m \in (0, \mu_{\mathbb{R}^+}]$, such that $E(u, \mathcal{K}) \leq 0$. However, this is forbidden by (12), which (combining with Lemma 3.1) concludes the proof. □

Proof of Theorem 2.1: Item (ii) Since by (13) the energy functional is lower bounded (whenever $\mu \leq \mu_{\mathbb{R}}$), from Lemma 3.1, it is sufficient to exhibit a function with a strictly negative energy (as the mass exceeds a certain threshold).

To this aim, fix $\mu \in (\mu_{\mathbb{R}^+}, \mu_{\mathbb{R}}]$ and let

$$u(x) := \begin{cases} c & \text{if } x \in \mathcal{K} \\ ce^{-\alpha x} & \text{if } x \in \mathcal{H}, \end{cases} \tag{18}$$

with $c, \alpha > 0$ satisfying the mass condition

$$\mu = \|u\|^2_{L^2(\mathcal{T})} = \int_{\mathcal{K}} c^2 \, dx + \int_{\mathcal{H}} c^2 e^{-2\alpha x} \, dx = c^2 L + \frac{c^2}{2\alpha} \tag{19}$$

(see also Fig. 5).

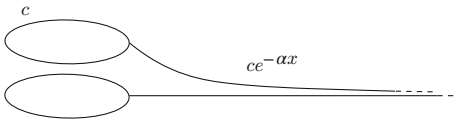

Fig. 5 Function introduced in the proof of Theorem 2.1: item (ii)

Hence, $u \in H^1_\mu(\mathcal{T})$ and its energy reads

$$E(u, \mathcal{K}) = \frac{c^2\alpha}{4} - \frac{c^6 L}{6}. \tag{20}$$

Now, by (19)

$$\alpha = \frac{c^2}{2(\mu - c^2 L)},$$

so that

$$E(u, \mathcal{K}) = \frac{c^4}{8(\mu - c^2 L)} - \frac{c^6 L}{6} = \frac{c^4}{2}\Big(\frac{1}{4(\mu - c^2 L)} - \frac{c^2 L}{3}\Big).$$

Therefore, imposing $E(u, \mathcal{K}) < 0$ reduces to determine whether exists (or not) a value c such that

$$\frac{1}{4(\mu - c^2 L)} - \frac{c^2 L}{3} < 0,$$

namely, whether exists (or not) a value $\Lambda := c^2 L$ such that

$$\Lambda^2 - \mu\Lambda + \frac{3}{4} < 0.$$

However, the previous inequality is satisfied whenever

$$\frac{\mu - \sqrt{\mu^2 - 3}}{2} < \Lambda < \frac{\mu + \sqrt{\mu^2 - 3}}{2},$$

provided that

$$\mu^2 - 3 \geq 0 \qquad \Leftrightarrow \qquad \mu \geq \sqrt{3}\,. \tag{21}$$

Henceforth, setting $\mu_2 := \sqrt{3}$, for every $\mu \in [\mu_2, \mu_{\mathbb{R}}]$, there exists $u \in H^1_\mu(\mathcal{T})$ such that $E(u, \mathcal{K}) < 0$. □

References

1. R. Adami, C. Cacciapuoti, D. Finco, D. Noja, Fast solitons on star graphs, *Rev. Math. Phys.* **23** (2011), no. 4, 409–451.
2. R. Adami, C. Cacciapuoti, D. Finco, D. Noja, Variational properties and orbital stability of standing waves for NLS equation on a star graph, *J. Differential Equations* **257** (2014), no. 10, 3738–3777.

3. R. Adami, C. Cacciapuoti, D. Finco, D. Noja, Constrained energy minimization and orbital stability for the NLS equation on a star graph, *Ann. Inst. H. Poincaré Anal. Non Linéaire* **31** (2014), no. 6, 1289–1310.
4. R. Adami, C. Cacciapuoti, D. Finco, D. Noja, Stable standing waves for a NLS on star graphs as local minimizers of the constrained energy, *J. Differential Equations* **260** (2016), no. 10, 7397–7415.
5. R. Adami, S. Dovetta, One-dimensional versions of three dimensional system: Ground states for the NLS on the spatial grid, *Rend. Mat. Appl.* **39** (2018), no. 7, 181-194.
6. R. Adami, S. Dovetta, E. Serra, P. Tilli, Dimensional crossover with a continuum of critical exponents for NLS on doubly periodic metric graphs, *Anal. PDE* **12** (2019), no. 6, 1597-1612.
7. R. Adami, E. Serra, P. Tilli, NLS ground states on graphs, *Calc. Var. Partial Differential Equations* **54** (2015), no. 1, 743–761.
8. R. Adami, E. Serra, P. Tilli, Threshold phenomena and existence results for NLS ground states on metric graphs, *J. Funct. Anal.* **271** (2016), no. 1, 201–223.
9. R. Adami, E. Serra, P. Tilli, Negative energy ground states for the L^2-critical NLSE on metric graphs, *Comm. Math. Phys.* **352** (2017), no. 1, 387–406.
10. R. Adami, E. Serra, P. Tilli, Nonlinear dynamics on branched structures and networks., *Riv. Math. Univ. Parma (N.S.)* **8** (2017), no. 1, 109–159.
11. R. Adami, E. Serra, P. Tilli, Multiple positive bound states for the subcritical NLS equation on metric graphs, *Calc. Var. Partial Differential Equations* **58** (2019), no. 5, 16pp.
12. G. Berkolaiko, P. Kuchment, *Introduction to quantum graphs*, Mathematical Surveys and Monographs 186, American Mathematical Society, Providence, RI, 2013.
13. W. Borrelli, R. Carlone, L. Tentarelli, Nonlinear Dirac equation on graphs with localized nonlinearities: bound states and nonrelativistic limit, SIAM J. Math. An. **51** (2019), no. 2, 1046-1081.
14. C. Cacciapuoti, Existence of the ground state for the NLS with potential on graphs, *Mathematical Problems in Quantum Physics*, 155–172, Contemporary Mathematics 717, American Mathematical Society, Providence, RI, 2018.
15. C. Cacciapuoti, D. Finco, D. Noja, Topology-induced bifurcations for the nonlinear Schrödinger equation on the tadpole graph, *Phys. Rev. E (3)* **91** (2015), no. 1, article number 013206, 8 pp.
16. C. Cacciapuoti, D. Finco, D. Noja, Ground state and orbital stability for the NLS equation on a general starlike graph with potentials, *Nonlinearity* **30** (2017), no. 8, 3271–3303.
17. T. Cazenave, Semilinear Schrödinger equations, Courant Lecture Notes in Mathematics 10, American Mathematical Society, Providence, RI, 2003.
18. S. Dovetta, Existence of infinitely many stationary solutions of the L^2-subcritical and critical NLSE on compact metric graphs, *J. Differential Equations* **264** (2018), no. 7, 4806–4821.
19. A. Duca, Global exact controllability of the bilinear Schrödinger potential type models on quantum graphs, arXiv:1710.06022v2 [math.OC] (2017).
20. S. Gilg, D.E. Pelinovsky, G. Schneider, Validity of the NLS approximation for periodic quantum graphs, *NoDEA Nonlinear Differential Equations Appl.* **23** (2016), no. 6, article number 63, 30 pp.
21. S. Gnutzmann, U. Smilansky, S. Derevyanko, Stationary scattering from a nonlinear network, *Phys. Rev. A* **83** (2011), no. 3, article number 033831.
22. S. Gnutzmann, D. Waltner, Stationary waves on nonlinear quantum graphs: general framework and canonical perturbation theory, *Phys. Rev. E* **93** (2016), no. 3, article number 032204, 19 pp.
23. Y. Li, F. Li, J. Shi, Ground states of nonlinear Schrödinger equation on star metric graphs, *J. Math. Anal. Appl.* **459** (2018), no. 2, 661–685.
24. J.L. Marzuola, D.E. Pelinovsky, Ground state on the dumbbell graph, *Appl. Math. Res. Express. AMRX* (2016), no. 1, 98–145.
25. D. Mugnolo, D. Noja, C. Seifert, Airy-type evolution equations on star graphs, *Anal. PDE* **11** (2018), no. 7, 1625–1652.

26. D. Noja, Nonlinear Schrödinger equation on graphs: recent results and open problems, *Philos. Trans. R. Soc. Lond. Ser. A Math. Phys. Eng. Sci.* **372** (2014), no. 2007, article number 20130002, 20 pp.
27. D. Noja, D. Pelinovsky, G. Shaikhova, Bifurcations and stability of standing waves in the nonlinear Schrödinger equation on the tadpole graph, *Nonlinearity* **28** (2015), no. 7, 2343–2378.
28. D. Noja, S. Rolando, S. Secchi, Standing waves for the NLS on the double-bridge graph and a rational-irrational dichotomy, *J. Differential Equations* **266** (2019), no. 1, 147–178.
29. D.E. Pelinovsky, G. Schneider, Bifurcations of standing localized waves on periodic graphs, *Ann. Henri Poincaré* **18** (2017), no. 4, 1185–1211.
30. E. Serra, L. Tentarelli, Bound states of the NLS equation on metric graphs with localized nonlinearities, *J. Differential Equations* **260** (2016), no. 7, 5627–5644.
31. E. Serra, L. Tentarelli, On the lack of bound states for certain NLS equations on metric graphs, *Nonlinear Anal.* **145** (2016), 68–82.
32. L. Tentarelli, NLS ground states on metric graphs with localized nonlinearities, *J. Math. Anal. Appl.* **433** (2016), no. 1, 291–304.

An Asymptotic Expansion of the Trace of the Heat Kernel of a Singular Two-particle Contact Interaction in One-dimension

Sebastian Egger

Abstract The regularized trace of the heat kernel of a one-dimensional Schrödinger operator with a singular two-particle contact interaction being of Lieb-Liniger type is considered. We derive a complete small-time asymptotic expansion in (fractional) powers of the time, t. Most importantly, we do not invoke standard parametrix constructions for the heat kernel. Instead, we first derive the large-energy expansion of the regularized trace of the resolvent for the considered operator. Then, we exploit that the resolvent may be obtained by a Laplace transformation of the heat semi-group, and an application of a suitable inverse Watson lemma eventually delivers the small-t asymptotic expansion of the heat-kernel trace.

1 Introduction

The classical heat kernel is the kernel of an integral operator generating the semi-group of the heat equation on domains or manifolds. Given sufficient regularity of the boundary and assuming that the volume of the domain is finite one may conclude that the heat semi-group is a trace class operator. Mercer's famous theorem tells then that its trace may be calculated by integrating the heat kernel along its diagonal.

Minakshisundaram and Pleijel showed in their celebrated work [40, 41], that the classical heat kernel possesses a complete small-time (small-t) asymptotic expansion in (fractional) powers of t. They were also able to show that its coefficients bear topological and metric information of the underlying domain or manifold. Most notable here is the heat-kernel approach to the profound Atiyah-Singer index theorem [2, 3, 22], which links a specific coefficient of the heat-kernel expansion to the topological and analytic index, respectively, of an elliptic operator acting on sections of a corresponding vector bundle.

S. Egger (✉)
Department of Mathematics, Technion-Israel Institute of Technology, Haifa, Israel
e-mail: egger@tx.technion.ac.il

F. M. Atay et al. (eds.), *Discrete and Continuous Models in the Theory of Networks*, Operator Theory: Advances and Applications 281,
https://doi.org/10.1007/978-3-030-44097-8_6

Another and very interesting aspect pointed out in [40, 41] is that the small-t asymptotics of the trace of the heat kernel and the meromorphic properties of the spectral ζ-function corresponding to the generating Laplacian of the heat equation are very closely related. From a physical point of view, the spectral ζ-function is an important object in statistical physics and quantum mechanics to calculate, e.g., path integrals (Brownian motion) [31], spectral determinants in lattice QCD, or the Casimir force in QED, see, e.g. [19, 34].

A standard approach to find an asymptotic expansion of the trace of the heat kernel is to derive a parametrix, i.e., a local small-t asymptotic expansion for the solution of the heat equation, and then integrate its position dependent coefficients along their diagonals. The advantage of this method is that it's rather universally applicable and the coefficients may be identified as *local invariants* of the underlying domain or manifold. Due to the overwhelming number of remarkable results we refer here (and references therein) to [8, 23, 32, 52–54, 58] for the heat-kernel expansion in particular and to [1, 4, 16, 17, 27, 37, 45, 47] for related modern results regarding asymptotic properties of the heat kernel.

On metric graphs the trace of the heat kernel was first studied by Roth [50], deriving an exact (Selberg-like) trace formula for it. After that, the (one-particle) heat kernel has experienced an accelerated attention and analogous questions has been asked to the manifold case [7, 15, 21, 28, 35, 42–44, 48]. The motivation of studying contact interactions in many-particle physics for one-dimensional systems dates back to the famous Lieb-Liniger model [38], used to test Bogoliubov's perturbation theory for Bose gases. Since then many-particle contact interactions in one-dimension and graphs are well established for testing and modeling famous phenomenons such as superconductivity or Bose-Einstein condensation [10–12, 18, 20, 30, 51]. For the importance of one-dimensional contact interactions in physics and recent experimental implementations we refer to [14]. Those above exciting results inspired us to consider as a very first example the small-t asymptotics of the trace of the heat kernel for a simple but non-standard Lieb-Liniger type system of a singular but non-constant contact interaction on the real line, $\mathbb{R}$.

More precisely, the operator which we consider is the one-dimensional two-particle Schrödinger operator given by the formal expression

$$-\Delta_\rho := -\partial_{x_1}^2 - \partial_{x_2}^2 + \rho(x_1, x_2)\delta(x_1 - x_2)\,, \tag{1}$$

with $L^2(\mathbb{R}^2)$ as the two-particle Hilbert space and a position dependent δ-potential modulated by a potential ρ. We assume that the modulating potential, ρ, is smooth and possesses compact support. The heat semi-group, $\mathrm{e}^{t\Delta_\rho}$, satisfies $\partial_t \mathrm{e}^{t\Delta_\rho}|_{t=0} = \Delta_\rho$ in a strong sense, and the heat kernel, $k^\rho(t)(\cdot,\cdot)$, $t \in \mathbb{R}$, is the integral kernel generating $\mathrm{e}^{t\Delta_\rho}$ by

$$(\mathrm{e}^{t\Delta_\rho}\psi)(\boldsymbol{x}) = \int_{\mathbb{R}^2} k^\rho(t)(\boldsymbol{x}, \boldsymbol{y})\psi(\boldsymbol{y})\mathrm{d}\boldsymbol{y}\,. \tag{2}$$

However, since the underlying configuration space is non-compact the Schrödinger operator (1) possesses an essential spectrum, and we have to regularize the heat semi-group in order to make it a trace-class operator.

In this paper, we follow the method of [7] and don't derive a parametrix expansion for the heat semi-group. Instead, we exploit that the resolvent and the heat semi-group are related via a Laplace transformation. This approach is similar to [32], where the authors used the so-called Agmon-Kannai method to derive an asymptotic expansion for the resolvent kernel of the corresponding Schrödinger operator. The Agmon-Kannai method, in turn, is a tool to obtain a series representation of the resolvent with operator-valued coefficients and is based on a recursive construction involving commutators of the free and the full resolvent of the considered operator [46].

We don't use the Agmon-Kannai method here, but we exploit that the resolvent of our system allows a rather explicit representation in terms of suitable integral operators which is based on a more-general formula of Kreĭn. We start by first establishing an asymptotic expansion for large but negative energies of the regularized trace of the resolvent. Then, we use a suitable version of the converse Watson lemma to deduce the small-t asymptotics of the regularized trace of the heat semi-group (and heat kernel). In general, our method is taking advantage of the symmetry properties of the underlying system, and the advantage of our method is that it allows a compact, explicit and quick formulation of the heat-kernel coefficients.

Finally, we refer to Appendix 1, where we recall standard notations and definitions used in this paper.

2 Preliminaries

We begin our investigations by implementing a rigorous version of the formal Schrödinger operator (1). To obtain a well-defined operator in $L^2(\mathbb{R}^2)$ corresponding to this operator it is convenient to associate with (1) a quadratic form being complete and semi-bounded from below. Then, there is a unique self-adjoint operator corresponding to the quadratic form [55, Section 4.2], which then may be regarded as a rigorous version of (1).

To get the quadratic form of the operator (1) we first realize that due to the δ-potential the modulation potential ρ has only to be known on the diagonal (one-dimensional submanifold)

$$D := \{(x, x) : \ x \in \mathbb{R}\} \subset \mathbb{R}^2 . \tag{3}$$

Now, using the identification $\rho(x, x) = \rho(x)$ we restrict our considerations in this paper to compactly supported and smooth potential, i.e., $\rho \in C_0^\infty(\mathbb{R})$. To identify the associated quadratic form and operator we are proceeding as in [9, Section 3.1], replacing the interval $[0, 1]$ with $\mathbb{R}$ to obtain our case related to (1). We follow the steps of [9, Section 3.1] and to do so, we use D and partition $\mathbb{R}^2$ into the two disjoint

open sets D_+ and D_- by

$$\mathbb{R}^2 = D_- \dot\cup D \dot\cup D_+ , \quad D_+ = \{(x_1, x_2) : \ x_1 < x_2\} , \quad D_- := \{(x_1, x_2) : \ x_1 > x_2\} . \tag{4}$$

Moreover, since D is a straight line, and hence a smooth curve, we may define the trace maps see, e.g. [29, Theorem 1.5.1.1]

$$\mathrm{bv}_\pm : H^1(D_\pm) \to H^{\frac{1}{2}}(D). \tag{5}$$

Both above maps are continuous linear maps. In the same way, the gradients

$$\nabla : H^2(D_\pm) \to H^1(D_\pm) \oplus H^1(D_\pm) \tag{6}$$

are well-defined and continuous maps. Therefore, the inward normal derivatives, $\partial_{\boldsymbol{n}}$, w.r.t. the boundary D of the domains $D_\pm$ act as

$$\partial_{\boldsymbol{n}} : H^2(D_+) \oplus H^2(D_-) \to H^{\frac{1}{2}}(D) \oplus H^{\frac{1}{2}}(D) , \tag{7}$$

and are well-defined by

$$\partial_{\boldsymbol{n}}(\psi_+ \oplus \psi_-) := \psi_{\boldsymbol{n},+} \oplus \psi_{\boldsymbol{n},-} , \tag{8}$$

and

$$\psi_{\boldsymbol{n},\pm} := \mp(\partial_{x_1} - \partial_{x_2})\psi_\pm . \tag{9}$$

With these technical tools at hand, we may now use [9, p. 6] allowing a proper identification of the two-particle and one-dimensional Schrödinger operator in (1) with a one-particle and two-dimensional operator acting on $\mathbb{R}^2$. For the readers convenience we denote this operator by $-\Delta_\rho$ as well. The functions of the corresponding operator domain, $D(\Delta_\rho)$, obey the following regularity and boundary conditions. If $\psi \in D(\Delta_\rho)$ then $\psi \in H^2(D_+) \oplus H^2(D_-) \subset L^2(\mathbb{R}^2)$ and the following boundary conditions are satisfied in a L^2-sense [9, p. 6]:

$$\mathrm{bv}_+ \psi = \mathrm{bv}_- \psi =: \Psi , \quad \psi_{\boldsymbol{n},+} + \psi_{\boldsymbol{n},-} = \rho\Psi . \tag{10}$$

Moreover, by Bolte and Kerner [9, p. 6] the operator $-\Delta_\rho$ is associated with the quadratic form $(q_\rho, H^1(\mathbb{R}^2))$ defined by

$$q_\rho(\psi) := \int_{\mathbb{R}^2} \langle \nabla\psi, \nabla\psi \rangle_{\mathbb{R}^2} \mathrm{d}\boldsymbol{x} + \int_D \rho\Psi \mathrm{d}x , \tag{11}$$

where we used (4). On the other hand, given $(q_\rho, H^1(\mathbb{R}^2))$ then the associated operator is $-\Delta_\rho$ and is self-adjoint and bounded from below [13, Theorem 4.2]. We denote by $\lambda_{\min,\rho} := \inf\{\lambda \in \mathbb{R} : \lambda \in \sigma(-\Delta_\rho)\}$ the bottom of the spectrum $\sigma(-\Delta_\rho)$ of the Schrödinger operator, and we recall the well-known fact $\lambda_{\min,0} = 0$.

3 The Resolvent Kernel

At the beginning of this section, we derive an explicit expression of the resolvent, $\lambda \notin \sigma(-\Delta_\rho)$,

$$R_\rho(\lambda) := (-\Delta_\rho - \lambda)^{-1}\,. \tag{12}$$

To do so, we follow [13], and in the following, we choose $\sqrt{\lambda} = k \in \mathbb{C}$ such that $\operatorname{Im} k > 0$. We introduce the integral kernels

$$G_0(k)(x_1, x_2, y_1, y_2) := \frac{1}{2\pi} K_0(-\mathrm{i}k\sqrt{(x_1 - y_1)^2 + (x_2 - y_2)^2})\,, \tag{13}$$

and

$$g(k)(x, y) := \frac{1}{2\pi} K_0(-\mathrm{i}\sqrt{2}k|x - y|)\,. \tag{14}$$

The integral kernel $G_0(k)$ corresponds for $\operatorname{Im} k > 0$ to a bounded operator $R_0(k) : L^2(\mathbb{R}^2) \to L^2(\mathbb{R}^2)$ and $g(k)$ to a bounded operator $\mathfrak{g}(k) : L^2(\mathbb{R}) \to L^2(\mathbb{R})$, respectively. That may be deduced from the asymptotic behavior of the K_0-Bessel function for large arguments [39, p. 139]. It is worth mentioning that the logarithmic singularity of the K_0-Bessel function at the origin [39, p, 65], doesn't affect the boundedness of R_0 and $\mathfrak{g}$ due to Young's inequality. Note that $R_0(k)$ is the (free) resolvent of the pure Laplacian on $\mathbb{R}^2$. To write down the resolvent explicitly we need one more integral operator connecting $L^2(\mathbb{R}^2)$ and $L^2(\mathbb{R})$. We introduce

$$b(k)(x, y_1, y_2) := \frac{1}{2\pi} K_0(-\mathrm{i}k\sqrt{(x - y_1)^2 + (x - y_2)^2})\,, \tag{15}$$

and those integral kernel generates for $\operatorname{Im} k > 0$ a bounded operator $\mathfrak{b}(k) : L^2(\mathbb{R}^2) \to L^2(\mathbb{R})$. Finally, we make the simple observation that any potential $\rho \in C_0^\infty(\mathbb{R})$, or only $\rho \in L^\infty(\mathbb{R})$, generates a bounded multiplication operator $\rho : L^2(\mathbb{R}) \to L^2(\mathbb{R})$.

With these operators at hand, we now invoke [13, Corollary 2.1] saying that the resolvent $R_\rho(\lambda)$ may be written as

$$R_\rho(\lambda) = R_0(k) - \mathfrak{b}\left(\overline{k}\right)^* (\mathbb{1} + \rho\mathfrak{g}(k))^{-1} \rho b(k)\,, \tag{16}$$

where we put $k = \sqrt{\lambda}$. In the following, it is convenient to denote by C_α, $\alpha < \frac{\pi}{2}$, the cone around the positive imaginary axis $\mathrm{i}\mathbb{R}^+$ and with opening angle 2α, i.e.,

$$C_\alpha := \left\{ z \in \mathbb{C} : \ |\arg(z) - \frac{\pi}{2}| < \alpha \right\} . \tag{17}$$

Then, for $k \in C_\alpha$, $\alpha < \frac{\pi}{2}$, and $|k|$ large enough one has [13, Corollary 2.2],

$$\|\rho \mathfrak{g}(k)\| < 1 . \tag{18}$$

Now, we introduce the regularized resolvent $R_\rho^{\mathrm{reg}}(k)$, $k \in C_\alpha$, $\alpha < \frac{\pi}{2}$, and $|k|$ sufficiently large, defined as $R_\rho^{\mathrm{reg}}(k) := R_\rho(k^2) - R_0(k^2)$. Due to the semi-boundedness of q_ρ (and q_0) the operator $R_\rho^{\mathrm{reg}}(k)$ exists for $k \in C_\alpha$, $\alpha < \frac{\pi}{2}$ and $|k|$ sufficiently large. We will show that $R_\rho^{\mathrm{reg}}(k)$ is also a trace class operator. For this, it is advantageous to 'shift' a square root of the potential in (16) from right to left. This will eventually reveal that the supports of the integral kernels are compact w.r.t. appropriate variables, and will be exploited to estimate the integrals from above. Specifically, the following rearrangement of $R_\rho^{\mathrm{reg}}(k)$ is possible.

Lemma 3.1 *For $k \in C_\alpha$, $\alpha < \frac{\pi}{2}$, and $|k|$ sufficiently large, we have*

$$R_\rho^{\mathrm{reg}}(k) = -\left(\sqrt{|\rho|}\mathfrak{b}\left(\overline{k}\right)\right)^* (\mathbb{1} + \operatorname{sgn}\rho\sqrt{|\rho|}\mathfrak{g}(k)\sqrt{|\rho|})^{-1} \operatorname{sgn}\rho\sqrt{|\rho|}\mathfrak{b}(k) . \tag{19}$$

Proof Using (18) we may write $(\mathbb{1} + \rho\mathfrak{g}(k))^{-1}$ as a Neumann series. Now,

$$(\rho\mathfrak{g}(k))^n \rho = \sqrt{|\rho|}(\operatorname{sgn}\rho\sqrt{|\rho|}\mathfrak{g}(k)\sqrt{|\rho|})^n \operatorname{sgn}\rho\sqrt{|\rho|} \tag{20}$$

for every $n \in \mathbb{N}_0$ proves the claim. □

3.1 Trace Class Property of the Regularized Resolvent

Now, we are in the position to prove that the regularized resolvent is actually a trace class operator.

Proposition 3.2 *For $k \in C_\alpha$, $\alpha < \frac{\pi}{2}$, and $|k|$ sufficiently large, $R_\rho^{\mathrm{reg}}(k)$ is a trace class operator.*

Proof We want to employ [55, Satz 3.23] saying that it's enough to show that $R_\rho^{\mathrm{reg}}(k)$ can be factorized as

$$R_\rho^{\mathrm{reg}}(k) = AB \tag{21}$$

by two Hilbert-Schmidt operators $A : L^2(\mathbb{R}) \to L^2(\mathbb{R}^2)$ and $B : L^2(\mathbb{R}^2) \to L^2(\mathbb{R})$. Looking at (19) we are tempted to identify

$$A = -\left(\sqrt{|\rho|}\mathfrak{b}\left(\overline{k}\right)\right)^* , \tag{22}$$

and

$$B = (\mathbb{1} + \operatorname{sgn}\rho\sqrt{|\rho|}\mathfrak{g}(k)\sqrt{|\rho|})^{-1}\operatorname{sgn}\rho\sqrt{|\rho|}\mathfrak{b}(k) . \tag{23}$$

Indeed, by [55, Satz 3.18] the Hilbert-Schmidt property is closed under taking the adjoint. Moreover, by [55, Satz 3.20] we may neglect the operator $(\mathbb{1} + \operatorname{sgn}\rho\sqrt{|\rho|}\mathfrak{g}(k)\sqrt{|\rho|})^{-1}\operatorname{sgn}\rho$, and it remains to show that $\sqrt{|\rho|}\mathfrak{b}(k)$ is of Hilbert-Schmidt class. We proceed to show that the integral kernel of $\sqrt{|\rho|}\mathfrak{b}(k)$ is in $L^2(\mathbb{R}\times\mathbb{R}^2)$ which then proves by [55, Satz 3.19] the claim. We recall (15) and calculate

$$\begin{aligned}
&(2\pi)^2 \int_{\mathbb{R}}\int_{\mathbb{R}^2} |\rho(x)||b(k)(x,y_1,y_2)|^2 \mathrm{d}x\mathrm{d}y_1\mathrm{d}y_2 \\
&\quad = \int_{\operatorname{supp}\rho}\int_{B_R(\mathbf{0})} |\rho(x)||K_0\left(-\mathrm{i}k\sqrt{(x-y_1)^2+(x-y_2)^2}\right)|^2 \mathrm{d}x\mathrm{d}y_1\mathrm{d}y_2 \\
&\qquad + \int_{\operatorname{supp}\rho}\int_{\mathbb{R}^2\setminus B_R(\mathbf{0})} |\rho(x)||K_0\left(-\mathrm{i}k\sqrt{(x-y_1)^2+(x-y_2)^2}\right)|^2 \mathrm{d}x\mathrm{d}y_1\mathrm{d}y_2 ,
\end{aligned} \tag{24}$$

where $B_R(\mathbf{0})$ is a ball with sufficient large radius R such that

$$x \in \operatorname{supp}\rho \quad \Rightarrow \quad y_1 \neq x \quad \text{or} \quad y_2 \neq x \tag{25}$$

holds in $\mathbb{R}^2 \setminus B_R(\mathbf{0})$. Such a radius, R, exists as the support of ρ is bounded. By the same reason and due to the asymptotic behavior (80) we have that

$$\begin{aligned}
&\int_{\operatorname{supp}\rho}\int_{B_R(\mathbf{0})} |\rho(x)||K_0\left(-\mathrm{i}k\sqrt{(x-y_1)^2+(x-y_2)^2}\right)|^2 \mathrm{d}x\mathrm{d}y_1\mathrm{d}y_2 \\
&\quad < C\int_{\operatorname{supp}\rho}\int_{B_R(\mathbf{0})} |\ln(kr)|^2 r\mathrm{d}r\mathrm{d}x < \infty
\end{aligned} \tag{26}$$

with some $C > 0$. By (81) a similarly estimates to (26) also holds for the second integral on the r.h.s. in (24) proving the claim. □

In order to evaluate the trace of the heat kernel, we want to employ a generalized version of Mercer's theorem. To achieve this, we first have to show that the heat

kernel exists and then to work out suitable continuity and decay properties satisfied by the integral kernel.

Lemma 3.3 *Given $k \in C_\alpha$, $\alpha < \frac{\pi}{2}$, and $|k|$ sufficiently large, $R_\rho^{\mathrm{reg}}(k)$ is an integral operator with an continuous and exponentially decaying kernel for large arguments.*

Proof First, we choose for our convenience an appropriate $-\mathrm{i}k \in \mathbb{R}^+$, and the remaining cases may then be similarly proven. With a similar argument as in the proof of Proposition 3.2, using the (absolute) integrability of the logarithm, we may regard $\sqrt{|\rho|}\mathfrak{b}(k)$ as a map

$$\tilde{b} : (\mathbb{R}^2, \|\cdot\|_{\mathbb{R}^2}) \to L^2(\mathbb{R}), \tag{27}$$

defined by

$$(\tilde{b}(y_1, y_2))(x) := \sqrt{|\rho(x)|}b(k)(x, y_1, y_2). \tag{28}$$

To see that $\tilde{b}$ is continuous we first take into account that the support of ρ is finite and therefore we only have to investigate singular points of (28) w.r.t. the argument. Looking at (15) we see that the singularity is in the logarithm of (80) where $x = y_1 = y_2$. We may choose $y_1 = y_2 = 0$, $y_1' = y_2' =: y' > 0$ and the other cases are similar. We are going to use that for every $\epsilon > 0$ there is a $\delta(\epsilon)$ such that

$$\begin{aligned} &\|(0,0) - (y', y')\|_{\mathbb{R}^2} \le \delta(\epsilon), \text{ and } (x,x) \notin B_{2\delta(\epsilon)}(0,0) \\ &\quad \Rightarrow \ |\ln\|(x,x)\|_{\mathbb{R}^2} - \ln\|(y'-x, y'-x)\|_{\mathbb{R}^2}| \le \epsilon. \end{aligned} \tag{29}$$

Hence, choosing ϵ suitable small gives

$$\begin{aligned} &\int_{\mathrm{supp}\,\rho} |\ln\|(x,x)\|_{\mathbb{R}^2} - \ln\|(y'-x, y'-x)\|_{\mathbb{R}^2}|^2 \mathrm{d}x \\ &= \int_{\{(x,x)\notin B_{2\delta(\epsilon)}(0,0)\}\cap \mathrm{supp}\,\rho} |\ln\|(x,x)\|_{\mathbb{R}^2} - \ln\|(y'-x, y'-x)\|_{\mathbb{R}^2}|^2 \mathrm{d}x \\ &\quad + \int_{\{(x,x)\in B_{2\delta(\epsilon)}(0,0)\}\cap \mathrm{supp}\,\rho} |\ln\|(x,x)\|_{\mathbb{R}^2} - \ln\|(y'-x, y'-x)\|_{\mathbb{R}^2}|^2 \mathrm{d}x \\ &\le C\epsilon + C' \int_0^{2\delta(\epsilon)} |\ln|1 - \frac{y'}{x}||^2 \mathrm{d}x, \\ &\le C\epsilon + C' \int_{y'(2\delta(\epsilon))^{-1}}^{\infty} \frac{y'}{x^2} |\ln|1-x||^2 \mathrm{d}x = C\epsilon + \mathrm{O}(y'), \end{aligned} \tag{30}$$

where in the last line we performed the substitution $x \to \frac{y}{x}$, and we used [49, pp. 240,241]. Observing that $C, C' > 0$ only depend on the size of $|\operatorname{supp}\rho|_1$ and choosing y' sufficiently close 0 proves the claim.

In the same way as above, we view $(\sqrt{|\rho|}\mathfrak{b}(\overline{k}))^*$ as a continuous map from $(\mathbb{R}^2, \|\cdot\|_{\mathbb{R}^2})$ to $L^2(\mathbb{R})$. This gives the same integral kernel $\tilde{b}$ as in (28) since $-ik \in \mathbb{R}^+$ and then the K_0-Bessel function is real valued, but the $\mathbb{R}^2$-variables are now indicated by (x_1, x_2). We denote for convenience, see (19),

$$q = (\mathbb{1} + \operatorname{sgn}\rho\sqrt{|\rho|}\mathfrak{g}(k)\sqrt{|\rho|})^{-1} : L^2(\mathbb{R}) \to L^2(\mathbb{R}), \tag{31}$$

and since q is continuous we observe that the integral kernel $r_\rho(k)((x_1, x_2), (y_1, y_2))$ of $R_\rho^{\mathrm{reg}}(k)$ is given by

$$r_\rho(k)((x_1, x_2), (y_1, y_2)) = \langle \tilde{b}(x_1, x_2), q\tilde{b}(y_1, y_2)\rangle_{L^2(\mathbb{R})}. \tag{32}$$

Now, the algebraic identity

$$\begin{aligned}
&r_\rho(k)((x_1, x_2), (y_1, y_2)) - r_\rho(k)((x_1', x_2'), (y_1', y_2)')\\
&= \langle \tilde{b}(x_1, x_2), q\tilde{b}(y_1, y_2)\rangle_{L^2(\mathbb{R})} - \langle \tilde{b}(x_1', x_2'), q\tilde{b}(y_1', y_2')\rangle_{L^2(\mathbb{R})}\\
&= \langle (\tilde{b}(x_1, x_2) - \tilde{b}(x_1', x_2')), q\tilde{b}(y_1, y_2)\rangle_{L^2(\mathbb{R})} + \langle \tilde{b}(x_1', x_2'), q(\tilde{b}(y_1, y_2) - \tilde{b}(y_1', y_2'))\rangle_{L^2(\mathbb{R})},
\end{aligned} \tag{33}$$

and a suitable application of Hölder's inequality prove the first part of the claim.

To see the exponential decay we recall that the operators $\tilde{b}$ in (32) involve the kernel $\sqrt{|\rho(x)|}b(k)(x, y_1, y_2)$ given in (15). As before, it's enough to assume $x \in \operatorname{supp}\rho$, and since the support of ρ is finite we have for sufficiently large $\|(y_1, y_2)\|_{\mathbb{R}^2}$ the inequality

$$\|(y_1 - x, y_2 - x)\|_{\mathbb{R}^2} > \frac{1}{2}\|(y_1, y_2)\|_{\mathbb{R}^2}. \tag{34}$$

We obtain, using Hölder's inequality,

$$\begin{aligned}
|r_\rho(k)((x_1, x_2), (y_1, y_2))| &= |\langle \tilde{b}(x_1, x_2), q\tilde{b}(y_1, y_2)\rangle_{L^2(\mathbb{R})}|\\
&\leq \|\tilde{b}(x_1, x_2)\|_{L^2(\mathbb{R})}\|q\|\|\tilde{b}(y_1, y_2)\|_{L^2(\mathbb{R})},
\end{aligned} \tag{35}$$

where $\|q\|$ is the L^2-operator norm of q. For sufficiently large $\|(y_1, y_2)\|_{\mathbb{R}^2}$ we may use (81) for (15). Together with (34) we then obtain

$$\begin{aligned}
\|\tilde{b}(y_1, y_2)\|_{L^2(\mathbb{R})} &\leq C \int_{\operatorname{supp}\rho} \mathrm{e}^{-k\sqrt{(x-y_1)^2+(x-y_2)^2}}\mathrm{d}x\\
&\leq C'\mathrm{e}^{-k\frac{1}{2}\sqrt{y_1^2+y_2^2}}
\end{aligned} \tag{36}$$

with some $C, C' > 0$. Plugging (36) in (35) proves the second part of the claim. □

Having established the existence of a (continuous) integral kernel we take over the notation of the above proof. We denote for $k \in C_\alpha$, $\alpha < \frac{\pi}{2}$, and $|k|$ sufficiently large, the integral kernel of $R_\rho^{\mathrm{reg}}(k)$ by $r_\rho(k)(\cdot,\cdot)$.

The following proposition tells us how we may calculate the trace of the regularized resolvent.

Proposition 3.4 *The trace of the regularized resolvent may be calculated by, $k \in C_\alpha$, $\alpha < \frac{\pi}{2}$, and $|k|$ sufficiently large,*

$$\mathrm{Tr}\, R_\rho^{\mathrm{reg}}(k) = \int_{\mathbb{R}^2} r_{\mathrm{reg}}^\rho(k)(\boldsymbol{x},\boldsymbol{x})\mathrm{d}\boldsymbol{x}\,. \tag{37}$$

Proof The claim follows by an application of [24, p. 117] saying that the properties of $R_\rho^{\mathrm{reg}}(k)$ and of its kernel $r_{\mathrm{reg}}^\rho(k)$ derived in Proposition 3.2 and Lemma 3.3 are sufficient to deduce the claim. □

The above (trace-class) result tempts us to define the regularized trace of the resolvent as the trace of the regularized resolvent

Definition 3.5 The regularized trace of the resolvent $R_\rho(\lambda)$ is defined as

$$\mathrm{Tr}_{\mathrm{reg}}\, R_\rho(\lambda) := \mathrm{Tr}\, R_\rho^{\mathrm{reg}}(\sqrt{\lambda})\,, \tag{38}$$

with λ such that $k = \sqrt{\lambda}$ satisfies the assumption of Proposition 3.4.

3.2 An Asymptotic Analysis of the Trace of the Regularized Resolvent

To determine the asymptotic expansion of the trace of the regularized resolvent we have to introduce a couple of auxiliary objects and notations permitting a closed presentation.

We start with defining a diffeomorphism, $n \in \mathbb{N}_0$,

$$\phi : \mathbb{R}^{n+1} \to \mathbb{R}^{n+1}\,, \tag{39}$$

by

$$\begin{aligned} w_l &= \phi(y_0,\ldots,y_n)_l = y_l - y_{l+1}\,, \quad l \in \{0,\ldots,n-1\}\,,\\ w_n &= \phi(y_0,\ldots,y_n)_n = y_n + y_0\,. \end{aligned} \tag{40}$$

Note that for $n = 0$ we have $w_0 = 2y_0$. The inverse map (diffeomorphism)

$$\phi^{-1} : \mathbb{R}^{n+1} \to \mathbb{R}^{n+1} \tag{41}$$

reads as

$$y_l = \phi^{-1}(w_0, \ldots, w_n)_l = \frac{1}{2}[\sum_{m=l}^{n} w_m - \sum_{l=0}^{l-1} w_m], \quad l \in \{0, \ldots, n\}, \tag{42}$$

and, in particular, for $n = 0$ we have $y_0 = \frac{1}{2}w_0$. Moreover, we are going to utilize the following (combinatorial) set of maps, $n \in \mathbb{N}_0$,

$$S_n := \begin{cases} \{s : \quad s : \{0, \ldots, n-1\} \to \{1, -1\}\}, & n \in \mathbb{N}, \\ \emptyset, & n = 0. \end{cases} \tag{43}$$

In addition, we employ the multy-index notation

$$\alpha^n := (\alpha_0, \ldots, \alpha_{n-1}), \quad \alpha_l \in \mathbb{N}_0, \quad l \in \{0, \ldots, n-1\}. \tag{44}$$

together with

$$|\alpha^n| := \sum_{l=0}^{n-1} \alpha_l. \tag{45}$$

We remark here that α^n is only defined for $n \neq 0$.

For any $\rho \in C_0^\infty(\mathbb{R})$ the maps ϕ^{-1} in (41) and $s \in S_n$, $n \in \mathbb{N}_0$, in (43) are employed to generate a smooth and compactly supported map $\rho_{n,s}$ from $\mathbb{R}^{n+1}$ to $\mathbb{R}$, i.e., $\rho_{n,s} \in C_0^\infty(\mathbb{R}^{n+1}, \mathbb{R})$, defined by, $(w_0, \ldots, w_n) \in \mathbb{R}^{n+1}$,

$$\rho_{n,s}(w_0, \ldots, w_n) := \begin{cases} \prod_{l=0}^{n} \rho((\phi^{-1}(s(0)w_0, \ldots, s(n-1)w_{n-1}, w_n))_l), & n \in \mathbb{N}, \\ \rho(\frac{w_0}{2}), & n = 0. \end{cases} \tag{46}$$

Our asymptotic analysis also deploys the following notations of partial derivatives of $\rho_{n,s}$, using (46) and (44),

$$\partial_{\alpha^n} \rho_{n,s}(w_0, \ldots, w_{n-1}, w_n) := (\frac{\partial^{|\alpha^n|}}{\partial_{w_0}^{\alpha_0} \ldots \partial_{w_{n-1}}^{\alpha_{n-1}}} \rho_{n,s})(w_0, \ldots, w_{n-1}, w_n). \tag{47}$$

Finally, fixing $\rho \in C_0^\infty(\mathbb{R})$, the following functions will turn out of particular interest

$$c_{\alpha^n,s,l} = \begin{cases} \int\limits_{\mathbb{R}^{+n}} \int\limits_{\mathbb{R}} \frac{\mathrm{d}\xi \mathrm{d}t_0 \ldots \mathrm{d}t_{n-1}}{(1+\xi^2)^{\frac{3}{2}} (\sqrt{2}((\cosh(t_0)+\mathrm{i}\xi s(n-1)))^{\alpha_0^n+1} \ldots (\sqrt{2}(\cosh(t_{n-1})+\mathrm{i}\xi s(n-1)))^{\alpha_{n-1}^n+1}}, & n \in \mathbb{N}, \\ \int\limits_{\mathbb{R}} \frac{\mathrm{d}\xi}{(1+\xi^2)^{\frac{3}{2}}}, & n = 0, l = 0, \\ 0, & \text{else}, \end{cases} \tag{48}$$

and, $l \in \mathbb{N}_0$,

$$b_{n,l} := \begin{cases} \sum\limits_{\substack{|\alpha^n|=l, \\ s \in S_n}} c_{\alpha^n,s,l} \int\limits_{\mathbb{R}} \partial_{\alpha^n} \rho_{n,s}(0, \ldots, 0, y) \mathrm{d}y, & n \in \mathbb{N}, \\ \int\limits_{\mathbb{R}} 2\rho(\frac{y}{2}) \mathrm{d}y, & n = 0, l = 0, \\ 0, & \text{else}, \end{cases} \tag{49}$$

where we incorporated [25, 3.251 11.] and $S_0 = \emptyset$, (43). We remark that by [25, 3.252 11.]

$$c_{\alpha^0,s,0} = 2. \tag{50}$$

Equipped with the above identities, we are now able to determine the large-λ asymptotic expansion of the regularized trace of the resolvent. For this, we remind that C_α is a sector with opening angle α around the positive imaginary axis, (17).

Theorem 3.6 *The regularized trace of the resolvent* $\mathrm{Tr}_{\mathrm{reg}} R_\rho(\lambda)$ *possesses for* $|\lambda| \to \infty$ *and* $k := \sqrt{-\lambda} \in C_\alpha$ *with* $\alpha < \frac{\pi}{2}$ *a complete asymptotic expansion in integer powers of* k *of the form*

$$\mathrm{Tr}_{\mathrm{reg}} R_\rho(-\lambda) \sim \sum_{m=0}^{\infty} b_m \lambda^{-(\frac{m}{2}+1)}, \tag{51}$$

where the coefficients b_m *are given by*

$$b_m = \frac{1}{8} \sum_{\substack{n,l, \\ l+n=m}} (-2\pi)^{-(n+1)} b_{n,l}. \tag{52}$$

The first two coefficients read as

$$b_0 = -\frac{1}{4\pi}\int_{\mathbb{R}} \rho(y)\mathrm{d}x\,, \quad b_1 = \frac{\sqrt{2}}{32}\int_{\mathbb{R}} \rho(y)^2\mathrm{d}y\,. \tag{53}$$

Remark 3.7 The condition on λ implies that λ has to be in a cone around the positive axis $\mathbb{R}^+$ with opening angle smaller than 2π. Moreover, we point out that for $m \geq 2$ integrals of derivatives of ρ appear in (52) for b_m.

Proof For our convenience we choose $k = \sqrt{-\lambda}$ and consider only the case $\tilde{k} := -\mathrm{i}k \in \mathbb{R}^+$, $|k|$ sufficiently large. The general case $k \in C_\alpha$ may be treated analogously. We also remark that in the following every interchange of the order of integration is justified by Fubini's theorem [5, 23.7 Corollary].

We are going to use the resolvent representation (16). First, we expand $(\mathbb{1} + \rho\mathfrak{g}(k))^{-1}$ into a Neumann series and attain

$$\begin{aligned}\mathrm{Tr}_{\mathrm{reg}}\, R_\rho(-\lambda) &= -\,\mathrm{Tr}(\mathfrak{b}\left(\overline{k}\right)^* (\mathbb{1} + \rho\mathfrak{g}(k))^{-1}\rho\mathfrak{b}(k)) \\ &= \sum_{n=0}^{\infty}(-1)^{n+1}\,\mathrm{Tr}(\mathfrak{b}\left(\overline{k}\right)^* (\rho\mathfrak{g}(k))^n\rho\mathfrak{b}(k))\,.\end{aligned} \tag{54}$$

It is possible to get a large-k asymptotic expansion of $\mathrm{Tr}(\mathfrak{b}\left(\overline{k}\right)^* (\rho\mathfrak{g}(k))^n\rho\mathfrak{b}(k))$ for every $n \in \mathbb{N}_0$, and then we rearrange the terms w.r.t. powers of $\tilde{k}$ in (54). To see the first part of the afore mentioned, we use the integral kernels (14) and (15) for $\mathfrak{b}(k)$ and $\mathfrak{g}(k)$, and we use the notation $Y = (y_0, y_1, \ldots, y_n) \in \mathbb{R}^{n+1}$, giving

$$\begin{aligned}&\mathrm{Tr}(\mathfrak{b}\left(\overline{k}\right)^* (\rho\mathfrak{g}(k))^n\rho\mathfrak{b}(k)) \\ &= (2\pi)^{-(n+2)}\int_{\mathbb{R}^2}\int_{\mathbb{R}^{n+1}} K_0(\tilde{k}\sqrt{(x_1-y_0)^2+(x_2-y_0)^2})\rho(y_0) * \ldots \\ &\quad \ldots * K_0(\sqrt{2}\tilde{k}|y_0-y_1|)\rho(y_{n-1})K_0(\sqrt{2}\tilde{k}|y_{n-1}-y_n|) * \ldots \\ &\quad \ldots * \rho(y_n)K_0(\tilde{k}\sqrt{(y_n-x_1)^2+(y_n-x_2)^2})\mathrm{d}Y\mathrm{d}x_1\mathrm{d}x_2\,.\end{aligned} \tag{55}$$

Now, by slight abuse of notation, we apply the (orthogonal) coordinate transformation

$$(x_1, x_2) \to \frac{1}{\sqrt{2}}(x_1 + x_2, x_1 - x_2)\,, \tag{56}$$

followed by an insertion of (82) in (55), using the notation $T = (t_0, \dots, t_{n-1}) \in \mathbb{R}^{+n}$, and (92) in (55) which yields

$$\begin{aligned}
&\mathrm{Tr}(\mathfrak{b}\left(\overline{k}\right)^* (\rho\mathfrak{g}(k))^n \rho\mathfrak{b}(k)) \\
&\quad = (2\pi)^{-(n+2)} \int_{\mathbb{R}^n} \int_{\mathbb{R}^{n+1}} \int_{\mathbb{R}^2} K_0(\tilde{k}\sqrt{(x_1 - \sqrt{2}y_0)^2 + x_2^2})\rho(y_0) * \dots \\
&\qquad \dots * \mathrm{e}^{-\sqrt{2}\tilde{k}|y_0 - y_1|\cosh(t)} \rho(y_{n-1}) \mathrm{e}^{-\sqrt{2}\tilde{k}|y_{n-1} - y_n|\cosh(t)} * \dots \\
&\qquad \dots * \rho(y_n) K_0(\tilde{k}\sqrt{(\sqrt{2}y_n - x_1)^2 + x_2^2}) \mathrm{d}x_1 \mathrm{d}x_2 \mathrm{d}Y \mathrm{d}T \\
&\quad = \frac{\pi}{2\tilde{k}^2} (2\pi)^{-(n+2)} \int_{\mathbb{R}^{+n}} \int_{\mathbb{R}} \int_{\mathbb{R}^{n+1}} \frac{\mathrm{e}^{-\mathrm{i}\sqrt{2}\tilde{k}\xi(y_0 - y_n)}}{(1+\xi^2)^{\frac{3}{2}}} \rho(y_0) \mathrm{e}^{-\sqrt{2}\tilde{k}|y_0 - y_1|\cosh(t_0)} * \dots \\
&\qquad \dots * \rho(y_{n-1}) \mathrm{e}^{-\sqrt{2}\tilde{k}|y_{n-1} - y_n|\cosh(t_{n-1})} \rho(y_n) \mathrm{d}Y \mathrm{d}\xi \mathrm{d}T \,.
\end{aligned} \tag{57}$$

For $n = 0$ we directly calculate the trace and obtain

$$\begin{aligned}
\mathrm{Tr}(\mathfrak{b}\left(\overline{k}\right)^* \rho\mathfrak{b}(k)) &= \frac{1}{8\pi\tilde{k}^2} \int_{\mathbb{R}} \int_{\mathbb{R}} \frac{1}{(1+\xi^2)^{\frac{3}{2}}} \rho(y_0) \mathrm{d}\xi \mathrm{d}y_0 \\
&= \frac{1}{4\pi\tilde{k}^2} \int_{\mathbb{R}} \rho(y_0) \mathrm{d}y_0 \,,
\end{aligned} \tag{58}$$

where in the last line we used [25, 3.252 11.]. For $n \neq 0$ we want to invoke for our asymptotic analysis the integration by parts method. For this, it is expedient to first use (41) as an appropriate substitution of variables. This transformation implies

$$\sum_{l=0}^{n-1} w_l = y_0 - y_n \,, \tag{59}$$

and the determinant of the Jacobian $\det J(\phi^{-1})$ of this coordinate transformation is constant, and given by $\det J(\phi^{-1}) = \frac{1}{2}$. Hence, changing the variables in (57), using (40), (59) and $W = (w_0, \dots, w_{n-1}) \in \mathbb{R}^n$, delivers

$$\begin{aligned}
&\int_{\mathbb{R}^{+n}} \int_{\mathbb{R}} \int_{\mathbb{R}^{n+1}} \frac{\mathrm{e}^{-\mathrm{i}\tilde{k}\xi(y_0 - y_n)}}{(1+\xi^2)^{\frac{3}{2}}} \rho(y_0) \mathrm{e}^{-\sqrt{2}\tilde{k}|y_0 - y_1|\cosh(t_0)} * \dots \\
&\qquad \dots * \rho(y_{n-1}) \mathrm{e}^{-\sqrt{2}\tilde{k}|y_{n-1} - y_n|\cosh(t_{n-1})} \rho(y_n) \mathrm{d}Y \mathrm{d}\xi \mathrm{d}T
\end{aligned}$$

$$
\begin{aligned}
&= \frac{1}{2} \int\limits_{\mathbb{R}^{+n}} \int\limits_{\mathbb{R}} \int\limits_{\mathbb{R}} \int\limits_{\mathbb{R}^{n+1}} \frac{1}{(1+\xi^2)^{\frac{3}{2}}} \rho(\phi^{-1}(w_0, \dots, w_n)_0) \mathrm{e}^{-\sqrt{2}\tilde{k}(|w_0| \cosh(t_0) + \mathrm{i}\xi w_0)} * \dots \\
&\quad \dots * \rho(\phi^{-1}(w_0, \dots, w_n)_{n-1}) \mathrm{e}^{-\sqrt{2}\tilde{k}(|w_{n-1}| \cosh(t_{n-1}) + \mathrm{i}\xi w_{n-1})} * \\
&\quad * \rho(\phi^{-1}(w_0, \dots, w_n)_n) \mathrm{d}W \mathrm{d}w_n \mathrm{d}\xi \mathrm{d}T \\
&= \sum_{s \in S_n} \frac{1}{2} \int\limits_{\mathbb{R}^{+n}} \int\limits_{\mathbb{R}} \int\limits_{\mathbb{R}} \int\limits_{\mathbb{R}^n} \frac{1}{(1+\xi^2)^{\frac{3}{2}}} * \dots \\
&\quad \dots * \mathrm{e}^{-\sqrt{2}\tilde{k}(\mathrm{sgn}(w_0) \cosh(t_0) + \mathrm{i}\xi) w_0} \dots \mathrm{e}^{-\sqrt{2}\tilde{k}(\mathrm{sgn}(w_{n-1}) \cosh(t_{n-1}) + \mathrm{i}\xi) w_{n-1}} * \\
&\quad * \prod_{l=0}^{n} \rho((\phi^{-1}(w_0, \dots, w_{n-1}, w_n))_l) \mathrm{d}W \mathrm{d}w_n \mathrm{d}\xi \mathrm{d}T \\
&= \sum_{s \in S_n} \frac{1}{2} \int\limits_{\mathbb{R}^{+n}} \int\limits_{\mathbb{R}} \int\limits_{\mathbb{R}} \int\limits_{\mathbb{R}^{+n}} \frac{1}{(1+\xi^2)^{\frac{3}{2}}} \rho_{n,s}(w_0, \dots, w_n) * \\
&\quad * \mathrm{e}^{-\sqrt{2}\tilde{k}(\cosh(t_0) + \mathrm{i}\xi s(0)) w_0} \dots \mathrm{e}^{-\sqrt{2}\tilde{k}(\cosh(t_{n-1}) + \mathrm{i}\xi s(n-1)) w_{n-1}} \mathrm{d}W \mathrm{d}w_n \mathrm{d}\xi \mathrm{d}T \,.
\end{aligned}
\tag{60}
$$

It is for the following integration by parts method important that in the last line of (60) only the variables w_l with $l \in \{0, \dots, n-1\}$ appear in the exponential function. We perform an integration by parts w.r.t. the W variables. The obtained terms which don't possess any W integrals anymore may then be ordered w.r.t. the powers of $\tilde{k}$. Using our notation (45) and (47), we obtain, $l \in \mathbb{N}_0$,

$$
\begin{aligned}
&\int\limits_{\mathbb{R}^{+n}} \int\limits_{\mathbb{R}} \int\limits_{\mathbb{R}} \int\limits_{\mathbb{R}^{+n}} \frac{1}{(1+\xi^2)^{\frac{3}{2}}} \rho_{n,s}(w_0, \dots, w_n) * \\
&\quad * \mathrm{e}^{-\sqrt{2}\tilde{k}(\cosh(t_0) + \mathrm{i}\xi \rho(0)) w_0} \dots \mathrm{e}^{-\sqrt{2}\tilde{k}(\cosh(t_{n-1}) + \mathrm{i}\xi s(n-1)) w_{n-1}} \mathrm{d}W \mathrm{d}w_n \mathrm{d}\xi \mathrm{d}T \\
&= \sum_{\substack{\alpha^n, \\ |\alpha^n| \le l}} \tilde{k}^{-|\alpha^n| - n} \int\limits_{\mathbb{R}^{+n}} \int\limits_{\mathbb{R}} \int\limits_{\mathbb{R}^+} \frac{1}{(1+\xi^2)^{\frac{3}{2}}} \partial_{\alpha^n} \rho_{n,s}(0, \dots, 0, w_n) * \\
&\quad * \frac{\mathrm{d}w_n \mathrm{d}\xi \mathrm{d}T}{(\sqrt{2}(\cosh(t_0) + \mathrm{i}\xi s(n-1)))^{\alpha_0^n + 1} \dots (\sqrt{2}(\cosh(t_{n-1}) + \mathrm{i}\xi s(n-1)))^{\alpha_{n-1}^n + 1}} \\
&\quad + \mathrm{O}(\tilde{k}^{-(l+n+1)}) \,.
\end{aligned}
\tag{61}
$$

The last line follows by integration by parts and observing that every partial derivative evaluated at $(0, \dots, 0, w_n)$ is generated exactly once. Moreover, we used that the T and ξ integration don't affect the order estimate $\mathrm{O}(\tilde{k}^{-(l-n+1)})$.

Now, sorting (61) w.r.t. powers of $\tilde{k}$ by making use of our definitions (48) and (49) we get

$$\mathrm{Tr}(\mathfrak{b}\,(\overline{k})^*\,(\rho\mathfrak{g}(k))^n\rho\mathfrak{b}(k)) = \frac{1}{8\tilde{k}^2}\frac{1}{(2\pi)^{n+1}}\sum_{l'=0}^{l}\frac{1}{\tilde{k}^{l'+n}}b_{n,l'} + O(\tilde{k}^{-(l+n+1)})\,. \tag{62}$$

Note that (62) is conform with (58) for $l = n = 0$.

Finally, we use (54) plugging in there the asymptotic expansion (62), and we sort the obtained sum again w.r.t. to powers of $\tilde{k}$. This then yields the asymptotic expansion w.r.t. powers of $\mathrm{i}\tilde{k} = k = \sqrt{-\lambda}$, (52). The calculations of the first two coefficients are as follows

$$b_0 = -\frac{1}{16\pi}b_{0,0}\,, \quad b_1 = -\frac{1}{16\pi}b_{0,1} + \frac{1}{32\pi^2}b_{1,0}\,, \tag{63}$$

and it remains to calculate the three coefficients in (63) by (49). The first two ones are simple and given by, (49),

$$b_{0,0} = 4\int_{\mathbb{R}}\rho(y)\mathrm{d}y\,, \quad b_{0,1} = 0\,, \tag{64}$$

where we used (50). For $b_{1,0}$ we get by (49)

$$b_{1,0} = c_{\alpha^n,s_+,0}\int_{\mathbb{R}}\rho_{0,s_+}(0,y)\mathrm{d}y + c_{\alpha^n,s_-,0}\int_{\mathbb{R}}\rho_{0,s_-}(0,y)\mathrm{d}y\,, \tag{65}$$

where $s_+(0) := 1$ and $s_-(0) := -1$. We have for $|\alpha^1| = 0$ the simple relations

$$\rho_{0,s_\pm}(0,y) = (\rho(\frac{1}{2}y))^2\,, \tag{66}$$

and, $|\alpha^1| = 0$,

$$c_{\alpha^1,s_\pm,0} = \frac{1}{\sqrt{2}}\int_{\mathbb{R}^+}\int_{\mathbb{R}}\frac{1}{(\xi^2+1)^{\frac{3}{2}}}\frac{\cosh(t_0)\mp\mathrm{i}\xi}{\cosh(t_0)^2+\xi^2}\mathrm{d}t_0\mathrm{d}\xi\,. \tag{67}$$

Taking into account that the imaginary part cancels out in (67) we are only interested on the real part of (67) given by [49, 2.5.49. 3.],

$$c_{\alpha^1,s_\pm,0} = \mathrm{Re}\,c_{\alpha^1,s_\pm,0} = \frac{\pi}{\sqrt{2}}\int_{\mathbb{R}}\frac{1}{(1+\xi^2)^2}\mathrm{d}\xi = \frac{\pi^2}{2\sqrt{2}}\,. \tag{68}$$

Hence, inserting (68) and (66) into (65) gives

$$b_{1,0} = \frac{\pi^2}{\sqrt{2}} \int_{\mathbb{R}} \rho(\frac{1}{2}x)^2 \mathrm{d}x = \sqrt{2}\pi^2 \int_{\mathbb{R}} \rho(x)^2 \mathrm{d}x \,. \tag{69}$$

Now, plugging (69) and (64) into (63) proves the claim. □

Regarding Theorem 3.6, we make the following remark.

Remark 3.8 On the r.h.s. of formula (48) only the real part is essential as the imaginary part vanishes.

4 The Asymptotic Expansion of the Regularized Trace of the Heat Kernel

Armed with all the results inferred in our paper so far we are now in the position to deduce the existence of the heat kernel and to conclude the small-t asymptotic expansion of the regularized trace of the heat semi-group $\mathrm{e}^{t\Delta_\rho}$ (and heat kernel).

We are going to exploit that the resolvent of a contraction semi-group admits a representation as a Laplace transformation of the heat semi-group [56, Satz VII.4.10]. As for the resolvent, the heat semi-group $\mathrm{e}^{t\Delta_\rho}$ isn't a trace-class operator due to the presence of an essential spectrum of $-\Delta_\rho$. Again, we may regularize the trace of the heat semi-group analogously to Definition 3.5 by subtracting the free heat semi-group, i.e., $\{\mathrm{e}^{t\Delta_\rho}\}_{\mathrm{reg}} := \mathrm{e}^{t\Delta_\rho} - \mathrm{e}^{t\Delta_0}$, $t > 0$.

To see that $\{\mathrm{e}^{t\Delta_\rho}\}_{\mathrm{reg}}$ is trace class as well, and how we may calculate its trace, we prove the following lemma.

Lemma 4.1 *The operator* $\{\mathrm{e}^{t\Delta_\rho}\}_{\mathrm{reg}}$ *is for* $t > 0$ *a trace-class integral operator with kernel* $k^\rho_{\mathrm{reg}}(t)(\cdot,\cdot) \in C^\infty(\mathbb{R}^2 \times \mathbb{R}^2) \cap L^\infty(\mathbb{R}^2 \times \mathbb{R}^2)$. *Its trace is given by*

$$\mathrm{Tr}\{\mathrm{e}^{t\Delta_\rho}\}_{\mathrm{reg}} = \int_{\mathbb{R}^2} k^\rho_{\mathrm{reg}}(t)(\boldsymbol{x},\boldsymbol{x})\mathrm{d}\boldsymbol{x} \,. \tag{70}$$

Proof With the same Dunford-Pettis argument as in [36, Lemma 6.1] we may infer that $\{\mathrm{e}^{t\Delta_\rho}\}_{\mathrm{reg}}$ is an integral operator possessing a smooth and bounded kernel for $t > 0$. We shall use the Dunford-Taylor integral identity [33, Section IX.1.6],

$$\{\mathrm{e}^{t\Delta_\rho}\}_{\mathrm{reg}} = \frac{\mathrm{i}}{2\pi} \int_\gamma \mathrm{e}^{-\lambda t} R^{\mathrm{reg}}_\rho(\sqrt{\lambda})\mathrm{d}\lambda \,, \tag{71}$$

where γ is a suitable contour encircling the spectrum of $-\Delta_\rho$ in a positively orientated way. With a similar method as in the proof of Lemma 3.3 we may infer

that $R_\rho^{\mathrm{reg}}(\sqrt{\lambda})$ is continuous in trace norm for suitable γ's. Furthermore, due to the asymptotics (51) we conclude that the integral converges in trace norm. Now, [55, Satz 3.22] proves the first part of the claim. The second part my be proven analogously to Proposition 3.4 incorporating the above properties of the integral kernel $k_{\mathrm{reg}}^\rho(t)$. □

It is reasonable to define the regularized trace of the heat semi-group (and heat kernel) analogously to (38).

Definition 4.2 The regularized trace of the heat semi-group (heat kernel) is defined as

$$\mathrm{Tr}_{\mathrm{reg}}\, \mathrm{e}^{t\Delta_\rho} := \mathrm{Tr}\{\mathrm{e}^{t\Delta_\rho}\}_{\mathrm{reg}} = \int_{\mathbb{R}^2} k_{\mathrm{reg}}^\rho(t)(\boldsymbol{x},\boldsymbol{x})\mathrm{d}\boldsymbol{x}\,, \quad t>0\,. \tag{72}$$

We are now ready to present the result concerning our desired small-t asymptotic expansion of the regularized trace of the heat semi-group (heat kernel).

Theorem 4.3 *Let $\rho \in C_0^\infty(\mathbb{R})$. Then, the regularized trace of the heat semi-group resp. heat kernel possesses a complete asymptotic expansion in powers of t given by, $t \to 0$,*

$$\mathrm{Tr}_{\mathrm{reg}}\, \mathrm{e}^{t\Delta_\rho} \sim \sum_{n=0}^{\infty} a_n t^{\frac{n}{2}}\,, \tag{73}$$

where

$$a_{2n} = \frac{b_{2n}}{n!}\,,\ n\in\mathbb{N}_0\,, \quad a_{2n+1} = \frac{n!2^{2n+1}b_{2n+1}}{(2n+1)!\sqrt{\pi}}\,,\ n\in\mathbb{N}_0\,, \tag{74}$$

and the b_n's are given in (52).

Proof In view of Lemma 4.1, we may utilize the well-known identity [56, Satz VII.4.10],

$$\mathrm{Tr}_{\mathrm{reg}}\, R_\rho(-\lambda) = \int_{\mathbb{R}^+} \mathrm{e}^{-\lambda t}\, \mathrm{Tr}_{\mathrm{reg}}\, \mathrm{e}^{t\Delta_\rho}\mathrm{d}t\,, \tag{75}$$

with $\mathrm{Re}\,\lambda > 0$ and $\lambda > |\lambda_{\min,\rho}|$ (sufficiently large). Now, we want to apply the converse Watson lemma, Lemma 2.5. For this, we observe that the condition $|\arg(|\lambda_{\min,\sigma}| - \lambda|) \le \frac{\pi}{2}$ is equivalent to $k \in C_\alpha$ with $\alpha \le \frac{\pi}{4}$. Hence, we may apply Lemma 4.1 and use the asymptotic expansion of $\mathrm{Tr}_{\mathrm{reg}}\, R_\sigma(-\lambda)$ in Theorem 3.6.

Comparing (51) with (98) we infer that $\lambda_n = \frac{n}{2} + 1$. Finally, we use [39, pp. 2,3] to calculate

$$\Gamma(n + \frac{3}{2}) = (n + \frac{1}{2})\Gamma(n + \frac{1}{2}) = \frac{(2n+1)\sqrt{\pi}}{n!2^{2n+1}}\,, \tag{76}$$

and we plug (76) together with the b_n's, (52), in (98). That reveals the identity (74). □

We end this paper with a comparison of our heat kernel asymptotics with known results for a Schrödinger operator on $\mathbb{R}^2$, however, with a smooth potential, V. Using the Theorems 4.3 and 3.6 we obtain for our system the leading asymptotic estimate

$$\mathrm{Tr}_{\mathrm{reg}}\, \mathrm{e}^{t\Delta_\sigma} = -\frac{1}{4\pi}\int\limits_{\mathbb{R}} \sigma(x)\mathrm{d}x + \frac{\sqrt{2}\sqrt{t}}{16\sqrt{\pi}}\int\limits_{\mathbb{R}} \sigma^2(x)\mathrm{d}x + \mathrm{O}(t)\,, \quad t \to 0\,. \tag{77}$$

On the other hand, for a Schrödinger operator of the form $-\Delta + V(\cdot)$ with $V \in C_0^\infty(\mathbb{R}^2)$ the result on [32, p, 405] is (using an analogous notation), $t \to 0^+$,

$$\mathrm{Tr}_{\mathrm{reg}}\, \mathrm{e}^{t(\Delta - V(\cdot))} = -\frac{1}{4\pi}\int\limits_{\mathbb{R}^2} V(\boldsymbol{x})\mathrm{d}\boldsymbol{x} + \frac{t}{24\pi}\int\limits_{\mathbb{R}^2} (3V^2(\boldsymbol{x}) - \Delta V(\boldsymbol{x}))\mathrm{d}\boldsymbol{x}\,. \tag{78}$$

We see that the first coefficients and the power of t agree, but not the second coefficient and the corresponding power of t owing to the fact that the potential is supported only on a codimension one submanifold.

Acknowledgments The author is very grateful to Ram Band for helpful discussions and comments and he is indebted to Frank Steiner for pointing out various useful relations of Bessel functions. The work has been supported by ISF (Grant No. 494/14).

Appendix 1: Notations

First, we introduce some notations and denote by $\langle\cdot,\cdot\rangle_{\mathbb{R}^2}$ and $\|\cdot\|_{\mathbb{R}^2}$ the standard inner product and the standard Euclidean norm on $\mathbb{R}^2$, respectively. To ease notation we denote by bold letters points in $\mathbb{R}^2$, e.g., $\boldsymbol{x} = (x_1, x_2)$. We put $0 \le \arg z < 2\pi$ as the range of the argument for $z \in \mathbb{C}$, and set the branch cut of the square root $\sqrt{\cdot}$ on $\mathbb{R}^+$ such that $\sqrt{z} = \mathrm{i}\sqrt{|z|}$ for $-z \in \mathbb{R}^+$. By $|\cdot|_1$ we denote the one-dimensional Hausdorff measure. The spectrum of an operator O is denoted by $\sigma(O)$ and by $\|O\|$ we refer to the standard operator norm [55, Sections 2.1, 5.1]. Moreover, we use standard notations for the set of n-times continuously differentiable functions (possessing compact support), $C^n(\mathbb{R}^m)$ ($C_0^n(\mathbb{R}^m)$), on $\mathbb{R}^m$, and for the set of square Lebesgue-integrable functions, $L^2(\mathbb{R}^m)$, on $\mathbb{R}^m$.

We put the Fourier transform Ff of a suitable function f on $\mathbb{R}$ as

$$(Ff)(\xi) := \frac{1}{\sqrt{2\pi}} \int_{\mathbb{R}} \mathrm{e}^{-\mathrm{i}\xi x} f(x) \mathrm{d}x \,. \tag{79}$$

We also remind that by Plancherel's theorem the Fourier transform generates a unitary map on $L^2(\mathbb{R})$ [26, Section 2.2.3]. In addition, by $\Gamma(\cdot)$ we identify the Gamma function and by $K_0(\cdot)$ the K_0-Bessel function (Mcdonald function)) [39, pp. 1,66].

Appendix 2: Integral Identities for the K_0-Macdonald Function

First, we remind the asymptotic behavior of the K_0-Macdonald function for large and small arguments, γ Euler-Mascheroni constant [39, p. 69],

$$K_0(z) = -(\ln(\frac{z}{2}) + \gamma)(1 + \mathrm{O}(z)) \,, \quad -z \neq \mathbb{R}^+ \,, \tag{80}$$

and [39, p. ,139], $\delta > 0$,

$$K_0(z) = \sqrt{\frac{\pi}{2z}} \mathrm{e}^{-z} (1 + \mathrm{O}(z^{-1})) \,, \quad |z| \to \infty \,, \quad |\arg z| < \frac{3}{2}\pi - \delta \,. \tag{81}$$

In addition, we invoke for our analysis the following integral identity [39, p. 85], $x, \xi \in \mathbb{R}$,

$$K_0(\sqrt{x^2 + \xi^2}) = \int_0^\infty \mathrm{e}^{-x \cosh(t)} \cos(\xi \sinh(t)) \mathrm{d}t \,. \tag{82}$$

The following easy lemma will be used.

Lemma 2.1 *For $\kappa > 0$ and $\eta \in \mathbb{R}$ we have, $\xi \in \mathbb{R}$,*

$$(F\mathrm{e}^{-\kappa|\cdot-\eta|})(\xi) = \sqrt{\frac{2}{\pi}} \frac{2\kappa}{\kappa^2 + \xi^2} \mathrm{e}^{-\mathrm{i}\mu\xi} \,. \tag{83}$$

Proof We first treat the case $\eta = 0$:

$$\begin{aligned}(F\mathrm{e}^{-\kappa|\cdot|})(\xi) &= \frac{1}{\sqrt{2\pi}}\int_{\mathbb{R}} \mathrm{e}^{\mathrm{i}x\xi}\mathrm{e}^{-\kappa|x|}\mathrm{d}x = \frac{1}{\sqrt{2\pi}}\int_{\mathbb{R}^+} (\mathrm{e}^{\mathrm{i}x\xi}+\mathrm{e}^{-\mathrm{i}x\xi})\mathrm{e}^{-\kappa|x|}\mathrm{d}x \\ &= \sqrt{\frac{2}{\pi}}\frac{\kappa}{\kappa^2+\xi^2}\,.\end{aligned} \tag{84}$$

Now, for $\eta \neq 0$ we use the identity $(Ff(\cdot-\mu))(\xi) = (Ff)(\xi)\mathrm{e}^{-\mathrm{i}\mu\xi}$ giving (83). □

Proposition 2.2 *For y, y', $x_2 \in \mathbb{R}$ we have*

$$\begin{aligned}&\int_{\mathbb{R}} K_0(k\sqrt{(x_1-y)^2+x_2^2})K_0(k\sqrt{(x_1-y')^2+x_2^2})\mathrm{d}x_1 \\ &= \frac{2}{\pi k}\int_{\mathbb{R}}\int_{\mathbb{R}^+}\int_{\mathbb{R}^+} \frac{\cosh(t)\cosh(t')\cos(x_2\sinh(t))\cos(x_2\sinh(t'))}{((\cosh(t))^2+\xi^2)((\cosh(t'))^2+\xi^2)}\mathrm{e}^{-\mathrm{i}\xi(y-y')}\mathrm{d}t\mathrm{d}t'\mathrm{d}\xi\,.\end{aligned} \tag{85}$$

Proof We use Plancherel's theorem and Lemma 2.1 to calculate

$$\begin{aligned}&\int_{\mathbb{R}} \mathrm{e}^{-k|x_1-(y-y')|\cosh(t)}\mathrm{e}^{-k|x_1|\cosh(t')}\mathrm{d}x_1 \\ &\quad= \frac{2}{\pi}\int_{\mathbb{R}} \frac{k^2\cosh(t)\cosh(t')}{((k\cosh(t))^2+\xi^2)((k\cosh(t'))^2+\xi^2)}\mathrm{e}^{-\mathrm{i}\xi(y-y')}\mathrm{d}\xi\,.\end{aligned} \tag{86}$$

Now, we use (82) and then Fubini's theorem [5, 23.7 Corollary], for an interchange of the x_1, t and t' integration. Moreover, we are going to use the coordinate transformation $\xi \to k\xi$ giving

$$\begin{aligned}&\int_{\mathbb{R}} K_0(k\sqrt{(x_1-y)^2+x_2^2})K_0(k\sqrt{(x_1-y')^2+x_2^2})\mathrm{d}x_1 \\ &= \int_{\mathbb{R}}\int_{\mathbb{R}^+}\int_{\mathbb{R}^+} \mathrm{e}^{-k|x_1-(y-y')|\cosh(t)}\cos(kx_2\sinh(t))\mathrm{e}^{-k|x_1|\cosh(t')}\cos(kx_2\sinh(t'))\mathrm{d}t\mathrm{d}t\mathrm{d}x_1 \\ &= \frac{2}{\pi k}\int_{\mathbb{R}}\int_{\mathbb{R}^+}\int_{\mathbb{R}^+} \frac{\cosh(t)\cosh(t')\cos(kx_2\sinh(t))\cos(kx_2\sinh(t'))}{((\cosh(t))^2+\xi^2)((\cosh(t'))^2+\xi^2)}\mathrm{e}^{-\mathrm{i}k\xi(y-y')}\mathrm{d}t\mathrm{d}t'\mathrm{d}\xi\,.\end{aligned} \tag{87}$$

□

We investigate the decay properties of the integral in (85) for large x_2. To ease notation we introduce

$$F(t,t',\xi) := \frac{\cosh(t)\cosh(t')}{((\cosh(t))^2+\xi^2)((\cosh(t'))^2+\xi^2)}\,, \tag{88}$$

and we obtain

Lemma 2.3 *The following estimate*

$$\begin{aligned}&\left|\int_{\mathbb{R}}\int_{\mathbb{R}^+}\int_{\mathbb{R}^+} F(t,t',\xi)\cos(kx_2\sinh(t))\cos(kx_2\sinh(t'))\mathrm{e}^{-\mathrm{i}\xi(y-y')}\mathrm{d}t\mathrm{d}t'\mathrm{d}\xi\right| \\ &\quad\le \frac{1}{(kx_2)^2}\int_{\mathbb{R}^+}\int_{\mathbb{R}^+}\frac{\left|(\partial_{t,t'}F(t,t',\xi))\right|}{\cosh(t)\cosh(t')}\mathrm{d}t\mathrm{d}t'\mathrm{d}\xi\end{aligned} \tag{89}$$

holds.

Proof We first observe that F, $\partial_l F$, $l = t, t'$, and $\partial_{t,t'}F$ are integrable. Then, we treat the t integration with the integration by parts method and arrive at

$$\begin{aligned}\int_{\mathbb{R}^+} F(t,t',\xi)\cos(kx_2\sinh(t))\mathrm{d}t &= \int_{\mathbb{R}^+}\frac{F(t,t',\xi)\cosh(t)}{\cosh(t)}\cos(kx_2\sinh(t))\mathrm{d}t \\ &= \frac{1}{kx_2}\int_{\mathbb{R}^+}\frac{(\partial_t F(t,t',\xi))}{\cosh(t)}\sin(kx_2\sinh(t))\mathrm{d}t\,.\end{aligned} \tag{90}$$

Doing the same w.r.t. the t' integration and exploiting that $|\sin(\tau)| \le |\mathrm{e}^{\mathrm{i}\tau}| = |\mathrm{e}^{-\xi(y-y')}| = 1$, $\tau \in \mathbb{R}$, gives

$$\begin{aligned}&\left|\int_{\mathbb{R}^+} F(t,t',\xi)\cos(kx_2\sinh(t))\cos(kx_2\sinh(t'))\mathrm{e}^{-\mathrm{i}k\xi(y-y')}\mathrm{d}t\mathrm{d}t'\mathrm{d}\xi\right| \\ &\quad= \frac{1}{(kx_2)^2}\left|\int_{\mathbb{R}^+}\frac{\partial_{t,t'}F(t,t',\xi)}{\cosh(t)\cosh(t')}\sin(kx_2\sinh(t))\sin(kx_2\sinh(t'))\mathrm{e}^{-\mathrm{i}k\xi(y-y')}\mathrm{d}t\mathrm{d}t'\mathrm{d}\xi\right| \\ &\quad\le \frac{1}{(kx_2)^2}\int_{\mathbb{R}^+}\frac{\left|\partial_{t,t'}F(t,t',\xi)\right|}{\cosh(t)\cosh(t')}\mathrm{d}t\mathrm{d}t'\mathrm{d}\xi\,.\end{aligned} \tag{91}$$

□

We are now able to perform an x_2-integration in (85), and we remark that in the following appearing integrals the order of integration is cruical.

Proposition 2.4 *For y, $y' \in \mathbb{R}$ we have*

$$\begin{aligned}&\int_{\mathbb{R}}\int_{\mathbb{R}} K_0(k\sqrt{(x_1-y)^2+x_2^2})K_0(k\sqrt{(x_1-y')^2+x_2^2})\mathrm{d}x_1\mathrm{d}x_2\\ &=\int_{\mathbb{R}}\frac{\pi}{2k^2(1+\xi^2)^{\frac{3}{2}}}\mathrm{e}^{-\mathrm{i}k\xi(y-y')}\mathrm{d}\xi\,.\end{aligned}\tag{92}$$

Proof Due to Lemma 2.3 the x_2-integral exists. We perform in (85) the substitution $t, t' \to \operatorname{arsinh}(t), \operatorname{arsinh}(t')$, use $(\frac{\mathrm{d}}{\mathrm{d}t}\sinh(t)) = (\cosh(\operatorname{arsinh}(t)))^{-1} = (\sqrt{1+t^2})^{-1}$, $\cos(x)\cos(y) = \frac{1}{2}(\cos(x+y)+\cos(x-y))$ and make the substitution $x_2 \to \frac{x_2}{k}$. This gives

$$\begin{aligned}&\int_{\mathbb{R}}\int_{\mathbb{R}^{+2}}\int_{\mathbb{R}}\frac{\cosh(t)\cosh(t')\cos(kx_2\sinh(t))\cos(kx_2\sinh(t'))}{((\cosh(t))^2+\xi^2)((\cosh(t'))^2+\xi^2)}\mathrm{e}^{-\mathrm{i}k\xi(y-y')}\mathrm{d}\xi\mathrm{d}t\mathrm{d}t'\mathrm{d}x_2\\ &=\frac{1}{k}\int_{\mathbb{R}}\int_{\mathbb{R}^{+2}}\int_{\mathbb{R}}\frac{\cos(x_2(t+t'))+\cos(x_2(t-t'))}{2(t^2+1+\xi^2)(t'^2+1+\xi^2)}\mathrm{e}^{-\mathrm{i}k\xi(y-y')}\mathrm{d}\xi\mathrm{d}t\mathrm{d}t'\mathrm{d}x_2\,.\end{aligned}\tag{93}$$

Due to decay property proven in Lemma 2.3 it is not hard to see that we may extend the setting on [6, p. 36] to our case. Hence, we may use the δ-identity [6, pp. 33,34],

$$\frac{1}{2\pi}\int_{\mathbb{R}}\cos(\xi(x-x_0))\mathrm{d}\xi = \delta(x-x_0)\,.\tag{94}$$

We arrive at

$$\begin{aligned}&\int_{\mathbb{R}} K_0(k\sqrt{(x_1-y)^2+x_2^2})K_0(k\sqrt{(x_1-y')^2+x_2^2})\mathrm{d}x_1\mathrm{d}x_2\\ &=\int_{\mathbb{R}^+}\int_{\mathbb{R}}\frac{2}{k^2(t^2+1+\xi^2)^2}\mathrm{e}^{-\mathrm{i}k\xi(y-y')}\mathrm{d}\xi\mathrm{d}t\\ &=\int_{\mathbb{R}}\frac{\pi}{2k^2(1+\xi^2)^{\frac{3}{2}}}\mathrm{e}^{-\mathrm{i}k\xi(y-y')}\mathrm{d}\xi\,,\end{aligned}\tag{95}$$

where in the last line we used [25, 3.241 4.]. □

2.1 A Converse Watson Lemma

To connect the large-λ (or large-k) asymptotics of the resolvent with the small-t asymptotics of the heat kernel the following lemma will be used, which may be obtained by replacing a_n by $\frac{a_n}{\Gamma(\lambda_n)}$ on [57, p. 31].

Lemma 2.5 (Converse Watson Lemma) *Let f be a continuous function in $(0,\infty)$, $f(t) = 0$ for $t < 0$, and $\mathrm{e}^{-c\cdot} f(\cdot) \in L^1(0,\infty)$. Let F be the Laplace transform of f, i.e.,*

$$F(z) := \int_0^\infty f(t)\mathrm{e}^{-zt}\mathrm{d}t\,. \tag{96}$$

If F possesses the uniform asymptotic expansion

$$F(z) \sim \sum_{n=0}^{\infty} a_n z^{-\lambda_n}\,, \quad |z| \to \infty,\ \arg(z-c) \le \frac{\pi}{2}\,, \tag{97}$$

and $\lambda_n \to \infty$ monotonously as $n \to \infty$, then

$$f(t) \sim \sum_{n=0}^{\infty} \frac{a_n}{\Gamma(\lambda_n)} t^{\lambda_n - 1}\,, \quad t \to 0^+\,. \tag{98}$$

References

1. W. Arendt, R. Nittka, W. Peter, and F. Steiner. Weyl's Law: Spectral Properties of the Laplacian in Mathematics and Physics. In *Mathematical Analysis of Evolution, Information, and Complexity*. Wiley-Blackwell, 2009.
2. M. Atiyah, R. Bott, and V. K. Patodi. On the heat equation and the index theorem. *Invent. Math.*, 19:279–330, 1973.
3. M. Atiyah, R. Bott, and V. K. Patodi. Errata to: "On the heat equation and the index theorem" (Invent. Math. **19** (1973), 279–330). *Invent. Math.*, 28:277–280, 1975.
4. R. F. Bass, M. Kassmann, and T. Kumagai. Symmetric jump processes: localization, heat kernels and convergence. *Ann. Inst. Henri Poincaré Probab. Stat.*, 46:59–71, 2010.
5. H. Bauer. *Measure and integration theory*. Walter de Gruyter & Co., Berlin, 2001.
6. P. Blanchard and E. Brüning. *Mathematical methods in physics*. Birkhäuser/Springer, Cham, 2015.
7. J. Bolte, S. Egger, and R. Rueckriemen. Heat-kernel and resolvent asymptotics for Schrödinger operators on metric graphs. *Appl. Math. Res. Express. AMRX*, pages 129–165, 2015.
8. J. Bolte and S. Keppeler. Heat kernel asymptotics for magnetic Schrödinger operators. *J. Math. Phys.*, 54:112104, 13, 2013.
9. J. Bolte and J. Kerner. Quantum graphs with two-particle contact interactions. *J. Phys. A*, 46:045207, 14, 2013.

10. J. Bolte and J. Kerner. Bose-Einstein condensation on quantum graphs. In *Mathematical results in quantum mechanics*, pages 221–226. World Sci. Publ., Hackensack, NJ, 2015.
11. J. Bolte and J. Kerner. Instability of Bose-Einstein condensation into the one-particle ground state on quantum graphs under repulsive perturbations. *J. Math. Phys.*, 57:043301, 9, 2016.
12. J. Bolte and J. Kerner. Many-particle quantum graphs: A review. *arXiv e-prints*, 2018. https://arxiv.org/abs/1805.00725.
13. J. F. Brasche, P. Exner, Y. A. Kuperin, and P. Seba. Schrödinger operators with singular interactions. *J. Math. Anal. Appl.*, 184:112–139, 1994.
14. M. A. Cazalilla, R. Citro, T. Giamarchi, E. Orignac, and M. Rigol. One dimensional bosons: From condensed matter systems to ultracold gases. *Rev. Mod. Phys.*, 83:1405–1466, Dec 2011.
15. G. Chinta, J. Jorgenson, and A. Karlsson. Heat kernels on regular graphs and generalized Ihara zeta function formulas. *Monatsh. Math.*, 178:171–190, 2015.
16. D. Daners. Heat kernel estimates for operators with boundary conditions. *Math. Nachr.*, 217:13–41, 2000.
17. B. Devyver. A Gaussian estimate for the heat kernel on differential forms and application to the Riesz transform. *Math. Ann.*, 358:25–68, 2014.
18. S. Egger and J. Kerner. Scattering properties of two singularly interacting particles on the half-line. *Rev. Math. Phys.*, 29(10):1750032, 37, 2017.
19. G. Esposito. New results in heat-kernel asymptotics on manifolds with boundary. In *The Casimir effect 50 years later (Leipzig, 1998)*. World Sci. Publ., River Edge, NJ, 1999.
20. R. L. Frank, C. Hainzl, R. Seiringer, and J. P. Solovej. Derivation of Ginzburg-Landau theory for a one-dimensional system with contact interaction. In *Operator methods in mathematical physics*, volume 227 of *Oper. Theory Adv. Appl.*, pages 57–88. Birkhäuser/Springer Basel AG, Basel, 2013.
21. B. Gaveau, M. Okada, and T. Okada. Explicit heat kernels on graphs and spectral analysis. In *Several complex variables (Stockholm, 1987/1988)*. Princeton Univ. Press, Princeton, NJ, 1993.
22. P. B. Gilkey. Curvature and the eigenvalues of the Laplacian for elliptic complexes. *Advances in Math.*, 10:344–382, 1973.
23. P. B. Gilkey. *Asymptotic formulae in spectral geometry*. Chapman & Hall/CRC, Boca Raton, FL, 2004.
24. I. C. Gohberg and M. G. Kreĭn. *Introduction to the theory of linear nonselfadjoint operators*. American Mathematical Society, Providence, R.I., 1969.
25. I. S. Gradshteyn and I. M. Ryzhik. *Table of integrals, series, and products*. Elsevier/Academic Press, Amsterdam, 2007.
26. L. Grafakos. *Classical Fourier analysis*. Springer, New York, 2014.
27. A. Grigor'yan. *Heat kernel and analysis on manifolds*, volume 47. American Mathematical Society, Providence, RI; International Press, Boston, MA, 2009.
28. A. Grigor'yan and A. Telcs. Sub-Gaussian estimates of heat kernels on infinite graphs. *Duke Math. J.*, 109:451–510, 2001.
29. P. Grisvard. *Elliptic problems in nonsmooth domains*. Pitman (Advanced Publishing Program), Boston, MA, 1985.
30. J. M. Harrison, J. P. Keating, J. M. Robbins, and A. Sawicki. n-particle quantum statistics on graphs. *Comm. Math. Phys.*, 330(3):1293–1326, 2014.
31. S. W. Hawking. Zeta function regularization of path integrals in curved spacetime. *Comm. Math. Phys.*, 55:133–148, 1977.
32. M. Hitrik and I. Polterovich. Regularized traces and Taylor expansions for the heat semigroup. *J. London Math. Soc. (2)*, 68:402–418, 2003.
33. T. Kato. *Perturbation theory for linear operators*. Springer-Verlag New York, Inc., New York, 1966.
34. K. Kirsten. Spectral functions in mathematics and physics. In *Trends in theoretical physics, II (Buenos Aires, 1998)*. Amer. Inst. Phys., Woodbury, NY, 1999.

35. V. Kostrykin, J. Potthoff, and R. Schrader. Heat kernels on metric graphs and a trace formula. In *Adventures in mathematical physics*, Contemp. Math. Amer. Math. Soc., Providence, RI, 2007.
36. V. Kostrykin and R. Schrader. Laplacians on metric graphs: eigenvalues, resolvents and semigroups. In *Quantum graphs and their applications*, Contemp. Math. Amer. Math. Soc., Providence, RI, 2006.
37. H. Kovařík and D. Mugnolo. Heat kernel estimates for Schrödinger operators on exterior domains with Robin boundary conditions. *Potential Analysis*, 48:159–180, 2018.
38. E. H. Lieb and W. Liniger. Exact analysis of an interacting bose gas. i. the general solution and the ground state. *Phys. Rev.*, 130:1605–1616, May 1963.
39. W. Magnus, F. Oberhettinger, and R. P. Soni. *Formulas and theorems for the special functions of mathematical physics*. Springer-Verlag New York, Inc., New York, 1966.
40. S. Minakshisundaram. A generalization of Epstein zeta functions. With a supplementary note by Hermann Weyl. *Canadian J. Math.*, 1:320–327, 1949.
41. S. Minakshisundaram and A. Pleijel. Some properties of the eigenfunctions of the Laplace-operator on Riemannian manifolds. *Canadian J. Math.*, 1:242–256, 1949.
42. D. Mugnolo. Gaussian estimates for a heat equation on a network. *Netw. Heterog. Media*, 2:55–79, 2007.
43. D. Mugnolo. *Semigroup methods for evolution equations on networks*. Springer, Cham, 2014.
44. T. Okada. Asymptotic behavior of skew conditional heat kernels on graph networks. *Canad. J. Math.*, 45:863–878, 1993.
45. Y. Pinchover. Some aspects of large time behavior of the heat kernel: an overview with perspectives. In *Mathematical physics, spectral theory and stochastic analysis*, Oper. Theory Adv. Appl. Birkhäuser/Springer Basel AG, Basel, 2013.
46. I. Polterovich. A commutator method for computation of heat invariants. *Indag. Math. (N.S.)*, 11:139–149, 2000.
47. O. Post and R. Rückriemen. Locality of the heat kernel on metric measure spaces. *Complex Anal. Oper. Theory*, 12:729–766, 2018.
48. R. Pröpper. Heat kernel bounds for the Laplacian on metric graphs of polygonal tilings. *Semigroup Forum*, 86(2):262–271, 2013.
49. A. P. Prudnikov, Y. A. Brychkov, and O. I. Marichev. *Integrals and series. Vol. 1*. Gordon & Breach Science Publishers, New York, 1986.
50. J.-P. Roth. Spectre du laplacien sur un graphe. *C. R. Acad. Sci. Paris Sér. I Math.*, 296:793–795, 1983.
51. R. Seiringer, J. Yngvason, and V. A. Zagrebnov. Disordered Bose Einstein condensates with interaction. In *XVIIth International Congress on Mathematical Physics*, pages 610–619. World Sci. Publ., Hackensack, NJ, 2014.
52. M. van den Berg. On the trace of the difference of Schrödinger heat semigroups. *Proc. Roy. Soc. Edinburgh Sect. A*, 119:169–175, 1991.
53. M. van den Berg, P. Gilkey, K. Kirsten, and R. Seeley. Heat trace asymptotics with singular weight functions. *Comm. Anal. Geom.*, 17:529–563, 2009.
54. D. V. Vassilevich. Heat kernel expansion: user's manual. *Phys. Rep.*, 388:279–360, 2003.
55. J. Weidmann. *Lineare Operatoren in Hilberträumen. Teil 1*. B. G. Teubner, Stuttgart, 2000.
56. D. Werner. *Funktionalanalysis*. Springer-Verlag, Berlin, 2000.
57. R. Wong. *Asymptotic approximations of integrals*. Society for Industrial and Applied Mathematics (SIAM), Philadelphia, PA, 2001.
58. E. M. E. Zayed. Short-time asymptotics of the heat kernel on bounded domain with piecewise smooth boundary conditions and its applications to an ideal gas. *Acta Math. Appl. Sin. Engl. Ser.*, 20:215–230, 2004.

Modeling Dynamic Coupling in Social Interactions

Merle T. Fairhurst

Abstract Whether negotiating the price of an item in a foreign marketplace or temporally coordinating actions within a musical ensemble, the basis of any social interaction must be the exchange of relevant information allowing for co-actors to become more or less aligned in body and mind. Although in humans, there are obvious daily examples of verbal exchanges, from infancy and beyond, we depend significantly on non-verbal exchanges. In most cases of social interaction, it is these non-verbal exchanges such as a hand gesture, a shift of gaze, a change in action timing, that allow us to predict, respond and adapt to one another, that is to become aligned. Both the experience and the process of becoming aligned is dynamic in nature, that is alignment happens and the degree of alignment changes across time. As such, an improved understanding of how we do things together, requires both a revised theoretical construct and dynamic timecourse models for predicting social behaviour between interconnected agents. The following is a summary of the work done as part of the interdisciplinary cooperation Group "Discrete and Continuous Models in the theory of Networks" at the Centre for Interdisciplinary Research (ZiF, Bielefeld University) to devise appropriate dynamic timecourse models. These models will be based on theoretical concepts of alignment as well as empirical testing of healthy individuals in which traditional measures of the degree of coupling will be used to compare instances where group size and richness of available social information is varied. Of specific interest will be phase transitions along a spectrum of self-organisation (negotiation, alignment, uncoupling). It is intended that the models will be used in conjunction with and compared with acquired and simulated data. Exploring the exchange of non-verbal information in a network of interconnected agents and bridging the gap between cognitive neuroscience and mathematics, this paper puts forward specific ways in which the use of dynamic timecourse modelling can further our understanding of the cognitive and neural

M. T. Fairhurst (✉)
Faculty of Philosophy, Ludwig Maximilian University, Munich, Germany

Munich Center for Neuroscience, Ludwig Maximilian University, Munich, Germany
e-mail: m.fairhurst@lmu.de

F. M. Atay et al. (eds.), *Discrete and Continuous Models in the Theory of Networks*, Operator Theory: Advances and Applications 281,
https://doi.org/10.1007/978-3-030-44097-8_7

underpinnings of social interactions. Specifically, findings will be translated to extend existing general sociological concepts of group behaviour and dynamics as well as specific applications in networks of individuals ranging from small groups like a string quartet or a football team to a large crowd at a political rally.

1 Introduction

From rowers to dancers, musicians to construction workers, social interactions require individuals working or playing together to coordinate intentions and actions. A central function of the human brain is to mediate these social interactions, whether for communication or more physical examples of joint action [1]. How one brain interacts with another has been said to depend on social cognition, theoretical models of which can be summarized as being based broadly in either mindreading or non-mindreading accounts, with an historical bias on the former [2]. With concepts such as 'theory of mind' or simulation, these mindreading models suggest that one creates a representation of another's thoughts or actions by inferring, simulating or projecting the behavior of another to respond appropriately. These more representationalist theories align social cognition with social understanding where a model of how someone might act allows for intersubjectivity. As elegantly described by Frith and Frith [3], these representations of another's actions, mental state, intentions or goals create shared representations of self and other [4] and can be very useful for the alignment of cooperating individuals. Calls from those working in the field of social cognition and neuroscience however have stipulated the need for the use and study of more interactive tasks in which information is exchanged in real time between interacting [5, 6]. In more interactive tasks, individuals are required to predict, respond and adapt to another person's actions in a so-called second person perspective [7]. This is certainly true in instances where the task demands the precise synchronisation of one person's movements with another's. Temporal synchronization is an essential part of many forms of social interaction where one must coordinate the timing of one's actions with an external stimulus, say for instance the tones produced by a fellow musician [8]. Beyond the obvious musical examples, consider for example an Olympic rowing team that speeds up to overtake a competing team based on the rhythmical calls of the coxswain or, when trying to navigate a busy sidewalk, you adapt your walking pace (and trajectory) to avoid colliding with other walkers. The process of synchronizing relies heavily on an interdependence or coupling of the actions and indeed intentions of the interacting agents: "will you go first, or shall I?", "are you slowing down, should I?".

Interestingly, in both the theoretical account of social cognition and in the preceding description of the temporal synchronisation of joint actions, one notices a tension between and the need for both interactive, online adaptation (***are*** you slowing down?) and feedforward, predictive mechanisms (***will*** you go first?) for interacting individuals to coordinate successfully. To date, the use of temporal

synchronisation tasks has been used to more generally describe the instances in which interacting agents/individuals were either "in" or "out" of synch (e.g. playing the musical piece temporally together) [9]. From personal experience though, we encounter a far broader and richer range of types of social interaction [10]. It is, one might say, the getting in synch, that motivates us to engage in social interactions: not the fact that we reach a certain goal (optimal temporal synchronisation) but rather that we are doing something together through time. The dynamic nature of social interactions, that the way we interact with others evolves through time, is something less likely to be captured by many of the more observational social cognition paradigms. Moreover, even sensorimotor synchronisation tasks where individuals coordinate across time, are often described using limited correlational methods. In the following, with a focus on sensorimotor synchronisation (SMS) tasks, we discuss the potential advantage offered by model-based computational approaches. By probing both the nature of the exchange and the nature of the information that is exchanged between interacting agents, we describe how we will create and test (based on real data and a minimalist theory of alignment) models of changing degrees of coupling within a network of coordinating individuals in dynamic interactions. More generally, these models and the theoretical advances they will facilitate may better characterise the self-organising character of the individuals within the network.

2 Coupling and Information Exchange

Early investigations of social cognition have employed observation tasks in which participants assessed a recorded social interaction between two other people [11–13]. These third person perspective designs however offer little insight into more direct or second person interactive social situations which require individuals to adapt and coordinate their actions in real time. Others have therefore implemented online gaming paradigms where participants play with an invisible, virtual partner [14–17]. Naturally, these designs offer the advantage of allowing one side of the interacting dyad to be controlled by the experimenter. With the advent of so-called two-brain social neuroscience, setups involving dyads of interacting agents have allowed for the measurement of temporal coordination behaviour, subsequent affiliation and associated brain activity to detail the nature of dyadic interactions [18]. Even the most recent studies of coordination or cooperation however tend to be limited by the choice of the task and, as a result, the lack of ongoing, objective outcome measures that quantify the degree of coupling, that is the relationship strength between interacting individuals.

Along with others, we have suggested the need for a shift in focus to studying and measuring the nature of the interaction rather than a focus on the task (identifying joint tasks that model social interaction) [10]. Specifically, we have suggested that rather than determine whether a certain interaction is social by virtue of the task used, we propose that quantifying the degree and nature coupling between

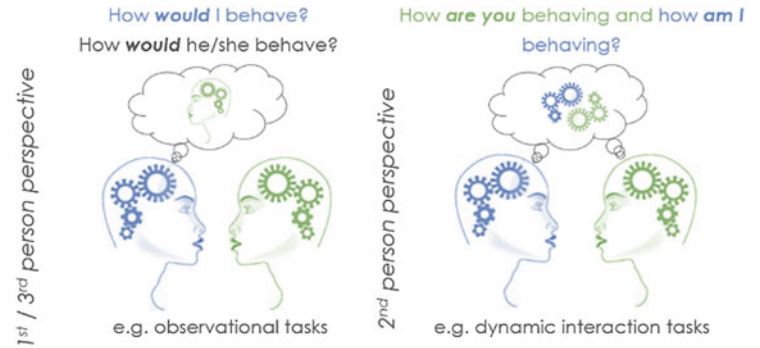

Fig. 1 A second person perspective account of social cognition. Future models of social cognition as well as the experimental paradigms used to test these should allow for both observational and predictive (how would I/she behave in this context) as well as online, dynamically interactive

interacting individuals, allows one to describe social interactions in terms of a spectrum ranging minimal or weak instances of coupling (e.g. walking in step along a pavement without consciously adapting to one another, much like the physical coupling observed in birds or fireflies and other dynamical systems) to strong and rich instances of coupling (e.g. group music making where alignment is seen at intentional, mental, emotional and physical levels). In so doing one can differentiate between two cases: imagine, for example, two people sitting side by side on an airplane, raising their glasses in a coordinated fashion. This temporally correlated, one shot, coordinated behaviour however need not rely on or result from a bidirectional or reciprocal exchange of information but simply be an inadvertent coincidence and as such would not correspond to a coupling between the two systems but rather to a lack of independence between them. The major risk would be to draw incorrect inferences as to the social nature of this observed behaviour based on what could be described as "the spectre of 'spurious' correlations" [19] (Fig. 1).

3 Dynamic Exchanges and Coupling in Sensorimotor Synchronisation

A more enactive description of social cognition suggests that in most interactions, socially relevant information is monitored and extracted [20, 21] which has aptly been described as *participatory sense making* [22]. In these situations where individuals actively and directly interact with one another, it has been put forward that this reciprocal information exchange establishes a subject-subject relationship (rather than a subject-object relationship) and as such a so-called second-person perspective is taken [7, 23]. Moreover, it has been suggested that in ongoing dynamic scenarios, a more interactive form of social exchange is required [24].

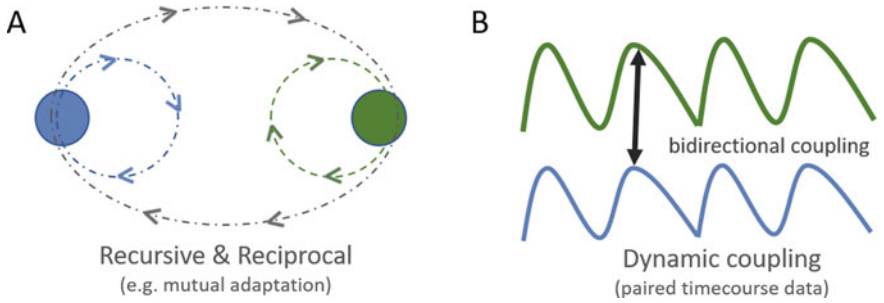

Fig. 2 Dynamic social interactions. Exploring the more interactive exchange of information in tasks such as those require temporal coordination across time will allow for a better description and quantification of the coupling of paired timecourses from interacting agents. The recursive information exchange that results in coupling may produce patterns of reciprocal adaptation

To successfully coordinate, rather than merely predicting how a partner *might* act, ongoing predictions and appropriate responses are derived based on how the partner *is* behaving and how the behavior of one partner changes over time with respect to the actions of the other. This coordination behaviour is a prime example of reciprocity, that is the mutual adaptation of interacting agents through the reciprocal exchange of information (Fig. 2a). The behaviour of one player results in a change in behaviour of the other in a reciprocal fashion.

This adaptive behavior significantly overlaps conceptually with the sensorimotor coupling and subsequent physical alignment which has been extensively studied within the field of sensorimotor research [25]. From the same body of literature, it has been shown that this reciprocal exchange of information results in physical alignment, which in turn results in greater degrees of affiliation and greater mental alignment [26–28]. In the ecological example of group music making, the sight of a conductor's baton or the tone onset of a fellow player prompts other players to commence their part. In these instances of temporal synchronisation and coordination as well as real-world scenarios they model, observed physical alignment in time and space is said to depend on cognitive models of adaptation [8, 28, 29] and thus on reciprocal interactions [30–32]. Using simplified models of interaction, cognitive theories of enaction and dynamical system approaches have been used to describe the dynamical coupling of cognitive agents with their environment and other agents. These paradigms therefore offer various advantages including the relevance of the findings to our understanding of the development and functioning of the social brain [33].

Experimentally, SMS is typically studied in a reduced fashion by requiring an individual to coordinate simple movements, such as finger taps [34], with an auditory sequence produced by a computer or a co-acting partner [8]. The instruction is typically to synchronize simple movements, such as finger taps, as accurately and precisely as possible with a pacing signal. Through variations on a theme, this task has been varied to include pacing signals that are isochronous (unchanging), at

varying tempos and others that include intermittent tempo perturbations. In all cases however, the instructed task infers and results in a coupling of two timecourses: that of the pacing signal and that of the human tapper (see Fig. 2b). These tasks have been expanded to investigate the SMS behavior of interacting, mutually adaptive dyads with measured coordination of a human tapper with either a virtual [35] or another human partner [36]. In each case, the information exchanged is, by design, reduced to temporal onset information. It should be noted that similar work has explored other, richer forms of non-verbal sensory information exchange, for example by including visual cues through face-to-face contact. By recording the tapping behavior of both partners, provide an objective read-out of the interaction.

How factors such as the richness of available coordination cues (e.g. only auditory information or both auditory and visual information) or the nature of the partner with whom one is tapping (e.g. leader vs. follower, tracker vs. predictor or minimally or overly adaptive) alters tapping behaviour is typically measured as a function of synchronization performance. Most basically, synchronisation tasks and measures have been used to model and describe instances in which interacting dyads were simply either "in" or "out" of synch [9]. Typically, this will include descriptions of measures of the mean asynchrony which can be used as an inverse measure of SMS accuracy, and the variability (i.e., standard deviation) of the signed asynchronies which serves an inverse measure of SMS precision. Measures of synchrony, influence, error correction mechanisms (26) and individual synchronization strategies are all easily derived from the simple self and other tap onsets [8]. Though not necessarily captured by current methodologies, the dynamic nature of these tasks potentially allows one to experimentally measure coordination across time including going beyond a mere description of whether (overall) interacting individuals are "in sync" but instead to describe, for example, phase shifts from coupled to uncoupled states (see Sect. 6).

4 Quantifying Interactive Coupling

A host of methods exist for quantifying the coupling that results from a dynamic, exchange of information between socially interacting individuals. Typically, these methods use concurrently acquired pairs of data and probe them with analyses which compare and correlate the timeseries [37, 38]. Mutual information is a quantity that measures the mutual dependence of the two random variables. Intuitively, it measures the information content that the two variables share, that is, how much knowing one of these variables reduces uncertainty about the other [39]. This method has therefore successfully been employed by our group as a measure of interpersonal coordination [40]. Both behavioural and brain data have been investigated using mutual information and cross-recurrence quantification (CRQA). For example, work by Konvalinka and colleagues implemented CRQA methods to explore commonalities in arousal levels, as a measure of emotional contagion (or influence). Specifically, they investigated synchronization of galvanic

skin responses between firewalkers and spectators [41]. Similarly, neural coupling between interacting individuals has previously been investigated using hyper phase locking value as a measure of synchrony [42].

From the SMS literature, one finds a diverse array of methods that are systematically used to quantify the strength of serial dependencies between successive asynchronies during paced finger tapping [43]. In instances of temporal coordination, participating individuals must respond and adapt to changes in behavior made by their partner(s) but this will be most efficiently done if combining the reactive error corrections processes with anticipatory, predictive mechanisms (e.g. [44, 45]. This work has provided insight into both the adaptive and predictive mechanisms that underlie coordination during SMS tasks. From the adaptive side, error correction estimates have been obtained by fitting models to asynchrony time series [29, 45–48] and used as a proxy for degree of coupling [49, 50]. Looking more towards the predictive aspect of temporal coordination during SMS, using temporal data from the inter-tap-intervals (ITIs from the human tapper) and inter-onset-intervals (IOIs of the pacing signal), Pecenka and Keller (2011) used the ratio between the lag-0 and lag-1 cross-correlations of ITIs and IOIs (a prediction-tracking P/T ratio) as a measure of prediction in SMS with tempo changing tapping tasks [51]. Based on several studies, it has been shown that a PT-ratio larger than 1 reflects an individual's tendency to predict tempo changes, while a ratio smaller than 1 indicates a tendency to copy (track) tempo changes. The PT-ratio has been found to correlate positively with musical experience, tapping abilities and neural activation in brain networks comprising cortico-cerebellar motor-related areas and medial cortical areas [51, 52]. Extending the original (adaptive) correction models [53], van der Steen and colleagues employed simulation techniques to create and test the Adaptation and Anticipation Model (ADAM) of SMS which incorporates both reactive and predictive elements [45].

5 Applying Dynamic Timecourse Models to Sensorimotor Synchronisation Data

To date, concurrently acquired pairs of data have typically been probed with analyses which compare and correlate the timeseries [42]. However, within the SMS literature, there have been successful applications of models to describe the nature of the interaction between coordinating individuals. A model is a (theoretical) machine that itself outputs a timeseries. If the model's output matches or resembles the measured behavioural or neural output to a reasonable extent, then the machine is "a good model" and can be used to test specific hypotheses regarding cognitive processing related to the task. The use of a dynamical model offers various advantages over more traditional approaches which are purely information-theoretic, i.e. that is one doesn't need to know how the system works. In mutual information, for example, one simply observes signals and calculates how much

information from one variable is contained in the second variable. Two random variables are independent if and only if their mutual information is zero. As part of an ongoing collaboration, bridging the gap between neuroscience and mathematics, we are developing a set of specialized prediction-based models to more specifically investigate coordination behavior in SMS tasks. These methods will be used to probe both behavioral and neural data to quantify the degree of coupling between the interacting agents but also, more importantly, to identify what precisely within the individual timecourses becomes coupled (e.g. amplitude, phase). Different factors such as the nature of the partner and the nature of the information exchanged can contribute to the observation of a temporally coherent link between two dynamical systems.

5.1 Nature of the Partner

Based on a Kuramoto model of dynamical systems [54], the first model under development investigates the interdependence of the two information streams (shared between two interacting agents, player 1 and player 2). This would be compared against experimental data from finger tapping experiments of human-metronome, human-virtual partner or human-human dyads. We posit firstly that player 1's response will depend on a comparison of his/her state and that of their interacting partner and secondly that the importance or weighting ("k") of this comparison should differ between leaders and followers. From existing SMS literature, the nature of the individuals that make up the interacting dyad can affect synchronisation strategies, tapping behaviour and synchronisation performance [49, 50]. By varying the model, we can test for example whether the temporal "leader" within the pair predicts or has some quantifiable influence over the observed behavior of the co-acting partner.

5.2 Nature of the Information Being Exchanged

This weighting ("k") may also vary as a function of the reliability of the information pertaining to "other". Previous SMS studies have explored differences in synchronisation performance as a function of the type of sensory information that is exchanged [55–57]. While the Kuramoto model is valid in cases in which individuals are always aware of the movements of the other, our second Winfree-based model allows for relative phase adjustments based on varying "other" information [58]. The width of the function ($f(\theta_1)$) can be varied as the richness/availability of socially relevant cues is manipulated. Specifically, one can imagine ecological instances and experimental setups in which agents have varying degrees of access to their partner and as such socially relevant information that aids coordination may or may not be available (e.g. playing a video game with someone online, tapping studies in which the participant either sees, hears or sees and hears their partner).

Both of these models can logically be extended using a time-delay function which assumes and explores the effect of a temporal (processing) delay in the information shared between interacting partners [59, 60]. This enhancement of the models may more accurately describe brain processing specifically in terms of the known importance of this type of delay in the sensorimotor loop. Beyond this, we may add further parameters, as suggested by theoretical shifts as well as further relevant empirical work.

6 Network Structures in Sensorimotor Synchronisation Tasks

As this project continues to evolve, the timecourse models will need to be developed in such a way as to capture various aspects of social behavioural dynamics that have been cursorily introduced above but which will become ever more important with the use of tasks that rely on interactive and iterative exchanges between the coordinating agents. These will include a more specific description of the way in which information is exchanged reciprocally between agents and how these will vary as a function of the size of the interacting groups (and considering cases of interaction beyond the simple dyad). This extension of the project will almost certainly require network-based methods which provide a rigorous framework and structure to the aggregate of pairwise relationships between individuals

6.1 Phase Shifts, Decoupling and the Importance of Transitions

A clear advantage of exploring dynamic social interactions is that they allow for a more comprehensive description of the evolution over time of an interaction between social agents. Two strangers decide to dance together at a party. Not knowing each other, their physical distance may impair clear, reliable sensorimotor coordination (through an impoverished exchange of useful sensory cues). Perhaps as the dance continues, as they stand closer together, as they start to understand how each other moves, such as how they signal a change in direction (to avoid another couple), the exchange of information is greater and richer as is the degree of coupling. Even in the reduced SMS finger tapping tasks, such phase shifts can be observed in the raw timecourse data and future models should attempt to capture these transitions (Fig. 3).

Of particular interest, new models might be used to further explore the concept of uncoupling (or “Exit from synchrony”, see Fig. 4a) [61]. By way of inspiration, Dahan and colleagues have already suggested and tested a modelling approach which goes beyond other rather extensive work on so-called zero-phase synchrony. A further rationale for exploring these phase shifts might be that the resulting

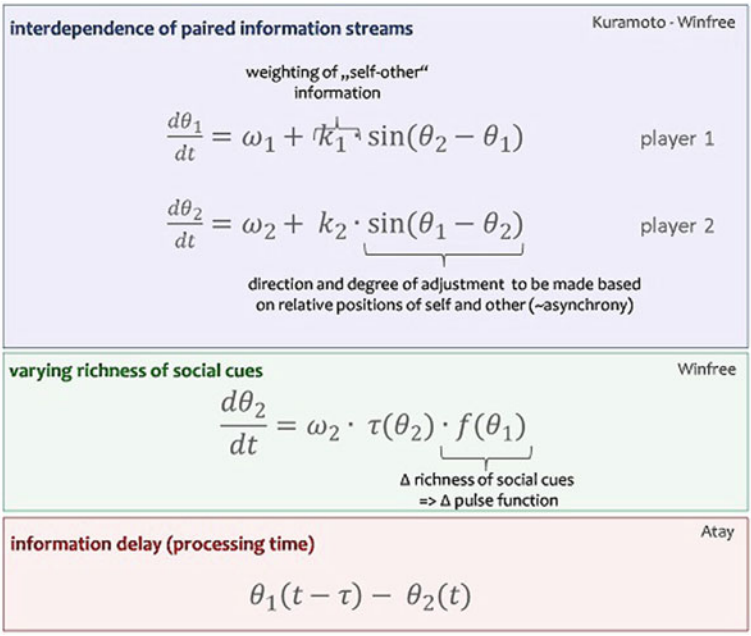

Fig. 3 Dynamic timecourse models. Proposed timecourse models to better capture both the nature of the exchange of information between interacting agents

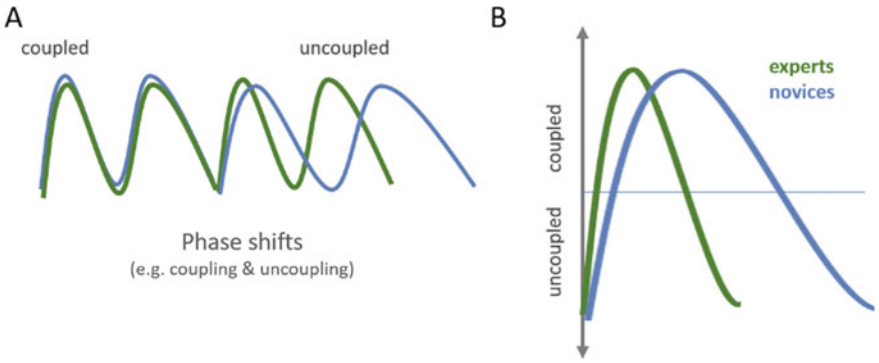

Fig. 4 Phase shifts in dynamic social interactions. (**a**) In most social scenarios, individuals may transition between states of coupling and uncoupling. (**b**) The nature of the transitions, including the slope of the change from a coupled to uncoupled stated, may provide further details as the nature of the information exchange and partners exchanging this information

changes in degrees of coupling may vary as a function of learning or experience, something that could be tested experimentally. This would build on work by Lior and colleagues that shows that the slope of these transitions may vary as a function of expertise (Fig. 4b) [62].

6.2 Beyond the Dyad

In the preceding paragraphs and as a reflection of the state of the art in social cognition, most studies of temporal coordination explore dyadic interactions. Only a few human studies have explored group interactions beyond the dyad, for example looking at phase correction in a string quartet [63]. From personal experience, we encounter a far broader and richer range of social interactions with varying degrees of coupling [10]. Imagine how coupling may differ in a context where we coordinate with larger groups of partners such as in a musical ensemble. The first violinist sets the tempo for the others to follow but with a handover of the melodic line to the cello, the group structure and the specific nature of the coupling links between the players changes as a result. Recent work by Alderisio and colleagues neatly shows how models might help to understand the self-organisation of groups coordinating a hand motion through visual exchanges of information [64].

As part of a new line of research, we have started investigating how individuals coordinate their actions in a group walking task [65]. While coordinating one's footsteps with those of others, we hypothesize that the nature of who and how many individuals we are walking with, how much sensory information we have about their movements and how close we feel or physically are to our partners, will vary not only our synchronisation performance but also objective and subjective measures of coupling: that is the relationship strength between the interacting agents.

Much like the more basic SMS tasks described previously, the group walking paradigm requires participants to walk in synchrony with a pacing tone while listening to the sounds of eight virtual "others" walking around them (Fig. 5a). The sensorimotor synchronization task therefore is a dynamic, goal directed activity during which individuals must coordinate their actions with a pacing signal but may be swayed by the sounds of the group of others. This new paradigm offers a new set of questions that might be answered by more advanced dynamic modelling approaches. These might include exploring the nature of the links between the human walker and the pacing signal and how this weakens as a function of the varying synchronicity of the group of virtual others (Fig. 5b). With the overwhelming power of the group, will the human walker opt instead to follow the temporal leader of the group or perhaps an average of the group and the pacing signal and couple to this timeseries?

As group size increases, the complexity of the multi-way interactions that may be involved must be captured sufficiently by the appropriate network models [66]. Many of the basic models are lacking in their ability to depict, for example, functional sub-groups or indeed whether the exchange of information between interacting agents occurred across all members of the group, or whether they

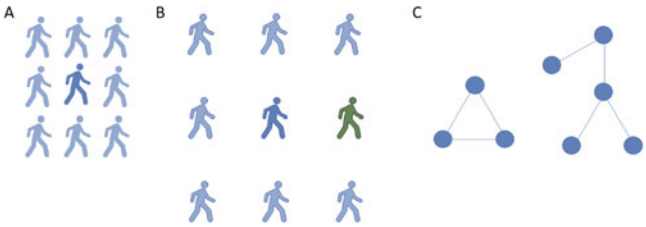

Fig. 5 Interacting in groups. Using an extension of basic SMS paradigms in which a simple motor response is triggered by a sensory cue, (**a**) we present a group walking task in which a human participant (dark blue figure) is instructed to walk in synchrony with a pacing signal while listening to the sound of an array of (8) virtual partners (light blue). (**b**) The design allows for iterations in which the exchange of information and coupling across time may vary as function of the presence of a global leader (green figure), (**c**) number of virtual partners or distance between interacting agents

occurred as several independent pairwise transfers of information. Future iterations of the proposed dynamic timecourse models must look at implementing more complex network frameworks to analyse higher order social interactions.

6.3 Reciprocity, Recursivity and Group Structural Organisation

Our proposal for using SMS paradigms as a proxy for real-world social interactions rests on the premise that in these (as in most social scenarios), we coordinate with others through the exchange of knowledge among members of social groups, and specifically via dyadic networks. Traditional computational models of SMS and the dynamic timecourse models introduced in the previous section aim to elucidate the nature of these exchanges. We have introduced and used the term coupling (for a review and further analysis of the usefulness of the term, see [67]) to describe the strength of the connections between interacting members of a group. This coupling however may vary in the degree of reciprocity, that is to say that the strength of the overall coupling between two individuals need not be symmetrical in nature (e.g. an interaction between a leader and a follower, see [49]). Additionally, as the nature of the task may vary over the course of an interaction, one might see changes in the degree of reciprocity between two individuals as they instead uncouple and become coupled with another agent.

An existing SMS paradigm requires two human tappers to first synchronise with a pacing signal (synchronisation phase) and then, when the external timekeeper is removed, to continue at the original tempo as previously prescribed by the pacing signal (Fig. 6). In the two-person version of this task, we see a clear opportunity to explore structural re-organisation of the three-vertice network. Coupling during the synchronisation phase for both P1 and P2 will consist of strong bonds with

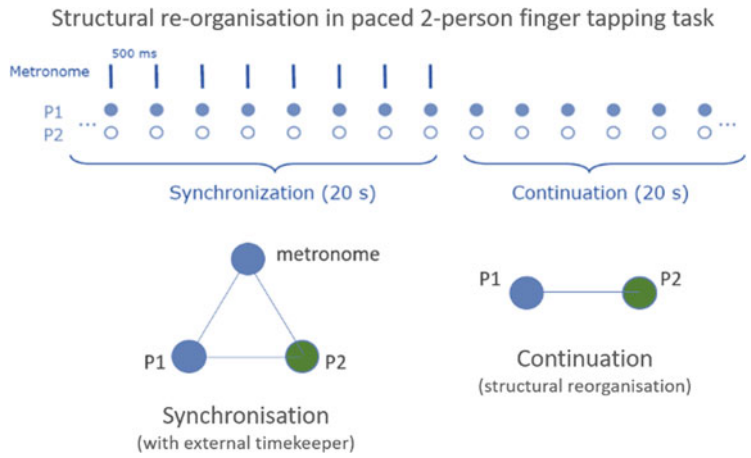

Fig. 6 Structural reorganization of interacting social agents. Depending on the reliability of the partner as well as the instructed task, the degree of coupling and who/what one couples with may vary across time

the external pacing signal (metronome-P1 and metronome-P2) and weaker bonds between the human tappers (P1-P2). By contrast, in the continuation phase, the tappers might show a decoupling from the metronome and instead show increased coupling between each other (P1-P2).

7 Conclusions

Every day we coordinate our intentions and actions with others. In many interactive tasks, this may require us not only to predict, respond and adapt to another person's actions but to precisely synchronize our movements with theirs and to do so in a recursive manner. The development and use of novel network-based modelling approaches is essential to our pushing beyond both dyadic interactions and binary descriptions of the rich timeseries data that is made available through, for example, sensorimotor synchronisation paradigms.

References

1. Hari, R., Henriksson, L., Malinen, S. & Parkkonen, L. Centrality of Social Interaction in Human Brain Function. *Neuron* **88**, (2015).
2. Hutto, D. D., Herschbach, M. & Southgate, V. Editorial: Social Cognition: Mindreading and Alternatives. *Rev. Philos. Psychol.* **2**, 375–395 (2011).
3. Frith, U. & Frith, C. D. Development and neurophysiology of mentalizing. *Philos. Trans. R. Soc. Lond. B. Biol. Sci.* **358**, 459–473 (2003).

4. Decety, J. & Grèzes, J. The power of simulation: Imagining one's own and other's behavior. *Brain Res.* **1079**, 4–14 (2006).
5. Di Paolo, E. & De Jaegher, H. The interactive brain hypothesis. *Front. Hum. Neurosci.* **6**, 1–16 (2012).
6. De Jaegher, H. Social understanding through direct perception? Yes, by interacting. *Conscious. Cogn.* **18**, 535–542 (2009).
7. Schilbach, L. *et al.* Toward a second-person neuroscience. *Behav. Brain Sci.* **36**, 393–414 (2013).
8. Repp, B. H. & Su, Y.-H. Sensorimotor synchronization: a review of recent research (2006–2012). *Psychon. Bull. Rev.* **20**, 403–452 (2013).
9. Fairhurst, M. T., Janata, P. & Keller, P. E. Being and Feeling in Sync with an Adaptive Virtual Partner: Brain Mechanisms Underlying Dynamic Cooperativity. *Cereb. Cortex* **23**, 2592–2600 (2013).
10. Gallotti, M., Fairhurst, M. T. & Frith, C. D. Alignment in social interactions. *Conscious. Cogn.* **48**, 253–261 (2017).
11. Pierno, A. C., Becchio, C., Turella, L., Tubaldi, F. & Castiello, U. Observing social interactions: The effect of gaze. *Soc. Neurosci.* **3**, 51–59 (2008).
12. Iacoboni, M. *et al.* Watching social interactions produces dorsomedial prefrontal and medial parietal BOLD fMRI signal increases compared to a resting baseline. *Neuroimage* **21**, 1167–1173 (2004).
13. Saxe, R. & Kanwisher, N. People thinking about thinking people. The role of the temporo-parietal junction in & quot;theory of mind& quot;. *Neuroimage* **19**, 1835–42 (2003).
14. Gallagher, H. L., Jack, A. I., Roepstorff, A. & Frith, C. D. Imaging the intentional stance in a competitive game. *Neuroimage* **16**, 814–21 (2002).
15. Fukui, H. *et al.* The neural basis of social tactics: An fMRI study. *Neuroimage* **32**, 913–20 (2006).
16. Kircher, T. *et al.* Online mentalising investigated with functional MRI. *Neurosci. Lett.* **454**, 176–81 (2009).
17. Rilling, J. K. *et al.* The neural correlates of the affective response to unreciprocated cooperation. *Neuropsychologia* **46**, 1256–66 (2008).
18. Konvalinka, I. & Roepstorff, A. The two-brain approach: how can mutually interacting brains teach us something about social interaction? *Front. Hum. Neurosci.* **6**, 215 (2012).
19. Jackson, D. A. & Somers, K. M. The spectre of "spurious" correlations. *Oecologia* **86**, 147–151 (1991).
20. Adolphs, R. Cognitive neuroscience: Cognitive neuroscience of human social behaviour. *Nat. Rev. Neurosci.* **4**, 165–178 (2003).
21. Adolphs, R. How do we know the minds of others? Domain-specificity, simulation, and enactive social cognition. *Brain Res.* **1079**, 25–35 (2006).
22. De Jaegher, H. & Di Paolo, E. Participatory sense-making: An enactive approach to social cognition. *Phenomenol. Cogn. Sci.* **6**, 485–507 (2007).
23. Schilbach, L. A second-person approach to other minds. *Nat. Rev. Neurosci.* **11**, 449 (2010).
24. De Jaegher, H., Di Paolo, E. & Gallagher, S. Can social interaction constitute social cognition? *Trends Cogn. Sci.* **14**, 441–447 (2010).
25. Keller, P. E. Synchronization. in *Music in the Social and Behavioral Sciences: An Encyclopedia* (ed. Thompson, W. F.) 1088–1091 (Sage Publications Inc., 2014).
26. Sciences, B., Hove, M. J. & Risen, J. L. It's All in the Timing: Interpersonal Synchrony Increases Affiliation. *Soc. Cogn.* **27**, 949–960 (2009).
27. Rabinovich, M. I., Huerta, R., Varona, P. & Afraimovich, V. S. Transient Cognitive Dynamics, Metastability, and Decision Making. *PLoS Comput. Biol.* **4**, e1000072 (2008).
28. Wiltermuth, S. S. & Heath, C. Synchrony and Cooperation. *Psychol. Sci.* (2009). doi:10.1111/j.1467-9280.2008.02253.x
29. Elliott, M. T., Chua, W. L. & Wing, A. M. Modelling single-person and multi-person event-based synchronisation. *Curr. Opin. Behav. Sci.* **8**, 167–174 (2016).
30. D'Ausilio, A., Novembre, G., Fadiga, L. & Keller, P. E. What can music tell us about social interaction? *Trends Cogn. Sci.* **19**, 111–4 (2015).

31. Keller, P. E., Novembre, G. & Hove, M. J. Rhythm in joint action: psychological and neurophysiological mechanisms for real-time interpersonal coordination. *Philos. Trans. R. Soc. B Biol. Sci.* **369**, 20130394–20130394 (2014).
32. Tognoli, E. & Kelso, J. A. S. The coordination dynamics of social neuromarkers. *Front. Hum. Neurosci.* **9**, 563 (2015).
33. Obhi, S. S. & Cross, E. *Shared representations: sensorimotor foundations of social life*.
34. Michon, J. A. *Timing in temporal tracking.* (Van Gorcum/Inst. For Perception RVO-TNO, 1967).
35. Repp, B. H. & Keller, P. E. Adaptation to tempo changes in sensorimotor synchronization: effects of intention, attention, and awareness. *Q. J. Exp. Psychol. A.* **57**, 499–521 (2004).
36. Novembre, G., Knoblich, G., Dunne, L. & Keller, P. E. Interpersonal synchrony enhanced through 20 Hz phase-coupled dual brain stimulation. *Soc. Cogn. Affect. Neurosci.* **12**, 662 (2017).
37. Dumas, G. Towards a two-body neuroscience. *Commun. Integr. Biol.* **4**, 349–352 (2011).
38. Dumas, G., Laroche, J. & Lehmann, A. Your body, my body, our coupling moves our bodies. *Front. Hum. Neurosci.* **8**, 1004 (2014).
39. Shannon, C. E. A Mathematical Theory of Communication. *Bell Syst. Tech. J.* **27**, 379–423 (1948).
40. Ragert, M., Schroeder, T. & Keller, P. E. Knowing too little or too much: the effects of familiarity with a co-performer's part on interpersonal coordination in musical ensembles. *Front. Psychol.* **4**, 368 (2013).
41. Konvalinka, I. *et al.* Synchronized arousal between performers and related spectators in a fire-walking ritual. *Proc. Natl. Acad. Sci. U. S. A.* **108**, 8514–8519 (2011).
42. Dumas, G., Nadel, J., Soussignan, R., Martinerie, J. & Garnero, L. Inter-brain synchronization during social interaction. *PLoS One* **5**, (2010).
43. Pressing. Error Correction Processes in Temporal Pattern Production. *J. Math. Psychol.* **42**, 63–101 (1998).
44. Repp, B. H. & Keller, P. E. Sensorimotor synchronization with adaptively timed sequences. *Hum. Mov. Sci.* **27**, 423–456 (2008).
45. van der Steen, M. C. (Marieke) & Keller, P. E. The ADaptation and Anticipation Model (ADAM) of sensorimotor synchronization. *Front. Hum. Neurosci.* **7**, 253 (2013).
46. Jacoby, N. & Repp, B. H. A general linear framework for the comparison and evaluation of models of sensorimotor synchronization. *Biol. Cybern.* **106**, 135–154 (2012).
47. Repp, B. H., Keller, P. E. & Jacoby, N. Quantifying phase correction in sensorimotor synchronization: empirical comparison of three paradigms. *Acta Psychol. (Amst).* **139**, 281–90 (2012).
48. Schulze, H.-H., Cordes, A. & Vorberg, D. Keeping Synchrony While Tempo Changes: Accelerando and Ritardando. *Music Percept. An Interdiscip. J.* **22**, 461–477 (2005).
49. Fairhurst, M. T., Janata, P. & Keller, P. E. Leading the follower: an fMRI investigation of dynamic cooperativity and leader-follower strategies in synchronization with an adaptive virtual partner. *Neuroimage* **84**, 688–697 (2014).
50. Fairhurst, M. T., Janata, P. & Keller, P. E. Being and Feeling in Sync with an Adaptive Virtual Partner: Brain Mechanisms Underlying Dynamic Cooperativity. *Cereb. Cortex* **23**, 2592–2600 (2013).
51. Pecenka, N. & Keller, P. E. The role of temporal prediction abilities in interpersonal sensorimotor synchronization. *Exp. Brain Res.* **211**, 505–515 (2011).
52. Pecenka, N., Engel, A. & Keller, P. E. Neural correlates of auditory temporal predictions during sensorimotor synchronization. *Front. Hum. Neurosci.* **7**, 380 (2013).
53. Vorberg, D. Synchronization in duet performance: testing the two-person phase error correction model. in *Tenth Rhythm Perception and Production Workshop* (2005).
54. Kuramoto, Y. *Chemical Oscillations, Waves, and Turbulence*. **19**, (Springer Berlin Heidelberg, 1984).

55. Hove, M. J., Fairhurst, M. T., Kotz, S. A. & Keller, P. E. Synchronizing with auditory and visual rhythms: An fMRI assessment of modality differences and modality appropriateness. *Neuroimage* **67**, 313–321 (2013).
56. Goebl, W. & Palmer, C. Synchronization of Timing and Motion Among Performing Musicians. *Music Percept.* **26**, 427–438 (2009).
57. Konvalinka, I., Vuust, P., Roepstorff, A. & Frith, C. D. C. D. Follow you, follow me: continuous mutual prediction and adaptation in joint tapping. *Q. J. Exp. Psychol.* **63**, 2220–2230 (2010).
58. Winfree, A. T. *The Geometry of Biological Time*.
59. Atay, F. M. The consensus problem in networks with transmission delays. doi:10.1098/rsta.2012.0460
60. Atay, F. M. *Complex time-delay systems: theory and applications*. (Springer, 2010).
61. Dahan, A., Noy, L., Hart, Y., Mayo, A. & Alon, U. Exit from Synchrony in Joint Improvised Motion. *PLoS One* **11**, e0160747 (2016).
62. Hart, Y., Noy, L., Feniger-Schaal, R., Mayo, A. E. & Alon, U. Individuality and Togetherness in Joint Improvised Motion. *PLoS One* **9**, e87213 (2014).
63. Wing, A. M., Endo, S., Bradbury, A. & Vorberg, D. Optimal feedback correction in string quartet synchronization. *J. R. Soc. Interface* **11**, 20131125 (2014).
64. Alderisio, F., Fiore, G., Salesse, R. N., Bardy, B. G. & Bernardo, M. di. Interaction patterns and individual dynamics shape the way we move in synchrony. *Sci. Rep.* **7**, 6846 (2017).
65. Fairhurst, M. F., Tajadura-Jiménez, A., Keller, P. E. & Deroy, O. The sound of us walking together in time and space: Exploring how temporal coupling affects represented body size, peripersonal and interpersonal space in group interactions. in *International multisensory research forum - Annual meeting* Poster presentation (2018).
66. Greening, B. R., Pinter-Wollman, N. & Fefferman, N. H. Higher-Order Interactions: Understanding the knowledge capacity of social groups using simplicial sets. *Curr. Zool.* **61**, 114–127 (2015).
67. Fairhurst, M. & Dumas, G. Reciprocity and alignment: quantifying coupling in dynamic interactions. doi:10.31234/OSF.IO/NMG4X

A Note on Cheeger Inequalities for Piecewise Flat Surfaces

Huabin Ge, Bobo Hua, and Aijin Lin

Abstract Any geometric triangulation of a compact surface with a flat cone metric induces a weighted graph structure and the associated discrete Laplacian is called cotangent Laplacian. In this note, we introduce some geometric quantities, so-called the Cheeger constant and their higher order versions, to control the eigenvalues of cotangent Laplacians.

1 Introduction

Let S be a compact surface, V a finite subset of S, and g a flat cone metric on S whose cone points are contained in V. We call the triple (S, V, g) a piecewise flat surface, PF surface in short. Let $\mathcal{T} = (V, E, F)$ be a (topological) triangulation of (S, V) with the vertex set V, edge set E and face set F of (S, V). The couple $(\mathcal{T}, l)$ is called a geometric triangulation of (S, V, g) if $\mathcal{T}$ is a triangulation and

$$\begin{aligned} l : E &\to (0, +\infty) \\ \overline{ij} &\mapsto l_{ij} \end{aligned}$$

H. Ge (✉)
School of Mathematics, Renmin University of China,
Beijing, People's Republic of China
e-mail: hbge@ruc.edu.cn

B. Hua
School of Mathematical Sciences, LMNS, Fudan University, Shanghai,
People's Republic of China

Shanghai Center for Mathematical Sciences, Fudan University, Shanghai,
People's Republic of China
e-mail: bobohua@fudan.edu.cn

A. Lin
Department of Mathematics, National University of Defense Technology, Changsha, Hunan,
People's Republic of China
e-mail: linaijin@nudt.edu.cn

F. M. Atay et al. (eds.), *Discrete and Continuous Models in the Theory of Networks*, Operator Theory: Advances and Applications 281,
https://doi.org/10.1007/978-3-030-44097-8_8

such that the metric obtained by gluing Euclidean triangles of side length l_{ij}, l_{jk}, l_{ki} for all $\{i, j, k\} \in F$ along the edges is isometric to the metric g, see e.g. [4] for the definition of gluing metrics. We consider the so-called cotangent (discrete) Laplacian on $(\mathcal{T}, l)$, which has been extensively studied in the literature, see e.g. [3, 9–11, 18, 19]. In this note, we study eigenvalue problems for cotangent Laplacians on PF surfaces. As is well-known, the main difficulty for studying the cotangent Laplacian is the lack of the maximum principle. To circumvent it, we adopt an idea of using the existence of Delaunay triangulations of PF surfaces, see e.g. [2, 8, 13, 21].

For the Laplace-Beltrami operator on a closed manifold, Cheeger [6] introduced an isoperimetric constant, now called Cheeger constant, to estimate the first nontrivial eigenvalue. This estimate has been generalized to the setting of graphs by Dodziuk [12] and Alon-Milman [1] respectively. Recently, Lee, Oveis Gharan and Trevisan [17] proved the Cheeger-type estimates for higher eigenvalues. In this note, we introduce various Cheeger constants and derive Cheeger-type estimates for higher eigenvalues of contangent Laplacians, see Theorem 6 in Sect. 3. There are close relations between eigenvalues of the Laplacian on a smooth manifold and those of the (discrete) Laplacian on some proper discretization of the manifold, see e.g. [5].

2 The Setting of Weighted Graph

A finite *weighted graph* G is a triple (V, w, μ) where V is a finite set of *vertices*, $w : V \times V \to \mathbb{R}$ is an *edge weight* which satisfies $w_{ij} = w_{ji}$ for all $i, j \in V$ and $\mu : V \to (0, \infty)$ is *vertex measure*. Note that in our setting, the edge weight w_{ij} could be negative. If $w_{ij} \neq 0$, we say that vertices i and j are *connected* by an edge with the weight w_{ij} and write $i \sim j$. We denote by $E := \{\overline{ij} : i \sim j\}$ the set of (undirected) edges. For any vertex $i \in V$, we define the weighted degree at i by $\mathrm{Deg}(i) = \frac{1}{\mu_i} \sum_{j \in V : j \sim i} w_{ij}$ and set

$$D_w := \sup_{i \in V} \mathrm{Deg}(i). \tag{1}$$

So that w and μ can be regarded as (signed) measures on E and V respectively: For any $\Omega \subset V$, its μ-measure is defined by $\mu(\Omega) := \sum_{i \in \Omega} \mu_i$; for any $A \subset E$, its w-measure is given by $w(A) := \sum_{\overline{ij} \in A} w_{ij}$. We denote by $\ell^2(V, \mu)$ the Hilbert space with inner product $\langle f, g \rangle := \sum_{i \in V} f_i g_i \mu_i$ for any functions f, g on V. In this note, we fix the vertex measure μ and let the edge measure w vary in cases. The canonical choice of the vertex measure is $\mu \equiv 1$, which corresponds to the combinatorial setting. For simplicity, we will indicate the dependence of the edge measure w and omit that of the vertex measure μ in the following.

For a weighted graph (V, w, μ), we denote, as usual, by $C(V)$ the set of real functions defined on V. For any $f \in C(V)$ we define the Dirichlet energy of f by

$$D^w(f) := \sum_{\overline{ij} \in E} w_{ij}(f_i - f_j)^2,$$

which only depends on the edge measure w. In this note, we only consider weighted graphs satisfying the following positivity property:

$$D^w(f) \geq 0, \quad \forall f \in C(V). \tag{Positivity}$$

This defines a nonnegative quadratic form on $\ell^2(V, \mu)$ which by variational method induces an operator Δ_w, called the Laplacian on (V, w, μ),

$$\Delta_w f_i = \frac{1}{\mu_i} \sum_{j \sim i} w_{ij}(f_j - f_i), \quad \forall f \in C(V), i \in V, \tag{2}$$

satisfying

$$D^w(f) = -\langle f, \Delta_w f \rangle, \quad \forall f \in C(V).$$

One readily sees that Δ_w is nonnegative self-adjoint operator on $\ell^2(V, \mu)$. We denote by

$$0 = \lambda_1^w \leq \lambda_2^w \leq \lambda_3^w \cdots \leq \lambda_N^w,$$

the eigenvalues of Δ_w where $N = \sharp V$. The Rayleigh quotient characterization of λ_k^w reads as

$$\lambda_k^w = \min_{\substack{W \subset C(V), \\ \dim W = k}} \max_{\substack{f \in W, \\ f \neq 0}} \frac{D^w(f)}{\|f\|^2_{\ell^2(V,\mu)}}. \tag{3}$$

For any subsets A, B, we write the set of edges between A and B as

$$E(A, B) := \{\overline{ij} \in E : i \in A, j \in B\}.$$

For any $\Omega \subset V$, its edge boundary is defined as $\partial\Omega := E(\Omega, V \setminus \Omega)$. The Cheeger constant of the weighted graph (V, w, μ) is defined by

$$h_w = \inf_{\Omega \subset V,\, \mu(\Omega) \leq \frac{1}{2}\mu(V)} \frac{w(\partial\Omega)}{\mu(\Omega)}. \tag{4}$$

In other words, h is the largest constant such that $w(\partial\Omega) \geq h_w \mu(\Omega)$ for any subset Ω of V satisfying $\mu(\Omega) \leq \frac{1}{2}\mu(V)$. Moreover, for $1 \leq k \leq \sharp V$, the *k-way Cheeger constant* of (V, w), see e.g. [15, 17], is defined as

$$h_{k,w} = \min_{S_1,S_2,\cdots,S_k} \max_{1\leq j\leq k} \frac{w(\partial S_j)}{\mu(S_j)}, \tag{5}$$

where the minimum is taken over the collection of all nonempty, disjoint subsets $\{S_j\}_{j=1}^k$ in V. Note that the Cheeger constant h_w, defined in (4), is equal to $h_{2,w}$.

For weighted graphs (V, w, μ) with nonnegative edge weights, i.e. $w_{ij} \geq 0$ for $i, j \in V$. The well-known Cheeger-Buser type inequality states that

$$\frac{h_w^2}{2D_w} \leq D_w - \sqrt{D_w^2 - h_w^2} \leq \lambda_2^w \leq 2h_w, \tag{6}$$

where D_w is defined in (1).

Furthermore, a higher order Cheeger estimate was proved by Lee, Oveis Gharan and Trevisan [17, Theorem 1.1], see also [14, Theorem 5.1].

Theorem 1 ([17]) *Let (V, w, μ) be a weighted graph with nonnegative edge weights. Then there exists a universal constant C such that for any $1 \leq k \leq \sharp V$,*

$$\frac{C}{k^4 D_w} h_{k,w}^2 \leq \lambda_k^w \leq 2h_{k,w}, \tag{7}$$

where $h_{k,w}$ is defined in (5) and D_w is defined in (1).

3 Graphs Induced by Geometric Triangulations

Given a compact connected surface S and a finite non-empty set $V \subset S$, we call (S, V) a marked surface. Define a PL metric on (S, V) as a flat cone metric g on S whose cone points are contained in V. The triple (S, V, g) will be referred to as a PF surface. For instance, the boundary of a compact convex polyhedral in $\mathbb{R}^3$ is a PL metric on the 2-sphere with all its vertices as cone points. For our purposes, we fix a vertex measure $\mu : V \to (0, \infty)$.

Let $\mathcal{T} = (V, E, F)$ be a (topological) triangulation of (S, V) with the vertex set V, edge set E and face set F of (S, V). The pair $(\mathcal{T}, l)$ is called a geometric triangulation if $\mathcal{T}$ is a triangulation and

$$\begin{aligned} l : E &\to (0, +\infty) \\ \overline{ij} &\mapsto l_{ij} \end{aligned}$$

is an edge length function which assigns each edge $\{ij\} \in E$ the length l_{ij} such that for each triangle $\{ijk\} \in F$ it satisfies the triangle inequalities for l_{ij}, l_{jk} and l_{ik}. In this way, we identify each triangle $\{ijk\} \in F$ in $\mathcal{T}$ with a Euclidean triangle with edge length given by l_{ij}, l_{jk}, l_{ik} and glue them together along common edges. This induces a PL-metric g on (S, V). In this note, given a PF surface (S, V, g), we consider all geometric triangulations $(\mathcal{T}, l)$ which induces the given metric g, and call them geometric triangulations of (S, V, g).

From now on, we fix a PF surface (S, V, g). Let $(\mathcal{T}, l)$ be a geometric triangulation of (S, V, g). One can define an edge weight $w^{\cot} : E \to \mathbb{R}$ as follows. For each edge $\overline{ij}$ in E, set

$$w_{ij}^{\cot} = \begin{cases} \frac{1}{2}\cot\alpha_{ij}^{k}, & \text{if } \overline{ij} \text{ is a boundary edge,} \\ \frac{1}{2}(\cot\alpha_{ij}^{k} + \cot\alpha_{ij}^{l}), & \text{if } \overline{ij} \text{ is an interior edge.} \end{cases} \tag{8}$$

This induces a weighted graph $(V, w^{\cot}, \mu)$. Note that the weights $w_{ij}^{\cot}$ might be negative when $\alpha_{ij}^{k} + \alpha_{ij}^{l} > \pi$ which causes some difficulties in analysis, where α_{ij}^{k} denotes the angle at the vertex k in the triangle $\{i, j, k\}$. In particular, the maximum principle doesn't apply in this case. As in Sect. 2, for the weighted graph (V, w, μ) the Dirichlet energy of a function f is given by

$$D^{w^{\cot}}(f) = \sum_{\overline{ij} \in E} w_{ij}^{\cot}(f_i - f_j)^2.$$

This is a nonnegative quadratic form. In fact, one can extend the function f on V to S, $f_{\mathcal{T}} : S \to \mathbb{R}$, by the piecewise linear interpolation of f, i.e. $f_{\mathcal{T}}$ is linear on each face of $\mathcal{T}$. Then one readily check that

$$D^{w^{\cot}}(f) = \frac{1}{2}\int_S |\nabla f_{\mathcal{T}}|^2. \tag{9}$$

Note that $D(f) = 0$ if and only if f is constant. For the weights in (8), we have the cotangent (discrete) Laplacian

$$\Delta_{w^{\cot}} f_i = \frac{1}{\mu_i}\sum_{j \sim i} w_{ij}^{\cot}(f_j - f_i), \ i \in V, \tag{10}$$

which is self-adjoint in $\ell^2(V, \mu)$, often called finite element discrete Laplacian [3, 9–11, 18, 19]. This type of discrete Laplacian is often used in discrete geometry, computational geometry and especially in the field of engineering. It plays a central role in many areas, such as signal and image processing and numerical analysis of geometric PDEs on surfaces. Xu [22, 23] proved that suitably "normalized" cotangent discrete Laplacians converge to the smooth Laplace-Beltrami operator

as the size of surface mesh goes to zero. We denote by

$$0 = \lambda_1^{w^{\cot}} \leq \lambda_2^{w^{\cot}} \leq \cdots \leq \lambda_N^{w^{\cot}},$$

the eigenvalues of the cotangent Laplacian $\Delta_{w^{\cot}}$ where $N = \sharp V$.

The aim of the note is to estimate the eigenvalues by geometric quantities. In order to get the upper bound for the eigenvalues of cotangent Laplacian, we introduce a modified Cheeger constant. For the edge weight $w^{\cot} : E \to \mathbb{R}$, we define the *absolute-value weight* $|w^{\cot}| : E \to \mathbb{R}$, by $|w^{\cot}|_{ij} = |w_{ij}^{\cot}|$ for any $i, j \in V$. For $1 \leq k \leq \sharp V$, the k-way Cheeger constant of $(V, w^{\cot})$ is defined as

$$\widetilde{h}_{k,w^{\cot}} = \min_{S_1,S_2,\cdots,S_k} \max_{1\leq j\leq k} \frac{w^{\cot}(\partial S_j) + \sum_{1\leq l\leq k, l\neq j} |w^{\cot}|(E(S_l, S_j))}{\mu(S_j)}, \tag{11}$$

where the minimum is taken over the collection of all nonempty, disjoint subsets $\{S_j\}_{j=1}^k$ in V. One readily sees that $\widetilde{h}_{k,w^{cot}} \leq 2h_{k,|w^{cot}|}$.

Theorem 2 *Let $(\mathcal{T}, l)$ be a geometric triangulation of (S, V, g). Then for any $2 \leq k \leq \sharp V$,*

$$\lambda_k^{w^{\cot}} \leq \widetilde{h}_{k,w^{\cot}},$$

where $\widetilde{h}_{k,w^{\cot}}$ is defined as in (11).

Proof Let $\{S_j\}_{j=1}^k$ attains the minimum in (11). We write $T = V \setminus (\cup_{j=1}^k S_j)$. For any $a_j \in \mathbb{R}$, $j = 1, \cdots, k$, set

$$f(x) = \begin{cases} a_j, & x \in S_j \\ 0, & \text{otherwise,} \end{cases}$$

Then by the min-max characterization (3) of $\lambda_k^{w^{\cot}}$, we have

$$\begin{aligned}
\lambda_k^{w^{\cot}} &\leq \max_{\substack{a_i\in\mathbb{R}, 1\leq i\leq k,\\ \sum_i a_i^2\neq 0}} \frac{\sum_{1\leq j<l\leq k}(a_j - a_l)^2 w^{\cot}(E(S_j, S_l)) + \sum_j a_j^2 w^{\cot}(E(S_j, T))}{\sum_j a_j^2 \mu(S_j)}, \\
&= \max_{\substack{a_i\in\mathbb{R}, 1\leq i\leq k,\\ \sum_i a_i^2\neq 0}} \frac{\sum_j a_j^2 w^{\cot}(\partial S_j) - 2\sum_{j<l} a_j a_l w^{\cot}(E(S_j, S_l))}{\sum_j a_j^2 \mu(S_j)} \\
&\leq \max_{\substack{a_i\in\mathbb{R}, 1\leq i\leq k,\\ \sum_i a_i^2\neq 0}} \frac{\sum_j a_j^2 \left(w^{\cot}(\partial S_j) + \sum_{1\leq l\leq k, l\neq j} |w^{\cot}|(E(S_l, S_j))\right)}{\sum_j a_j^2 \mu(S_j)} \\
&\leq \widetilde{h}_{k,w^{\cot}}.
\end{aligned}$$

This proves the theorem. □

For any PF surface (S, V, g), there exists a cotangent Laplacian of particular interests, introduced by Bobenko, and Springborn [2]. We say that a geometric triangulation $(\mathcal{T}_D, l_D)$ of (S, V, g) is a Delaunay triangulation if for any interior edge $\overline{ij}$,

$$\alpha_{ij}^k + \alpha_{ij}^l \leq \pi, \text{ where } \{ijk\}, \{ijl\} \in F. \tag{12}$$

The existence of Delaunay triangulation for a PF surface (S, V, g) can be obtained by the edge flipping algorithm, see e.g. Proposition 12 in [2]. As before, for $(\mathcal{T}_D, l_D)$ we write the weights w_{ij}^* for any $\overline{ij} \in E$ as in (8) and obtain the weighted graph (V, w^*, μ) and the corresponding cotangent Laplacian Δ_{w^*} as in (10). It is easy to check that the weights w^* are nonnegative by (12). One can show that the weighted graph structure (V, w^*, μ) is independent of the choice of Delaunay triangulation which may not be unique. In fact, there exists a unique Delaunay tessellation on the PF surface (S, V, g) whose faces are polygons in $\mathbb{R}^2$ satisfying the property that all vertices on any face are co-circular. Any Delaunay triangulation of (S, V, g) is obtained from the Delaunay tessellation by triangulating all non-triangular faces. We refer to [13] and [16] for more discussions on Delaunay tessellations and Delaunay triangulations on surfaces. Hence, any two Delaunay triangulations of (S, V, g) differ only by a finite steps of edge flipping. Hence the edge weight w_{ij}^* for any edge $\overline{ij}$ which triangulates a non-triangular face in the Delaunay tessellation vanishes. So that all Delaunay triangulations induce unique edge weights w^* and hence a unique Laplacian Δ_{w^*}. We denote by

$$D^{w^*}(f) = \sum_{\overline{ij} \in E} w_{ij}^* (f_i - f_j)^2,$$

the Dirichlet energy of a function of f for a Delaunay triangulation, and by

$$0 = \lambda_1^{w^*} \leq \lambda_2^{w^*} \leq \cdots \leq \lambda_N^{w^*},$$

the eigenvalues of the corresponding Laplacian where $N = \sharp V$.

Rippa [20] proved that the Dirichlet energy of a function of a Delaunay triangulation attains the minimum among all geometric triangulations for a PF surface (S, V, g).

Theorem 3 ([20]) *Let $(\mathcal{T}, l)$ be a geometric triangulation of (S, V, g) and $(\mathcal{T}_D, l_D)$ be a Delaunay triangulation of (S, V, g). Then for any function f on V,*

$$D^{w^{\cot}}(f) \geq D^{w^*}(f).$$

We adopt the arguments as in [7] to obtain the comparison result for these associated eigenvalues.

Theorem 4 *Let $(\mathcal{T}, l)$ be a geometric triangulation of (S, V, g) and $(\mathcal{T}_D, l_D)$ be a Delaunay triangulation of (S, V, g). Then for any $1 \leq k \leq \sharp V$,*

$$\lambda_k^{w^{\cot}} \geq \lambda_k^{w^*}.$$

Proof This follows from the min-max characterization of k-th eigenvalue (3) and Theorem 3. □

Since the weights w^* are nonnegative, by Theorem 1 we have the following corollary.

Corollary 5 *Let $(\mathcal{T}_D, l_D)$ be a Delaunay triangulation of (S, V, g). Then there exists a universal constant C such that for any $2 \leq k \leq \sharp V$,*

$$\frac{C}{k^4 D_{w^*}} h_{k,w^*}^2 \leq \lambda_k^{w^*} \leq 2h_{k,w^*}. \tag{13}$$

By combining the results in Theorems 2, 4 and Corollary 5, we obtain the following theorem.

Theorem 6 *Let $(\mathcal{T}, l)$ be a geometric triangulation of (S, V, g) and $(\mathcal{T}_D, l_D)$ be a Delaunay triangulation of (S, V, g). Then for any $2 \leq k \leq \sharp V$,*

$$\frac{C}{k^4 D_{w^*}} h_{k,w^*}^2 \leq \lambda_k^{w^{\cot}} \leq \widetilde{h}_{k,w^{\cot}},$$

where h_{k,w^*} is defined as in (5), $\widetilde{h}_{k,w^{\cot}}$ is defined as in (11) and D_{w^*} is defined as in (1).

In particular, for the first nontrivial eigenvalue $\lambda_{2,w^{\cot}}$, we obtain the following estimate by Theorems 2, 4 and the Cheeger estimate (6).

Theorem 7 *Let $(\mathcal{T}, l)$ be a geometric triangulation of (S, V, g) and $(\mathcal{T}_D, l_D)$ be a Delaunay triangulation of (S, V, g). Then*

$$\frac{h_{w^*}^2}{2D_{w^*}} \leq D_{w^*} - \sqrt{D_{w^*}^2 - h_{w^*}^2} \leq \lambda_2^{w^{\cot}} \leq \widetilde{h}_{2,w^{\cot}}.$$

Acknowledgments H. Ge is supported by NSFC (no. 11871094). B. Hua is supported by NSFC (nos. 11831004 and 11926313). A. Lin is supported by NSFC (no. 11401578) and Scientific Research Program Funds of NUDT (no. ZK18-03-30).

References

1. N. Alon, V. Milman, λ_1, *isoperimetric inequalities for graphs, and superconcentrators*, J. Combin. Theory Ser. B 38 (1985), no. 1, 73–88.
2. A. Bobenko, B. Springborn, *A discrete Laplace-Beltrami operator for simplicial surfaces*, Discrete Comput. Geom., 38 (2007), no. 4, 740–756.
3. M. Botsch, L. Kobbelt, *An intuitive framework for real time freeform modeling*, ACM Trans. Graph. 23 (2004), no.3, 630–634.
4. D. Burago, Yu. Burago, and S. Ivanov. *A course in metric geometry*, volume 33 of *Graduate Studies in Mathematics*. American Mathematical Society, Providence, RI, 2001.
5. D. Burago, S. Ivanov and Y. Kurylev, *A graph discretization of the Laplace-Beltrami operator*, J. Spectr. Theory 4 (2014), 675–714.
6. J. Cheeger, *A lower bound for the smallest eigenvalue of the Laplacian*, in: Problems in Analysis, Papers Dedicated to Salomon Bochner, 1969, Princeton Univ. Press, Princeton, NJ, 1970, pp. 195–199.
7. R. Chen, Y. Xu, C. Gotsman, L. Liu, *A spectral characterization of the Delaunay triangulation*, Comput. Aided Geom. Design 27 (2010), no. 4, 295–300.
8. B.N. Delaunay, Sur la sphère vide. Izv. Akad. Nauk SSSR, Otd. Mat. Estestv. Nauk 7 (1934), 793–800.
9. M. Desbrun, M. Meyer, P.Schröder, A.H. Barr, *Implicit fairing of irregular meshes using diffusion and curvature flow*, In: SIGGRAPH99, pp. 317–324, 1999.
10. R.J. Duffin, *Distributed and lumped networks*, J. Math. Mech. 8(5), 793–826 (1959).
11. G. Dziuk, *Finite elements for the Beltrami operator on arbitrary surfaces*, In: Hildebrandt, S., Leis, R. (eds.) Partial Differential Equations and Calculus of Variations. Lecture Notes in Mathematics, vol. 1357, pp. 142–155. Springer, Berlin (1988).
12. J. Dodziuk, *Difference equations, isoperimetric inequality and transience of certain random walks*, Trans. Amer. Math. Soc., 284 (1984), no.2, 787–794.
13. C. Indermitte, Th.M. Liebling, M. Troyanov, H. Clemenvon, *Voronoi diagrams on piecewise flat surfaces and an application to biological growth*, Theor. Comput. Sci. 263 (2001), 263–274.
14. Carsten Lange, Shiping Liu, Norbert Peyerimhoff and Olaf Post, *Frustration index and Cheeger inequalities for discrete and continuous magnetic Laplacians*, Calculus of Variations and Partial Differential Equations, 54 (2015), no. 4, 4165–4196.
15. Shiping Liu, *Multi-way dual Cheeger constants and spectral bounds of graphs*, Advances in Mathematics 268 (2015), 306–338.
16. G. Leibon, D. Letscher, *Delaunay triangulations and Voronoi diagrams for Riemannian manifolds*, In: Proceedings of the Sixteenth Annual Symposium on Computational Geometry, Hong Kong, 2000, pp. 341–349. ACM, New York (2000)
17. J. R. Lee, S. Oveis Gharan and L. Trevisan, Multi-way spectral partitioning and higher-order Cheeger inequalities, STOC'12-Proceedings of the 2012 ACM Symposium on Theory of Computing, 1117–1130, ACM, New York, 2012.
18. U. Pinkall, K. Polthier,*Computing discrete minimal surfaces and their conjugates*, Exp. Math. 2 (1993), no. 1, 15–36
19. K. Polthier, *Computational aspects of discrete minimal surfaces*, In: J. Hass, D. Hoffman, A. Jaffe, H. Rosenberg, R. Schoen, M. Wolf, (Eds.), Proc. of the Clay Summer School on Global Theory of Minimal Surfaces, 2002.
20. S. Rippa, *Minimal roughness property of the Delaunay triangulation*, Comput. Aided Geom. Design 7 (1990), 489–497.
21. I. Rivin, *Euclidean structures on simplicial surfaces and hyperbolic volume*, Ann. of Math., 139 (1994), 553–580.
22. G. Xu, *Convergence of discrete Laplace-Beltrami operators over surfaces*, Comput. Math. Appl. 48 (2004), no. 3–4, 347–360.
23. G. Xu, *Discrete Laplace-Beltrami operators and their convergence*, Comput. Aided Geom. Design 21 (2004), no. 8, 767–784.

Unravelling Topological Determinants of Excitable Dynamics on Graphs Using Analytical Mean-field Approaches

Marc-Thorsten Hütt and Annick Lesne

Abstract We present our use of analytical mean-field approaches in investigating how the interplay between graph topology and excitable dynamics produce spatio-temporal patterns. We first detail the derivation of mean-field equations for a few simple model situations, mainly 3-state discrete-time excitable dynamics with an absolute or a relative excitation threshold. Comparison with direct numerical simulation shows that their solution satisfactorily predicts the steady-state excitation density. In contrast, they often fail to capture more complex dynamical features, however we argue that the analysis of this failure is in itself insightful, by pinpointing the key role of mechanisms neglected in the mean-field approach. Moreover, we show how second-order mean-field approaches, in which a topological object (e.g. a cycle or a hub) is considered as embedded in a mean-field surrounding, allow us to go beyond the spatial homogenization currently associated with plain mean-field calculations. The confrontation between these refined analytical predictions and simulation quantitatively evidences the specific contribution of this topological object to the dynamics.

Keywords Network dynamics · Analytical approaches · Simulation

This work has been completed in the framework of the ZiF programme *Discrete and continuous models in the theory of networks*.

M.-T. Hütt (✉)
Department of Life Sciences and Chemistry, Jacobs University Bremen, Bremen, Germany
e-mail: m.huett@jacobs-university.de

A. Lesne
Sorbonne Université, CNRS, Laboratoire de Physique Théorique de la Matière Condensée, LPTMC, Paris, France

Institut de Génétique Moléculaire de Montpellier, University of Montpellier, CNRS, Montpellier, France
e-mail: annick.lesne@sorbonne-universite.fr

F. M. Atay et al. (eds.), *Discrete and Continuous Models in the Theory of Networks*, Operator Theory: Advances and Applications 281,
https://doi.org/10.1007/978-3-030-44097-8_9

Mathematics Subject Classification (2010) Primary 05C82; Secondary 92C42

1 Introduction

The original mean-field approach has been introduced in statistical physics for the analysis of ferromagnetism [28]. Its insight is to approximately describe the effect of specific couplings between a given atom and its neighbors (actually all reduced to their spin) as the influence of their average magnetization, acting as an homogeneous external magnetic field (the *mean field*). It has lead to a general class of methods, involving similar 'mean-field' ansatzes [19, 20]. In the context of dynamics on graphs, it has for example been applied to self-organized criticality [8], reaction-diffusion processes on networks for one-component [7] and multi-component systems [27], voter model [26], or excitable dynamics [6, 17, 18]. A general discussion of the accuracy of such methods can be found in [14] and the monograph [2]. The forest-fire model in [15] is the first attempt to take into account graph topology in a mean-field approach, via shortcut density.

In all dynamic models where nodes of the graph can be in a finite number of states, the general spirit of mean-field approaches is a space-implicit description in terms of the probability (in physical terms, the density) of each state. Such approaches provide an average view over space, initial conditions and stochasticity of the dynamics, based on ignoring spatial correlations and inhomogeneities. The validity of mean-field approximations thus requires weak correlations and statistical homogeneity. While standard mean-field approaches in continuous systems are shown to be valid above a critical dimension d_c, the situation is different on a graph, where mean-field failure is presumed to originate in the inherent heterogeneities of its topology and the way they influence the dynamics. In the context of processes on graphs, mean-field equations are usually not derived bottom-up from a microscopic stochastic description, but rather proposed straightforwardly in view of the qualitative features of the local dynamics, e.g. how many excited neighbors are required to excite a node in case of excitable dynamics [3, 4, 24, 25].

We will present in Sect. 2 the derivation of mean-field equations for two instances of discrete-time excitable dynamics on graphs. In both models, a node i of the graph can be either susceptible S, excited E, or refractory R. The dynamics is defined as a 3-state cellular automaton $S \to E \to R \to S$ according to the following rules: an excited node at time t becomes refractory at time $t+1$, a refractory node at time t becomes susceptible at time $t+1$ with a recovery probability p (else it remains refractory), and a susceptible node becomes excited according to the state at time t of the neighboring nodes on the graph. For the *absolute threshold model*, a susceptible node at time t becomes excited at time $t+1$ if it has at least q excited neighbors (we will mostly consider the simplest case $q = 1$), while for the *relative threshold model*, a susceptible node becomes excited at time $t+1$ if at least a fraction κ of its neighbors are excited at time t. Additionally, spontaneous excitations can occur at susceptible nodes with probability f per time step. When

$p < 1$ (stochastic recovery) and/or $f > 0$ (spontaneous excitations), the dynamics is stochastic. An additional level of stochasticity comes from the randomness of initial conditions. What thus makes sense is to describe average behaviors. These two models are reminiscent of SIS and SIR models [4, 16], however no simple mapping can be drawn (excitation propagation is a stochastic step in SIS and SIR, involving a transmission probability), and their behaviors differ. As for the underlying graphs, we actually consider *ensembles of graphs* defined by current models, from Erdős-Rényi random graphs [10] to Barabási-Albert scale-free graphs [1] to Molloy-Reed configuration model that samples graphs with any prescribed degree distribution, to hierarchical or modular complex networks [5].

To evaluate the validity of a mean-field approach and its limits, we have compared in Sect. 3 the analytical mean-field predictions and the numerical implementation of our two models of excitable dynamics on graphs. Failure of a mean-field approach means that either correlations between the nodes, or local network features, or both, matter. We will discuss the insights than can be gained from the analysis of this failure. Section 4 is devoted to the analytical strategies we have devised to go beyond basic mean-field approaches and take into account some specific topological features of the graph, in order to gain some general understanding of the interplay between graph topology and its excitable dynamics.

2 Mean-field Equations for Excitable Dynamics on Graphs

2.1 *Principle of Mean-field Approximation(s)*

Denoting $x_i(t)$ the state of node i at discrete time t, the standard mean-field approach for describing the average graph dynamics actually comprises two different approximations, whatever the considered model of dynamics. The first one is a *spatial de-correlation* of the node states when computing statistical averages: $\langle x_i(t)x_j(t)\rangle \approx \langle x_i(t)\rangle\langle x_j(t)\rangle$. The second one is a *spatial homogenization*, considering that $\langle x_i(t)\rangle$ is independent of the node i. These two approximations will allow us to derive autonomous, deterministic and space-implicit equations for the densities $c_\alpha(t) = \text{Prob}[x_i(t) = \alpha]$, with here $\alpha = E, S, R$.

2.2 *Absolute Threshold $q = 1$ for Excitation Propagation*

Mean-field dynamics is derived by identifying the probability that a given neighbor is not excited with the average and node-independent quantity $1 - c_E(t)$. A decorrelation approximation lies in considering an average quantity, while its node-independence amounts to an homogenization. Another homogenization arises in replacing the number of direct neighbors of a node (that is, its degree) with

the average degree $\langle k \rangle$. This latter approximation is applied in particular to the probability that a node has at least an excited neighbor at time t, which is the condition for its excitation by neighbors in the absolute-threshold model. This probability is accordingly estimated as $1 - B(0, \langle k \rangle, c_E(t))$, where the binomial distribution can be explicitly expressed $B(0, \langle k \rangle, c_E(t)) = (1 - c_E(t))^{\langle k \rangle}$. This probability has then to be multiplied by $(1 - f)$ (no overriding spontaneous excitation) and by the homogenized probability $c_S(t)$ that the node is susceptible. Overall, mean-field evolution equations for the state densities are:

$$\begin{cases} c_E(t+1) = c_S(t) \left[f + (1-f)[1 - (1 - c_E(t))^{\langle k \rangle}] \right] \\ c_R(t+1) = c_E(t) + (1-p) c_R(t) \\ c_S(t+1) = 1 - c_E(t+1) - c_R(t+1) \end{cases} \tag{2.1}$$

In the regimes where $c_E(t) \ll 1$, the term $1 - (1 - c_E(t))^{\langle k \rangle}$ simply reduces to $\langle k \rangle \; c_E(t)$. Note that the average degree $\langle k \rangle$ is usually not an integer: while the probabilistic reasoning makes sense only for integral $\langle k \rangle$, the resulting formula can be interpolated and extended to any real value of $\langle k \rangle$.

Fixed points of (2.1), i.e. $c_\alpha(t+1) = c_\alpha(t) = c_\alpha^*$ for $\alpha = E, S, R$, correspond to steady states. For all mean-field fixed points, we have the equations: $p \; c_R^* = c_E^*$ and $p(1 - c_S^*) = c_E^*(1+p)$, whatever the excitation probability model and the value of f. For $f = 0$, there is a trivial (unstable) fixed point ($c_E^o = 0, c_R^o = 0, c_S^o = 1$) whatever the value of p. Still for $f = 0$, there is also a non trivial fixed point:

$$c_E^* = \frac{p\,(\langle k \rangle - 1)}{\langle k \rangle (p+1)}, \qquad c_S^* = \frac{1}{\langle k \rangle}, \qquad c_R^* = \frac{\langle k \rangle - 1}{\langle k \rangle (p+1)} \tag{2.2}$$

provided the consistency condition $\langle k \rangle c_E^* \ll 1$ holds. Else we have to solve numerically the non-linear equation:

$$c_E^* = \left[1 - c_E^*(1 + 1/p) \right] \left[f + (1-f)[1 - (1 - c_E^*)^{\langle k \rangle}] \right] \tag{2.3}$$

2.3 Relative Threshold κ for Excitation Propagation

In case of a relative excitation threshold κ, the most basic mean-field approximation states that a susceptible node of degree k gets excited if its average number of excited neighbors, $k c_E$, is larger than $k\kappa$, that is if $c_E \geq \kappa$ whatever the node degree k. This leads to the simple evolution equations, where H is the Heaviside function:

$$\begin{cases} c_E(t+1) = c_S(t) \, [f \; + \; (1-f) H[c_E(t) - \kappa]] \\ c_R(t+1) = c_E(t) + (1-p) c_R(t) \\ c_S(t+1) = 1 - c_E(t+1) - c_R(t+1) \end{cases} \tag{2.4}$$

A refined set of equations can be obtained using combinatoric probabilistic arguments, and considering for all nodes the same homogenized degree, equal to the average degree $\langle k \rangle$. We define $\bar{n}_\kappa$ as the smallest integer larger or equal to $\kappa \langle k \rangle$, that is, $\bar{n}_\kappa = \lceil \kappa \langle k \rangle \rceil$. Excitation propagation at a susceptible node then requires that it has at least $\bar{n}_\kappa$ excited neighbors, whatever its actual degree. The mean-field evolution equations for a relative excitation threshold κ then coincide with those obtained for an absolute excitable threshold $q = \bar{n}_\kappa$. The factor $[1 - (1 - c_E(t))^{\langle k \rangle}]$ in the above mean-field evolution Eqs. (2.1) is now to be replaced with:

$$\sum_{j=0}^{\lceil \langle k \rangle \rceil - \bar{n}_\kappa} \binom{\lceil \langle k \rangle \rceil}{\bar{n}_\kappa + j} c_E(t)^{\bar{n}_\kappa + j} (1 - c_E(t))^{\lceil \langle k \rangle \rceil - \bar{n}_\kappa - j} \tag{2.5}$$

Note that $\langle k \rangle$ is usually not an integer, and has to be replaced by $\lceil \langle k \rangle \rceil$ for the binomial coefficient to make sense. For $\kappa \to 0$, we have $\bar{n}_\kappa = 1$, and the mean-field equations for an absolute threshold $q = 1$ are satisfactorily recovered. Overall, we obtain the coupled equations:

$$\begin{cases} c_E(t+1) = f c_S(t) \\ \qquad +(1-f) c_S(t) \sum_{j=0}^{\lceil \langle k \rangle \rceil - \bar{n}_\kappa} \binom{\lceil \langle k \rangle \rceil}{\bar{n}_\kappa + j} c_E(t)^{\bar{n}_\kappa + j} (1 - c_E(t))^{\lceil \langle k \rangle \rceil - \bar{n}_\kappa - j} \\ c_R(t+1) = c_E(t) + (1-p) c_R(t) \\ c_S(t+1) = 1 - c_E(t+1) - c_R(t+1) \end{cases} \tag{2.6}$$

When $c_E(t) \ll 1$, the term for $j = 0$ dominates and the above sum can be replaced in the numerical implementation by the proxy:

$$\binom{\lceil \langle k \rangle \rceil}{\bar{n}_\kappa} c_E(t)^{\bar{n}_\kappa} \tag{2.7}$$

For $f = 0$, the evolution described by the simple Eqs. (2.4) has a non trivial stable fixed point:

$$c_E^* = \frac{p}{2p+1}, \qquad c_S^* = \frac{p}{2p+1}, \qquad c_R^* = \frac{1}{2p+1} \tag{2.8}$$

provided $\kappa < c_E^*$, i.e. $\kappa < p/(2p+1)$. When $\kappa > p/(2p+1)$, the stable fixed point becomes: $c_E^* = 0$, $c_S^* = 1$, $c_R^* = 0$. When the evolution is described by the refined mean-field equations (2.6) with the simplification (2.7), the fixed points in the absence of spontaneous excitations ($f = 0$) correspond to the solutions of:

$$c_E^* = \binom{\lceil \langle k \rangle \rceil}{\bar{n}_\kappa} (c_E^*)^{\bar{n}_\kappa} (1 - c_E^*(1 + 1/p)) \tag{2.9}$$

satisfying he condition $0 \leq c_E^* \leq p/(p+1)$, so that $c_R^* \geq 0$ and $c_S^* \geq 0$. This yields a trivial fixed point ($c_E^o = 0, c_R^o = 0, c_S^o = 1$) whatever the value of p. This fixed point is stable for $\bar{n}_\kappa \geq 2$ (the stability analysis is easily done by reducing the evolution to two coupled equations, e.g. for $c_E(t)$ and $c_R(t)$, and determining for which values of κ the eigenvalues of the Jacobian matrix have a modulus strictly lower than 1). For $\bar{n}_\kappa = 1$, i.e. for $\kappa < 1/\langle k \rangle$, the stable fixed point is associated to the nontrivial solution of (2.9).

For $f > 0$, we have to numerically solve the fixed point equations. However, at small f, a simple approximation is to identify the average excitation density with $c_E^o = f$ (instead of $c_E^o = 0$) at large values of κ, while the non trivial value c_E^* at low values of κ is considered to be unaffected by a small rate of spontaneous excitations. The good accuracy of these various analytical predictions for the steady-state excitation density is presented below n Sect. 3 and associated figures.

2.4 Evolution for Degree Classes

In the basic mean-field equations (2.1) and (2.6), graph topology is involved only through the average degree $\langle k \rangle$. It is possible to better take into account a broad degree distribution by considering degree classes, that is, subsets of nodes of a given degree. We denote $c_E(k,t)$ the average excitation density of nodes of degree k (and similarly $c_S(k,t)$ and $c_R(k,t)$, for susceptible and refractory states). In the mean-field approximation for an excitable dynamics with absolute threshold $q = 1$, a node in the class of degree k has $k\, c_E(t)$ excited neighbors and a probability equal to $1 - (1 - c_E(t)]^k$ to have at least one excited neighbor: some node heterogeneity is now included in the mean-field dynamics. Evolution equations become:

$$\begin{cases} c_E(k,t+1) = c_S(k,t)\left[f + (1-f)\left[1 - (1 - c_E(t)\right]^k\right] \\ c_R(k,t+1) = c_k E(k,t) + (1-p) c_R(k,t) \\ c_S(k,t+1) = 1 - c_E(k,t+1) - c_R(k,t+1) \end{cases} \tag{2.10}$$

The overall excitation density is related to these partial densities by the relation $\sum_k \rho(k)\, c_E(k,t) = c_E(t)$ directly involving the degree distribution $\rho(k)$. However, several mean-field approximations are still present: at the dynamic level, we still ignore correlations between the states of the nodes, and at the network level, we neglect degree-degree correlations and consider the degree-average state for neighboring nodes.

In case of excitable dynamics with a relative threshold κ, we introduce $n_\kappa(k)$ as the smallest integer larger or equal to κk. The equation for $c_E(k,t)$ is the same as

for an absolute threshold $q = n_\kappa(k)$:

$$c_E(k, t+1) = f\ c_S(k,t) + (1-f)\ c_S(k,t) \sum_{j=n_\kappa(k)}^{k} \binom{k}{j} c_E(t)^j (1-c_E(t))^{k-j} \tag{2.11}$$

In a finite graph (hence having a bounded maximal degree), equations for an absolute threshold $q = 1$ are recovered in the limit $\kappa \to 0$, when all $n_\kappa(k)$ reduce to 1.

A refinement is to take into account degree-degree correlations (see e.g. [4, 23] for application to SIS epidemic model and [27] for application to diffusion-annihilation process). An analysis of mean-field validity in the case where degree-degree correlations cannot be ignored is presented in [14], suggesting that the mean first-neighbor degree d is a good predictor of the validity (the more reliable the larger d); d reduces to the average degree $\langle k \rangle$ in uncorrelated networks. Degree-degree correlations are described by the conditional probability $\rho(k'|k)$ that the degree of a neighbor of a node of degree k is k'. For an excitable model with absolute threshold $q = 1$, the probability for a node of degree k to have at least an excited neighbor becomes $1 - (1 - \sum_{k'} \rho(k'|k)\ c_E(k', t))^k$, replacing $1 - (1 - c_E(t))^k$ in (2.10). The mean excitation field of a node, $\sum_{k'} \rho(k'|k)\ c_E(k', t) \equiv c_E(\mathrm{nn}(k), t)$, now depends on the node degree k. This modification of $c_E(t)$ into a degree-dependent local field $c_E(\mathrm{nn}(k), t)$ also holds in (2.11) for the model with a relative excitation threshold κ.

2.5 *Pair-correlation Equations*

Identifying the probability that two neighboring nodes are simultaneously excited with $[c_E(t)]^2$ is often too crude. This approximation can be circumvented by introducing a quantity $c_{E,E}(t)$, describing the probability that two neighbors are simultaneously excited, and similar quantities for the other pair correlations [9, 22]. The evolution of state densities $c_\alpha(t)$ can be written in a less approximate way by involving these additional variables. For an excitable model with an absolute threshold $q = 1$, it comes:

$$c_E(t+1) = f c_S(t) + (1-f) c_S(t) \left[1 - \left(1 - \frac{c_{E,S}(t)}{c_S(t)} \right)^{\langle k \rangle} \right] \tag{2.12}$$

$$c_R(t+1) = c_E(t) + (1-p) c_R(t) \tag{2.13}$$

$$c_S(t+1) = 1 - c_E(t+1) - c_R(t+1) \tag{2.14}$$

While spatial homogenization remains, the mean-field decorrelation approximation is relaxed and displaced at a higher order. The approximation is now involved in a closure relation of the form $\langle xxyy\rangle = \langle xx\rangle\langle yy\rangle$ required to get an autonomous set of equations of evolution for the pair-correlations, as follows:

$$\begin{aligned} c_{E,S}(t+1) &= fp\, c_{S,R}(t) + (1-f)p\, \frac{c_{S,R}(t)c_{E,S}(t)}{c_S(t)} \\ &+(1-f)f c_{S,S}(t)\left(1-\frac{c_{E,S}(t)}{c_S(t)}\right)^{\langle k\rangle-1} \\ &+(1-f)^2 c_{S,S}(t)\left(1-\frac{c_{E,S}(t)}{c_S(t)}\right)^{\langle k\rangle-1}\left[1-\left(1-\frac{c_{E,S}(t)}{c_S(t)}\right)^{\langle k\rangle-1}\right] \end{aligned} \tag{2.15}$$

This evolution equation for $c(E, S, t)$ contains four terms: the probability that in a pair of neighbors (S, R), the first one gets spontaneously excited and the second one recovers; the probability that in a pair of neighbors (S, S), the first one gets excited due to its excited neighbors and the second one recovers; the probability that in a pair of neighbors (S, S), the first one gets spontaneously excited and the second one escapes both spontaneous and neighbor-induced excitation and remains susceptible; the probability that in a pair of neighbors (S, S), the first one gets excited due to its excited neighbors and the second one escapes both spontaneous and neighbor-induced excitation and remains susceptible. Similar equations can be written for the other joint densities $c_{E,R}$ and $c_{S,R}$:

$$\begin{aligned} c_{E,R}(t+1) &= c_{S,R}(t)\left[(1-p)f+(1-p)(1-f)\left[1-\left(1-\frac{c_{E,S}(t)}{c_S(t)}\right)^{\langle k\rangle}\right]\right] \\ &+c_{E,S}(t)\left[(f+(1-f)\left[1-\left(1-\frac{c_{E,S}(t)}{c_S(t)}\right)^{\langle k\rangle}\right]\right] \end{aligned} \tag{2.16}$$

$$\begin{aligned} c_{S,R}(t+1) &= c_{S,R}(t)\,(1-p)(1-f)\left(1-\frac{c_{E,S}(t)}{c_S(t)}\right)^{\langle k\rangle} + (1-p)p\, c_{R,R}(t) \\ &+ p\, c_{E,R}(t) + (1-f)\, c_{E,S}(t)\left(1-\frac{c_{E,S}(t)}{c_S(t)}\right)^{\langle k\rangle} \end{aligned} \tag{2.17}$$

supplemented with the equations $c_S(t+1) = 1 - c_E(t+1) - c_R(t+1)$, $c_{S,S}(t+1) = c_S(t+1) - c_{S,E}(t+1) - c_{S,R}(t+1)$ and similar relationships for $c_{E,E}(t+1)$ and $c_{R,R}(t+1)$. Such pair-correlation equations have been used for instance to investigate co-activation and pinpoint its topological determinants, through a comparison of analytical predictions and numerical simulations [17].

3 Successes and Failures of Mean-field Approaches: Numerical Checks

3.1 A Remarkable Power to Predict Excitation Density in Random Graphs

An implicit step in the practical use of mean-field approaches is to identify empirical space averages that can be measured in experiments and simulation, with the statistical averages $c_\alpha(t)$ involved in the equations (here $\alpha = E, S, R$). The validity of this identification directly follows from the applicability of the law of large numbers, which has the same conditions of validity as the mean-field approximations, namely it also requires weak correlations and statistical homogeneity.

To evaluate the validity of mean-field approximations, we implemented numerically the two models of excitable dynamics on graph described in the introduction. They are specially suitable for a numerical analysis, since they actually take the form of three-state cellular automata. The initial condition is generally taken at random, with equal fractions of susceptible, excited and refractory nodes spanning the graph. All the spatio-temporal correlations and network heterogeneities are by construction taken into account in the simulation. We compared the steady-state mean-field excitation density c_E^* predicted analytically and its numerical value, observed in the simulation after discarding initial transients and performing a suitable time average.

As seen on Fig. 1, for excitable dynamics on a highly connected random graph (Erdős-Rényi graph of average degree 10), the simulated time-average excitation density lies around the mean-field prediction, with some fluctuations of relatively low amplitude. The goodness of the basic mean-field approach on highly connected random graphs relies (1) on the spatial homogeneity of these graphs, (2) the fact that they are locally similar to a tree, and (3) the large enough number of neighbors. Consequently it is respectively valid (1) to identify the node degrees with the average degree, (2) to consider that there is no correlations between the states of node neighbors as if the topology around each node were star-like, and (3) to identify the excitation probability of the neighbors of a given node with the average excitation density. When the graph connectivity decreases, the prediction quality decreases, as seen on Fig. 2.

Considering scale-free graphs yields a prediction quality similar to that observed for low-connectivity random graph, as seen on Fig. 3. However, a marked difference is the range and nature of fluctuations, which now exhibit spikes. This latter feature is presumably due to the spatial heterogeneity of the network, where nodes of both small and high degree are present, and the fact that high-degree nodes may nucleate coherent waves of activation (see below, Sect. 4.3 and [17]).

In the case of a relative excitation threshold, Fig. 4 shows the good agreement of both the mean-field prediction (2.8) and the stationary solution of mean-field equations (2.6) and (2.7) with the numerical steady-state. Both correctly predicts the exchange of stability between the non-trivial fixed point and the value $c_E^o = f$

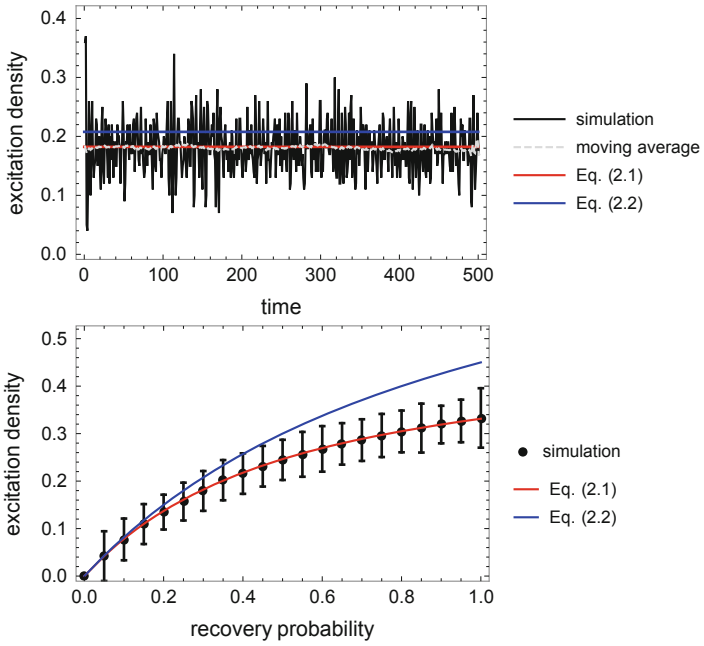

Fig. 1 Mean-field excitation density and its simulated counterpart on a highly connected random graph, for an absolute excitation threshold $q = 1$. Simulation has been performed with a spontaneous excitation rate $f = 0.01$, on a random graph (Erdős-Rényi) with 100 nodes and 500 links. The upper panel displays a simulated trajectory for a recovery probability $p = 0.3$ (highly fluctuating black line), its moving average (light grey dashes), the approximate fixed point given by (2.2) and the steady-state solution of mean-field equations (2.1). The lower panel compares the excitation density obtained in the simulation, the fixed point (2.2) and the steady-state solution of (2.1) for varying values of the recovery probability p. Error bars on simulation points have been obtained from the last 250 time steps of a 500 time-step simulation starting from random initial conditions

corresponding to the extinction of excitation propagation. We have shown in [11] that a sustained activity (corresponding to the non trivial steady state) occurs up to a value κ_m that can be roughly estimated from the graph topology as the maximal degree k_{max} of the graph, in agreement with the upper bound $1/\langle k \rangle$ (larger that $1/k_{max}$) predicted here using mean-field analysis. The observed lower bound c_E^* can be explained as a fluctuation effect: the actual number of excited neighbors of a node of degree k can be higher than kc_E^*, which accommodates excitation propagation for relative threshold values higher than $\kappa = c_E^*$.

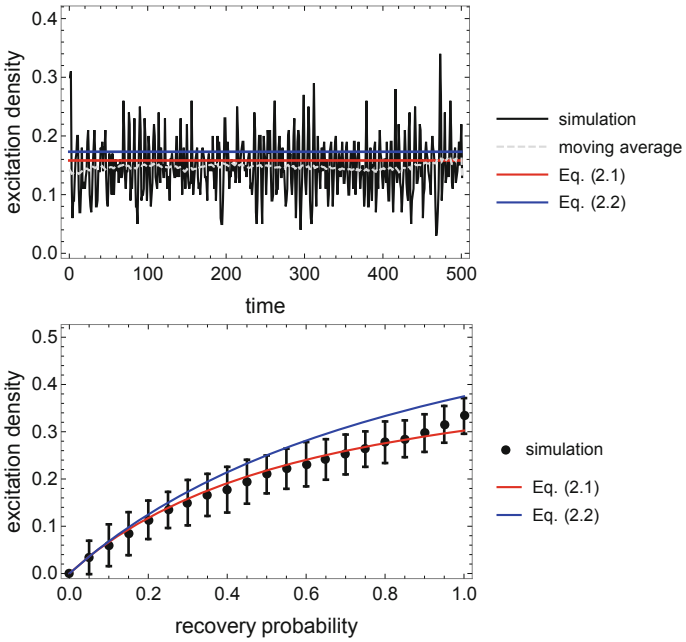

Fig. 2 Mean-field excitation density and its simulated counterpart on a low-connectivity random graph, for an absolute excitation threshold $q = 1$. Same as Fig. 1 now on a random graph (Erdős-Rényi) with 100 nodes and 200 links

3.2 Insightful Failures

Numerical simulations, Fig. 3, show that basic mean-field equations fail to describe the full complexity of excitable dynamics on graphs with a very broad degree distribution. They miss self-organized formation of coherent patterns of excitation, responsible of the spikes apparent on the time evolution of the overall excitation density. In showing the limits of considering the same average degree for all nodes, they indirectly demonstrate the central role of hubs in the dynamics of scale-free graphs. Actually, a sounder approximation is to consider that hubs act as organizing centers of the excitable dynamics, see Sect. 4.3. An another numerical observation is the fact that plain mean-field description accounts for the excitation density but not at all for the correlation between co-activation patterns and graph topology [21]. Finally, mean-field equations provide an average view of the dynamics: they do not reflect dynamical features of individual trajectories.

Mean-field analysis alone is not reliable enough to grasp understanding of dynamics on complex networks. In general there is no internal way to delineate which results are correct and which are by far different from the actual behavior. On the other hand, numerical simulation alone is often as complex and intricate as an experiment on the real system, and it may prove difficult to dissect and identify

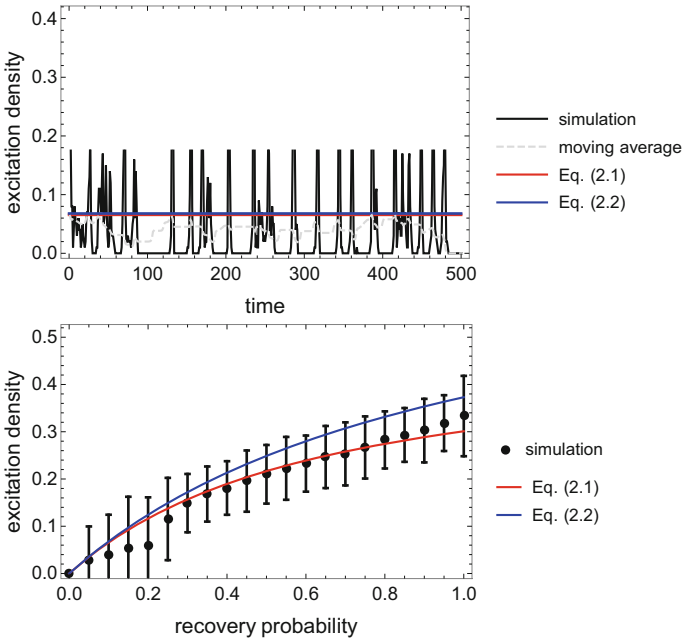

Fig. 3 Mean-field excitation density and its simulated counterpart on a scale-free graph for an absolute excitable threshold $q = 1$. Same as Fig. 2 now on a a scale-free graph (Barabási-Albert) with 100 nodes and 197 links (corresponding to $m = 2$ links being added per node during preferential attachment)

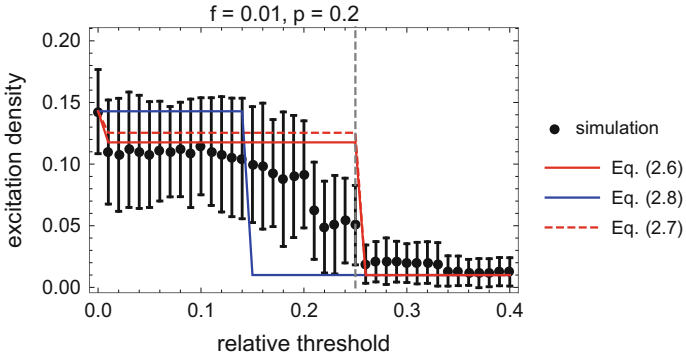

Fig. 4 Mean-field excitation density and its simulated counterpart on a random graph, in case of relative excitation threshold. Simulation has been performed with a recovery probability $p = 0.2$, a spontaneous excitation rate $f = 0.01$, on a random graph (Erdős-Rényi) with 100 nodes and 200 links. The time-averaged excitation density obtained in the simulation (black dots) is compared for various values of the relative threshold κ with the fixed point (2.8) and the steady-state solution of mean-field equations (2.6) and (2.7). Error bars on simulation points have been obtained from the last 250 time steps of a 500 time-step simulation starting from random initial conditions. The first step (blue line, Eq. (2.8)) is located at $\kappa = p/(2p + 1)$ and the second step (red continuous and dashed lines, Eqs. (2.6) and (2.7)) is at the higher value $\kappa = 1/\langle k \rangle$, indicated by the gray dashed vertical line

the local features and basic mechanisms responsible of the observed behavior. We claim that a reliable understanding can be gained by the conjunction of mean-field analysis and numerical simulation.

4 Second-Order Mean-field Approach for Topological Devices

4.1 Principle

Mean-field approaches described above all involved a spatial homogenization over the nodes (or subsets of nodes) of the graph. This is obviously a critical gap for investigating the interplay between graph topology and excitable dynamics. To circumvent this gap, we devised a refined analytical approach involving a more detailed account of the topology. The contribution of a specific topological motif (for instance a triangle, a cycle, a shell of nodes at the same distance from a given hub, a module) to the overall dynamical behavior can be computed by considering it as a device embedded in a surrounding described by mean-field densities. This approach amounts to use a second-order mean-field approximation, in which the (local) probability that neighbors of the motif are excited is given by the (global) steady-state mean-field excitation density c_E^*.

This general idea of mean-field for embedded devices is specially fruitful when considering the contribution of cycles (i.e. closed paths) to the overall dynamical behavior. Indeed, cycles are a feature not accounted in standard nor even in refined (pair-correlations or degree-classes) mean-field approaches, while they play a key role in excitable dynamics by contributing to excitation amplification and sustained activity [11–13]. In the case of an absolute excitation threshold $q = 1$, we detail below in Sect. 4.2 how to compute the average success rate of a cycle, by considering that it is embedded in a mean-field environment. We also sketch below in Sect. 4.3 the application of this methodology to study co-activation, by using a shell model around a hub [17].

4.2 Excitation of a Cycle

In a cycle of length L (i.e. a closed path of L nodes), a cycling excitation vanishes as soon as it meets a refractory node. Only long cycles can persistently store excitation: cycles should be long enough so that excitation always faces a susceptible substrate. Quantitatively, the probability π_L that a site R as recovered after $L-2$ steps, in time to accommodate the cycling excitation, should be close enough to 1. The simple

computation (which ignores the correlations with the surroundings) yields $\pi_L = \sum_{j=0}^{L-3}(1-p)^j p = 1-(1-p)^{L-2}$. Failure of re-excitation thus occurs on average after a time

$$\tau_{break}(p, L) = \frac{1}{(1-\pi_L)} = \frac{1}{(1-p)^{L-2}} \tag{4.1}$$

The quantity $\tau(L, p) = L - 1 + \tau_{break}(p, L)$ provides an estimate of the average runtime of the cycle. Using a similar reasoning, the probability that there is exactly N re-excited nodes in a row in the cycle is $\pi_L^N(1-\pi_L)$. The time after which failure of re-excitation occurs thus follows exactly a geometric distribution with parameter $1-\pi_L$. Accordingly, the corresponding variance, which coincides with the variance of the cycle runtime, is equal to $\pi_L/(1-\pi_L)^2$. In particular, $\pi_L = p$ for a triangle ($L = 3$), and the runtime is predicted to be equal to $2 + 1/(1-p)$ with a standard deviation $\sqrt{p/(1-p)^2}$. The good accuracy of this simple analysis is shown on Fig. 5.

A more detailed analysis shows that a cycle that is initially all susceptible and receives an excitation does not trigger a cycling excitation. It should also contain a refractory node, otherwise two waves of excitation will propagate in opposite direction and ultimately annihilate, which does not correspond to a cycling excitation. The probability that excitation of a cycle sets in is thus difficult to compute, as it essentially depends on the initial condition of the cycle. This difficulty has been circumvented above by computing the number of re-excitations N_{reex}, defined as the number of excitations following in a row the completion of a cycle. $N_{reex} = 1$ if the cycle excitation only closes onto itself, $N_{reex} = L + 1$ if a second

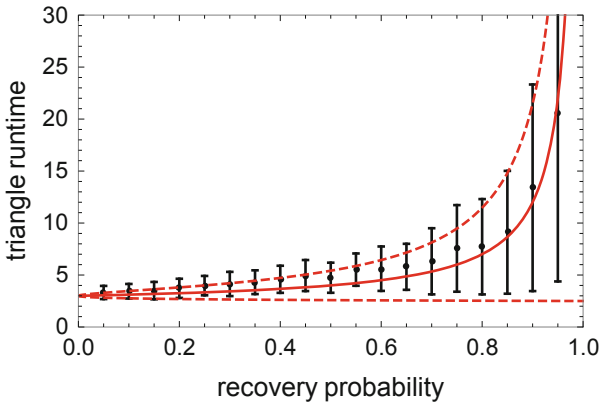

Fig. 5 Cycling excitation in a triangle. Considering the runtime of an excitation in a triangle, with initial condition (E, S, R), the figure compares the analytical prediction of this runtime $\tau(L, p) = L - 1 + \tau_{break}(L, p)$ for $L = 3$, with $\tau_{break}(L, p)$ given in (4.1), continuous red line, plus/minus the corresponding standard deviation $\sqrt{p/(1-p)^2}$, dashed red lines, with the simulation result (black dots). Errors bars on the numerical estimates have been computed with 100 runs

full turn is completed. N_{reex} is a number that is not a multiple of L in case of incomplete turns.

We can provide a refined estimate of the probability of continued excitation of a cycle, i.e. re-excitation of its nodes, using the second-order mean-field methodology described above. For simplicity we consider the case with no spontaneous excitations ($f = 0$). To get re-excited nodes, we have to consider that they do not fail to recover in time, and once recovered, that they do not receive a perturbing external excitations. Considering all the possible timings j between 1 and $L-2$ steps for the recovery, and the subsequent absence of external inputs during the $L-2-j$ remaining steps, we obtain the probability $\gamma(L, p)$ of a re-excitation:

$$\gamma(L, p) = \sum_{j=1}^{L-2} p(1-p)^{j-1}[(1-c_E^*)^{\langle k\rangle-2}]^{L-2-j}$$

$$= p \times \frac{[(1-c_E^*)^{\langle k\rangle-2}]^{L-2} - (1-p)^{L-2}}{(1-c_E^*)^{\langle k\rangle-2} - (1-p)} \tag{4.2}$$

Note that for a triangle, $L = 3$, the sum (correctly) contains a single term, yielding $\gamma(L, p) = p$: there is no way to perturb a cycling excitation along a triangle ESR except by a lack of recovery, the effect of which is analyzed in Fig. 5. In this mean-field approach, $\gamma(L, p)^N$ is the cumulative probability to have at least N re-excitations in a row, while the probability to have exactly N re-excitations in a row is $(1-\gamma(L, p))\gamma(L, p)^N$. The average number of re-excitations following cycle completion becomes:

$$\langle N_{reex}\rangle = \frac{\gamma(L, p)}{1-\gamma(L, p)} = \tau_{break} - 1 \tag{4.3}$$

In particular, (4.1) is recovered for a triangle, with $L = 3$ and $\gamma(L, p) = p$. Under the assumption that re-excitations dominate cycle activity, i.e. the cycle completion is followed by several turns of cycling re-excitation, this mean-field computation also gives the probability that at a given time a L-cycle is active, equal to $\gamma(L, p)^L$. The computation (4.2) involves several mean-field approximations: the probability of excitation of a cycle neighbor is taken equal to the steady-state mean-field excitation density c_E^*, the correlations between the states of the cycle neighbors are ignored, and the degree of cycle nodes are replaced by the average degree $\langle k\rangle$. This latter approximation could be eliminated by considering explicitly the degrees $(k_1, \ldots, k_L)$ of the cycle nodes. The probability of N re-excitations following cycle completion is then given by:

$$P(N, L, p) = \prod_{\alpha=1}^{N} \left[\sum_{j=1}^{L-2} p(1-p)^{j-1}[(1-c_E^*)^{k_\alpha-2}]^{L-2-j} \right] \tag{4.4}$$

where the label α of the degree should be understood modulo L, starting from the node having received the excitation. If another excitation enters the cycle at some susceptible node before the cycling excitation arrives, a phase slip is observed [12].

4.3 Shell Model of Hub-induced Co-activation

In the case of an excitable dynamics with an absolute threshold $q = 1$, the qualitative analysis of the dynamics suggests that hubs act as sources of excitation, spreading any single excitation they have received from their numerous neighbors. To quantitatively check whether this phenomenon actually dominates the dynamics, we considered the graph as a set of nested shells centered on the strongest hub [17]. Nodes belonging to the same shell are by definition at the same distance to the hub (Fig. 6). We first estimate the probability of excitation of the hub, of degree k_{hub}, by identifying it with the mean-field excitation density c_E^* for an average degree $\langle k \rangle = k_{hub}$, given in (2.2):

$$c_E(hub) = c_E^*(k_{hub}) \tag{4.5}$$

Comparison of this prediction and numerical simulation for hubs of various degrees is shown on Fig. 7, as a function of their degree k_{hub}.

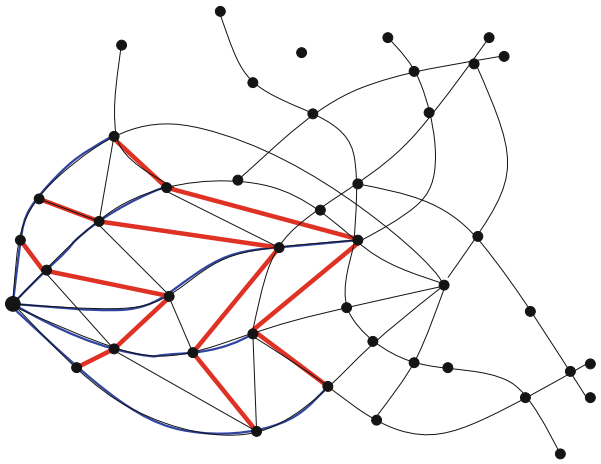

Fig. 6 Shell model for analytical estimation of co-activation. When the graph has a broad degree distribution, the excitable dynamics with an absolute threshold $q = 1$ is presumably dominated by the presence of hubs. We thus propose to represent the graph as a nested set of shells (bold red) centered around the strongest hub. Co-activation is then approximated as the synchronous activation of nodes in the same shell by an excitation propagating from the hub

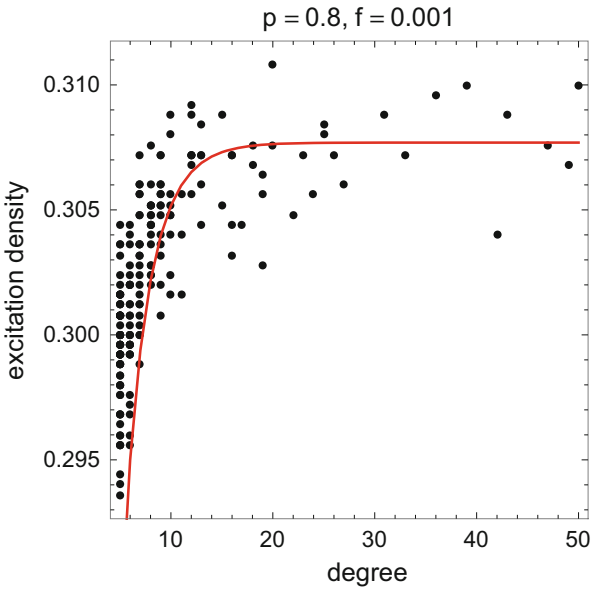

Fig. 7 Prediction of the steady-state excitation density of a node as a function of its degree. The figure compares the prediction (4.5), red line, and the simulation result for various nodes (scatter plot, black dots). The simulation has been performed for the excitable model with an absolute threshold $q = 1$, with $p = 0.8$ and $f = 0.001$, on a scale-free graph (Barabási-Albert) with 100 nodes and 985 links (corresponding to $m = 5$ links being added per node during preferential attachment)

Once the hub gets excited, nodes of the same shell will be reached at the same time by the excitation wave propagating from the hub. Accordingly, they will get excited jointly provided they are both in a susceptible state when the excitation wave arrives. The probability of such an event for a given pair of nodes, presumed to be the main contribution to the probability of their co-activation, can be computed in the mean-field approximation. We have to express that each node of the two paths from the hub to the considered nodes is susceptible when the excitation wave arrives. When ignoring pair correlations, the co-activation probability of any given pair of nodes in shell n can be written:

$$Q_n = c^*_{hub}(E)[c^*(S)]^{2n} \tag{4.6}$$

The comparison of this analytical prediction with the co-activation probability observed in the simulation has shown that excitations are more strongly coordinated in space and time than accounted in the derivation of (4.6). Dynamic correlations between neighbors should also be taken into account, for instance using the pair-correlation mean-field equations detailed above in Sect. 2.5, see [17] for details.

5 Conclusion

Mean-field approaches provide an analytical way to get some insights on excitable dynamics on graphs. They involve a closure relation, namely they ignore some correlations, and some kind of spatial homogenization, namely they also ignore most spatial structures and heterogeneities. Sometimes, a self-consistent validity check is possible. However, we claim that the most interesting insights come from either the agreement or the discrepancies between mean-field predictions and what is observed in numerical experiments. In this regard, analytical approaches are used as null models, as a way of hypothesis testing, to check the validity of their assumptions by comparing their predictions with direct simulation. Mean-field approaches presented above thus offer a sequence of nested null models, increasingly taking into account graph topological features.

Our previous and present investigations have shown that the validity and accuracy of mean-field approaches strongly depend on the observable. They are in general satisfactory for describing excitation density, but of more limited validity for investigating complex features like co-activation or sustained activity. Mean-field failure reveals the presence and key role of collective patterns of activity. When these collective patterns are rooted in some topological motifs, we propose a methodology based on mean-field-embedded devices, that is, the detailed description of the activity of a subset of nodes, given that their surrounding is described by mean-field densities. Beyond the examples detailed above for excitable dynamics with an absolute threshold $q = 1$, we also successfully implemented this mean-field methodology in the case of a relative excitation threshold, for instance to compute the contribution of multiple excitations meeting at a node and increasing the probability that this node gets excited and propagates the excitation [11]. This original methodology circumvents the limitation coming from the spatial homogenization involved in more basic mean-field approaches, and provides an analytical access to the interplay between dynamics and the underlying network topology. Joining these analytical results and simulation at the same time validates our analytical understanding and guides the interpretation of the detailed numerical results.

Mean-field approaches can be applied to a variety of other dynamical processes on graphs. What we have described using the formalism of graphs and excitable dynamics can be extended to numerous other settings, for instance reaction-diffusion on a structured substrate, in surface chemistry, or colonization-extinction processes on a heterogeneous landscape, in ecology.

Acknowledgments The authors warmly thank Delio Mugnolo, Fatihcan Atay and Pavel Kurasov, organizers of the ZiF programme *Discrete and continuous models in the theory of networks*, and ZiF (Center for Interdisciplinary Research) in Bielefeld for hospitality during this programme. This work was also funded by the French Centre National de la Recherche Scientifique (CNRS), programme InFIniTI of the Mission for Interdisciplinarity, grant 238301 (to A.L.).

References

1. BARABASI, A., AND ALBERT, R. Emergence of scaling in random networks. *Science 286*, 5439 (1999), 509.
2. BARRAT, A., BARTHELEMY, M., AND VESPIGNANI, A. *Dynamical processes on complex networks*. Cambridge University Press, 2008.
3. BARTHÉLEMY, M. Spatial networks. *Physics Reports 499*, 1–3 (2011), 1–101.
4. BARTHELEMY, M., BARRAT, A., PASTOR-SATORRAS, R., AND VESPIGNANI, A. Dynamical patterns of epidemic outbreaks in complex heterogeneous networks. *Journal of Theoretical Biology 235*, 2 (2005), 275–288.
5. BOCCALETTI, S., LATORA, V., MORENO, Y., CHAVEZ, M., AND HWANG, D. Complex networks: Structure and dynamics. *Physics Reports 424*, 4 (2006), 175–308.
6. CARVUNIS, A., LATAPY, M., LESNE, A., MAGNIEN, C., AND PEZARD, L. Dynamics of three-state excitable units on Poisson vs. power-law random networks. *Physica A: Statistical Mechanics and its Applications* (2006).
7. CATANZARO, M., BOGUÑÁ, M., AND PASTOR-SATORRAS, R. Diffusion-annihilation processes in complex networks. *Physical Review E 71*, 5 (2005), 056104.
8. CHRISTENSEN, K., FLYVBJERG, H., AND OLAMI, Z. Self-organized critical forest-fire model: Mean-field theory and simulation results in 1 to 6 dimenisons. *Physical Review Letters 71*, 17 (1993), 2737.
9. DANGERFIELD, C., ROSS, J., AND KEELING, M. Integrating stochasticity and network structure into an epidemic model. *Journal of the Royal Society Interface 6*, 38 (2009), 761–774.
10. ERDÖS, P., AND RÉNYI, A. On random graphs, i. *Publicationes Mathematicae (Debrecen) 6* (1959), 290–297.
11. FRETTER, C., LESNE, A., HILGETAG, C. C., AND HÜTT, M.-T. Topological determinants of self-sustained activity in a simple model of excitable dynamics on graphs. *Scientific reports 7* (2017), 42340.
12. GARCIA, G. C., LESNE, A., HILGETAG, C. C., AND HÜTT, M.-T. Role of long cycles in excitable dynamics on graphs. *Physical Review E 90*, 5 (2014), 052805.
13. GARCIA, G. C., LESNE, A., HÜTT, M., AND HILGETAG, C. C. Building blocks of self-sustained activity in a simple deterministic model of excitable neural networks. *Frontiers in Computational Neuroscience 6* (2012), 50.
14. GLEESON, J. P., MELNIK, S., WARD, J. A., PORTER, M. A., AND MUCHA, P. J. Accuracy of mean-field theory for dynamics on real-world networks. *Physical Review E 85*, 2 (2012), 026106.
15. GRAHAM, I., AND MATTHAI, C. C. Investigation of the forest-fire model on a small-world network. *Physical Review E 68* (2003), 036109.
16. HETHCOTE, H. W. Mathematics of infectious diseases. *SIAM Review 42* (2000), 599.
17. HÜTT, M., AND LESNE, A. Interplay between topology and dynamics in excitation patterns on hierarchical graphs. *Frontiers in Neuroinformatics 3* (2009).
18. HÜTT, M.-T., JAIN, M., HILGETAG, C. C., AND LESNE, A. Stochastic resonance in discrete excitable dynamics on graphs. *Chaos, Solitons and Fractals 45* (2012), 611–618.
19. LANDAU, L. D., AND LIFSHITZ, E. M. *Statistical physics*. Pergamon Press, London, 1958.
20. LESNE, A., AND LAGUËS, M. *Scale invariance: From phase transitions to turbulence*. Springer, Paris, 2011.
21. MÜLLER-LINOW, M., MARR, C., AND HÜTT, M. Topology regulates the distribution pattern of excitations in excitable dynamics on graphs. *Physical Review E 74*, 1 (July 2006), 1–7.
22. MURRELL, D. J., DIECKMANN, U., AND LAW, R. On moment closures for population dynamics in continuous space. *Journal of theoretical biology 229*, 3 (2004), 421–432.
23. PASTOR-SATORRAS, R., AND VESPIGNANI, A. Epidemic spreading in scale-free networks. *Physical Review Letters 86* (2001), 3200–3203.
24. ROY, M., AND PASCUAL, M. On representing network heterogeneities in the incidence rate of simple epidemic models. *Ecological Complexity 3*, 1 (2006), 80–90.

25. SIMOES, M., DA GAMA, M. T., AND NUNES, A. Stochastic fluctuations in epidemics on networks. *Journal of The Royal Society Interface 5*, 22 (2008), 555–566.
26. VAZQUEZ, F., AND EGUÍLUZ, V. M. Analytical solution of the voter model on uncorrelated networks. *New Journal of Physics 10*, 6 (2008), 063011.
27. WEBER, S., AND PORTO, M. Multicomponent reaction-diffusion processes on complex networks. *Physical Review E 74*, 4 (2006), 046108.
28. WEISS, P. La variation du ferromagnétisme avec la température [in French]. *Comptes Rendus 143* (1906), 1136–1139.

Spectral Zeta Functions

Anders Karlsson

Abstract This paper discusses the simplest examples of spectral zeta functions, especially those associated with graphs, a subject which has not been much studied. The analogy and the similar structure of these functions, such as their parallel definition in terms of the heat kernel and their functional equations, are emphasized. Another theme is to point out various contexts in which these non-classical zeta functions appear. This includes Eisenstein series, the Langlands program, Verlinde formulas, Riemann hypotheses, Catalan numbers, Dedekind sums, and hypergeometric functions. Several open-ended problems are suggested with the hope of stimulating further research.

1 Introduction

Euler observed the following product formula:

$$\sum_{n=1}^{\infty} \frac{1}{n^s} = \prod_p (1 - p^{-s})^{-1}$$

where the product is taken over the prime numbers. This function of the complex variable s is called the Riemann zeta function, denoted $\zeta(s)$, and the expressions above are convergent for $\mathrm{Re}(s) > 1$. The right hand side inspired several generalizations, by Artin, Hasse, Weil, Selberg, Ihara, Artin, Mazur, Ruelle, and others, see

Supported in part by the Swiss NSF, grant 20020 153127.

A. Karlsson (✉)
Section de mathématiques, Université de Genève, 2-4 Rue du Lièvre, Genève 4, Suisse

Matematiska institutionen, Uppsala universitet, Uppsala, Sweden
e-mail: anders.karlsson@unige.ch,anders.karlsson@math.uu.se

F. M. Atay et al. (eds.), *Discrete and Continuous Models in the Theory of Networks*, Operator Theory: Advances and Applications 281,
https://doi.org/10.1007/978-3-030-44097-8_10

[IK04, Te10] and references therein. The most far-reaching frameworks for Euler products might be provided by the insights of Grothendieck and Langlands. The left hand side found generalizations by Dirichlet, Dedekind, Hurwitz, Epstein and others in number theory, but also in another direction in the work of Carleman [Ca34], later extended in [MP49], where instead of the integers one takes Laplacian eigenvalues:

$$\sum_{\lambda \neq 0} \frac{1}{\lambda^s}$$

convergent in some right half-plane. The purpose of the present note is to survey a few recent investigations of these latter functions, *spectral zeta functions*, in cases where the Laplacian is less classical, instead coming from graphs or p-adics. As in one of Riemann's arguments, to get the analytic continuation one rather defines the zeta function via the heat kernel, so the Mellin transform of the heat trace (removing the constant term whenever necessary) and divide by $\Gamma(s)$. This has the advantage of also making sense when the spectrum has continuous part.

One intriguing aspect that we mention is the functional equation of the type s vs $1-s$ that appears also for these non-classical zeta functions. Notably one has

$$\xi_{\mathbb{Z}}(1-s) = \xi_{\mathbb{Z}}(s),$$

see below, and the equivalence of certain asymptotic functional equations to the Riemann hypotheses for $\zeta(s)$ and certain Dirichlet L-functions [FK17, F16].

Although there are a few instances in the literature where such function are introduced for graphs, it seems that the first more systematic effort to study spectral zeta functions of graphs appear in my paper with Friedli [FK17]. As it turns out, via asymptotic considerations, these functions are intimately related to certain zeta functions from number theory. In what follows we will moreover point out that spectral zeta functions for graphs appear *incognito* in, or are connected to, a rich set of topics:

- Eisenstein series, continuous spectrum of surfaces, Langlands program,
- Riemann hypotheses
- Dedekind sums and Verlinde formulas,
- hypergeometric functions of Appell and Lauricella
- Catalan numbers
- Fuglede-Kadison determinants

Although each of these connections may not be of central importance for the corresponding topic, still, in view of the variety of such appearances, I think that the subject of graph spectral zeta functions deserves more attention. This note can also be viewed as a modest update to parts of the discussion in Jorgenson-Lang [JL01] originally entitled *Heat kernels all over the place*. Throughout the text, I will suggest some questions and further directions for research.

I would like the thank the organizers, Mugnolo, Atay and Kurasov, for the very stimulating workshop *Discrete and continuous models in the theory of networks,* at the ZIF, Bielefeld, 2017, and for their invitation. I thank Fabien Friedli, Mårten Nilsson and the referee for corrections.

2 Continuous Case

2.1 $\mathbb{R}$ *and* $\mathbb{R}/\mathbb{Z}$

This case has been recorded in so many places and there is no need to repeat it here. But for comparison with the other contexts, we recall the formulas. The heat kernel on $\mathbb{R}$ is

$$K_{\mathbb{R}}(t,x) = \frac{1}{\sqrt{4\pi t}} e^{-x^2/t}.$$

The heat kernel on the circle $\mathbb{R}/\mathbb{Z}$ is

$$K_{\mathbb{R}/\mathbb{Z}}(t,x) = \sum_{n\in\mathbb{Z}} e^{-4\pi^2 n^2 t} e^{2\pi i n x}.$$

This expression comes from spectral considerations and equals the following periodization (i.e. one sums over the discrete group $\mathbb{Z}$ to obtain a function on the quotient $\mathbb{R}/\mathbb{Z}$, like in the proof of the Poisson summation formula):

$$\frac{1}{\sqrt{4\pi t}} \sum_{m\in\mathbb{Z}} e^{-(x+n)^2/4t}.$$

Setting $x = 0$ in the former expression, removing 1, and taking the Mellin transform and dividing by $\Gamma(s)$ yields

$$\zeta_{\mathbb{R}/\mathbb{Z}}(s) := 2 \cdot 4^{-s} \pi^{-2s} \zeta(2s),$$

which is the spectral zeta function of the circle $\mathbb{R}/\mathbb{Z}$. If we replace s by $s/2$ we have

$$2 \cdot (2\pi)^{-s} \zeta(s).$$

By defining the completed zeta function (in particular by multiplying back the gamma factor)

$$\xi(s) := \frac{1}{2} 2^s \pi^{s/2} \Gamma(s/2) \zeta_{\mathbb{R}/\mathbb{Z}}(s/2)$$

and equating the two heat kernel expressions (Poisson summation formula) one gets the fundamental functional equation in this form

$$\xi(1-s) = \xi(s),$$

known in the physics literature as the reflection formula for $\zeta(s)$.

The identity with the two heat kernel expressions are known to contain moreover a wealth of theorems, such as the modularity of theta functions and the law of quadratic reciprocity, see [K12] for a discussion.

2.2 A Few Comments on Further Examples

As recalled in the introduction the definition of spectral zeta function was perhaps first in [Ca34], in fact he had more general functions using also the eigenfunctions. This was used for the study of asymptotic properties of the spectrum using techniques from analytic number theory. Another application is for the purpose of defining determinants of Laplacians, in topology this was done by Seeley, Ray and Singer in the definition of analytic torsion, see [R97], and in physics by Dowker, Critchley, and Hawking [DC76, Ha77], useful in several contexts, see [E12]. A referee suggested that in this context one can also make reference to the important heat kernel approach to index theorems, see [BGV92], and to the connection with Arakelov geometry, see [So92].

The determinant of the Laplacian is defined in the following way, assuming the analytic continuation of the zeta function to $s = 0$,

$$\det \Delta_X := e^{-\zeta_X'(0)}.$$

For the numbers $1, 2, 3, \ldots$ (essentially the circle spectrum) the corresponding determinant, which formally would be $1 \cdot 2 \cdot 3 \ldots = \infty!$, has the value $\sqrt{2\pi}$ thanks to the corresponding well-known special value of $\zeta(s)$, and this value is coherent with the asymptotics of the factorial function $n!$ by de Moivre and Stirling. In fact it was exactly this constant that Stirling determined.

For tori the corresponding spectral zeta function are Epstein zeta functions. There are also some studies of spheres with explicit formulas. Osgood, Phillips, Sarnak [OPS88] showed that the determinant of the Laplacian is a proper function on the moduli spaces of Riemann surfaces, and could conclude that the set of isospectral surfaces is pre-compact. In string theory it was important to study how the determinant of laplacian changes when varying the metric on surfaces.

Spectral functions of Riemannian manifolds will appear in the limit of spectral zeta functions for certain sequences of graphs. The first more substantial example, the case of tori, can be found in [FK17].

3 Discrete Case

To avoid confusion, let me right away emphasize that I am not considering the Ihara zeta function or any related function. Therefore I do not give references for this zeta function, other than the book by Terras [Te10], our paper [CJK15] and another recent reference for the Ihara zeta function of quantum graphs [Sm07].

On the other hand, what is more relevant in our context here, but will not be discussed, are the spectral zeta functions of quantum metric graphs studied by Harrison, Kirsten and Weyand, see [HK11, HWK16, HW18] and references therein. The paper [HW18] even discusses the spectral zeta functions of discrete graphs exactly in our sense.

Other related papers on spectral functions of (especially finite cyclic) graphs are those of Knill [Kn13, Kn18] which contain a wealth of interesting ideas, and some considerations close to topics in [FK17] (we do not however understand his Theorem 1c in [Kn13], the convergence to a non-vanishing function in the critical strip, see also his Theorem 10; for us this limiting function is the Riemann zeta function which of course has zeros.) Knill also defines a function $c(s)$ that coincides with our $\zeta_{\mathbb{Z}}(s)$ perhaps without connecting it to the graph $\mathbb{Z}$. The asymptotics for cyclic graphs considered in [Kn13] and [FK17] were also deduced in [Si04]. The re-proof of Euler's formulas for $\zeta(2n)$ via such asymptotics also appears in [CJK10], but also here there are earlier references, for example [W91], in view of the form of Verlinde's formulas, discussed below.

3.1 $\mathbb{Z}$ *and* $\mathbb{Z}/n\mathbb{Z}$

Using the heat kernel on $\mathbb{Z}$ in terms of the I-Bessel function, see for example [KN06] where it is rediscovered, the spectral zeta function of the graph $\mathbb{Z}$ is

$$\zeta_{\mathbb{Z}}(s) = \frac{1}{\Gamma(s)} \int_0^\infty e^{-2t} I_0(2t) t^s \frac{dt}{t}, \tag{1}$$

where it converges as it does for $0 < Re(s) < 1/2$. From this definition it is not immediate that it admits a meromorphic continuation and a functional equation very similar to classical zetas. However, the following was shown in [FK17]:

Theorem 1 *For all $s \in \mathbb{C}$ it holds that*

$$\zeta_{\mathbb{Z}}(s) = \frac{1}{4^s \sqrt{\pi}} \frac{\Gamma(1/2 - s)}{\Gamma(1 - s)}.$$

The function

$$\xi_{\mathbb{Z}}(s) = 2^s \cos(\pi s/2) \zeta_{\mathbb{Z}}(s/2),$$

is entire and satisfies for all $s \in \mathbb{C}$

$$\xi_{\mathbb{Z}}(s) = \xi_{\mathbb{Z}}(1-s).$$

Jérémy Dubout [Du16] observed that in fact one can write this function as follows:

$$\zeta_{\mathbb{Z}}(s) = \binom{-2s}{-s}. \tag{2}$$

This makes a connection to the **Catalan numbers**

$$C_n = \frac{1}{n+1}\binom{2n}{n}$$

which are ubiquitous in combinatorics (214 such manifestations are listed in the book by Stanley [St12]).

Problem Could the other $\zeta_{\mathbb{Z}^d}(-n)$ be thought of as generalizations of the Catalan numbers?

Note also that (2) immediately shows, what is not a priori clear from the definition (1), that at negative integers this zeta function takes rational (indeed integral) values. This is analogous to Riemann zeta function and other Dedekind zeta functions, by theorems of Hecke, Klingen, Siegel, Deligne and Ribet. I refer to [Du16] for a fuller discussion on this topic in the graph setting.

Eisenstein series are functions which appear already in classical number theory as well as in the spectral theory of surfaces with cusps. Our function $\zeta_{\mathbb{Z}}(s)$ can be seen to be an important fudge factor (also called scattering determinant) for the Eisenstein series, this comes from Selberg but he does not realize that it is itself a spectral zeta function and writes just $\sqrt{\pi}\Gamma(s-1/2)/\Gamma(s)$, see [Se56] We think that $\zeta_{\mathbb{Z}}(s)$ is undeniably present, the question is whether its appearance is incidental or part of a general structure. Evidence for the more structural picture could be that for surfaces $\mathbb{Z}$ appears as the fundamental group of the cusps. This leads to the question whether in higher dimensional Eisenstein series, for example in Langlands' work [La76], other graph spectral zeta functions occur. In this context, the **Langlands program,** we observe that our function $\zeta_{\mathbb{Z}}(s)$ (or products thereof) is essentially the value in the Bhanu-Murty-Gindikin-Karpelevich formula at the archimedian place, see [Bh60, FGKP16, Ch. 8] related to the Harish-Chandra c-function.

Problem Understand the role played by $\zeta_{\mathbb{Z}}(s)$, and perhaps other spectral zeta functions, in the theory of Eisenstein series and the Langlands program. For example, $\zeta_{\mathbb{Z}}(s)$ and all the p-adic zeta functions in the last section might appear together in the Langlands constant term, or Langlands p-adic Gindikin-Karpelevich formula in [La71].

The spectral zeta function of the finite cyclic graph $\mathbb{Z}/n\mathbb{Z}$ (see e.g. [CJK10, FK17] for details) is

$$\zeta_{\mathbb{Z}/n\mathbb{Z}}(s) = \frac{1}{4^s}\sum_{k=1}^{n-1}\frac{1}{\sin^{2s}(\pi k/n)}.$$

There exists some literature on finite trigonometric sums, which in our context appears as the special values

$$\zeta_{\mathbb{Z}/n\mathbb{Z}}(m)$$

for integral m. Some of these special values are recorded in [FK17]. In particular since we can transform $\sin^{-2} z$ to $\cot^2 z$ we have special cases of **Dedekind sums** (which again leads into the theory of Eisenstein series as I learnt from Claire Burrin), see [Z73]. In another context, in the first of the **Verlinde formulas**, such sums appear, see [Sz93, Z96] for mathematical discussions. Let $\mathcal{N}_{\mathrm{g,n,d}}$ denote the moduli space of semi-stable n-dimensional vector bundles over a fixed Riemann surface of genus g and having as determinant bundle a fixed line bundle of degree d. The formula reads

$$\dim_{\mathbb{C}} H^0(\mathcal{N}_{\mathrm{g},2,0},\mathcal{L}^{\mathrm{m}}) = \frac{(\mathrm{m}+2)^{\mathrm{g}-1}}{2^{\mathrm{g}-1}}\sum_{\mathrm{k}=1}^{\mathrm{m}+1}\frac{1}{\sin^{2\mathrm{g}-2}\frac{\pi \mathrm{k}}{\mathrm{m}+2}}.$$

The right hand side can in our terminology be written as

$$(m+2)^{g-1}2^{g-1}\zeta_{\mathbb{Z}/(m+2)\mathbb{Z}}(g-1).$$

The lead term in the asymptotics as $m \to \infty$ was considered by Witten [W91] to evaluate the volume of the moduli space in question and here the well-known special values $\zeta(2(g-1))$ of the Riemann zeta function appears. This is consistent with the results in [FK17] and indeed earlier in a numerical analysis paper [Si04].

Problem Is the appearance of the special values of spectral zeta function of cyclic graphs just a coincidence, or are there other cases of the Verlinde formulas that allow interpretations as spectral zeta functions of graphs? If so, this would be intriguing and demand for an explanation.

In [FK17], using some of the methods in [CJK10, CJK12], we study the asymptotics of the spectral zeta function of $\mathbb{Z}^{\mathrm{d}}/A_n\mathbb{Z}^d$ as $n \to \infty$ motivated in particular by statistical physics. One sees there how in the asymptotics, the spectral zeta functions of the infinite graphs and manifold spectral zeta functions appear. In [FK17] and [F16] relations to analytic number theory are discussed. Notably there are reformulations of the **Riemann hypothesis** and the generalized Riemann hypothesis for certain Dirichlet L-functions. For example in [F16]: Let $m \geq 3$ and let χ be a

primitive and even Dirichlet character modulo m. For $n \geq 1$, define the cyclic graph L-function

$$L_n(s, \chi) := \sum_{k=1}^{mn-1} \frac{\chi(k)}{\sin^s(\pi k/mn)}.$$

Let $\Lambda_n(s, \chi) = n^{-s}(\pi/k)^{s/2}\Gamma(s/2)L_n(s, \chi)$. Recall the classical Dirichlet L-function

$$L(s, \chi) = \sum_{k=1}^{\infty} \frac{\chi(k)}{k^s}.$$

Friedli's theorem relates the Riemann hypothesis, on the location of the zeros of this latter function to a functional relation for the graph functions that imitates the well-known one for L itself. (This extension of [FK17] seems to me rather surprising.)

Theorem 2 ([F16]) *The following two statements are equivalent:*

1. *For all s with $0 < Re(s) < 1$ and $Im(s) \geq 8$ we have*

$$\lim_{n\to\infty} \frac{|\Lambda_n(s, \chi)|}{|\Lambda_n(1 - s, \overline{\chi})|} = 1;$$

2. *In the region $0 < Re(s) < 1$ and $Im(s) \geq 8$, all zeros of $L(s, \chi)$ have real part $1/2$.*

The first statement holds in any case for all s where L does not vanish. The appearance of a restriction on the imaginary part has a substantial reason, see Lemma 3.1 in the proof of the theorem in [F16]. A related lemma with a similar restriction was proved in the case of the Riemann zeta function and the restriction was shown to be essential [FK17].

3.2 A Few Comments on Further Examples

As it is pointed out in [FK17] the spectral zeta functions of such fundamental infinite graphs as the regular trees T_{q+1} and the standard lattices $\mathbb{Z}^d$ lead into **hypergeometric functions** of several variables, more precisely, specializations of these functions.

The spectral zeta function of $\mathbb{Z}^d$ is

$$\zeta_{\mathbb{Z}^d}(s) = \frac{d^{-s+1/2}}{\sqrt{2\pi}} \frac{\Gamma((s+1)/2)}{\Gamma(s)} F_C^{(d)}(s/2, (s+1)/2; 1, 1, \ldots, 1; 1/d^2, 1/d^2, \ldots, 1/d^2),$$

where $F_C^{(d)}$ is one of the Lauricella hypergeometric functions in d variables.

Problem It is remarked in [Ex76, p. 49] that no integral representation of Euler type has been found for F_C. We note that if one instead of the heat kernel starts with the spectral measure in defining $\zeta_{\mathbb{Z}^d}(s)$, we do get such an integral representation, at least for special parameters. Does this lead to the missing Euler-type integral representation formula?

The $(q+1)$-regular tree (or Bethe lattice in physics parlance) is the universal covering of $(q+1)$-regular graphs and is therefore a fundamental graph. In [FK17] an expression for the corresponding zeta function is found, interestingly via an Euler-type integral that Picard considered and which leads into Appell's hypergeometric function F_1:

$$\zeta_{T_{q+1}}(s) = \frac{q(q+1)}{(q-1)^2(\sqrt{q}-1)^{2s}} F_1(3/2, s+1, 1, 3; u, v),$$

with $u = -4\sqrt{q}/(\sqrt{q}-1)^2$ and $v = 4\sqrt{q}/(\sqrt{q}+1)^2$.

Problem What functional equations do these spectral zeta functions have? In view of the many symmetries that such hypergeometric functions have, could one hope for an s vs $1-s$ symmetry or similar identities?

The determinant of the Laplacian (of course removing the trivial eigenvalue 0 from the product) of a finite graph is known to count the number of spanning trees (with a root) of the graph. This is called Kirchhoff's matrix-tree theorem. For infinite graphs the corresponding determinant is sometimes related to Mahler measures (in number theory) and more generally to **Fuglede-Kadison determinants** (in operator algebras). See [Ly10, CJK10, CJK12] for more about these connections. A famous value is the determinant of the graph $\mathbb{Z}^2$ which is $4/\pi$ times Catalan's constant; one my wonder if there are other such values in terms of special values of Dirichlet L-functions.

4 Totally Disconnected Case

4.1 $\mathbb{Q}_p$ *and* $\mathbb{Q}_p/\mathbb{Z}_p$

This follows [CZ17] and the recent master thesis of Mårten Nilsson [Ni18], see these two sources for further references. Let $\mathbb{Q}_p$ denote the p-adic numbers and $\mathbb{Z}_p$ the p-adic integers. Let dy be the Haar measure on the locally compact additive group $\mathbb{Q}_p$ normalized so that the measure of $\mathbb{Z}_p$ is 1. The Taibleson-Vladimirov Laplacian can

be defined like pseudo-differential operators via the Fourier transform, alternatively it is explicitly given as an integral as follows:

$$\Delta f(x) = \frac{p^2-1}{1-p^{-3}} \int_{\mathbb{Q}_p} \frac{f(x)-f(y)}{|x-y|_p^3} dy$$

for suitable functions $f : \mathbb{Q}_p \to \mathbb{C}$. This gives rise in the usual ways to a heat equation and a heat kernel, which in this case turns out to be:

$$K_p(x,t) = \sum_{k=-\infty}^{\infty} \left(e^{-tp^{2k}} - e^{-tp^{2k+2}} \right) p^k C_{p^{-k}}(x),$$

where C_{p^n} denotes the characteristic function of the the ball $B_{p^n} = \left\{ x \in \mathbb{Q}_p : |x|_p \leq p^n \right\}$. There is another formula for this function:

$$K_p(x,t) = \sum_{m=0}^{\infty} \frac{(-1)^m t^m}{m!} \frac{1-p^{2m}}{1-p^{-2m-1}} |x|_p^{-2m-1},$$

valid for $x \neq 0$. Now passing to the quotient $\mathbb{Q}_p/\mathbb{Z}_p$ (which is analogous to the periodization done above and is here an integral over $\mathbb{Z}_p$), and after that taking the Mellin transform dividing by $\Gamma(s)$, leads to the corresponding spectral zeta function which is

$$\zeta_p(s) = (1-p^{-1}) \frac{p^{1-2s}}{1-p^{1-2s}} = \frac{p^{1-2s}-p^{-2s}}{1-p^{1-2s}} = \frac{p-1}{p^{2s}-p}.$$

Here we complete this function in the following manner:

$$\xi_p(s) = \sin(2\pi s) p^s \zeta_p(s),$$

then we obtain a functional equation of the usual type in the most symmetric form:

$$\xi_p(1-s) = \xi_p(s).$$

Since the zeta functions became so simple this relation is more trivial than what we saw in the other contexts. But still, we see a pattern: From the line $\mathbb{R}$ and the circle $\mathbb{R}/\mathbb{Z}$, to the graphs $\mathbb{Z}$ and $\mathbb{Z}/\mathrm{n}\mathbb{Z}$, and now $\mathbb{Q}_p$ and $\mathbb{Q}_p/\mathbb{Z}_p$, their associated spectral zeta functions have a non-obvious symmetry s vs $1-s$.

In another direction taking the Laplace transform of the two heat kernel expressions, Nilsson derives an identity valid for $Re(s) > (p/|x|_p)^2$:

$$\frac{1}{s|x|_p} \sum_{m=0}^{\infty} \frac{(-1)^m}{s^m |x|_p^{2m}} \frac{1-p^{2m}}{1-p^{-2m-1}} = \sum_{k=-\infty}^{\infty} \frac{p^2-1}{(1+p^{2k}s)(p^2+p^{2k}s)} p^k C_{p^k}(x).$$

Specializing to certain x gives an identity without p-adics, but only involving ordinary integers. For example, with $x = 1$ and $s > p^2$,

$$\frac{1}{s}\sum_{m=0}^{\infty}\frac{(-1)^m}{s^m}\frac{1-p^{2m}}{1-p^{-2m-1}} = \sum_{k=0}^{\infty}\frac{p^2-1}{(1+p^{2k}s)(p^2+p^{2k}s)}\cdot p^k.$$

It is natural to compare these considerations with the celebrated **Tate's thesis**, where Tate in particular after a Mellin transform, obtains for each p the local Euler factor $(1-p^{-s})^{-1}$, instead of our $\zeta_p(s)$. This brings us back to the first paragraph of this paper.

References

[BGV92] Berline, Nicole; Getzler, Ezra; Vergne, Michèle, Heat kernels and Dirac operators. Grundlehren der Mathematischen Wissenschaften [Fundamental Principles of Mathematical Sciences], 298. Springer-Verlag, Berlin, 1992. viii+369 pp.

[Bh60] Bhanu Murti, T. S. Plancherel's measure for the factor-space SL(n;R)/SO(n;R). Dokl. Akad. Nauk SSSR 133 503--506 (Russian); translated as Soviet Math. Dokl. 1 1960 860–862.

[Ca34] Carleman, Torsten, Propriétés asymptotiques des fonctions fondamentales des membranes vibrantes, Comptes rendus du VIIIe Congrès des Math. Scand. Stockholm, 1934, pp. 34–44

[CZ17] Chacón-Cortés, L. F.; Zúñiga-Galindo, W. A. Heat traces and spectral zeta functions for p-adic Laplacians. Reprinted in St. Petersburg Math. J. 29 (2018), no. 3, 529–544. Algebra i Analiz 29 (2017), no. 3, 144–166.

[CJK15] Chinta, G.; Jorgenson, J.; Karlsson, A. Heat kernels on regular graphs and generalized Ihara zeta function formulas. Monatsh. Math. 178 (2015), no. 2, 171–190.

[CJK10] Chinta, Gautam; Jorgenson, Jay; Karlsson, Anders Zeta functions, heat kernels, and spectral asymptotics on degenerating families of discrete tori. Nagoya Math. J. 198 (2010), 121–172.

[CJK12] Chinta, Gautam; Jorgenson, Jay; Karlsson, Anders Complexity and heights of tori. Dynamical systems and group actions, 89–98, Contemp. Math., 567, Amer. Math. Soc., Providence, RI, 2012.

[DC76] Dowker, J. S.; Critchley, Raymond Scalar effective Lagrangian in de Sitter space. Phys. Rev. D (3) 13 (1976), no. 2, 224–234Dowker. S. and Critchley, Raymond, Effective Lagrangian and energy-momentum tensor in de Sitter space, J. Phys. Rev. D 13, 3224, 1976

[Du16] Dubout, J., Spectral zeta functions of graphs, their symmetries and extended Catalan numbers, arXiv:1909.01659

[E12] Elizalde, Emilio, Ten physical applications of spectral zeta functions. Second edition. Lecture Notes in Physics, 855. Springer, Heidelberg, 2012. xiv+227 pp.

[Ex76] Exton, Harold *Multiple hypergeometric functions and applications.* Foreword by L. J. Slater. Mathematics & its Applications. Ellis Horwood Ltd., Chichester; Halsted Press [John Wiley & Sons, Inc.], New York-London-Sydney, 1976. 312 pp.

[FGKP16] Fleig, Philipp; Gustafsson, Henrik P. A.; Kleinschmidt, Axel; Persson, Daniel Eisenstein series and automorphic representations. With applications in string theory. Cambridge Studies in Advanced Mathematics, 176. Cambridge University Press, Cambridge, 2018. xviii+567 pp.

[F16] Friedli, Fabien, A functional relation for L-functions of graphs equivalent to the Riemann hypothesis for Dirichlet L-functions. J. Number Theory 169 (2016), 342–352.
[FK17] Friedli, Fabien; Karlsson, Anders Spectral zeta functions of graphs and the Riemann zeta function in the critical strip. Tohoku Math. J. (2) 69 (2017), no. 4, 585–610.
[HK11] Harrison, J. M.; Kirsten, K. Zeta functions of quantum graphs. J. Phys. A 44 (2011), no. 23, 235301, 29 pp.
[HWK16] Harrison, J. M.; Weyand, T. and Kirsten, K., Zeta functions of the Dirac operator on quantum graphs Journal of Mathematical Physics 57, 102301 (2016);
[HW18] Harrison, Jonathan; Weyand, Tracy, Relating zeta functions of discrete and quantum graphs. Lett. Math. Phys. 108 (2018), no. 2, 377–390.
[Ha77] Hawking, S. W. Zeta function regularization of path integrals in curved spacetime. Comm. Math. Phys. 55 (1977), no. 2, 133–148.
[IK04] Iwaniec, Henryk; Kowalski, Emmanuel, Analytic number theory. American Mathematical Society Colloquium Publications, 53. American Mathematical Society, Providence, RI, 2004. xii+615 pp.
[JL01] Jorgenson, Jay; Lang, Serge, The ubiquitous heat kernel. Mathematics unlimited—2001 and beyond, 655–683, Springer, Berlin, 2001.
[K12] Karlsson, Anders, Applications of heat kernels on abelian groups: $\zeta(2n)$, quadratic reciprocity, Bessel integrals. Number theory, analysis and geometry, 307–320, Springer, New York, 2012.
[KN06] Karlsson, Anders; Neuhauser, Markus, Heat kernels, theta identities, and zeta functions on cyclic groups. Topological and asymptotic aspects of group theory, 177–189, Contemp. Math., 394, Amer. Math. Soc., Providence, RI, 2006.
[Kn13] Knill, Oliver, The zeta function for circular graphs, https://arxiv.org/abs/1312.4239
[Kn18] Knill, Oliver, An elementary dyadic Riemann hypothesis, https://arxiv.org/pdf/1801.04639.pdf
[La71] Langlands, Robert P. Euler products. A James K. Whittemore Lecture in Mathematics given at Yale University, 1967. Yale Mathematical Monographs, 1. Yale University Press, New Haven, Conn.-London, 1971. v+53 pp.
[La76] Langlands, R. On the functional equations satisfied by Eisenstein series. Lecture Notes in Mathematics, Vol. 544. Springer-Verlag, Berlin-New York, 1976.
[Ly10] Lyons, Russell, Identities and inequalities for tree entropy. Combin. Probab. Comput. 19 (2010), no. 2, 303–313.
[MP49] Minakshisundaram, S.; Pleijel, Å. Some properties of the eigenfunctions of the Laplace-operator on Riemannian manifolds. Canadian J. Math. 1, (1949). 242–256.
[Ni18] Nilsson, M. The Vladimirov Heat Kernel in the Program of Jorgenson-Lang, master thesis, Uppsala University, 2018
[OPS88] Osgood, B.; Phillips, R.; Sarnak, P. Compact isospectral sets of surfaces. J. Funct. Anal. 80 (1988), no. 1, 212–234.
[R97] Rosenberg, Steven The Laplacian on a Riemannian manifold. An introduction to analysis on manifolds. London Mathematical Society Student Texts, 31. Cambridge University Press, Cambridge, 1997. x+172 pp.
[Se56] Harmonic analysis and discontinuous groups in weakly symmetric Riemannian spaces with applications to Dirichlet series. J. Indian Math. Soc. B 20, (1756). 47–87.
[Si04] Sidi, Avram, Euler-Maclaurin expansions for integrals with endpoint singularities: a new perspective. Numer. Math. 98 (2004), no. 2, 371–387.
[Sm07] Smilansky, Uzy, Quantum chaos on discrete graphs. J. Phys. A 40 (2007), no. 27, F621–F630.
[So92] Soulé, C. Lectures on Arakelov geometry. With the collaboration of D. Abramovich, J.-F. Burnol and J. Kramer. Cambridge Studies in Advanced Mathematics, 33. Cambridge University Press, Cambridge, 1992. viii+177 pp.
[Sz93] Szenes, András, Hilbert polynomials of moduli spaces of rank 2. Vector bundles. I. Topology 32 (1993), no. 3, 587–597.

[St12] Stanley, Richard P. Catalan numbers. Cambridge University Press, New York, 2015. viii+215 pp.

[Te10] Terras, Audrey, Zeta Functions of Graphs: A Stroll through the Garden. Cambridge Studies in Advanced Mathematics 128. Cambridge University Press, 2010

[W91] Witten, Edward On quantum gauge theories in two dimensions. Comm. Math. Phys. 141 (1991), no. 1, 153–209.

[Z73] Zagier, Don Higher dimensional Dedekind sums. Math. Ann. 202 (1973), 149–172.

[Z96] Zagier, Don Elementary aspects of the Verlinde formula and of the Harder-Narasimhan-Atiyah-Bott formula. Proceedings of the Hirzebruch 65 Conference on Algebraic Geometry (Ramat Gan, 1993), 445–462, Israel Math. Conf. Proc., 9, Bar-Ilan Univ., Ramat Gan, 1996.

A Family of Diameter-Based Eigenvalue Bounds for Quantum Graphs

J. B. Kennedy

Abstract We establish a sharp lower bound on the first non-trivial eigenvalue of the Laplacian on a metric graph equipped with natural (i.e., continuity and Kirchhoff) vertex conditions in terms of the diameter and the total length of the graph. This extends a result of, and resolves an open problem from, [J. B. Kennedy, P. Kurasov, G. Malenová and D. Mugnolo, Ann. Henri Poincaré **17** (2016), 2439–2473, Section 7.2], and also complements an analogous lower bound for the corresponding eigenvalue of the combinatorial Laplacian on a discrete graph. We also give a family of corresponding lower bounds for the higher eigenvalues under the assumption that the total length of the graph is sufficiently large compared with its diameter. These inequalities are sharp in the case of trees.

Keywords Quantum graphs · Spectral geometry of quantum graphs · Bounds on spectral gaps

2010 Mathematics Subject Classification 34B45 (34L15, 35P15, 81Q35)

1 Introduction

Let $\mathcal{G}$ be a connected, compact metric graph with a finite number of edges and let $-\Delta$ denote the Laplacian operator on $L^2(\mathcal{G})$ with natural (i.e., continuity and Kirchhoff) vertex conditions.[1] Since $-\Delta$ can be shown by standard means to be a

[1]We recall that these conditions are also called standard, Neumann–Kirchhoff or even just Neumann conditions in the literature.

J. B. Kennedy (✉)
Grupo de Física Matemática, Faculdade de Ciências, Universidade de Lisboa, Campo Grande, Lisboa, Portugal
e-mail: jbkennedy@fc.ul.pt

F. M. Atay et al. (eds.), *Discrete and Continuous Models in the Theory of Networks*, Operator Theory: Advances and Applications 281,
https://doi.org/10.1007/978-3-030-44097-8_11

self-adjoint operator with compact resolvent, one obtains the existence of a discrete sequence of eigenvalues of this operator, which we think of as eigenvalues of the *quantum graph* itself, having the form

$$0 = \mu_1(\mathcal{G}) < \mu_2(\mathcal{G}) \leq \mu_3(\mathcal{G}) \leq \ldots \to \infty; \tag{1.1}$$

the corresponding eigenfunctions may be chosen to form an orthonormal basis of $L^2(\mathcal{G})$. We refer to the monographs [12, 30] and the seminal review article [20] as well as Sect. 2 for more details.

It is a major preoccupation of spectral geometry to investigate how the sequence of eigenvalues (1.1) of a differential operator such as the Laplacian depends on the structure, be it total size, shape, degree of connectivity etc., of the underlying object on which it is defined. For operators on domains and manifolds, this goes back at least to conjectures of Saint Venant and Lord Rayleigh in the mid-to-late nineteenth century (see [33]; we refer also to [21, 22] for more modern overviews of the field). In the case of quantum graphs, that is, metric graphs with a differential operator defined on them, the first work in this direction appeared about 30 years ago [32], where it was proved that the first non-trivial eigenvalue $\mu_2(\mathcal{G})$ of the Laplacian with natural conditions on a graph whose total length, i.e., the sum of all its edge lengths, is $L > 0$ satisfies

$$\mu_2(\mathcal{G}) \geq \frac{\pi^2}{L^2}, \tag{1.2}$$

the right-hand side corresponding to the first non-trivial eigenvalue on an interval of the same total length L as $\mathcal{G}$. After a lull in the 1990s and early 2000s, in the last few years there seems to have been an explosion of interest in the topic, as witnessed by the long list of works establishing bounds on some or all of the eigenvalues (1.1), for example in terms of the total length, diameter, number of edges or vertices, edge connectivity,... of the graph, or establishing properties of extremising graphs realising the bounds, or developing tools with which the eigenvalues can be manipulated, or else considering similar problems for related nonlinear operators. We refer to [1–4, 6, 8, 10, 11, 16, 18, 24–27, 34–36] and mention in particular the generalisation of (1.2) to the higher eigenvalues [18]

$$\mu_k(\mathcal{G}) \geq \frac{\pi^2(k-1)^2}{L^2}, \tag{1.3}$$

with equality if and only if $\mathcal{G}$ is an *equilateral k-star*, a graph consisting of k edges of equal length L/k, all joined together at exactly one common vertex.

The goal of the present contribution is to give lower a bound on $\mu_k(\mathcal{G})$ in terms of the total length $L \in (0, \infty)$ of the graph $\mathcal{G}$ and its diameter

$$D := \operatorname{diam}(\mathcal{G}) := \sup\{\operatorname{dist}(x, y) : x, y \in \mathcal{G}\} \in (0, L],$$

where the distance is with respect to the canonical (Euclidean) metric in $\mathcal{G}$, i.e., the shortest Euclidean path within $\mathcal{G}$ connecting the points x and y, and the supremum is in fact a maximum since $\mathcal{G}$ is assumed to be compact.

For $k = 2$, this problem was first studied in [24, Section 7.2], where a non-trivial but non-sharp lower bound for μ_2 was given, and the question of obtaining the best possible bound was left open (see Remark 7.3(a) there). Here, by using some more advanced tools developed recently in [10] (which we call *surgery principles*), we can give a complete answer: our main theorem is as follows.

Theorem 1.1 *Assume that $\mathcal{G}$ is a connected, compact metric graph with a finite number of edges of total length $L > 0$ and diameter $\operatorname{diam}(\mathcal{G}) = D \in (0, L)$. Then $\mu_2(\mathcal{G})$ is larger than the square ω^2 of the smallest positive solution $\omega > 0$ of the transcendental equation*

$$\cos\left(\frac{\omega D}{2}\right) = \frac{\omega(L-D)}{2} \sin\left(\frac{\omega D}{2}\right); \tag{1.4}$$

the number ω^2 satisfies the two-sided bound

$$\frac{1}{LD} < \omega^2 < \frac{12}{LD}. \tag{1.5}$$

Equality is never attained on any fixed graph, but there is a sequence of graphs $\mathcal{D}_n$ each of length L and diameter D such that $\mu_2(\mathcal{D}_n) \to \omega^2$ as $n \to \infty$.

To describe our result for the higher eigenvalues μ_k, $k \geq 3$, we first recall that the *(first) Betti number* $\beta = \beta(\mathcal{G})$ of the graph $\mathcal{G}$ is defined to be the number of independent cycles of $\mathcal{G}$; equivalently, if $\mathcal{G}$ has E edges and V vertices, then it is given by $\beta = E - V + 1$. In particular, we have $\beta = 0$ if and only if $\mathcal{G}$ is a tree. We will require that L be "large" compared with D in the sense that the quantity

$$\gamma(L, D, k, \beta) := \begin{cases} \frac{L}{k-\beta} - \frac{D}{2} & \text{if } k > \beta, \\ \frac{L}{k} - \frac{D}{2} & \text{otherwise,} \end{cases} \tag{1.6}$$

will be assumed to be positive.

Theorem 1.2 *Assume that $\mathcal{G}$ is a connected, compact metric graph with a finite number of edges of total length $L > 0$ and diameter $\operatorname{diam}(\mathcal{G}) = D \in (0, L)$, and that the quantity $\gamma = \gamma(L, D, k, \beta)$ defined by (1.6) is strictly positive. Further assume that no loop[2] in $\mathcal{G}$ is longer than D. Then $\mu_k(\mathcal{G})$ is larger than the square $\omega_{k,\beta}^2$ of the smallest positive solution $\omega = \omega_{k,\beta} > 0$ of the transcendental equation*

$$\cos\left(\frac{\omega D}{2}\right) = \omega\gamma \sin\left(\frac{\omega D}{2}\right); \tag{1.7}$$

[2]By a *loop* we mean an edge which starts and ends at the same vertex, possibly after the suppression of vertices of degree two. A precise definition is given in [13, Definition 3.1].

the number $\omega^2_{k,\beta}$ satisfies the two-sided bound

$$\frac{2}{D\gamma + \frac{D^2}{2}} \leq \omega^2 \leq \frac{2}{D\gamma - \frac{D^2}{6}}. \tag{1.8}$$

There is a sequence of tree graphs $\mathcal{T}_n$ each of length L and diameter D such that $\mu_k(\mathcal{T}_n) \to \omega^2_{k,0}$ as $n \to \infty$.

While Theorem 1.2 is essentially optimal for trees, we expect that improvements may be possible if $\beta \geq 1$. We give some remarks to this effect in Sect. 5.

To describe concrete sequences $\mathcal{D}_n$ and $\mathcal{T}_n$ of optimisers, and at the same time to explain the meaning of (1.4) and (1.7), we first need to introduce a particular class of graphs, which will also play a role in the proofs.

Definition 1.3 Fix suitable numbers $n \in \mathbb{N}$, $n \geq 2$, and $0 < D \leq L$. We denote by

$$\mathcal{S}_n = \mathcal{S}(L, D, n)$$

the unique star graph having $n + 1$ edges, total length L and total diameter D, such that there is one distinguished edge e_0 of length $\ell_0 = (nD - L)/(n - 1)$ and n identical edges of length $\ell_1 = (L - D)/(n - 1)$ each, all joined at a common vertex (see Fig. 1).

Of interest will be the smallest eigenvalue

$$\lambda_1(\mathcal{S}_n)$$

of the Laplacian with a Dirichlet (zero) condition at the degree-one vertex v_0 at the end of e_0 and natural conditions at all other vertices (see Sect. 2 for more details on our notation). Observe that, for fixed L and D, as $n \to \infty$ the length ℓ_0 of the edge e_0 to D, and the other edges contract to a point: in the limit, we have an interval of length D with a kind of point mass of size $L - D$ at one endpoint. Henceforth, whenever we speak of stars, we shall *always mean stars of this form*.

The link to Theorem 1.1 is that the graphs $\mathcal{S}_n$ with length $L/2$ and diameter $D/2$ are the "building blocks" for a sequence of limiting domains $\mathcal{D}_n$. More precisely, we can form $\mathcal{D}_n$ by gluing together two copies of $\mathcal{S}_n$ at their respective Dirichlet vertices (the corresponding domain, a *symmetric star dumbbell* in the language of

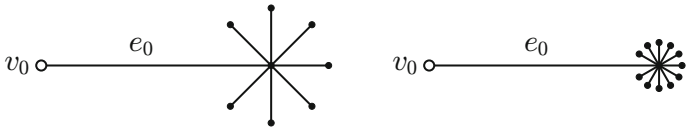

Fig. 1 The stars $\mathcal{S}_7$ (left) and $\mathcal{S}_{11}$ (right), for given L and D. The white circles at v_0 indicate Dirichlet vertex conditions

[24, Section 7.2], is pictured in Fig. 3 in Sect. 3); we then have $\mu_2(\mathcal{D}_n) = \lambda_1(\mathcal{S}_n)$ and each copy of $\mathcal{S}_n$ corresponds to a nodal domain of the eigenfunction of $\mu_2(\mathcal{D}_n)$ (see Sect. 3 for more details). Similarly, the domains $\mathcal{T}_n$ can be formed by taking k copies of $\mathcal{S}_n$ (each now with length L/k and diameter $D/2$) and joining them at their common Dirichlet vertex; then $\mu_k(\mathcal{T}_n) = \lambda_1(\mathcal{S}_n)$. As $n \to \infty$, the $\mathcal{T}_n$ converge to an equilateral k-star with diameter D and a point mass of size γ at each vertex of degree one, thus recalling the equilateral k-stars which were the optimisers in the inequality (1.3).

The next proposition summarises the properties of these stars $\mathcal{S}_n$, and in particular provides a rigorous justification of the formulae (1.4) and (1.7); it also implies the bounds on ω^2 given in (1.5) in Theorem 1.1, and on $\omega^2_{k,\beta}$ in (1.8) in Theorem 1.2 (where $\mathcal{S}_n$ is chosen to have diameter $D/2$ and length $L/(k-\beta)$ if $k > \beta$ or L/k otherwise).

Proposition 1.4 *Suppose $L > 0$ and $D \in (0, L]$ are given and, for $n \geq 2$, $\mathcal{S}_n$ is the star graph described in Definition 1.3 having length L and diameter D. Denote by $\lambda_1(\mathcal{S}_n)$ the first eigenvalue of the Laplacian on $\mathcal{S}_n$ with a Dirichlet condition at the degree one vertex v_0 of the edge e_0 and natural conditions at all other vertices. Then*

(1) the sequence $(\lambda_1(\mathcal{S}_n))_{n\geq 1}$ is strictly decreasing in n, and as $n \to \infty$, the eigenvalue $\lambda_1(\mathcal{S}_n)$ converges from above to the square ω^2 of the smallest positive solution $\omega > 0$ of the transcendental equation

$$\cos(\omega D) = \omega(L - D)\sin(\omega D); \tag{1.9}$$

(2) the number ω^2 from (1) is the smallest (strictly) positive eigenvalue of the problem

$$\begin{aligned} -u''(x) &= \omega^2 u(x) \qquad \text{in } (0, D), \\ u(0) &= 0, \\ u''(D) + \frac{2}{L-D}u'(D) &= 0; \end{aligned} \tag{1.10}$$

(3) for fixed L, the number ω^2 from (1) is a strictly decreasing function of $D \in (0, L]$;

(4) the number ω^2 from (1) satisfies the bounds

$$\frac{4}{LD} < \frac{4}{LD - \frac{D^2}{2}} \leq \omega^2 \leq \frac{48}{3LD - 2D^2} < \frac{48}{LD}.$$

The condition in (1.10), which is usually called a *generalised Wentzell*-type boundary condition, reflects the concentration of mass at one endpoint of the star $\mathcal{S}_n$ as $n \to \infty$. (The term *Wentzell boundary condition* is usually used to describe

the situation where the differential operator, in this case the Laplacian, itself appears in the boundary condition. We refer to [5, 31] for more information in the case of the Laplacian on domains.)

Remark 1.5

(a) The *stars* $\mathcal{S}_n$ are not the only building blocks we could use to construct suitable $\mathcal{D}_n$ and $\mathcal{T}_n$: in principle, we simply need a sequence of domains converging in an appropriate sense to an interval of given diameter, with a suitable point mass at one end described by the Wentzell condition in (1.10). These could, for example, be suitably chosen *stowers* (see [8, Example 1.5]) with one long edge e_0 and short loops in place of short pendant edges. We will use stars as they are easier to handle in our context.

(b) In [24, Section 7.2], in place of (1.4) the lower bound is the square $\tilde{\omega}^2$ of the smallest positive solution of

$$\cos(2\tilde{\omega}D) = (L - 2D)\tilde{\omega}\sin(2\tilde{\omega}D)$$

as long as $D \leq L/2$; this number satisfies $\tilde{\omega}^2 > 1/(2LD)$.[3] There, proofs of statements corresponding to Proposition 1.4(1) and (2) are given (in a slightly different form). The derivation of Eq. (1.10) from (1.9) is also described there; see [24, Remark 7.3(c)]. However, the proof of Theorem 1.1 uses an essentially different set of tools from the proof of the corresponding main result [24, Theorem 7.2]. Indeed, here we will make use of both a new transplantation principle and an Hadamard-type length perturbation formula (see Sect. 2 for details).

Finally, we remark that Theorem 1.1 and Proposition 1.4 recall very much results for the first non-trivial eigenvalue of *discrete* graph Laplacians (this eigenvalue is often called the *algebraic connectivity* of the discrete graph), in terms of the number of vertices of the graph–the discrete equivalent of its size, i.e., length–as well as the (now integer-valued) diameter. We reproduce the statements here in our language for ease of comparison.

Proposition 1.6 ([17], Corollary 3.3) *Let* T *be any (discrete) tree with diameter* $D \geq 3$ *and* $V \geq 4$ *vertices. Assume that* $V - D$ *is odd. Then the smallest non-trivial discrete Laplacian eigenvalue of* T *is at least as large as that of a symmetric star dumbbell formed by a chain of edges ("handle") of length* $D-2$*, with* $(V-D+1)/2$ *pendant edges attached to each end. (If* $V - D$ *is even, one edge must be removed from one of the pendant stars.)*

In fact, it seems plausible to expect that this result should hold for all graphs on V vertices, not only trees (just as our result holds independently of the topology of the graph). To the best of our knowledge this has not been proved; however, there

[3] There was an arithmetic error in the upper bound in [24, Remark 7.3(a)]; namely, it was too small by a factor of 4.

is a slightly older result which is valid for all graphs, which very much recalls our estimate (1.5), and which is at least asymptotically optimal as $V \to \infty$.

Proposition 1.7 ([29], Theorem 4.2 and Example After It) *Let* G *be any discrete graph with diameter* $D \geq 1$ *and* $V \geq 2$ *vertices. Then its smallest non-trivial Laplacian eigenvalue is at least as large as* $4/(DV)$*. Equality is achieved in the limit as* $V \to \infty$ *for fixed* D *by discrete analogues of the symmetric star dumbbells described in Proposition 1.6.*

In fact, this bound was extended very recently to infinite discrete graphs equipped with a probability measure in place of the usual one (so that the total "length" is one) and finite diameter; see [28, Corollary 3.7]. It would be interesting to know whether the latter result could be extended to quantum graphs, and to know what happens in the case of the higher eigenvalues. We thank Delio Mugnolo for bringing these results to our attention.

In Sect. 2 we will recall from [10] the elementary but powerful technical tools we will need for the proofs; for the sake of readability we will provide proof sketches here but refer to [10] for full details. In Sect. 3 we give the proof of Proposition 1.4 together with a detailed analysis of the stars $\mathcal{S}_n$ as well as their counterparts, the symmetric star dumbbells $\mathcal{D}_n$, and how their eigenvalues depend on parameters like length and diameter. These will be needed in the proofs of Theorem 1.1 and 1.2, which are in Sect. 4. Finally, in Sect. 5, we discuss the role of some of the assumptions in Theorem 1.2, and the possibility that they may be weakened.

2 Background Results: Surgical Tools

In this section we recall both the formal definition of the Laplacian on a quantum graph and the characterisation of its eigenvalues, as well as the "surgery" tools we shall need from [10].

Formally, the metric graph $\mathcal{G}$ is taken to consist of a set of edges $\mathcal{E} = \{e_1, \dots, e_M\}$, each of which may be identified with an interval $e_j \sim [0, \ell_j]$, $j = 1, \dots, M$, and a set of vertices $\mathcal{V} = \{v_1, \dots, v_N\}$; we write $e_i \sim e_j$ if e_i and e_j are adjacent (share a vertex), and in a slight abuse of notation $e \sim v$ if the vertex v is incident with the edge e, and $e \sim vw$ if e runs from v to w (i.e., both are incident with e). We always assume our graph to be connected, but *we explicitly allow it to have loops* ($e \sim vv$ for some $v \in \mathcal{V}$) and multiple edges running between two given vertices; in the latter case we speak of *parallel* edges. A *pendant edge* is any edge which ends at a vertex of degree one; the latter may be referred to as a *pendant vertex*.

We consider the operator associated with the bilinear form $a : H^1(\mathcal{G}) \times H^1(\mathcal{G}) \to \mathbb{R}$,

$$a(f, g) := \int_{\mathcal{G}} f' g' \, \mathrm{d}x \equiv \sum_{e \in \mathcal{E}} \int_e f' g' \, \mathrm{d}x, \tag{2.1}$$

where

$$L^2(\mathcal{G}) \simeq \bigoplus_{e\in\mathcal{E}} L^2(e), \qquad H^1(\mathcal{G}) = \{f \in L^2(\mathcal{G}) : f' \in L^2(\mathcal{G})\}.$$

Here f' is to be interpreted in the distributional sense, and the space $H^1(\mathcal{G}) \hookrightarrow C(\mathcal{G})$ in particular encodes both the vertex incidence relations and the vertex conditions. Indeed, the corresponding operator is given by the negative Laplacian (negative of the second derivative) on each edge. Its operator domain consists of those H^1-functions which, in addition to being automatically continuous across the vertices as members of $H^1(\mathcal{G})$, also satisfy the Kirchhoff condition

$$\sum_{e\sim v} f|'_e(v) = 0$$

at every vertex $v \in \mathcal{V}$, where $f|'_e$ is the derivative of the function along the edge e pointing into v. The associated smallest non-trivial eigenvalue $\mu_2(\mathcal{G})$, often also called the *spectral gap* since $\mu_1(\mathcal{G}) = 0$, admits the variational characterisation[4]

$$\mu_2(\mathcal{G}) = \inf\left\{\frac{\int_{\mathcal{G}} |f'|^2\,\mathrm{d}x}{\int_{\mathcal{G}} |f|^2\,\mathrm{d}x} : 0 \neq f \in H^1(\mathcal{G}),\ \int_{\mathcal{G}} f\,\mathrm{d}x = 0\right\} \tag{2.2}$$

with equality if and only if f is a corresponding eigenfunction, which we will tend to denote by ψ. For the higher eigenvalues, the usual min-max characterisation of Courant–Fischer type is available: we have

$$\mu_k(\mathcal{G}) = \inf_{M\subset H^1(\mathcal{G})} \max_{0\neq f\in M} \frac{\int_{\mathcal{G}} |f'|^2\,\mathrm{d}x}{\int_{\mathcal{G}} |f|^2\,\mathrm{d}x}, \tag{2.3}$$

where the infimum is taken over all subspaces of $H^1(\mathcal{G})$ of dimension k, and equality is achieved by any set M consisting of k linearly independent eigenfunctions corresponding to $\mu_1, \ldots, \mu_k$ (see [10, Sections 2 and 4.1], also for a characterisation of the sets achieving equality in (2.3), which is more complicated than for μ_2 and seems little known).

If instead we wish to consider the Laplacian with Dirichlet (zero) vertices on a subset $\mathcal{V}_\mathcal{D} \subset \mathcal{V}$, our form is still given by (2.1) but our form domain changes to $H^1_0(\mathcal{G}) := \{f \in H^1(\mathcal{G}) : f(v) = 0 \text{ for all } v \in \mathcal{V}_\mathcal{D}\}$ (the set $\mathcal{V}_\mathcal{D}$ being clear from the

[4]Note that we use the numbering convention from [10]. Both the notation and the numbering condition in [24] are different; there, $\lambda_1(\mathcal{G}) > 0$ is the smallest non-trivial eigenvalue of the Laplacian with natural vertex conditions.

context). In this case, we will denote the eigenvalues by $0 < \lambda_1(\mathcal{G}) < \lambda_2(\mathcal{G}) \leq \ldots$, where the smallest eigenvalue is given by

$$\lambda_1(\mathcal{G}) = \inf \left\{ \frac{\int_{\mathcal{G}} |f'|^2 \, \mathrm{d}x}{\int_{\mathcal{G}} |f|^2 \, \mathrm{d}x} : f \in H_0^1(\mathcal{G}) \right\}; \tag{2.4}$$

again, there is equality if and only if f is a corresponding eigenfunction. As is standard, we shall call the quotient appearing in (2.2)–(2.4) the *Rayleigh quotient* (of the function f).

Finally, if ψ is an eigenfunction associated with any one of the eigenvalues $\mu_k(\mathcal{G})$ or $\lambda_k(\mathcal{G})$, $k \geq 1$, then we call the closures of the connected components of the set

$$\{x \in \mathcal{G} : \psi(x) \neq 0\}$$

the *nodal domains* of the function ψ. (Any edges on which ψ vanishes identically are considered not to lie in any nodal domain.) If $k \geq 2$, then ψ must change sign in $\mathcal{G}$, since it is orthogonal in $L^2(\mathcal{G})$ to the eigenfunction associated with the smallest eigenvalue, which does not change sign and can easily be shown not to vanish anywhere (except on the set of Dirichlet vertices in the case of λ_1).

We refer to both the monographs [12, 20, 30] as well as the introductions and preliminary sections of [10, 11, 24] etc. for more details on these preliminaries.

We now collect the tools that we will need in the sequel. These are all based purely on the variational characterisations (2.2), (2.4) of the eigenvalues; most are from [10] although some have appeared in various guises throughout the recent literature. We start with the most elementary, which we take from [10, Theorem 3.4] but which has also appeared elsewhere.

Lemma 2.1 *Suppose the graph $\widetilde{\mathcal{G}}$ is formed from $\mathcal{G}$ by gluing together two vertices $v_1, v_2 \in \mathcal{V}(\mathcal{G})$, i.e., every edge that had v_1 or v_2 as an endpoint in $\mathcal{G}$ has a new common vertex $v_0 \in \mathcal{V}(\widetilde{\mathcal{G}})$. Then $\lambda_k(\widetilde{\mathcal{G}}) \geq \lambda_k(\mathcal{G})$ and $\mu_k(\widetilde{\mathcal{G}}) \geq \mu_k(\mathcal{G})$ for all $k \geq 1$. For λ_1 (corresp. μ_2) equality holds if and only if there is an eigenfunction ψ of $\lambda_1(\mathcal{G})$ (corresp. $\mu_2(\mathcal{G})$) such that $\psi(v_1) = \psi(v_2)$. In this case, the image of ψ under the gluing procedure remains an eigenfunction of $\lambda_1(\widetilde{\mathcal{G}})$ (corresp. $\mu_2(\widetilde{\mathcal{G}})$).*

Proof The inequality follows from the identification of $H^1(\widetilde{\mathcal{G}})$ as a subspace of $H^1(\mathcal{G})$, but such that the form (2.1) itself is the same. The characterisation of equality follows from the fact that the minimum in (2.2) (corresp. (2.4)) is achieved if and only if the function is a corresponding eigenfunction. This is also a special case of [10, Theorem 3.4]; the inequality itself has appeared in multiple places including [12, Theorem 3.1.8]. □

Lemma 2.2 *Suppose the graph $\widetilde{\mathcal{G}}$ is formed from $\mathcal{G}$ by lengthening an edge in $\mathcal{G}$. Then $\lambda_1(\widetilde{\mathcal{G}}) \leq \lambda_1(\mathcal{G})$ and $\mu_2(\widetilde{\mathcal{G}}) \leq \mu_2(\mathcal{G})$. Each of the inequalities is strict if there is a corresponding eigenfunction on $\mathcal{G}$ which does not vanish identically on the edge in question.*

Proof This is contained in [10, Corollary 3.12(1)]. □

Lemma 2.3 *Suppose ψ is an eigenfunction corresponding to $\mu_k(\mathcal{G})$, $k \geq 2$, and suppose ψ has $m \geq 2$ nodal domains, which we denote by $\mathcal{G}_1, \ldots, \mathcal{G}_m$. If we equip each of the $\mathcal{G}_i$ with Dirichlet conditions on the (finite) set $\mathcal{G}_i \cap \{x \in \mathcal{G} : \psi(x) = 0\}$, then $\mu_k(\mathcal{G}) = \lambda_1(\mathcal{G}_i)$ and $\psi|_{\mathcal{G}_i}$ is an eigenfunction corresponding to $\lambda_1(\mathcal{G}_i)$, for all $i = 1, \ldots, m$.*

Proof Fix $i = 1, \ldots, m$. Since $\psi|_{\mathcal{G}_i} \in H_0^1(\mathcal{G}_i)$ is a valid test function on $\mathcal{G}_i$, whose Rayleigh quotient is seen to be equal to its Rayleigh quotient on $\mathcal{G}$, i.e., $\mu_k(\mathcal{G})$. Thus $\mu_k(\mathcal{G}) \geq \lambda_1(\mathcal{G}_i)$. Conversely, since $\psi|_{\mathcal{G}_i}$ satisfies the strong form of the eigenvalue equation, including the zero condition, it must be an eigenfunction of $\lambda_j(\mathcal{G}_i)$ for *some* $j \geq 1$. But it does not change sign on $\mathcal{G}_i$; in fact, it is strictly different from zero everywhere on $\mathcal{G}_i$ outside the set of Dirichlet vertices. Now $\lambda_1(\mathcal{G}_i)$ is immediately seen to have an eigenfunction φ_i not changing sign on $\mathcal{G}_i$ (if φ is an eigenfunction, just replace it by $|\varphi|$ in (2.4)). Hence the $L^2(\mathcal{G}_i)$-inner product of $\psi|_{\mathcal{G}_i}$ and φ_i is not zero. Since both are eigenfunctions of the same Dirichlet eigenvalue problem, they must belong to the same eigenspace. It follows that $\psi|_{\mathcal{G}_i}$ corresponds to $\lambda_1(\mathcal{G}_i)$ and $\mu_k(\mathcal{G}) = \lambda_1(\mathcal{G}_i)$. □

We also have the following statement, which is complementary to Lemma 2.3 and an immediate consequence of the min-max principle (2.3). It relates $\mu_k(\mathcal{G})$ to *k-partitions* of $\mathcal{G}$. In the context of domains and manifolds, there is a large literature relating such partitions to the eigenvalues of the underlying domain or manifold and the nodal count of the associated eigenfunctions. We refer to [14] for a recent survey; for quantum graphs less has been done, but we refer to [7, 23].

Lemma 2.4 *Suppose $\mathcal{H}_1, \mathcal{H}_2, \ldots, \mathcal{H}_k$ form a* partition *of $\mathcal{G}$, that is, $\mathcal{H}_1, \mathcal{H}_2, \ldots, \mathcal{H}_k$ are closed graphs whose intersection is at most a finite set. Assume that $\partial\mathcal{H}_i = \{x \in \mathcal{G} : x \in \mathcal{H}_i \cap \overline{\mathcal{G} \setminus \mathcal{H}_i}\}$ is equipped with Dirichlet conditions, $i = 1, 2, \ldots, k$. Then $\mu_k(\mathcal{G}) \leq \max\{\lambda_1(\mathcal{H}_1), \lambda_1(\mathcal{H}_2), \ldots, \lambda_1(\mathcal{H}_k)\}$.*

Proof Denote by $\varphi_i \in H_0^1(\mathcal{H}_i)$ any eigenfunction corresponding to $\lambda_1(\mathcal{H}_i)$, $i = 1, \ldots, k$. Extend φ_i by zero on the rest of $\mathcal{G}$ to obtain a function $\tilde{\varphi}_i$ in $H^1(\mathcal{G})$ whose Rayleigh quotient is still $\lambda_1(\mathcal{H}_i)$. Note that for $i \neq j$ the sets where $\tilde{\varphi}_i \neq 0$ and $\tilde{\varphi}_j \neq 0$ are disjoint in $\mathcal{G}$, so in particular the functions are linearly independent. The desired inequality now follows immediately upon taking $M := \operatorname{span}\{\tilde{\varphi}_1, \ldots, \tilde{\varphi}_k\}$ in (2.3). □

We already observed that when $k = 2$, any corresponding eigenfunction ψ has (at least) two nodal domains. In the case $k \geq 3$, the precise number of nodal domains will be important to us. We thus recall the following general result from [9, Theorem 2.6].

Lemma 2.5 *Fix $k \geq 1$ and suppose $\mu_k(\mathcal{G})$ is simple and its eigenfunction ψ does not vanish at any vertex $v \in \mathcal{V}$. Then the number m of nodal domains of ψ is bounded by*

$$k - \beta \leq m \leq k, \tag{2.5}$$

where we recall that $\beta = |\mathcal{E}| - |\mathcal{V}| + 1$ is the (first) Betti number of $\mathcal{G}$.

We now give two surgery lemmata which will be central to the proof of Theorem 1.1. The first shows us that altering a graph by transferring "mass" from where its eigenfunction is smaller to where it is larger lowers the eigenvalue, and is adapted from [10, Theorem 3.18(1)].

Lemma 2.6 (Transplantation Lemma) *Suppose $\psi \geq 0$ is an eigenfunction corresponding to $\lambda_1(\mathcal{G})$. Suppose there is a vertex $v \in \mathcal{V}(\mathcal{G})$ and edges $e_1, \ldots, e_k \in \mathcal{E}(\mathcal{G})$ such that*

$$\sup\{\psi(x) : x \in e_1 \cup \ldots \cup e_k\} \leq \psi(v), \tag{2.6}$$

and the total length of these edges is $|e_1| + \ldots + |e_k| = \ell > 0$. Form a new graph $\widetilde{\mathcal{G}}$ from $\mathcal{G}$ by deleting the edges $e_1, \ldots, e_k$ (deleting also any vertices of degree one) and inserting new pendant edges at v and/or lengthening existing edges in $\mathcal{G}$ to which v is incident; any Dirichlet vertices in $\mathcal{G}$ not deleted should be preserved in $\widetilde{\mathcal{G}}$. Suppose that the total length of the additions and extensions is equal to or greater than ℓ. Then $\lambda_1(\widetilde{\mathcal{G}}) \leq \lambda_1(\mathcal{G})$. The inequality is strict provided $\psi(v) > 0$.

By *deleting an edge*, we always mean removing the edge in question *without* gluing its endpoints together; in particular, this process could disconnect the graph. See Fig. 2.

Proof This is actually an easy special case of [10, Theorem 3.18(1)], which is also valid for μ_2, for more general transplantation procedures, and for more general vertex conditions. Here, this follows simply by constructing a test function

$$\varphi(x) := \begin{cases} \psi(x) & \text{if } x \in \mathcal{G} \cap \widetilde{\mathcal{G}}, \\ \psi(v) & \text{if } x \in \widetilde{\mathcal{G}} \setminus \mathcal{G}. \end{cases}$$

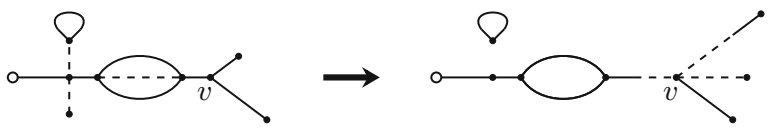

Fig. 2 The graph on the left is transformed into the graph on the right by transplantation to v. On the left, the dashed lines indicate the edges to be deleted, while on the right, they represent the insertion of new, and lengthening of existing, edges. These are chosen in such a way that the total length is preserved, or increased

Then condition (2.6) guarantees that $\|\varphi\|_{L^2(\widetilde{\mathcal{G}})} \geq \|\psi\|_{L^2(\mathcal{G})}$; while since φ is constant on $\widetilde{\mathcal{G}} \setminus \mathcal{G}$ and identical to ψ elsewhere, we obviously have $\|\varphi'\|_{L^2(\widetilde{\mathcal{G}})} \leq \|\psi\|_{L^2(\mathcal{G})}$. The inequality now follows from (2.4).

The strictness if $\psi(v) > 0$ holds because in this case φ, being locally equal to a nonzero constant, cannot be an eigenfunction of $\widetilde{\mathcal{G}}$; hence it has strictly larger Rayleigh quotient than $\lambda_1(\widetilde{\mathcal{G}})$. □

We finish with a perturbation formula giving the rate of change of a simple eigenvalue with respect to a perturbation of the edge lengths; such a formula is often referred to as being of *Hadamard type*, by way of analogy with the formulae for the derivative of an eigenvalue on a domain with respect to shape perturbations. The following formula has appeared in the literature multiple times, possibly beginning with [19].

Lemma 2.7 (Hadamard-Type Formula) *Let λ be a simple eigenvalue of the Laplacian (with either all natural or some natural and some Dirichlet vertices), with eigenfunction ψ normalised to have L^2-norm 1. Then the quantity*

$$\mathscr{E}_e := \lambda\psi(x)^2 + \psi'(x)^2, \qquad x \in e, \tag{2.7}$$

is constant on each edge $e \in \mathcal{E}$. Moreover,

(1) The derivative of λ with respect to the edge length $|e|$ exists and equals

$$\frac{d\lambda}{d|e|} = -\mathscr{E}_e.$$

(2) In particular, the rate of change of λ with respect to lengthening e_1 and shortening e_2 by the same amount is strictly negative if and only if

$$\mathscr{E}_{e_1} > \mathscr{E}_{e_2}.$$

The quantity (2.7) is called the *Prüfer amplitude* (of the eigenfunction ψ on the edge e).

Proof The formula in (1) may be found in [19], [15, Appendix A] and [8, Lemma 5.2] (probably among others). Part (2) is an immediate application, and can at any rate be found, together with (1), in [10, Section 3.2]. □

3 Properties of Stars and Dumbbells

In addition to the stars $\mathcal{S}_n$ of Definition 1.3 we will need a second, related class of graphs, which also appeared in [24].

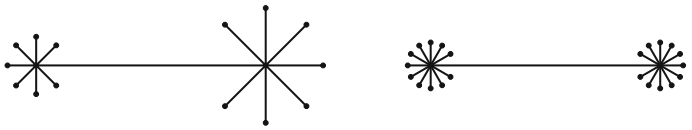

Fig. 3 A star dumbbell with $n = 7$ (left); the symmetric star dumbbell $\mathcal{D}_{11}$ (right): the handle has length $(11D - L)/10$, while all 22 short pendant edges have length $(L - D)/20$ each

Definition 3.1

(1) Fix suitable numbers $n \in \mathbb{N}$ and $\ell_0 > 0$, $\ell_1, \ell_2 \geq 0$. A *star dumbbell* will for us be a graph consisting of a finite edge (a *handle*) e_0 of length ℓ_0 connecting two distinct vertices v_1 and v_2, to each of which are attached n *pendant edges* each of length ℓ_1 at v_1, and a further n pendant edges of length ℓ_2 at v_2. We will denote such a graph by $\mathcal{D} = \mathcal{D}(\ell_0, \ell_1, \ell_2, n)$. The set of n pendant edges at v_i of length ℓ_i each will be denoted by $\mathcal{P}_i$, $i = 1, 2$.

(2) A *symmetric star dumbbell* is a star dumbbell with the additional property that $\ell_1 = \ell_2$.

See Fig. 3. If $L > 0$ and $D \in (0, L)$ are fixed, for $n \geq 2$ sufficiently large the symmetric star dumbbell of the form

$$\mathcal{D}_n = \mathcal{D}_n(L, D) := \mathcal{D}\left(\frac{nD - L}{n - 1}, \frac{L - D}{2(n - 1)}, \frac{L - D}{2(n - 1)}, n\right) \tag{3.1}$$

has total length L and diameter D, and is seen to consist of two identical copies of $\mathcal{S}_n = \mathcal{S}(\frac{L}{2}, \frac{D}{2}, n)$ imagined as being glued together at their respective Dirichlet vertices.

The link between $\mathcal{S}_n$ and $\mathcal{D}_n$ is made more precise in Lemma 3.4; first, we need two lemmata describing the relevant eigenfunctions of $\mathcal{S}_n$ and $\mathcal{D}_n$.

Lemma 3.2 *Let $\mathcal{S} = \mathcal{S}(L, D, n)$ be any star with $n \geq 2$ and $0 < D \leq L$. The eigenfunction associated with $\lambda_1(\mathcal{S})$, when chosen positive, is strictly increasing away from the Dirichlet vertex v_0, with vanishing derivative only at the Kirchhoff vertices of degree one, and is invariant with respect to permutations of the n identical edges of length ℓ_1.*

Proof Note that $\lambda_1(\mathcal{S})$ is simple as it is the smallest eigenvalue and denote by ψ the corresponding eigenfunction, chosen non-negative in $\mathcal{S}$. Let $e_1, \ldots, e_n$ be the n equal edges of length ℓ_1; then the function $\varphi \in H^1(\mathcal{S})$ given by the average value

$$\varphi = \frac{1}{n} \sum_{j=1}^{n} \psi|_{e_j}$$

on each of $e_1, \ldots, e_n$ and $\varphi|_{e_0} = \psi|_{e_0}$ is invariant under permutations of the edges $e_1, \ldots, e_n$, and immediately seen to satisfy the (classical) eigenvalue equation for $\lambda_1(\mathcal{S})$. Since $\lambda_1(\mathcal{S})$ is simple, the only possibility is that $\varphi = \psi$ everywhere.

To show that ψ is strictly monotone, it suffices to show that ψ' cannot vanish identically at any interior point (at the central vertex v_1, this means ruling out $\psi|'_{e_j}(v_1) = 0$ edgewise). Since ψ cannot change sign on $\mathcal{S}$, nor be identically equal to a nonzero constant on a set of positive measure, if ψ' vanishes, then ψ has a strict interior maximum. In this case, it must reach a non-negative local minimum at either an interior point of one of the edges or a (Neumann–Kirchhoff) vertex v. In the first case, the (one-dimensional) maximum principle is violated directly. In the second case, since we certainly have $\psi|'_{e_j}(v) = 0$ for all edges $e_j \sim v$, we may equally apply the one-dimensional maximum principle to obtain a contradiction. □

Lemma 3.3 *Suppose $\mathcal{D} = \mathcal{D}(\ell_0, \ell_1, \ell_2, n)$ is any star dumbbell, $\ell_0, \ell_1, \ell_2 > 0$, $n \geq 1$. Assume that $\ell_0 > \max\{\ell_1, \ell_2\}$, i.e., the handle is longer than the pendant edges,* or *that $\ell_1 = \ell_2$, i.e., $\mathcal{D}$ is symmetric. Then $\mu_2(\mathcal{D})$ is simple and its eigenfunction ψ, unique up to scalar multiples, is invariant with respect to permutations of the edges within each pendant collection of edges $\mathcal{P}_i$, $i = 1, 2$.*

Proof Fix one of the $\mathcal{P}_i$. Then we may choose a basis of $L^2(\mathcal{D})$ made of eigenfunctions such that each either takes the value 0 at the central vertex v_i of $\mathcal{P}_i$ (the eigenfunction is "odd"), or it is invariant with respect to permutations of the edges in $\mathcal{P}_i$ (it is "even"). (Indeed, if ψ is any eigenfunction and $e_1, \ldots, e_n$ are the edges of $\mathcal{P}_i$, then it suffices to consider instead the eigenfunction $(\psi|_{e_1} + \ldots + \psi|_{e_n})/n$ as in Lemma 3.2, together with its orthogonal complement in the span of ψ.) We do this for both $\mathcal{P}_i$.

Equipped with this basis, we note that the eigenfunctions which are "even" with respect to both $\mathcal{P}_i$ are all simple within the space of all such "even" eigenfunctions, since their value at any point depends only on that point's position along any path of $\mathcal{D}$ realising the diameter (and thus they correspond to one-dimensional problems). Hence, to prove the lemma, it is sufficient to show that the smallest non-constant of these has a smaller eigenvalue than any of the "odd" eigenfunctions, each of the latter being supported without loss of generality only on one of the $\mathcal{P}_i$. Indeed, under the assumption $\ell_1 \geq \ell_2$, the smallest eigenvalue associated with an odd eigenfunction is π^2/ℓ_1^2, corresponding to an eigenfunction each of whose two nodal domains corresponds to exactly one pendant edge of $\mathcal{S}_1$. If $\ell_0 > \ell_1$ or if $\ell_1 = \ell_2$, an elementary calculation shows that the (unique) zero of the even eigenfunction ψ with the smallest eigenvalue must lie in the interior of the handle e_0. In particular, each edge of $\mathcal{P}_1$ is strictly contained in one the nodal domains of ψ; and thus the eigenvalue of ψ is strictly smaller than π^2/ℓ_1^2. □

Lemma 3.4 *Fix $0 < D \leq L$ and $n \geq 2$. Denote by $\mathcal{D}_n(L, D)$ the symmetric star dumbbell with total length L and diameter D. Then*

$$\mu_2(\mathcal{D}_n(L, D)) = \lambda_1\left(\mathcal{S}\left(\frac{L}{2}, \frac{D}{2}, n\right)\right)$$

and the two copies of $\mathcal{S}(\frac{L}{2}, \frac{D}{2}, n)$ *embedded in* $\mathcal{D}_n(L, D)$ *are the two nodal domains of the eigenfunction corresponding to* $\mu_2(\mathcal{D}_n(L, D))$.

Proof This follows immediately from Lemmata 3.2 and 3.3, the latter in the form valid for symmetric star dumbbells. Alternatively, this statement is contained implicitly in [24, Proof of Lemma 7.6]. □

With this background, we can now give the proof of Proposition 1.4. As mentioned in the introduction, (1) and (2) were proved in [24] (in a slightly different form), and to avoid repetition of the somewhat tedious calculations we will not give their proofs again here.

Proof of Proposition 1.4

(1) and (2) For all $n \geq 2$, as shown in Lemma 3.4, we have

$$\lambda_1(\mathcal{S}_n) = \mu_2(\mathcal{D}_n)$$

where $\mathcal{D}_n$ is the symmetric star graph having total length $2L$ and diameter $2D$. The statements (1) and (2) now follow from [24, Lemma 7.6 and its proof] and [24, Remark 7.3(c)], respectively, bearing in mind that $\mathrm{diam}(\mathcal{D}_n) = 2D$ and $|\mathcal{D}_n| = 2L$. For an alternative proof of (1), see Lemma 3.5(1).

(3) We introduce the notation

$$F(\omega, D) := \cos(\omega D) - \omega(L - D)\sin(\omega D).$$

and wish to show that the derivative of ω with respect to D is negative when $L > D$:

$$\frac{\partial \omega}{\partial D} = -\frac{\partial F}{\partial D} \Big/ \frac{\partial F}{\partial \omega} = \frac{\omega \sin(\omega D) - \omega \sin(\omega D) + \omega^2 (L - D)\cos(\omega D)}{-D \sin(\omega D) - (L - D)\sin(\omega D) - \omega(L - D)D\cos(\omega D)}$$
$$= -\frac{\omega^2 (L - D)\cos(\omega D)}{L \sin(\omega D) + \omega(L - D)D\cos(\omega D)}.$$

Using the relation $\cos(\omega D) = \omega(L - D)\sin(\omega D)$, i.e., $F(\omega, D) \equiv 0$, which in particular implies that neither $\cos(\omega D)$ nor $\sin(\omega D)$ can be zero, we have

$$\frac{\partial \omega}{\partial D} = -\frac{\omega^3 (L - D)^2 \sin(\omega D)}{(L + \omega^2 (L - D)^2 D)\sin(\omega D)} = -\frac{\omega^3 (L - D)^2}{L + \omega^2 (L - D)^2 D} < 0$$

since $\omega > 0$ by assumption.

(4) See [24, Remark 7.3(a) and proof of Theorem 7.2]. □

We next give two lemmata showing how the eigenvalues of stars and star dumbbells depend on changes in the parameters (total length, diameter etc.). The key tool in both is the Hadamard formula, Lemma 2.7.

Lemma 3.5

(1) For fixed $L > 0$ and $D \in (0, L)$, the function

$$n \mapsto \lambda_1 (\mathcal{S}(L, D, n))$$

is strictly decreasing in $n \geq 2$.

(2) For fixed $L > 0$ and $n \geq 2$, the function

$$D \mapsto \lambda_1(\mathcal{S}(L, D, n))$$

is strictly decreasing in $D \in (0, L)$.

(3) Fix $L > 0$, $D > 0$ and $n \geq 2$. Then for each $L_1 > L$ there exists $n_1 \geq n$ such that

$$\lambda_1(\mathcal{S}(L_1, D, n_1)) < \lambda_1(\mathcal{S}(L, D, n)).$$

Proof

(1) Although this could be derived from an analysis of the corresponding secular equation, cf. the proof of Proposition 1.4, we will show how it can be obtained via the transplantation lemma 2.6. Essentially the same proof will also yield (3).

Fix any numbers $n_2 > n_1 \geq 2$. Denote by ψ the eigenfunction of $\lambda_1(\mathcal{S}(L, D, n_1))$, chosen positive, by v_1 the central vertex (i.e., of degree $n_1 + 1$) of $\mathcal{S}(L, D, n_1)$, and by

$$\ell_1 := \frac{L - D}{n_1 - 1} > \frac{L - D}{n_2 - 1} =: \ell_2$$

the lengths of the identical edges of $\mathcal{S}(L, D, n_1)$ and $\mathcal{S}(L, D, n_2)$, respectively. Now by Lemma 3.2, we know that ψ takes on the same value at the n_1 points at distance ℓ_2 to a degree one Kirchhoff vertex of $\mathcal{S}(L, D, n_1)$. Hence, by Lemma 2.1, if we glue these points together to create a new vertex v_2 of degree $2n_1$ (see Fig. 4), $\lambda_1(\mathcal{S}(L, D, n_1))$ is unaffected and ψ is still the eigenfunction; in particular, it is still a monotonically increasing function of the distance to the Dirichlet vertex.

We now create $\mathcal{S}(L, D, n_2)$ out of this graph by deleting $n_1 - 1$ of the n_1 parallel edges of length $\ell_2 - \ell_1$ each between v_1 and v_2 and, in their place, inserting $n_2 - n_1$ pendant edges of length ℓ_2 each at v_2. Since ψ was smaller on the deleted parallel edges than at v_2, Lemma 2.6 yields

$$\lambda_1(\mathcal{S}(L, D, n_2)) \leq \lambda_1(\mathcal{S}(L, D, n_1)).$$

In fact, since $\psi(v_2) > 0$ by Lemma 3.2, this inequality is strict.

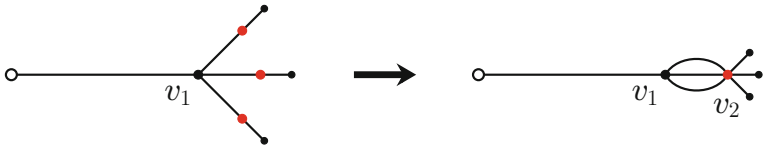

Fig. 4 The star $\mathcal{S}(L, D, n_1)$ with the points to be glued together marked in red (left); the graph obtained after the gluing (right). To create $\mathcal{S}(L, D, n_2)$ out of the right-hand graph, we remove all but one of the edges between v_1 and v_2 and, in their place, create new pendant edges at the red vertex v_2

(2) We use the Hadamard formula, Lemma 2.7. Write $\mathcal{S}$ for $\mathcal{S}(L, D, n)$, for given L, D, n. Noting that the simple eigenvalue λ_1 is a differentiable function of the edge lengths at $\mathcal{S}$, if we write ℓ_0 for the length of the Dirichlet edge e_0 and ℓ_1 for the common length of each of the other n edges, then we see that

$$\frac{d}{dD}\lambda_1(\mathcal{S}) = \frac{d}{d\ell_0}\lambda_1(\mathcal{S}) - n\left(\frac{1}{n}\cdot\frac{d}{d\ell_1}\lambda_1(\mathcal{S})\right) \tag{3.2}$$

since increasing D while holding L and n constant is equivalent to lengthening e_0 while shortening the n other edges by $1/n$th of that amount each. As before, let v_1 denote the central vertex, $e_1, \ldots, e_n$ the n identical edges and ψ the eigenfunction. By Lemma 2.7, we have

$$\frac{d}{d\ell_0}\lambda_1(\mathcal{S}) = -\mathscr{E}_{e_0} = -\left(\lambda_1(\mathcal{S})\psi(v_1)^2 + \psi|'_{e_0}(v_1)^2\right),$$

where we recall $\psi|'_{e_0}(v_1)$ is the (normal) derivative of ψ on e_0 at v_1; while by Lemma 2.7, the continuity–Kirchhoff condition at v_1 and the symmetry property of ψ from Lemma 3.2,

$$\frac{d}{d\ell_1}\lambda_1(\mathcal{S}) = -\left(\lambda_1(\mathcal{S})\psi(v_1)^2 + \psi|'_{e_j}(v_1)^2\right) = -\left(\lambda_1(\mathcal{S})\psi(v_1)^2 + \left(\frac{1}{n}\psi|'_{e_0}(v_1)\right)^2\right)$$

(for any fixed $j = 1, \ldots, n$). Inserting these expressions into (3.2), we obtain

$$\frac{d}{dD}\lambda_1(\mathcal{S}) = \left(\frac{1}{n^2} - 1\right)\psi|'_{e_0}(v_1)^2.$$

This last expression is strictly negative since $n \geq 2$ and ψ' does not vanish at v_1 on any edge with which v_1 is incident by Lemma 3.2.

(3) The proof is similar to the proof of (1), so we only sketch it. Choose any $n_1 \geq n$ such that the n_1 identical edges of $\mathcal{S}(L_1, D, n_1)$ are shorter than the n identical edges of $\mathcal{S}(L, D, n)$, that is, such that

$$\frac{L_1 - D}{n_1 - 1} < \frac{L - D}{n - 1}.$$

As in (1), we may glue the n vertices of $\mathcal{S}(L, D, n)$ at distance $(L_1 - D)/(n_1 - 1)$ from a degree one Kirchhoff vertex to form v_2 without affecting the eigenvalue or eigenfunction. We may now transplant the surplus parallel edges from v_1 to v_2 to pendant edges at v_2 of the right length to create $\mathcal{S}(L_1, D, n_1)$ and strictly lower the eigenvalue in the process.

□

Lemma 3.6 *For fixed total length L, fixed $\ell_0 \geq \ell > 0$ and fixed $n \geq 1$ consider the family of star dumbbells $\mathcal{D} = \mathcal{D}(\ell_0, \ell_1, \ell - \ell_1, n)$, where $\ell_1 \in [0, \ell]$. Then*

(1) $\frac{d}{d\ell_1}\mu_2(\mathcal{D})$ exists for all $\ell_1 \in (0, \ell)$ and is strictly negative if $\ell_1 \in (0, \ell/2)$ and strictly positive if $\ell_1 \in (\ell/2, \ell)$.

(2) In particular, $\mu_2(\mathcal{D})$ reaches its unique global minimum over $\ell_1 \in [0, \ell]$ at $\ell_1 = \ell/2$.

In words, a symmetric star dumbbell has the lowest first eigenvalue among all star dumbbells having the same total length, diameter and number of pendant edges at each side. While the proof is similar to (parts of) the proof of Lemma 3.5, the latter lemma does not directly imply Lemma 3.6 because, while the nodal domains of the eigenfunction of $\mu_2(\mathcal{D})$ will be stars, it would require more work to study their dependence on the edge lengths of $\mu_2(\mathcal{D})$; so instead we give a direct proof.

Proof

(1) The existence of the derivative follows immediately from Lemma 2.7, which is applicable since $\mu_2(\mathcal{D})$ is always simple by Lemma 3.3. By symmetry, it suffices to restrict attention to $\ell_1 \in (0, \ell/2)$ and prove that

$$\frac{d}{d\ell_1}\mu_2(\mathcal{D}) < 0 \qquad \text{if } \ell \in (0, \ell_1/2). \tag{3.3}$$

Denote by ψ the corresponding eigenfunction, which is unique up to scalar multiples by Lemma 3.3. Then by Lemma 2.7 ψ is identical on all edges within each of the stars, and to prove (3.3) it suffices to prove that if e_1 is an edge in $\mathcal{P}_1$ and e_2 is an edge in $\mathcal{P}_2$, then $\ell_1 = |e_1| < |e_2| = \ell_2$ implies $\mathscr{E}_{e_1} > \mathscr{E}_{e_2}$. By Lemma 2.7, this in turn is equivalent to showing

$$\mu_2(\mathcal{D})\psi(v_1)^2 + \psi|'_{e_1}(v_1)^2 > \mu_2(\mathcal{D})\psi(v_2)^2 + \psi|'_{e_2}(v_2)^2,$$

$i = 1, 2$. Denote by e_0 the handle, so that e_1 and e_0 are adjacent at v_1, and e_2 and e_0 are adjacent at v_2. Note that since $\ell_0 \geq \ell > \max\{\ell_1, \ell - \ell_1\}$ the eigenfunction ψ has exactly one zero, and this is on the handle e_0.

Claim The zero of ψ is strictly closer to v_2 than v_1.

To prove the claim: if the claim does not hold, then, supposing the star $\mathcal{D}^+ := \{x \in \mathcal{D} : \psi(x) \geq 0\}$ to contain $\mathcal{P}_2$, and noting that $\mu_2(\mathcal{D}) = \lambda_1(\mathcal{D}^+)$ by Lemma 2.3, we may reflect $\mathcal{D}^+$ across the set $\{x \in \mathcal{D} : \psi(x) = 0\}$ to obtain a

new (symmetric) star dumbbell $\widetilde{\mathcal{D}}$ such that, by symmetry, $\mu_2(\widetilde{\mathcal{D}}) = \lambda_1(\mathcal{D}^+)$. But the handle of $\widetilde{\mathcal{D}}$ is at least as long as e_0 and, since $\ell_1 < \ell/2$, the pendant edges of its other star are strictly longer than those of $\mathcal{D}$. But by Lemma 2.2, this means that $\mu_2(\widetilde{\mathcal{D}}) < \mu_2(\mathcal{D})$, a contradiction. This proves the claim.
It follows from the claim that $\psi(v_1)^2 > \psi(v_2)^2$; correspondingly, since, again, the Prüfer amplitude is constant on each edge, we also have $\psi|'_{e_0}(v_1)^2 < \psi|'_{e_0}(v_2)^2$, so that

$$-(n-1)\psi|'_{e_0}(v_1)^2 > -(n-1)\psi|'_{e_0}(v_2)^2. \tag{3.4}$$

Now by the Kirchhoff condition and the fact that ψ is identical on all pendant edges within each star,

$$\begin{aligned}\mu_2(\mathcal{D})\psi(v_1)^2 + n\psi|'_{e_1}(v_1)^2 &= \mu_2(\mathcal{D})\psi(v_1)^2 + \psi|'_{e_0}(v_1)^2 \\ &= \mu_2(\mathcal{D})\psi(v_2)^2 + \psi|'_{e_0}(v_2)^2 = \mu_2(\mathcal{D})\psi(v_2)^2 + n\psi|'_{e_2}(v_2)^2.\end{aligned}$$

Adding (3.4) yields

$$\mu_2(\mathcal{D})\psi(v_1)^2 + \psi|'_{e_1}(v_1)^2 > \mu_2(\mathcal{D})\psi(v_2)^2 + \psi|'_{e_2}(v_2)^2,$$

as desired.

(2) This follows immediately from (1), also using the continuity of μ_2 as $\ell_1 \to 0$ or ℓ, for fixed ℓ_0 and n. □

We finish this section with a kind of symmetrisation or balancing result for stars which we will need for the proof of Theorem 1.2. This is closely related to the minimisation result of Lemma 3.6(2) when combined with Lemma 3.4.

Lemma 3.7 *Suppose $\mathcal{S}_1$ and $\mathcal{S}_2$ are stars with diameter D_1, D_2 and total length $L_1 \geq D_1$, $L_2 \geq D_2$, respectively. Assume that both stars have n identical shorter edges (each of length $(L_1 - D_1)/n \geq 0$ and $(L_2 - D_2)/n \geq 0$, respectively).*[5] *Denote by $\mathcal{S}^*$ the star with diameter $(D_1 + D_2)/2$, total length $(L_1 + L_2)/2$, and n identical shorter edges, and by $\mathcal{D}^*$ the symmetric star dumbbell with diameter $D_1 + D_2$ and total length $L_1 + L_2$, formed by gluing together two copies of $\mathcal{S}^*$ at their respective vertices. Then*

$$\max\{\lambda_1(\mathcal{S}_1), \lambda_1(\mathcal{S}_2)\} \geq \mu_2(\mathcal{D}^*) = \lambda_1(\mathcal{S}^*). \tag{3.5}$$

The inequality is strict if $\mathcal{S}_1 \neq \mathcal{S}_2$.

[5] When we say *shorter*, we are including the assumption that these edges are shorter than the respective $(n+1)$st edges equipped with the Dirichlet condition; that is, $\frac{L_i - D_i}{2(n-1)} \leq \frac{nD_i - L_i}{n-1}$, $i = 1, 2$.

Proof We glue $\mathcal{S}_1$ and $\mathcal{S}_2$ together at their Dirichlet points to create a (non-symmetric) star dumbbell $\mathcal{D}$ having total length $L_1 + L_2$ and diameter $D_1 + D_2$. By Lemma 2.4 we have $\mu_2(\mathcal{D}) \leq \max\{\lambda_1(\mathcal{S}_1), \lambda_1(\mathcal{S}_2)$. Denote by $\mathcal{D}^*$ the symmetric star dumbbell having the same length and diameter as $\mathcal{D}$. Then $\mu_2(\mathcal{D}^*) \leq \mu_2(\mathcal{D})$ by Lemma 3.6(2). Appealing to Lemma 3.4 completes the proof of (3.5).

Now suppose that $\mathcal{S}_1 \neq \mathcal{S}_2$. We consider two cases: (1) the respective shorter edges have different lengths, i.e., $L_1 - D_1 \neq L_2 - D_2$. In this case, $\mathcal{D} \neq \mathcal{D}^*$ and Lemma 3.6(2) yields the strict inequality $\mu_2(\mathcal{D}^*) < \mu_2(\mathcal{D})$; or (2) we have $L_1 - D_1 = L_2 - D_2$ so that $\mathcal{D} = \mathcal{D}^*$. In this case, since $\mathcal{S}_1 \neq \mathcal{S}_2$, we may assume without loss of generality that $L_1 < L_2$. In this case, $\mathcal{S}_1$ is strictly contained in the star $\mathcal{S}^*$ having length $(L_1 + L_2)/2$ and diameter $(D_1 + D_2)/2$, that is, $\mathcal{S}^*$ can be obtained from $\mathcal{S}_1$ by strictly lengthening the edge of the latter equipped with the Dirichlet vertex. The strictness statement in Lemma 2.2 now yields $\lambda_1(\mathcal{S}^*) < \lambda_1(\mathcal{S}_1)$. □

4 Proof of the Main Theorems

We now turn to the proof of Theorems 1.1 and 1.2. The key to both is the following observation.

Lemma 4.1 *Suppose $\mathcal{H}$ is a connected, compact graph with a finite number of edges, and with total length $L > 0$ and equipped with a non-empty set of Dirichlet vertices $\mathcal{V}_\mathcal{D}$, and set*

$$d := \sup_{x \in \mathcal{H}} \operatorname{dist}(x, \mathcal{V}_\mathcal{D}).$$

Let $\mathcal{S}_n = \mathcal{S}(L, d, n)$ be the star having $n \geq 2$ identical edges, total length L and diameter d. Then there exists $n_0 \geq 1$ such that

$$\lambda_1(\mathcal{S}_n) \leq \lambda_1(\mathcal{H}) \tag{4.1}$$

for all $n \geq n_0$. Equality in (4.1) for some $n \geq 1$ implies that $L = d$ and $\mathcal{H}$ is a path graph (interval) of length d with a Dirichlet condition at one endpoint and a Neumann condition at the other.

We explicitly remark that $\mathcal{H}$ is itself allowed to be a star graph of the type we are considering; in this case, the lemma contains a proof of the statement that $\lambda_1(\mathcal{S}_n) < \lambda_1(\mathcal{S}_m)$ if $n > m$ is sufficiently large (where D and L are fixed).

Proof We may assume without loss of generality that $\mathcal{V}_\mathcal{D} = \{v_0\}$ consists of a single vertex of degree possibly larger than one, by formally gluing together all vertices in $\mathcal{V}_\mathcal{D}$ if necessary. Denote by ψ the eigenfunction of $\lambda_1(\mathcal{H})$, chosen positive, and let v be any point in $\mathcal{H}$ at which $\psi \in H^1(\mathcal{H}) \hookrightarrow C(\mathcal{H})$ reaches a global maximum in $\mathcal{H}$; we assume without loss of generality that v is a vertex.

By definition of d, there exists a path $\mathfrak{p}$ in $\mathcal{H}$ from v to v_0 which has no self-intersections and length at most d. Assume that $\mathcal{H}$ is itself not a path (i.e., not an interval), so that $\mathfrak{p} \neq \mathcal{H}$ and $|\mathfrak{p}| < L$. Fix $n_0 \geq 1$, to be specified precisely later, but large enough that $n_0 > \deg v$ and the shortest edge in $\mathcal{H}$ is longer than

$$\varepsilon := \frac{L - |\mathfrak{p}|}{n_0} > 0.$$

We let $\widetilde{\mathcal{S}}$ be the star having one edge of length $|\mathfrak{p}| - \varepsilon$ (equipped with a Dirichlet condition at the far end) and n shorter edges of length ε each: then by construction, $|\widetilde{\mathcal{S}}| = L$ and $\operatorname{diam}(\widetilde{\mathcal{S}}) = |\mathfrak{p}| \leq d$.

We claim that $\lambda_1(\widetilde{\mathcal{S}}) < \lambda_1(\mathcal{H})$; we will use the transplantation principle, Lemma 2.6, to prove this. The lemma will then follow from Lemma 3.5: more precisely, part (2) yields the inequality $\lambda_1(\mathcal{S}_{n_0}) \leq \lambda_1(\widetilde{\mathcal{S}})$, while part (1) yields $\lambda_1(\mathcal{S}_n) \leq \lambda_1(\mathcal{S}_{n_0})$ for $n \geq n_0$.

To prove the claim, we look at the value

$$m := \max\{\psi(x) : x \in \mathcal{H} \text{ and } \operatorname{dist}(x, v) = \varepsilon\} > 0.$$

We glue together all points $x \in \mathcal{H}$ such that $\psi(x) = m$ (of which there are only finitely many), to create a new vertex v_ε. In accordance with Lemma 2.1, this does not affect λ_1 or ψ, so in a slight abuse of notation we will call the new graph $\mathcal{H}$.

Now the set $\{\psi \geq m\} \subset \mathcal{H}$ consists of a *pumpkin* (collection of parallel edges) running from v_ε to v, such that each edge of this pumpkin has length at most ε; and v still lies on $\mathfrak{p}$ (or, more precisely, on its image under the gluing, which we will still denote by $\mathfrak{p}$). Note that the number of edges of this pumpkin is simply $\deg v < n_0$.

We now apply the transplantation lemma 2.6. We remove every edge of $\mathcal{H}$ not on $\mathfrak{p}$ and not part of the pumpkin between v_ε and v. In their place we first lengthen any edges between v_ε and v if necessary, so that each has exactly length ε. We then attach additional pendant edges each of length ε to v_ε until the new graph has total length L. (Note that the choice of ε and the fact that the pumpkin has fewer than n_0 edges means that there is always enough material being transplanted to guarantee that all these edges can be made to have length exactly ε.)

We finally de-glue (cut through) v to produce a graph having only pendant edges at v_ε. This graph is by construction $\widetilde{\mathcal{S}}$, and we have

$$\lambda_1(\widetilde{\mathcal{S}}) \leq \lambda_1(\mathcal{H}) \tag{4.2}$$

by Lemmata 2.1 (applied in reverse) and 2.6. But under the assumption that $\mathcal{H}$ was not a path graph, the transplantation was nontrivial and so Lemma 2.6 in fact yields strict inequality in (4.2). Combined with our earlier statements, this completes the proof. □

We can now give the proof of Theorem 1.1. In fact, in light of Proposition 1.4, more precisely, the fact that $\lambda_1(\mathcal{S}_n)$ forms a decreasing sequence in n, which converges to ω^2, it suffices to prove:

Theorem 4.2 *Suppose $\mathcal{G}$ is any, connected compact graph with a finite number of edges, and with total length $L > 0$ and diameter $D \in (0, L)$. Then there exists some $n \geq 1$ such that the star graph $\mathcal{S}_n$ having total length $L/2$ and diameter $D/2$ satisfies*

$$\lambda_1(\mathcal{S}_n) < \mu_2(\mathcal{G}).$$

Proof of Theorem 4.2, and hence of Theorem 1.1 Let ψ be any eigenfunction associated with $\mu_2(\mathcal{G})$ and denote by $\mathcal{G}^+$ and $\mathcal{G}^-$ any two nodal domains of ψ. Then, by Lemma 2.3,

$$\mu_2(\mathcal{G}) = \lambda_1(\mathcal{G}^+) = \lambda_1(\mathcal{G}^-)$$

(where the Dirichlet vertices correspond to the points where $\psi = 0$), and with $\psi|_{\mathcal{G}^\pm}$ being the corresponding eigenfunctions. Moreover, $|\mathcal{G}^+| + |\mathcal{G}^-| \leq L$ and, if

$$\begin{aligned} d^+ &:= \sup\{\mathrm{dist}(x, \mathcal{V}_{\mathcal{D}}(\mathcal{G}^+)) : x \in \mathcal{G}^+\} \\ &\equiv \sup\{\mathrm{dist}(x, \{\psi = 0\}) : x \in \mathcal{G}^+\} \\ d^- &:= \sup\{\mathrm{dist}(x, \mathcal{V}_{\mathcal{D}}(\mathcal{G}^-)) : x \in \mathcal{G}^-\} \end{aligned} \tag{4.3}$$

(where it makes no difference whether we take the distance in $\mathcal{G}$ or in $\mathcal{G}^\pm$), then, since the distance from any point in $\mathcal{G}^+$ to any point in $\mathcal{G}^-$ is at most $D = \mathrm{diam}(\mathcal{G})$, we have

$$d^+ + d^- \leq D.$$

By Lemma 4.1, there exist stars $\mathcal{S}_n^+$ and $\mathcal{S}_n^-$ (for some n sufficiently large, which is the same for both stars) with total lengths $|\mathcal{G}^+|$ and $|\mathcal{G}^-|$ and diameters d^+ and d^-, respectively, such that $\lambda_1(\mathcal{S}_n^\pm) \leq \lambda_1(\mathcal{G}^\pm)$. By Lemma 3.5(2) and (3), we may in fact assume without loss of generality that $|\mathcal{S}_n^+| + |\mathcal{S}_n^-| = L$ and $d^+ + d^- = D$ (possibly at the cost of making n larger). Now, by Lemma 3.7 (or by a direct application of Lemmata 2.4 and 3.6(2) to the union of $\mathcal{S}_n^+$ and $\mathcal{S}_n^-$), we conclude that

$$\mu_2(\mathcal{G}) \geq \max\{\lambda_1(\mathcal{S}_n^+), \lambda_1(\mathcal{S}_n^-)\} \geq \lambda_1(\mathcal{S}_n), \tag{4.4}$$

where $\mathcal{S}_n$ is now the star with length $L/2$ and diameter $D/2$.

It remains to prove that at least one inequality in (4.4) is strict. Since $D < L$ by assumption, $\mathcal{G}$ is not a path. Suppose first that at least one of its nodal domains $\mathcal{G}^\pm$

is also not a path. If neither is a path with one Dirichlet and one Neumann endpoint, then Lemma 4.1 already yields the strict inequality

$$\mu_2(\mathcal{G}) > \max\{\lambda_1(\mathcal{S}_n^+), \lambda_1(\mathcal{S}_n^-)\}.$$

If one is a path with one Dirichlet and one Neumann endpoint, say $\mathcal{G}^+$, then since the same is not true of $\mathcal{G}^-$, the star $\mathcal{S}_n^+$ is trivially equal to the path $\mathcal{G}^+$, while $\mathcal{S}_n^-$ is nontrivial (not a path). Since $\mathcal{S}_n^+ \neq \mathcal{S}_n^-$, Lemma 3.7 implies that the second inequality in (4.4) is strict.

Finally, we deal with the case where $\mathcal{G}$ is not a path but it only has nodal domains which are paths: in this case, we must have $|\mathcal{G}^+| + |\mathcal{G}^-| < L$ and hence $|\mathcal{S}_n^+| + |\mathcal{S}_n^-| < L$. Assuming $\mathcal{S}_n$ still to have length $L/2$, strict inequality in Lemma 3.5(3) leads to strict inequality in the second inequality in (4.4). □

We conclude with the proof of Theorem 1.2.

Proof of Theorem 1.2 Suppose first that $\mu_k(\mathcal{G})$ is simple and its eigenfunction ψ does not vanish identically on any edge of $\mathcal{G}$. Then by Lemma 2.5 ψ has $m \geq k - \beta$ nodal domains $\mathcal{G}_1, \ldots, \mathcal{G}_m$, which by Lemma 2.3 satisfy

$$\mu_k(\mathcal{G}) = \lambda_1(\mathcal{G}_1) = \ldots = \lambda_1(\mathcal{G}_m)$$

(with the Dirichlet vertices at the points where $\psi = 0$, and $\psi|_{\mathcal{G}_i}$ is, up to scalar multiples, the unique eigenfunction on $\mathcal{G}_i$, $i = 1, \ldots, m$. Note that

$$\sum_{i=1}^{m} |\mathcal{G}_i| = L$$

since ψ does not vanish identically on any edge. For each i, analogous to (4.3), set

$$d_i := \sup\{\mathrm{dist}(x, \mathcal{V}_{\mathcal{D}}(\mathcal{G}_j)) : x \in \mathcal{G}_i\};$$

then, as in the case $k = 2$, for each pair $i \neq j$, we have

$$d_i + d_j \leq D; \tag{4.5}$$

Fix $n \geq 1$ sufficiently large. Then by Lemma 4.1, for each i there exists a star $\mathcal{S}_n^i$ (as usual having n identical shorter sides and one longer Dirichlet side) such that $|S_n^i| = |\mathcal{G}_i|$, $\mathrm{diam}(\mathcal{S}_n^i) = d_i$, and $\mu_k(\mathcal{G}) \geq \lambda_1(\mathcal{S}_n^i)$.

Now choose any pair $i_1 \neq j_1$ and apply Lemma 3.7 to $S_n^{i_1}$ and $S_n^{j_1}$, replacing them with the resulting stars which have the same total length and whose sum of diameters is the same, but which have smaller eigenvalues. Now choose a different pair $(i_2, j_2) \neq (i_1, j_1)$ and repeat.

Repeating this process arbitrarily often and passing to the limit, the stars converge (and their eigenvalues converge from above) to m copies of the star $\mathcal{S}_n$ with total

length L/m and diameter no larger than $D/2$ (by (4.5)); by Lemma 3.5(2) we may assume without loss of generality that actually $\operatorname{diam}(\mathcal{S}_n) = D/2$; and by Lemma 3.7, we also have

$$\mu_k(\mathcal{G}) \geq \max\{\lambda_1(\mathcal{S}_n^1), \ldots, \lambda_1(\mathcal{S}_n^m)\} \geq \lambda_1(\mathcal{S}_n).$$

Since $m \geq k - \beta$ and, by Lemma 3.5(3), $\lambda_1(\mathcal{S}_n)$ is a decreasing function of increasing its length $L/m \mapsto L/(k-\beta)$ if its diameter $D/2$ is fixed (possibly at the cost of increasing n at the same time), we obtain the statement of the theorem under the assumption that $\mu_k(\mathcal{G})$ is simple and ψ does not vanish identically on any edge.

In the general case, we use a standard approximation argument. Let $\mathcal{G}$ be a connected, compact graph with a finite number of edges, such that $\mathcal{G}$ does not contain any loops longer than D. Firstly, if $\mathcal{G}$ does in fact contain any loops, we cut through the midpoint of each loop. Our assumption on the maximal loop length implies that this does not change either L or D and can only lower μ_k by Lemma 2.1. So we may assume without loss of generality that $\mathcal{G}$ does not contain any loops at all.

Now, by [13, Theorem 3.6], there exists a sequence of graphs $\mathcal{G}_i$ having the same topology as $\mathcal{G}$, such that all edge lengths of $\mathcal{G}_i$ converge to those of $\mathcal{G}$, meaning in particular that $D_i := \operatorname{diam}(\mathcal{G}_i) \to D$ and $L_i := |\mathcal{G}_i| \to L$; and, for each i, we have that $\mu_k(\mathcal{G}_i)$ is simple and its eigenfunction does not vanish identically on any edge of $\mathcal{G}_i$. Now $\mu_k(\mathcal{G}_i)$ satisfies the eigenvalue bound of Theorem 1.2 for all i (with L_i and D_i in place of L and D); but, since this bound depends smoothly on L and D, passing to the limit we obtain the desired bound for $\mathcal{G}$. □

5 Concluding Remarks

The idea of the proofs of Theorems 1.1 and 1.2 consists in comparing each of the nodal domains of a graph $\mathcal{G}$ (more precisely, the nodal domains of a given eigenfunction ψ associated with $\mu_k(\mathcal{G})$) with a corresponding star graph having the same total length and a possibly smaller diameter; this is the idea behind Lemma 4.1. To obtain the overall infimum, the balancing results of Sect. 3 show that the minimum over the m stars obtained from the m nodal domains of ψ is achieved when the stars all have the same total length (L/m each) and diameter ($D/2$ each). These copies can be pasted together at their respective Dirichlet vertices to form the graphs which, in the limit, converge to m-stars with point masses of size $L/m - D/2$ at each pendant vertex. The assumption that L be sufficiently large compared with D is, we believe, natural: it is necessary to ensure that these point masses actually have positive mass; in the borderline case where $L/m = D/2$, we obtain exactly the equilateral star which in accordance with (1.3) is minimising for $\mu_m(\mathcal{G})$ among all graphs $\mathcal{G}$ having given total length but without any constraint on the diameter.

The shortcoming in Theorem 1.2 is that in general we cannot expect that $m = k$, i.e., that the eigenfunction ψ have k nodal domains. Instead, we rely on the (sharp) lower bound $m \geq k - \beta$ in Lemma 2.5, which is also only valid "generically", that is, possibly after an arbitrarily small perturbation of the edge lengths, and for graphs without loops (in the presence of loops, there will always be special eigenfunctions supported on the loops, which cannot be eliminated by a perturbation argument).

In the case of trees, Lemma 2.5 and hence Theorem 1.2 is sharp; all we lose via the edge perturbation argument is the ability to conclude that the inequality is always strict, that is, that there is no actual tree whose eigenvalue is equal to the square of the solution of (1.7). (However, we strongly expect this conclusion to be true.)

For non-trees, we do not expect Theorem 1.2 to be sharp. Indeed, simple examples such as loops and tadpoles suggest that Theorem 1.2 should be true in a sharper form, namely without the presence of β and without the assumption that $\mathcal{G}$ not contain any long loops:

Conjecture 5.1 Let $\mathcal{G}$ be *any* connected, compact graph with total length L and diameter D, where $L/k > D/2$. Then $\mu_k(\mathcal{G})$ is strictly larger than the square of the smallest positive solution $\omega > 0$ of the equation

$$\cos\left(\frac{\omega D}{2}\right) = \omega\left(\frac{L}{k} - \frac{D}{2}\right)\sin\left(\frac{\omega D}{2}\right). \tag{5.1}$$

(Here, again, we see the necessity of the assumption $L/k > D/2$ in (5.1) in order for this result to make sense.)

In other contexts, such as the proof of (1.3) or the related [11, Theorem 4.7], one typically circumvents the problem of having too few nodal domains by first cutting through cycles in $\mathcal{G}$ to obtain a tree with the same total length, smaller eigenvalues (cf. Lemma 2.1), and (generically) the correct number of nodal domains. Here, this is generally impossible since by cutting through a cycle one may increase the total diameter (see Fig. 5 for an example). Actually, one only needs to guarantee the weaker property (4.5) of the nodal domains of the cut graph, but there seems no reasonable way to arrange this.

We therefore leave Conjecture 5.1 as an open problem; we also leave completely open the question of determining what happens when the assumption $L/k > D/2$ is not satisfied.

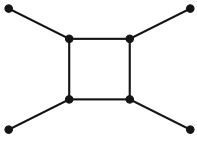

Fig. 5 An example of a graph with a cycle, such that cutting the cycle at any point would increase the diameter

Acknowledgments The work of the author was supported by the Fundação para a Ciência e a Tecnologia, Portugal, via the program "Investigador FCT", reference IF/01461/2015, and project PTDC/MAT-CAL/4334/2014, as well as by the Center for Interdisciplinary Research (ZiF) in Bielefeld, Germany, within the framework of the cooperation group on "Discrete and continuous models in the theory of networks". The author would like to extend his warmest thanks to Gregory Berkolaiko, Pavel Kurasov and Delio Mugnolo for innumerable discussions and much inspiration over the last few years, including in the context of the current work. He wishes to thank Delio Mugnolo in particular for pointing out an analogous result from the discrete literature (Proposition 1.7), Pavel Kurasov for helpful advice in the context of Proposition 1.4, and the anonymous referee for a number of constructive suggestions, including the encouragement to consider the case of the higher eigenvalues.

References

1. R. Adami, E. Serra and P. Tilli, *Negative energy ground states for the L^2-critical NLSE on metric graphs*, Comm. Math. Phys. **352** (2017), 387–406.
2. R. Adami, E. Serra, and P. Tilli, *Lack of ground state for NLSE on bridge-type graphs*, pp. 1–11 in D. Mugnolo (ed.), Mathematical Technology of Networks (Proc. Bielefeld 2013), volume 128 of *Proc. Math. & Stat.*, Springer, Cham, 2015.
3. R. Adami, E. Serra and P. Tilli, *NLS ground states on graphs*, Calc. Var. **54** (2015), 743–761.
4. M. Aizenman, H. Schanz, U. Smilansky, and S. Warzel, *Edge switching transformations of quantum graphs*, Acta Phys. Polon. A **132** (2017), 1699–1703.
5. W. Arendt, G. Metafune, D. Pallara, and S. Romanelli, *The Laplacian with Wentzell–Robin boundary conditions on spaces of continuous functions*, Semigroup Forum **67** (2003), 247–261.
6. S. Ariturk, *Eigenvalue estimates on quantum graphs*, preprint (2016), arXiv:1609.07471.
7. R. Band, G. Berkolaiko, H. Raz and U. Smilansky, *The number of nodal domains on quantum graphs as a stability index of graph partitions*, Comm. Math. Phys. **311** (2012), 815–832.
8. R. Band and G. Lévy, *Quantum graphs which optimize the spectral gap*, Ann. Henri Poincaré **18** (2017), 3269–3323.
9. G. Berkolaiko, *A lower bound for nodal count on discrete and metric graphs*, Comm. Math. Phys. **278** (2008), 803–819.
10. G. Berkolaiko, J. B. Kennedy, P. Kurasov and D. Mugnolo, *Surgery principles for the spectral analysis of quantum graphs*, Trans. Amer. Math. Soc. **372** (2019), 5153–5197.
11. G. Berkolaiko, J. B. Kennedy, P. Kurasov and D. Mugnolo, *Edge connectivity and the spectral gap of combinatorial and quantum graphs*, J. Phys. A: Math. Theor. **50** (2017), 365201.
12. G. Berkolaiko and P. Kuchment, *Introduction to quantum graphs*. Math. Surveys and Monographs vol. 186, American Mathematical Society, Providence, RI, 2013.
13. G. Berkolaiko and W. Liu, *Simplicity of eigenvalues and non-vanishing of eigenfunctions of a quantum graph*, J. Math. Anal. Appl. **445** (2017), 803–818.
14. V. Bonnaillie-Noël and B. Helffer, *Nodal and spectral minimal partitions – the state of the art in 2016*, Chapter 10 in A. Henrot (ed.), *Shape optimization and spectral theory*, De Gruyter Open, Warsaw-Berlin, 2017.
15. Y. Colin de Verdière, *Semi-classical measures on quantum graphs and the Gauß map of the determinant manifold*, Ann. Henri Poincaré **16** (2015), 347–364.
16. S. Dovetta, *Existence of infinitely many stationary solutions of the L^2-subcritical and critical NLSE on compact metric graphs*, J. Differential Equations **264** (2018), 4806–4821.
17. S. Fallat and S. Kirkland, *Extremizing algebraic connectivity subject to graph theoretic constraints*, Electron. J. Linear Algebra **3** (1998), 48–74.
18. L. Friedlander, *Extremal properties of eigenvalues for a metric graph*, Ann. Inst. Fourier (Grenoble) **55** (2005), 199–211.

19. L. Friedlander, *Genericity of simple eigenvalues for a metric graph*, Israel J. Math. **146** (2005), 149–156.
20. S. Gnutzmann and U. Smilansky, *Quantum graphs: Applications to quantum chaos and universal spectral statistics*, Adv. Phys. **55** (2006), 527–625.
21. A. Henrot (ed.), *Shape optimization and spectral theory*, De Gruyter Open, Warsaw-Berlin, 2017.
22. A. Henrot, *Minimization problems for eigenvalues of the Laplacian*, J. Evol. Equ. **3** (2003), 443–461.
23. J. B. Kennedy, P. Kurasov, C. Lena and D. Mugnolo, *A theory of spectral partitions of metric graphs*, preprint (2020), arXiv:2005.01126.
24. J. B. Kennedy, P. Kurasov, G. Malenová and D. Mugnolo, *On the spectral gap of a quantum graph*, Ann. Henri Poincaré **17** (2016), 2439–2473.
25. J. B. Kennedy and D. Mugnolo, *The Cheeger constant of a quantum graph*, Conference proceedings of the joint 87th annual meeting of the GAMM and Deutsche Mathematiker-Vereinigung, PAMM **16** (2016), 875–876.
26. P. Kurasov and S. Naboko, *Rayleigh estimates for differential operators on graphs*, J. Spectr. Theory **4** (2014), 211–219.
27. P. Kurasov, G. Malenová, and S. Naboko, *Spectral gap for quantum graphs and their edge connectivity*, J. Phys. A: Math. Theor. **46** (2013), 275309.
28. D. Lenz, M. Schmidt and P. Stollmann, *Topological Poincaré type inequalities and bounds on the infimum of the spectrum for graphs*, preprint (2018), arXiv:1801.09279.
29. B. Mohar, *Eigenvalues, diameter, and mean distance in graphs*, Graphs Combin. **7** (1991), 53–64.
30. D. Mugnolo, *Semigroup Methods for Evolution Equations on Networks*, Springer-Verlag, Berlin 2014.
31. D. Mugnolo and S. Romanelli, *Dynamic and generalized Wentzell node conditions for network equations*, Math. Meth. Appl. Sci. **30** (2007), 681–706.
32. S. Nicaise, *Spectre des réseaux topologiques finis*, Bull. Sci. Math. (2) **111** (1987), 401–413.
33. L. E. Payne, *Isoperimetric inequalities and their applications*, SIAM Rev. **9** (1967), 453–488.
34. L. M. Del Pezzo and J. D. Rossi, *The first eigenvalue of the p-Laplacian on quantum graphs*, Anal. Math. Phys. **6** (2016), 365–391.
35. J. Rohleder, *Eigenvalue estimates for the Laplacian on a metric tree*, Proc. Amer. Math. Soc. **145** (2017), 2119–2129.
36. J. Rohleder and C. Seifert, *Spectral monotonicity for Schrödinger operators on metric graphs*, to appear in F. M. Atay et al. (eds.), Discrete and Continuous Models in the Theory of Networks, Operator Theory: Advances and Applications 281, preprint arXiv:1804.01827.

Missing-Level Statistics in Chaotic Microwave Networks Versus Level Statistics of Partially Chaotic Systems

Michał Ławniczak, Małgorzata Białous, Vitalii Yunko, Szymon Bauch, and Leszek Sirko

Abstract We present experimental and numerical studies of level statistics in incomplete spectra obtained with fully connected microwave networks simulating quantum chaotic graphs with preserved time reversal symmetry. We demonstrate that, if resonance frequencies are randomly removed from the spectra, the experimental results for the short-range and long-range spectral fluctuations are in good agreement with theoretical predictions of the missing-level statistics for the systems with preserved time reversal symmetry. The same behavior of the short-range spectral fluctuations, e.g., the nearest-neighbor spacing distribution and the integrated nearest-neighbor spacing distribution may be also observed for complete spectra in partially chaotic systems. Using the Rosenzweig-Porter model which interpolates between the chaotic and regular behavior we demonstrate that in a such case the long-range spectral fluctuations differ significantly from the ones predicted by the missing-level statistics.

Keywords 05.40.-a · 05.45.Mt · 05.45.Tp · 03.65.Sq

1 Introduction

The theory of quantum chaotic systems [1–3] have accounted for better understanding of experimental results obtained in real physical systems in the presence of dissipation, openness and missing energy levels. In accordance with the Bohigas-Giannoni-Schmit (BGS) conjecture [4] it was established that the fluctuations in the spectra of quantum chaotic systems coincide with those of the eigenvalues of random matrices [5] from the Gaussian orthogonal ensemble (GOE) and the Gaussian unitary ensemble (GUE) for classically chaotic systems with and without time-reversal symmetry (TRS). For quantum systems with classically regular

M. Ławnicza (✉) · M. Białous · V. Yunko · S. Bauch · L. Sirko
Institute of Physics, Polish Academy of Sciences, Warsaw, Poland
e-mail: lawni@ifpan.edu.pl

F. M. Atay et al. (eds.), *Discrete and Continuous Models in the Theory of Networks*, Operator Theory: Advances and Applications 281,
https://doi.org/10.1007/978-3-030-44097-8_12

dynamics the energy levels behave as if they were drawn from a Poissonian random process [6].

A large number of theoretical and numerical studies devoted to the problems of quantum and wave chaos have been performed so far, yet not all non-generic features in the spectra of the real physical systems are fully understood. Experimental approaches to understanding of the unsolved problems are feasible with microwave cavities simulating two-dimensional (2D) quantum billiards [7–14] and one-dimensional (1D) microwave networks simulating quantum graphs [15–19], respectively. It is possible because of the formal analogies between the scalar Helmholtz equation and the Telegraph equation and the two- and one-dimensional Schrödinger equations, respectively. One should point out that the introduction of one-dimensional microwave networks simulating quantum graphs extended considerably the knowledge on quantum chaotic systems. The other systems which lead to deeper understanding of chaotic systems include Rydberg atoms strongly driven by microwave fields [20–26].

It should be noticed that wave chaos can be also studied using three-dimensional (3D) microwave cavities [27]. However, in this case there is no direct analogy between the 3D vectorial Helmholtz equation and the Schrödinger equation.

Quantum graphs were introduced by Linus Pauling [28] more than eighty years ago. They provide a very useful tool for modelling many different systems, eg., quantum wires [29], optical waveguides [30] and mesoscopic quantum systems [31, 32]. Quantum graphs consist of vertices connected by 1D bonds (edges). For graphs with bonds of incommensurable lengths the BGS conjecture was proven rigourously [33, 34]. This was also confirmed experimentally with help of microwave networks [15, 16, 35–40].

In order to perform statistical analysis of the spectral properties of quantum systems the complete sequences of eigenvalues belonging to the same symmetry class are indispensable [4, 41]. Recently, a new, effective procedure to obtain information on the degree of chaoticity of a classical system from the spectral properties of the corresponding quantum system was developed for incomplete sequences of levels [42–44]. Incomplete spectra pose major problems in real physical systems like, e.g., nuclei and molecules [45–48], which have to be overcome, so such procedures are indispensable [49, 50]. The effect of missing levels is particularly large for long-range spectral fluctuations. R. A. Molina et. al. demonstrated numerically [51] that the power spectrum [52–56] is a powerful statistical measure to discriminate between deviations caused by missing levels and by the mixing of symmetries.

In this paper we present a numerical analysis of missing level statistics for quantum systems with preserved time reversal symmetry. In the analysis we use as basis incomplete experimental spectra obtained with fully connected six-vertex microwave network where, additionally, some resonance frequencies were randomly removed. Moreover, we show that the same behavior of the short-range spectral correlations as observed in the case of incomplete spectra may be observed for complete spectra in partially chaotic systems. Using the Rosenzweig-Porter model which interpolates between the GOE and Poisson behavior we demonstrate

that in a such situation the long-range correlation functions differ significantly from the ones predicted by the missing-level statistics.

2 Experimental Setup and Measurements

In order to perform one-port measurements of the scattering matrix S_{11} we used the experimental setup consisting of the Agilent E8364B vector network analyzer (VNA) and a microwave network connected to the VNA via the HP 85133-616 microwave flexible cable, see Fig. 1. Quantum graphs with TRS are simulated experimentally by networks of coaxial cables coupled by junctions at vertices. The coaxial cables (SMA-RG402) consist of an outer concentric conductor of inner radius $r_2 = 0.15$ cm, which surrounds dielectric material (Teflon) and an inner conductor of radius $r_1 = 0.05$ cm. The dielectric constant of Teflon obtained from the measurements is $\varepsilon \simeq 2.06$. The cut-off frequency of the TE_{11} mode below which only the fundamental TEM can propagate in the cable is $\nu_c \simeq \frac{c}{\pi(r_1+r_2)\sqrt{\varepsilon}} \simeq 33$ GHz [15, 57]. In the experiment we used fully connected, six-vertex microwave networks which were composed of fifteen bonds (coaxial cables), four phase shifters, five five-arm joints and one six-arm joint connected to the VNA via a flexible microwave cable. The geometric lengths of the four bonds was varied with phase shifters (Advanced Technical Materials PNR P1507D) to obtain 10 different realizations of networks. On should point out that not the geometric lengths L_i but the optical length $L_i^{opt} = L_i\sqrt{\varepsilon}$, of the microwave cables yield the lengths of the bonds in the corresponding quantum graph. The total optical length of the networks $L^{opt} = \sum_{i=1}^{15} L_i^{opt} \simeq 7.04 \pm 0.02$ m was kept constant.

The scattering matrix S_{11} of the networks was measured in the frequency window 1.0–5.7 GHz. Figure 2 shows an example of the measured reflection spectrum in the frequency window: 4.0–5.0 GHz. According to the Weyl's formula given in [17] $\overline{N} = 2L^{opt}\nu/c$, where c is the speed of light in the vacuum and ν is microwave frequency, about 220 resonances should be measured in the frequency range 1–5.8 GHz. However, we found that on average, in all 10 network realizations, about 3.5% of resonances were not detected, giving the fraction of observed resonances (levels) $\varphi = 0.965 \pm 0.005$ [50]. There are two main reasons for missing resonances in microwave networks: overlapping with other resonances, which increases with frequency and their small amplitudes. Despite of that the experiments with microwave networks provide a unique chance for getting almost complete sequences of resonance frequencies.

Before starting with the analysis of spectral properties, the resonance frequencies need to be rescaled (unfolded) to eliminate system specific properties like the total optical length L^{opt} of the graph. This is done using Weyl's formula. The unfolded eigenvalues determined from the resonance frequencies are given by $\epsilon_i = 2L^{opt}\nu_i/c$.

Fig. 1 The six-vertex microwave network containing four phase shifters. The connection to a vector network analyzer (VNA) is shown with the arrow

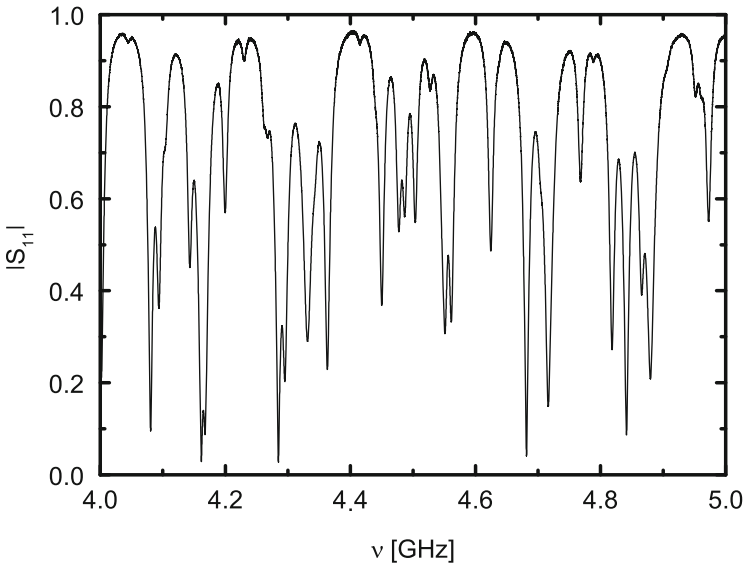

Fig. 2 An example of the reflection spectra $|S_{11}|$ measured for a microwave network in the frequency range: 4.0–5.0 GHz

To test more comprehensively the missing level statistics we generated new data series from the experimental spectra by randomly removing from them resonance frequencies, yielding sequences with the fraction of observed levels $\varphi = 0.81 \pm 0.01$. The random removal of resonance frequencies was achieved with a Matlab random number generator. These new data were rescaled to the mean spacing unity [50] of adjacent resonance frequencies.

The most common measure of the short-range spectral correlations is the nearest-neighbor spacing distribution NNSD describing the distribution of the spacings between adjacent eigenvalues $s_i = \epsilon_{i+1} - \epsilon_i$ in terms of their mean value $\langle s \rangle$ and the integrated nearest-neighbor spacing distribution INNSD. For long-range spectral correlations we present the spectral rigidity $\Delta_3(L)$ which corresponds to the least square deviation of the integrated spectral density of the unfolded ϵ_i from the straight line being the best fit of it in an interval of length L. We also consider the power spectrum, i.e., the square modulus of the Fourier transform of the deviation $\delta_q = \epsilon_{q+1} - \epsilon_1 - q$ of the spacing between an eigenvalue and its $(q+1)$st nearest neighbor from its average value q.

3 Missing Level Statistics

In the experimental investigations [47–49] the completeness of energy spectra is a rare situation. The problem of missing levels can be circumvented in open systems by using the scattering matrix formalism. The fluctuation properties of the scattering matrix elements provide sensitive measures for the chaoticity, e.g., in terms of Wigner reaction matrix, the enhancement factor [14, 16, 58] or their correlation functions [59, 60].

For closed or weakly open systems analytical expressions were derived for incomplete spectra based on RMT in Ref. [50]. The fraction of observed resonances is characterized by the parameter φ, where $0 < \varphi \leq 1$. For such systems the nearest-neighbor spacing distribution $p(s)$ can be expressed in terms of the $(n+1)$st nearest-neighbor spacing distribution $P(n, \frac{s}{\varphi})$

$$p(s) = \sum_{n=0}^{\infty} (1-\varphi)^n P(n, \frac{s}{\varphi}). \tag{1}$$

For the GOE systems the first term in Eq. (1) is approximated by

$$P(0, \frac{s}{\varphi}) = \frac{\pi}{2} \frac{s}{\varphi} \exp\left[-\frac{\pi}{4} \left(\frac{s}{\varphi} \right)^2 \right]. \tag{2}$$

In the case of complete sequences, $\varphi = 1$, $P(0, s)$ reduces to the Wigner surmise formula for the NNSD.

The second term $P(1, \frac{s}{\varphi})$ is defined by the formula

$$P(1, \frac{s}{\varphi}) = \frac{8}{3\pi^3}\left(\frac{4}{3}\right)^5\left(\frac{s}{\varphi}\right)^4 \exp\left[-\frac{16}{9\pi}\left(\frac{s}{\varphi}\right)^2\right]. \tag{3}$$

For the complete spectra, $\varphi = 1$, $P(1, s)$ gives the NNSD of the symplectic ensemble with $\langle s\rangle = 2$.

The higher spacing distributions $P(n, \frac{s}{\varphi})$ for $n = 2, 3, \ldots$ are well approximated by their Gaussian asymptotic forms, centered at $n + 1$

$$P(n, \frac{s}{\varphi}) = \frac{1}{\sqrt{2\pi V^2(n)}} \exp\left[-\frac{(\frac{s}{\varphi} - n - 1)^2}{2V^2(n)}\right], \tag{4}$$

with the variances

$$V^2(n) \simeq \Sigma^2(L = n) - \frac{1}{6}. \tag{5}$$

The number variance $\Sigma^2(L)$ in the Eq. (5) is the variance of the number of levels contained in an interval of length L [5].

The integrated nearest-neighbor spacing distribution $I(s)$ plays also an important role in the spectral analysis of the experimental data. It is used to distinguish between the systems possessing or lacking time-reversal symmetry, e.g., described by the GOE and GUE ones, where the sensitive dependence of $I(s)$ at small level separations s is important.

$$I(s) = \int_0^s p(s')ds'. \tag{6}$$

The spectral rigidity $\Delta_3(L)$ is a measure of the long-range fluctuation properties in the spectra. In the presence of missing levels [50] the spectral rigidity $\delta_3(L)$ may be expressed in terms of those for the complete spectra $\Delta_3(L)$,

$$\delta_3(L) = (1 - \varphi)\frac{L}{15} + \varphi^2\Delta_3\left(\frac{L}{\varphi}\right). \tag{7}$$

The results obtained for the discussed above measures are presented in Fig. 3. The NNSD, the INNSD and the spectral rigidity are displayed in the panels (a), (b) and (c) respectively. The results obtained for the NNSD after removing certain number of resonances from the experimental spectra to achieve $\varphi = 0.81 \pm 0.01$, respectively, are presented by the histogram (black in color). In the preparation of the histogram about 1780 eigenvalues from all 10 network realizations were taken into account. The results were obtained by averaging the statistical measures obtained for the individual networks. The red dash-dot, black solid and broken lines

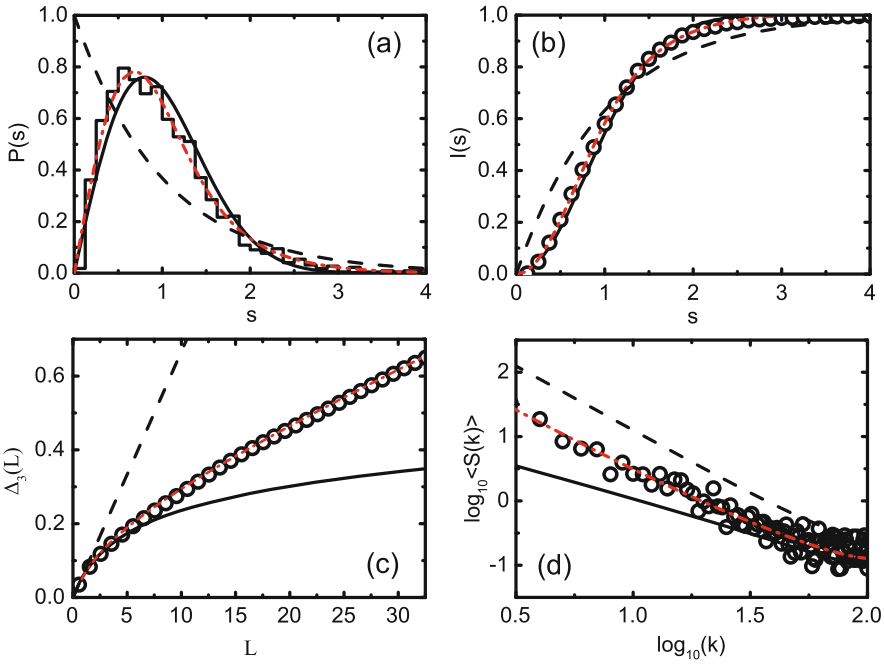

Fig. 3 The nearest-neighbor spacing distribution, the integrated nearest-neighbor spacing distribution, the spectral rigidity, and the average power spectrum for $\varphi = 0.81 \pm 0.01$ are shown in the panels (**a**), (**b**), (**c**), and (**d**) respectively. The modified experimental data are denoted by bars in the panel (**a**) and by empty circles in the panels (**b**), (**c**) and (**d**). They are compared with the results calculated from the Eqs. (1), (6), (7), and (9), respectively, for the fraction of observed levels $\varphi = 0.81 \pm 0.01$ (red dash-dot lines). The RMT prediction for GOE for $\varphi = 1$ and Poisson distribution are denoted by black solid and broken lines, respectively

denote the theoretical results based on random matrix theory (RMT) for incomplete $\varphi = 0.81$, complete $\varphi = 1$ series and Poisson distribution, respectively.

4 Power Spectrum of Levels Fluctuations

The power spectrum $P(k) = |\tilde{\delta}_k|^2$ is the Fourier transform of $\delta_q = \epsilon_{i+q} - \epsilon_i - q$ from "time" q to k for the sequence of N levels

$$\tilde{\delta}_k = \frac{1}{\sqrt{N}} \sum_{q=0}^{N-1} \delta_q \exp\left(-\frac{2\pi i k q}{N}\right). \tag{8}$$

when considering a sequence of N levels. It was shown in Refs. [52, 53], that for $\tilde{k} = k/N \ll 1$ the power spectrum of levels fluctuations for complete level sequences

exhibits a power law dependence $\langle S(\tilde{k})\rangle \propto (\tilde{k})^{-\alpha}$. Here, for regular systems $\alpha = 2$ and for chaotic ones $\alpha = 1$ regardless whether time reversal symmetry is preserved or not. The power spectrum and the power law behavior were studied numerically in Refs. [54, 61–63] and experimentally in microwave billiards in Refs. [42, 55]. It was also successfully applied to the measured molecular resonances in ^{166}Er and ^{168}Er [46].

It is important to point out that in practice a priori knowledge about the fraction of observed levels φ is not always possible. Therefore, additionally to the discussed above spectral rigidity of the spectrum other sensitive tests of missing levels are of great value. It was demonstrated in Refs. [42, 43] that the power spectrum of levels fluctuations can be used as such a remarkably sensitive measure. An analytical expression for the power spectrum of levels fluctuations in the case of incomplete spectra is given in Ref. [51],

$$\langle s(\tilde{k})\rangle = \frac{\varphi}{4\pi^2}\left[\frac{K\left(\varphi\tilde{k}\right)-1}{\tilde{k}^2} + \frac{K\left(\varphi\left(1-\tilde{k}\right)\right)-1}{(1-\tilde{k})^2}\right] + \frac{1}{4\sin^2(\pi\tilde{k})} - \frac{\varphi^2}{12}, \tag{9}$$

which for $\varphi = 1$ yields the formula for complete spectra $\langle S(\tilde{k})\rangle$ [52, 53]. Here, $0 \leq \tilde{k} \leq 1$ and $K(\tau)$ is the spectral form factor, which equals $K(\tau) = 2\tau - \tau\log(1+2\tau)$ for the GOE systems.

The average power spectrum $\langle s(\tilde{k})\rangle$ for the fraction of observed levels $\varphi = 0.81 \pm 0.01$ is shown with empty circles in the panel (d) in Fig. 3. The RMT prediction for GOE for the fraction of observed levels $\varphi = 0.81$, calculated from the Eq. (9), $\varphi = 1$, and Poisson distribution are denoted by red dash-dot, black solid, and broken lines, respectively. One should point out that the power spectrum obtained for the incomplete experimental spectra of networks with broken TRS are presented in Refs. [42, 44].

The inspection of the results presented in Fig. 3 reveals that for all measures, namely for the nearest-neighbor spacing distribution, the integrated nearest-neighbor spacing distribution, the spectral rigidity and the power spectrum, the experimental results are in good agreement with the RMT prediction for GOE.

5 Transition between GOE and Poisson Behavior: Rosenzweig-Porter Model

We would like to point out that the NNSD obtained for the incomplete spectra (missing-level statistics) may be very similar to the one calculated for the complete spectra in partially chaotic systems. To analyze such a situation we applied the

Rosenzweig-Porter random matrix model [64] which is often used to describe the transition between GOE and Poisson behavior. We show that even in the case of good agreement of the short-range correlation functions obtained in the Rosenzweig-Porter model with the experimental and theoretical short-range missing-level correlations, the long-range correlation functions obtained in this model differ significantly from the ones predicted by the experiment and the missing-level statistics. The Rosenzweig-Porter random-matrix model depends on a parameter κ. It interpolates between random matrix ensembles, GOE for $\kappa = N$ and Poisson for $\kappa = 0$, with N denoting the dimension of the random matrices $\hat{H}$ with matrix elements

$$\hat{H}_{ij} = \hat{G}_{ij}\left[\delta_{ij} + \frac{\kappa}{N}(1 - \delta_{ij})\right],\ i, j = 1, \ldots., N. \tag{10}$$

Here, the quantities $\hat{G}_{ij}$ denote the entries of a real symmetric matrix from the GOE. The parameter κ is defined in such a way that it does not depend on the dimension N of $\hat{H}$. We determined the value of $\kappa = 4.35 \pm 0.55$ by fitting the NNSD from the Rosenzweig-Porter model to the experimental one obtained for the fraction of observed levels $\varphi = 0.81 \pm 0.01$. In the calculations we generated ensembles of 99 random matrices with dimensions $N = 1000$. In the unfolding procedure we used the polynomial of the fifth order.

In the panels (a) and (b) in Fig. 4 we compare the results for the NNSD (bars) and the INNSD (empty circles) based on the Rosenzweig-Porter model (Eq. (10)) with the results obtained from the RMT calculations for $\varphi = 0.81 \pm 0.01$, $\varphi = 1$, and Poisson distribution, which are denoted by red dash-dot, black solid, and broken lines, respectively. One can easily see very good agreement between the results based on the Rosenzweig-Porter model and the missing level statistics with $\varphi = 0.81 \pm 0.01$. We would like to point out that missing-level statistics are in very good agreement with the experimental data presented in Fig. 3. In the panels (c) and (d) in Fig. 4 we show the δ_3 statistic and the power spectrum obtained from the Rosenzweig-Porter calculations (empty circles) with the parameter $\kappa = 4.35 \pm 0.55$. In both cases the Rosenzweig-Porter model fails to reproduce the experimental long-range correlations obtained for $\varphi = 0.81 \pm 0.01$. In the case of the δ_3 statistic the departure towards Poisson distribution is seen for $L > 25$. The power spectrum is especially sensitive on the value of the parameter k. For $\log(k) < 1.0$ the results based on the Rosenzweig-Porter model are already very close to Poisson distribution.

6 Conclusions

We compared the the short-range and long-range correlations calculated for incomplete experimental spectra of the six-vertex microwave networks with preserved time reversal symmetry with the fraction of observed levels $\varphi = 0.81 \pm 0.01$ to the

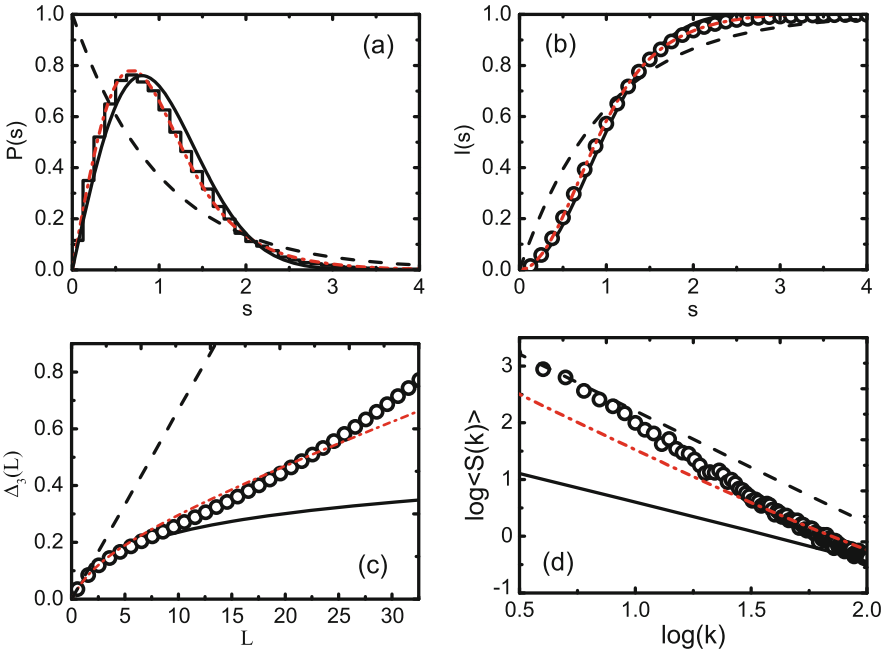

Fig. 4 The nearest-neighbor spacing distribution, the integrated nearest-neighbor spacing distribution, the spectral rigidity, and the average power spectrum calculated in the Rosenzweig-Porter model (Eq. (9)) with $k = 4.35 \pm 0.55$ are shown in the panels (**a**), (**b**), (**c**), and (**d**), respectively. The Rosenzweig-Porter model data are denoted by bars in the panel (**a**) and by empty circles in the panels (**b**), (**c**), and (**d**). The RMT prediction for GOE for the fraction of observed levels $\varphi = 0.81 \pm 0.01$, $\varphi = 1$, and for Poisson distribution are denoted by red dash-dot, black solid, and broken lines, respectively

respective analytical formulas for missing-level statistics. The agreement between the modified experimental data (randomly removed levels) and the analytical formulas for all discussed statistical measures are good or very good which clearly shows the power of missing-level statistics. Using the Rosenzweig-Porter model (Eq. (9)) we show that the same behavior of the short-range correlations may be observed for complete spectra in partially chaotic systems. However, the Rosenzweig-Porter model fails to reproduce the experimental long-range correlations such as the spectral rigidity and the power spectrum. This property of the Rosenzweig-Porter model may be used as a tool for distinguishing between the chaotic systems with the incomplete spectra and the partially chaotic ones with the complete spectra.

This work was partially supported by the National Science Centre, Poland, grant UMO-2016/23/B/ST2/03979.

References

1. J. M. G. Gómez, K. Kar, V. K. B. Kota, R. A. Molina, A. Relaño, and J. Retamosa, (doi.org/10.1016/j.physrep.2010.11.003.) Phys. Rep. **499**, 103 (2011).
2. H. A. Weidenmüller and G. E. Mitchell, (doi.org/10.1103/RevModPhys.81.539) Rev. Mod. Phys. **81**, 539 (2009).
3. F. Haake, (ISBN 3-540-67723-2) *Quantum Signatures of Chaos* (Springer-Verlag, Heidelberg, 2001).
4. O. Bohigas, M. J. Giannoni, and C. Schmit, (doi.org/10.1103/PhysRevLett.52.1) Phys. Rev. Lett. **52**, 1 (1984).
5. M. L. Mehta, (ISBN 0124880517) *Random Matrices* (Academic Press, London, 1990).
6. M.V. Berry and M. Tabor, (10.1098/rspa.1977.0140) Proc. R. Soc. A **356**, 375 (1977).
7. L. Sirko, P.M. Koch, and R. Blümel, (doi:10.1103/PhysRevLett.78.2940) Phys. Rev. Lett. **78**, 2940 (1997).
8. H.-J. Stöckmann, (ISBN-10 0521027152) *Quantum Chaos: An Introduction* (Cambridge University Press, Cambridge, 2000).
9. Y. Hlushchuk, A. Błędowski, N. Savytskyy, L. Sirko, (PACS Ref: 05.45.Mt) Physica Scripta **64**, 192 (2001).
10. R. Blümel, P.M. Koch, L. Sirko, (doi:10.1023/A:1017590503566) Found. Phys. **31**, 269 (2001).
11. N. Savytskyy, A. Kohler, S. Bauch, R. Blümel, and L. Sirko, (doi.org/10.1103/PhysRevE.64.036211) Phys. Rev. E **64**, 036211 (2001).
12. S. Hemmady, X. Zheng, E. Ott, T. M. Antonsen and S. M. Anlage, (doi.org/10.1103/PhysRevLett.94.014102) Phys. Rev. Lett. **94**, 014102 (2005).
13. B. Dietz and A. Richter, (doi.org/10.1063/1.4915527) CHAOS **25**, 097601 (2015).
14. M. Ławniczak, M. Białous, V. Yunko, S. Bauch, and L. Sirko, (doi.org/10.1103/PhysRevE.91.032925) Phys. Rev. E **91**, 032925 (2015).
15. O. Hul, S. Bauch, P. Pakoński, N. Savytskyy, K. Życzkowski, and L. Sirko, (doi:10.1103/PhysRevE.69.056205) Phys. Rev. E **69**, 056205 (2004).
16. M. Ławniczak, S. Bauch, O. Hul, and L. Sirko, (doi:10.1103/PhysRevE.81.046204) Phys. Rev. E **81**, 046204 (2010).
17. T. Kottos, U. Smilansky, (doi.org/10.1103/PhysRevLett.79.4794) Phys. Rev. Lett. **79**, 4794 (1997).
18. T. Kottos, U. Smilansky, (doi.org/10.1006/aphy.1999.5904) Ann. Phys. **274**, 76 (1999).
19. P. Pakoński, K. Życzkowski, M. Kuś (PACS numbers: 04.45.Mt, 02.10.Yn) J. Phys. A **34** 9303 (2001).
20. R. Blümel, A. Buchleitner, R. Graham, L. Sirko, U. Smilansky, and H. Walther, (doi.org/10.1103/PhysRevA.44.4521) Phys. Rev. A **44**, 4521 (1991).
21. M. Bellermann, T. Bergemann, A. Haffmann, P. M. Koch, and L. Sirko, (doi:10.1103/PhysRevA.46.5836) Phys. Rev. A **46**, 5836 (1992).
22. L. Sirko, S. Yoakum, A. Haffmans, and P. M. Koch, (doi:10.1103/PhysRevA.47.R782) Phys. Rev. A **47**, R782 (1993).
23. L. Sirko and P. M. Koch, Appl. Phys. B **60**, S195 (1995)
24. L. Sirko, A. Haffmans, M. R. W. Bellermann, and P. M. Koch, (doi:10.1209/epl/i1996-00318-5) Europhysics Letters **33**, 181 (1996).
25. L. Sirko, S.A. Zelazny, and P. M. Koch, (doi.org/10.1103/PhysRevLett.87.043002) Phys. Rev. Lett. **87**, 043002 (2001).
26. L. Sirko and P. M. Koch, (doi:10.1103/PhysRevLett.89.274101) Phys. Rev. Lett. **89**, 274101 (2002).
27. S. Deus, P. M. Koch, and L. Sirko, (doi.org/10.1103/PhysRevE.52.1146) Phys. Rev. E **52**, 1146 (1995).
28. L. J. Pauling, Chem. Phys. **4**, 673 (1936).
29. J. A. Sanchez-Gil, V. Freilikher, I. Yurkevich, and A. A. Maradudin, Phys. Rev. Lett. **80**, 948 (1998).

30. R. Mittra, S. W. Lee, (ASIN: B0006C0E1M) *Analytical Techniques in the Theory of Guided Waves* (Macmillan, NY, 1971).
31. D. Kowal, U. Sivan, O. Entin-Wohlman, and Y. Imry, (doi.org/10.1103/PhysRevB.42.9009) Phys. Rev. B **42**, 9009 (1990).
32. Y. Imry, *Introduction to Mesoscopic Physics* (Oxford, NY, 1996).
33. S. Gnutzmann and A. Altland, (DOI:10.1103/PhysRevLett.93.194101) Phys. Rev. Lett. **93**, 194101 (2004).
34. Z. Pluhař and H. A. Weidenmüller, (doi.org/10.1103/PhysRevLett.112.144102) Phys. Rev. Lett. **12**, 144102 (2014).
35. M. Ławniczak, O. Hul, S. Bauch, P. Seba, and L. Sirko, (doi.org/10.1103/PhysRevE.77.056210) Phys. Rev. E **77**, 056210 (2008).
36. M. Ławniczak, S. Bauch, O. Hul, and L. Sirko, (doi: 10.1088/0031-8949/2011/T143/014014) Phys. Scr. **T143**, 014014 (2011).
37. O. Hul, M. Ławniczak, S. Bauch, A. Sawicki, M. Kuś, L. Sirko, (doi.org/10.1103/PhysRevLett.109.040402) Phys. Rev. Lett **109**, 040402 (2012).
38. M. Ławniczak, A. Sawicki, S. Bauch, M. Kuś, and L. Sirko, (doi:10.1103/PhysRevE.89.032911) Phys. Rev E **89,** 032911 (2014).
39. M. Allgaier, S. Gehler, S. Barkhofen, H.-J. Stöckmann, and U. Kuhl, (doi:10.1103/PhysRevE.89.022925) Phys. Rev. E **89**, 022925 (2014).
40. M. Ławniczak, S. Bauch, and L. Sirko, in (ISBN-10: 1466590432) *Handbook of Applications of Chaos Theory*, eds. Christos Skiadas and Charilaos Skiadas (CRC Press, Boca Raton, USA, 2016), p. 559.
41. O. Bohigas, R. U. Haq, and A. Pandey, (doi.org/10.1007/978-94-009-7099-1-179) in *Nuclear Data for Science and Technology*, ed. by K. H. Böckhoff (Reidel, Dordrecht, 1983).
42. M. Białous, V. Yunko, S. Bauch, M. Ławniczak, B. Dietz, and L. Sirko, (DOI:10.1103/PhysRevLett.117.144101) Phys. Rev. Lett. **117**, 144101 (2016).
43. B. Dietz, V. Yunko, M. Białous, S. Bauch, M. Ławniczak, and L. Sirko, (doi.org/10.1103/PhysRevE.95.052202) Phys. Rev. E **95**, 052202 (2017).
44. M. Ławniczak, M. Białous, V. Yunko, S. Bauch, B. Dietz, and L. Sirko, Acta Phys. Pol. A **132**, 1672 (2017).
45. A. Frisch, M. Mark, K. Aikawa, F. Ferlaino, J. Bohn, C. Makrides, A. Petrov, and S. Kotochigova, (DOI:10.1038/nature13137) Nature (London) **507**, 475 (2014).
46. J. Mur-Petit and R. A. Molina, (DOI:10.1103/PhysRevE.92.042906) Phys. Rev. E **92**, 042906 (2015).
47. H. I. Liou, H. S. Camarda, and F. Rahn, Phys. Rev. C **5**, 1002 (1972).
48. T. Zimmermann, H. Köppel, L. S. Cederbaum, G. Persch, and W. Demtröder, (PACS numbers: 03.65.6e, 05.40.+j, 05.45.+b, 33.20.Kf) Phys. Rev. Lett. **61**, 3 (1988).
49. U. Agvaanluvsan, G. E. Mitchell, J. F. Shriner Jr., M. Pato, (doi.org/10.1103/PhysRevC.67.064608) Phys. Rev. C **67**, 064608 (2003).
50. O. Bohigas and M. P. Pato, (doi.org/10.1016/j.physletb.2004.05.065) Phys. Lett. B **595**, 171 (2004).
51. R.A. Molina, J. Retamosa, L. Muñoz, A. Relaño, and E. Faleiro, (doi.org/10.1016/j.physletb.2006.10.058) Phys. Lett. B **644**, 25 (2007).
52. A. Relaño, J.M.G. Gómez, R. A. Molina, J. Retamosa, and E. Faleiro, (doi.org/10.1103/PhysRevLett.89.244102) Phys. Rev. Lett. **89**, 244102 (2002).
53. E. Faleiro, J. M. G. Gómez, R. A. Molina, L. Muñoz, A. Relaño, and J. Retamosa, (DOI:10.1103/PhysRevLett.93.244101) Phys. Rev. Lett. **93**, 244101 (2004).
54. J. M. G. Gómez, A. Relaño, J. Retamosa, E. Faleiro, L. Salasnich, M. Vraničar, and M. Robnik, (DOI: 10.1103/PhysRevLett.94.084101) Phys. Rev. Lett. **94**, 084101 (2005).
55. E. Faleiro, U. Kuhl, R.A. Molina, L. Muñoz, A. Relaño, and J. Retamosa, (doi:10.1016/j.physleta.2006.05.029) Phys. Lett. A **358**, 251 (2006).
56. R. Riser, V. Al. Osipov, E. Kanzieper, (DOI:10.1103/PhysRevLett.118.204101) Phys. Rev. Lett. **118**, 204101 (2017).

57. D. S. Jones, (Library of Congress Catalogue Card Number 62-19277) *Theory of Electromagnetism* (Pergamon Press, Oxford, 1964), p. 254.
58. M. Ławniczak, S. Bauch, and L. Sirko, in Handbook of Applications of Chaos Theory, eds. Christos Skiadas and Charilaos Skiadas (CRC Press, Boca Raton, USA, 2016), p. 559.
59. B. Dietz, T. Friedrich, H. L. Harney, M. Miski-Oglu, A. Richter, F. Schäfer, J. Verbaarschot, and H. A. Weidenmüller, (PACS numbers: 24.60.Ky, 05.45.Mt, 11.30.Er, 85.70.Ge) Phys. Rev. Lett. **103**, 064101 (2009).
60. B. Dietz, T. Friedrich, H. L. Harney, M. Miski-Oglu, A. Richter, F. Schäfer and H. A. Weidenmüller, (doi:10.1103/PhysRevE.81.036205) Phys. Rev. E **81**, 036205 (2010).
61. L. Salasnich, Phys. Rev. E **71**, 047202 (2005).
62. M. S. Santhanam and J. N. Bandyopadhyay, Phys. Rev. Lett. **95**, 114101 (2005).
63. A. Relaño, Phys. Rev. Lett. **100**, 224101 (2008).
64. N. Rosenzweig and C. E. Porter, Phys. Rev. **120**, 1698 (1960).

Signatures, Lifts, and Eigenvalues of Graphs

Shiping Liu, Norbert Peyerimhoff, and Alina Vdovina

Abstract We study the spectra of cyclic signatures of finite graphs and the corresponding cyclic lifts. Starting from a bipartite Ramanujan graph, we prove the existence of an infinite tower of 3-cyclic lifts, each of which is again Ramanujan.

1 Introduction

Constructing infinite families of (optimal) expander graphs is a very challenging topic both in mathematics and computer science, which has received extensive attentions, see e.g. [23]. Bilu and Linial [5] succeeded in constructing expander graphs by taking 2-lift operations iteratively. In particular, they relate 2-lifts of a base graph $G = (V, E)$ with signatures $s : E \to \{+1, -1\}$ on the set of edges E, and reduce the construction problem to finding a signature s whose signed adjacency matrix A^s has a small spectral radius. Furthermore, Bilu and Linial conjectured that every d-regular graph G has a signature $s : E \to \{+1, -1\}$ such that all the eigenvalues of A^s have absolute value at most the Ramanujan bound, $2\sqrt{d-1}$. In a recent breakthrough, Marcus, Spielman and Srivastava [25, 27] proved Bilu and Linial's conjecture for bipartite graphs affirmatively, by which they obtained an infinite family of bipartite Ramanujan graphs for every degree larger than 2 via taking 2-lift operations iteratively, starting with a complete bipartite graph.

S. Liu (✉)
School of Mathematical Sciences, University of Science and Technology of China, Hefei, China
e-mail: spliu@ustc.edu.cn

N. Peyerimhoff
Department of Mathematical Sciences, Durham University, Durham, UK
e-mail: norbert.peyerimhoff@durham.ac.uk

A. Vdovina
School of Mathematics, Statistics and Physics, Newcastle University, Newcastle-upon-Tyne, UK
e-mail: alina.vdovina@ncl.ac.uk

F. M. Atay et al. (eds.), *Discrete and Continuous Models in the Theory of Networks*, Operator Theory: Advances and Applications 281,
https://doi.org/10.1007/978-3-030-44097-8_13

In this note, by considering more general groups of signatures, especially cyclic groups, we prove that for each $i \in \{1, 2, \ldots, k-1\}$ where $k \geq 2$, every d-regular graph G has a k-cyclic signature s such that the maximal eigenvalue of the i-th power of its k-cyclic signed adjacency matrix $A^{s,i}$ in the sense of Hadamard product is at most $2\sqrt{d-1}$ (see Theorem 2 in Sect. 5 for the general case). This generalizes Marcus, Spielman and Srivastava's result for $\{+1, -1\}$-signed adjacency matrices. In particular, this enables us to show that every bipartite Ramanujan graph G can be used as the starting point of an infinite tower of 3-cyclic lifts, $\cdots \to G_k \to G_{k-1} \to G_{k-2} \to \cdots \to G_1 = G$, where each G_i is again Ramanujan (Theorem 4 in Sect. 5).

Besides constructing expander graphs, the ideas around (general) signatures and lifts of graphs have been developed from various motivations, e.g. social psychology, Heawood map-coloring problem, matroid theory, mathematical physics. We defer a brief historical review about these interesting developments to Sect. 3.

We emphasize that the set of 3-cyclic lifts is a restrictive class of 3-lifts, which we like to explain briefly. Let $G = (V, E)$ be a finite graph. For any two vertices $u, v \in V$, we denote the corresponding edge by $\{u, v\} \in E$ if it exists. One can assign an orientation to it, say, directing from u to v, in which case, we write $e = (u, v)$. The same edge with the opposite orientation is then written as $\bar{e} := (v, u)$. The set of oriented edges is denoted by E^{or}. A 3-cyclic signature is a map $s : E^{or} \to \{1, \xi, \overline{\xi}\}$, where $\xi = e^{2\pi i/3} \in \mathbb{C}$ and $\overline{\xi}$ is the conjugate of ξ, such that

$$s(\bar{e}) = \overline{s(e)}, \quad \text{for all } e = (u, v) \in E^{or}. \tag{1.1}$$

For every oriented edge $e = (u, v) \in E^{or}$, the three possible values of $s(e)$ correspond to different local cyclic lifts, as shown in the following figures.

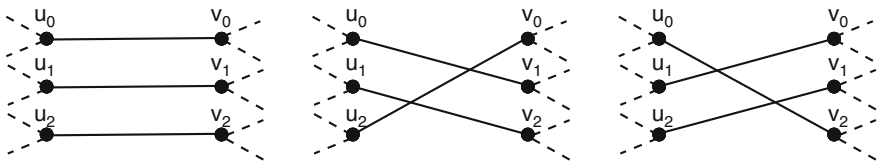

$s(e) = 1$ $\quad$ $s(e) = \xi$ $\quad$ $s(e) = \overline{\xi}$

Let $A, A^s, \widehat{A}$ be the adjacency matrices of a graph G, its signature s, and the corresponding lift $\widehat{G}$, respectively. We will show that the eigenvalues $\sigma(\widehat{A})$ of $\widehat{A}$ satisfy (Lemma 1)

$$\sigma(\widehat{A}) = \sigma(A) \sqcup \sigma(A^s) \sqcup \sigma(\overline{A^s}), \tag{1.2}$$

where $\sqcup$ is the multiset union and $\overline{A^s}$ is the conjugate of A^s.

We prove the existence of our construction by applying the method of interlacing families in [25] and mixed characteristic polynomials in [26] to our setting. The

proof does not work for k-cyclic lifts, when $k \geq 4$. In this case, we have to find a signature s, such that all Hadamard powers of the associated signed adjacency matrix A^s have simultaneously all their eigenvalues in the Ramanujan interval (see Lemma 1). For $k = 3$, we only need to ensure that there is one signed adjacency matrix A^s which satisfies this property. This is due to the fact that (1.1) implies that A^s is Hermitian and hence $\sigma(A^s) = \sigma(\overline{A^s})$. We like to mention that the k-cyclic lifts of a bipartite Ramanujan graph are a very special class and it is remarkable that such special lifts are sufficient to conclude that there are Ramanujan graphs in this class in the case $k = 3$.

In this note, we consider the existence problem of cyclic signatures with particular spectral properties. For the special signature group $\{+1, -1\}$ more spectral theory of signed matrices can be found, e.g., in the survey paper [35]. In [24], we extend results on Cheeger type constants and related spectral estimates, developed in [4], to the more general case of cyclic signatures.

Subsequent to the appearance of our note in arXiv in December 2014, Chandrasekaran and Velingker [7] showed the existence of 4-cyclic lifts that preserve the Ramanujan property for bipartite graphs. The case of arbitrary r-lifts was proved by Hall, Puder and Sawin [17]. It is still an open question whether there is always a cyclic r-lift preserving the Ramanujan property for arbitrary r and whether the bipartiteness condition can be dropped.

2 Basic Notions and General Framework

Given a group Γ, which is usually finite, a general signature is defined as follows.

Definition 1 A signature of $G = (V, E)$ is a map $s : E^{or} \to \Gamma$ satisfying

$$s(\bar{e}) = s(e)^{-1}, \quad \text{for all } e \in E^{or}. \tag{2.1}$$

For an oriented edge $e = (u, v) \in E^{or}$, we call $s(e)$ its signature, and write s_{uv}, alternatively. The signature of a cycle $C := (u_1, u_2)(u_2, u_3) \cdots (u_{l-1}, u_l)(u_l, u_1)$ is defined as the conjugacy class of the element

$$s_{u_1u_2} s_{u_2u_3} \cdots s_{u_{l-1}u_l} s_{u_lu_1} \in \Gamma. \tag{2.2}$$

Definition 2 A signature s of G is called balanced if the signature of every cycle in G is the identity element $\mathrm{id} \in \Gamma$.

Switching a signature s by a function $\theta : V \to \Gamma$ means replacing s by s^θ, which is given by

$$s^\theta(e) := \theta(u) s(e) \theta(v)^{-1}, \quad \text{for all } e = (u, v) \in E^{or}. \tag{2.3}$$

Two signatures s and s' of G are called switching equivalent if there exists a function $\theta : V \to \Gamma$ such that $s' = s^\theta$. Switching equivalence between signatures is an equivalence relation. We denote the corresponding switching class of a signature s by $[s]$. Observe that being balanced is a switching invariant property.

Proposition 1 ([34, Corollary 3.3]) *A signature s of G is balanced if and only if it is switching equivalent to the signature s_{id}, where $s_{id}(e) := id$, for all $e \in E^{or}$.*

Signatures have interesting connections with lifts of graphs. In particular, we consider the permutation signatures, i.e. the maps $s : E^{or} \to \mathcal{S}_k$, where $\mathcal{S}_k$ denotes the group of permutations of $\{1, 2, \ldots, k\}$. The k-lift $\widehat{G} = (\widehat{V}, \widehat{E})$ of $G = (V, E)$ corresponding to the permutation signature $s : E^{or} \to \mathcal{S}_k$ is defined as follows: The vertex set $\widehat{V}$ is given by the Cartesian product $V \times \{1, 2, \ldots, k\}$. For any $u \in V$, we call $\{u_i := (u, i)\}_{i=1}^k \subseteq \widehat{V}$ the fiber over u. Every edge $(u, v) \in E^{or}$ gives rise to the k edges $(u_i, v_{s_{uv}(i)})$, $i = 1, 2, \ldots, k$, in $\widehat{E}^{or}$.

Theorem 1 ([15, Theorems 1 and 2] and [34, Theorem 9.1]) *Let G be a finite graph. There is a 1-to-1 correspondence between the isomorphism classes of k-lifts of G and the switching classes of signatures of G with values in $\mathcal{S}_k$.*

In particular, if two permutation signatures are switching equivalent, then the corresponding two k-lifts of G are isomorphic. Observe that the k-lift of G corresponding to a balanced permutation signature is composed of k disjoint copies of G.

3 Historical Background

In 1953, Harary [18] introduced the concept of a signed graph, which is a graph $G = (V, E)$ with a signature $s : E \to \{+1, -1\}$, and the notion of balance (Definition 2) in this setting. Harary was motivated by certain problems in social psychology, see also [6, 19, 20]. The switching equivalence of signatures was then described by the social psychologists Abelson and Rosenberg [1], and later discussed mathematically by Zaslavsky [34].

Another source of the ideas around signatures and lifts is the Heawood map-coloring problem [21] asking for the chromatic number of a surface with positive genus, which is an extension of the famous four-color problem. The Heawood map-coloring problem is equivalent to finding the imbedding of every complete graph into a surface with the smallest possible genus [33]. Gustin [16] introduced the concept of a current graph in order to solve this imbedding problem, which was proved to be very important for the final solution due to Ringel and Youngs [29, 30]. In the 1970s, Gross and Alpert [12, 13] developed Gustin's current graph theory into full topological generality and interpreted Gustin's method to construct an imbedding of a complete graph into a surface as a lift (or covering in topological terminology) of an imbedding of a smaller graph. Gross [11] further introduced the

concept of a (reduced) voltage graph, which is a graph $G = (V, E)$ with a signature defined in Definition 1 (Gross called it a voltage assignment). A voltage graph can be considered as a dual graph of a current graph when both are imbedded into a certain surface. Gross associated to each signature $s : E^{or} \to \Gamma$ an n-lift of the graph G with $n = |\Gamma|$, the order of Γ. Observe that voltage graphs are natural extensions of signed graphs of Harary. One advantage of voltage graphs over current graphs is that their correspondence to lifts is independent of graph imbeddings, and the concept of a voltage graph makes the understanding of certain aspects of the solution of the Heawood map-coloring problem easier [14].

In [15], Gross and Tucker considered voltage graphs with $\Gamma = \mathcal{S}_k$ and established their correspondence to all k-lifts of G. In [11], a cycle is called satisfying Kirchhoff's Voltage Law (KVL) if its signature is equal to the identity (compare with balance). Both KVL and its dual, the Kirchhoff's Current Law (KCL) in the current graph theory [16], play crucial roles in the corresponding lift and imbedding theory.

In 1982, motivated by a counting problem of the chambers of classical root systems, Zaslavsky [34] introduced the concepts of balance and switching equivalence of signatures into Gross and Tucker's theory on permutation signatures and lifts, and he formulated the explicit 1-to-1 correspondence given in Theorem 1 above.

Connections between permutation signatures and lifts were also discussed by Amit and Linial [3], and they employed them to introduce a new model of random graphs. Friedman [8] first used such a random model in the quest of finding larger Ramanujan graphs from smaller ones. This work stimulated an extensive study on the spectral theory of random k-lifts, see the recent work of Puder [28] and the references therein.

Agarwal, Kolla and Madan [2, Section 1.1] pointed out that another motivation of considering permutation signatures and lifts is the famous Unique Game Conjecture of Khot. The permutations assigned to each oriented edge satisfying (2.1) appear naturally in the context of this conjecture.

We were led to consider general signatures and lifts by the notion of a discrete magnetic Laplacian studied in Sunada [32] (see also Shubin [31] and the references therein). This operator, originating from physics, is defined on a graph where every oriented edge has a signature in the unitary group $U(1)$ such that (2.1) holds. Sunada [32] discussed switching equivalent signatures under a different terminology, cohomologous weight functions.

4 Cyclic Signature, Lifts and Adjacency Matrices

Let $S_k^1 := \{\xi^l \mid 0 \le l \le k-1\}$ be the cyclic group generated by the primitive k-th root of unity, $\xi = e^{2\pi i/k} \in \mathbb{C}$. We consider cyclic signatures, that is, maps $s : E^{or} \to S_k^1$. The corresponding signed adjacency matrix A^s is a matrix with entries $(A^s)_{uv} = s_{uv}$ if $\{u, v\} \in E$ and 0 otherwise, where $u, v \in V$. A^s is Hermitian

and has, therefore, only real eigenvalues with eigenvectors orthogonal w.r.t. the inner product $\langle a, b\rangle = \sum_{i=1}^{k} a_i \bar{b}_i$.

The lift $\widehat{G}$ of G corresponding to a k-cyclic signature is called a k-cyclic lift. In particular, every edge $(u, v) \in E^{or}$ with $s_{uv} = \xi^l$, for some $l \in \{0, 1, \ldots, k-1\}$, gives rise to the following k edges in $\widehat{G}$:

$$(u_i, v_{i+l \pmod k}), i = 0, 1, \ldots, k-1.$$

The adjacency matrix $\widehat{A}$ of $\widehat{G}$ can be written as

$$\widehat{A} = \begin{pmatrix} A_0 & A_1 & A_2 & \cdots & A_{k-1} \\ A_{k-1} & A_0 & A_1 & \cdots & A_{k-2} \\ A_{k-2} & A_{k-1} & A_0 & \cdots & A_{k-3} \\ \vdots & \vdots & \vdots & \ddots & \vdots \\ A_1 & A_2 & A_3 & \cdots & A_0 \end{pmatrix}, \tag{4.1}$$

where A_l is the adjacency matrix for the oriented edges $s^{-1}(\xi^l)$ and $A_l = A_{k-l}^T$. For $i \in \{0, 1, 2, \ldots, k-1\}$, let $A^{s,i}$ be the Hermitian matrix with entries

$$(A^{s,i})_{uv} := ((A^s)_{uv})^i = (s_{uv})^i,$$

where $u, v \in V$. In particular, we have $A^{s,0} = A$, $A^{s,1} = A^s$. Observe that

$$A^{s,i} = \sum_{l=0}^{k-1} \xi^{il} A_l, \tag{4.2}$$

and

$$A^{s,i} = \overline{A^{s,k-i}}. \tag{4.3}$$

Lemma 1 *The spectrum of $\widehat{A}$ is given by*

$$\sigma(\widehat{A}) = \bigsqcup_{l=0}^{k-1} \sigma(A^{s,i}), \tag{4.4}$$

where the notion $\bigsqcup$ stands for the multiset union.

Remark 1 This is an extension of Bilu and Linial [5, Lemma 3.1]. We will call $\bigsqcup_{l=1}^{k-1} \sigma(A^{s,i})$ the *new eigenvalues* of the lift. Lemma 1 was formulated in a slightly different form in [2, Theorem 5]. For the reader's convenience, we present a proof here.

Proof For any $i \in \{0, 1, \ldots, k-1\}$, let w_i be an eigenvector of $A^{s,i}$ with eigenvalue λ, i.e., $A^{s,i} w_i^T = \lambda w_i^T$. Set $\widehat{w}_i := (w_i, \xi^i w_i, \xi^{2i} w_i, \ldots, \xi^{(k-1)i} w_i)$. We check that

$$\widehat{A}\widehat{w}_i^T = \begin{pmatrix} \sum_{l=0}^{k-1} A_l \xi^{il} w_i^T \\ \sum_{l=0}^{k-1} A_l \xi^{i(l+1)} w_i^T \\ \vdots \\ \sum_{l=0}^{k-1} A_l \xi^{i(l+k-1)} w_i^T \end{pmatrix} = \begin{pmatrix} A^{s,i} w_i^T \\ A^{s,i} \xi^i w_i^T \\ \vdots \\ A^{s,i} \xi^{i(k-1)} w_i^T \end{pmatrix} = \lambda \widehat{w}_i^T. \tag{4.5}$$

Therefore, λ is also an eigenvalue of $\widehat{A}$ with eigenvector $\widehat{w}_i$.

Moreover, we have for any two eigenvectors w_i, w_j of $A^{s,i}, A^{s,j}$, respectively, where $i \neq j$,

$$\langle \widehat{w}_i, \widehat{w}_j \rangle = \langle w_i, w_j \rangle (1 + \xi^{i-j} + \xi^{2(i-j)} + \cdots + \xi^{(k-1)(i-j)}) = 0. \tag{4.6}$$

Note that the number of mutually orthogonal eigenvectors of $\{A^{s,i}\}_{i=0}^{k-1}$ is $k|V|$. Therefore, we have $\sigma(\widehat{A}) = \bigsqcup_{l=0}^{k-1} \sigma(A^{s,i})$. □

As a consequence of Lemma 1 and (4.3), most of the new eigenvalues have even multiplicity.

Lemma 2 *Let G be a finite bipartite graph. Then, for any $i \in \{0, 1, \ldots, k-1\}$ and any $s : E^{or} \to S_k^1$, the spectrum $\sigma(A^{s,i})$ is symmetric w.r.t. zero.*

Proof First observe that for every $A^{s,i}$, there exists two square matrix A_1, A_2 such that

$$A^{s,i} = \begin{pmatrix} 0 & A_1 \\ A_2 & 0 \end{pmatrix}. \tag{4.7}$$

Furthermore, $A^{s,i}$ is Hermitian and has only real eigenvalues. Let λ be an eigenvalue of $A^{s,i}$ with eigenvector $w := (w_1, w_2)^T$. Then we have

$$A_1 w_2 = \lambda w_1, \quad A_2 w_1 = \lambda w_2, \tag{4.8}$$

and we can check directly that $-\lambda$ is an eigenvalue of $A^{s,i}$ with the eigenvector $(w_1, -w_2)^T$. □

The following lemma is an extension of the corresponding result for signatures $s : E^{or} \to \{+1, -1\}$ in [35, Proposition II.3].

Lemma 3 *Let s and s' be switching equivalent. Then for each $i \in \{0, 1, \ldots, k-1\}$, the matrices $A^{s,i}$ and $A^{s',i}$ are unitary equivalent, and hence have the same spectrum.*

Proof Let $\theta : V \to S_k^1$ be the function such that $s'_{uv} = \theta(u)s_{uv}\overline{\theta(v)}$, for all $e = (u, v) \in E^{or}$. Set $D^i(\theta)$ be the diagonal matrix with entries $(D^i(\theta))_{uu} = \theta(u)^i$, where $u \in V$. We can check that

$$A^{s',i} = D^i(\theta)A^{s,i}\overline{D^i(\theta)}. \tag{4.9}$$

□

A set of i edges is called an i-matching if no two of them share a common vertex. If m_i denotes the number of i-matchings in G, then the matching polynomial of G is defined as (see [10])

$$\mu_G(x) := \sum_{i=0}^{\lfloor \frac{N}{2} \rfloor} (-1)^i m_i x^{n-2i}. \tag{4.10}$$

Now we consider the signature s as a random variable with the following properties. The signature of $(u, v) \in E^{or}$ and its inverse (v, u) are chosen independently from the other oriented edges. The signature s_{uv} is chosen uniformly from S_k^1 and this choice determines the value of $s_{vu} = \overline{s_{uv}}$, as well. We have the following proposition, extending a result of Godsil and Gutman [10, Corollary 2.2] (see also [25]).

Proposition 2 *For any $i \in \{1, 2, \ldots, k-1\}$, the expectation of the characteristic polynomial of $A^{s,i}$ satisfies*

$$\mathbb{E}_s(\det(xI - A^{s,i})) = \mu_G(x). \tag{4.11}$$

Proof We denote by $\mathrm{Sym}(S)$ the set of permutations of a set S, and by $[N]$ the set $\{1, 2, \ldots, N\}$. Let $(-1)^{|\eta|}$ denote the signature of a permutation $\eta \in \mathrm{Sym}([N])$. For $l \in \{0, 1, 2, \ldots, N\}$, we define a subset P_l of $\mathrm{Sym}([N])$ to be

$$P_l := \{\eta \in \mathrm{Sym}([\mathrm{N}]) : \text{the number of indices } i \in [N] \text{ s. t. } \eta(i) \neq i \text{ is equal to } l\}.$$

Next, we calculate the characteristic polynomials of $A^{s,i}$:

$$\begin{aligned}
\det(xI - A^{s,i}) &= \sum_{\eta \in \mathrm{Sym}([N])} (-1)^{|\eta|} \prod_{j=1}^{N} (xI - A^{s,i})_{j,\eta(j)} \\
&= \sum_{l=0}^{N} \sum_{\eta \in P_l} (-1)^{|\eta|} x^{N-l} \prod_{\substack{j=1 \\ \eta(j) \neq j}}^{N} (-A^{s,i})_{j,\eta(j)} \\
&= \sum_{l=0}^{N} x^{N-l} \sum_{\substack{S \subseteq [N] \\ |S|=l}} \sum_{\substack{\pi \in \mathrm{Sym}(S) \\ \pi(i) \neq i \, \forall i \in S}} (-1)^{|\pi|} \prod_{j \in S} (-A^{s,i})_{j,\pi(j)}.
\end{aligned}$$

Observe that

$$\mathbb{E}_s((-A^{s,i})_{j,\pi(j)}) = -\frac{1}{k}\sum_{l=0}^{k-1}\xi^{il} = 0, \tag{4.12}$$

and

$$\mathbb{E}_s((-A^{s,i})_{j,\pi(j)}(-A^{s,i})_{\pi(j),j}) = \frac{1}{k}\sum_{l=0}^{k-1}\xi^{il}\overline{\xi^{il}} = 1. \tag{4.13}$$

Hence, we obtain

$$\begin{aligned}\mathbb{E}_s(\det(xI - A^{s,i})) =& \sum_{l=0}^{N} x^{N-l} \sum_{\substack{S\subseteq[N]\\ |S|=l,\, l \text{ even}}} \sum_{\substack{\pi\in \mathrm{Sym}(S)\\ \pi(i)\neq i, \pi^2(i)=i\ \forall i\in S}} (-1)^{\frac{l}{2}} \\ =& \mu_G(x).\end{aligned}$$

□

Heilmann and Lieb [22] proved that for every graph G, $\mu_G(x)$ has only real roots and all these roots have absolute value at most $2\sqrt{d-1}$, where d is the maximal vertex degree of G. A refinement in the irregular case was proved by Godsil [9] leading to the following result presented in [25, Lemma 3.5].

Proposition 3 *Let T be the universal cover of the graph G. Then the roots of $\mu_G(x)$ are bounded in absolute value by the spectral radius $\rho(T)$ of T.*

5 Ramanujan Properties

The following theorem is a generalization of [25, Theorem 5.3].

Theorem 2 *Let $G = (V, E)$ be a finite connected graph. Then for any $i \in \{1, 2, \ldots, k-1\}$, there exists a cyclic signature $s_0^i : E^{or} \to S_k^1$ such that*

$$\lambda_{max}(A^{s_0^i,i}) \leq \rho(T), \tag{5.1}$$

that is, all the eigenvalues of $A^{s_0^i,i}$ are at most the spectral radius $\rho(T)$ of the universal covering tree T of G.

Remark 2 Note that by Lemma 3, all the signatures in the switching class $[s_0^i]$ fulfill (5.1).

For each $i \in \{1, 2, \ldots, k-1\}$, we consider the following family of characteristic polynomials:

$$\{f^{s,i} := \det(xI - A^{s,i}) \mid s : E^{or} \to S_k^1\}. \tag{5.2}$$

By Propositions 2 and 3, it is enough to prove the following property of (5.2):

there exists one polynomial of (5.2) whose largest root is no greater than the largest root of the sum of all polynomials in (5.2). (5.3)

However, this property can not hold for an arbitrary family of polynomials. We apply the method of *interlacing families*, developed by Marcus, Spielman and Srivastava [25–27] to prove property (5.3).

First observe that for every signature $s : E^{or} \to S_k^1$, $f^{s,i}$ is a real-rooted degree N polynomial with leading coefficient one. Let $\lambda_1(f^{s,i}) \le \lambda_2(f^{s,i}) \le \cdots \le \lambda_N(f^{s,i})$ be the N roots of $f^{s,i}$. If there exists a sequence of real numbers $\alpha_1 \le \alpha_2 \le \cdots \le \alpha_{N-1}$ such that

$$\lambda_1(f^{s,i}) \le \alpha_1 \le \lambda_2(f^{s,i}) \le \alpha_2 \le \cdots \le \alpha_{N-1} \le \lambda_N(f^{s,i}) \quad \forall s : E^{or} \to S_k^1, \tag{5.4}$$

then we say that $\{f^{s,i}\}_s$ has a *common interlacing*. If the family of polynomials (5.2) could be proved to have a common interlacing, then property (5.3) would hold by [25, Lemma 4.2].

A systematic way to establish the existence of a common interlacing is given in the following lemma (see, e.g., [25, Lemma 4.5]).

Lemma 4 *Let $g^1, g^2, \ldots, g^l$ be polynomials of the same degree with positive leading coefficients. Then $g^1, g^2, \ldots, g^l$ have a common interlacing if and only if $\sum_{i=1}^l p_i g^i$ is real-rooted for all convex combinations, $p_i \ge 0$, $\sum_{i=1}^l p_i = 1$.*

In fact, in order to prove (5.3), we do not prove that the polynomials $\{f^{s,i}\}_s$ have a common interlacing but that they form an *interlacing family* introduced by Marcus, Spielman and Srivastava, for which we only need to consider special convex combinations of $\{f^{s,i}\}_s$ instead of all.

Definition 3 (Interlacing Families [25]) Let $S_1, \ldots, S_m$ be finite index sets and for every assignment $(s_1, \ldots, s_m) \in S_1 \times S_2 \times \cdots \times S_m$, let $g^{s_1,\ldots,s_m}(x)$ be a real-rooted degree N polynomial with positive leading coefficient. For a partial assignment $(s_1, \ldots, s_q) \in S_1 \times \cdots \times S_l$ with $1 \le q < m$, we define

$$g^{s_1,\ldots,s_q} := \sum_{s_{q+1} \in S_{q+1}, \ldots, s_m \in S_m} g^{s_1,\ldots,s_q,s_{q+1},\ldots,s_m},$$

and

$$g^{\emptyset} := \sum_{s_1 \in S_1, \ldots, s_m \in S_m} g^{s_1, \ldots, s_m}.$$

The family of polynomials $\{g^{s_1,\ldots,s_m}\}_{s_1,\ldots,s_m}$ is called an *interlacing family* if, for all $q \in \{0, 1, \ldots, m-1\}$ and all given parameters $s_1 \in S_1, \ldots, s_q \in S_q$, the family of polynomials

$$\{g^{s_1,\ldots,s_q,t}\}_{t \in S_{q+1}}$$

has a common interlacing.

Marcus, Spielman and Srivastava [25, Theorem 4.4] proved the following theorem.

Theorem 3 *Let $S_1, \ldots, S_m$ be finite index sets and let $\{g^{s_1,\ldots,s_m}\}_{s_1,\ldots,s_m}$ be an interlacing family of polynomials. Then there exists $(s_1, \ldots, s_m) \in S_1 \times \cdots \times S_m$ such that the largest root of $g^{s_1,\ldots,s_m}$ is no greater than the largest root of $g^{\emptyset}$.*

In order to prove property (5.3) using Theorem 3, we still need to prove the following proposition.

Proposition 4 *For each $i \in \{1, 2, \ldots, k-1\}$, the family of polynomials $\{f^{s,i} \mid s : E^{or} \to S_k^1\}$ is an interlacing family.*

Proof For notational convenience, let $e_1, \ldots, e_m$ be all the oriented edges in E^{or} and $s_1, \ldots, s_m$ their associated signatures, respectively. Then we can write the family of polynomials of this proposition as

$$\{f^{s,i}\}_{s=(s_1,\ldots,s_m)\in(S_k^1)^m}.$$

Let $p_1^l, \ldots, p_m^l$, $l = 0, 1, \ldots, k-1$ be nonnegative real numbers satisfying

$$\sum_{l=0}^{k-1} p_j^l = 1, \quad \text{for } j = 1, 2, \ldots, m. \tag{5.5}$$

In order to prove this proposition, it is sufficient to prove that the following polynomial is real-rooted for all possible choices of $\{p_j^l\}$ satisfying (5.5),

$$\sum_{s=(s_1,\ldots,s_m)\in(S_k^1)^m} \left(\prod_{j=1}^{m} p_j^{l(s_j)} \right) f^{s,i}(x), \tag{5.6}$$

where $l(s_j) \in \{0, 1, \ldots, k-1\}$ satisfies $s_j = \xi^{l(s_j)}$. In fact, if this real-rootedness is true, for each $q \in \{0, \ldots, m-1\}$ and fixed $s_1 \in S_k^1, \ldots, s_q \in S_k^1$, we can apply Lemma 4 to (5.6) with

$$p_{q+1}^l \geq 0, \text{ for } l = 0, 1, \ldots, k-1, \sum_{l=0}^{k-1} p_{q+1}^l = 1;$$

$$p_{q+2}^l = \cdots = p_m^l = \frac{1}{k}, \text{ for } l = 0, 1, \ldots, k-1;$$

$$p_j^l = \begin{cases} 1, \text{ if } s_j = \xi^l; \\ 0, \text{ otherwise,} \end{cases} \text{ for } j = 1, 2, \ldots, q,$$

to conclude that $\{f^{(s_1,\ldots,s_q,t),i}\}_{t \in S_k^1}$ has a common interlacing and hence Proposition 4 holds by Definition 3.

Now we start to prove the real-rootedness of the polynomial (5.6). Observe that the matrix $A^{s,i}$ can be written as follows:

$$A^{s,i} = \sum_{j=1}^{m} r_j^i \cdot (r_j^i)^* - D. \tag{5.7}$$

In the above equation, we use the following notations: D is the diagonal matrix with $D_{uu} = d_u$, for each $u \in V$; $r_j^i \in \mathbb{C}^N$ is a column vector associated to the signature s_j of the oriented edge e_j. If $e_j = (u, v)$ for $u, v \in V$, we have

$$r_j^i := (0, \ldots, 0, \alpha_j^i, 0, \ldots, 0, \overline{\alpha_j^i}, 0, \ldots, 0)^T, \tag{5.8}$$

where the non-zero entries are at the u-th and v-th positions, respectively, and $(\alpha_j^i)^2 = (s_j)^i$. We use the notation that $(r_j^i)^* := (\overline{r_j^i})^T$ for simplicity.

For each edge $e_j \in E^{or}$, we consider its signature s_j as a random variable with values chosen randomly from S_k^1. All the m random variables $s_1, \ldots, s_m$ are independent with possibly different distributions. In this viewpoint, the values $\{p_j^l\}_{l=0}^{k-1}$ in (5.5) represent the distribution of s_j. Accordingly, the vectors $\{r_j^i\}_{j=1}^m$ are a set of independent finite-valued random column vectors in $\mathbb{C}^N$. Then, the polynomial (5.6) is equal to the following expectation of characteristic polynomial:

$$\mathbb{E}(f^{s,i}) = \mathbb{E}(\det(xI - A^{s,i})) = \mathbb{E}\left(\det\left(xI + D - \sum_{j=1}^{m} r_j^i \cdot (r_j^i)^*\right)\right). \tag{5.9}$$

If the graph G is regular with vertex degree d, we have $D = dI$. Therefore $\mathbb{E}(f^{s,i})$ is the expectation of characteristic polynomials of a sum of independent rank one Hermitian matrices (with a shift of all roots by $-d$). In the terminology of [26],

the right hand side of (5.9) without the matrix D is called the *mixed characteristic polynomial* of the matrices

$$A_j^i := \mathbb{E}(r_j^i \cdot (r_j^i)^*), \quad j = 1, 2, \ldots, m. \tag{5.10}$$

Note that all the above matrices A_j^i are positive semi-definite. Then by [26, Corollary 4.4], the mixed characteristic polynomial of positive semi-definite matrices is real-rooted. This proves the real-rootedness of (5.9) in the regular case and hence the proposition.

In the case that G is irregular, we can obtain the real-rootedness of (5.9) by modifying the arguments of [26, Corollary 4.4]. For convenience, we outline the proof here. A proof similar to the one of [26, Theorem 4.1] yields

$$\begin{aligned}&\mathbb{E}\left(\det\left(xI + x'D - \sum_{j=1}^m r_j^i \cdot (r_j^i)^*\right)\right)\\ &= \prod_{j=1}^m (1 - \partial_{z_j}) \det\left(xI + x'D + \sum_{j=1}^m z_j A_j^i\right)\Bigg|_{z_1=\cdots=z_m=0}.\end{aligned}$$

Therefore, we obtain

$$\begin{aligned}&\mathbb{E}(f^{s,i}) = \mathbb{E}\left(\det\left(xI + D - \sum_{j=1}^m r_j^i \cdot (r_j^i)^*\right)\right)\\ &= \prod_{j=1}^m (1 - \partial_{z_j}) \det\left(xI + x'D + \sum_{j=1}^m z_j A_j^i\right)\Bigg|_{z_1=\cdots=z_m=0,x'=1}.\end{aligned}$$

Note that $\det(xI + x'D + \sum_{j=1}^m z_j A_j^i)$ is real stable by [26, Proposition 3.6] and we conclude the real stability of $\mathbb{E}(f^{s,i})$ by [26, Corollary 3.8 and Proposition 3.9]. Since real stability coincides with real rootedness in the case of univariate polynomials, we conclude that $\mathbb{E}(f^{s,i})$ is real-rooted. For more details, see [26]. □

Theorem 4 *Let G be a finite connected bipartite graph. Then there exists a 3-cyclic lift $\widehat{G}$ of G such that all its new eigenvalues lie in the Ramanujan interval $[-\rho(T), \rho(T)]$, where $\rho(T)$ is the spectral radius of the universal covering T of G. In particular, when G is d-regular, the interval is $[-2\sqrt{d-1}, 2\sqrt{d-1}]$.*

Proof By Lemma 1, the new eigenvalues of the 3-cyclic lift $\widehat{G}$ are eigenvalues of either $A^{s,1} = A^s$ or $A^{s,2}$. From (4.3) we know $A^{s,2} = \overline{A^s}$. Since A^s is Hermitian, we obtain $\sigma(A^{s,2}) = \sigma(A^s)$ for any choice of $s : E^{or} \to S_3^1$. Applying Theorem 2,

we can find an $s_0 : E^{or} \to S_3^1$ such that

$$\lambda_{max}(A^{s_0}) \leq \rho(T). \tag{5.11}$$

By Lemma 2, $\sigma(A^s)$ is symmetric w.r.t. to zero since G is bipartite. Therefore, we arrive at

$$|\lambda_i(A^{s_0})| \leq \rho(T), \quad |\lambda_i(A^{s_0,2})| \leq \rho(T), \text{ for } i = 1, 2, \ldots, N. \tag{5.12}$$

This proves the corollary. □

Starting from the complete bipartite graph $G_1 := K_{d,d}$, we can apply Theorem 4 repeatedly to obtain an infinite tower of 3-cyclic lifts $\cdots \to G_k \to G_{k-1} \to G_{k-2} \to \cdots \to G_1$ with each G_i being Ramanujan.

As we have commented in the Introduction, the above method of finding an infinite family of Ramanujan graphs does not work for k-lifts with $k \geq 4$. In this case, one needs to find a proper signature s_0 which works simultaneously for all $i \in \{1, 2, \ldots, k-1\}$ in Theorem 2.

Acknowledgments We thank Stefan Dantchev for bringing the reference [2] to our attention. We acknowledge the support of the EPSRC Grant EP/K016687/1.

References

1. R. P. Abelson and M. J. Rosenberg, Symbolic psycho-logic: A model of attitudinal cognition, Behavioral Sci. 3 (1958), 1–13.
2. N. Agarwal, A. Kolla, V. Madan, Small lifts of expander graphs are expanding, arXiv: 1311.3268v1, November 2013.
3. A. Amit, N. Linial, Random graph coverings I: General theory and graph connectivity, Combinatorica 22 (2002), no. 1, 1–18.
4. F. M. Atay, S. Liu, Cheeger constants, structural balance, and spectral clustering analysis for signed graphs, Discrete Math. 343 (2020), no. 1, 111616, 26 pp.
5. Y. Bilu, N. Linial, Lifts, discrepancy and nearly optimal spectral gap, Combinatorica 26 (2006), no. 5, 495–519.
6. D. Cartwright, F. Harary, Structural balance: a generalization of Heider's theory, Psychol. Rev. 63 (1956), no. 5, 277–293.
7. K. Chandrasekaran, A. Velingker, Shift lifts preserving Ramanujan property, Linear Algebra and its Applications 529 (2017), 199–214.
8. J. Friedman, Relative expanders or weakly relatively Ramanujan graphs, Duke Math. J. 118 (2003), no. 1, 19–35.
9. C. D. Godsil, Matchings and walks in graphs, J. Graph Theory 5 (1981), no. 3, 285–297.
10. C. D. Godsil, I. Gutman, On the matching polynomial of a graph, Algebraic methods in graph theory, Vol. I, II (Szeged, 1978), pp. 241–249, Colloq. Math. Soc. János Bolyai, 25, North-Holland, Amsterdam-New York, 1981.
11. J. L. Gross, Voltage graphs, Discrete Math. 9 (1974), 239–246.
12. J. L. Gross, S. R. Alpert, Branched coverings of graph imbeddings, Bull. Amer. Math. Soc. 79 (1973), 942–945.

13. J. L. Gross, S. R. Alpert, The topological theory of current graphs, J. Combinatorial Theory Ser. B 17 (1974), 218–233.
14. J. L. Gross, T. W. Tucker, Quotients of complete graphs: revisiting the Heawood map-coloring problem, Pacific J. Math. 55 (1974), 391–402.
15. J. L. Gross, T. W. Tucker, Generating all graph coverings by permutation voltage assignments, Discrete Math. 18 (1977), no. 3, 273–283.
16. W. Gustin, Orientable embedding of Cayley graphs, Bull. Amer. Math. Soc. 69 (1963), 272–275.
17. C. Hall, D. Puder, W. F. Sawin, Ramanujan coverings of graphs, Adv. Math. 323 (2018), 367–410.
18. F. Harary, On the notion of balance of a signed graph, Michigan Math. J. 2 (1953), no. 2, 143–146.
19. F. Harary, Structural duality, Behavioral Sci. 2 (1957), no. 4, 255–265.
20. F. Harary, On the measurement of structural balance, Behavioral Sci. 4 (1959), 316–323.
21. P. J. Heawood, Map colour theorem, Quart. J. Math. Oxford Ser. 2 24 (1890), 332–338.
22. O. J. Heilmann, E. H. Lieb, Theory of monomer-dimer systems, Comm. Math. Phys. 25 (1972), 190–232.
23. S. Hoory, N. Linial, A. Wigderson, Expander graphs and their applications, Bull. Amer. Math. Soc. 43 (2006), no. 4, 439–561.
24. C. Lange, S. Liu, N. Peyerimhoff, O. Post, Frustration index and Cheeger inequalities for discrete and continuous magnetic Laplacians, Calc. Var. Partial Differential Equations 54 (2015), no. 4, pp. 4165–4196.
25. A. W. Marcus, D. A. Spielman, N. Srivastava, Interlacing families I: Bipartite Ramanujan graphs of all degrees, Proceedings of FOCS, 529–537, 2013; Ann. of Math. (2) 182 (2015), no. 1, 307–325.
26. A. W. Marcus, D. A. Spielman, N. Srivastava, Interlacing families II: Mixed characteristic polynomials and the Kadison-Singer Problem, Ann. of Math. (2) 182 (2015), no. 1, 327–350.
27. A. W. Marcus, D. A. Spielman, N. Srivastava, Ramanujan graphs and the solution of the Kadison-Singer problem, Proceedings of the International Congress of Mathematicians-Seoul 2014. Vol. III, 363–386, Kyung Moon Sa, Seoul, 2014.
28. D. Puder, Expansion of random graphs: new proofs, new results, Invent. Math. 201 (2015), no. 3, 845–908.
29. G. Ringel, Map color theorem, Die Grundlehren der mathematischen Wissenschaften in Einzeldarstellungen, Band 209, Springer-Verlag, New York-Heidelberg, 1974.
30. G. Ringel, J. W. T. Youngs, Solution of the Heawood map-coloring problem, Proc. Nat. Acad. Sci. U.S.A. 60 (1968), 438–445.
31. M. A. Shubin, Discrete magnetic Laplacian, Comm. Math. Phys. 164 (1994), no. 2, 259–275.
32. T. Sunada, A discrete analogue of periodic magnetic Schrödinger operators, Geometry of the spectrum (Seattle, WA, 1993), 283–299, Contemp. Math., 173, Amer. Math. Soc., Providence, RI, 1994.
33. J. W. T. Youngs, The Heawood Map Coloring Conjecture, Chapter 12 in Graph Theory and Theoretical Physics (F. Harary, ed.), pp. 313–354, Academic Press, London, 1967.
34. T. Zaslavsky, Signed graphs, Discrete Appl. Math. 4 (1982), no. 1, 47–74.
35. T. Zaslavsky, Matrices in the theory of signed simple graphs, Advances in discrete mathematics and applications: Mysore, 2008, 207–229, Ramanujan Math. Soc. Lect. Notes Ser., 13, Ramanujan Math. Soc., Mysore, 2010.

Strong Isoperimetric Inequality for Tessellating Quantum Graphs

Noema Nicolussi

Abstract We investigate isoperimetric constants of infinite tessellating metric graphs. We introduce a curvature-like quantity, which plays the role of a metric graph analogue of discrete curvature notions for combinatorial tessellating graphs. Based on the definition in [26], we then prove a lower estimate and a criterium for positivity of the isoperimetric constant.

Keywords Quantum graph · Tiling · Tessellation · Isoperimetric inequality

2010 Mathematics Subject Classification Primary 34B45; Secondary 35P15, 81Q35

1 Introduction

Isoperimetric constants, which relate surface area and volume of sets, are among the most fundamental tools in spectral geometry of manifolds and graphs. They first appeared in this context in [7], where Cheeger obtained a lower bound on the spectral gap of Laplace–Beltrami operators. For discrete Laplacians on graphs, versions of Cheeger's inequality are known in various settings, e.g. [1–3, 9, 10, 13, 23, 30, 32]. They find application in many fields (such as the study of expander graphs and random walks on graphs, see [28] and [38] for more information) and consequently, there is a very large interest in graph isoperimetric constants.

Research supported by the Austrian Science Fund (FWF) under Grants P28807 and W1245.

N. Nicolussi (✉)
Faculty of Mathematics, University of Vienna, Vienna, Austria
e-mail: noema.nicolussi@univie.ac.at

F. M. Atay et al. (eds.), *Discrete and Continuous Models in the Theory of Networks*, Operator Theory: Advances and Applications 281,
https://doi.org/10.1007/978-3-030-44097-8_14

In the case of *tessellating graphs* (i.e. edge graphs of tessellations of $\mathbb{R}^2$), they have been investigated using certain notions of *discrete curvature* (see for example [17, 24, 34, 37, 39]). On the other hand, the idea of plane graph curvature already appears earlier in several unrelated works [14, 20, 36] and was also employed to describe other geometric properties, for instance discrete analogues of the Gauss–Bonnet formula and the Bonnet–Myers theorem, e.g. [4, 8, 19, 22, 24, 36].

Another framework for isoperimetric constants are *metric graphs* $\mathcal{G}$, i.e. combinatorial graphs $\mathcal{G}_d = (\mathcal{V}, \mathcal{E})$ with vertex set $\mathcal{V}$ and edge set $\mathcal{E}$, where each edge $e \in \mathcal{E}$ is identified with an interval $I_e = (0, |e|)$ of length $0 < |e| < \infty$. Topologically, $\mathcal{G}$ may be considered as a "network" of intervals glued together at the vertices. The analogue of the Laplace–Beltrami operator for metric graphs is the *Kirchhoff–Neumann Laplacian* $\mathbf{H}$ (also known as a *quantum graph*). It acts as an edgewise (negative) second derivative $f_e \mapsto -\frac{d^2}{dx_e^2} f_e$, $e \in \mathcal{E}$, and is defined on edgewise H^2-functions satisfying continuity and Kirchhoff conditions at the vertices (we refer to [5, 6, 11, 35] for more information and references; see also [12] for the case that $\mathcal{G}$ is infinite). A well-known result for *finite metric graphs* (i.e. $\mathcal{V}$ and $\mathcal{E}$ are finite sets) is a spectral gap estimate for $\mathbf{H}$ in terms of an isoperimetric constant due to Nicaise [33] (see also [25, 27]).

In this work, we are interested in *infinite metric graphs* (infinitely many vertices and edges). A notion of an isoperimetric constant $\alpha(\mathcal{G})$ in this context was introduced recently in [26] (see (2.5) below for a precise definition) together with the following Cheeger-type estimate

$$\frac{1}{4}\alpha(\mathcal{G})^2 \leq \lambda_0(\mathbf{H}) \leq \frac{\pi^2}{2\,\inf_{e\in\mathcal{E}} |e|}\alpha(\mathcal{G}), \tag{1.1}$$

which holds for every connected, simple, locally finite, infinite metric graph. Here $\lambda_0(\mathbf{H}) := \inf \sigma(\mathbf{H})$ is the bottom of the spectrum of $\mathbf{H}$.

However, let us stress that explicit computation of isoperimetric constants in general is a difficult problem (known to be NP-hard for combinatorial graphs [31]). Hence the question arises, whether one can find bounds on $\alpha(\mathcal{G})$ in terms of less complicated quantities. On the other hand, the definition of $\alpha(\mathcal{G})$ is purely combinatorial and moreover $\alpha(\mathcal{G})$ is related to the isoperimetric constant $\alpha_{\mathrm{comb}}(\mathcal{G}_d)$ of the combinatorial graph $\mathcal{G}_d$ (see [26] for further details). This strongly suggests to use discrete methods for further study. For combinatorial tessellating graphs, such tools are available in the form of discrete curvature and it is natural to ask whether similar techniques also apply to metric graphs. Moreover, the class of plane graphs contains important examples such as trees and edge graphs of regular tessellations.

Motivated by this, the subject of our paper are isoperimetric constants of *infinite tessellating metric graphs* (see Definition 2.1). Our main contribution is the definition of a *characteristic value* $c(\cdot)$ of the edges of a given metric graph (see (2.9)), which takes over the role of the classical discrete curvature (up to sign convention; as opposed to e.g. [17, 22, 24], our results on $\alpha(\mathcal{G})$ are formulated in terms of positive curvature). In the simple case of equilateral metric graphs (i.e.

$|e| = 1$ for all $e \in \mathcal{E}$), c coincides with the characteristic edge value introduced by Woess in [37]. Moreover, for a finite tessellating metric graph (Corollary 3.9),

$$\sum_{e\in\mathcal{E}} -c(e)|e| = 1, \tag{1.2}$$

which can be interpreted as a metric graph analogue of the combinatorial Gauss–Bonnet formula known in the discrete case (see e.g. [22]).

In terms of these characteristic values, we then formulate our two main results: Theorem 3.1 contains a criterium for positivity of $\alpha(\mathcal{G})$ based on the averaged value of $c(\cdot)$ on large subgraphs $\widetilde{\mathcal{G}} \subset \mathcal{G}$. In Theorem 3.3, we obtain explicit lower bounds on $\alpha(\mathcal{G})$. A simplified version of this estimate is the following inequality:

$$\alpha(\mathcal{G}) \geq \inf_{e\in\mathcal{E}} c(e). \tag{1.3}$$

Theorem 3.3 can be interpreted as a metric graph analogue of the estimate in [24, Theorem 1] and a result by McKean in the manifold case [29].

Finally, we demonstrate the use of our theory by examples. First, we consider the case of equilateral (p, q)-regular graphs. Here, $\alpha(\mathcal{G})$ is closely related to $\alpha_{\mathrm{comb}}(\mathcal{G}_d)$ and hence can be computed explicitly. It turns out for large p and q, the estimate in Theorem 3.3 is quite close to the actual value. Second, we show how to construct an example where $\alpha(\mathcal{G})$ and $\alpha_{\mathrm{comb}}(\mathcal{G}_d)$ behave differently.

Let us finish the introduction by describing the structure of the paper. In Sect. 2, we recall a few basic notions and give a precise definition of infinite tessellating metric graphs. Moreover, we review the definition of $\alpha(\mathcal{G})$ and define the characteristic values. Section 3 contains our main results and proofs. In the final section, we consider examples.

2 Preliminaries

2.1 (Combinatorial) Planar Graphs

Let $\mathcal{G}_d = (\mathcal{V}, \mathcal{E})$ be an infinite, unoriented graph with countably infinite sets of vertices $\mathcal{V}$ and edges $\mathcal{E}$. For a vertex $v \in \mathcal{V}$, we set

$$\mathcal{E}_v := \{e \in \mathcal{E} |\ e \text{ is incident to } v\} \tag{2.1}$$

and denote by $\deg(v) := \#\mathcal{E}_v$ the *combinatorial degree* of $v \in \mathcal{V}$. Throughout the paper, $\#A$ denotes the number of elements of a given set A. We will always assume that $\mathcal{G}_d$ is connected, simple (no loops or multiple edges) and locally finite ($\deg(v) < \infty$ for all $v \in \mathcal{V}$).

Moreover, we suppose that $\mathcal{G}_d$ is *planar* and consider a fixed planar embedding. Hence $\mathcal{G}_d$ can be regarded as a subset of the plane $\mathbb{R}^2$, which we assume to be closed. Denote by $\mathcal{T}$ the set of *faces* of $\mathcal{G}_d$, i.e. the closures of the connected components of $\mathbb{R}^2 \setminus \mathcal{G}_d$. Note that unbounded faces of $\mathcal{G}_d$ are included in $\mathcal{T}$ as well. Motivated by the next definition, we will refer to the elements $T \in \mathcal{T}$ as the *tiles* of $\mathcal{G}_d$.

Definition 2.1 A planar graph $\mathcal{G}_d$ is *tessellating* if the following additional conditions hold:

(i) $\mathcal{T}$ is locally finite, i.e. each compact subset K in $\mathbb{R}^2$ intersects only finitely many tiles.
(ii) Each bounded tile $T \in \mathcal{T}$ is a closed topological disc and its boundary ∂T consists of a finite cycle of at least three edges.
(iii) Each unbounded tile $T \in \mathcal{T}$ is a closed topological half-plane and its boundary ∂T consists of a (countably) infinite chain of edges.
(iv) Each edge $e \in \mathcal{E}$ is contained in the boundary of precisely two different tiles.
(v) Each vertex $v \in \mathcal{V}$ has degree ≥ 3.

Here, a subset $A \subseteq \mathbb{R}^2$ is called a closed topological disc (half-plane) if it is the image of the closed unit ball in $\mathbb{R}^2$ (the closed upper half-plane) under a homeomorphism $\phi\colon \mathbb{R}^2 \to \mathbb{R}^2$. For a tile $T \in \mathcal{T}$, we define

$$\mathcal{E}_T := \{e \in \mathcal{E} |\ e \subseteq \partial T\}, \qquad d_{\mathcal{T}}(T) := \#\mathcal{E}_T, \tag{2.2}$$

where the latter is called the *degree of a tile* $T \in \mathcal{T}$. Notice that according to Definition 2.1(ii), $d_{\mathcal{T}}(T) \geq 3$ for all $T \in \mathcal{T}$.

The above assumptions (i)–(v) imply that $\mathcal{T}$ is a *locally finite tessellation* of $\mathbb{R}^2$, i.e. a locally finite, countable family of closed subsets $T \subset \mathbb{R}^2$ such that the interiors are pairwise disjoint and $\bigcup_{T\in\mathcal{T}} T = \mathbb{R}^2$. In addition, $\mathcal{G}_d = (\mathcal{V}, \mathcal{E})$ coincides with the edge graph of the tessellation in the following sense: by calling a connected component of the intersection of at least two tiles $T \in \mathcal{T}$ a $\mathcal{T}$-vertex, if it has only one point and a $\mathcal{T}$-edge otherwise, we recover the vertex and edge sets $\mathcal{V}$ and $\mathcal{E}$.

For a finite subgraph $\widetilde{\mathcal{G}} \subset \mathcal{G}_d$, let $\mathcal{F}(\widetilde{\mathcal{G}})$ be the set of *bounded faces* of $\widetilde{\mathcal{G}}$, i.e. the closures of all bounded, connected components of $\mathbb{R}^2 \setminus \widetilde{\mathcal{G}}$. By local finiteness, each bounded face of $\widetilde{\mathcal{G}}$ is a finite union of bounded tiles $T \in \mathcal{T}$. Moreover, define $\mathcal{P}(\widetilde{\mathcal{G}})$ as the set of tiles $T \in \mathcal{T}$ with $\partial T \subseteq \widetilde{\mathcal{G}}$. Note that always

$$\mathcal{P}(\widetilde{\mathcal{G}}) \subseteq \mathcal{F}(\widetilde{\mathcal{G}}).$$

2.2 Metric Graphs

After assigning each edge $e \in \mathcal{E}$ a finite length $|e| \in (0, \infty)$, we obtain a *metric graph* $\mathcal{G} := (\mathcal{V}, \mathcal{E}, |\cdot|) = (\mathcal{G}_d, |\cdot|)$. Let us stress that in general $|e|$ is not related to the length of the Jordan arc in $\mathbb{R}^2$ representing the edge $e \in \mathcal{E}$. For a subgraph

$\widetilde{\mathcal{G}} = (\widetilde{\mathcal{V}}, \widetilde{\mathcal{E}}) \subset \mathcal{G}$, define its *boundary vertices* by

$$\partial_{\mathcal{G}} \widetilde{\mathcal{G}} := \left\{ v \in \widetilde{\mathcal{V}} \mid \deg_{\widetilde{\mathcal{G}}}(v) < \deg(v) \right\}, \tag{2.3}$$

where $\deg_{\widetilde{\mathcal{G}}}(v)$ denotes the degree of a vertex $v \in \widetilde{\mathcal{V}}$ with respect to $\widetilde{\mathcal{G}}$. For a given finite subgraph $\widetilde{\mathcal{G}} \subset \mathcal{G}$ we then set

$$\deg(\partial_{\mathcal{G}} \widetilde{\mathcal{G}}) := \sum_{v \in \partial_{\mathcal{G}} \widetilde{\mathcal{G}}} \deg_{\widetilde{\mathcal{G}}}(v). \tag{2.4}$$

Following [26], the *isoperimetric constant* of a metric graph $\mathcal{G}$ is then defined by

$$\alpha(\mathcal{G}) := \inf_{\widetilde{\mathcal{G}}} \frac{\deg(\partial_{\mathcal{G}} \widetilde{\mathcal{G}})}{\operatorname{mes}(\widetilde{\mathcal{G}})} \in [0, \infty), \tag{2.5}$$

where the infimum is taken over all finite, connected subgraphs $\widetilde{\mathcal{G}} \subset \mathcal{G}$ and $\operatorname{mes}(\widetilde{\mathcal{G}})$ denotes the measure (the "total length") of $\widetilde{\mathcal{G}}$ with respect to the edge length function $|\cdot|$, $\operatorname{mes}(\widetilde{\mathcal{G}}) := \sum_{e \in \widetilde{\mathcal{E}}} |e|$. We will say that the metric graph $\mathcal{G}$ satisfies the *strong isoperimetric inequality* if $\alpha(\mathcal{G}) > 0$.

Recall that for a combinatorial graph $\mathcal{G}_d = (\mathcal{V}, \mathcal{E})$ the *(combinatorial) isoperimetric constant* $\alpha_{\mathrm{comb}}(\mathcal{G}_d)$ is defined by (see, e.g., [10])

$$\alpha_{\mathrm{comb}}(\mathcal{G}_d) = \inf_{U \subset \mathcal{V}} \frac{\#\{e \in \mathcal{E} \mid e \text{ connects } U \text{ and } \mathcal{V} \setminus U\}}{\sum_{v \in U} \deg(v)}, \tag{2.6}$$

where the infimum is taken over all finite subsets $U \subset \mathcal{V}$. There is a close connection between $\alpha_{\mathrm{comb}}(\mathcal{G}_d)$ and $\alpha(\mathcal{G})$ and we refer for further details to [26].

We also need the following quantities. The *weight* $m(v)$ of a vertex $v \in \mathcal{V}$ is given by

$$m(v) = \sum_{e \in \mathcal{E}_v} |e|. \tag{2.7}$$

Clearly, $m(v)$ equals the measure (the "length") of the star $\mathcal{E}_v$. The *perimeter* $p(T)$ of a tile $T \in \mathcal{T}$ is defined as

$$p(T) := \begin{cases} \sum_{e \in \mathcal{E}_T} |e|, & T \in \mathcal{T} \text{ is bounded} \\ \infty, & T \in \mathcal{T} \text{ is unbounded} \end{cases}. \tag{2.8}$$

For every $e \in \mathcal{E}$, we define its *characteristic value* $c(e)$ by

$$c(e) := \frac{1}{|e|} - \sum_{v : v \in e} \frac{1}{m(v)} - \sum_{T : e \subseteq \partial T} \frac{1}{p(T)}. \tag{2.9}$$

Here we employ the convention that whenever ∞ appears in a denominator, the corresponding fraction $1/p$ has to be interpreted as zero if p is infinite. Let us mention that for equilateral metric graphs $\mathcal{G}$ (i.e. $|e| \equiv 1$ for all $e \in \mathcal{E}$), the characteristic value $c(e)$ coincides with the characteristic edge value introduced in [37] in the context of combinatorial graphs.

Finally, we need the following class of subgraphs of $\mathcal{G}$. A subgraph $\widetilde{\mathcal{G}} = (\widetilde{\mathcal{V}}, \widetilde{\mathcal{E}}) \subset \mathcal{G}$ is called *star-like*, if it can be written as a finite, connected union of stars. More precisely,

$$\widetilde{\mathcal{E}} = \bigcup_{v \in \widetilde{U}} \mathcal{E}_v$$

for some finite, connected vertex set $\widetilde{U} \subseteq \widetilde{\mathcal{V}}$.

Also, for a finite subgraph $\widetilde{\mathcal{G}} \subset \mathcal{G}$, we define its *interior graph* $\widetilde{\mathcal{G}}_{\mathrm{int}} = (\widetilde{\mathcal{V}}_{\mathrm{int}}, \widetilde{\mathcal{E}}_{\mathrm{int}})$ as the set of interior vertices $v \in \widetilde{\mathcal{V}}_{\mathrm{int}} := \widetilde{\mathcal{V}} \setminus \partial\widetilde{\mathcal{G}}$ together with all edges between such vertices. We say that $\widetilde{\mathcal{G}}$ is *complete*, if $\mathcal{F}(\widetilde{\mathcal{G}}_{\mathrm{int}}) = \mathcal{P}(\widetilde{\mathcal{G}}_{\mathrm{int}})$, or equivalently if every bounded face of $\widetilde{\mathcal{G}}_{\mathrm{int}}$ consists of exactly one tile $T \in \mathcal{T}$. Let us denote the class of star-like complete subgraphs by $\mathcal{S}(\mathcal{G})$.

3 Strong Isoperimetric Inequality for Tessellating Quantum Graphs

Now we are in position to formulate our main results. Our first theorem relates the positivity of the isoperimetric constant with the positivity of the characteristic values of a metric graph.

Theorem 3.1 *Let $\mathcal{G} = (\mathcal{V}, \mathcal{E}, |\cdot|)$ be a tessellating metric graph having infinite volume,* $\mathrm{mes}(\mathcal{G}) = \sum_{e\in\mathcal{E}} |e| = \infty$. *If*

$$\ell^*(\mathcal{G}) := \sup_{e\in\mathcal{E}} |e| < \infty \tag{3.1}$$

and

$$\liminf_{\mathrm{mes}(\widetilde{\mathcal{G}})\to\infty} \frac{1}{\mathrm{mes}(\widetilde{\mathcal{G}})} \sum_{e\in\widetilde{\mathcal{E}}} c(e)|e| = \liminf_{\mathrm{mes}(\widetilde{\mathcal{G}})\to\infty} \frac{\sum_{e\in\widetilde{\mathcal{E}}} c(e)|e|}{\sum_{e\in\widetilde{\mathcal{E}}} |e|} > 0, \tag{3.2}$$

then $\alpha(\mathcal{G}) > 0$. Here, the lim inf *is taken over all star-like complete subgraphs $\widetilde{\mathcal{G}} \in \mathcal{S}(\mathcal{G})$.*

Remark 3.2

(i) Let us mention that (3.1) is necessary for the strong isoperimetric inequality to hold for an arbitrary metric graph since (see, e.g., [26, Remark 3.3])

$$\alpha(\mathcal{G}) \leq \frac{2}{\ell^*(\mathcal{G})}. \tag{3.3}$$

(ii) If $\mathrm{mes}(\mathcal{G}) = \sum_{e\in\mathcal{E}} |e| < \infty$, then the lower bound

$$\alpha(\mathcal{G}) \geq \frac{2}{\mathrm{mes}(\mathcal{G})} > 0 \tag{3.4}$$

holds. In fact, if $\mathcal{G}$ is tessellating, then $\deg(\partial\widetilde{\mathcal{G}}) \geq 2$ for every finite subgraph $\widetilde{\mathcal{G}} \subset \mathcal{G}$ and (3.4) follows immediately from (2.5).

(iii) Theorem 3.1 can be seen as the analogue of [37, Theorem 1].

(iv) As we will see below, the proof of Theorem 3.1 implies the explicit estimate

$$\alpha(\mathcal{G}) \geq \min\left\{\frac{2}{\ell^*(\mathcal{G})}, \inf_{\widetilde{\mathcal{G}}\in\mathcal{S}} \frac{1}{\mathrm{mes}(\widetilde{\mathcal{G}})} \sum_{e\in\widetilde{\mathcal{E}}} c(e)|e|\right\}, \tag{3.5}$$

however, the conditions in Theorem 3.1 are weaker than positivity of the right-hand side in (3.5).

The next result shows that pointwise estimates for the characteristic values also yield lower estimates for the isoperimetric constant. To this end, introduce the following quantities

$$M(\mathcal{G}) := \sup_{v\in\mathcal{V}} \frac{m(v)}{\inf_{e\in\mathcal{E}_v} |e|}, \qquad P(\mathcal{G}) := \sup_{T\in\mathcal{T}} \frac{p(T)}{\inf_{e\in\mathcal{E}_T} |e|}, \tag{3.6}$$

and set

$$K(\mathcal{G}) := 1 - \frac{1}{M(\mathcal{G})} - \frac{2}{P(\mathcal{G})} - \frac{1}{(M(\mathcal{G})-2)P(\mathcal{G})}. \tag{3.7}$$

Theorem 3.3 *Let $\mathcal{G} = (\mathcal{V}, \mathcal{E}, |\cdot|)$ be a tessellating metric graph. Suppose*

$$c_*(\mathcal{G}) := \inf_{e\in\mathcal{E}} c(e) > 0. \tag{3.8}$$

Then

$$\alpha(\mathcal{G}) \geq \frac{c_*(\mathcal{G})}{K(\mathcal{G})} > 0. \tag{3.9}$$

Theorem 3.3 can be considered as the metric graph analogue of the corresponding estimate for combinatorial graphs in [24, Theorem 1].

Remark 3.4 The following obvious estimates

$$M(\mathcal{G}) \geq \sup_{v\in\mathcal{V}} \deg(v) \geq 3, \qquad P(\mathcal{G}) \geq \sup_{T\in\mathcal{T}} d_{\mathcal{T}}(T) \geq 3, \tag{3.10}$$

imply that $K(\mathcal{G}) \leq 1$. Moreover, one can show that $K(\mathcal{G}) > 0$ if $c_*(\mathcal{G}) > 0$. Indeed, noting that

$$m(v) \leq \deg(v)\ell^*(\mathcal{G}), \qquad p(T) \leq d_{\mathcal{T}}(T)\ell^*(\mathcal{G}),$$

we easily get the rough estimate

$$c_*(\mathcal{G}) \leq \frac{1}{\ell^*(\mathcal{G})}\Big(1 - \frac{2}{\deg^*(\mathcal{G})} - \frac{2}{d^*_{\mathcal{T}}(\mathcal{G})}\Big), \tag{3.11}$$

where $\deg^*(\mathcal{G}) := \sup_{v\in\mathcal{V}} \deg(v)$ and $d^*_{\mathcal{T}}(\mathcal{G}) := \sup_{T\in\mathcal{T}} d_{\mathcal{T}}(T)$. On the other hand,

$$\begin{aligned} K(\mathcal{G}) &= \frac{1}{2}\Big(1 - \frac{2}{M(\mathcal{G})} - \frac{2}{P(\mathcal{G})}\Big) + \frac{1}{2} - \frac{1}{P(\mathcal{G})} - \frac{1}{(M(\mathcal{G})-2)P(\mathcal{G})} \\ &\geq \frac{1}{2}\Big(1 - \frac{2}{\deg^*(\mathcal{G})} - \frac{2}{d^*_{\mathcal{T}}(\mathcal{G})}\Big) + \frac{1}{2} - \frac{1}{d^*_{\mathcal{T}}(\mathcal{G})} - \frac{1}{(\deg^*(\mathcal{G})-2)d^*_{\mathcal{T}}(\mathcal{G})}. \end{aligned}$$

If $c_*(\mathcal{G}) > 0$, then so is the right-hand side in (3.11) which implies

$$\begin{aligned} K(\mathcal{G}) &> \frac{1}{2} - \frac{1}{d^*_{\mathcal{T}}(\mathcal{G})} - \frac{1}{(\deg^*(\mathcal{G})-2)d^*_{\mathcal{T}}(\mathcal{G})} \\ &> \frac{1}{\deg^*(\mathcal{G})} - \frac{1}{(\deg^*(\mathcal{G})-2)d^*_{\mathcal{T}}(\mathcal{G})} \geq 0. \end{aligned}$$

To prove Theorems 3.1 and 3.3, we first show that we can restrict in (2.5) to star-like complete subgraphs.

Lemma 3.5 *Let $\mathcal{G} = (\mathcal{V}, \mathcal{E}, |\cdot|)$ be a tessellating metric graph. Then*

$$\alpha(\mathcal{G}) = \min\Big\{\frac{2}{\ell^*(\mathcal{G})}, \alpha_{\mathcal{S}}(\mathcal{G})\Big\}, \tag{3.12}$$

where

$$\alpha_{\mathcal{S}}(\mathcal{G}) := \inf_{\widetilde{\mathcal{G}}\in\mathcal{S}} \frac{\deg(\partial\widetilde{\mathcal{G}})}{\operatorname{mes}(\widetilde{\mathcal{G}})}. \tag{3.13}$$

Proof

(i) First, we show that it suffices to consider subgraphs that are either star-like or consist of a single edge. Let $\widetilde{\mathcal{G}} = (\widetilde{\mathcal{V}}, \widetilde{\mathcal{E}})$ be a finite, connected subgraph of $\mathcal{G}$ and $\widetilde{\mathcal{V}}_{\text{int}} = \widetilde{\mathcal{V}} \setminus \partial\widetilde{\mathcal{G}}$. We split $\widetilde{\mathcal{V}}_{\text{int}} = \bigcup_{i=1}^{n} \mathcal{V}_i$ into a finite, disjoint union of connected vertex sets $\mathcal{V}_i$. Let $\mathcal{G}_i = (\mathcal{V}_i, \mathcal{E}_i) \subset \mathcal{G}$ be the subgraph with edge set

$$\mathcal{E}_i = \bigcup_{v \in \mathcal{V}_i} \mathcal{E}_v.$$

By construction, each $\mathcal{G}_i$ is star-like and each edge $e \in \mathcal{E}$ belongs to at most one $\mathcal{G}_i$. Let $\mathcal{E}_r = \widetilde{\mathcal{E}} \setminus \bigcup_{i=1}^{n} \mathcal{E}_i$ be the remaining edges. Then

$$\operatorname{mes}(\widetilde{\mathcal{G}}) = \sum_{i=1}^{n} \operatorname{mes}(\mathcal{G}_i) + \sum_{e \in \mathcal{E}_r} |e|.$$

Moreover, both vertices of an edge $e \in \mathcal{E}_r$ are in $\partial\widetilde{\mathcal{G}}$ and $\partial\mathcal{G}_i = \partial\widetilde{\mathcal{G}} \cap \mathcal{V}_i$. Hence

$$\deg(\partial\widetilde{\mathcal{G}}) = \sum_{v \in \partial\widetilde{\mathcal{G}}} \sum_{i=1}^{n} \deg_{\mathcal{G}_i}(v) + 2\#\mathcal{E}_r = \sum_{i=1}^{n} \deg(\partial\mathcal{G}_i) + 2\#\mathcal{E}_r.$$

This finally implies

$$\frac{\deg(\partial\widetilde{\mathcal{G}})}{\operatorname{mes}(\widetilde{\mathcal{G}})} = \frac{\sum_{i=1}^{n} \deg(\partial\mathcal{G}_i) + 2\#\mathcal{E}_r}{\sum_{i=1}^{n} \operatorname{mes}(\mathcal{G}_i) + \sum_{e \in \mathcal{E}_r} |e|} \geq \min_{\substack{i=1,\dots,n,\\ e \in \mathcal{E}_r}} \left\{ \frac{\deg(\partial\mathcal{G}_i)}{\operatorname{mes}(\mathcal{G}_i)}, \frac{2}{|e|} \right\}.$$

(ii) To complete the proof, it suffices to construct for every star-like subgraph $\widetilde{\mathcal{G}}$ a star-like, complete subgraph $\widehat{\mathcal{G}} \in \mathcal{S}(\mathcal{G})$ with $\widehat{\mathcal{G}} \supseteq \widetilde{\mathcal{G}}$ and $\deg(\partial\widetilde{\mathcal{G}}) \geq \deg(\partial\widehat{\mathcal{G}})$. Let $\widetilde{\mathcal{G}}_{\text{int}} = (\widetilde{\mathcal{V}}_{\text{int}}, \widetilde{\mathcal{E}}_{\text{int}})$ be the interior graph of $\widetilde{\mathcal{G}}$. Denote by $\mathcal{F}_0$ the set of bounded, open components of $\mathbb{R}^2 \setminus \widetilde{\mathcal{G}}_{\text{int}}$ and by $\mathcal{F} = \{F = \overline{f} \mid f \in \mathcal{F}_0\}$ the bounded faces of $\widetilde{\mathcal{G}}_{\text{int}}$. The idea is to add "edges contained in bounded faces". Define the subgraph $\widehat{\mathcal{G}} = (\widehat{\mathcal{V}}, \widehat{\mathcal{E}})$ by its edge set

$$\widehat{\mathcal{E}} = \widetilde{\mathcal{E}} \cup \bigcup_{v \in f:\ f \in \mathcal{F}_0} \mathcal{E}_v.$$

If an edge $e \in \mathcal{E}$ is incident to a vertex $v \in f$ with $f \in \mathcal{F}_0$, then its other vertex lies in $F = \overline{f}$. Hence $\deg_{\widehat{\mathcal{G}}}(v) = \deg_{\widetilde{\mathcal{G}}}(v)$ for every vertex v with $v \notin K := \bigcup_{F \in \mathcal{F}} F$. On the other hand, every vertex $v \in K$ belongs to $\widehat{\mathcal{G}}$ and satisfies $\deg_{\widehat{\mathcal{G}}}(v) = \deg_{\mathcal{G}}(v)$. Indeed, if $v \in F = \overline{f}$, then either $v \in f$ or $v \in \partial f \subseteq \widetilde{\mathcal{G}}_{\text{int}}$.

This implies $\partial\widehat{\mathcal{G}} \subseteq \partial\widetilde{\mathcal{G}}$ and $\deg(\partial\widetilde{\mathcal{G}}) \geq \deg(\partial\widehat{\mathcal{G}})$. Moreover, $\widehat{\mathcal{E}} = \cup_{v\in\widehat{U}}\mathcal{E}_v$, where

$$\widehat{U} = \widetilde{\mathcal{V}}_{\text{int}} \cup \bigcup_{f\in\mathcal{F}_0} \{v \in \mathcal{V} |\ v \in f\}.$$

Also, $\widehat{U}$ is finite by local finiteness and connected since $\widetilde{\mathcal{G}}$ is star-like and $\partial f \subseteq \widetilde{\mathcal{G}}_{\text{int}}$ for $f \in \mathcal{F}_0$. It remains to show that $\widehat{\mathcal{G}}$ is complete. Let $\widehat{F}$ be a bounded face of the interior graph $\widehat{\mathcal{G}}_{\text{int}}$. Suppose $T \in \mathcal{T}$ with $T \subseteq \widehat{F}$. Then $T \subseteq \widehat{F} \subseteq F$ for some bounded face F of $\widetilde{\mathcal{G}}_{\text{int}}$. In particular, $e \subseteq K$ for every edge $e \subseteq \partial T$. But every vertex $v \in K$ belongs to $\widehat{\mathcal{G}}_{\text{int}}$, and hence $\partial T \subseteq \widehat{\mathcal{G}}_{\text{int}}$ and $\widehat{F} = T$.

■

Remark 3.6 Combining (3.12) with (3.3), one concludes that the inequality

$$\frac{2}{\ell^*(\mathcal{G})} \leq \alpha_{\mathcal{S}}(\mathcal{G}) = \inf_{\widetilde{\mathcal{G}}\in\mathcal{S}} \frac{\deg(\partial\widetilde{\mathcal{G}})}{\text{mes}(\widetilde{\mathcal{G}})} \tag{3.14}$$

implies that

$$\alpha(\mathcal{G}) = \frac{2}{\ell^*(\mathcal{G})}. \tag{3.15}$$

In Example 4.3, we provide an explicit construction of a graph satisfying (3.14).

The next lemma contains the connection between $c(e)$ and $\alpha(\mathcal{G})$.

Lemma 3.7 *The following inequality*

$$\sum_{e\in\widetilde{\mathcal{E}}} c(e)|e| \leq \deg(\partial_{\mathcal{G}}\widetilde{\mathcal{G}}) \tag{3.16}$$

holds for any star-like, complete subgraph $\widetilde{\mathcal{G}} \in \mathcal{S}(\mathcal{G})$.

Proof Let $\widetilde{\mathcal{G}}_{\text{int}} = (\widetilde{\mathcal{V}}_{\text{int}}, \widetilde{\mathcal{E}}_{\text{int}})$ be the interior graph and $\mathcal{E}^b := \widetilde{\mathcal{E}} \setminus \widetilde{\mathcal{E}}_{\text{int}}$ the remaining edges. Then

$$\begin{aligned}\sum_{e\in\widetilde{\mathcal{E}}} c(e)|e| &= \sum_{e\in\widetilde{\mathcal{E}}} 1 - \sum_{v\in\widetilde{\mathcal{V}}} \frac{\text{mes}(\mathcal{E}_v \cap \widetilde{\mathcal{E}})}{m(v)} - \sum_{T\in\mathcal{T}} \frac{\text{mes}(\mathcal{E}_T \cap \widetilde{\mathcal{E}}_{\text{int}})}{p(T)} - \sum_{T\in\mathcal{T}} \frac{\text{mes}(\mathcal{E}_T \cap \mathcal{E}^b)}{p(T)} \\ &= \#\mathcal{E}^b + \#\widetilde{\mathcal{E}}_{\text{int}} - \#\widetilde{\mathcal{V}}_{\text{int}} - \#\mathcal{P}(\widetilde{\mathcal{G}}_{\text{int}}) \\ &\quad - \sum_{v\in\partial\widetilde{\mathcal{G}}} \frac{\text{mes}(\mathcal{E}_v \cap \widetilde{\mathcal{E}})}{m(v)} - \sum_{T\in\mathcal{T},\, \mathcal{E}_T\not\subseteq\widetilde{\mathcal{E}}_{\text{int}}} \frac{\text{mes}(\mathcal{E}_T \cap \widetilde{\mathcal{E}}_{\text{int}})}{p(T)} - \sum_{T\in\mathcal{T}} \frac{\text{mes}(\mathcal{E}_T \cap \mathcal{E}^b)}{p(T)},\end{aligned}$$

where $\mathcal{P}(\widetilde{\mathcal{G}}_{\text{int}})$ is the set of tiles $T \in \mathcal{T}$ with $\mathcal{E}_T \subseteq \widetilde{\mathcal{E}}_{\text{int}}$. By Euler's formula (see, e.g., [16])

$$\#\widetilde{\mathcal{E}}_{\text{int}} - \#\widetilde{\mathcal{V}}_{\text{int}} - \#\mathcal{F}(\widetilde{\mathcal{G}}_{\text{int}}) = -1,$$

Because $\widetilde{\mathcal{G}}$ is complete, $\mathcal{F}(\widetilde{\mathcal{G}}_{\text{int}}) = \mathcal{P}(\widetilde{\mathcal{G}}_{\text{int}})$ and $\sum |e|c(e)$ is equal to

$$\#\mathcal{E}^b - 1 - \sum_{v\in\partial\widetilde{\mathcal{G}}} \frac{\text{mes}(\mathcal{E}_v \cap \widetilde{\mathcal{E}})}{m(v)} - \sum_{T\in\mathcal{T},\, \mathcal{E}_T\not\subseteq\widetilde{\mathcal{E}}_{\text{int}}} \frac{\text{mes}(\mathcal{E}_T \cap \widetilde{\mathcal{E}}_{\text{int}})}{p(T)} - \sum_{T\in\mathcal{T}} \frac{\text{mes}(\mathcal{E}_T \cap \mathcal{E}^b)}{p(T)}.$$

Since $\widetilde{\mathcal{G}}$ is star-like, there are no edges $e \in \widetilde{\mathcal{E}}$ with both vertices in $\partial\widetilde{\mathcal{G}}$. Therefore, $\#\mathcal{E}^b = \deg(\partial\widetilde{\mathcal{G}})$ and the proof is complete. ∎

Remark 3.8 For future reference, observe that

$$\begin{aligned}\sum_{v\in\partial\widetilde{\mathcal{G}}} \frac{\text{mes}(\mathcal{E}_v \cap \widetilde{\mathcal{E}})}{m(v)} + \sum_{T\in\mathcal{T},\, \mathcal{E}_T\not\subseteq\widetilde{\mathcal{E}}_{\text{int}}} \frac{\text{mes}(\mathcal{E}_T \cap \widetilde{\mathcal{E}}_{\text{int}})}{p(T)} + \sum_{T\in\mathcal{T}} \frac{\text{mes}(\mathcal{E}_T \cap \mathcal{E}^b)}{p(T)} \\ \geq \sum_{v\in\partial\widetilde{\mathcal{G}}} \frac{\deg_{\widetilde{\mathcal{G}}}(v)}{M(\mathcal{G})} + \sum_{T\in\mathcal{T},\, \mathcal{E}_T\not\subseteq\widetilde{\mathcal{E}}_{\text{int}}} \frac{\#(\mathcal{E}_T \cap \widetilde{\mathcal{E}}_{\text{int}})}{P(\mathcal{G})} + \sum_{T\in\mathcal{T}} \frac{\#(\mathcal{E}_T \cap \mathcal{E}^b)}{P(\mathcal{G})}.\end{aligned}$$

This implies the following estimate

$$\begin{aligned}\sum_{e\in\widetilde{\mathcal{E}}} c(e)|e| \leq \deg(\partial\widetilde{\mathcal{G}})\Big(1 - \frac{1}{M(\mathcal{G})} - \frac{2}{P(\mathcal{G})}\Big) \\ - \frac{1}{P(\mathcal{G})} \sum_{e\in\widetilde{\mathcal{E}}_{\text{int}}} \#\big\{T \mid e \in \mathcal{E}_T \text{ and } \mathcal{E}_T \not\subseteq \widetilde{\mathcal{E}}_{\text{int}}\big\}\end{aligned} \tag{3.17}$$

for every star-like, complete subgraph $\widetilde{\mathcal{G}} \in \mathcal{S}(\mathcal{G})$.

Corollary 3.9 *Let $\mathcal{G} = (\mathcal{V}, \mathcal{E}, |\cdot|)$ be a finite tessellating metric graph, that is a finite graph satisfying all the assumptions of Sect. 2.1 except (iii) of Definition 2.1. Then*

$$\sum_{e\in\mathcal{E}} -c(e)|e| = 1. \tag{3.18}$$

Proof By Euler's formula

$$\begin{aligned}\sum_{e\in\mathcal{E}} c(e)|e| &= \#\mathcal{E} - \sum_{v\in\mathcal{V}} \frac{\text{mes}(\mathcal{E} \cap \mathcal{E}_v)}{m(v)} - \sum_{T\in\mathcal{T}} \frac{\text{mes}(\mathcal{E} \cap \mathcal{E}_T)}{p(T)} \\ &= \#\mathcal{E} - \#\mathcal{V} - \#\mathcal{F}(\mathcal{G}) = -1.\end{aligned}$$

∎

Remark 3.10 Formula (3.18) can be seen as the analogue of the combinatorial Gauss–Bonnet formula known for combinatorial graphs (see [22, Proposition 1]). Let us also mention that the difference in the right-hand side arises from our convention $p(T) = \infty$ for unbounded $T \in \mathcal{T}$.

Theorem 3.1 now follows from Lemma 3.5 and 3.7 together with the inequality $\deg(\partial\widetilde{\mathcal{G}}) \geq 1$ for $\widetilde{\mathcal{G}} \in \mathcal{S}(\mathcal{G})$. Moreover, we can already deduce (see (3.5) and (3.11)) the basic estimate

$$\alpha(\mathcal{G}) \geq c_*(\mathcal{G}). \tag{3.19}$$

By improving this bound further we finally obtain Theorem 3.3.

Proof of Theorem 3.3 We start by providing a basic inequality. By Remark 3.4, we have $K(\mathcal{G}) > 0$. Let $\deg^*(\mathcal{G}) := \sup_{v\in\mathcal{V}} \deg(v)$. Then using (3.10) and (3.11), a lengthy but straightforward calculation implies

$$\frac{c_*(\mathcal{G})}{K(\mathcal{G})} \leq \frac{\deg^*(\mathcal{G}) - 2}{\deg^*(\mathcal{G}) - 1} \frac{1}{\ell^*(\mathcal{G})}. \tag{3.20}$$

Hence by Lemma 3.5, it suffices to show that

$$\frac{\deg(\partial\widetilde{\mathcal{G}})}{\mathrm{mes}(\widetilde{\mathcal{G}})} \geq \frac{c_*(\mathcal{G})}{K(\mathcal{G})} \tag{3.21}$$

for every $\widetilde{\mathcal{G}} = (\widetilde{\mathcal{V}}, \widetilde{\mathcal{E}}) \in \mathcal{S}(\mathcal{G})$.

We will obtain (3.21) by induction over $\#\widetilde{\mathcal{V}}_{\mathrm{int}}$. If $\#\widetilde{\mathcal{V}}_{\mathrm{int}} = 1$, that is, $\widetilde{\mathcal{V}}_{\mathrm{int}} = \{v\}$ for some $v \in \mathcal{V}$, then $\widetilde{\mathcal{G}}$ "consists of a single star". More precisely, $\widetilde{\mathcal{E}} = \mathcal{E}_v$ and (3.20) implies

$$\frac{\deg(\partial\widetilde{\mathcal{G}})}{\mathrm{mes}(\widetilde{\mathcal{G}})} \geq \frac{\deg(v)}{\deg(v)\ell^*(\mathcal{G})} \geq \frac{c_*(\mathcal{G})}{K(\mathcal{G})}.$$

Now suppose $\#\widetilde{\mathcal{V}}_{\mathrm{int}} = n \geq 2$ and (3.21) holds for all $\widehat{\mathcal{G}} \in \mathcal{S}(\mathcal{G})$ with $\#\widehat{\mathcal{V}}_{\mathrm{int}} < n$. We distinguish two cases:

(i) First, assume

$$\#\{u \in \partial\widetilde{\mathcal{G}} |\ u \text{ is connected to } v\} \leq \deg^*(\mathcal{G}) - 2$$

for all $v \in \widetilde{\mathcal{V}}_{\mathrm{int}}$. In view of (3.17), define

$$\mathcal{E}_i := \{e \in \widetilde{\mathcal{E}}_{\mathrm{int}} |\ \#\{T |\ e \in \mathcal{E}_T \text{ and } \mathcal{E}_T \not\subseteq \widetilde{\mathcal{E}}_{\mathrm{int}}\} = i\}$$

for $i \in \{1, 2\}$. Then

$$\sum_{e \in \widetilde{\mathcal{E}}_{\text{int}}} \#\{T |\, e \in \mathcal{E}_T \text{ and } \mathcal{E}_T \not\subseteq \widetilde{\mathcal{E}}_{\text{int}}\} = \#\mathcal{E}_1 + 2\#\mathcal{E}_2 = \sum_{v \in \widetilde{\mathcal{V}}_{\text{int}}} \delta(v),$$

where $\delta(v) := \#(\mathcal{E}_v \cap \mathcal{E}_1)/2 + \#(\mathcal{E}_v \cap \mathcal{E}_2)$ for all $v \in \mathcal{V}$.

Now assume that $v \in \widetilde{\mathcal{V}}_{\text{int}}$ and that v is connected to at least one vertex in $\partial\widetilde{\mathcal{G}}$. Since $\widetilde{\mathcal{G}}$ is star-like and $\#\widetilde{\mathcal{V}}_{\text{int}} \geq 2$, v is connected to another vertex in $\widetilde{\mathcal{V}}_{\text{int}}$ and hence there exists an interior edge $e \in \widetilde{\mathcal{E}}_{\text{int}}$ incident to v. Going through the edges incident to v in counter-clockwise direction starting from e, denote by e_+ the "last" edge incident to v with $e_+ \in \widetilde{\mathcal{E}}_{\text{int}}$. Define e_- analogously by going clockwise. Then $e_\pm \in \mathcal{E}_1 \cup \mathcal{E}_2$. Moreover, if $e_+ = e_-$, then $e = e_+ = e_- \in \mathcal{E}_2$. Thus $\delta(v) \geq 1$ for every such $v \in \widetilde{\mathcal{V}}_{\text{int}}$. Since $\widetilde{\mathcal{G}}$ is star-like,

$$\begin{aligned}\sum_{v \in \widetilde{\mathcal{V}}_{\text{int}}} \delta(v) &\geq \frac{1}{\deg^*(\mathcal{G}) - 2} \sum_{v \in \widetilde{\mathcal{V}}_{\text{int}}} \#\{u \in \partial\widetilde{\mathcal{G}} |\, u \text{ is connected to } v\} \\ &\geq \frac{1}{M(\mathcal{G}) - 2} \deg(\partial\widetilde{\mathcal{G}}),\end{aligned}$$

and (3.21) follows from (3.17).

(ii) Assume that $\#\{u \in \partial\widetilde{\mathcal{G}} |\, u \text{ is connected to } v\} \geq \deg^*(\mathcal{G}) - 1$ for some vertex $v \in \widetilde{\mathcal{V}}_{\text{int}}$. Since $\#\widetilde{\mathcal{V}}_{\text{int}} \geq 2$, this implies $\deg(v) = \deg^*(\mathcal{G})$ and that v is connected to exactly one $w \in \widetilde{\mathcal{V}}_{\text{int}}$. We "cut out" the $\deg^*(\mathcal{G}) - 1$ edges between v and $\partial\widetilde{\mathcal{G}}$ and define $\widehat{\mathcal{G}} = (\widehat{\mathcal{V}}, \widehat{\mathcal{E}})$ by its edge set

$$\widehat{\mathcal{E}} = \widetilde{\mathcal{E}} \setminus \{e \in \mathcal{E} |\, e \text{ connects } v \text{ and } \partial\widetilde{\mathcal{G}}\}.$$

Then $\widehat{\mathcal{G}}$ is again star-like and complete. Its interior graph $\widehat{\mathcal{G}}_{\text{int}} = (\widehat{\mathcal{V}}_{\text{int}}, \widehat{\mathcal{E}}_{\text{int}})$ is given by $\widehat{\mathcal{V}}_{\text{int}} = \widetilde{\mathcal{V}}_{\text{int}} \setminus \{v\}$ and $\widehat{\mathcal{E}}_{\text{int}} = \widetilde{\mathcal{E}}_{\text{int}} \setminus \{e_{v,w}\}$, where $e_{v,w}$ is the edge between v and w. In particular, $\widehat{\mathcal{G}}$ satisfies (3.21).

Now assume (3.21) fails for $\widetilde{\mathcal{G}}$. Then

$$\deg(\partial\widetilde{\mathcal{G}})(\text{mes}(\widetilde{\mathcal{G}}) - \text{mes}(\widehat{\mathcal{G}})) \leq (\deg^*(\mathcal{G}) - 2)\text{mes}(\widetilde{\mathcal{G}})$$

by (3.20). Consequently,

$$\begin{aligned}\frac{\deg(\partial\widehat{\mathcal{G}})}{\text{mes}(\widehat{\mathcal{G}})} = \frac{\#\widehat{\mathcal{E}} - \#\widehat{\mathcal{E}}_{\text{int}}}{\text{mes}(\widehat{\mathcal{G}})} &= \frac{\#\widetilde{\mathcal{E}} - \#\widetilde{\mathcal{E}}_{\text{int}} - \deg^*(\mathcal{G}) + 2}{\text{mes}(\widehat{\mathcal{G}})} \\ &= \frac{\deg(\partial\widetilde{\mathcal{G}}) - \deg^*(\mathcal{G}) + 2}{\text{mes}(\widehat{\mathcal{G}})} \leq \frac{\deg(\partial\widetilde{\mathcal{G}})}{\text{mes}(\widetilde{\mathcal{G}})} < \frac{c_*(\mathcal{G})}{K(\mathcal{G})},\end{aligned}$$

which is a contradiction. ∎

4 Examples

In this section, we illustrate the use of our results in three examples.

4.1 (p,q)-Regular Graphs

Let $p \in \mathbb{Z}_{\geq 3}$ and $q \in \mathbb{Z}_{\geq 3} \cup \{\infty\}$. A tessellating (combinatorial) graph $\mathcal{G}_d = (\mathcal{V}, \mathcal{E})$ is called (p, q)-*regular*, if $\deg(v) = p$ for all $v \in \mathcal{V}$ and $d_{\mathcal{T}}(T) = q$ for all $T \in \mathcal{T}$. Let $\mathcal{G}_{p,q}$ denote both the corresponding combinatorial graph and the associated equilateral metric graph, that is, we put $|e| \equiv 1$ for all $e \in \mathcal{E}_{p,q} = \mathcal{E}(\mathcal{G}_{p,q})$. Notice that $\mathcal{G}_{p,\infty}$ is an infinite p-regular tree $\mathbb{T}_p$ (also known as a *Cayley tree* or a *Bethe lattice*).

Next, by (2.9), we get

$$c(e) = 1 - \frac{2}{p} - \frac{2}{q} =: c_{p,q}, \tag{4.1}$$

for all $e \in \mathcal{E}_{p,q}$, and the *vertex curvature* of the combinatorial graph $\mathcal{G}_{p,q}$ (see for example [8, 17, 37]) is given by

$$\kappa(v) = 1 - \frac{\deg(v)}{2} + \sum_{T: v \in T} \frac{1}{d_{\mathcal{T}}(T)} = 1 - \frac{p}{2} + \frac{p}{q} = -\frac{p}{2}\, c_{p,q}, \tag{4.2}$$

for all $v \in \mathcal{V}$.

Since strictly positive vertex curvature implies that $\mathcal{G}_d$ has only finitely many vertices (see [8, Theorem 1.7]), the characteristic value should satisfy $c_{p,q} \geq 0$. Clearly, $c_{p,q} = 0$ exactly when $(p, q) \in \{(4, 4), (3, 6), (6, 3)\}$ and in these cases $\mathcal{G}_{p,q}$ is isomorphic to the square, hexagonal or triangle lattice in $\mathbb{R}^2$. If $c_{p,q} > 0$, then $\mathcal{G}_{p,q}$ is isomorphic to the edge graph of a tessellation of the Poincaré disc H^2 with regular q-gons of interior angle $2\pi/p$ (see [15, Remark 4.2.] and [21]). In the latter case, Theorem 3.3 implies $\alpha(\mathcal{G}_{p,q}) > 0$ and the estimate

$$\alpha(\mathcal{G}_{p,q}) \geq \frac{q(p-2)c_{p,q}}{q(p-1)c_{p,q} + 1} = \frac{p-2}{p-1} \times \begin{cases} \frac{1}{1+(q(p-1)\, c_{p,q})^{-1}}, & q < \infty \\ 1, & q = \infty \end{cases}. \tag{4.3}$$

Notice that in the case $q = \infty$, equality holds true in (4.3) (see, e.g., [26, Example 8.3]).

It is well-known that (see [15, 18]),

$$\alpha_{\mathrm{comb}}(\mathcal{G}_{p,q}) = \frac{p-2}{p} \sqrt{1 - \frac{4}{(p-2)(q-2)}}. \tag{4.4}$$

By (a slight modification of) [26, Lemma 4.1],

$$\alpha(\mathcal{G}) = \frac{2\alpha_{\mathrm{comb}}(\mathcal{G}_d)}{\alpha_{\mathrm{comb}}(\mathcal{G}_d)+1} \tag{4.5}$$

for every equilateral metric graph $\mathcal{G} = (\mathcal{V}, \mathcal{E}, |\cdot|)$ with underlying combinatorial graph $\mathcal{G}_d = (\mathcal{V}, \mathcal{E})$. Hence

$$\alpha(\mathcal{G}_{p,q}) = \frac{p-2}{p-1+\frac{p}{2}\left(\sqrt{\frac{(p-2)(q-2)}{pq-2(p+q)}}-1\right)} = \frac{p-2}{p-1} \times \begin{cases} \frac{1}{1+\delta(q(p-1)\,c_{p,q})^{-1}}, & q<\infty \\ 1, & q=\infty \end{cases}, \tag{4.6}$$

where

$$\delta := \frac{pq-2(p+q)}{2}\left(\sqrt{1+\frac{4}{pq-2(p+q)}}-1\right) \le 1.$$

Comparing (4.6) with (4.3), we conclude that the error in the estimate (4.3) is uniformly of order $\frac{1}{(pq)^2}$.

Finally, let us mention that using (4.5), we can turn (4.3) into a lower estimate for $\alpha_{\mathrm{comb}}(\mathcal{G}_{p,q})$ as well. After a short calculation, we recover Theorem 1 from [24],

$$\alpha_{\mathrm{comb}}(\mathcal{G}_{p,q}) \ge \frac{p-2}{p}\left(1-\frac{2}{(p-2)(q-2)-2}\right). \tag{4.7}$$

4.2 Another Example

Denote by $\mathbb{Z}^2_+$ the square lattice of the upper half-plane, i.e. the combinatorial graph with vertex set $\mathbb{Z}\times\mathbb{Z}_{\ge 0}$ and two vertices connected if and only if they are connected in the square lattice $\mathbb{Z}^2 = \mathbb{Z}\times\mathbb{Z}$. Fix $k \in \mathbb{Z}_{\ge 3}$ and let $\mathcal{G}_k$ be the graph obtained from $\mathbb{Z}^2_+$ by attaching to each vertex $v \in \mathbb{Z}\times\{0\}$ an infinite k-regular tree (see Fig. 1).

To assign edge lengths, we first define a partition of the edge set $\mathcal{E}_k$. We denote by $\mathcal{E}_{k,\mathrm{tree}}$ the set of edges $e \in \mathcal{E}_k$ belonging to one of the attached trees. Also, let

$$\mathcal{V}_n = \{(z,n)|\ z\in\mathbb{Z}\} = \mathbb{Z}\times\{n\}, \qquad n\in\mathbb{Z}_{\ge 0},$$

be the vertices on the "n-th horizontal line". For $n \in \mathbb{Z}_{\ge 0}$, we define $\mathcal{E}^+_{k,n}$ as the set of "vertical" edges between the n-th horizontal line $\mathcal{V}_n$ and the $(n+1)$-th horizontal line $\mathcal{V}_{n+1}$, and $\mathcal{E}^-_{k,n}$ as the set of "horizontal" edges connecting vertices

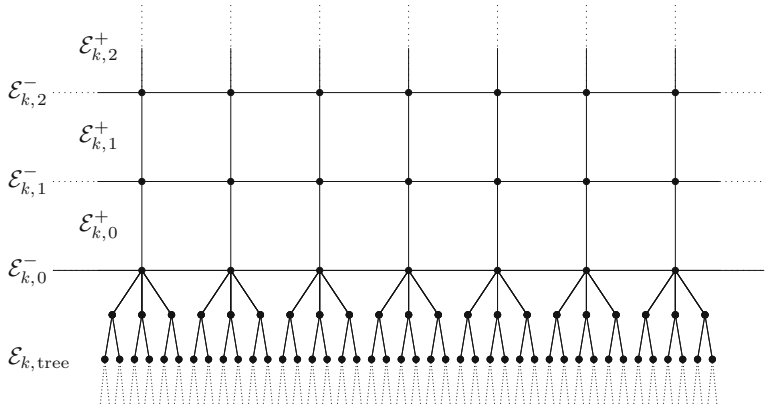

Fig. 1 $\mathcal{G}_k$ for $k = 3$

in the n-th horizontal line $\mathcal{V}_n$ (see Fig. 1). Finally, we equip $\mathcal{G}_k$ with edge lengths in the following way:

$$|e| = \begin{cases} 1, & e \in \mathcal{E}_{k,\mathrm{tree}} \\ \frac{1}{(2n+2)^2}, & e \in \mathcal{E}^-_{k,n} \\ \frac{1}{(2n+3)^2}, & e \in \mathcal{E}^+_{k,n} \end{cases}. \tag{4.8}$$

Now let us compute the characteristic values. First of all, for all $e \in \mathcal{E}_{k,\mathrm{tree}}$ we have the estimate

$$\inf_{e \in \mathcal{E}_{k,\mathrm{tree}}} c(e) = 1 - \frac{2}{k} = \frac{k-2}{k}.$$

Next, taking into account that $k \geq 3$, we get

$$c(e) = 4 - \frac{2}{k + 2\frac{1}{4} + \frac{1}{9}} - \frac{1}{\frac{1}{4} + 2\frac{1}{9} + \frac{1}{16}} = \frac{164}{77} - \frac{2}{k + \frac{11}{18}} > 1$$

for all $e \in \mathcal{E}^-_{k,0}$, and

$$c(e) = 9 - \frac{1}{k + 2\frac{1}{4} + \frac{1}{9}} - \frac{1}{\frac{1}{9} + \frac{1}{25} + 2\frac{1}{16}} - \frac{2}{\frac{1}{4} + 2\frac{1}{9} + \frac{1}{16}} = \frac{8955}{5467} - \frac{1}{k + \frac{11}{18}} > 1$$

for $e \in \mathcal{E}^+_{k,0}$. Moreover, after lengthy but straightforward calculations one can see that

$$c(e) > 1$$

for all $e \in \mathcal{E}_{k,n}^{\pm}$ with $n \geq 1$. Thus we obtain

$$c_*(\mathcal{G}_k) = \inf_{e \in \mathcal{E}_{k,\text{tree}}} c(e) = \frac{k-2}{k} > 0, \tag{4.9}$$

and hence, by Theorem 3.3, $\alpha(\mathcal{G}_k) > 0$.

Now let us compute $K(\mathcal{G}_k)$. If $v \in \mathcal{V}_n$ with $n \geq 1$, then

$$\begin{aligned} \sup_{v \in \bigcup_{n\geq 1} \mathcal{V}_n} \frac{m(v)}{\inf_{e\in\mathcal{E}_v} |e|} &= \sup_{n\geq 1} (2n+3)^2 \left(\frac{1}{(2n+1)^2} + \frac{2}{(2n+2)^2} + \frac{1}{(2n+3)^2} \right) \\ &= \left(1 + \frac{2}{3}\right)^2 + 2\left(1 + \frac{1}{4}\right)^2 + 1 = \frac{497}{72} = 6.902\dot{7}. \end{aligned}$$

For $v \in \mathcal{V}_0$, we obtain

$$\frac{m(v)}{\inf_{e\in\mathcal{E}_v} |e|} = 9\left(k + 2\frac{1}{4} + \frac{1}{9}\right) = 9k + \frac{11}{2}.$$

Moreover, for the remaining vertices $v \in \mathcal{V}$ belonging to one of the attached trees,

$$\frac{m(v)}{\inf_{e\in\mathcal{E}_v} |e|} = k.$$

By assumption, $k \geq 3$ and hence $M(\mathcal{G}_k) = 9k + \frac{11}{2}$. In addition, $P(\mathcal{G}_k) = \infty$ since $\mathcal{T}$ contains unbounded tiles. Thus we obtain

$$K(\mathcal{G}_k) = 1 - \frac{1}{M(\mathcal{G}_k)} = \frac{18k+9}{18k+11}, \tag{4.10}$$

and Theorem 3.3 implies the lower estimate

$$\alpha(\mathcal{G}_k) \geq \frac{18k+11}{18k+9}\frac{k-2}{k}.$$

Our next goal is to derive an upper estimate. Denote by $\mathcal{T}$ the k-regular tree attached to the origin $o = (0,0) \in \mathbb{R}^2$. For $l \in \mathbb{Z}_{\geq 2}$, let $\widetilde{\mathcal{G}}_l$ be the subgraph consisting of all vertices in $\mathcal{T}$ that can be reached from o with a path using at most l edges and all edges between such vertices. Then it is straightforward to verify

$$\text{mes}(\widetilde{\mathcal{G}}_l) = \sum_{j=0}^{l-1} k(k-1)^j = \frac{k((k-1)^l - 1)}{k-2}, \quad \deg(\partial\widetilde{\mathcal{G}}_l) = k + k(k-1)^{l-1},$$

and as a consequence,

$$\lim_{l\to\infty} \frac{\deg(\partial\widetilde{\mathcal{G}}_l)}{\mathrm{mes}(\widetilde{\mathcal{G}}_l)} = \frac{k-2}{k-1} = \alpha(\mathbb{T}_k),$$

where $\mathbb{T}_k$ is the equilateral, k-regular tree (see Example 4.1 or [26, Example 8.3]). This implies the two-sided estimate

$$\frac{18k+11}{18k+9}\frac{k-2}{k} \le \alpha(\mathcal{G}_k) \le \frac{k-2}{k-1}.$$

In particular, $\alpha(\mathcal{G}_k) \to 1$ for $k \to \infty$.

Remark 4.1 The two above examples demonstrate the use of Theorem 3.3 in two different situations. First of all, let us mention that by [26, Corollary 4.4.] the metric graph $\mathcal{G}$ satisfies the strong isoperimetric inequality if $\ell^*(\mathcal{G}) < \infty$ and the combinatorial isoperimetric constant $\alpha_{\mathrm{comb}}(\mathcal{G}_d)$ is positive,

$$\alpha_{\mathrm{comb}}(\mathcal{G}_d) > 0.$$

In Example 4.1, the positivity of $\alpha_{\mathrm{comb}}(\mathcal{G}_{p,q})$ is known (see (4.4)) and hence it is a priori clear that $\alpha(\mathcal{G}) > 0$. However, Example 4.1 shows that in certain situations Theorem 3.3 gives a good quantitative estimate.

On the other hand, in Example 4.2 we have $\alpha_{\mathrm{comb}}(\mathcal{G}_k) = 0$ (since obviously $\alpha_{\mathrm{comb}}(\mathbb{Z}^2_+) = 0$), however, $\alpha(\mathcal{G}) > 0$. In particular, Theorem 3.3 shows that the isoperimetric constants of the combinatorial and metric graph behave differently.

4.3 Non-equilateral p-Regular Trees

We conclude with an example showing the use of Remark 3.6. For $p \in \mathbb{Z}_{\ge 6}$, let $\mathbb{T}_p$ be the equilateral, p-regular tree from Example 4.1. Fix an edge $\hat{e} \in \mathcal{E}(\mathbb{T}_p)$. In the following, we will consider $\mathbb{T}_p$ equipped with another choice of edge lengths. Define the metric graph $\mathcal{T}_p := (\mathbb{T}_p, |\cdot|)$ by assigning

$$|e| := \begin{cases} p, & e = \hat{e} \\ 1, & e \in \mathcal{E}(\mathbb{T}_p) \setminus \{\hat{e}\} \end{cases}.$$

Let $\widetilde{\mathcal{G}} \in \mathcal{S}(\mathcal{T}_p)$ be a star-like complete subgraph. If $\hat{e} \notin \widetilde{\mathcal{E}}$, then $\mathrm{mes}(\widetilde{\mathcal{G}}) = \#\widetilde{\mathcal{E}}$. If $\hat{e} \in \widetilde{\mathcal{E}}$, then $\widetilde{\mathcal{V}}_{\mathrm{int}} \neq \varnothing$ since $\widetilde{\mathcal{G}}$ is star-like. Hence

$$\mathrm{mes}(\widetilde{\mathcal{G}}) = \#\widetilde{\mathcal{E}} + p - 1 \le 2\#\widetilde{\mathcal{E}}.$$

Thus we conclude from (4.6) and Lemma 3.5 that

$$\alpha_{\mathcal{S}}(\mathcal{T}_p) = \inf_{\widetilde{\mathcal{G}}\in\mathcal{S}} \frac{\deg(\partial\widetilde{\mathcal{G}})}{\operatorname{mes}(\widetilde{\mathcal{G}})} \geq \frac{1}{2} \inf_{\widetilde{\mathcal{G}}\in\mathcal{S}} \frac{\deg(\partial\widetilde{\mathcal{G}})}{\#\widetilde{\mathcal{E}}} = \frac{1}{2}\alpha(\mathbb{T}_p) = \frac{1}{2}\frac{p-2}{p-1} \geq \frac{2}{5}$$

for all $p \geq 6$. On the other hand, $\ell^*(\mathcal{T}_p) = p \geq 6$ by assumption. Hence Remark 3.6 implies

$$\alpha(\mathcal{T}_p) = \frac{2}{\ell^*(\mathcal{T}_p)} = \frac{2}{p}.$$

Acknowledgments I thank Aleksey Kostenko for helpful discussions throughout the preparation of this article and Delio Mugnolo for useful comments and hints with respect to the literature.

References

1. N. Alon, *Eigenvalues and expanders*, Combinatorica, **6**, no. 2, 83–96 (1986).
2. N. Alon and V. D. Milman, λ_1, *isoperimetric inequalities for graphs, and superconcentrators*, J. Combin. Theory, Ser. B **38**, 73–88 (1985).
3. F. Bauer, M. Keller, and R. K. Wojciechowski, *Cheeger inequalities for unbounded graph Laplacians*, J. Eur. Math. Soc. **17**, 259–271 (2015).
4. O. Baues and N. Peyerimhoff, *Curvature and geometry of tessellating plane graphs*, Discrete Comput. Geom. **25**, 141–159 (2001).
5. G. Berkolaiko, R. Carlson, S. Fulling, and P. Kuchment, *Quantum Graphs and Their Applications*, Contemp. Math. 415, Amer. Math. Soc., Providence, RI, 2006.
6. G. Berkolaiko and P. Kuchment, *Introduction to Quantum Graphs*, Amer. Math. Soc., Providence, RI, 2013.
7. J. Cheeger, *A lower bound for the smallest eigenvalue of the Laplacian*, in: "Problems in Analysis" (Papers dedicated to Salomon Bochner, 1969), Princeton Univ. Press, Princeton, NJ, 195–199 (1970).
8. M. DeVos and B. Mohar, *An analogue of the Descartes-Euler formula for infinite graphs and Higuchi's conjecture*, Trans. Amer. Math. Soc. **359**, 3287–3300 (2007).
9. J. Dodziuk, *Difference equations, isoperimetric inequality and transience of certain random walks*, Trans. Amer. Math. Soc. **284**, 787–794 (1984).
10. J. Dodziuk and W. S. Kendall, *Combinatorial Laplacians and isoperimetric inequality*, in: K. D. Elworthy (ed.), "From local times to global geometry, control and physics" (Coventry, 1984/85), pp. 68–74, Pitman Res. Notes Math. Ser. **150**, Longman Sci. Tech., Harlow, 1986.
11. P. Exner, J. P. Keating, P. Kuchment, T. Sunada, and A. Teplyaev, *Analysis on Graphs and Its Applications*, Proc. Symp. Pure Math. **77**, Providence, RI, Amer. Math. Soc., 2008.
12. P. Exner, A. Kostenko, M. Malamud, and H. Neidhardt, *Spectral theory of infinite quantum graphs*, Ann. Henri Poincaré **19**, no. 11, 3457–3510 (2018).
13. K. Fujiwara, *The Laplacian on rapidly branching trees*, Duke. Math. J. **83**, no. 1, 191–202 (1996).
14. M. Gromov, *Hyperbolic groups*, Essays in group theory, Math. Sci. Res. Inst. Publ. **8**, 75–263 (1987).
15. O. Häggström, J. Jonasson, and R. Lyons, *Explicit isoperimetric constants and phase transitions in the random-cluster model*, Ann. Pobab. **30**(1), 443–473 (2002).
16. F. Harary, *Graph Theory*, Addison Wesley, 1969.

17. Y. Higuchi, *Combinatorial curvature for planar graphs.*, J. Graph Theory **38**(4), 220–229 (2001).
18. Y. Higuchi and T. Shirai, *Isoperimetric constants of* (d, f)*-regular planar graphs*, Interdiscip. Inform. Sci. **9**(2), 221–228 (2003).
19. B. Hua, J. Jost, and S. Liu, *Geometric analysis aspects of infinite semiplanar graphs with nonnegative curvature*, J. reine angew. Math. **700**, 1–36 (2015).
20. M. Ishida, *Pseudo-curvature of a graph*, lecture at "Workshop on topological graph theory", Yokohama National University, 1990.
21. B. Iversen, *Hyperbolic Geometry*, London Math. Soc. Student Texts, Cambridge Univ. Press, Cambridge, 1992.
22. M. Keller, *Curvature, geometry and spectral properties of planar graphs*, Discrete Comput. Geom. **46**(3), 500–525 (2011).
23. M. Keller and D. Mugnolo, *General Cheeger inequalities for p-Laplacians on graphs*, Nonl. Anal. **147**, 80–95 (2016).
24. M. Keller and N. Peyerimhoff, *Cheeger constants, growth and spectrum of locally tessellating planar graphs*, Math. Z., **268**(3–4),871–886 (2011).
25. J. B. Kennedy, P. Kurasov, G. Malenová, and D. Mugnolo, *On the spectral gap of a quantum graph*, Ann. Henri Poincaré **7**, 2439–2473 (2016).
26. A. Kostenko and N. Nicolussi, *Spectral estimates for infinite quantum graphs*, Calc. Var. PDEs, to appear, arXiv:1711.02428 (2017).
27. P. Kurasov, *On the spectral gap for Laplacians on metric graphs*, Acta Phys. Pol. A, **124**, 1060–1062 (2013).
28. A. Lubotzky, *Expander graphs in pure and applied mathematics*, Bull. Amer. Math. Soc. **49**, no. 1, 113–162 (2012).
29. H. P. McKean, *An upper bound to the spectrum of* Δ *on a manifold of negative curvature*, J. Differential Geometry **4**, 359–366 (1970).
30. B. Mohar, *Isoperimetric inequalities, growth, and the spectrum of graphs*, Linear Algebra Appl. **103**, 119–131 (1988).
31. B. Mohar, *Isoperimetric numbers of graphs*, J. Combin. Theory Ser. B **47**(3), 274–291 (1989).
32. B. Mohar, *Isoperimetric numbers and spectral radius of some infinite planar graphs*, Mathematica Slovaca **42**(4), 411–425 (1992).
33. S. Nicaise, *Spectre des réseaux topologiques finis*, Bull. Sci. Math., II. Sér., **111**, 401–413 (1987).
34. B. Oh, *Duality properties of strong isoperimetric inequalities on a planar graph and combinatorial curvatures*, Discrete Comput. Geom. **51**(4), 859–884 (2014).
35. O. Post, *Spectral Analysis on Graph-Like Spaces*, Lect. Notes in Math. **2039**, Springer-Verlag, Berlin, Heidelberg, 2012.
36. D. A. Stone, *A combinatorial analogue of a theorem of Myers*, Illinois J. Math. **20**(1), 12–21 (1976).
37. W. Woess, *A note on tilings and strong isoperimetric inequality*, Math. Proc. Cambridge Phil. Soc. **124**, 385–393 (1998).
38. W. Woess, *Random Walks on Infinite Graphs and Groups*, Cambridge Univ. Press, Cambridge, 2000.
39. A. Żuk, *On the norms of the random walks on planar graphs*, Ann. Inst. Fourier (Grenoble) **47**(5), 1463–1490 (1997).

Spectral Monotonicity for Schrödinger Operators on Metric Graphs

Jonathan Rohleder and Christian Seifert

Abstract We study the influence of certain geometric perturbations on the spectra of self-adjoint Schrödinger operators on compact metric graphs. Results are obtained for permutation invariant vertex conditions, which, amongst others, include δ and δ'-type conditions. We show that adding edges to the graph or joining vertices changes the eigenvalues monotonically. However, the monotonicity properties may differ from what is known for the previously studied cases of Kirchhoff (or standard) and δ-conditions and may depend on the signs of the coefficients in the vertex conditions.

Keywords Metric graphs · Schrödinger operators · Spectrum · Surgery principles

2010 Mathematics Subject Classification 34B45, 35P15 (primary), 47A10, 47B25, 81Q35 (secondary)

1 Introduction

Differential operators on metric graphs, also called quantum graphs, have been studied extensively during the last two decades, see e.g. the two monographs [3, 15] and the references therein. An aspect which came into focus rather recently is the behavior of the spectrum of Laplacians (or more general Schrödinger operators) on metric graphs under perturbations of the geometry and topology, see, e.g, [7, 13]. These so-called surgery principles appear to be a natural and very useful tool for

J. Rohleder (✉)
Matematiska Institutionen, Stockholms Universitet, Stockholm, Sweden
e-mail: jonathan.rohleder@math.su.se

C. Seifert
TU Hamburg, Institut für Mathematik, Hamburg, Germany
e-mail: christian.seifert@tuhh.de

F. M. Atay et al. (eds.), *Discrete and Continuous Models in the Theory of Networks*, Operator Theory: Advances and Applications 281,
https://doi.org/10.1007/978-3-030-44097-8_15

spectral investigation. They were applied successfully to derive Faber–Krahn type inequalities for graph Laplacians and eigenvalue estimates depending on various quantities of the graph such as the total length, the number of edges or vertices, the diameter or the Betti number, see [1, 2, 4, 8–11, 14, 16], where Kirchhoff (also called standard), δ, or Dirichlet conditions at the vertices were treated.

In the present paper two types of perturbations of the graph are considered for a more general class of vertex conditions. More specifically, for a compact metric graph Γ we focus on the change of the eigenvalues of a self-adjoint Schrödinger operator H in $L^2(\Gamma)$ when either

(i) an edge is added to the graph, or
(ii) two vertices of the graph are joined into a single vertex.

For the case of Kirchhoff or δ vertex conditions it is known that the eigenvalues behave non-increasing under the perturbation (i) if the additional edge connects a vertex of Γ to a new vertex of degree one while no general monotonicity principle is valid if the new edge connects two previously existing vertices, see [13]. For the graph transformation (ii), the eigenvalues of Schrödinger operators subject to Kirchhoff or δ-conditions are known to move non-decreasingly.

In order to study eigenvalue monotonicity under the graph transformations (i) and (ii) for more general couplings, one needs to specify how vertex conditions change; actually, each of these transformations leads to an increase of the vertex degree of certain vertices. Hence, we will consider the question only for those vertex conditions which admit a canonical or *natural* extension to a larger vertex degree. This is the case if the vertex conditions are permutation invariant, i.e., different edges incident to the same vertex are not distinguished by the vertex conditions. Permutation invariant vertex conditions include δ- and δ'-type conditions. They are discussed in detail and classified in Sect. 2 below; cf. Classification 2.3.

In the main results of this paper we observe that different types of permutation invariant vertex conditions behave differently under the considered transformations. Section 3 is devoted to the transformation (i). It turns out that there is a class of conditions for which, in contrast to Kirchhoff or δ-conditions, all eigenvalues behave monotonically non-increasing if an edge is added connecting two previously present vertices; this class includes so-called anti-Kirchhoff as well as δ'-type conditions, see Theorem 3.2. Moreover, in Theorem 3.5 it is shown that for all permutation invariant vertex conditions the eigenvalues behave non-increasingly if an edge connecting the specified vertex to a new vertex of degree one is added. These observations are complemented by examples. In Sect. 4 the behavior of the eigenvalues under the transformation (ii) is studied. It turns out that this transformation divides the permutation invariant conditions into three classes: those for which joining two vertices leads to non-decreasing eigenvalues (as for Kirchhoff and δ-conditions), those for which it leads, conversely, to non-increasing eigenvalues, and those for which the monotonicity properties depend on the signs of the coefficients in the vertex conditions. The latter applies e.g. to δ'-type conditions. The different classes of permutation invariant vertex conditions according to Classification 2.3 are treated in Theorems 4.1, 4.2 and 4.5. We would like to mention that all results depend

only on the vertex conditions at those vertices which are changed by the graph transformation. At all other vertices, general self-adjoint conditions are allowed.

The proofs of our results are all variational comparing Rayleigh quotients, which is a standard method in obtaining eigenvalue estimates. In fact, estimates on the quadratic form associated to the Schrödinger operator on suitable finite-dimensional subspaces together with an application of the min-max principle yield the desired estimates for the eigenvalues.

After conceiving the paper we learned about the manuscript [5] dealing also with monotonicity properties for the spectrum of the Laplacian with Kirchhoff, δ, and Dirichlet boundary conditions, but for a larger toolkit of surgery principles.

2 Schrödinger Operators with Permutation Invariant Vertex Conditions

In this section we introduce the operators under consideration. First we recall some general facts on self-adjoint vertex (or coupling) conditions. After that we restrict our considerations to a subclass, the permutation invariant conditions, which is suitable for the questions under investigation.

Let Γ be a finite, compact metric graph, i.e. a graph consisting of a finite vertex set $V := V(\Gamma)$ and a finite edge set $E := E(\Gamma)$ that is, additionally, equipped with a length function $L\colon E \to (0, \infty)$. We identify each edge $e \in E$ with the interval $[0, L(e)] \subseteq \mathbb{R}$ and obtain a natural metric on Γ. For each $e \in E$ we say that e has initial vertex v_i and terminal vertex v_t if e is incident to v_i and v_t such that v_i is identified with the zero endpoint of $[0, L(e)]$ and v_t is identified with the endpoint $L(e)$; note that v_i and v_t coincide if e is a loop. Furthermore, for each vertex $v \in V$ we denote by $E_{v,\mathrm{i}} \subseteq E$ ($E_{v,\mathrm{t}} \subseteq E$) the set of edges for which v is the initial vertex (terminal vertex) and by $\deg(v) = |E_{v,\mathrm{i}}| + |E_{v,\mathrm{t}}|$ the degree of v. Finally, by $L^2(\Gamma)$ we denote the usual L^2-space on Γ, which coincides with the direct sum $\bigoplus_{e\in E} L^2(0, L(e))$. For $f \in L^2(\Gamma)$ we denote by f_e the restriction of f to some edge $e \in E$. Moreover, for $k = 1, 2, \ldots$ we make use of the Sobolev spaces

$$\widetilde{H}^k(\Gamma) := \bigoplus_{e\in E} H^k(0, L(e)),$$

equipped with the standard Sobolev norms and inner products. Moreover, a function $f \in \widetilde{H}^1(\Gamma)$ is called continuous at a vertex $v \in V$ if for any two edges $e, \hat{e} \in E$ incident to v the values of f_e and $f_{\hat{e}}$ at v coincide.

In the following we consider Schrödinger operators in $L^2(\Gamma)$ acting as

$$(\mathcal{L}f)_e = -f_e'' + q_e f_e, \quad e \in E, \tag{2.1}$$

with a real-valued potential q; for simplicity, we assume that $q \in L^\infty(\Gamma)$. Sometimes we will impose mild sign conditions on q; cf. Remark 3.7.

In order to write down vertex conditions we make use of the following abbreviations. For any vertex $v \in V$ we fix enumerations $\{e_1, \dots, e_l\}$ and $\{e_{l+1}, \dots e_m\}$ of $E_{v,\mathrm{i}}$ and $E_{v,\mathrm{t}}$, respectively, where $l = |E_{v,\mathrm{i}}|$ and $m = \deg(v)$. For each sufficiently regular $f \in L^2(\Gamma)$ we write

$$F(v) := \begin{pmatrix} f_{e_1}(0) \\ \vdots \\ f_{e_l}(0) \\ f_{e_{l+1}}(L(e_{l+1})) \\ \vdots \\ f_{e_m}(L(e_m)) \end{pmatrix} \quad \text{and} \quad F'(v) := \begin{pmatrix} f'_{e_1}(0) \\ \vdots \\ f'_{e_l}(0) \\ -f'_{e_{l+1}}(L(e_{l+1})) \\ \vdots \\ -f'_{e_m}(L(e_m)) \end{pmatrix}.$$

Note that $F(v)$ is well-defined whenever $f \in \widetilde{H}^1(\Gamma)$ and $F'(v)$ is well-defined for $f \in \widetilde{H}^2(\Gamma)$. The latter denotes the collection of derivatives pointing out of v into the edges. The following description of all self-adjoint incarnations of $\mathcal{L}$ in $L^2(\Gamma)$ with local vertex conditions is standard, see, e.g., [3, Theorem 1.4.4].

Proposition 2.1 *Let Γ be a finite, compact metric graph, let $q \in L^\infty(\Gamma)$ be real-valued and let $\mathcal{L}$ be the Schrödinger differential expression in (2.1). For each vertex $v \in V$ let $P_{v,\mathrm{D}}$, $P_{v,\mathrm{N}}$ and $P_{v,\mathrm{R}}$ be orthogonal projections in $\mathbb{C}^{\deg(v)}$ with mutually orthogonal ranges such that $P_{v,\mathrm{D}} + P_{v,\mathrm{N}} + P_{v,\mathrm{R}} = I$ and let Λ_v be a self-adjoint, invertible operator in $\operatorname{ran} P_{v,\mathrm{R}}$. Then the operator H in $L^2(\Gamma)$ given by*

$$\begin{aligned} Hf &= \mathcal{L}f, \\ \operatorname{dom} H &= \Big\{ f \in \widetilde{H}^2(\Gamma) : P_{v,\mathrm{D}} F(v) = 0,\ P_{v,\mathrm{N}} F'(v) = 0, \\ &\qquad P_{v,\mathrm{R}} F'(v) = \Lambda_v P_{v,\mathrm{R}} F(v) \text{ for each } v \in V \Big\}, \end{aligned}$$

is self-adjoint (and each self-adjoint realization of $\mathcal{L}$ in $L^2(\Gamma)$ subject to local vertex conditions can be written in this form). Furthermore, the closed quadratic form h corresponding to the operator H is given by

$$\begin{aligned} h[f] &= \int_\Gamma |f'|^2 \mathrm{d}x + \int_\Gamma q|f|^2 \mathrm{d}x + \sum_{v \in V} \big\langle \Lambda_v P_{v,\mathrm{R}} F(v),\, P_{v,\mathrm{R}} F(v) \big\rangle, \\ \operatorname{dom} h &= \Big\{ f \in \widetilde{H}^1(\Gamma) : P_{v,\mathrm{D}} F(v) = 0 \text{ for each } v \in V \Big\}. \end{aligned}$$

Recall that by a standard compact embedding argument the spectrum of the Hamiltonian H on the compact graph Γ is always purely discrete and bounded from below, see, e.g., [12, Corollary 10 and Theorem 18]. In the following we denote by

$$\lambda_1(H) \le \lambda_2(H) \le \dots$$

the eigenvalues of H in non-decreasing order, counted with multiplicities. We remark that all eigenvalues are non-negative if $q \geq 0$ and Λ_v is non-negative for each vertex v. If H acts as the Laplacian, i.e. $q = 0$ identically on Γ, and the vertex conditions are Kirchhoff conditions at every vertex then $\lambda_1(H) = 0$ and the multiplicity of $\lambda_1(H)$ coincides with the number of connected components of Γ.

The focus of this paper is on the behavior of the spectrum under a change of the graph, namely adding extra edges to a vertex or joining two vertices. For general vertex conditions there is no natural extension in the case that edges are added to a vertex. However, such an extension exists if the vertex conditions are *permutation invariant*, that is, they do not distinguish between the edges incident to the vertex. However, the only subspaces of $\mathbb{C}^{\deg(v)}$ being invariant under all permutations are $\{0\}$, $\mathbb{C}^{\deg(v)}$, $\operatorname{span}\{(1,1,\dots,1)^\top\}$ and $(\operatorname{span}\{(1,1,\dots,1)^\top\})^\perp$. Therefore in the following we assume that each of the orthogonal projections $P_{v,\mathrm{D}}$, $P_{v,\mathrm{N}}$ and $P_{v,\mathrm{R}}$ involved in the vertex conditions projects onto one of these subspaces. The orthogonal projections onto $\operatorname{span}\{(1,1,\dots,1)^\top\}$ and $(\operatorname{span}\{(1,1,\dots,1)^\top\})^\perp$ are given by the $d \times d$-matrices

$$\mathcal{P} := \mathcal{P}_d = \begin{pmatrix} \frac{1}{d} & \cdots & \frac{1}{d} \\ \vdots & & \vdots \\ \frac{1}{d} & \cdots & \frac{1}{d} \end{pmatrix} \quad \text{and} \quad \mathcal{Q} := \mathcal{Q}_d = \begin{pmatrix} \frac{d-1}{d} & -\frac{1}{d} & \cdots & -\frac{1}{d} \\ -\frac{1}{d} & \ddots & \ddots & \vdots \\ \vdots & \ddots & \ddots & -\frac{1}{d} \\ -\frac{1}{d} & \cdots & -\frac{1}{d} & \frac{d-1}{d} \end{pmatrix},$$

where $d := \deg(v)$. Moreover, in order to make the conditions permutation invariant we assume that Λ_v is the multiplication by a constant. Note that, under these assumptions, if one of the projections is the identity (and, thus, the others are zero) then the vertex conditions do not reflect the connectivity of the graph but degenerate to decoupled Dirichlet, Neumann or Robin conditions. As we are not interested in this situation, we are left with the following assumption for the vertices to be changed. It comprises all permutation invariant vertex conditions that do not decouple the vertex.

Hypothesis 2.2 For a given vertex $v \in V$ we assume that $P_{v,\mathrm{D}}, P_{v,\mathrm{N}}, P_{v,\mathrm{R}} \in \{0, \mathcal{P}, \mathcal{Q}\}$ such that $P_{v,\mathrm{D}}$, $P_{v,\mathrm{N}}$ and $P_{v,\mathrm{R}}$ are mutually distinct. Moreover, we assume that Λ_v is the operator of multiplication by a constant in $\operatorname{ran} P_{v,\mathrm{R}}$.

Considering the vertex conditions in Proposition 2.1 under the additional assumption of Hypothesis 2.2 leads to a total of six different classes of conditions. They are described in the following.

Classification 2.3 Let Hypothesis 2.2 hold for some vertex $v \in V$. Then the vertex conditions at v have one of the following forms.

I. The first two cases correspond to $P_{v,\mathrm{D}} = \mathcal{Q}$.

(a) If $P_{v,\mathrm{N}} = \mathcal{P}$ and $P_{v,\mathrm{R}} = 0$ we get *Kirchhoff conditions*

$$f \text{ is continuous at } v \quad \text{and} \quad \sum_{j=1}^{\deg(v)} F_j'(v) = 0.$$

(b) For $P_{v,\mathrm{N}} = 0$, $P_{v,\mathrm{R}} = \mathcal{P}$ and Λ_v acting as multiplication by $\frac{\alpha_v}{\deg(v)}$ for some real $\alpha_v \neq 0$ we have *δ-conditions*

$$f \text{ is continuous at } v \quad \text{and} \quad \sum_{j=1}^{\deg(v)} F_j'(v) = \alpha_v f(v).$$

II. The next two cases are $P_{v,\mathrm{N}} = \mathcal{Q}$.

(a) If $P_{v,\mathrm{D}} = \mathcal{P}$ and $\mathcal{P}_{v,\mathrm{R}} = 0$ we have conditions which are known as *anti-Kirchhoff*, namely, the vector $F'(v)$ is constant and

$$\sum_{j=1}^{\deg(v)} F_j(v) = 0.$$

(b) If $P_{v,\mathrm{D}} = 0$, $P_{v,\mathrm{R}} = \mathcal{P}$ and Λ_v is multiplication by $\frac{\deg(v)}{\beta_v}$ for some real $\beta_v \neq 0$ we get *δ'-type conditions*, i.e., the vector $F'(v)$ is constant (let $f'(v)$ denote an arbitrary component of it) and

$$\sum_{j=1}^{\deg(v)} F_j(v) = \beta_v f'(v).$$

III. The remaining cases correspond to $P_{v,\mathrm{R}} = \mathcal{Q}$.

(a) For $P_{v,\mathrm{D}} = \mathcal{P}$, $P_{v,\mathrm{N}} = 0$ and Λ_v being multiplication with real $C_v \neq 0$ the conditions can be written as

$$\sum_{j=1}^{\deg(v)} F_j(v) = 0 \quad \text{and} \quad F_j'(v) - F_k'(v) = C_v(F_j(v) - F_k(v))$$

for all $j, k \in \{1, \dots, \deg(v)\}$.

(b) If $P_{v,\mathrm{D}} = 0$, $P_{v,\mathrm{N}} = \mathcal{P}$ and Λ_v is multiplication by $\frac{1}{D_v}$ for a real $D_v \neq 0$ we get

$$\sum_{j=1}^{\deg(v)} F_j'(v) = 0 \quad \text{and} \quad F_j(v) - F_k(v) = D_v(F_j'(v) - F_k'(v))$$

for all $j, k \in \{1, \dots, \deg(v)\}$.

Remark 2.4 The conditions of type III in Classification 2.3 appear less frequently in the literature. However, for instance the conditions III (b) were proposed in [6] as an alternative to the δ'-type conditions II (b) in the description of quantum particles on graphs, and their physical properties were discussed there.

As all proofs in the following sections will be based on calculations involving quadratic forms, we provide the following lemma. Its proof is a simple calculation and is left to the reader.

Lemma 2.5 *Let Γ be a finite, compact metric graph, let H be a self-adjoint Schrödinger operator in $L^2(\Gamma)$ as in Proposition 2.1, and let h be the corresponding quadratic form. Furthermore, let $v \in V$ and let the vertex conditions for H at v be given in terms of $P_{v,\mathrm{D}}$, $P_{v,\mathrm{N}}$, $P_{v,\mathrm{R}}$ and Λ_v. Assume that Hypothesis 2.2 holds for v. Then the following assertions hold for each $f \in \operatorname{dom} h$, where the types refer to Classification 2.3.*

(i) *If the conditions at v are of type I (a) then f is continuous at v and*

$$\left\langle \Lambda_v P_{v,\mathrm{R}} F(v),\, P_{v,\mathrm{R}} F(v) \right\rangle = 0.$$

(ii) *If the conditions at v are of type I (b) then f is continuous at v and*

$$\left\langle \Lambda_v P_{v,\mathrm{R}} F(v),\, P_{v,\mathrm{R}} F(v) \right\rangle = \alpha_v |f(v)|^2.$$

(iii) *If the conditions at v are of type II (a) then $\sum_{j=1}^{\deg(v)} F_j(v) = 0$ and*

$$\left\langle \Lambda_v P_{v,\mathrm{R}} F(v),\, P_{v,\mathrm{R}} F(v) \right\rangle = 0.$$

(iv) *If the conditions at v are of type II (b) then f does not satisfy any vertex conditions at v and*

$$\left\langle \Lambda_v P_{v,\mathrm{R}} F(v),\, P_{v,\mathrm{R}} F(v) \right\rangle = \frac{1}{\beta_v} \left| \sum_{j=1}^{\deg(v)} F_j(v) \right|^2.$$

(v) *If the conditions at v are of type III (a) then $\sum_{j=1}^{\deg(v)} F_j(v) = 0$ and*

$$\left\langle \Lambda_v P_{v,\mathrm{R}} F(v),\, P_{v,\mathrm{R}} F(v) \right\rangle = C_v \sum_{j=1}^{\deg(v)} |F_j(v)|^2.$$

(vi) *If the conditions at v are of type III (b) then f does not satisfy any vertex conditions at v and*

$$\left\langle \Lambda_v P_{v,\mathrm{R}} F(v),\, P_{v,\mathrm{R}} F(v) \right\rangle = \frac{1}{D_v} \left(\sum_{j=1}^{\deg(v)} |F_j(v)|^2 - \frac{1}{\deg(v)} \left| \sum_{j=1}^{\deg(v)} F_j(v) \right|^2 \right).$$

3 Attaching Edges

In this section we study the question how the spectrum of a graph Hamiltonian changes when we attach additional edges (or, more generally, whole graphs) to certain vertices of a given graph. This question was studied earlier for the Laplacian with Kirchhoff vertex conditions and the first positive eigenvalue (the spectral gap) in [13]. We provide two theorems depending on the conditions at those vertices where the additional edge or graph is attached. In order to avoid making the presentation over-complicated, in the theorems of this section we treat only the case of the Laplacian, i.e., the negative second derivative with zero potentials on the edges and discuss only adding one edge, either connecting two vertices of the original graph or a vertex of the original graph and a new vertex. We then discuss the general case of Schrödinger operators as well as attaching whole graphs in Remark 3.7 below.

The notion in the following definition will be used below when graph transformations lead to an increase of the degree of a vertex.

Definition 3.1 At a graph vertex v of degree d let vertex conditions satisfying Hypothesis 2.2 be given, that is, $P_{v,\mathrm{D}}, P_{v,\mathrm{N}}, P_{v,\mathrm{R}} \in \{0, \mathcal{P}_d, \mathcal{Q}_d\}$ are distinct and Λ_v acts as multiplication with a constant in $\operatorname{ran} P_{v,\mathrm{R}}$. Then the *natural extension* of these conditions to a vertex $\widetilde{v}$ of degree $\widetilde{d} > d$ is obtained by replacing $\mathcal{P}_d$ by $\mathcal{P}_{\widetilde{d}}$ and $\mathcal{Q}_d$ by $\mathcal{Q}_{\widetilde{d}}$ and letting $\Lambda_{\widetilde{v}}$ be the multiplication operator in $\operatorname{ran} P_{\widetilde{v},\mathrm{R}}$ with the constant corresponding to the same interaction strength as for Λ_v; i.e. multiplication with $\frac{\alpha_v}{\widetilde{d}}$ in case I (b), with $\frac{\widetilde{d}}{\beta_v}$ in case II (b), with C_v in case III (a) and with $\frac{1}{D_v}$ in case III (b).

We point out that proceeding from vertex conditions satisfying Hypothesis 2.2 to their natural extensions does not change the type of the conditions according to Classification 2.3.

The following theorem deals with adding an edge connecting two vertices v_1 and v_2 of a graph. The admissible vertex conditions include δ'-type and anti-Kirchhoff conditions.

Theorem 3.2 *Let Γ be a finite, compact metric graph, let v_1, v_2 be two distinct vertices of Γ and let H be the Laplacian in $L^2(\Gamma)$ subject to arbitrary local, self-adjoint vertex conditions at each vertex $v \in V \setminus \{v_1, v_2\}$, see Proposition 2.1, and having at each of the vertices v_1 and v_2 conditions either of type II (a) or II (b) or III (a) according to Classification 2.3 (not necessarily the same type at v_1 and v_2). Let $\widetilde{\Gamma}$ be the graph obtained from Γ by adding an extra edge of an arbitrary, finite length connecting v_1 and v_2, see Fig. 1. Moreover, let $\widetilde{H}$ be the Laplacian in $L^2(\widetilde{\Gamma})$ having the same vertex conditions as H on all $v \in V \setminus \{v_1, v_2\}$ and with the natural extension of the vertex conditions for H at v_1 and v_2. Then*

$$\lambda_k(\widetilde{H}) \leq \lambda_k(H)$$

holds for all $k \in \mathbb{N}$.

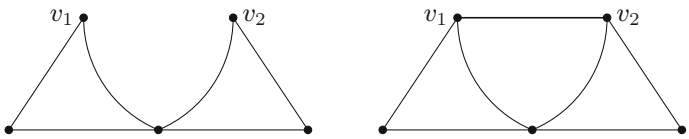

Fig. 1 The transformation of Theorem 3.2. Left: Γ, right: $\widetilde{\Gamma}$, i.e. attaching an edge connecting v_1 and v_2

Proof Let us denote by h and $\widetilde{h}$ the quadratic forms on $L^2(\Gamma)$ and $L^2(\widetilde{\Gamma})$ corresponding to the operators H and $\widetilde{H}$, respectively, see Proposition 2.1. Let $k \in \mathbb{N}$ and let $\mathcal{F}$ be a k-dimensional subspace of $\operatorname{dom} h$ such that

$$h[f] \leq \lambda_k(H) \int_\Gamma |f|^2 \mathrm{d}x \quad \text{for all } f \in \mathcal{F}.$$

For each $f \in \mathcal{F}$ denote by $\widetilde{f}$ the extension of f by zero to $\widetilde{\Gamma}$. Then the space $\widetilde{\mathcal{F}}$ formed by these extensions is k-dimensional, and $\widetilde{\mathcal{F}} \subset \operatorname{dom} \widetilde{h}$ as the conditions for h at v carry over to the corresponding conditions for $\widetilde{h}$. Moreover, for each $\widetilde{f} \in \widetilde{\mathcal{F}}$ we have

$$\begin{aligned}\widetilde{h}[\widetilde{f}] = \int_\Gamma |f'|^2 \mathrm{d}x + \sum_{v \in V \setminus \{v_1, v_2\}} \big\langle \Lambda_v P_{v,\mathrm{R}} F(v),\, P_{v,\mathrm{R}} F(v) \big\rangle \\ + \big\langle \widetilde{\Lambda}_{v_1} \widetilde{P}_{v_1,\mathrm{R}} \widetilde{F}(v_1),\, \widetilde{P}_{v_1,\mathrm{R}} \widetilde{F}(v_1) \big\rangle + \big\langle \widetilde{\Lambda}_{v_2} \widetilde{P}_{v_2,\mathrm{R}} \widetilde{F}(v_2),\, \widetilde{P}_{v_2,\mathrm{R}} \widetilde{F}(v_2) \big\rangle.\end{aligned} \tag{3.1}$$

Let us look at the term for v_1 in more detail. Our aim is to show

$$\big\langle \widetilde{\Lambda}_{v_1} \widetilde{P}_{v_1,\mathrm{R}} \widetilde{F}(v_1),\, \widetilde{P}_{v_1,\mathrm{R}} \widetilde{F}(v_1) \big\rangle = \big\langle \Lambda_{v_1} P_{v_1,\mathrm{R}} F(v_1),\, P_{v_1,\mathrm{R}} F(v_1) \big\rangle. \tag{3.2}$$

Indeed, if the conditions at v_1 are of type II (a) then $P_{v_1,\mathrm{R}} = 0$ and $\widetilde{P}_{v_1,\mathrm{R}} = 0$ so that (3.2) follows. If the conditions at v_1 are of type II (b) then by Lemma 2.5 (iv)

$$\begin{aligned}\big\langle \widetilde{\Lambda}_v \widetilde{P}_{v_1,\mathrm{R}} \widetilde{F}(v_1),\, \widetilde{P}_{v_1,\mathrm{R}} \widetilde{F}(v_1) \big\rangle &= \frac{1}{\beta_{v_1}} \Big| \sum_{j=1}^{d+1} \widetilde{F}_j(v) \Big|^2 = \frac{1}{\beta_{v_1}} \Big| \sum_{j=1}^{d} F_j(v) \Big|^2 \\ &= \big\langle \Lambda_{v_1} P_{v_1,\mathrm{R}} F(v_1),\, P_{v_1,\mathrm{R}} F(v_1) \big\rangle,\end{aligned}$$

where d is the degree of v_1 in Γ. This is (3.2). Finally, if the conditions at v_1 are of type III (a) then Lemma 2.5 (v) gives

$$\begin{aligned}\big\langle \widetilde{\Lambda}_v \widetilde{P}_{v_1,\mathrm{R}} \widetilde{F}(v_1),\, \widetilde{P}_{v_1,\mathrm{R}} \widetilde{F}(v_1) \big\rangle &= C_{v_1} \sum_{j=1}^{d+1} \big| \widetilde{F}_j(v) \big|^2 = C_{v_1} \sum_{j=1}^{d} \big| F_j(v) \big|^2 \\ &= \big\langle \Lambda_{v_1} P_{v_1,\mathrm{R}} F(v_1),\, P_{v_1,\mathrm{R}} F(v_1) \big\rangle,\end{aligned}$$

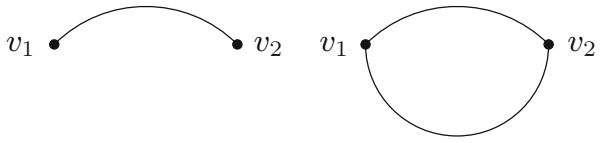

Fig. 2 The graphs in Example 3.3. Left: Γ, right: $\widetilde{\Gamma}$

which is again (3.2). Finally, combining (3.1) with (3.2) and its analogous counterpart for v_1 replaced by v_2 we get

$$\widetilde{h}[\widetilde{f}] = h[f] \leq \lambda_k(H) \int_\Gamma |f|^2 \mathrm{d}x = \lambda_k(H) \int_{\widetilde{\Gamma}} |\widetilde{f}|^2 \mathrm{d}x \quad \text{for all } \widetilde{f} \in \widetilde{\mathcal{F}},$$

which by the min-max principle implies the assertion of the theorem. ∎

The following example shows that Theorem 3.2 may fail for other conditions satisfying Hypothesis 2.2. For Kirchhoff conditions this example was discussed in [13, Example 1].

Example 3.3 Let Γ be the graph with two vertices v_1, v_2 and one edge of length 1 connecting these two, see Fig. 2. Let H be the Laplacian in $L^2(\Gamma)$ with a δ-condition of strength $\alpha \in \mathbb{R}$ at v_1 and a Kirchhoff condition at v_2. Note that both vertices have degree one; hence, the condition at v_1 is a Robin boundary condition and the one at v_2 is Neumann. Note further that for $\alpha = 0$ the condition at v_1 is Neumann, too. Moreover, let $\widetilde{\Gamma}$ be the graph obtained from Γ by adding another edge of length $\ell > 0$ that also connects v_1 to v_2, and let $\widetilde{H}$ be the Laplacian in $L^2(\widetilde{\Gamma})$ subject to the natural extensions of the conditions for H, namely a δ-condition of strength α at v_1 and a Kirchhoff condition at v_2. We look at two different cases.

If $\alpha = 0$ (see [13, Example 1]) then $\lambda_k(H) = \pi^2(k-1)^2$ for all $k \in \mathbb{N}$, and $\widetilde{H}$ is unitarily equivalent to the Laplacian on an interval of length $1 + \ell$ with periodic boundary conditions, which implies $\lambda_1(\widetilde{H}) = 0$ and $\lambda_{2k}(\widetilde{H}) = \lambda_{2k+1}(\widetilde{H}) = \frac{4\pi^2}{(1+\ell)^2} k^2$ for all $k \in \mathbb{N}$. Hence for $\ell < 1$ we observe $\lambda_2(\widetilde{H}) > \lambda_2(H)$, whereas for $\ell \geq 1$ we obtain $\lambda_k(\widetilde{H}) \leq \lambda_k(H)$ for all $k \in \mathbb{N}$ (and even a strict inequality for $k > 2$; for $\ell > 1$ the inequality is strict also for $k = 2$).

If $\alpha = 1$ then simple calculations yield $\lambda_1(H) \approx 0.74017$. Furthermore, letting $\ell = 0.1$ one obtains $\lambda_1(\widetilde{H}) \approx 0.83156$, that is, $\lambda_1(H) < \lambda_1(\widetilde{H})$. Hence, adding an edge may increase the eigenvalues also for $\alpha \neq 0$.

We would like to point out that we did not find an example for conditions of type III (b) violating the assertion of Theorem 3.2. We provide a further example that shows that the inequality in Theorem 3.2 can be strict for all $k \in \mathbb{N}$ simultaneously.

Example 3.4 Let Γ and $\widetilde{\Gamma}$ be as in the previous example, where the edge length in Γ is 1 and the edge lengths in $\widetilde{\Gamma}$ are 1 and $\ell > 0$, and let H and $\widetilde{H}$ be the Laplacians in $L^2(\Gamma)$ and $L^2(\widetilde{\Gamma})$, respectively, with type II (a) (anti-Kirchhoff) coupling conditions at both v_1 and v_2. For Γ this results in Dirichlet boundary conditions and, hence,

$\lambda_k(H) = \pi^2 k^2$ for all $k \in \mathbb{N}$. Moreover, $\widetilde{H}$ is unitarily equivalent to the Laplacian $\widehat{H}$ on the interval $[0, 1+\ell]$ with conditions $f(1-)+f(1+) = 0, -f'(1-) = f'(1+)$, $f(0) + f(1+\ell) = 0$ and $f'(0) = -f'(1+\ell)$. Hence, f is an eigenfunction of $\widehat{H}$ if and only if g defined by $g = f$ on $[0, \ell)$ and $g = -f$ on $(\ell, 1+\ell]$ is an eigenfunction of the Laplacian on $[0, 1+\ell]$ with periodic boundary conditions. We conclude that $\lambda_1(\widetilde{H}) = 0$ and $\lambda_{2k}(\widetilde{H}) = \lambda_{2k+1}(\widetilde{H}) = \frac{4\pi^2}{(1+\ell)^2}k^2$ for all $k \in \mathbb{N}$. Thus, $\lambda_k(\widetilde{H}) < \lambda_k(H)$ for all $k \in \mathbb{N}$, independent of the choice of ℓ.

In the next theorem we show that adding an edge connecting an old vertex to a new vertex of degree one does in most cases lead to a non-increase of all eigenvalues. For the special case of Kirchhoff vertex conditions this was discussed in [13, Theorem 2], see also [16, Proposition 3.1]. For the sake of completeness we indicate the proof also for this case.

Theorem 3.5 *Let Γ be a finite, compact metric graph, let v_1 be a vertex of Γ and let H be the Laplacian in $L^2(\Gamma)$ subject to arbitrary local, self-adjoint vertex conditions at each vertex $v \in V \setminus \{v_1\}$, see Proposition 2.1, and with a condition satisfying Hypothesis 2.2 at v_1. Let $\widetilde{\Gamma}$ be the graph obtained from Γ by adding an extra edge of an arbitrary, finite length connecting v_1 with a new vertex v_2 (i.e., $v_2 \notin V$ and v_2 has degree one in $\widetilde{\Gamma}$), see Fig. 3. Moreover, let $\widetilde{H}$ be the Laplacian in $L^2(\widetilde{\Gamma})$ having the same vertex conditions as H on all $v \in V \setminus \{v_1\}$, with the natural extension of the vertex conditions for H at v_1 and with any self-adjoint, local conditions at v_2. If the conditions at v_1 are of type I (a), I (b) or III (b) we assume in addition that the condition of $\widetilde{H}$ at v_2 is a δ (i.e. Robin) condition with $\alpha_{v_2} \leq 0$. Then*

$$\lambda_k(\widetilde{H}) \leq \lambda_k(H)$$

holds for all $k \in \mathbb{N}$.

Proof If the condition at v_1 is of type II (a), II (b) or III (a) then the proof is literally the same as for Theorem 3.2, and the result is independent of the boundary condition at the new vertex v_2. For the remaining cases let $k \in \mathbb{N}$ and let $\mathcal{F}$ be as in the proof of Theorem 3.2. If the condition at v_1 is of type I (Kirchhoff or δ) then each $f \in \mathcal{F}$ is continuous at v_1 and we define $\widetilde{f}$ to be the extension of f to $\widetilde{\Gamma}$ having the constant

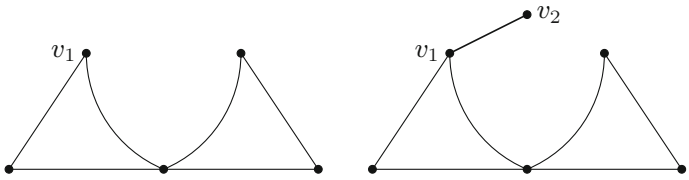

Fig. 3 The transformation of Theorem 3.5. Left: Γ, right: $\widetilde{\Gamma}$, i.e. adding an extra edge connecting v_1 and a new vertex v_2

value $f(v_1)$ on the new edge, and $\widetilde{\mathcal{F}}$ to be the collection of all such extensions of $f \in \mathcal{F}$. As the condition of $\widetilde{H}$ at v_2 is δ, it follows $\widetilde{\mathcal{F}} \subset \operatorname{dom} \widetilde{h}$. Moreover, by Lemma 2.5 (i) or (ii),

$$\begin{aligned}\left\langle \widetilde{\Lambda}_{v_1} \widetilde{P}_{v_1,\mathrm{R}} \widetilde{F}(v_1), \widetilde{P}_{v_1,\mathrm{R}} \widetilde{F}(v_1) \right\rangle &= \alpha_{v_1} |\widetilde{f}(v_1)|^2 = \alpha_{v_1} |f(v_1)|^2 \\ &= \left\langle \Lambda_{v_1} P_{v_1,\mathrm{R}} F(v_1), P_{v_1,\mathrm{R}} F(v_1) \right\rangle \end{aligned} \tag{3.3}$$

holds for the coefficient $\alpha_{v_1} \in \mathbb{R}$ of the condition at v_1. Moreover, at v_2 we have

$$\left\langle \widetilde{\Lambda}_{v_2} \widetilde{P}_{v_2,\mathrm{R}} \widetilde{F}(v_2), \widetilde{P}_{v_2,\mathrm{R}} \widetilde{F}(v_2) \right\rangle = \alpha_{v_2} |\widetilde{f}(v_2)|^2 \leq 0. \tag{3.4}$$

We plug (3.3) and (3.4) into (3.1), which remains valid in this situation, and obtain

$$\widetilde{h}[\widetilde{f}] \leq h[f] \leq \lambda_k(H) \int_\Gamma |f|^2 \mathrm{d}x \leq \lambda_k(H) \int_{\widetilde{\Gamma}} |\widetilde{f}|^2 \mathrm{d}x \quad \text{for all } \widetilde{f} \in \widetilde{\mathcal{F}}. \tag{3.5}$$

If the condition at v_2 is of type III (b) then for each $f \in \mathcal{F}$ we denote by $\widetilde{f}$ the extension to $\widetilde{\Gamma}$ being constantly equal to

$$\frac{1}{d} \sum_{j=1}^{d} F_j(v_1)$$

on the new edge, where d is the degree of v_1 in Γ. As above, we denote by $\widetilde{\mathcal{F}}$ the space of these extensions of all functions in $\mathcal{F}$. Then by Lemma 2.5 (vi)

$$\begin{aligned}\left\langle \widetilde{\Lambda}_{v_1} \widetilde{P}_{v_1,\mathrm{R}} \widetilde{F}(v_1), \widetilde{P}_{v_1,\mathrm{R}} \widetilde{F}(v_1) \right\rangle &= \frac{1}{D_{v_1}} \left(\sum_{j=1}^{d+1} |\widetilde{F}_j(v_1)|^2 - \frac{1}{d+1} \left| \sum_{j=1}^{d+1} \widetilde{F}_j(v_1) \right|^2 \right) \\ &= \frac{1}{D_{v_1}} \left(\sum_{j=1}^{d} |F_j(v_1)|^2 + \frac{1}{d^2} \left| \sum_{j=1}^{d} F_j(v_1) \right|^2 - \frac{1}{d+1} \left| \sum_{j=1}^{d} F_j(v_1) + \frac{1}{d} \sum_{j=1}^{d} F_j(v_1) \right|^2 \right) \\ &= \frac{1}{D_{v_1}} \left(\sum_{j=1}^{d} |F_j(v_1)|^2 - \frac{1}{d} \left| \sum_{j=1}^{d} F_j(v_1) \right|^2 \right) \\ &= \left\langle \Lambda_{v_1} P_{v_1,\mathrm{R}} F(v_1), P_{v_1,\mathrm{R}} F(v_1) \right\rangle. \end{aligned}$$

Together with

$$\left\langle \widetilde{\Lambda}_{v_2} \widetilde{P}_{v_2,\mathrm{R}} \widetilde{F}(v_2), \widetilde{P}_{v_2,\mathrm{R}} \widetilde{F}(v_2) \right\rangle = \alpha_{v_2} |\widetilde{f}(v_1)|^2 \leq 0$$

and (3.1) we arrive again at (3.5). As $\dim \widetilde{\mathcal{F}} = k$, the min-max principle implies the assertion of the theorem. ∎

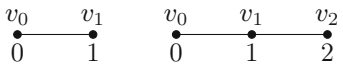

Fig. 4 The graphs in Example 3.6. Left: Γ, right: $\widetilde{\Gamma}$

The following example shows that in case we impose a Robin boundary condition with a positive coefficient or a Dirichlet boundary condition at the new vertex v_2, the assertion of the previous theorem may be false.

Example 3.6 Let Γ be the graph consisting of two vertices v_0 and v_1 and one edge connecting the two vertices, which is parametrised by the interval $(0, 1)$; cf. Fig. 4. Let us impose Kirchhoff conditions at v_0 and v_1. Since the degree is one in both cases, these conditions correspond to Neumann boundary conditions for H at 0 and at 1. Hence, $\lambda_k(H) = (k-1)^2\pi^2$ for all $k \in \mathbb{N}$. Now, let us add an edge of length one, which connects v_1 with v_2, see Fig. 4. At the vertex v_2 we impose either the condition $f'(2) + \alpha f(2) = 0$ for some $\alpha > 0$ or a Dirichlet condition. Then the spectrum of $\widetilde{H}$ is nonnegative and it is easy to see by solving the respective boundary value problem that $\lambda_1(\widetilde{H}) \neq 0$. Hence

$$\lambda_1(\widetilde{H}) > 0 = \lambda_1(H),$$

which shows that the assertion of Theorem 3.5 is not valid here.

Let us add some concluding remarks on generalizations of the results of this section.

Remark 3.7

(a) As the proofs show, the statements of Theorem 3.2 and Theorem 3.5 remain true if the Laplacian on Γ is replaced by a Schrödinger operator with a real-valued potential $q \in L^\infty(\Gamma)$. Furthermore, the statement of Theorem 3.2 remains valid if an arbitrary bounded, measurable, real-valued potential is introduced on the new edge, and the same is true for Theorem 3.5 if the conditions at v_1 are of type II (a), II (b) or III (a). In the remaining cases of Theorem 3.5 it is easy to see that the statement remains true if the potential $q_{\widetilde{e}}$ on the new edge $\widetilde{e}$ satisfies

$$\int_0^{L(\widetilde{e})} q_{\widetilde{e}}\,\mathrm{d}x \leq 0.$$

(b) Instead of just adding one edge in Theorem 3.2, the result remains valid when one attaches a whole compact metric graph to a subset $V_0 \subset V$ provided the conditions at each vertex of V_0 have one of the types II (a), II (b) or III (a). Also in the situation of Theorem 3.5 we can add a whole compact metric graph to one vertex, but in that case appropriate assumptions on the vertex conditions of the attached graph need to be imposed. We do not discuss this here in more detail.

4 Joining Vertices

In this section we study the behavior of eigenvalues when joining two vertices (with the same type of conditions) and merging their coupling conditions appropriately. In the following we say that two vertices v_1, v_2 of a graph are *joined* to one vertex v_0 if v_1 and v_2 are removed from Γ and, instead, a vertex v_0 with

$$E_{v_0,\mathrm{i}} := E_{v_1,\mathrm{i}} \cup E_{v_2,\mathrm{i}} \quad \text{and} \quad E_{v_0,\mathrm{t}} := E_{v_1,\mathrm{t}} \cup E_{v_2,\mathrm{t}}$$

is introduced. We point out that the process of joining two vertices does not affect the edge set of a metric graph. In particular, each function on the original graph can be identified naturally with a function on the new graph where v_1 and v_2 are joined to v_0, and vice versa. In particular, we will identify the spaces $L^2(\Gamma)$ and $L^2(\widetilde{\Gamma})$ if $\widetilde{\Gamma}$ was obtained from Γ by joining two vertices.

We start with the case of conditions of type I, i.e., Kirchhoff or δ-conditions. This situation was treated in [8, Theorem 2]. For completeness we include its simple proof here. We allow nonzero potentials on the edges as well as arbitrary self-adjoint conditions at the vertices that are not changed, which does not complicate the proof.

Theorem 4.1 *Let Γ be a finite, compact metric graph and let H be a Schrödinger operator in $L^2(\Gamma)$ with real-valued potential $q \in L^\infty(\Gamma)$ and local, self-adjoint vertex conditions at the vertices; cf. Proposition 2.1. Assume that v_1, v_2 are two distinct vertices of Γ and that the vertex conditions of H at v_1 and v_2 are of type I according to Classification 2.3, i.e. of δ-type with coefficients $\alpha_{v_1}, \alpha_{v_2} \in \mathbb{R}$ (coefficient zero corresponds to a Kirchhoff condition). Denote by $\widetilde{\Gamma}$ the graph obtained from Γ by joining v_1 and v_2 to form one single vertex v_0. Let $\widetilde{H}$ be the self-adjoint Schrödinger operator in $L^2(\widetilde{\Gamma})$ with potential q having the same vertex conditions as H at all vertices apart from v_0 and satisfying a δ-type condition with coefficient $\alpha_{v_0} := \alpha_{v_1} + \alpha_{v_2}$ at v_0. Then*

$$\lambda_k(H) \leq \lambda_k(\widetilde{H}) \tag{4.1}$$

holds for all $k \in \mathbb{N}$.

Proof Let h and $\widetilde{h}$ be the quadratic forms corresponding to the operators H and $\widetilde{H}$, respectively (see Proposition 2.1). For the inequality (4.1) it suffices to show the inequality for the quadratic forms, i.e., $\operatorname{dom}\widetilde{h} \subset \operatorname{dom} h$ and $h[f] \leq \widetilde{h}[f]$ for all $f \in \operatorname{dom}\widetilde{h}$. In fact, each function in $\operatorname{dom}\widetilde{h}$ is continuous at each vertex of $\widetilde{\Gamma}$ which clearly implies continuity at each vertex of Γ. In particular, each $f \in \operatorname{dom}\widetilde{h}$ satisfies $f(v_0) = f(v_1) = f(v_2)$, and by Lemma 2.5 (i) or (ii) we get

$$\widetilde{h}[f] - h[f] = \alpha_{v_0}|f(v_0)|^2 - \alpha_{v_1}|f(v_1)|^2 - \alpha_{v_2}|f(v_2)|^2 = 0,$$

which leads to the assertion. ∎

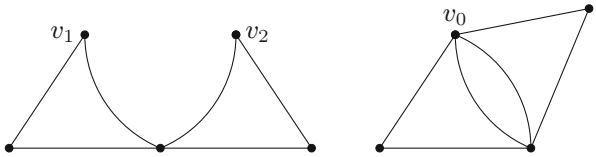

Fig. 5 The transformation of Theorems 4.1, 4.2 and 4.5. Left: Γ, right: $\widetilde{\Gamma}$, i.e. joining the vertices v_1 and v_2 to a new vertex v_0

In the next theorem we show that joining two vertices of type II can have a different effect on the eigenvalues, depending on the signs of the coupling coefficients. Recall that f satisfies conditions of type II at some vertex v if $F'(v)$ is a constant vector (let us call an arbitrary component $f'(v)$) and

$$\sum_{j=1}^{\deg(v)} F_j(v) = \beta_v f'(v). \tag{4.2}$$

These are δ'-type conditions for $\beta_v \neq 0$ and anti-Kirchhoff conditions for $\beta_v = 0$.

Theorem 4.2 *Let Γ be a finite, compact metric graph and let H be a Schrödinger operator in $L^2(\Gamma)$ with real-valued potential $q \in L^\infty(\Gamma)$ and local, self-adjoint vertex conditions at the vertices; cf. Proposition 2.1. Assume that v_1, v_2 are two distinct vertices of Γ and that each of the vertex conditions of H at v_1 and v_2 is of type II according to Classification 2.3, with coefficients $\beta_{v_1}, \beta_{v_2} \in \mathbb{R}$. Denote by $\widetilde{\Gamma}$ the graph obtained from Γ by joining v_1 and v_2 to form one single vertex v_0 (see Fig. 5) and let $\widetilde{H}$ be the self-adjoint Schrödinger operator in $L^2(\widetilde{\Gamma})$ with potential q, having the same vertex conditions as H at all vertices apart from v_0 and satisfying conditions of the form (4.2) at $v = v_0$ with coefficient $\beta_{v_0} := \beta_{v_1} + \beta_{v_2}$ at v_0. Then the following assertions hold.*

(i) *If $\beta_{v_1}, \beta_{v_2} > 0$ then $\lambda_k(\widetilde{H}) \leq \lambda_k(H)$ for all $k \in \mathbb{N}$.*
(ii) *If $\beta_{v_1}, \beta_{v_2} < 0$ then $\lambda_k(H) \leq \lambda_k(\widetilde{H})$ for all $k \in \mathbb{N}$.*
(iii) *If $\beta_{v_1} \cdot \beta_{v_2} < 0$ and $\beta_{v_0} > 0$ then $\lambda_k(H) \leq \lambda_k(\widetilde{H})$ for all $k \in \mathbb{N}$.*
(iv) *If $\beta_{v_1} \cdot \beta_{v_2} < 0$ and $\beta_{v_0} < 0$ then $\lambda_k(\widetilde{H}) \leq \lambda_k(H)$ for all $k \in \mathbb{N}$.*
(v) *If $\beta_{v_1} \cdot \beta_{v_2} < 0$ and $\beta_{v_0} = 0$ then $\lambda_k(H) \leq \lambda_k(\widetilde{H})$ for all $k \in \mathbb{N}$.*
(vi) *If $\beta_{v_1} \cdot \beta_{v_2} = 0$ then $\lambda_k(\widetilde{H}) \leq \lambda_k(H)$ for all $k \in \mathbb{N}$.*

The proof of this theorem relies on the following simple lemma.

Lemma 4.3 *Let $a, b \in \mathbb{C}$, $p, q, r > 0$, $\frac{1}{p} + \frac{1}{q} = \frac{1}{r}$. Then*

$$r|a+b|^2 \leq p|a|^2 + q|b|^2.$$

Proof Let $y > 0$. Then the Cauchy–Schwarz inequality yields

$$|a+b|^2 = \left| \left\langle \begin{pmatrix} \sqrt{y}a \\ \frac{b}{\sqrt{y}} \end{pmatrix}, \begin{pmatrix} \frac{1}{\sqrt{y}} \\ \sqrt{y} \end{pmatrix} \right\rangle \right|^2 \leq \left(y|a|^2 + \frac{|b|^2}{y} \right) \left(\frac{1}{y} + y \right)$$
$$= \left(1+y^2\right)|a|^2 + \left(\frac{1}{y^2}+1\right)|b|^2.$$

Let $y := \sqrt{\frac{p}{q}} > 0$. Then $1 + y^2 = 1 + \frac{p}{q} = \frac{p}{r}$ and $\frac{1}{y^2} + 1 = \frac{q}{p} + 1 = \frac{q}{r}$, and the desired inequality follows. ∎

Proof of Theorem 4.2 As in the proof of the previous theorem we show inequalities for the quadratic forms h and $\widetilde{h}$ corresponding to H and $\widetilde{H}$, respectively, under the different conditions. These form inequalities will immediately imply the statements. Let us first discuss the assertions (i)–(iv). These are the cases where the conditions for H at both v_1 and v_2 are of type II (b) and the same holds for the conditions for $\widetilde{H}$ at v_0. In particular, for functions in the form domain of h no conditions are imposed at v_1 and v_2, and the same holds for $\widetilde{h}$ and v_0. Hence the domains of h and $\widetilde{h}$ coincide. For $f \in \operatorname{dom} h = \operatorname{dom} \widetilde{h}$ let us set

$$a := \sum_{j=1}^{\deg(v_1)} F_j(v_1) \quad \text{and} \quad b := \sum_{j=1}^{\deg(v_2)} F_j(v_2). \tag{4.3}$$

Then

$$a + b = \sum_{j=1}^{\deg(v_0)} F_j(v_0)$$

and

$$\widetilde{h}[f] - h[f] = \frac{1}{\beta_{v_0}}|a+b|^2 - \frac{1}{\beta_{v_1}}|a|^2 - \frac{1}{\beta_{v_2}}|b|^2. \tag{4.4}$$

Now the assertions (i)–(iv) can be derived as follows:

(i) If both $\beta_{v_1}, \beta_{v_2} > 0$ (and hence $\beta_{v_0} > 0$) we set $p := \frac{1}{\beta_{v_1}}$, $q := \frac{1}{\beta_{v_2}}$ and $r := \frac{1}{\beta_{v_0}}$, and Lemma 4.3 together with (4.4) yields $\widetilde{h}[f] \leq h[f]$. Hence, $\widetilde{h} \leq h$.

(ii) If $\beta_{v_1}, \beta_{v_2} < 0$ (and hence $\beta_{v_0} < 0$) then Lemma 4.3 applied with $p = -\frac{1}{\beta_{v_1}}$, $q = -\frac{1}{\beta_{v_2}}$ and $r = -\frac{1}{\beta_{v_0}}$ and (4.4) yield $h[f] \leq \widetilde{h}[f]$ and, hence, $h \leq \widetilde{h}$.

(iii) If $\beta_{v_1} > 0$ and $\beta_{v_2} < 0$ such that $\beta_{v_0} = \beta_{v_1} + \beta_{v_2} > 0$ we set $p := \frac{1}{\beta_{v_0}}$, $q := -\frac{1}{\beta_{v_2}}$ and $r := \frac{1}{\beta_{v_1}}$, and by Lemma 4.3 we obtain

$$\frac{1}{\beta_{v_1}}|a|^2 = r|a|^2 = r|a+b-b|^2 \le p|a+b|^2 + q|b|^2 = \frac{1}{\beta_{v_0}}|a+b|^2 - \frac{1}{\beta_{v_2}}|b|^2.$$

Hence (4.4) yields $\widetilde{h}[f] \ge h[f]$, that is, $h \le \widetilde{h}$.

(iv) If $\beta_{v_1} > 0$ and $\beta_{v_2} < 0$ such that $\beta_{v_0} = \beta_{v_1} + \beta_{v_2} < 0$ we set $p := -\frac{1}{\beta_{v_0}}$, $q := \frac{1}{\beta_{v_1}}$ and $r := -\frac{1}{\beta_{v_2}}$. Then by Lemma 4.3 we obtain

$$-\frac{1}{\beta_{v_2}}|b|^2 = r|b|^2 = r|a+b-a|^2 \le p|a+b|^2 + q|a|^2 = -\frac{1}{\beta_{v_0}}|a+b|^2 + \frac{1}{\beta_{v_1}}|a|^2.$$

Together with (4.4) this gives $\widetilde{h}[f] \le h[f]$, that is, $\widetilde{h} \le h$.

It remains to treat the cases where zero appears as a coefficient. Under the conditions of (v), let $f \in \operatorname{dom}\widetilde{h}$. Then clearly $f \in \operatorname{dom} h$ (which does not require any conditions at v_1 or v_2) and with a and b defined in (4.3) we have $a + b = 0$. Thus

$$\widetilde{h}[f] - h[f] = -\frac{1}{\beta_{v_1}}|a|^2 - \frac{1}{\beta_{v_2}}|b|^2 = -\Big(\frac{1}{\beta_{v_1}} + \frac{1}{\beta_{v_2}}\Big)|a|^2 = 0$$

as $\beta_{v_2} = -\beta_{v_1}$. Hence $h \le \widetilde{h}$, which implies (v).

For the remaining assertion (vi) let us first look at the case $\beta_{v_1} = 0$, $\beta_{v_2} \ne 0$. In this situation let $f \in \operatorname{dom} h$. Then clearly $f \in \operatorname{dom}\widetilde{h}$ (no condition at v_0 is required since $\beta_{v_0} \ne 0$) and in the above notation we have $a = 0$. Then

$$\widetilde{h}[f] - h[f] = \frac{1}{\beta_{v_0}}|a+b|^2 - \frac{1}{\beta_{v_2}}|b|^2 = \frac{1}{\beta_{v_2}}|b|^2 - \frac{1}{\beta_{v_2}}|b|^2 = 0.$$

Thus $\widetilde{h} \le h$. The case $\beta_{v_1} \ne 0$, $\beta_{v_2} = 0$ is analogous. In the final case that $\beta_{v_0} = \beta_{v_1} = \beta_{v_2} = 0$ let $f \in \operatorname{dom} h$. Then in the above notation we have $a = b = 0$ and, in particular, $a + b = 0$ which implies $f \in \operatorname{dom}\widetilde{h}$. Moreover, we see directly $h[f] - \widetilde{h}[f] = 0$. Thus $\widetilde{h} \le h$. This completes the proof. ∎

We provide an example where a strict inequality appears in the setting of Theorem 4.2 (vi).

Example 4.4 Let Γ be the graph with two vertices and one edge of length 1 connecting these two and let H be the Laplacian in $L^2(\Gamma)$ with type II (a) (anti-Kirchhoff) couplings at both vertices; since the degree of the vertices is 1, this results in Dirichlet boundary conditions. Hence, $\lambda_k(H) = \pi^2 k^2$ for $k \in \mathbb{N}$. Now, let us join the two vertices, see Fig. 6.

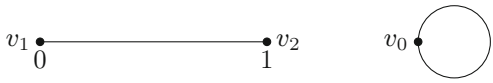

Fig. 6 Left: Γ, right: $\widetilde{\Gamma}$

Then $\widetilde{H}$ is unitarily equivalent to the Laplacian on the interval $[0, 1]$ with conditions $f'(0) = -f'(1)$ and $f(0) = -f(1)$, i.e. anti-periodic boundary conditions. Hence, $\lambda_{2k-1}(\widetilde{H}) = \lambda_{2k}(\widetilde{H}) = \pi^2(2k-1)^2$ for all $k \in \mathbb{N}$. Thus, the inequality between the eigenvalues is strict for the even indices and an equality for the odd indices.

The following last theorem of this section deals with joining vertices with conditions of type III (a) or (b). In view of the form of these conditions summing up the corresponding coefficients does not seem appropriate. Instead we join vertices with the same strength of interaction.

Theorem 4.5 *Let Γ be a finite, compact metric graph and let H be a Schrödinger operator in $L^2(\Gamma)$ with real-valued potential $q \in L^\infty(\Gamma)$ and local, self-adjoint coupling conditions at the vertices; cf. Proposition 2.1. Assume that v_1, v_2 are two distinct vertices of Γ such that the vertex conditions of H at v_1 and v_2 are either both of type III (a) according to Classification 2.3, with coefficients $C_{v_1} = C_{v_2} \in \mathbb{R}$ or both of type III (b) with coefficients $D_{v_1} = D_{v_2} \neq 0$. Denote by $\widetilde{\Gamma}$ the graph obtained from Γ by joining v_1 and v_2 to form one single vertex v_0. Let $\widetilde{H}$ be the self-adjoint Schrödinger operator in $L^2(\widetilde{\Gamma})$ with potential q having the same vertex conditions as H at all vertices apart from v_0 and satisfying, at v_0, conditions of the same form as H satisfies at v_1 and v_2, with $C_{v_0} := C_{v_1} = C_{v_2}$ or $D_{v_0} := D_{v_1} = D_{v_2}$, respectively, at v_0. Then the following assertions hold.*

(i) *If the conditions at v_1, v_2, v_0 are of type III (a) then $\lambda_k(\widetilde{H}) \leq \lambda_k(H)$ for all $k \in \mathbb{N}$.*
(ii) *If the conditions at v_1, v_2, v_0 are of type III (b) with coefficient $D_{v_0} > 0$ then $\lambda_k(H) \leq \lambda_k(\widetilde{H})$ for all $k \in \mathbb{N}$.*
(iii) *If the conditions at v_1, v_2, v_0 are of type III (b) with coefficient $D_{v_0} < 0$ then $\lambda_k(\widetilde{H}) \leq \lambda_k(H)$ for all $k \in \mathbb{N}$.*

Proof Let again h and $\widetilde{h}$ be the quadratic forms corresponding to H and $\widetilde{H}$, respectively. Let first the conditions at v_1, v_2, v_0 be of type III (a), let $f \in \operatorname{dom} h$, and let us set again

$$a := \sum_{j=1}^{\deg(v_1)} F_j(v_1) \quad \text{and} \quad b := \sum_{j=1}^{\deg(v_2)} F_j(v_2). \tag{4.5}$$

Then $a = b = 0$ and, hence, $a + b = 0$, so that $f \in \operatorname{dom}\widetilde{h}$. Moreover, by Lemma 2.5 (v),

$$\begin{aligned}\widetilde{h}[f] - h[f] &= C_{v_0} \sum_{j=1}^{\deg(v_0)} |F_j(v_0)|^2 - C_{v_1} \sum_{j=1}^{\deg(v_1)} |F_j(v_1)|^2 - C_{v_2} \sum_{j=1}^{\deg(v_2)} |F_j(v_2)|^2 \\ &= 0\end{aligned}$$

as $C_{v_0} = C_{v_1} = C_{v_2}$. Hence $\widetilde{h} \le h$, which implies (i).

Assume now that the conditions at v_1, v_2, v_0 are of type III (b). Then the domains of h and $\widetilde{h}$ coincide, and for each $f \in \operatorname{dom} h = \operatorname{dom}\widetilde{h}$ and a, b defined in (4.5), Lemma 2.5 (vi) yields

$$\begin{aligned}\widetilde{h}[f] - h[f] &= \frac{1}{D_{v_0}} \left(\sum_{j=1}^{\deg(v_0)} |F_j(v_0)|^2 - \frac{1}{\deg(v_0)} |a+b|^2 \right) \\ &\quad - \frac{1}{D_{v_1}} \left(\sum_{j=1}^{\deg(v_1)} |F_j(v_1)|^2 - \frac{1}{\deg(v_1)} |a|^2 \right) \\ &\quad - \frac{1}{D_{v_2}} \left(\sum_{j=1}^{\deg(v_2)} |F_j(v_2)|^2 - \frac{1}{\deg(v_2)} |b|^2 \right) \\ &= \frac{1}{D_{v_0}} \left(\frac{1}{\deg(v_1)} |a|^2 + \frac{1}{\deg(v_2)} |b|^2 - \frac{1}{\deg(v_0)} |a+b|^2 \right).\end{aligned}$$

As $\deg(v_0) = \deg(v_1) + \deg(v_2)$ we can apply Lemma 4.3 in order to see that the term in the brackets is always nonnegative. From this it follows that $h \le \widetilde{h}$ if $D_{v_0} > 0$ and $\widetilde{h} \le h$ if $D_{v_0} < 0$. This leads to the assertions (ii) and (iii). ∎

References

1. S. Ariturk, *Eigenvalue estimates on quantum graphs*, preprint, arXiv:1609.07471.
2. R. Band and G. Lévy, *Quantum graphs which optimize the spectral gap*, Ann. Henri Poincaré 18 (2017), 3269–3323.
3. G. Berkolaiko and P. Kuchment, Introduction to quantum graphs, Mathematical Surveys and Monographs 186, American Mathematical Society, Providence, RI, 2013.
4. G. Berkolaiko, J. Kennedy, P. Kurasov, and D. Mugnolo, *Edge connectivity and the spectral gap of combinatorial and quantum graphs*, J. Phys. A 50 (2017), 365201.
5. G. Berkolaiko, J. Kennedy, P. Kurasov, and D. Mugnolo, *Surgery principles for the spectral analysis of quantum graphs*, Trans. Amer. Math. Soc. 372 (2019), 5153–5197.
6. P. Exner, *Contact interactions on graph superlattices*, J. Phys. A 29 (1996), 87–102.
7. P. Exner and M. Jex, *On the ground state of quantum graphs with attractive δ-coupling*, Phys. Lett. A 376 (2012), 713–717.

8. G. Karreskog, P. Kurasov, and I. Trygg Kupersmidt, *Schrödinger operators on graphs: Symmetrization and Eulerian cycles*, Proc. Amer. Math. Soc. 144 (2016), 1197–1207.
9. J. Kennedy, *A sharp eigenvalue bound for quantum graphs in terms of their diameter*, to appear in Oper. Theory Adv. Appl. 281.
10. J. B. Kennedy, P. Kurasov, G. Malenová, and D. Mugnolo, *On the spectral gap of a quantum graph*, Ann. Henri Poincaré 17 (2016), 2439–2473.
11. A. Kostenko and N. Nicolussi, *Spectral estimates for infinite quantum graphs*, Calc. Var. Partial Differential Equations 58 (2019), paper no. 15.
12. P. Kuchment, *Quantum graphs: I. Some basic structures*, Waves Random Media 14 (2004), no. 1, S107–S128.
13. P. Kurasov, G. Malenová, and S. Naboko, *Spectral gap for quantum graphs and their connectivity*, J. Phys. A 46 (2013), 275309.
14. P. Kurasov and S. Naboko, *Rayleigh estimates for differential operators on graphs*, J. Spectral Theory 4 (2014), 211–219.
15. D. Mugnolo, Semigroup Methods for Evolution Equations on Networks, Springer, Berlin, 2014.
16. J. Rohleder, *Eigenvalue estimates for the Laplacian on a metric tree*, Proc. Amer. Math. Soc. 145 (2017), 2119–2129.

Random Graphs and Their Subgraphs

Klemens Taglieber and Uta Freiberg

Abstract Random graphs are more and more used for modeling real world networks such as evolutionary networks of proteins. For this purpose we look at two different models and analyze how properties like connectedness and degree distributions are inherited by differently constructed subgraphs. We also give a formula for the variance of the degrees of fixed nodes in the preferential attachment model and additionally draw a connection between weighted graphs and electrical networks.

1 Introduction

The modeling and analysis of random graphs is a good possibility to understand and examine real world networks. The first random graphs were introduced between 1959 and 1961 by Paul Erdős and Alfréd Rényi [4–6]. This model is connected to percolation theory which has several applications in physics. Up until today new models are developed such as the preferential attachment model which was worked out by László Barabási and Réka Albert [1] in 1999. This model is suitable for the modeling of most networks we are surrounded by such as the Internet, the World Wide Web or friendship networks. More and more random graphs are used in biology to analyze a variety of mechanisms like for example the spreading of epidemics or the evolution of proteins. Looking at protein networks the question arises if one can predict the not yet discovered proteins or even how the network and therefore the proteins will evolve.

At first we want to look at random graphs and their subgraphs and their different properties. We especially focus on the degree distributions which are calculated and plotted using `R` [9]. We will also compare subgraphs which are constructed in different ways and determine if this yields to different subgraphs. We finally look

K. Taglieber (✉) · U. Freiberg
Chemnitz University of Technology, Chemnitz, Germany
e-mail: klemens.taglieber@math.tu-chemnitz.de; uta.freiberg@math.tu-chemnitz.de

F. M. Atay et al. (eds.), *Discrete and Continuous Models in the Theory of Networks*, Operator Theory: Advances and Applications 281,
https://doi.org/10.1007/978-3-030-44097-8_16

at a protein network to find out if it can be constructed with one of the presented methods. The figures of graphs throughout the work are done with Gephi [2], a software for visualizing graphs and networks.

As an interesting intermezzo we generalize the results from [10] to weighted graphs.

We start in Sect. 2 by giving some basic definitions of graphs and random walks on graphs, as well as proving some relationships between graph theory and the theory of electrical networks. In Sect. 3 we introduce two models for constructing random graphs and analyze these graphs and their subgraphs concerning their degree distributions. We then investigate a protein network in Sect. 4 on the possibility of modeling it and finally in Sect. 5 we give an overview on further possibilities to model such protein networks.

2 Graphs

In this section we want to present some basic definitions and properties of graphs which are found in [3]. We will also introduce Markov chains on graphs and analyze some of their properties. Finally we look at graphs by interpreting them as electric networks to generalize the results from [10].

Definition 2.1 A *graph* G is a pair of disjoint sets (V, E) where $E \subseteq V \times V$ is consisting of unordered pairs of elements of V. The elements in V are called *nodes*, the elements of E *edges*. We call two nodes $x, y \in V$ *neighbors* if $\{x, y\} \in E$ and denote this with $x \sim y$.

We will only consider finite graphs here. A graph is called *finite* if V is only finitely large, i.e. $\#V < \infty$. For a finite graph with $\#V = n \in \mathbb{N}$ we denote $V = [n] := \{1, \ldots, n\}$.

Since in some cases we have more than one graph we will then denote V with $V(G)$ and E with $E(G)$.

Definition 2.2 Let $G = (V, E)$ be a graph with $V = [n]$ for some $n \in \mathbb{N}$. Its *adjacency matrix* is then an $n \times n$-matrix $A = (a_{xy})_{x,y \in V}$ where

$$a_{xy} := \mathbb{1}_{\{\{x,y\} \in E\}} := \begin{cases} 1, & \text{if } \{x, y\} \in E, \\ 0, & \text{otherwise.} \end{cases}$$

Definition 2.3 Let $G = (V, E)$ be a graph. The *degree* of a node $x \in V$ is given by

$$D(x) := \sum_{y \in V} \mathbb{1}_{\{\{x,y\} \in E\}} = \sum_{y \in V : y \sim x} 1 =: \sum_{y \sim x} 1.$$

By the definition of the adjacency matrix it follows directly for the degree of any node x that

$$D(x) = \sum_{y \in V} a_{xy}.$$

Definition 2.4 A *path* $P = (V(P), E(P))$ is a subgraph of $G = (V(G), E(G))$ with edge set $E(P) = \{\{x_0, x_1\}, \ldots, \{x_{k-1}, x_k\}\} \subseteq E(G)$ and vertex set $V(P) = \{x_0, \ldots, x_k\} \subseteq V(G)$. The length of P is given by the number of edges $k = \#E(P)$ it contains.

A path from x to y is a path with $x_0 = x$ and $x_k = y$. Let $G = (V, E)$ be a graph and $x, y \in V$ we then say that x and y are in the same component of G, if there exists a path from x to y.

If the graph G only consists of one component, we call it *connected*.

We now generalize our definitions to weighted graphs.

Definition 2.5 A *weighted graph* $G = (V, E, C)$ is a graph where we assign a weight $c_{xy} \in [0, \infty)$ to every pair $(x, y) \in V \times V$. We want the weights to be symmetric, hence $c_{xy} = c_{yx}$. The set of edges is then given by

$$E := \{\{x, y\} \in V \times V : c_{xy} > 0\}.$$

The weights $(c_{xy})_{x,y \in V}$, called conductances, give us analogously to the adjacency matrix the conductance matrix C of the graph.

Definition 2.6 Let $G = (V, E, C)$ be a weighted graph with edge weights $(c_{xy})_{x,y \in V}$, then the *conductance matrix* C of G is given by

$$C = (c_{xy})_{x,y \in V}.$$

Obviously the conductance matrix is symmetric. It is also possible to give an adjacency matrix for weighted graphs where $a_{xy} = \mathbb{1}_{\{c_{xy} > 0\}}$ for all $x, y \in V$.

Definition 2.7 Let $x \in V$ be a node of the weighted graph $G = (V, E, C)$ then the *generalized degree* of x–or *weight of node* x–is given by

$$\mu_x := \sum_{y \in V} c_{xy} = \sum_{y \sim x} c_{xy}.$$

If $c_{xy} \in \{0, 1\}$ for all $x, y \in V$ the graph is not weighted and it holds $\mu_x = D(x)$ for all $x \in V$.

2.1 Properties of Graphs and Markov Chains on Graphs

In the following we will consider a weighted graph $G = (V, E, C)$ with $V = [n]$, $E \subseteq V \times V$, where $\#E := m$, and conductance matrix C.

Definition 2.8 For all $x \in V$ let μ_x be the generalized degree of x. The *degree distribution* of G is then given by

$$\mathbb{P}(\mu_x \geq s) = \frac{1}{n} \sum_{y \in V} \mathbb{1}_{\{\mu_y \geq s\}}.$$

We call the degree distribution of G respectively the graph G itself scale free if for $s \in [0, \infty)$, some $c_n \in (0, \infty)$ and some $\tau > 1$ it holds that

$$\mathbb{P}(\mu_x \geq s) \asymp c_n s^{-(\tau-1)}.$$

Equivalently we can look at the total number of nodes with degree s or more denoted by $N_{\geq s}$ and get

$$N_{\geq s} \asymp \tilde{c}_n s^{-(\tau-1)} \text{ where } \tilde{c}_n \in (0, \infty).$$

For unweighted graphs it is sufficient to look at the number of nodes with exactly degree $k \in \mathbb{N}_0$ and the scale free property simplifies to $N_k \asymp \hat{c}_n k^{-\tau}$ for some $\hat{c}_n \in (0, \infty)$.

Definition 2.9 Let $G = (V, E, C)$ be a weighted graph with conductance matrix C and $(X_n)_{n \in \mathbb{N}_0}$ a homogeneous Markov chain with state space V. We then call $(X_n)_{n \in \mathbb{N}_0}$ *Markov chain on* G if its transition matrix $P = (p_{xy})_{x,y \in V}$ is for all $n \in \mathbb{N}$, $x, y \in V$ given by

$$p_{xy} = \mathbb{P}(X_n = y | X_{n-1} = x) := \frac{c_{xy}}{\sum_{z \sim x} c_{xz}} = \frac{c_{xy}}{\mu_x}.$$

Since the initial distribution of the Markov chain is not important here we will not worry about it.

Definition 2.10 The *hitting time of* $y \in V$ for the Markov chain $(X_n)_{n \in \mathbb{N}_0}$ on G is defined as

$$\tau_y := \inf\{n \geq 0 : X_n = y\}.$$

Definition 2.11 Let $G = (V, E, C)$ be a connected graph with $V = [n]$, $(X_n)_{n \in \mathbb{N}_0}$ a Markov chain on G and $x \in V$. We then call

$$\mathbb{E}^x(\tau_y) := \mathbb{E}(\tau_y | X_0 = x)$$

the *expected hitting time of* y *with start in* x.

For every $x \in V$ it obviously holds that $\mathbb{E}^x(\tau_x) = 0$.

Lemma 2.12 *For $x \neq y$ the expected hitting time of y with start in x satisfies*

$$\mathbb{E}^x(\tau_y) = 1 + \sum_{z \sim x} p_{xz} \mathbb{E}^z(\tau_y).$$

Proof By using the Markov property for the fourth equality we get

$$\begin{aligned}
\mathbb{E}^x(\tau_y) &= \mathbb{E}(\tau_y | X_0 = x) = \sum_{k \geq 1} k \mathbb{P}(\tau_y = k | X_0 = x) \\
&= \sum_{k \geq 1} k \sum_{z \sim x} \frac{\mathbb{P}(\tau_y = k, X_0 = x, X_1 = z)}{\mathbb{P}(X_0 = x)} \frac{\mathbb{P}(X_0 = x, X_1 = z)}{\mathbb{P}(X_0 = x, X_1 = z)} \\
&= \sum_{k \geq 1} k \sum_{z \sim x} \mathbb{P}(\tau_y = k | X_0 = x, X_1 = z) \mathbb{P}(X_1 = z | X_0 = x) \\
&= \sum_{z \sim x} p_{xz} \sum_{k \geq 1} k \mathbb{P}(\tau_y = k - 1 | X_0 = z) \\
&= \sum_{z \sim x} p_{xz} \mathbb{E}^z(\tau_y + 1) = 1 + \sum_{z \sim x} p_{xz} \mathbb{E}^z(\tau_y).
\end{aligned}$$

□

With the boundary condition $\mathbb{E}^y(\tau_y) = 0$ and Lemma 2.12 we get $T_x^y := \mathbb{E}^x(\tau_y)$ as the solution of

$$\begin{pmatrix} T_1^y \\ \vdots \\ T_n^y \end{pmatrix} = \begin{pmatrix} p_{11} & \cdots & p_{1n} \\ \vdots & \ddots & \vdots \\ p_{n1} & \cdots & p_{nn} \end{pmatrix} \cdot \begin{pmatrix} T_1^y \\ \vdots \\ T_n^y \end{pmatrix} + \begin{pmatrix} 1 \\ \vdots \\ 1 \end{pmatrix}. \tag{1}$$

Let $T^y := (T_1^y, \ldots, T_n^y)^T$, $\underline{1} := (1, \ldots, 1)^T \in \mathbb{R}^n$, then we can write Eq. (1) as

$$T^y = P \cdot T^y + \underline{1} \Leftrightarrow (P - I_n) \cdot T^y = -\underline{1},$$

hence the expected hitting times are the solution of an inhomogeneous system of linear equations.

By the linearity of expectations we can determine the commute time between two nodes. Let $\tau_x^y := \inf\{l \geq 0 : X_l = x \text{ and } \exists k \leq l \text{ with } X_k = y\}$ be the time the Markov chain $(X_n)_{n \in \mathbb{N}_0}$ needs to reach node y and then node x. The expected commute time $\mathbb{E}^x(\tau_x^y)$ is then given by

$$\mathbb{E}^x(\tau_x^y) = \mathbb{E}^x(\tau_y) + \mathbb{E}^y(\tau_x).$$

2.2 Graphs as Electrical Networks

As a short intermezzo we want to generalize the results of Tetali '91 [10] to weighted graphs. Therefore we want to consider the connected graph $G = (V, E, C)$ as an electrical network with n nodes and m edges. The graph itself is still undirected, even though at some points we will look at directed edges since the current on every edge is only flowing in one direction. When the direction of an edge is important we will consider (x, y) and (y, x) as two different edges. The conductances $(c_{xy})_{x,y\in V}$ are the upper threshold for the current on an edge and $r_{xy} = c_{xy}^{-1}$ is the resistance of the edge $\{x, y\}$. The weight of a node is still the sum over all conductances of incident edges to the node, hence

$$\mu_x = \sum_{y\sim x} c_{xy}.$$

For two adjacent nodes x and y we call i_{xy} the current flowing from x to y. Let $x, y \in V$ be two nodes we then call V_x the potential of x and V_y the potential of y. The potential between x and y is given by $V_{xy} := V_x - V_y$ and for $w, z \in V$ it holds

$$V_{wz} = V_w - V_z + V_y - V_y = V_w - V_y - (V_z - V_y) = V_{wy} - V_{zy}. \tag{2}$$

By Ohm's law, see for example [8], we have

$$V_{xy} = r_{xy} i_{xy} \text{ for } x \sim y, \tag{3}$$

and Kirchhoff's first law states that the current flowing into an inner node of the network is the same as the one flowing out of it, hence if the potential lies on x and y it holds for all $z \in V \setminus \{x, y\}$ that

$$\sum_{w\sim z} i_{wz} = 0. \tag{4}$$

We now can proof the following lemma.

Lemma 2.13 *Let $G = (V, E, C)$ be an electrical network with potentials $V_x > 0$ in x and $V_y = 0$ in y, hence current flowing from x to y. Then for all nodes $z \in V \setminus \{x, y\}$*

$$V_{zy} = \sum_{w\in V} p_{zw} V_{wy}.$$

Proof By Kirchhoff's first law (4) and Ohm's law (3) we get

$$\begin{aligned} 0 &\overset{(4)}{=} \sum_{w\sim z} i_{zw} \overset{(3)}{=} \sum_{w\sim z} \frac{V_{zw}}{r_{zw}} \\ &= \sum_{w\sim z} V_{zw} c_{zw} \overset{(2)}{=} \sum_{w\sim z} (V_{zy} - V_{wy}) c_{zw} \end{aligned}$$

$$= \sum_{w\sim z} V_{zy} c_{zw} - \sum_{w\sim z} V_{wy} c_{zw}$$
$$= V_{zy}\mu_z - \sum_{w\sim z} V_{wy} c_{zw}.$$

By solving for V_{zy} we get the desired statement

$$V_{zy} = \sum_{w\sim z} V_{wy} \frac{c_{zw}}{\mu_z} = \sum_{w\in V} p_{zw} V_{wy}.$$

□

We now want to draw a connection between random walks on graphs and electrical networks. We therefore define a random walk on G from x to y as the stopped Markov chain with start in x which is stopped when reaching y. Hence let $(X_n)_{n\in\mathbb{N}_0}$ be a Markov chain on G, τ_y the hitting time of y and

$$N_z^{xy} := \sum_{k=0}^{\tau_y - 1} \mathbb{1}_{\{X_k = z | X_0 = x\}} = \sum_{k=1}^{\tau_y - 1} \mathbb{1}_{\{X_k = z | X_0 = x\}} + \mathbb{1}_{\{z = x\}},\ z \in V \setminus \{y\}$$

the number of visits in z of a random walk from x to y.

Lemma 2.14 *Let $U_z^{xy} := \mathbb{E}(N_z^{xy})$ then for all $z \in V \setminus \{x, y\}$ we have*

$$U_z^{xy} = \sum_{w\in V} U_w^{xy} p_{wz}.$$

Proof Since $z \neq x, y$ for N_z^{xy} it holds

$$N_z^{xy} = \sum_{k=1}^{\tau_y - 1} \mathbb{1}_{\{X_k = z | X_0 = x\}} + \mathbb{1}_{\{z = y\}} = \sum_{k=1}^{\tau_y - 1} \mathbb{1}_{\{X_k = z | X_0 = x\}} + \mathbb{1}_{\{X_{\tau_y} = z | X_0 = x\}}$$
$$= \sum_{k=1}^{\tau_y} \mathbb{1}_{\{X_k = z | X_0 = x\}}.$$

With that and our notation $U_z^{xy} = \mathbb{E}(N_z^{xy})$ we get

$$U_z^{xy} = \mathbb{E}\left(\sum_{k=1}^{\tau_y} \mathbb{1}_{\{X_k = z | X_0 = x\}}\right)$$
$$= \sum_{n=0}^{\infty} \mathbb{E}\left(\sum_{k=1}^{\tau_y} \mathbb{1}_{\{X_k = z | X_0 = x\}} \,\middle|\, \tau_y = n\right) \mathbb{P}(\tau_y = n)$$

$$= \sum_{n=0}^{\infty} \sum_{k=1}^{n} \mathbb{E}\left(\mathbb{1}_{\{X_k=z|X_0=x\}}\right) \mathbb{P}(\tau_y = n) = \sum_{n=0}^{\infty} \sum_{k=1}^{n} p_{xz}^{(k)} \mathbb{P}(\tau_y = n)$$

$$= \sum_{n=0}^{\infty} \sum_{k=1}^{n} \sum_{w \in V} p_{xw}^{(k-1)} p_{wz} \mathbb{P}(\tau_y = n) = \sum_{w \in V} p_{wz} \sum_{n=0}^{\infty} \sum_{k=0}^{n-1} p_{xw}^{(k)} \mathbb{P}(\tau_y = n)$$

$$= \sum_{w \in V} p_{wz} \sum_{n=0}^{\infty} \sum_{k=0}^{n-1} \mathbb{E}\left(\mathbb{1}_{\{X_k=w|X_0=x\}}\right) \mathbb{P}(\tau_y = n)$$

$$= \sum_{w \in V} p_{wz} \mathbb{E}\left(\sum_{k=0}^{\tau_y - 1} \mathbb{1}_{\{X_k=w|X_0=x\}} \right) = \sum_{w \in V} p_{wz} U_w^{xy}.$$

□

By dividing both sides by μ_z we get

$$\frac{U_z^{xy}}{\mu_z} = \sum_{w \in V} \frac{U_w^{xy}}{\mu_w} \frac{c_{wz}}{\mu_z} \quad \text{for all } z \in V \setminus \{x, y\}.$$

With the property of lemma 2.13 for the potential

$$V_{zy} = \sum_{w \in V} p_{zw} V_{wy}$$

and by choosing $V_{yy} = 0$, $V_{xy} = \frac{U_z^{xy}}{\mu_x}$ we get by the uniqueness of harmonic functions that

$$V_{zy} = \frac{U_z^{xy}}{\mu_z} \quad \forall z \in V.$$

The current of an edge (w, z) equals

$$i_{wz} = \frac{V_{wz}}{r_{wz}} = V_{wy} c_{wz} - V_{zy} c_{wz} = \frac{U_w^{xy} c_{wz}}{\mu_w} - \frac{U_z^{xy} c_{wz}}{\mu_z} = U_w^{xy} p_{wz} - U_z^{xy} p_{zw}$$

and is therefore the expected number of times the random walk traverses the edge (w, z). A random walk starting in x is leaving this node effectively one time and hence the total current leaving x is 1. Respectively the total current flowing into y is also equal to 1, which means there's a unit current flowing through the network:

$$\sum_{w \sim x} i_{xw} = 1 = \sum_{z \sim y} i_{zy}.$$

This yields by Ohm's law (3) that the effective resistance between x and y–denoted by R_{xy}–is exactly the potential between these two nodes V_{xy}. Let $U_w = U_w^{xy} + U_w^{yx}$ be the number of times a random walk starting from x going to y and returning to x is visiting w. We then get

$$U_w = U_w^{xy} + U_w^{yx} = V_{wy}\mu_w - V_{wx}\mu_w = (V_{wy} + V_{xw})\mu_w = V_{xy}\mu_w = R_{xy}\mu_w,$$

where $U_w^{yx} = -V_{wx}\mu_w$ since the random walk is walking in the opposite direction in which the current flows. We also can write the expected hitting time $\mathbb{E}^x(\tau_y)$ as the expected number of times a random walk from x to y visits every node in the network, hence

$$\mathbb{E}^x(\tau_y) = \sum_{w \in V} U_w^{xy}.$$

Then for the commute time between x and y it holds

$$\begin{aligned} \mathbb{E}^x(\tau_x^y) = \mathbb{E}^x(\tau_y) + \mathbb{E}^y(\tau_x) &= \sum_{w \in V} U_w^{xy} + \sum_{w \in V} U_w^{yx} \\ &= \sum_{w \in V} U_w = R_{xy} \sum_{w \in V} \mu_w. \end{aligned} \tag{5}$$

The reciprocity in electrical networks gives us that the potential V_{zy} for a current flowing between x and y is the same as the potential V_{xy} if the current flows between z and y (see Fig. 1). For random walks we get that the number of visits in z proportional to its weight when walking from x to y is the same as the number of visits in x proportional to its weight when walking from z to y, hence

$$V_{zy} = \frac{U_z^{xy}}{\mu_z} = \frac{U_x^{zy}}{\mu_x} = V_{xy}.$$

With that we are able to proof our final theorem of this section.

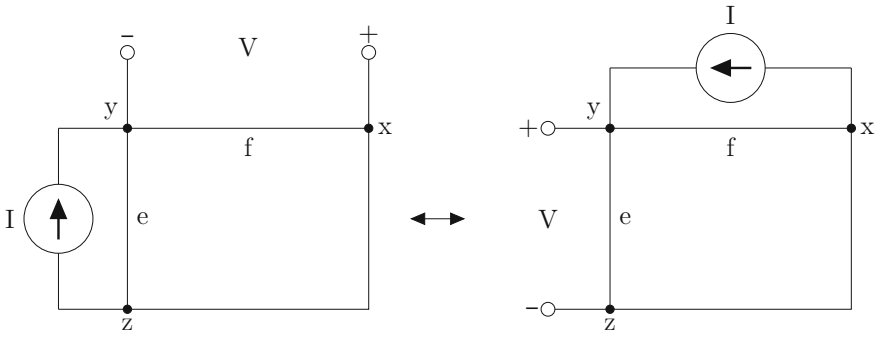

Fig. 1 Reciprocity in electrical networks (see [10])

Theorem 2.15 *Let $G = (V, E, C)$ be a finite graph with $n \in \mathbb{N}$ nodes. It then holds*

$$\sum_{(x,y)\in E} \mathbb{E}^x(\tau_y) \frac{c_{xy}}{\sum_{(w,u)\in E} c_{wu}} = n - 1.$$

Proof By using the reciprocity we get

$$\sum_{x\sim y} \frac{U_z^{xy} c_{xy}}{\mu_z} = \sum_{x\sim y} \frac{U_x^{zy} c_{xy}}{\mu_x} = \sum_{x\sim y} U_x^{zy} p_{xy} = \begin{cases} 1 & \text{for } z \neq y \\ 0 & \text{for } z = y \end{cases},$$

since the expected number of times y is reached from one of its neighbors is exactly 1 if the random walk does not start in y. Summing over all possible terminal nodes y yields

$$\sum_{y\in V} \sum_{x\sim y} \frac{U_z^{xy} c_{xy}}{\mu_z} = \sum_{y\in V} \mathbb{1}_{\{y\neq z\}} = n - 1, \ z \in V.$$

We can simplify this by considering two random walks, one going from x to y and the other on going from y to x. This gives us

$$\begin{aligned} n - 1 &= \sum_{y\in V} \sum_{x\sim y} \frac{U_z^{xy} c_{xy}}{\mu_z} = \sum_{(x,y)\in E} \frac{U_z^{xy} c_{xy}}{\mu_z} = \sum_{\{x,y\}\in E} \left(\frac{U_z^{xy} c_{xy}}{\mu_z} + \frac{U_z^{yx} c_{yx}}{\mu_z} \right) \\ &= \sum_{\{x,y\}\in E} \frac{U_z}{\mu_z} c_{xy} = \sum_{\{x,y\}\in E} \frac{R_{xy}\mu_z}{\mu_z} c_{xy} = \sum_{\{x,y\}\in E} R_{xy} c_{xy}. \end{aligned}$$

From equation (5) we know

$$\mathbb{E}^x(\tau_x^y) = R_{xy} \sum_{w\in V} \mu_w.$$

By multiplication with c_{xy} and summing over all edges we get

$$\sum_{\{x,y\}\in E} \mathbb{E}^x(\tau_x^y) c_{xy} = \left(\sum_{w\in V} \mu_w \right) \cdot \left(\sum_{\{x,y\}\in E} R_{xy} c_{xy} \right) = (n-1) \sum_{w\in V} \mu_w,$$

which yields

$$\frac{\sum_{\{x,y\}\in E} \mathbb{E}^x(\tau_x^y) c_{xy}}{\sum_{w\in V} \mu_w} = n - 1.$$

If we finally consider directed edges the desired equation follows:

$$\begin{aligned} n-1 &= \sum_{\{x,y\}\in E} \mathbb{E}^x(\tau_x^y)\frac{c_{xy}}{\sum_{w\in V}\sum_{u\sim w} c_{wu}} \\ &= \sum_{\{x,y\}\in E}\left(\mathbb{E}^x(\tau_y)\frac{c_{xy}}{\sum_{(w,u)\in E} c_{wu}} + \mathbb{E}^y(\tau_x)\frac{c_{yx}}{\sum_{(w,u)\in E} c_{wu}}\right) \\ &= \sum_{(x,y)\in E} \mathbb{E}^x(\tau_y)\frac{c_{xy}}{\sum_{(w,u)\in E} c_{wu}}. \end{aligned}$$

□

For unweighted graphs the statement of Theorem 2.15 simplifies to

$$\sum_{(x,y)\in E} \mathbb{E}^x(\tau_y)\frac{1}{2m} = n-1,$$

where m is the number of edges in the graph.

3 Models

There are different possibilities for modeling networks. We consider two models in order to analyze the resulting graphs. Firstly the Erdős-Rényi model in which every two nodes are independently of each other connected with the same probability and secondly the preferential attachment model where the probability of two nodes being connected depends on the current degrees of the nodes.

We also take a look at subgraphs of those random graphs in order to analyze if and how certain properties are inherited from the original graph. This is useful when considering networks where not the whole network is known like in the case of the protein network in Sect. 4.

3.1 The Erdős-Rényi Graph

An Erdős-Rényi graph is a graph $G = (V, E)$ with $V = [n], n \in \mathbb{N}$. Let $(Y_{ij})_{1\le i<j\le n}$ be i.i.d. random variables with $Y_{12} \sim Bin(1, p), p \in [0, 1]$. The edge set is then given by $E = \{\{i, j\} \in V \times V : Y_{ij} = 1\}$. Let

$$X_{ij} := \begin{cases} Y_{ij} & \text{if } i < j \\ 0 & \text{if } i = j \\ Y_{ji} & \text{if } i > j, \end{cases}$$

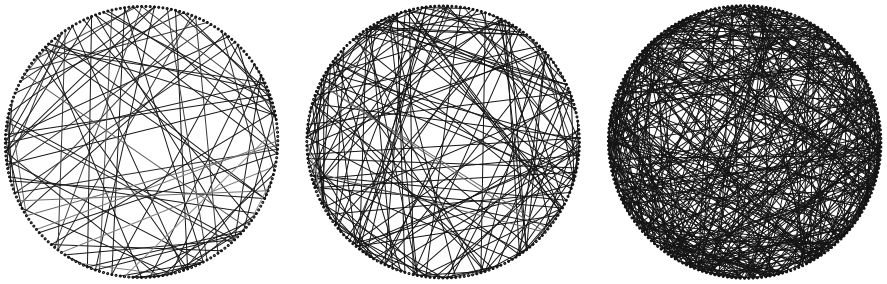

Fig. 2 Three Erdős-Rényi graphs with $n = 200$ nodes and edge probabilities $p = \frac{1}{200}, \frac{2}{200}, \frac{5}{200}$ (left to right)

then the adjacency matrix A of G is given by $A = (X_{ij})_{i,j \in V}$. In Fig. 2 are three different Erdős-Rényi graphs. By above construction it is obvious that the degree distribution of the Erdős-Rényi graph is again a binomial distribution, hence $D(i) \sim Bin(n-1, p)$ for all $i \in [n]$. Further we have the mean degree in an Erdős-Rényi graph given as $\mathbb{E}(D(i)) = (n-1)p$.

3.1.1 Subgraphs of Erdős-Rényi Graphs

We now want to analyze subgraphs of Erdős-Rényi graph and especially their degree distribution. We consider three different mechanisms for the constructions of our subgraphs. Let first $q \in [0, 1]$ be the probability for an edge from the graph G to be in the subgraph. We then decide for every edge of G independently if it should stay in the subgraph, i.e.

$$\mathbb{P}(D_{Sub}(i) = l | D(i) = k) = \binom{k}{l} q^l (1-q)^{k-l}, \ k \in \{0, \ldots, n-1\}, \ l \in \{0, \ldots, k\}.$$

where $D_{Sub}(i)$ denotes the degree of node $i \in [n]$ in the subgraph. Then by the law of total probability it follows

$$\begin{aligned} &\mathbb{P}(D_{Sub}(i) = l) \\ &= \sum_{k=0}^{n-1} \mathbb{P}(D_{Sub}(i) = l | D(i) = k) \mathbb{P}(D(i) = k) \\ &= \sum_{k=l}^{n-1} \binom{k}{l} q^l (1-q)^{k-l} \binom{n-1}{k} p^k (1-p)^{n-1-k} \end{aligned}$$

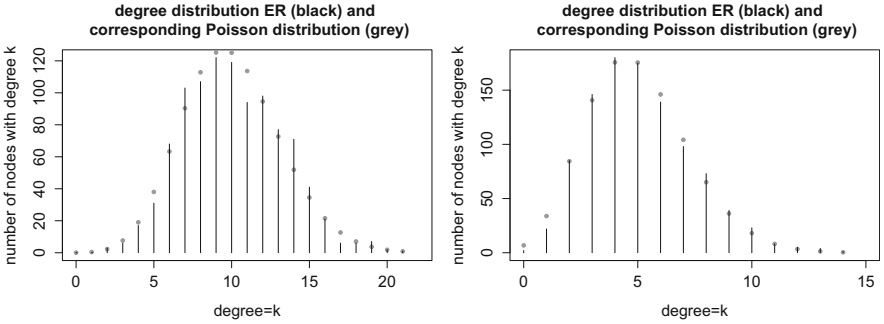

Fig. 3 On the left is the degree distribution of an Erdős-Rényi graph with $n = 1000$ nodes and $p = \frac{1}{100}$. The dots represent the corresponding Poisson distribution with $\lambda = (n-1)p = 9.99$. All Erdős-Rényi subgraphs are based on this Erdős-Rényi graph. On the right is the degree distribution of a subgraph constructed by selection of edges with probability $q = 0.5$ again with the corresponding Poisson distribution with $\lambda = (n-1)pq = 4.995$

$$= \binom{n-1}{l}(pq)^l \sum_{k=0}^{n-1-l} \binom{n-1-l}{k}(p-pq)^k(1-p)^{n-1-l-k}$$
$$= \binom{n-1}{l}(pq)^l(1-pq)^{n-1-l}.$$

Hence the degree distribution of the subgraph is again binomial with parameters $n-1$ and pq. The degree distributions of an Erdős-Rényi graph and the resulting subgraph are depicted in Fig. 3.

Next we construct subgraphs by deleting nodes from the graph. In this case we keep an edge if both adjacent nodes are also in the subgraph. One possibility to do this is to fix the number of nodes in the subgraph and then choosing the subgraph from the set of all subgraph with this number of nodes.

Hence let $G = (V, E)$ be an Erdős-Rényi graph with $V = [n]$. Let further $m \in [n]$ be the number of nodes in the subgraph and

$$\Omega_m := \left\{ \omega = (\omega_1, \ldots, \omega_n) \in \{0,1\}^n : \sum_{i=1}^{n} \omega_i = m \right\},$$

the set of all possibilities of choosing m nodes out of n nodes. Since every subgraph with m nodes has the same probability to be chosen it holds for all $\omega \in \Omega_m$

$$\mathbb{P}(\{\omega\}) = \frac{1}{\binom{n}{m}}.$$

We denote such a subgraph of the Erdős-Rényi graph by $G^m_{Sub} = (V^m_{Sub}, E^m_{Sub})$. Let $i \in V^m_{Sub}$ be a fixed node then the subset of Ω_m giving all combinations of the other $m-1$ nodes ist given by

$$\begin{aligned}\Omega^i_m &:= \{\omega \in \Omega_m : \omega_i = 1\} \\ &= \left\{ \omega = (\omega_1, \ldots, \omega_n) \in \{0,1\}^{i-1} \times \{1\} \times \{0,1\}^{n-i} : \sum_{j \in [n] \setminus i} \omega_j = m-1 \right\}.\end{aligned}$$

Since the number of elements in Ω^i_m is given by $\binom{n-1}{m-1}$ the conditional degree distribution of i is given by

$$\mathbb{P}(D_{Sub}(i) = l | D(i) = k) = \frac{\binom{n-1-k}{m-1-l}\binom{k}{l}}{\binom{n-1}{m-1}}.$$

By using the law of total probability again it holds for fixed $i \in V^m_{Sub}$

$$\begin{aligned}&\mathbb{P}(D_{Sub}(i) = l) \\ &= \sum_{k=0}^{n-1} \mathbb{P}(D_{Sub}(i) = l | D(i) = k) \mathbb{P}(D(i) = k) \\ &= \sum_{k=0}^{n-1} \frac{\binom{n-1-k}{m-1-l}\binom{k}{l}}{\binom{n-1}{m-1}} \binom{n-1}{k} p^k (1-p)^{n-1-k} \\ &= \sum_{k=0}^{n-1} \binom{n-m}{k-l} \binom{m-1}{l} p^{k-l+l} (1-p)^{n-1-(m-1)-(k-l)+m-1-l} \\ &= \binom{m-1}{l} p^l (1-p)^{m-1-l} \sum_{k=0}^{n-m} \binom{n-m}{k} p^k (1-p)^{n-m-k} \\ &= \binom{m-1}{l} p^l (1-p)^{m-1-l}.\end{aligned}$$

Hence we again have binomially distributed degrees with parameters $m-1$ and p.

We now want to choose nodes binomially distributed to stay in the subgraph. Let therefore be $q \in [0,1]$. We denote the resulting subgraph by $G^q_{Sub} = (V^q_{Sub}, E^q_{Sub})$. It then holds for $m \in \{0, \ldots, n\}$:

$$\mathbb{P}(\#V^q_{Sub} = m) = \binom{n}{m} q^m (1-q)^{n-m}.$$

Let again be $i \in V_{Sub}^q$ be a fixed node then it holds

$$\mathbb{P}(\#V_{Sub}^q = m) = \binom{n-1}{m-1} q^{m-1}(1-q)^{n-m},\ m \in \{1, \ldots, n\}$$

and the probability for node i in the subgraph to have degree l, given $D(i) = k$ in the graph and $\#V_{Sub}^q = m$ is

$$\mathbb{P}(D_{Sub}(i) = l | D(i) = k, \#V_{Sub}^q = m) = \begin{cases} \frac{\binom{n-1-k}{m-1-l}\binom{k}{l}}{\binom{n-1}{m-1}} & \text{for } i \in V_{Sub}^q, \\ 0 & \text{for } i \notin V_{Sub}^q. \end{cases}$$

By the law of total probability we get

$$\begin{aligned} &\mathbb{P}(D_{Sub}(i) = l | \#V_{Sub}^q = m) \\ &= \sum_{k=0}^{n-1} \mathbb{P}(D_{Sub}(i) = l | D(i) = k, \#V_{Sub}^q = m)\mathbb{P}(D(i) = k) \\ &= \sum_{k=0}^{n-1} \frac{\binom{n-1-k}{m-1-l}\binom{k}{l}}{\binom{n-1}{m-1}} \binom{n-1}{k} p^k (1-p)^{n-1-k} = \binom{m-1}{l} p^l (1-p)^{m-1-l}, \end{aligned}$$

which yields

$$\begin{aligned} &\mathbb{P}(D_{Sub}(i) = l) \\ &= \sum_{m=l+1}^{n} \mathbb{P}(D_{Sub}(i) = l | \#V_{Sub}^q = m)\mathbb{P}(\#V_{Sub}^q = m) \\ &= \sum_{m=l+1}^{n} \binom{m-1}{l} p^l (1-p)^{m-1-l} \binom{n-1}{m-1} q^{m-1}(1-q)^{n-m} \\ &= \binom{n-1}{l} (pq)^l \sum_{m=0}^{n-l-1} \binom{n-1-l}{m} (q-pq)^m (1-q)^{n-1-l-m} \\ &= \binom{n-1}{l} (pq)^l (1-pq)^{n-l-1}. \end{aligned}$$

Hence the degrees in G_{Sub}^q are again binomially distributed with parameters $n-1$ and pq (Fig. 4). If we now choose $q := \frac{m}{n}$ then G_{Sub}^m and G_{Sub}^q are comparable by

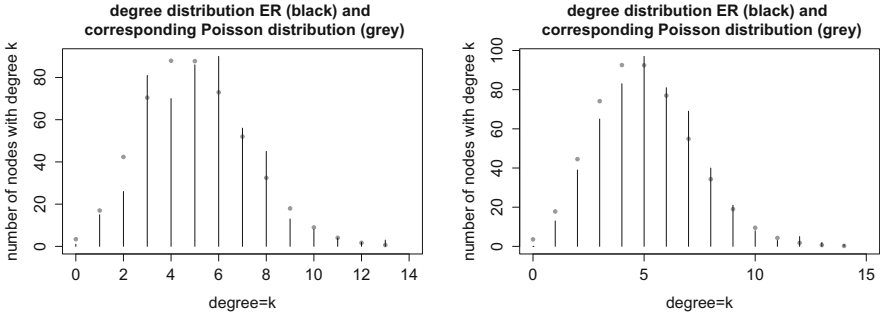

Fig. 4 On the left we see the degree distribution of a subgraph constructed by uniform selection of nodes with $m = 500$ together with the corresponding Poisson distribution with $\lambda = (m-1)p = 4.99$. On the right is the degree distribution of a subgraph constructed by binomial selection of nodes with probability $q = \frac{m}{n} = 0.5$ and the corresponding Poisson distribution with $\lambda = (n-1)pq = 4.995$

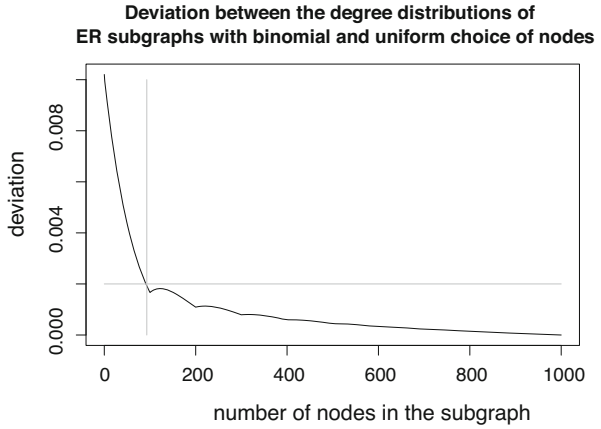

Fig. 5 Absolute deviation of the degree distributions by constructing the Erdős-Rényi subgraphs via the selection of nodes (black line). For subgraphs wit more than 93 nodes the absolute deviation of the two binomial distributions is smaller than 0.002

their number of nodes, because

$$\mathbb{E}(\#V_{Sub}^{q}) = nq = n\frac{m}{n} = m = \#V_{Sub}^{m} = \mathbb{E}(\#V_{Sub}^{m}).$$

Moreover the degree distributions are comparable as Fig. 5 shows. For an Erdős-Rényi graph with $n = 1000$ nodes and edge probability $p = 1/100$ we get, that the degree distributions of the subgraphs only differ significantly if the subgraphs have less than 10% of the nodes of the graph.

By the calculations of this section we see that subgraphs of an Erdős-Rényi graph constructed according to one of the above mechanisms have the same structure as the graph itself and can therefore again be modeled as Erdős-Rényi graphs.

3.2 The Preferential Attachment Model

There are different possibilities to define a preferential attachment model but the basic idea stays the same. All preferential attachment models consider a growing graph where the degrees of the existing nodes influence the probability of a new node connecting to them. In our model we will not allow self-loops, hence every new node really is connected to the existing graph.

For our model we fix $m \in \mathbb{N}$ and $\delta \in (-m, \infty)$. We then initialize our graph with one node with m self-loops. Here the self-loops are necessary to calculate the probabilities. Every new node has m edges which connect to existing nodes. At time $n \geq 2$ the n-th node is added to the graph.

Let $D^n(i)$ be the degree of node $i \leq n$ at time n and $PA_n^{(m,\delta)} = (V_n, E_n)$ the preferential attachment graph with parameters $m \geq 1$ and $\delta > -m$ at time n. Then the probability of node $n+1$ to connect to node i, hence the probability for $\{n+1, i\} \in E_n$ given $PA_n^{(m,\delta)}$, is given by

$$\mathbb{P}(\{n+1, i\} \in E_{n+1} | PA_n^{(m,\delta)}) := \frac{D^n(i) + \delta}{(2m+\delta)n} \text{ for } i \in [n],\ n \in \mathbb{N}.$$

Since we only consider finite graphs, we stop the construction when the graph has the desired size. By construction the graph is connected, due to the fact that we do not allow self-loops. In Fig. 6 we see four preferential attachment graphs with different parameters. This leads to different structural properties. Since m is responsible for the number of edges added with each node one will always get a tree for $m = 1$. The parameter δ controls the influence of the degrees on the connection probabilities. For δ close to $-m$ the probability for a new node to connect to a node with degree m is rather small which leads to a graph where early nodes are preferred and get a much higher degree than nodes added later on. For δ large the influence of the degrees on the connection probabilities is small which leads to a more homogeneous graph.

3.2.1 Properties of Preferential Attachment Graphs

We now want to look at the degree distribution and because we can not determine it exactly we are also interested in the expected degree and variance of the degree of fixed nodes. First we get that the mean degree in a preferential attachment graph of

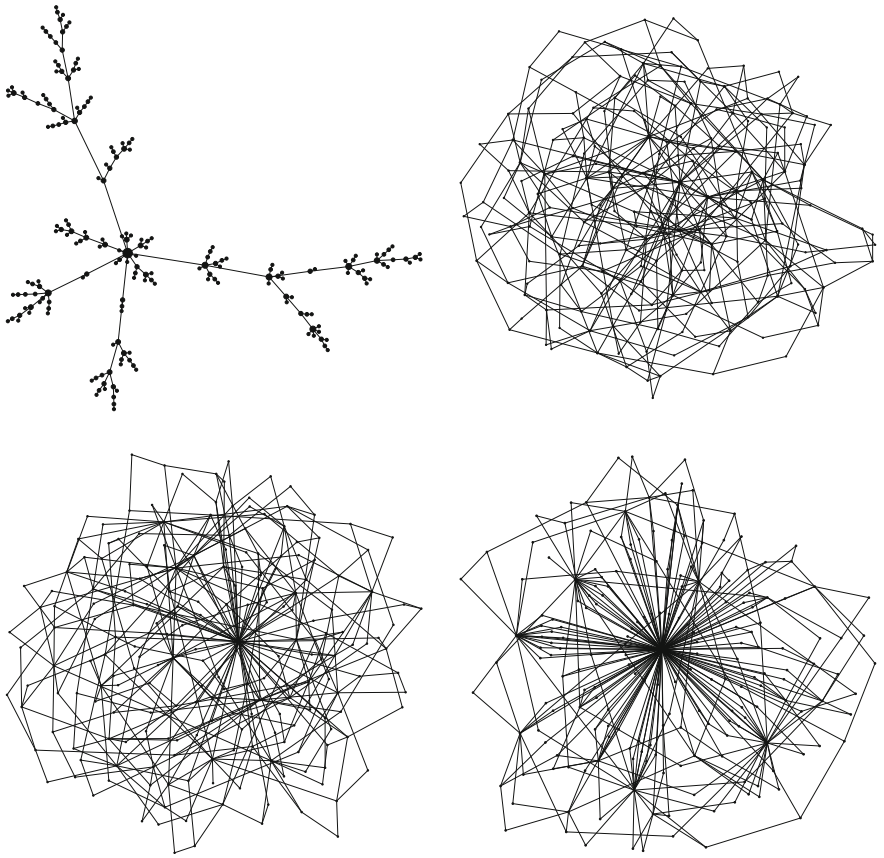

Fig. 6 Four preferential attachment graphs with $n = 200$ nodes and different values for m and δ. Upper left: $m = 1,\ \delta = 10$. Upper right: $m = 2,\ \delta = 10$. Lower left: $m = 2,\ \delta = 0$. Lower right: $m = 2,\ \delta = -1.5$

size n is given by

$$\frac{1}{n}\sum_{i=1}^{n} D^n(i) = \frac{2nm}{n} = 2m, \tag{6}$$

since every node adds m edges to the graph and the sum over all degrees is twice the number of edges. We are not able determine the degree distribution exactly, but it is possible to show that the degree distributions converge and to give the exact limit.

Let $P_k(n) := \frac{1}{n}\sum_{i=1}^{n} \mathbb{1}_{\{D^n(i)=k\}},\ k \in \mathbb{N}_0$ be the ratio of nodes with degree k at time n. Then $(P_k(n))_{k\geq 0}$ defines the degree distribution of $PA_n^{(m,\delta)}$. For

$m \geq 1,\ \delta > -m$ and all $k \in \mathbb{N}$ we define the sequence $(p_k)_{k\in\mathbb{N}}$ by

$$p_k := \begin{cases} 0 & \text{for } k \leq m-1, \\ \left(2+\frac{\delta}{m}\right)\frac{\Gamma(k+\delta)\Gamma(m+2+\delta+\frac{\delta}{m})}{\Gamma(m+\delta)\Gamma(k+3+\delta+\frac{\delta}{m})} & \text{for } k \geq m, \end{cases} \tag{7}$$

where $\Gamma(t) = \int_0^\infty x^{t-1}e^{-x}dx,\ t > 0$ is the Gamma function. For the degree distribution it then holds

$$P_k(n) \xrightarrow{\mathbb{P}} p_k, (n \to \infty).$$

This convergence is shown in [11]. The limit of the degree distributions is again a probability distribution by

Theorem 3.1 *The limit distribution $(p_k)_{k\geq m}$ is a probability distribution.*

Proof See [11]. □

Stirling's formula states

$$\frac{\Gamma(x+a)}{\Gamma(x)} \approx x^a.$$

By that we get for k sufficiently big

$$\begin{aligned} p_k &= \left(2+\frac{\delta}{m}\right)\frac{\Gamma(k+\delta)\Gamma(m+2+\delta+\frac{\delta}{m})}{\Gamma(m+\delta)\Gamma(k+3+\delta+\frac{\delta}{m})} \\ &= \left(2+\frac{\delta}{m}\right)\frac{\Gamma(m+2+\delta+\frac{\delta}{m})}{\Gamma(m+\delta)}\frac{\Gamma(k+\delta)}{\Gamma(k+\delta+3+\frac{\delta}{m})} \\ &\approx \left(2+\frac{\delta}{m}\right)\frac{\Gamma(m+2+\delta+\frac{\delta}{m})}{\Gamma(m+\delta)}k^{-(3+\frac{\delta}{m})} \\ &= c_{m,\delta}k^{-\tau}, \end{aligned}$$

where $c_{m,\delta} = (2+\frac{\delta}{m})\frac{\Gamma(m+2+\delta+\frac{\delta}{m})}{\Gamma(m+\delta)}$ and $\tau = 3+\frac{\delta}{m}$. Hence we get that the preferential attachment graph is scale free if the number of nodes is large.

Since we can not estimate the exact degree distribution we now look at the expectation and variance of the degrees of fixed nodes.

Theorem 3.2 *Let $m \geq 1,\ \delta > -m$, then for the expected degree of node $i \in [n]$ it holds*

$$\mathbb{E}(D^n(i)+\delta) = (m+\mathbb{1}_{\{i=1\}}m+\delta)\frac{\Gamma(n+\frac{m}{2m+\delta})\Gamma(i)}{\Gamma(i+\frac{m}{2m+\delta})\Gamma(n)}.$$

Proof Let $m \geq 1$ and $\delta > -m$ be fixed then

$$\begin{aligned}
\mathbb{E}(D^n(i) + \delta | D^{n-1}(i)) &= D^{n-1}(i) + \delta + \mathbb{E}(D^n(i) - D^{n-1}(i) | D^{n-1}(i)) \\
&= D^{n-1}(i) + \delta + m\mathbb{P}(\{n, i\} \in E_n | PA_{n-1}^{(m,\delta)}) \\
&= (D^{n-1}(i) + \delta) \frac{(2m + \delta)(n - 1 + \frac{m}{2m+\delta})}{(2m + \delta)(n - 1)} \\
&= (D^{n-1}(i) + \delta) \frac{n - 1 + \frac{m}{2m+\delta}}{n - 1},
\end{aligned}$$

and obviously

$$\mathbb{E}(D^i(i) + \delta) = m + \mathbb{1}_{\{i=1\}} m + \delta \quad \text{for all } i \geq 1.$$

For $\mathbb{E}(D^n(i) + \delta)$ it then follows recursively

$$\begin{aligned}
\mathbb{E}(D^n(i) + \delta) &= \mathbb{E}(\mathbb{E}(D^n(i) + \delta | D^{n-1}(i))) \\
&= \mathbb{E}(D^{n-1}(i) + \delta) \frac{n - 1 + \frac{m}{2m+\delta}}{n - 1} \\
&\vdots \\
&= \mathbb{E}(D^i(i) + \delta) \frac{n - 1 + \frac{m}{2m+\delta}}{n - 1} \cdot \ldots \cdot \frac{i + \frac{m}{2m+\delta}}{i} \\
&= (m + \mathbb{1}_{\{i=1\}} m + \delta) \frac{\Gamma(n + \frac{m}{2m+\delta})\Gamma(i)}{\Gamma(i + \frac{m}{2m+\delta})\Gamma(n)}.
\end{aligned}$$

□

Theorem 3.3 *Let $m \geq 1$, $\delta > -m$, then for the variance of the degree of a fixed node i at time n it holds*

$$\begin{aligned}
\mathrm{Var}(D^n(i)) = (m + \mathbb{1}_{\{i=1\}} m + \delta)^2 &\left[\prod_{j=i}^{n-1} (d_j - c_j) - \prod_{j=i}^{n-1} d_j \right] \\
&+ \sum_{j=i}^{n-1} \mathbb{E}(D^j(i) + \delta) \sqrt{m c_j} \prod_{k=j+1}^{n-1} (d_k - c_k),
\end{aligned}$$

where

$$c_j = \frac{m}{(2m+\delta)^2 j^2} \text{ and } d_j = \left(1 + \frac{m}{(2m+\delta)j}\right)^2, \forall 1 \leq j < n.$$

Proof Let $n \in \mathbb{N}$ and $i \leq n$ as well as $m \geq 1$ and $\delta > -m$ be fixed. To calculate the variance we use the well known identity

$$\mathrm{Var}(X) = \mathbb{E}(\mathrm{Var}(X|Y)) + \mathrm{Var}(\mathbb{E}(X|Y)),$$

where the conditional variance is given by

$$\mathrm{Var}(X|Y) := \mathbb{E}(X^2|Y) - \mathbb{E}(X|Y)^2.$$

It then holds for the variance of the degree of node i at time n

$$\begin{aligned}
\mathrm{Var}(D^n(i)) &= \mathrm{Var}(D^n(i) + \delta) \\
&= \mathbb{E}(\mathrm{Var}(D^n(i) + \delta | D^{n-1}(i))) + \mathrm{Var}(\mathbb{E}(D^n(i) + \delta | D^{n-1}(i))) \\
&= \underbrace{\mathbb{E}(\mathbb{E}((D^n(i) + \delta)^2 | D^{n-1}(i)))}_{I} - \underbrace{\mathbb{E}((\mathbb{E}(D^n(i) + \delta | D^{n-1}(i)))^2)}_{II} \\
&\quad + \underbrace{\mathrm{Var}(\mathbb{E}(D^n(i) + \delta | D^{n-1}(i)))}_{III}.
\end{aligned}$$

The different summands can be determined as follows.

(I):

$$\begin{aligned}
&\mathbb{E}[\mathbb{E}((D^n(i) + \delta)^2 | D^{n-1}(i))] \\
&= \mathbb{E}[\mathbb{E}((D^n(i) + \delta + D^{n-1}(i) - D^{n-1}(i))^2 | D^{n-1}(i))] \\
&= \mathbb{E}[(D^{n-1}(i) + \delta)^2] \\
&\quad + 2\mathbb{E}\left[(D^{n-1}(i) + \delta) m \frac{D^{n-1}(i) + \delta}{(2m+\delta)(n-1)}\right] \\
&\quad + \mathbb{E}[\mathbb{E}((D^n(i) - D^{n-1}(i))^2 | D^{n-1}(i))] \\
&= \underbrace{\mathbb{E}[(D^{n-1}(i) + \delta)^2]}_{= \mathbb{E}[\mathbb{E}((D^{n-1}(i)+\delta)^2 | D^{n-2}(i))]} \left(1 + \frac{2m}{(2m+\delta)(n-1)}\right) \\
&\quad + \underbrace{\mathbb{E}[\mathbb{E}((D^n(i) - D^{n-1}(i))^2 | D^{n-1}(i))]}_{IV}.
\end{aligned}$$

(II): With the calculations in the proof of Theorem 3.2 we get

$$\begin{aligned}
&\mathbb{E}[\mathbb{E}(D^n(i)+\delta|D^{n-1}(i))^2] \\
&= \mathbb{E}\left[\left((D^{n-1}(i)+\delta)\left(1+\frac{m}{(2m+\delta)(n-1)}\right)\right)^2\right] \\
&= \underbrace{\mathbb{E}[(D^{n-1}(i)+\delta)^2]}_{=\mathbb{E}[\mathbb{E}((D^{n-1}(i)+\delta)^2|D^{n-2}(i))]}\left(1+\frac{m}{(2m+\delta)(n-1)}\right)^2.
\end{aligned}$$

(III):

$$\begin{aligned}
&\mathrm{Var}[\mathbb{E}(D^n(i)+\delta|D^{n-1}(i))] \\
&= \mathrm{Var}\left[(D^{n-1}(i)+\delta)\left(1+\frac{m}{(2m+\delta)(n-1)}\right)\right] \\
&= \mathrm{Var}[D^{n-1}(i)+\delta]\left(1+\frac{m}{(2m+\delta)(n-1)}\right)^2.
\end{aligned}$$

(IV): For the calculation of

$$\mathbb{E}[\mathbb{E}((D^n(i)-D^{n-1}(i))^2|D^{n-1}(i))]$$

we use that, by construction, the number of edges between a new node and a node already in the graph is binomially distributed, hence

$$D^n(i)-D^{n-1}(i)|D^{n-1}(i) \sim \mathrm{Bin}(m,p), \text{ where } p := \frac{D^{n-1}(i)+\delta}{(2m+\delta)(n-1)}.$$

For $X \sim \mathrm{Bin}(m,p)$ one gets $\mathbb{E}(X^2) = mp(1-p)+(mp)^2$ and it follows

$$\begin{aligned}
&\mathbb{E}[\mathbb{E}((D^n(i)-D^{n-1}(i))^2|D^{n-1}(i))] \\
&= \mathbb{E}[D^{n-1}(i)+\delta]\frac{m}{(2m+\delta)(n-1)} \\
&\quad + \underbrace{\mathbb{E}[(D^{n-1}(i)+\delta)^2]}_{=\mathbb{E}[\mathbb{E}((D^{n-1}(i)+\delta)^2|D^{n-2}(i))]}\frac{m(m-1)}{(2m+\delta)^2(n-1)^2}.
\end{aligned}$$

We now introduce the following abbreviations for simplicity

$$\begin{aligned}
V_n &:= \mathrm{Var}(D^n(i)+\delta), \\
E_n &:= \mathbb{E}[\mathbb{E}((D^n(i)+\delta)^2|D^{n-1}(i))], \\
D_n &:= \mathbb{E}[D^n(i)+\delta].
\end{aligned}$$

By putting the results into the first equation of the proof and using the abbreviations we get

$$\begin{aligned}
V_n &= E_{n-1}\left(1+\frac{2m}{(2m+\delta)(n-1)}\right)+E_{n-1}\frac{m(m-1)}{(2m+\delta)^2(n-1)^2}\\
&\quad +D_{n-1}\frac{m}{(2m+\delta)(n-1)}-E_{n-1}\left(1+\frac{m}{(2m+\delta)(n-1)}\right)^2\\
&\quad +V_{n-1}\left(1+\frac{m}{(2m+\delta)(n-1)}\right)^2\\
&= -E_{n-1}\frac{m}{(2m+\delta)^2(n-1)^2}+D_{n-1}\frac{m}{(2m+\delta)(n-1)}\\
&\quad +V_{n-1}\left(1+\frac{m}{(2m+\delta)(n-1)}\right)^2.
\end{aligned}$$

For $j<n$ let

$$\begin{aligned}
c_j &:= \frac{m}{(2m+\delta)^2 j^2},\\
d_j &:= \left(1+\frac{m}{(2m+\delta)\,j}\right)^2.
\end{aligned}$$

Then we can calculate $\mathrm{Var}(D^n(i))$ with the following recursion formulas and termination conditions

$$\begin{aligned}
V_n &= E_{n-1}(-c_{n-1})+D_{n-1}\sqrt{mc_{n-1}}+V_{n-1}d_{n-1},\\
E_n &= E_{n-1}(d_{n-1}-c_{n-1})+D_{n-1}\sqrt{mc_{n-1}},
\end{aligned}$$

$$\begin{aligned}
V_i &= \mathrm{Var}(D^i(i)+\delta)=0,\\
E_i &= \mathbb{E}((D^i(i)+\delta)^2)=(m+\mathbb{1}_{\{i=1\}}m+\delta)^2.
\end{aligned}$$

Two steps of the recursion yield

$$\begin{aligned}
V_n &= E_{n-1}(-c_{n-1})+D_{n-1}\sqrt{mc_{n-1}}+V_{n-1}d_{n-1}\\
&= E_{n-2}(c_{n-1}c_{n-2}-c_{n-1}d_{n-2}-c_{n-2}d_{n-1})+D_{n-1}\sqrt{mc_{n-1}}\\
&\quad +D_{n-2}\sqrt{mc_{n-2}}(d_{n-1}-c_{n-1})+V_{n-2}d_{n-1}d_{n-2}\\
&= E_{n-2}[(d_{n-1}-c_{n-1})(d_{n-2}-c_{n-2})-d_{n-1}d_{n-2}]+D_{n-1}\sqrt{mc_{n-1}}\\
&\quad +D_{n-2}\sqrt{mc_{n-2}}(d_{n-1}-c_{n-1})+V_{n-2}d_{n-1}d_{n-2}
\end{aligned}$$

$$
\begin{aligned}
&= E_{n-3}(d_{n-3} - c_{n-3})[(d_{n-1} - c_{n-1})(d_{n-2} - c_{n-2}) - d_{n-1}d_{n-2}] \\
&\quad + D_{n-3}\sqrt{mc_{n-3}}[(d_{n-1} - c_{n-1})(d_{n-2} - c_{n-2}) - d_{n-1}d_{n-2}] \\
&\quad + D_{n-1}\sqrt{mc_{n-1}} + D_{n-2}\sqrt{mc_{n-2}}(d_{n-1} - c_{n-1}) - E_{n-3}c_{n-3}d_{n-1}d_{n-2} \\
&\quad + D_{n-3}\sqrt{mc_{n-3}}d_{n-1}d_{n-2} + V_{n-3}d_{n-1}d_{n-2}d_{n-3} \\
&= E_{n-3}[(d_{n-3} - c_{n-3})(d_{n-1} - c_{n-1})(d_{n-2} - c_{n-2}) - d_{n-1}d_{n-2}d_{n-3}] \\
&\quad + D_{n-1}\sqrt{mc_{n-1}} + D_{n-2}\sqrt{mc_{n-2}}(d_{n-1} - c_{n-1}) \\
&\quad + D_{n-3}\sqrt{mc_{n-3}}(d_{n-1} - c_{n-1})(d_{n-2} - c_{n-2}) + V_{n-3}d_{n-1}d_{n-2}d_{n-3}.
\end{aligned}
$$

Hence it follows

$$
\begin{aligned}
V_n &= V_i \prod_{j=i}^{n-1} d_j + E_i \left[\prod_{j=i}^{n-1} (d_j - c_j) - \prod_{j=i}^{n-1} d_j \right] \\
&\quad + \sum_{j=i}^{n-1} D_j \sqrt{mc_j} \prod_{k=j+1}^{n-1} (d_k - c_k) \\
&= (m + \mathbb{1}_{\{i=1\}}m + \delta)^2 \left[\prod_{j=i}^{n-1} (d_j - c_j) - \prod_{j=i}^{n-1} d_j \right] \\
&\quad + \sum_{j=i}^{n-1} D_j \sqrt{mc_j} \prod_{k=j+1}^{n-1} (d_k - c_k).
\end{aligned}
$$

□

In Fig. 7 the degrees are plotted with their expectations and variances.

3.2.2 Subgraphs of Preferential Attachment Graphs

Since we can not determine the degree distribution of the preferential attachment graphs, we will analyze them numerically. The constructions of the subgraphs are the same as for the Erdős-Rényi graphs.

We first look at the mean degree of subgraphs of preferential attachment graphs. For the construction of the subgraph we decide for every edge if it is deleted while keeping all nodes. Let therefore the probability for an edge of the graph to be kept in the subgraph be $q \in (0, 1)$. It then holds for fixed $i \in [n]$

$$
\mathbb{P}(D^n_{Sub}(i) = l | D^n(i) = k) = \binom{k}{l} q^l (1 - q)^{k-l} \text{ for } l \in \{0, \ldots, k\},\ k \leq n.
$$

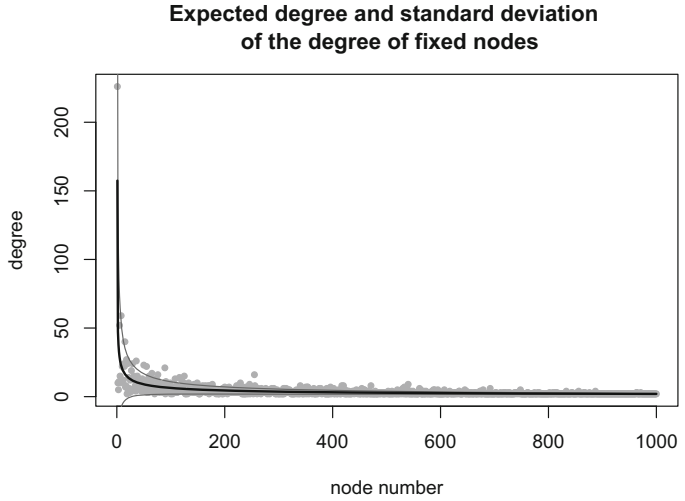

Fig. 7 The points are the degrees of the nodes in the order in which they were added to the graph. The thick black line is the expected degree of the nodes of a preferential attachment graph with $n = 1000$ nodes, $m = 2$ and $\delta = 0$. The thin lines are the standard deviation from the mean of the degrees

With that we can determine the degree distribution of the subgraph given the degree distribution of the graph by

$$\begin{aligned}\mathbb{P}(D^n_{Sub}(i) = l) &= \sum_{k=l}^{n-1} \mathbb{P}(D^n_{Sub}(i) = l | D^n(i) = k)\mathbb{P}(D^n(i) = k) \\ &= \sum_{k=l}^{n-1} \binom{k}{l} q^l (1-q)^{k-l} \frac{1}{n} \sum_{i=1}^{n} \mathbb{1}_{\{D^n(i)=k\}} \\ &= \frac{1}{n} \sum_{i=1}^{n} \binom{D^n(i)}{l} q^l (1-q)^{D^n(i)-l},\end{aligned}$$

where $D^n(i) \sim P_k(n)$. Hence for the mean degree it holds

$$\begin{aligned}\mathbb{E}(D^n_{Sub}(i)) &= \sum_{l=0}^{n-1} l \frac{1}{n} \sum_{i=1}^{n} \binom{D^n(i)}{l} q^l (1-q)^{D^n(i)-l} \\ &= \frac{1}{n} \sum_{i=1}^{n} \sum_{l=0}^{D^n(i)} l \binom{D^n(i)}{l} q^l (1-q)^{D^n(i)-l} \\ &= \frac{1}{n} \sum_{i=1}^{n} D^n(i) q = \frac{q}{n} 2\#E_n = 2mq.\end{aligned}$$

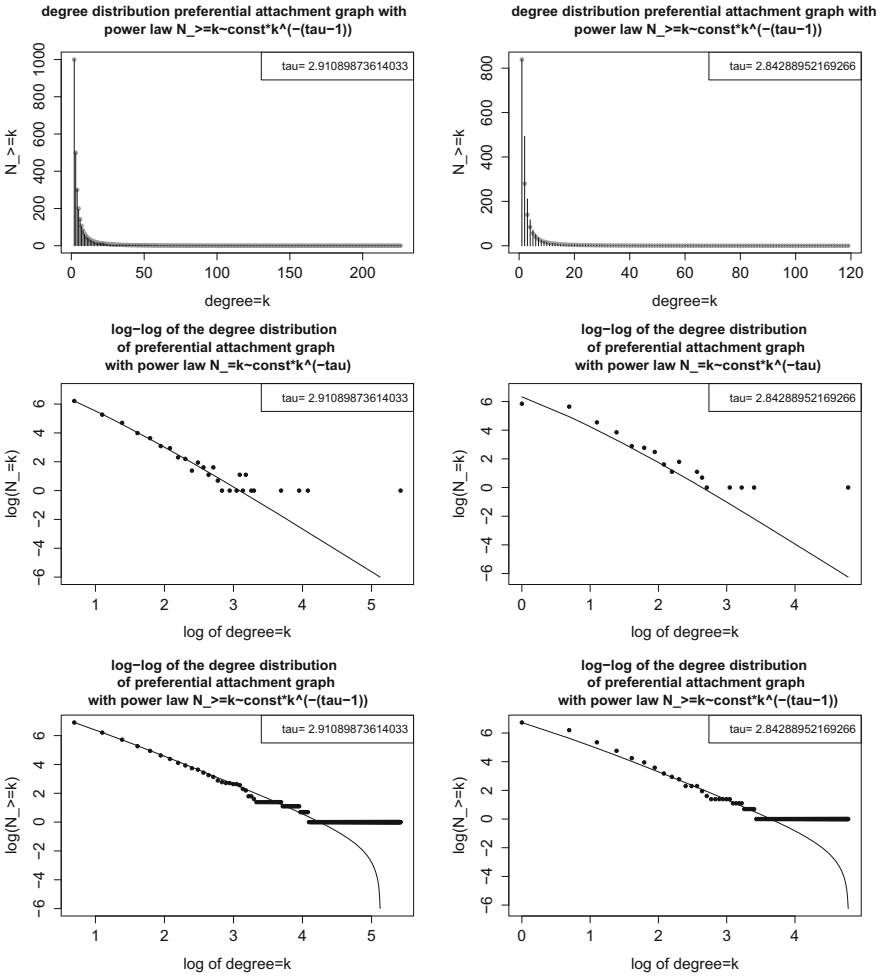

Fig. 8 On the left is the degree distribution of a PA graph with $n = 1000$, $m = 2$ and $\delta = 0$. This PA graph is used for the construction of all PA subgraphs and the analysis of the expected degrees. On the right is the degree distribution of a subgraph constructed by selection of edges with probability $p = 0.5$ and limit distribution $(p_k)_{k \geq m}$ with $n = 500$, $m = 1$ and $\delta = 0$. The dots in the top pictures represent the limit distribution $(p_k)_{k \geq m}$. In the lower four pictures $(p_k)_{k \geq m}$ is represented by the line. The preferential attachment graph is scale free with $\tau = 2.911$, the subgraph has power law exponent $\tau = 2.843$

Since we are not able to determine the exact degree distributions we calculated the empirical degree distributions. These are depicted in Fig. 8 for a preferential attachment graph and its subgraph by selection of edges together with the limit distribution from formula (7). By comparing the two degree distributions one sees that they are both scale free with approximately the same exponent. But the subgraph is not necessarily connected, whereas the preferential attachment graph

itself is by construction. Hence it is not possible to construct the subgraph with our preferential attachment model.

We now want to look at subgraphs of our preferential attachment graph which are constructed by deleting nodes. We again select the nodes in the two different ways we used for the Erdős-Rényi graphs. Hence we fix a number of nodes and choose a subgraph of that size uniformly at random out of the set of all subgraphs with that size. For the other mechanism we decide for every node independently of the others if we delete it. The empirical degree distributions are depicted in Fig. 9 together with the limit distribution from formula (7). One can see that the exponent τ of the power law stays approximately the same as in the preferential attachment graph but the subgraphs are again not necessarily connected which is a complex problem related to percolation theory. Additionally the mean degree does not have to be a multiplicity of 2 which is the case in our model. Hence its not possible to construct these subgraphs with our initial preferential attachment model used to construct the entire graph.

4 Protein Networks

We now want to analyze a protein network in order to decide if it can be constructed with our preferential attachment model. Proteins are sequences of amino acids. The length of most of them is between 250 and 420 amino acids. But there are some with lengths up to 27000 amino acids.

Proteins consist of up to 20 different amino acids. The order of the amino acids determines the structure and function of the protein. It is obvious that not every constellation of amino acids yields a biological sufficient protein. Yet proteins do not necessarily loose their functionality if only few of the amino acids are replaced.

It is possible to compare proteins regarding the order of their amino acids and assign scores according to their similarity. One could also look at the number of mutations between two proteins as a score.

Proteins of the same family can then be connected to form a network by connecting two proteins that differ by one mutation. The structure of such a network is depicted in Fig. 10. We therefore took class A β-lactamases of the TEM family which have a length between 200 and 300 amino acids. Figure 11 shows the degree distribution of the protein network which is scale free with $\tau = 2.641$. The question that arises is if we can model the protein network with our preferential attachment model. As we can see in Fig. 10 the graph is not connected and this actually is the case for the majority of discovered protein families. Yet by construction every graph coming from our preferential attachment model is connected. But since our network only contains discovered proteins it still could be possible to model it with our preferential attachment model if we had the full network with all connections.

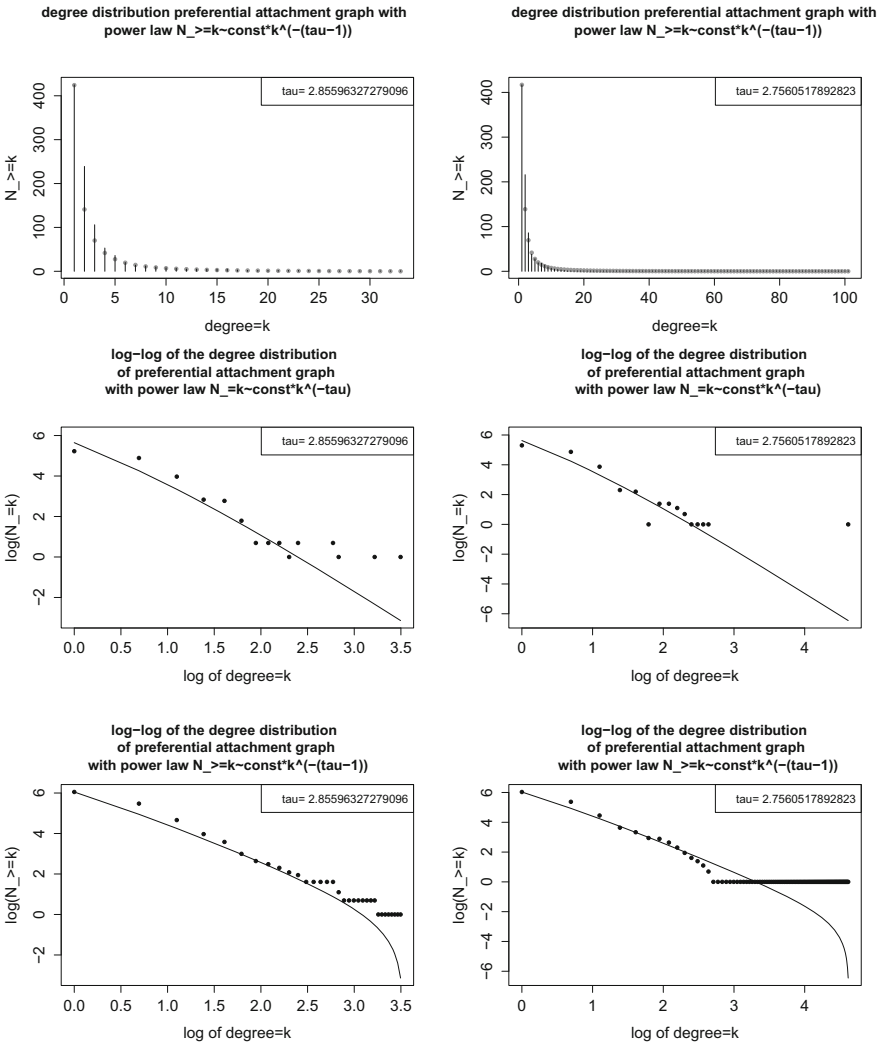

Fig. 9 Here we see the degree distributions of two subgraphs constructed by selection of nodes together with the corresponding limit distributions. On the left we have uniform selection of nodes with 500 nodes and on the right binomial selection of nodes with probability $q = 0.5$. The parameters of the limit distributions are in both cases given by $n = 500$, $m = 1$ and $\delta = 0$. Uniform selection of nodes yields a power law exponent $\tau = 2.847$, whereas the binomial selected subgraph is scale free with $\tau = 2.756$. We calculated m for the subgraphs by the identity $\#E = mn$. One can see that the limit distribution is a good approximation for the degree distribution in the beginning. The large deviation at the end is due to the small number of nodes and single nodes having a degree which occurs with a very small probability

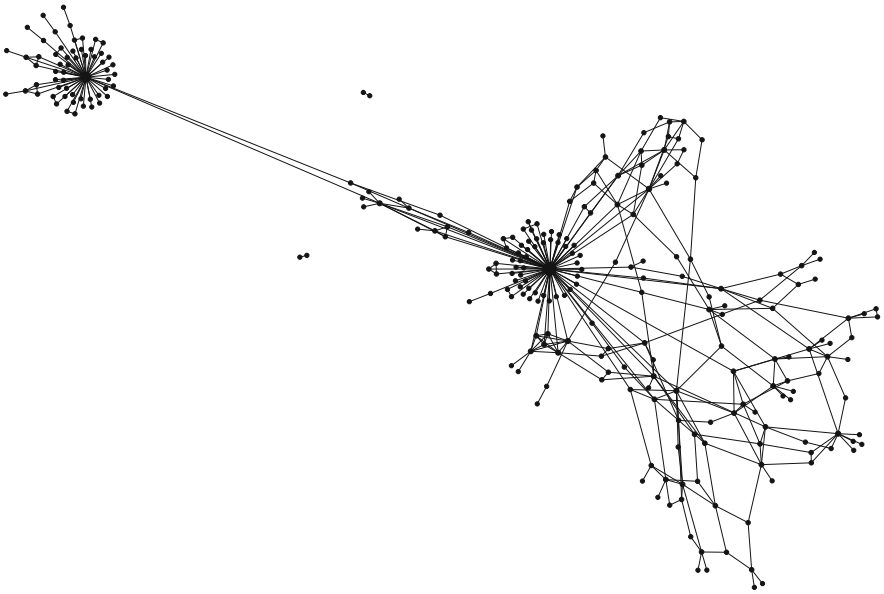

Fig. 10 Graphical illustration of a protein network of 263 class A β-lactamases of the TEM family where adjacent proteins differ by one mutation

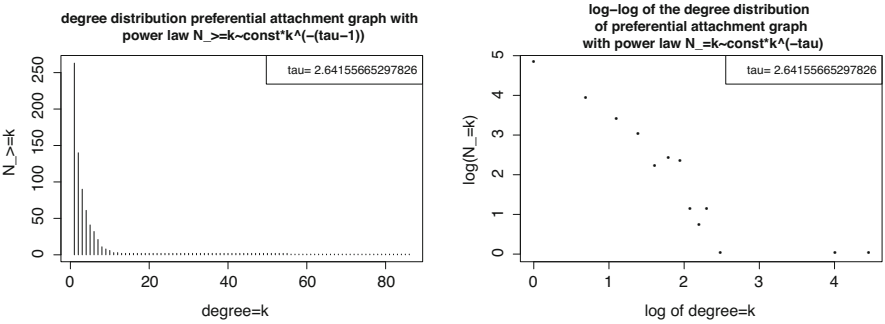

Fig. 11 Degree distribution of the protein network with $n = 263$ nodes and $\tau = 2.642$

Lets therefore look at the average degree in our network. It is given by

$$\frac{1}{n}\sum_{i=1}^{n} D(i) \approx 3.027,$$

which is not possible with our model since by Eq. (6) we always get an even degree. As stated before we are only looking at a subgraph of the network of all existing proteins of this family. Therefore it could still be possible to get the protein network

as a subgraph of a preferential attachment graph if the parameters are chosen carefully. Also one could think of a preferential attachment model which does not yield a connected graph.

5 Outlook

The discussion in Sect. 4 did not confirm that it is possible to model protein networks with our preferential attachment model. But like stated before there might be a solution to this by using a different preferential attachment approach which yields an unconnected graph with a random number of edges added every time a new node enters the graph.

Most protein networks are scale free but there are actually many possibilities to construct scale free graphs with different models such as the SN-Model introduced by Frisco in 2011 [7] where the nodes itself have a structure and are connected according to the differences in these structures. It is also possible to imitate the construction of proteins by using a Hidden Markov Model where the overlaying graph corresponds to the protein network.

References

1. A.-L. Barabási and R. Albert. Emergence of scaling in random networks. *Science*, 286(5439):509–512, 1999.
2. M. Bastian, S. Heymann, and M. Jacomy. Gephi: An open source software for exploring and manipulating networks, 2009. http://www.aaai.org/ocs/index.php/ICWSM/09/paper/view/154.
3. B. Bollobás. *Modern Graph Theory*. Springer, 1998.
4. P. Erdős and A. Rényi. On random graphs I. *Publ. Math. Debrecen*, 6:290–297, 1959.
5. P. Erdős and A. Rényi. On the evolution of random graphs. *Publ. Math. Inst. Hung. Acad. Sci.*, 5(1):17–60, 1960.
6. P. Erdős and A. Rényi. On the evolution of random graphs. *Bull. Inst. Internat. Statist.*, 38(4):343–347, 1961.
7. P. Frisco. Network model with structured nodes. *Physical Review*, 84(2):021931, 2011.
8. W. H. Hayt Jr., J. E. Kemmerly, and S. M. Durbin. *Engineering Circuit Analysis*. The McGraw-Hill Companies, Inc., 8. edition, 2012.
9. R Development Core Team. *R: A Language and Environment for Statistical Computing*. R Foundation for Statistical Computing, Vienna, Austria, 2008. ISBN 3-900051-07-0, http://www.R-project.org.
10. P. Tetali. Random walks and the effective resistance of networks. *Journal of Theoretical Probability*, 4(1):101–109, 1991.
11. R. van der Hofstad. *Random Graphs and Comples Networks Volume I*. Cambridge University Press, 2017.

Massive Modes for Quantum Graphs

H. A. Weidenmüller

Abstract The spectral two-point function of chaotic quantum graphs is expected to be universal. Within the supersymmetry approach, a proof of that assertion amounts to showing that the contribution of non-universal (or massive) modes vanishes in the limit of infinite graph size. Here we pay particular attention to the fact that the massive modes are defined in a coset space. Using the assumption that the spectral gap of the Perron-Frobenius operator remains finite in the limit, we then argue that the massive modes are indeed negligible.

1 Motivation

According to the Bohigas-Giannoni-Schmit (BGS) conjecture [1], the spectral fluctuation properties of Hamiltonian systems that are chaotic in the classical limit, coincide with those of the random-matrix ensemble in the same symmetry class (unitary, orthogonal, symplectic). Numerical simulations (see, f.i., Ref. [2]) strongly suggest that the BGS conjecture holds likewise for chaotic quantum graphs. Analytical arguments in support of the BGS conjecture for chaotic quantum graphs have been presented in several papers [3–6]. All these approaches use the supersymmetry formalism and a separation of the modes of the system into the universal (or massless or zero) mode and a number of massive modes. An essential part of the argument then consists in showing that the contribution of massive modes to all correlation functions vanishes in the limit of infinite graph size (number B of bonds to ∞). That leaves only the contribution of the zero mode, and universality of all correlation functions follows. The zero mode and the massive modes range in a non-linear space of cosets. That fact has not been addressed explicitly in previous work [3–6]. The problem has not gone unnoticed. Indeed, in Ref. [7] mathematical

H. A. Weidenmüller (✉)
Max-Planck-Institut für Kernphysik, Heidelberg, Germany
e-mail: hans.weidenmueller@mpi-hd.mpg.de

F. M. Atay et al. (eds.), *Discrete and Continuous Models in the Theory of Networks*, Operator Theory: Advances and Applications 281,
https://doi.org/10.1007/978-3-030-44097-8_17

aspects of the non-linearity of the coset space were discussed in detail without, however, establishing control of the contribution from the massive modes.

In the present paper we aim at filling that gap. We introduce the zero mode and the massive modes in a manner that is consistent with the non-linear coset structure. We do so using the strong assumption that in the limit $B \to \infty$, the spectrum of the Perron-Frobenius operator (defined in Eq. (2) below) has a finite gap that separates the eigenvalue $\lambda_1 = 1$ from the rest. In contrast, Refs. [3] and [4] pose only the weaker condition that the gap closes (for $B \to \infty$) no faster than $B^{-\alpha}$ with $0 \leq \alpha < 1/2$. That is perhaps a realistic requirement: Numerical simulations [2] suggest that chaotic graphs obeying Kirchhoff boundary conditions at each vertex possess universal spectral correlations even though the gap closes for large B. However, we doubt that, in the framework of a perturbative treatment of massive modes, there exists an easy way to turn the reasoning of Refs. [3, 4] into a convincing argument showing that the contribution of the massive modes vanishes in all orders. This is why we settle for the stronger assumption of a gap that remains finite in the limit of infinite graph size B. That assumption prevents us from keeping the local structure of the quantum graph fixed in the limit $B \to \infty$: To prevent the gap from closing, the graph connectivity must increase as the graph size is taken to infinity.

In Sect. 2 we recall some basic facts on chaotic graphs [2]. Section 3 forms the central piece of the paper. We introduce the universal mode and the massive modes in a manner that is consistent with the coset structure, and we express the effective action in terms of these variables. We use the fact that the spectrum of the Perron-Frobenius operator possesses a gap. In Sect. 4 we address the superintegrals over massive modes, and we argue that the contribution of these modes to the two-point correlation function vanishes in the limit of infinite graph size. We do so under rather restrictive assumptions concerning the matrix $\mathcal{B}$ that describes amplitude propagation on the quantum graph, see Sect. 2. We assume that the elements of $\mathcal{B}$ are all of order $1/\sqrt{2B}$, see Eq. (47). That implies that the fluctuations of the matrix elements about their mean values (defined by the unitarity of $\mathcal{B}$) are small (of order $1/\sqrt{2B}$). For a general proof of the BGS conjecture it would be necessary to lift that assumption.

We confine ourselves to the unitary case, to closed graphs, and to the two-point function (the correlation function of the retarded and the advanced Green's function).

2 Two-Point Function

To set the stage, we briefly summarize previous work [2–6] on chaotic quantum graphs. We consider connected simple graphs with V vertices and B bonds. Each bond has two directions $d = \pm$. The $2B$ directed bonds are labeled (bd). On every directed bond the Schrödinger wave carries the same wave number k and a direction-dependent magnetic phase ϕ_{bd} that breaks time-reversal invariance. Hermitean boundary conditions at vertex α (with $\alpha = 1, 2, \ldots, V$) cause incoming

and outgoing waves on the bonds linked to α to be related by a unitary vertex scattering matrix $\sigma^{(\alpha)}$. When arranged in directed-bond representation, the V scattering matrices $\sigma^{(\alpha)}$ form the $(2B)$-dimensional unitary bond scattering matrix $\Sigma^{(B)}$ with elements $\Sigma^{(B)}_{bd,b'd'}$. Amplitude propagation within the graph depends upon the unitary matrix

$$\mathcal{B}_{bd,b'd'} = \left(\sigma_1^D \Sigma^{(B)}\right)_{bd,b'd'} . \tag{1}$$

Here σ_1^D is the first Pauli spin matrix in two-dimensional directional space. It flips the direction of bonds, $(\sigma_1^D \Sigma^{(B)})_{bd,b'd'} = \Sigma^{(B)}_{b-d,b'd'}$. To see how σ_1^D arises (see Refs. [5, 6]) we consider a bond connecting vertices α and β. For vertex α the bond is denoted by $(\alpha, \beta) = (bd)$, for vertex β the bond is denoted by $(\beta, \alpha) = (b, -d)$. The two bond directions differ. To correctly describe amplitude propagation through the graph, the bond directions must match. That is achieved by multiplying $\Sigma^{(B)}$ with σ_1^D. The graph is classically chaotic if in the limit $B \to \infty$ of infinite graph size the spectrum of the Perron-Frobenius operator, i.e., of the matrix

$$\mathcal{F}_{bd,b'd'} = |\mathcal{B}_{bd,b'd'}|^2 \tag{2}$$

possesses a finite gap separating the leading eigenvalue $\lambda_1 = 1$ from all other eigenvalues λ_i (so that $|\lambda_i| \leq (1 - a)$ with $a > 0$). That is assumed throughout.

Unitary symmetry is realized by averaging separately and independently over the phases ϕ_{bd} ranging in the interval $[0, 2\pi]$. The averages are carried out using the supersymmetry method and the color-flavor transformation [8]. As a result, the two-point function is written as the derivative of a generating function, an integral in superspace. That function carries in the exponent the effective action $\mathcal{A}_{\text{eff}}$ given here in the form of Ref. [6] (see also Refs. [3, 4]),

$$\mathcal{A}_{\text{eff}} = -\text{STr}\ln(1 - Z\tilde{Z}) + \text{STr}\ln(1 - w_+\mathcal{B}_+ Z \mathcal{B}_-^\dagger w_- \tilde{Z}) . \tag{3}$$

Here $w_+ = w_-^* = \exp\{i\kappa\mathcal{L}\}$ where $\mathcal{L}$ is the diagonal matrix of bond lengths L_b, and where κ $(-\kappa)$ is the wave number increment in the retarded sector (the advanced sector, respectively). The matrices $\mathcal{B}_\pm$ are defined as

$$\mathcal{B}_\pm = (1 + j_\pm \frac{i\pi}{B}\sigma_3^s)\mathcal{B} , \tag{4}$$

with σ_3^s the third Pauli spin matrix in superspace. The average two-point function is obtained by differentiation of the generating function with respect to j_+ and j_- at $j_+ = 0 = j_-$.

The supermatrices $Z = \{\delta_{bb'}\delta_{dd'}Z_{bd;ss'}\}$ and $\tilde{Z} = \{\delta_{bb'}\delta_{dd'}\tilde{Z}_{bd;ss'}\}$ are diagonal in directed-bond space. For fixed indices (bd) the matrices Z and $\tilde{Z}$ each have dimension two and form part of a supermatrix of dimension four,

$$\begin{pmatrix} 0 & Z \\ \tilde{Z} & 0 \end{pmatrix} . \tag{5}$$

In Boson-Fermion block notation we have

$$Z = \begin{pmatrix} Z_{BB} & Z_{BF} \\ Z_{FB} & Z_{FF} \end{pmatrix}, \quad \tilde{Z} = \begin{pmatrix} \tilde{Z}_{BB} & \tilde{Z}_{BF} \\ \tilde{Z}_{FB} & \tilde{Z}_{FF} \end{pmatrix}, \tag{6}$$

where

$$Z_{BB} = \tilde{Z}_{BB}^* \,, \; Z_{FF} = -\tilde{Z}_{FF}^* \,, \; |Z_{BB}| < 1 \,. \tag{7}$$

The variable transformation $(1 + j_+ \frac{i\pi}{B} \sigma_3^s) Z \to Z$, $(1 + j_- \frac{i\pi}{B} \sigma_3^s) \tilde{Z} \to \tilde{Z}$ with Berezinian unity is used to simplify the source terms and, after differentiation with respect to j_+ and j_-, yields for the effective action

$$\mathcal{A} = -\mathrm{STr} \ln(1 - Z\tilde{Z}) + \mathrm{STr} \ln(1 - w_+ \mathcal{B} Z \mathcal{B}^\dagger w_- \tilde{Z}) \tag{8}$$

and for the source terms

$$\frac{\pi^2}{B^2} \Big(\mathrm{STr}\big[\sigma_3^s (1 - Z\tilde{Z})^{-1} Z \tilde{Z}\big] \, \mathrm{STr}\big[\sigma_3^s (1 - \tilde{Z}Z)^{-1} \tilde{Z} Z\big] + \mathrm{STr}\big[\sigma_3^s Z (1 - \tilde{Z}Z)^{-1} \sigma_3^s \tilde{Z} (1 - Z\tilde{Z})^{-1}\big] \Big) \,. \tag{9}$$

The terms (9) multiply $\exp\{-\mathcal{A}\}$ (Eq. (8)) under the superintegral over $(Z, \tilde{Z})$ with flat measure. That superintegral constitutes an exact representation of the average two-point function.

3 Effective Action

We introduce the universal mode and the massive modes. We express the effective action (8) and the source terms (9) as functions of these modes.

3.1 Coset Space

We first focus attention on the bare effective action, obtained from Eq. (8) by omission of κ, i.e., by putting $w_+ = 1 = w_-$,

$$\mathcal{A}_{\mathrm{bare}}(\tilde{Z}, Z) = -\mathrm{STr} \ln(1 - Z\tilde{Z}) + \mathrm{STr} \ln(1 - \mathcal{B} Z \mathcal{B}^\dagger \tilde{Z}). \tag{10}$$

Using an argument of Ref. [7] we show that $\mathcal{A}_{\mathrm{bare}}(\tilde{Z}, Z)$ is defined in a coset space. In retarded-advanced notation we define the matrices

$$\Lambda = \begin{pmatrix} 1 & 0 \\ 0 & -1 \end{pmatrix}, \quad M = \begin{pmatrix} \mathcal{B} & 0 \\ 0 & \mathcal{B}^\dagger \end{pmatrix}. \tag{11}$$

We expand the logarithms in Eq. (10), resume and obtain

$$\mathcal{A}_{\text{bare}} = -\text{STr}\ln\frac{2}{1+Q\Lambda} + \text{STr}\ln\left(1 - M\frac{Q\Lambda - 1}{Q\Lambda + 1}\right) \tag{12}$$

where

$$\begin{aligned} Q &= \begin{pmatrix} (1+Z\tilde{Z})(1-Z\tilde{Z})^{-1} & -2Z(1-\tilde{Z}Z)^{-1} \\ 2\tilde{Z}(1-Z\tilde{Z})^{-1} & -(1+\tilde{Z}Z)(1-\tilde{Z}Z)^{-1} \end{pmatrix} \\ &= g(Z)\Lambda(g(Z))^{-1} \end{aligned} \tag{13}$$

and

$$g(Z) = \begin{pmatrix} (1-Z\tilde{Z})^{-1/2} & Z(1-\tilde{Z}Z)^{-1/2} \\ \tilde{Z}(1-Z\tilde{Z})^{-1/2} & (1-\tilde{Z}Z)^{-1/2} \end{pmatrix}. \tag{14}$$

The supermatrices Z and $\tilde{Z}$ are diagonal in directed bond space and so is, therefore, Q.

We consider a specific set of bond indices (bd), omit these and work in four-dimensional superspace only. The matrix Q and the bare action $\mathcal{A}_{\text{bare}}$ remain unchanged under the transformation $g \to gk$ if k commutes with Λ. Therefore, Q and $\mathcal{A}_{\text{bare}}$ are defined in the coset superspace G/K where $g \in G = U(1,1|2)$ and $k \in K = U(1|1) \times U(1|1)$ with fundamental form $Q = g\Lambda g^{-1} = gk\Lambda k^{-1}g^{-1}$. Writing

$$g = \begin{pmatrix} A & B \\ C & D \end{pmatrix} \tag{15}$$

we find from Eq. (14)

$$\begin{aligned} Z(Q) &= B(g)(D(g))^{-1} = B(gk)(D(gk))^{-1}, \\ \tilde{Z}(Q) &= C(g)(A(g))^{-1} = C(gk)(A(gk))^{-1} \end{aligned} \tag{16}$$

for the local coordinates $(Z, \tilde{Z})$ of Q used in Eqs. (13). As briefly explained in the paragraph following Eq. (22), these and the other local coordinates introduced below are, however, not globally defined.

A group element $g_0 \in G$ acts on Q by $Q \to g_0 Q g_0^{-1}$ and on $g \in G$ by left multiplication. With

$$g_0 = \begin{pmatrix} A_0 & B_0 \\ C_0 & D_0 \end{pmatrix} \text{ and } g_0 g = \begin{pmatrix} A_0A + B_0C & A_0B + B_0D \\ D_0C + C_0A & D_0D + C_0B \end{pmatrix} \tag{17}$$

we obtain from Eqs. (16) for the local coordinates of $g_0 Q g_0^{-1}$

$$g_0 \cdot Z(Q) = (A_0 Z(Q) + B_0)(D_0 + C_0 Z(Q))^{-1},$$
$$g_0 \cdot \tilde{Z}(Q) = (D_0 \tilde{Z}(Q) + C_0)(A_0 + B_0 \tilde{Z}(Q))^{-1}. \tag{18}$$

3.2 Zero Mode Plus Fluctuations

Let $g_0 \in G$ in Eq. (17) be independent of the directed-bond indices (bd), and $Q_0 = g_0 \Lambda g_0^{-1}$. Following Eqs. (18) we define the zero mode (or universal mode) $(Y, \tilde{Y})$ by the local coordinates of Q_0,

$$Y = g_0 \cdot 0 = B_0 D_0^{-1}\ ,\ \ \tilde{Y} = g_0 \cdot \tilde{0} = C_0 A_0^{-1}\ . \tag{19}$$

Fluctuations about the zero mode are written in the sense of Eq. (18) as

$$Z_{bd} = g_0 \cdot \zeta_{bd}\ , \quad \tilde{Z}_{bd} = g_0 \cdot \tilde{\zeta}_{bd}\ . \tag{20}$$

Equations (20) transform the local variables $(Z, \tilde{Z})$ to the local variables $(Y, \tilde{Y})$ and $(\zeta, \tilde{\zeta})$. The latter are not gauge invariant. Therefore, we replace the supermatrices $(\zeta, \tilde{\zeta})$ by the gauge-invariant supermatrices $(\xi, \tilde{\xi})$ defined by

$$\xi = A_0 \zeta D_0^{-1}\ , \quad \tilde{\xi} = D_0 \tilde{\zeta} A_0^{-1}\ . \tag{21}$$

Suppressing the directed-bond indices we use Eqs. (18) (with ζ for $Z(Q)$ and $\tilde{\zeta}$ for $\tilde{Z}(Q)$) to express Z and $\tilde{Z}$ as given by Eqs. (20) as

$$Z = g_0 \cdot \zeta = (A_0 \zeta + B_0)(D_0 + C_0 \zeta)^{-1} = (Y + \xi)(1 + \tilde{Y}\xi)^{-1},$$
$$\tilde{Z} = g_0 \cdot \tilde{\zeta} = (D_0 \tilde{\zeta} + C_0)(A_0 + B_0 \tilde{\zeta})^{-1} = (\tilde{Y} + \tilde{\xi})(1 + Y\tilde{\xi})^{-1}. \tag{22}$$

The transformation (22) from the variables $(Z, \tilde{Z})$ to the variables $(Y, \tilde{Y})$ and $(\xi, \tilde{\xi})$ is somewhat analogous to the transformation from independent coordinates to center-of-mass and relative coordinates. Actually, the transformation (22) is more complicated than that because it has to respect the coset structure. We very briefly remark on the ensuing difficulties. The variables for our coset space G/K cannot be introduced in a globally well-defined way without using the mathematical machinery of an atlas of coordinate charts, transition functions, etc. Therefore, the gauge-independent variables $(Z, \tilde{Z})$, $(Y, \tilde{Y})$ and $(\xi, \tilde{\xi})$ are not globally defined but serve as good local coordinates. A simplification arises because we confine ourselves to small fluctuations of $(Z, \tilde{Z})$ about the "center-of-mass" coordinates $(Y, \tilde{Y})$. That is done by linearizing the transformation (20) in the new variables $(\zeta, \tilde{\zeta})$. Even in the linear regime we have to respect the coset structure, however.

We are greatly helped by our assumption that the spectrum of the Perron-Frobenius operator has a sufficiently large gap. By that assumption, the fluctuations of $(Z, \tilde{Z})$ about the "center-of-mass" coset $g_0 K$ with coordinates $(g_0 \cdot 0, g_0 \cdot \tilde{0})$ are small in a quantifiable sense, and the smallness allows us to treat the relative variables $(\zeta, \tilde{\zeta})$ approximately as vectors in the tangent space of G/K at $g_0 K$. Then the variables $(\xi, \tilde{\xi})$ also lie in a vector space. That is used in what follows.

Constraints are needed because only $(2B - 1)$ of the variables ζ and of the variables $\tilde{\zeta}$ appearing in Eqs. (20) (or of the variables ξ and $\tilde{\xi}$ appearing in Eqs. (21)) are independent. Using the assumption that $(\xi, \tilde{\xi})$ lie in a vector space we impose the constraints

$$\sum_{bd} \xi_{bd} = 0 = \sum_{bd} \tilde{\xi}_{bd} \,. \tag{23}$$

The transformation (22) with the constraints (23) introduces as new integration variables the coordinates $(Y, \tilde{Y})$ of the zero mode and the independent ones among the variables $(\xi, \tilde{\xi})$. The Berezinian of the transformation is unity.

3.3 Implementation of the New Variables

In order to express the effective action of Eq. (8) and the source terms (9) in terms of the modes $(Y, \tilde{Y})$ and $(\xi, \tilde{\xi})$, we derive an invariance property of the bare effective action, adapting to the present case an argument developed in Ref. [9] for a network model of the Integer Quantum Hall Effect. With the help of the definitions and results of Sect. 3.1 we show by explicit calculation that

$$\begin{aligned} &\mathrm{STr}\ln(1 - (g_0 \cdot Z)(g_0 \cdot \tilde{Z})) - \mathrm{STr}\ln(1 - \mathcal{B}(g_0 \cdot Z)\mathcal{B}^\dagger(g_0 \cdot \tilde{Z})) \\ &= \mathrm{STr}\ln(1 - Z\tilde{Z}) - \mathrm{STr}\ln(1 - \mathcal{B}Z\mathcal{B}^\dagger\tilde{Z}) \,. \end{aligned} \tag{24}$$

The invariance property (24) holds provided that $g_0 \cdot (\mathcal{B}Z\mathcal{B}^\dagger) = \mathcal{B}(g_0 \cdot Z)\mathcal{B}^\dagger$. We have not used any specific properties of the matrices $(Z, \tilde{Z})$. Therefore, Eq. (24) holds also for the matrices $(\zeta, \tilde{\zeta})$. We use Eq. (24) for the bare effective action of Eq. (10). We replace the variables $(Z, \tilde{Z})$ by the transformation (20) and apply the invariance property (24) to the resulting expression. That gives

$$\mathcal{A}_{\mathrm{bare}}(g_0 \cdot \zeta, g_0 \cdot \tilde{\zeta}) = \mathcal{A}_{\mathrm{bare}}(\zeta, \tilde{\zeta}) \,. \tag{25}$$

The matrices A_0 and D_0 in Eqs. (21) commute with $\mathcal{B}$. Therefore, $\mathcal{A}_{\mathrm{bare}}(\zeta, \tilde{\zeta}) = \mathcal{A}_{\mathrm{bare}}(\xi, \tilde{\xi})$, and we obtain

$$\mathcal{A}_{\mathrm{bare}}(\xi, \tilde{\xi}) = -\mathrm{STr}\ln(1 - \xi\tilde{\xi}) + \mathrm{STr}\ln(1 - \mathcal{B}\xi\mathcal{B}^\dagger\tilde{\xi}) \,. \tag{26}$$

We return to the full effective action (8). We are interested in values of κ that are of the order of the mean level spacing $\Delta = \pi / \sum_b L_b$. Therefore, we expand $\mathcal{A}$ up to terms of first order in κ. In the first-order terms we neglect the fluctuations by putting all $\xi = 0 = \tilde{\xi}$. Since $\mathcal{B}$ commutes with the zero-mode variables Y and $\tilde{Y}$ that gives

$$\mathcal{A} \approx \mathcal{A}_{\rm bare}(\xi, \tilde{\xi}) - \frac{2i\pi\kappa}{\Delta} \, {\rm STr}_s \frac{1}{1 - Y\tilde{Y}} \,, \tag{27}$$

with $\mathcal{A}_{\rm bare}$ given by Eq. (26). The index s indicates that the supertrace extends only over superspace. Being proportional to ${\rm STr}[g(Y)\Lambda(g(Y))^{-1}\Lambda] = {\rm STr}[Q\Lambda]$, the last term in Eq. (27) has the classical form for the symmetry-breaking term.

We turn to the source terms (9). The supermatrices $(Z, \tilde{Z})$ are diagonal in directed bond space; we consider a fixed value of (bd) and omit these indices. Then both Z and $\tilde{Z}$ have dimension two. We define the four-dimensional matrix $Q(\xi, \tilde{\xi})$ as in Eq. (13) but with the replacements $Z \to \xi$, $\tilde{Z} \to \tilde{\xi}$. With Λ defined in Eqs. (11), the source terms are written as

$$\begin{aligned}
&{\rm STr}_s\big[\sigma_3^s (1 - Z\tilde{Z})^{-1} Z\tilde{Z}\big] = -1 + {\rm STr}_s\big[\Sigma(Y, \tilde{Y}) Q(\xi, \tilde{\xi})\Lambda\big] \,, \\
&{\rm STr}_s\big[\sigma_3^s (1 - \tilde{Z}Z)^{-1} \tilde{Z}Z\big] = -1 + {\rm STr}_s\big[\Sigma'(Y, \tilde{Y}) Q(\xi, \tilde{\xi})\Lambda\big] \,, \\
&{\rm STr}_s\big[\sigma_3^s Z(1 - \tilde{Z}Z)^{-1} \sigma_3^s \tilde{Z}(1 - Z\tilde{Z})^{-1}\big] \\
&\quad = {\rm STr}_s\big[\Sigma(Y, \tilde{Y}) Q(\xi, \tilde{\xi})\Lambda \Sigma'(Y, \tilde{Y}) Q(\xi, \tilde{\xi})\Lambda\big] \,.
\end{aligned} \tag{28}$$

The index s indicates that the supertraces extend over superspace only. The supermatrices Σ and Σ' are defined as

$$\begin{aligned}
\Sigma(Y, \tilde{Y}) &= \frac{1}{2} \begin{pmatrix} (1 - Y\tilde{Y})^{-1} & 0 \\ 0 & (1 - \tilde{Y}Y)^{-1} \end{pmatrix} \begin{pmatrix} \sigma_3^s & \sigma_3^s Y \\ \tilde{Y}\sigma_3^s & \tilde{Y}\sigma_3^s Y \end{pmatrix} , \\
\Sigma'(Y, \tilde{Y}) &= \frac{1}{2} \begin{pmatrix} (1 - Y\tilde{Y})^{-1} & 0 \\ 0 & (1 - \tilde{Y}Y)^{-1} \end{pmatrix} \begin{pmatrix} Y\sigma_3^s\tilde{Y} & Y\sigma_3^s \\ \sigma_3^s\tilde{Y} & \sigma_3^s \end{pmatrix} .
\end{aligned} \tag{29}$$

It is a very convenient feature of expression (28) that the contributions from the universal mode $(Y, \tilde{Y})$ and from the massive modes $(\xi, \tilde{\xi})$ factorize. That separation can be carried a step further. We use the decomposition $Q(\xi_{bd}, \tilde{\xi}_{bd})\Lambda = [Q(\xi_{bd}, \tilde{\xi}_{bd})\Lambda - 1] + 1$. Supersymmetry must be broken for the same integration variable in both the advanced and the retarded sector to obtain a non-vanishing result. Therefore, terms linear in $(Q\Lambda - 1)$ vanish upon integration, and the contribution of the massive modes to the source terms is

$$\frac{\pi^2}{B^2} \Big\{ \sum_{bd} {\rm STr}_s \Big(\Sigma(Y, \tilde{Y}) [Q(\xi_{bd}, \tilde{\xi}_{bd})\Lambda - 1] \Sigma'(Y, \tilde{Y}) [Q(\xi_{bd}, \tilde{\xi}_{bd})\Lambda - 1] \Big)$$

$$+\sum_{bd}\mathrm{STr}_s\Big(\Sigma(Y,\tilde{Y})[Q(\xi_{bd},\tilde{\xi}_{bd})\Lambda-1]\Big)$$

$$\times\sum_{b'd'}\mathrm{STr}_s\Big(\Sigma'(Y,\tilde{Y})[Q(\xi_{b'd'},\tilde{\xi}_{b'd'})\Lambda-1]\Big)\Big\}. \tag{30}$$

It is our task to show that the integrals over the terms (30) with weight factor $\exp\{-\mathcal{A}_{\mathrm{bare}}(\xi,\tilde{\xi})\}$ and carried out for all $(\xi,\tilde{\xi})$ vanish for $B\to\infty$.

4 Evaluation

To argue in that direction we proceed as follows. We simplify the source terms (30) by a suitable variable transformation. We expand the bare effective action in powers of the new integration variables. Terms up to second order define Gaussian superintegrals. The exponential containing terms of higher order is expanded in a Taylor series. We perform the Gaussian superintegrals. We give an approximate estimate of the dependence on B of the terms so generated and on that basis argue that they vanish for $B\to\infty$.

We display the procedure for a single contribution to the source terms. The procedure applies likewise to the remaining terms without any additional difficulties and is not given here. We consider the last term in expression (30). We introduce block notation, writing

$$\Sigma=\begin{pmatrix}\Sigma_{++} & \Sigma_{+-}\\ \Sigma_{-+} & \Sigma_{--}\end{pmatrix} \tag{31}$$

and correspondingly for Σ' and for $Q(\xi_{bd},\tilde{\xi}_{bd})$. It is convenient to write μ for (bd) and ν for $(b'd')$. For the pair $\Sigma_{++}\ \Sigma'_{--}$ the relevant contribution is

$$\frac{\pi^2}{B^2}\Big\langle\sum_{\mu}\mathrm{STr}_s\Big(\Sigma_{++}[Q(\xi_\mu,\tilde{\xi}_\mu)\Lambda-1]_{++}\Big)$$

$$\times\sum_{\nu}\mathrm{STr}_s\Big(\Sigma'_{--}[Q(\xi_\nu,\tilde{\xi}_\nu)\Lambda-1]_{--}\Big)\Big\rangle. \tag{32}$$

The angular brackets denote the superintegration over all $(\xi,\tilde{\xi})$ with weight factor $\exp\{-\mathcal{A}_{\mathrm{bare}}\}$. According to Eqs. (13) we have $[Q(\xi,\tilde{\xi})\Lambda-1]_{++}=2\xi\tilde{\xi}(1-\xi\tilde{\xi})^{-1}$ and $[Q(\xi,\tilde{\xi})\Lambda-1]_{--}=2\tilde{\xi}\xi(1-\tilde{\xi}\xi)^{-1}$.

4.1 Variable Transformation

We simplify the form of the source term in expression (32) by defining for each set of directed bond indices the variable transformation

$$\xi = \psi(1 + \tilde{\psi}\psi)^{-1/2}, \quad \tilde{\xi} = \tilde{\psi}(1 + \psi\tilde{\psi})^{-1/2}, \tag{33}$$

with inverse transformation

$$\psi = \xi(1 - \tilde{\xi}\xi)^{-1/2}, \quad \tilde{\psi} = \tilde{\xi}(1 - \xi\tilde{\xi})^{-1/2}. \tag{34}$$

Calculation shows that the Berezinian of the variable transformation (33) is unity. Instead of the constraints (23) we impose

$$\sum_{\mu} \psi_{\mu} = 0 = \sum_{\mu} \tilde{\psi}_{\mu} \,. \tag{35}$$

To justify Eqs. (35) we observe that Eqs. (23) were introduced in an ad-hoc fashion to guarantee that only $(2B - 1)$ of the variables $(\zeta_{\mu}, \tilde{\zeta}_{\mu})$ and $(\xi_{\mu}, \tilde{\xi}_{\mu})$ are independent. Equations (35) serve that same purpose.

From Eqs. (33) we have $[Q(\xi, \tilde{\xi})\Lambda - 1]_{++} = 2\psi\tilde{\psi}$ and $[Q(\xi, \tilde{\xi})\Lambda - 1]_{--} = 2\tilde{\psi}\psi$. Expression (32) becomes

$$\frac{4\pi^2}{B^2} \sum_{\mu\nu} \left\langle \mathrm{STr}_s\big(\Sigma_{++}\, \psi_{\mu}\tilde{\psi}_{\mu}\big) \mathrm{STr}_s\big(\Sigma'_{--}\, \tilde{\psi}_{\nu}\psi_{\nu}\big) \right\rangle . \tag{36}$$

For the bare effective action of Eq. (26), the variable transformation (33) leads to

$$\begin{aligned} \mathcal{A}_{\mathrm{bare}}(\psi, \tilde{\psi}) &= +\mathrm{STr}\ln(1 + \psi\tilde{\psi}) \\ &\quad +\mathrm{STr}\ln\big(1 - \mathcal{B}\psi(1 + \tilde{\psi}\psi)^{-1/2}\mathcal{B}^{\dagger}\tilde{\psi}(1 + \psi\tilde{\psi})^{-1/2}\big) \\ &= \mathrm{STr}\big(\psi\tilde{\psi} - \mathcal{B}\psi\mathcal{B}^{\dagger}\tilde{\psi}\big) + \ldots \end{aligned} \tag{37}$$

where the dots indicate terms of higher order in ψ and $\tilde{\psi}$.

4.2 Gaussian Superintegrals

In the expansion of $\mathcal{A}_{\mathrm{bare}}$ in Eq. (37), we retain in the exponent only terms up to second order in $(\psi, \tilde{\psi})$ (last line of Eq. (37)). With $\mathcal{F}$ defined in Eq. (2) these can be written as

$$\mathcal{A}_0 = \sum_{\mu\nu} \mathrm{Str}_s\big[\psi_{\mu}(\delta_{\mu\nu} - \mathcal{F}_{\mu\nu})\tilde{\psi}_{\nu}\big]. \tag{38}$$

Equation (38) defines the Gaussian part $\mathcal{A}_0$ of the bare effective action. The Perron-Frobenius operator $\mathcal{F}$ is expanded in terms of its complex eigenvalues λ_k and left and right eigenvectors $\langle w_k|$ and $|u_k\rangle$ as

$$\mathcal{F} = \sum_k |u_k\rangle \lambda_k \langle w_k| \,. \tag{39}$$

These (non-real) eigenvectors satisfy the relations $\langle w_k|u_l\rangle = \delta_{kl}$. The matrix $\mathcal{F}$ is bistochastic, its elements are positive or zero. The graph is connected. It follows from the Perron-Frobenius theorem that there exists a non-degenerate eigenvalue $\lambda_1 = +1$. The associated left and right eigenvectors $\langle w_1|$ and $|u_1\rangle$ have the components $(1/\sqrt{2B})\{1, 1, \ldots, 1\}$. All other eigenvalues λ_i with $i \geq 2$ lie within or on the unit circle in the complex plane. As stated below Eq. (2), we assume that all other eigenvalues λ_i with $2 \leq i \leq 2B$ obey $|\lambda_i| \leq (1 - a)$ with $a > 0$ even in the limit $B \to \infty$. The matrix $|u_1\rangle\langle w_1|$ is an orthogonal projector. Equations (35) guarantee that $|u_1\rangle\langle w_1|$ does not contribute to the sum on the right-hand side of expression (38), confirming that the zero mode has been eliminated. We emphasize that fact by defining the complementary projector $\mathcal{P} = 1 - |u_1\rangle\langle w_1|$, and by writing expression (38) as

$$\mathcal{A}_0 = \sum_{\mu\nu} \mathrm{STr}_s \Big[\psi_\mu \Big(\mathcal{P}(1 - \mathcal{F})\mathcal{P} \Big)_{\mu\nu} \tilde{\psi}_\nu \Big] . \tag{40}$$

The bilinear form $\mathcal{A}_0$ defines the propagator of the theory. The factor $\exp\{-\mathcal{A}_0\}$ defines Gaussian superintegrals. The fundamental integral is

$$\int \mathrm{d}(\psi, \tilde{\psi}) \psi_{\mu;st} \tilde{\psi}_{\nu;t's'} \exp\{-\mathcal{A}_0\} = \delta_{ss'}\delta_{tt'}(-)^t \langle \mu|\mathcal{P}(1 - \mathcal{F})^{-1}\mathcal{P}|\nu\rangle \,. \tag{41}$$

We have written $\mu = (bd)$ as before. The range of the superindices (s, t) is $(0, 1)$ or, equivalently, (B, F).

The Taylor expansion of the exponential containing the dotted terms in expression (37) generates products of supertraces each containing powers of ψ and $\tilde{\psi}$. For the Gaussian integral over the product of these with the source term in expression (36) we use the general result

$$\begin{aligned} &\int \mathrm{d}(\psi, \tilde{\psi}) \prod_{i=1}^{n} \psi_{\mu_i;s_it_i} \tilde{\psi}_{\nu_i;t_i's_i'} \exp\{-\mathcal{A}_0\} \\ &\quad = \prod_{i=1}^{n} \sum_{\text{perm}} \prod_{j=1}^{n} \delta_{s_is_j'}\delta_{t_it_j'}(-)^{t_i} \langle \mu_i|\mathcal{P}(1 - \mathcal{F})^{-1}\mathcal{P}|\nu_j\rangle \,. \end{aligned} \tag{42}$$

The sum is over all permutations of $(1, 2, \ldots, n)$. The expressions generated by the Gaussian integrals (42) contain products of factors $\langle \mu|\mathcal{P}(1 - \mathcal{F})^{-1}\mathcal{P}|\nu\rangle$ and may

become very lengthy. We use the abbreviations

$$W_{\mu\nu} = \langle\mu|\mathcal{P}(1-\mathcal{F})^{-1}\mathcal{P}|\nu\rangle \text{ and, for } n>1\ , W^{(n)}_{\mu\nu} = \langle\mu|\mathcal{P}(1-\mathcal{F})^{-n}\mathcal{P}|\nu\rangle\ . \tag{43}$$

4.3 Qualitative Estimation

The integrals (42) generate products of matrix elements $W_{\mu\nu}$. Progress hinges on our ability to estimate the dependence of these matrix elements and of sums of their products on the dimension $(2B)$ of directed-bond space for $B \to \infty$. Postponing a strict treatment to future work, we here settle for the simple approximation of using averages based upon the completeness relation.

For the diagonal elements we use Eq. (39), the relation $\langle w_k|u_l\rangle = \delta_{kl}$, and the completeness relation and find

$$\langle\mu|\mathcal{P}(1-\mathcal{F})^{-1}\mathcal{P}|\mu\rangle \approx \frac{1}{2B}\sum_{\mu}\langle\mu|\mathcal{P}(1-\mathcal{F})^{-1}\mathcal{P}|\mu\rangle = \frac{1}{2B}\sum_{k\geq 2}\frac{1}{1-\lambda_k}\ . \tag{44}$$

Since $\mathcal{F}$ is real, the eigenvalues λ_k are either real or come in complex conjugate pairs. Therefore, the sum on the right-hand side is real. By assumption, the eigenvalues obey $|\lambda_k| \leq (1-a)$ with $a>0$. Therefore, the expression on the right-hand side is positive and for all B bounded from above by $1/a$. We accordingly estimate $W_{\mu\mu} = \langle\mu|\mathcal{P}(1-\mathcal{F})^{-1}\mathcal{P}|\mu\rangle$ by $1/a$. (Here and in what follows we use the word "estimate" in the non-technical sense of order-of-magnitude estimate). For terms with higher inverse powers of $(1-\mathcal{F})$ we find correspondingly $W^{(n)}_{\mu\mu} \approx 1/a^n$. The factor $1/a^n$ stems from the sum $\sum_k 1/(1-\lambda_k)^n$. In the limit $B\to\infty$ that sum exists for all n only if the gap in the spectrum of the Perron-Frobenius operator $\mathcal{F}$ does not close. That condition is also used in the estimates given below.

For the non-diagonal elements we have

$$\langle\mu|\mathcal{P}(1-\mathcal{F})^{-1}\mathcal{P}|\nu\rangle(1-\delta_{\mu\nu}) \approx \frac{1}{(2B)^2}\sum_{\mu\nu}\langle\mu|\mathcal{P}(1-\mathcal{F})^{-1}\mathcal{P}|\nu\rangle(1-\delta_{\mu\nu})\ . \tag{45}$$

Since $\sum_\mu\langle\mu|\mathcal{P} = \sqrt{2B}\langle w_1|\mathcal{P} = 0$ and $\sum_\mu \mathcal{P}|\mu\rangle = \sqrt{2B}\mathcal{P}|u_1\rangle = 0$, the first term of $(1-\delta_{\mu\nu})$ gives a vanishing contribution. For the second term we use Eq. (44) and find that the typical non-diagonal element $W_{\mu\nu}$ with $\mu\neq\nu$ is of order $1/((2B)a)$. For $W^{(n)}_{\mu\nu}$ with $\mu\neq\nu$ and $n>1$ we correspondingly have $W^{(n)}_{\mu\nu} \approx 1/((2B)a^n)$.

After integration and use of the order-of-magnitude estimate (44), the remaining terms in the expansion may carry a product of matrix elements of the form $\prod_{i=1}^n\langle\mu_i|\mathcal{P}(1-\mathcal{F})^{-1}\mathcal{P}|\mu_{i+1}\rangle$. In addition to the steps taken in Eqs. (44) and (45) we use the approximation $|\mu_i\rangle\langle\mu_i| \approx (1/(2B))\sum_\mu|\mu\rangle\langle\mu|$ for the intermediate

projectors $|\mu_i\rangle\langle\mu_i|$ with $2 \le i \le n$. That gives

$$\prod_{i=1}^{n}\langle\mu_i|\mathcal{P}(1-\mathcal{F})^{-1}\mathcal{P}|\mu_{i+1}\rangle = \prod_{i=1}^{n} W_{\mu_i\mu_{i+1}} \approx \frac{1}{a^n(2B)^{n-1}}\left(\delta_{\mu_1\mu_{n+1}} - \frac{1}{2B}\right). \quad (46)$$

The relation (46) holds likewise (with appropriate changes of the power of $1/a$) in cases where one or several of the denominators $(1-\mathcal{F})$ carry powers larger than unity.

For an estimate of the large-B dependence of expressions involving $\mathcal{B}$ or $\mathcal{B}^\dagger$, we use the unitarity relation $\sum_{\sigma=1}^{2B}\mathcal{B}^\dagger_{\rho\sigma}\mathcal{B}_{\sigma\rho} = 1$. It implies that in the ergodic limit we have

$$|\mathcal{B}_{\mu\nu}| \approx \frac{1}{\sqrt{2B}}\,. \quad (47)$$

The estimates (42), (46) and (47) provide us with the tools needed to give an order-of-magnitude estimate of the B-dependence of the source terms and the terms generated by the Taylor expansion of the higher-order terms in $\mathcal{A}_{\text{bare}}$.

4.4 Source Term

In expression (36) we first disregard contributions due to the Taylor expansion of higher-order terms in $\mathcal{A}_{\text{bare}}$. Equation (42) implies that the Gaussian integrals over products of factors $(\psi, \tilde{\psi})$ lead to pairwise contractions. In the source term (36) that results in the sum of two terms,

$$\begin{aligned}\left\langle \sum_{t_1}\psi_{\mu,s_1t_1}\tilde{\psi}_{\mu,t_1s_1'}\sum_{s_2}\tilde{\psi}_{\nu,t_2s_2}\psi_{\nu,s_2t_2'}\right\rangle \\ = \left\langle \sum_{t_1}\psi_{\mu,s_1t_1}\tilde{\psi}_{\mu,t_1s_1'}\right\rangle\left\langle \sum_{s_2}\tilde{\psi}_{\nu,t_2s_2}\psi_{\nu,s_2t_2'}\right\rangle \\ +(-)^{s_1+t_2}\sum_{t_1}\sum_{s_2}\left\langle \psi_{\mu,s_1t_1}\tilde{\psi}_{\nu,t_2s_2}\right\rangle\left\langle \tilde{\psi}_{\mu,t_1s_1'}\psi_{\nu,s_2t_2'}\right\rangle. \quad (48)\end{aligned}$$

According to Eq. (42) the first term vanishes, and the second term equals $W_{\mu\nu}W_{\nu\mu}\delta_{s_1s_1'}\delta_{t_2t_2'}$. We have $|\sum_\nu W_{\mu\nu}W_{\nu\mu}| \le ||WW||_{\text{op}} \le ||W||^2_{\text{op}} \le a^{-2}$. The double bars denote the operator norm. Hence $|\sum_\nu W_{\mu\nu}W_{\nu\mu}| \le (2B)/a^2$. The term (36) carries the factor $1/B^2$. For $B \to \infty$ it vanishes as $1/B$.

4.5 Higher-Order Contributions

Among the terms in expression (36) that arise from the Taylor expansion of higher-order terms in $\mathcal{A}_{\rm bare}$ in Eq. (37), we first address terms that originate from STr $\ln(1+\psi\tilde{\psi})$. Except for numerical factors the general term in the Taylor expansion has the form

$$\frac{4\pi^2}{B^2}\Big\langle \sum_{\mu\nu} \mathrm{STr}_s\big(\Sigma_{++}\,\psi_\mu\tilde{\psi}_\mu\big)\mathrm{STr}_s\big(\Sigma'_{--}\,\tilde{\psi}_\nu\psi_\nu\big)\prod_{i=1}^{m}\mathrm{STr}(\psi\tilde{\psi})^{n_i}\Big\rangle\,, \tag{49}$$

with integer $m \geq 1, n_i \geq 2$. Gaussian integration as in Eq. (42) leads to pairwise contraction of all factors ψ and $\tilde{\psi}$ and, thus, to $k = 2 + \sum_i n_i$ factors W. A non-vanishing result is obtained only if supersymmetry is violated in every supertrace in expression (49). Therefore, all supertraces in expression (49) must be linked by pairwise contractions. That, incidentally, is the reason why in Eq. (48) the first term on the right-hand side vanishes.

We consider two examples. For $m = 1, n_1 = 2$, the nonvanishing links yield two terms,

$$\begin{aligned}(1/B^2)\sum_{\mu\nu\rho} W_{\mu\nu}W_{\nu\rho}W_{\rho\mu}W_{\rho\rho} &= (1/B^2)\sum_{\rho} W^{(3)}_{\rho\rho}W_{\rho\rho}\,,\\ (1/B^2)\sum_{\mu\nu\rho} W_{\mu\rho}W_{\rho\mu}W_{\rho\nu}W_{\nu\rho} &= (1/B^2)\sum_{\rho} W^{(2)}_{\rho\rho}W^{(2)}_{\rho\rho}\,.\end{aligned} \tag{50}$$

In the first expression we use $W_{\rho\rho} \approx 1/a$, $W^{(3)}_{\rho\rho} \approx 1/a^3$. The sum over ρ yields a factor $(2B)$. Altogether the term is estimated as $1/((2B)a^4)$ and vanishes for $B \to \infty$. In the second expression we use $W^{(2)}_{\rho\rho} \approx 1/a^2$ and find the same result. For $m = 2, n_1 = 2 = n_2$ we correspondingly obtain the terms

$$\begin{aligned}&(1/B^2)\sum_{\rho\tau} W^{(3)}_{\rho\rho}W_{\rho\tau}W_{\tau\rho}W_{\tau\tau}\,,\ (1/B^2)\sum_{\rho\tau} W^{(3)}_{\tau\rho}(W_{\rho\tau})^2W_{\tau\rho}\,,\\ &(1/B^2)\sum_{\rho\tau} W^{(3)}_{\tau\rho}W_{\rho\tau}W_{\rho\rho}W_{\tau\tau}\,,\ (1/B^2)\sum_{\rho\tau} W^{(2)}_{\rho\tau}W^{(2)}_{\tau\rho}W_{\rho\tau}W_{\tau\rho}\,,\\ &(1/B^2)\sum_{\rho\tau} W^{(2)}_{\rho\rho}W^{(2)}_{\tau\tau}W_{\rho\tau}W_{\tau\rho}\,,\ (1/B^2)\sum_{\rho\tau} W^{(2)}_{\rho\tau}W^{(2)}_{\tau\rho}W_{\rho\rho}W_{\tau\tau}\,.\end{aligned} \tag{51}$$

We use the estimates (44, 46). The terms of leading order are the ones where two factors $W^{(n)}$ with $n = 1$ or $n = 2$ or $n = 3$ each carry identical indices. These are the terms number 1, 3, 5, 6. They vanish asymptotically as $1/(2B)$.

From these examples we deduce the following rules. (i) In expression (49), contraction of the four factors $(\psi_\mu, \tilde{\psi}_\mu)$ and $(\psi_\nu, \tilde{\psi}_\nu)$ with one another and with corresponding factors in the product over traces yields a nonvanishing result only

if it generates either two factors $W^{(2)}$ or a single factor $W^{(3)}$. These carry indices of the factors in the product over traces. For every pair (ρ, σ), the factors $W^{(2)}_{\rho\sigma}$ and $W^{(3)}_{\rho\sigma}$ are, both for $\rho = \sigma$ and for $\rho \neq \sigma$, of the same order in $1/(2B)$ as the factor $W_{\rho\sigma}$. For purposes of counting powers of $(2B)$ it suffices, therefore, to disregard the four factors $(\psi_\mu, \tilde{\psi}_\mu)$ and $(\psi_\nu, \tilde{\psi}_\nu)$ together with the summation over μ and ν and to consider only contractions within the product of supertraces. (ii) The terms of leading order in $1/(2B)$ are obtained by contracting, in every supertrace $\mathrm{STr}(\psi\tilde{\psi})^{n_i}$, $(n_i - 1)$ pairs $(\psi_\rho, \tilde{\psi}_\rho)$ with one another. That is because contraction of pairs of ψ's in the same (in different) supertraces generates factors $W_{\rho\rho} \propto 1/a$ ($W_{\rho\sigma} \propto 1/(2Ba)$ with $\rho \neq \sigma$, respectively). Contraction of pairs within the same supertrace generates $(n_i - 1)$ factors $W_{\rho\rho}$ and reduces each supertrace to $(1/a^{n_i - 1})\mathrm{STr}(\psi\tilde{\psi})$. These rules imply that the only remaining contractions in expression (49) are over the term

$$[\mathrm{STr}(\psi\tilde{\psi})]^m \to \sum_{\mu_1,\ldots,\mu_m} W_{\mu_1\mu_2} \times \ldots \times W_{\mu_m\mu_1} = \sum_{\mu_1} W^{(m)}_{\mu_1} \,. \tag{52}$$

To the extent that our approximations (of replacing fluctuating quantities by their averages) capture the qualitative aspects of the problem, we may conclude that expression (49) is of order $1/(2B)$ and vanishes for $B \to \infty$.

The general term in the Taylor expansion contains, in addition to the terms in expression (49), also products of supertraces that contain the elements of $\mathcal{B}$. Each such supertrace has the form $\mathrm{STr}[\mathcal{B}\psi(\tilde{\psi}\psi)^m\mathcal{B}^\dagger\tilde{\psi}(\psi\tilde{\psi})^n]^l$ with $l \geq 1$ and (m, n) zero or positive integer, see Eq. (37). In contracting factors ψ and $\tilde{\psi}$ we apply rule (ii). The terms of leading order are obtained by replacing in each supertrace $(\tilde{\psi}\psi)^m$ by $1/a^m$ and $(\psi\tilde{\psi})^n$ by $1/a^n$. We proceed likewise for the product of supertraces in expression (49). That reduces the general expression to

$$\frac{1}{B^2}\Bigg\langle \sum_{\mu\nu} \mathrm{STr}_s\big(\Sigma_{++}\,\psi_\mu\tilde{\psi}_\mu\big)\mathrm{STr}_s\big(\Sigma'_{--}\,\tilde{\psi}_\nu\psi_\nu\big) \times \Bigg\{[\mathrm{STr}(\psi\tilde{\psi})]^m \prod_{i=1}^{k} \mathrm{STr}\Big(\mathcal{B}\psi\mathcal{B}^\dagger\tilde{\psi}\Big)^{l_i}\Bigg\}\Bigg\rangle \,. \tag{53}$$

Here $m \geq 0$ and $l_i \geq 1$ for $i = 1, \ldots, m$. We require $k \geq 1$ as the case $k = 0$ has been considered above. We apply rule (i) and disregard the difference between factors $W^{(n)}$ and W in estimating the dependence of expression (53) on $1/(2B)$. In other words, we confine ourselves to contractions involving elements $(\psi, \tilde{\psi})$ in the curly brackets in expression (53). For $m = 0$, all supertraces carrying elements of $\mathcal{B}$ must be connected by pairwise contractions. That generates $\sum_i l_i$ factors W. Each such factor carries a pair of summation indices. No two summation indices in any of these factors are the same. Therefore, each factor W is of order $1/(2B)$. There are $\sum_i l_i$ elements of $\mathcal{B}$ and of $\mathcal{B}^\dagger$, each of order $1/\sqrt{2B}$. There are $2\sum_i l_i$ independent summations over directed-bond space. Together with the

prefactor $1/B^2$, we therefore expect expression (53) to be of order $1/(2B)^2$ for $m = 0$.

That expectation remains unaltered for $m > 0$. We show that first for $m = 1$, writing $\mathrm{STr}(\psi\tilde{\psi}) = \sum_\rho \mathrm{STr}_s(\psi_\rho\tilde{\psi}_\rho)$. Contraction links the factor ψ_ρ (the factor $\tilde{\psi}_\rho$) with some factor $\tilde{\psi}_\sigma$ (with some factor ψ_τ, respectively). Both $\tilde{\psi}_\sigma$ and ψ_τ occur in the product over i in expression (53). The result is $\sum_\rho W_{\rho\sigma} W_{\tau\rho} = W^{(2)}_{\tau\sigma}$ while for $m = 0$ contracting $\tilde{\psi}_\sigma$ and ψ_τ gives $W_{\tau\sigma}$. Since $W_{\tau\sigma}$ and $W^{(2)}_{\tau\sigma}$ are of the same order, the expressions (53) with $m = 0$ and with $m = 1$ are of the same order, too. The argument can straightforwardly be extended to $m \geq 2$. This concludes our heuristic reasoning that the general term containing matrix elements of $\mathcal{B}$ vanishes for $B \to \infty$ as $1/(2B)^2$.

5 Summary and Discussion

We have given a brief account of an approach to chaotic quantum graphs that aims at demonstrating the BGS conjecture using supersymmetry and the color-flavor transformation. We have paid particular attention to the treatment of the massive modes as these are defined in a coset space. We have used the assumption that the spectrum of the Perron-Frobenius operator possesses a finite gap even for infinite graph size. We have shown that the effective action and the source terms are given by Eqs. (26) and (27) and by Eq. (30), respectively.

To evaluate the resulting generating function, we have defined Gaussian superintegrals by expanding the effective action up to terms of second order. The remaining terms are expanded in a Taylor series. We have carried out the Gaussian superintegrals over the product of that series with the source terms. We have given order-of-magnitude estimates of the resulting expressions using averages based upon completeness and unitarity. Assuming that these approximations are valid, we are led to the conclusion that the contribution of massive modes to the two-point function vanishes for large graph size. Therefore, that function attains universal form.

The rough estimates in Sect. 4.3 are based on averages and require small fluctuations. That may be unsatisfactory. We are working on strict estimates. We hope to be able soon to report on these, combining that with a more detailed account of conceptual and technical aspects of the steps taken in Sect. 3 that were treated here only cursorily.

The author is much indebted to M. R. Zirnbauer. Without his numerous useful suggestions, especially concerning the developments in Sect. 3, this contribution would not have come into existence.

References

1. O. Bohigas, M. J. Giannonni, and C. Schmit, Phys. Rev. Lett. **52**, 1 (1984).
2. T. Kottos and U. Smilansky, Ann. Phys. **274** (1999) 76.
3. S. Gnutzmann and A. Altland, Phys. Rev. Lett. **93**, 014103 (2004).
4. S. Gnutzmann and A. Altland, Phys. Rev. E **72**, 056215 (2005).
5. Z. Pluhař and H. A. Weidenmüller, Phys. Rev. Lett. **110**, 034101 (2013); Phys. Rev. E **88**, 022902 (2013); Phys. Rev. Lett. **112**, 144102 (2014).
6. Z. Pluhař and H. A. Weidenmüller, J. Phys. A: Math. Theor. **48** (2015) 275102.
7. A. Altland, S. Gnutzmann, F. Haake, and T. Micklitz, Rep. Prog. Phys. **78** (2015) 086001.
8. M. R. Zirnbauer, J. Phys. A: Math. Gen. **29** (1996) 7113.
9. M. R. Zirnbauer, J. Math. Phys. **38** (1997) 2007 and arxiv:cond-mat/9701024.